SYNTHETIC STUDIES AND BIOLOGICAL ACTIVITY OF SPIROINDOLIZIDINE-OXINDOLE AND INDOLIZIDINE ALKALOIDS DERIVATIVE

By
MR. Artid BUAPHAN

A Thesis Submitted in Partial Fulfillment of the Requirements
for Doctor of Philosophy ORGANIC CHEMISTRY
Department of CHEMISTRY
Graduate School, Silpakorn University
Academic Year 2022

การศึกษาการสังเคราะห์และการออกฤทธิ์ทางชีวภาพของสไปโรอินโดลิซิดีนออกซินโดลและอินโดลิซิดีนอัลคาลอยด์ที่มีความหลากหลายทางโครงสร้าง

โดย
นายอาทิตย์ บัวผัน

วิทยานิพนธ์นี้เป็นส่วนหนึ่งของการศึกษาตามหลักสูตรปรัชญาดุษฎีบัณฑิต
สาขาวิชาเคมีอินทรีย์ แบบ 1.1 ปรัชญาดุษฎีบัณฑิต
ภาควิชาเคมี
บัณฑิตวิทยาลัย มหาวิทยาลัยศิลปากร
ปีการศึกษา 2565

SYNTHETIC STUDIES AND BIOLOGICAL ACTIVITY OF SPIROINDOLIZIDINE-OXINDOLE AND INDOLIZIDINE ALKALOIDS DERIVATIVE

By
MR. Artid BUAPHAN

A Thesis Submitted in Partial Fulfillment of the Requirements
for Doctor of Philosophy ORGANIC CHEMISTRY
Department of CHEMISTRY
Graduate School, Silpakorn University
Academic Year 2022

Title	SYNTHETIC STUDIES AND BIOLOGICAL ACTIVITY OF SPIROINDOLIZIDINE-OXINDOLE AND INDOLIZIDINE ALKALOIDS DERIVATIVE
By	MR. Artid BUAPHAN
Field of Study	ORGANIC CHEMISTRY
Advisor	Assistant Professor Punlop Kuntiyong, Ph.D.

Graduate School Silpakorn University in Partial Fulfillment of the Requirements for the Doctor of Philosophy

.....Dean of the Graduate School
(Assistant Professor Sathit Niratisai, Ph.D) (Acting)

Approved by

.....Chair person
(Assistant Professor Kanok-on Rayanil, Ph.D.)

.....Advisor
(Assistant Professor Punlop Kuntiyong, Ph.D.)

.....External Examiner
(Associate Professor Pitak Chuawong, Ph.D.)

60302802 : Major ORGANIC CHEMISTRY
Keyword : indoloquinolizidine; spiroindolizidine-oxindole; N-acyliminium ion cyclization; oxidative ring contraction; α-glucosidase; nitric oxide (NO)

MR. ARTID BUAPHAN : SYNTHETIC STUDIES AND BIOLOGICAL ACTIVITY OF SPIROINDOLIZIDINE-OXINDOLE AND INDOLIZIDINE ALKALOIDS DERIVATIVE THESIS ADVISOR : ASSISTANT PROFESSOR PUNLOP KUNTIYONG, Ph.D.

Spiroindolizidine-oxindole and indoloquinolizidine belong to an important class of alkaloids with variety of structures and biological activites. For example, rhynchophylline and mitraphylline, natural product isolated from the plant species *Uncaria* and *Mitragyna speciosa* 'Kratom' found in the region of Africa and South America and Southeast Asia especially in Thailand. *Uncaria* have 34 species in the world. In Southeast Asia, some of the traditional treatments for medicinal proposes such as ailments including cardiovascular and central nervous system such as lightheadedness, dizziness, convulsions, numbness and hypertension rely on extracts from *Uncaria* plants.

Another related indolizidine alkaloid is hirsutine, indoloquinolizidine alkaloid isolated from the plant species *Hirsutus* and *Uncaria* extraction, which have various biological activities used as a traditional medicine in China to cure convulsions analgesic and a sedative. Especially, hirsutine involved medical community to inhibit the growth of influenza A virus (subtype H_3N_2) with an EC_{50} value of 0.40-0.57 μg/mL. Hirsutine is 10-20 times more effective than ribavirin as drug.

Our objective of this research is to find ways to synthesize rhynchophylline and hirsutine analog in the form of enamide with functionality suitable for further synthesize spiroindolizidine-oxindole and indoloquinolizidine derivative, respectively. We used oxidative ring contraction and *N*-acyliminium ion cyclization, cope elimination, hydrogenation, and Micheal reacion as key reactions to construct spiroindolizidine-oxindole and indoloquinolizidine, respectively. Herein we reported the syntheses of spiroindolizidine-oxindole and indoloquinolizidine from commercial L-glutamic acid and tryptamine which have alkoxy instead of enamide that provided a less complication in synthetic route to study a reaction that could be provided for spiroindolizidine-oxindole and indoloquinolizidine derivative synthesis. We used *N*-acyliminium ion cyclization to construct the indoloquinolizidine for hirsutine analog. The oxidative ring contraction of indoloquinolizidine gave spiroindolizidine-oxindole. The *N*-dibenzylamino group in spiroindolizidine-oxindole and indoloquinolizidine was removed using cope elimination to provide a cyclic enamide as a key intermediate. Micheal reaction with various alcohol provided series of spiroindolizidine-oxindole] and indoloquinolizidine derivatives. These compounds active by values exhibit nitric oxide synthesis inhibition and induced nitric oxide synthase (iNOS) protein expression. Nitric oxide is an important cellular signaling molecule which is synthesized from L-arginine. It is a vital molecule that affects cell homeostasis in our body controlling movement of smooth muscle, activating innate immunity against some pathogens and triggering the inflammatory process. In part of chemical pretreatment spiroindolizidine-

oxindole and indoloquinolizidine significantly reduced active by values iNOS expression. It showed the most significant activity against nitric oxide (NO) production. It seemed like that this chemical could protect inflammation. The series of highly active indoloquinolizidines and spiro[indolizidine-oxindole derivatives were found to be inhibitors of α-glucosidase and therefore are potentially useful for treatment to delay the absorption of glucose after meals. Our synthetic indoloquinolizidines and spiroindolizidine-oxindole derivatives inhibited α-glucosidase with IC_{50} values between 13.83±0.01 and 900.44±0.01 μM. Among them, the indoloquinolizidine and spiroindolizidine-oxindole derivative displayed strong activity when compared with acarbose as positive control (an IC_{50} value of 106.09±0.03 μM).

ACKNOWLEDGEMENTS

I would like to express my sincere this opportunity to thank all the people in my life who have maintained me during my academic years in graduate school. I could not have completed this educated without their help.

First of all, I thank the Department of Chemistry, Faculty of Science, Silpakorn University for servicing my education. I would like to thank the Graduate School of Silpakorn University for giving advice on writing a thesis in the ithesis system. Thank you for giving me the experience and rational thinking so that I can develop my future career as a lecturer. More than help from an educational institution, I would like to thank staff from all sectors for their assistance with the laboratory and making this thesis possible.

I would like to thank Assistant Professor Punlop Kuntiyong, Ph.D., my advisor, for useful guidance and teaching. He is a perfect teacher. He helps me with my research and revision of this thesis.

To my committee, Associate Professor Pitak Chuawong, Ph.D., Assistant Professor Kanok-on Rayanil, Ph.D., I thank them for time and guidance during my time in graduate school.

Finally, I would like to thank my family for encouragement and supports throughout the period of studying in doctor of philosophy degree. I hope this thesis will be helpful to other researchers.

MR. Artid BUAPHAN

TABLE OF CONTENTS

Page

LIST OF SCHEME

Page

LIST OF FIGURE

Page

CHAPTER 1
INTRODUCTION

Background and Signification of the Research Problem

Human life (1) has changed more over the past century than in all the previously recorded span of human history. The world's population has increased than doubled because of our ability to synthesize drugs to control diseases acquired through knowledge of organic chemistry. Organic chemistry is the study of carbon-based compounds. Unlike most other elements, carbon can form strong bonds with carbon atoms and other elements through covalent bonds that can form chains and rings. The importance of carbon is a key element in the body of life on Earth. Most living creatures are made up of complex organic compounds that accomplish structural, chemical or genetic functions.

Prior to the expansion of the chemical industry in the late 19th and early 20th centuries, only natural compounds were used for medicinal purposes. Natural color compounds are used to dye clothes. For example, a purple dye derived from mollusks found in the Middle East, where fabrics have been used to dye fabrics since ancient times. Natural extracts are used as raw materials for perfumery, for instance, kaffir lime leaf extract. For centuries, roses and lavender have been used as main ingredients in perfumery.

In nature, there are many organic compounds that are obtained by extracting them from natural products. Three examples of organic compounds are in natural product. Nicotine comes from the tobacco plant, an addictive alkaloid. Citrus fruit contain vitamin C, essential for preventing scurvy. Morphine is derived from the opium poppy, a pain-relieving, addictive alkaloid. Natural product extracts have both benefits and disadvantages depending on their use. The structure of natural products of vitamin C, nicotine and morphine is shown in figure 1.

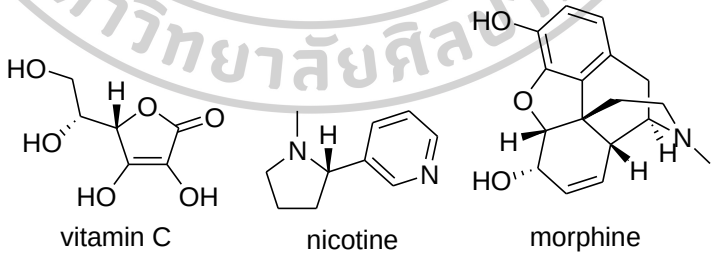

Figure 1 Structure of natural products of vitamin C, nicotine and morphine

Many natural products were first used with a lack of knowledge of their chemical composition. When organic chemistry advanced, chemists have studied how to work out the structure of compounds in natural products. For example, the therapeutic properties of lemons and other citrus fruits known for centuries but the chemical structure of vitamin C which is an active ingredient that was not prescribed until 1933. Today there is a recovery of interest in traditional remedies. And it is

working hard to identify important medicinal chemical compounds found in living organisms.

Once the structure is known, organic chemists will try to synthesize the compound in the laboratory. If the starting material is low cost and the synthesis process is simple enough. It may be converted to a more inexpensive material to produce compounds than to extract the compound from living organisms. The well-being of modern society is impossible without the many products of industrial organic synthesis. Our quality of life depends heavily on products in the pharmaceutical industry, such as disease fighting antibiotics and anti-inflammatory pain relievers.

Alkaloids (2) are a group of natural products that have nitrogen atoms and might contain of other elements such as oxygen, sulfur, chlorine, bromine and phosphorus in their molecules. Nitrogen atoms may exist in the form of amine, amine oxide, amide and imide. Alkaloids have diverse and important physiological effects on humans and other living organisms. Alkaloids are produced by a wide variety of organisms, including bacteria, fungi, plants and animals. Alkaloids are known for their versatile therapeutic potential such as anticancer, antimalarial, anesthetic and stimulant etc. Alkaloids were purified from crude extracts by extraction and chromatography.

According to the heterocyclic ring system and biosynthetic precursor Alkaloids are classified into different types such as indole, purine, quinoline, isoquinoline, tropane, imidazole, etc. The basic structure of the alkaloids above is shown in figure 2.

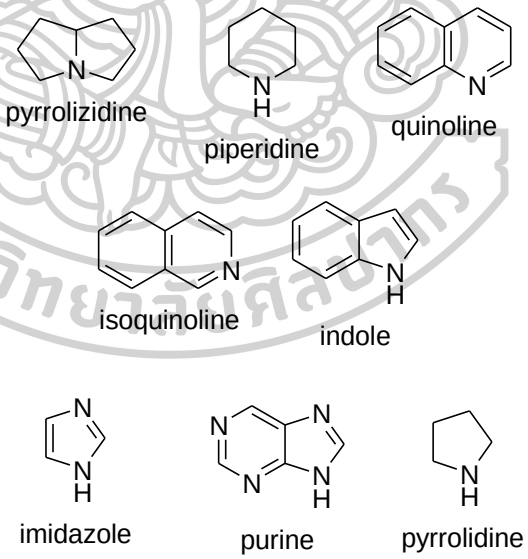

Figure 2 Basic structure of pyrrolizidine, piperidine, quinolone, isoquinoline, indole, imidazole, purine and pyrrolidine nucleus.

Alkaloids have the potential to be antiproliferative, antibacterial and antioxidant, which can be used for drug development in the pharmaceutical industry. The therapeutic potential of alkaloid expands its application in industry. There is a lot

of research on the pharmaceutical properties of various alkaloids extracted from living organisms.

Classification of alkaloids according to their carbon skeleton or biogenic precursor gives three types of alkaloids; (1) True alkaloids; this alkaloid is derived from amino acids and shares a nitrogen-containing heterocyclic ring. These alkaloids are highly reactive in nature and have potent biological activity. Structural characteristics form soluble salts. Many kinds are crystalline which combine with acids and form salts. Almost true alkaloids are bitter and hard. Their existence in plants occurs in three forms: in the free states, *N*-oxide and salt. (2) Protoalkaloids; this alkaloid is derived from amino acids but not part of the heterocyclic ring. These alkaloids are used for various health disorders such as mental illness, pain and neurosis. (3) Pseudoalkaloids; Simple structures of pseudoalkaloids are not directly from amino acids. These structures are connected to the amino acid path which is derived from by amination or transamination reaction from precursors or postcursors of amino acid. Due to the various biological activities and complexity of the structure, organic chemists were impulsion. In the organic chemistry society, a large number of alkaloid compounds have been studied in the synthesis. The total synthesis of bioactive alkaloids and their analogues has been reported. We are interested in the synthesis of the spiroindolizidine-oxindole and indolizidine alkaloids. The key reaction for this research is successful in the synthesis of indoloquinolizidine. The indoloquinolizidine is a part of the spiroindolizidine-oxindole and indolizidine structure. The two key reactions are *N*-acyliminium ion cyclization and oxidative rearrangement.

The *N*-acyliminium ion cyclization reaction (3) can be used as a key reaction in the synthesis of one to many ring structures, which can synthesize the core structure of various natural products. The *N*-acyliminium ion has been used as an important reaction in the synthesis of a wide variety of structures from the past to the present.

The *N*-acyliminium ion cyclization reaction involves iminium ion, which are important initial intermediate in organic synthesis where bonds between carbon-carbon atoms and carbon-heteroatom are formed. The atoms in which the compounds can be develop in cyclization reactions that formed by *N*-acyliminium ion. In contrast to the cyclization reaction that takes place by iminium cation through the Mannich reaction and the Pictet-Spengler reaction as shown in scheme 1 respectively.

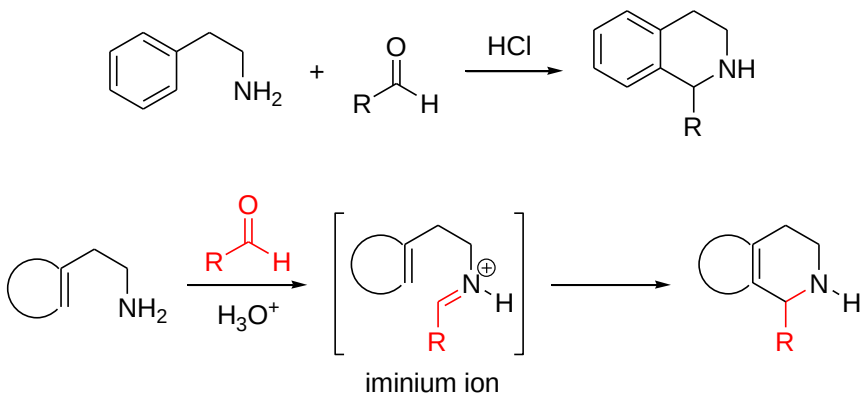

Scheme 1 Mannich reaction and Pictet-Spengler reaction, respectively.

The cyclization reaction takes place through *N*-acyliminium ion with very reactive intermediates of electron-deficient electrophiles which favorable attraction electrophiles toward weak nucleophiles of the carbonyl group on the nitrogen atom or double bond between carbon atoms such as aromatic and heteroaromatic compound. The *N*-acyliminium ion is reacting well including double and triple bonds. The *N*-acyliminium ion is more active electrophiles than *N*-akyliminium ion. The reasons for electrophilic used in α-amidoalkylation of various nucleophile compounds as shown in scheme 2.

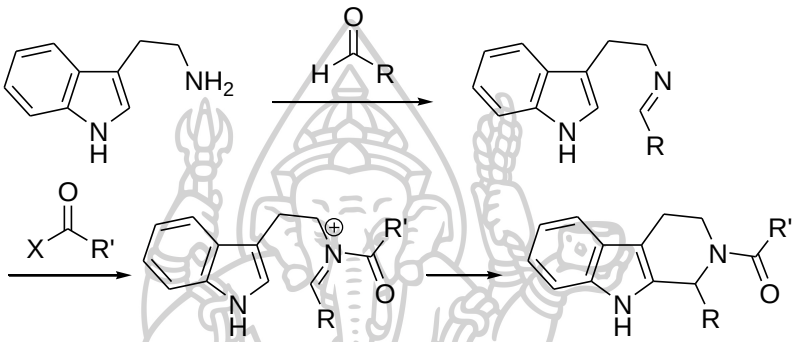

Scheme 2 Intramolecular cyclization of *N*-acyliminium ion

The two reactions involving *N*-acyliminium ion intermediate are Mannich and Pictet-Spengler reaction, where Pictet-Spengler reaction is a form of intramolecular reaction of Mannich reaction, which is the information given by Amé Pictet and Theodor Spengler in 1911. There are two main types of intermediates: *N*-acyliminium ion and *N*-alkyliminium ion with intermolecular and intramolecular addition respectively (Figure 3). The intramolecular of iminium cyclization focus on enantioelective to lead the formation of rings that can lead to the synthesis of polycyclic natural products.

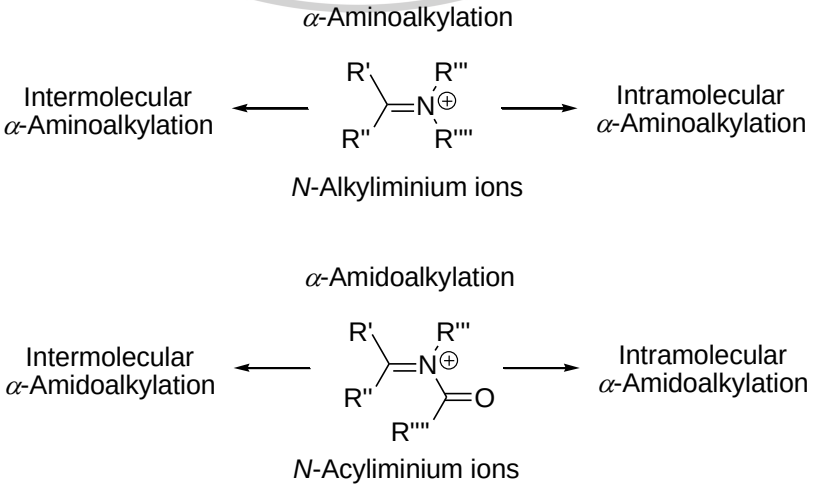

Figure 3 Intermediate of *N*-acyliminium ion and *N*-alkyliminium ion and related reaction

The *N*-acyliminium ion can be rearranged resulting in different stereochemical products. In later year, the *N*-acyliminium ion reaction in the molecule is formed by the hydroxylactam structure as part of the synthesis of natural products.

Formation of the *N*-acyliminium ion intermediate

There are three main structure of *N*-acyliminium ion formation. The first procedure is the most widely used form today constructed on the release of leaving group from the alpha position of acyl nitrogen under acidic conditions in reversible reaction. Subsequent, the nucleophile will attack alpha position of *N*-acyliminium ion intermediate to generate product (Scheme 3).

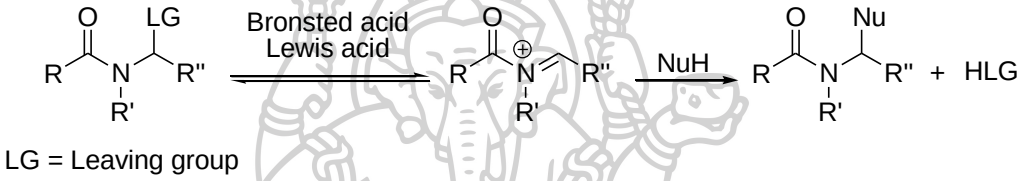

Scheme 3 Generation of *N*-acyliminium ion with release of leaving group

The common leaving group is the protonation of the hydroxyl group. But there are other leaving groups that use it, such as halogen, alkyloxy, aryloxy, acetoxy, alkylthio, arylthio, arylsulfonyl, carbamate and benzotriazolyl group. A variety of Lewis acids are used to create *N*-acyliminium ion intermediate such as iron(III) chloride ($FeCl_3$), tin(IV) chloride ($SnCl_4$), indium(III) chloride ($InCl_3$), boron trifluoride diethyl etherate ($BF_3{\cdot}OEt_2$), scandium(III) triflate ($Sc(OTf)_3$), indium(III) trifluoromethanesulfonate ($In(OTf)_3$), trimethylsilyl trifluoromethanesulfonate (TMSOTf), zinc trifluoromethanesulfonate ($Zn(OTf)_2$), copper(II) trifluoromethanesulfonate ($Cu(OTf)_2$) and silver trifluoromethanesulfonate (AgOTf). A diversity of Brønsted acids are used to geneate *N*-acyliminium ion intermediate such as formic acid, acetic acid (AcOH), sulfuric acid (H_2SO_4), *p*-toluenesulfonic acid (TsOH), Trifluoroacetic acid (TFA) and trifluoroacetic acid (CSA).

This second procedure has a synthetic *N*-acyliminium ion process intermediate by protonation of enamide compounds under acidic conditions. Next, the nucleophile will attack alpha position of *N*-acyliminium ion intermediate to generate product (Scheme 4).

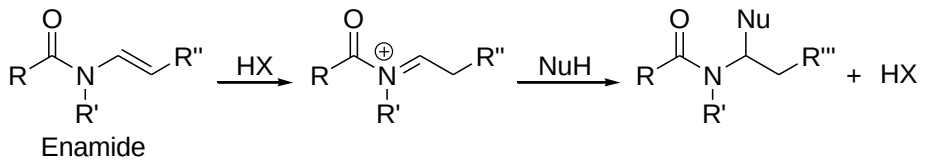

Scheme 4 Generation of *N*-acyliminium ion with protonation of enamide

The third procedure generated *N*-acyliminium ion by oxidation of the amide using the electrochemical principle, which is the form of Shono oxidation. The *N*-acyliminium ion formed a highly reactive intermediate, which reacts well with solvent with nucleophiles such as methanol and ethanol, to form *N*,*O*-acetal. The advantage of this reaction is irreversible reaction with nucleophiles (Scheme 5).

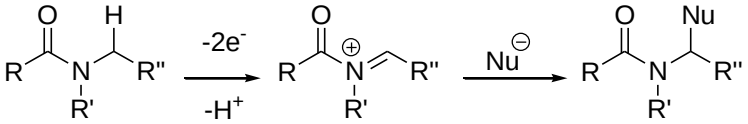

Scheme 5 Generation of *N*-acyliminium ion with anodic oxidation

Intramolecular cyclization depends reactivity of nucleophiles and the ability of iminium ion of each structure in various forms such as *N*-acyliminium, *N*-alkoxycarbonyliminium, *N*-carbamoyliminium, *N*-sulfonyliminium, *N*-phosphoryliminium and *N*,*N*-diacyliminium ions (Figure 4). This results in high diastereoselectivity, which is mainly influenced by the steric effect from substrates or auxiliaries compound. Chiral catalyst is consequence in high enantiomeric selectivity in stereochemistry.

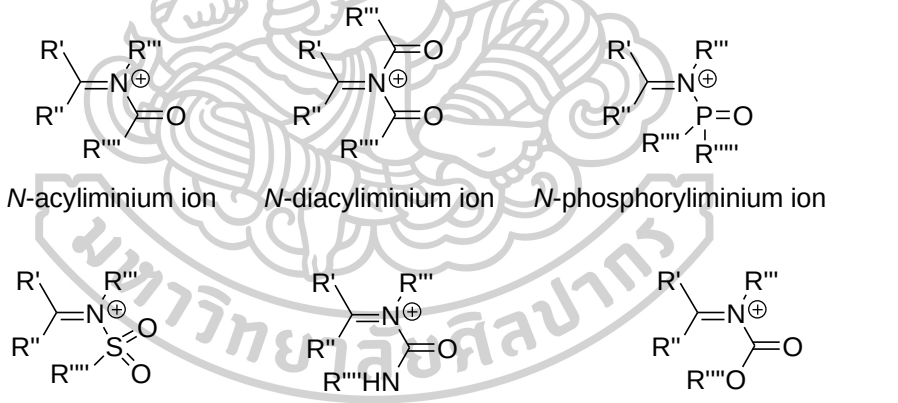

Figure 4 Structure of various iminium ions for cyclization

***N*-acyliminium cyclization for synthesis cyclic derivative**

The *N*-acyliminium ions intermediate are powerful reactive species for the formation of carbon-heteroatom and carbon-carbon bonds on the intramolecular. The *N*-acyliminium ion cyclization reactions have been used for the formation of structurally diverse skeletons of bicyclic, tricyclic and tetracyclic compound. The various precursors for cyclization reactions have been employed *N*-acyliminium ions derived for the assembly of structurally diverse skeletons.

Bicyclic skeletons by heteroatom nucleophiles

The tandem cyclization, diastereoselective ring expansion reaction have been used for the synthesis of bicyclic skeletons with fused rings or shared bonds by heteroatom nucleophiles through *N*-acyliminium ion intermediate. An example of structurally diverse compounds produced bicyclic compound through cyclization of *N*-acyliminium ion is shown by heteroatom nucleophiles in the figure 5.

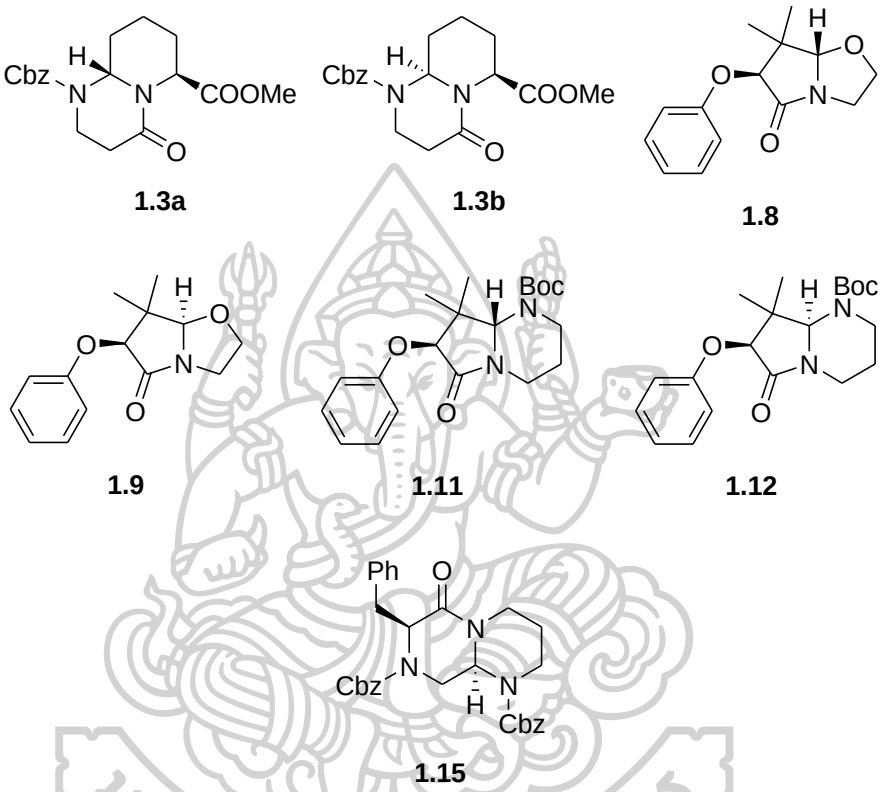

Figure 5 Structure synthesized bicyclic compounds from *N*-acyliminium cyclization by heteroatom nucleophiles

The products of different ring structures may be derived from a single reaction form which undergoes aza-Prins cyclization under the same conditions published by Blaauw and coworker which is the diastereoselective cationic tandem-cyclization of enantiomeric pure dipeptide compound **1.1** using 10 mol% *p*-toluenesulfonic acid (TsOH) in toluene. The *N*-acyliminium intermediate **1.2** was formed, leading to the synthesis of bicyclic *N*-heterocyclic compound **1.3a** and **1.3b** in 82% yield and 5:1 diastereomeric ratio by double cyclization (Scheme 6) (4), (5).

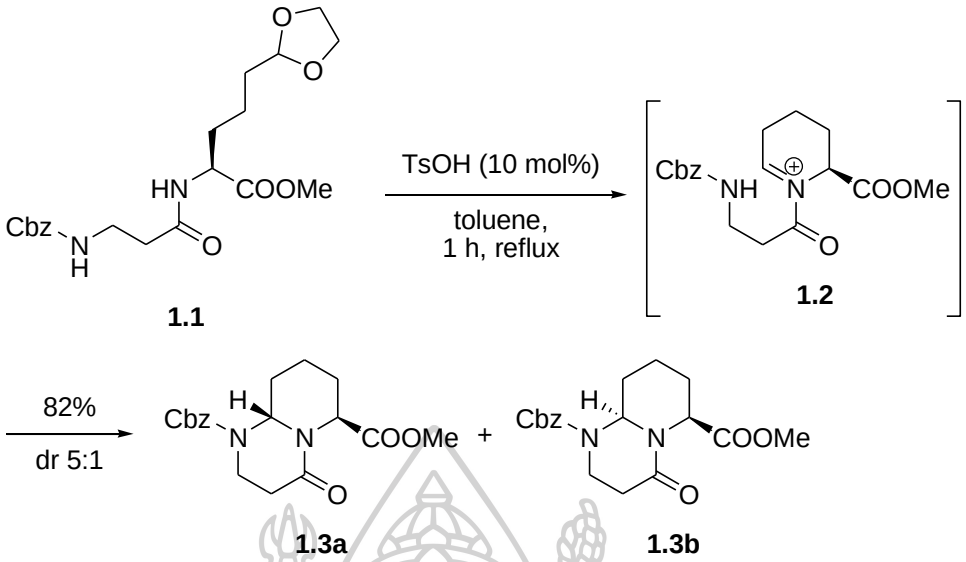

1.1 **1.2** **1.3a** **1.3b**

Scheme 6 Diastereoselective cationic tandem-cyclization through *N*-acyliminium ion intermediate

The intramolecular nucleophilic trapping of *N*-acyliminium ion intermediates by the hydroxyl moiety of *cis*-4-(1-chloro-1-methylethyl)-1-(ω-hydroxyalkyl)azetidin-2-ones were diastereoselectively converted into *trans*-1-aza-4-oxabicyclo[3.3.0]octan-8-ones and *trans*-1-aza-5-oxabicyclo[4.3.0]nonan-9-ones using with 1 equiv of silver tetrafluoroborate ($AgBF_4$) and pyridine in toluene of Kimpe. The research by Kimpe and coworker describes the diastereoselective ring expansion reaction of *cis*-4-(1-chloro-1-methylethyl)-1(ω-hydroxyalkyl)azetidin-2-ones **1.6** using silver tetrafluoroborate ($AgBF_4$) and pyridine dissolve in toluene. Formed through *N*-acyliminium ion intermediate **1.7** to produce bicyclic lactam **1.8** in 44% yield and **1.9** in 21% yield. In the same condition, diastereoselective ring expansion reaction of *N*-Boc azetidin-2-ones **1.6** was obtained bicyclic lactam **1.11** (54% yield) and **1.12** (14% yield) in higher trans diastereoselective explained by the steric hindrance of Boc group (Scheme 7) (6).

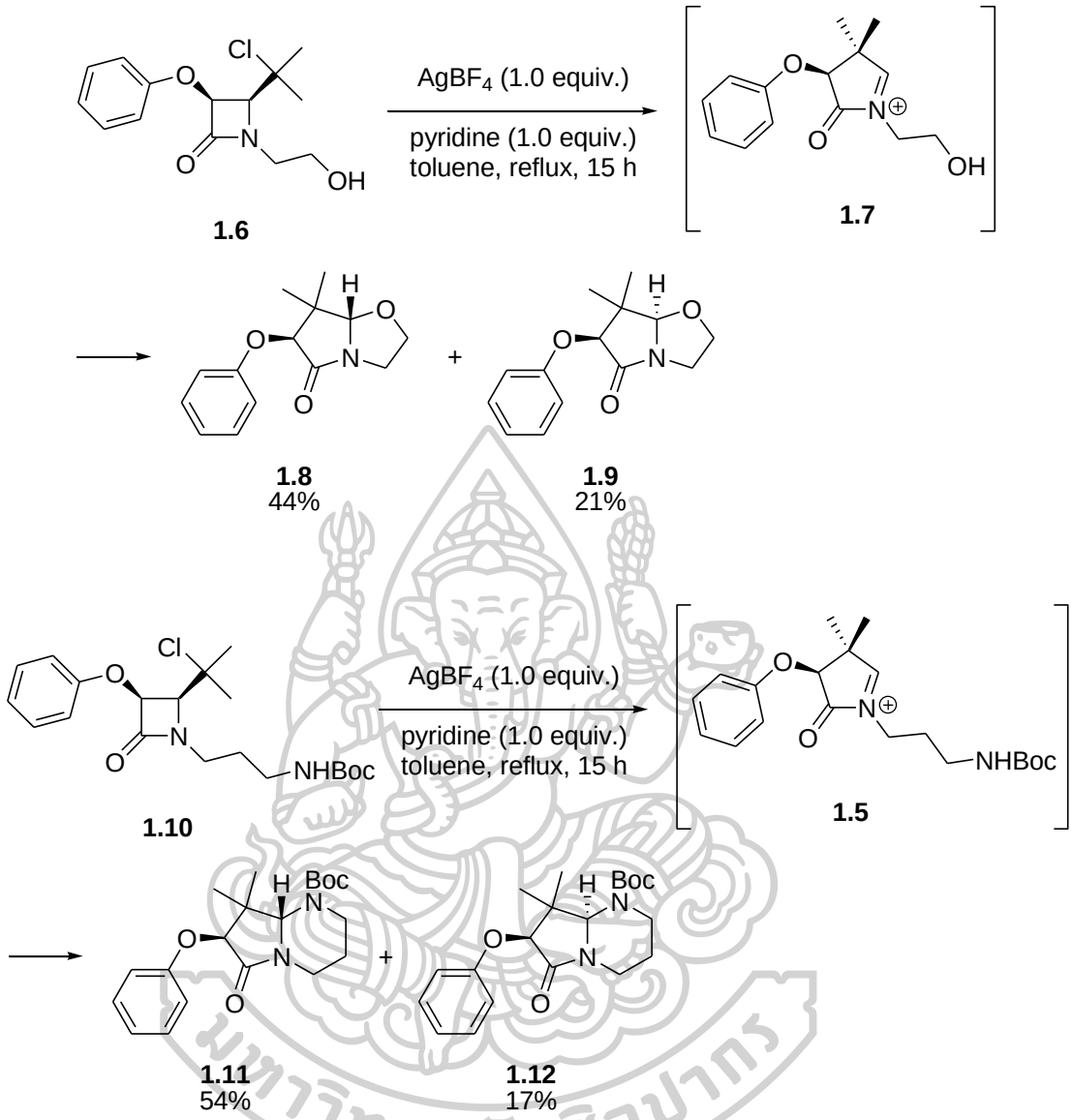

Scheme 7 Diastereoselective ring expansion reaction through *N*-acyliminium ion intermediate by Kimpe and coworker

An example of bicyclic compound formation is researched by Hruby and coworker. The amide-aldehyde condensation followed by cyclization between carbamate-tethered acetal compound **1.13** with formic acid are formed *N*-acyliminium ion intermediate **1.14** to give bicyclic compound **1.15** (89% yield) in single diastereomer as a result of thermodynamic control. The formation of diastereomer paid low energy chairlike conformation of bicyclic skeleton (Scheme 8) (7).

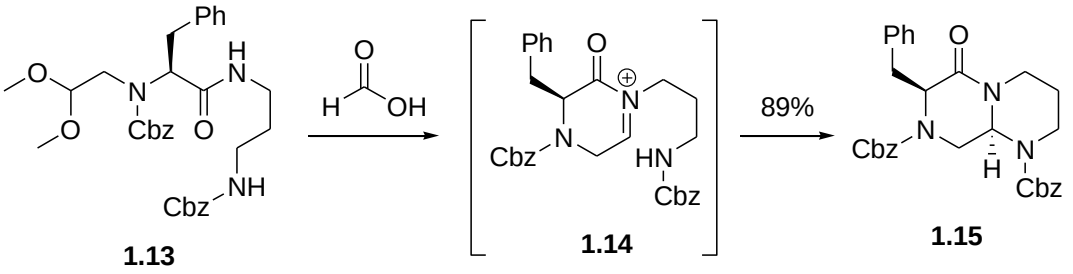

Scheme 8 Amide-aldehyde condensation through *N*-acyliminium ion intermediate by Hruby and coworkers

Bicyclic skeletons by alkene nucleophiles

The endo-trig cyclization followed by Friedel-Crafts or aza-Prins-Ritter, intramolecular Schmidt *N*-acyliminium ions cyclization, intramolecular tandem Michael/Mannich reaction have been used for the synthesis of bicyclic skeletons with fused rings or shared bonds by alkene nucleophiles through *N*-acyliminium ion intermediate. An example of structurally diverse compounds produced bicyclic compound through cyclization of *N*-acyliminium ion by alkene nucleophiles is shown in the figure 6.

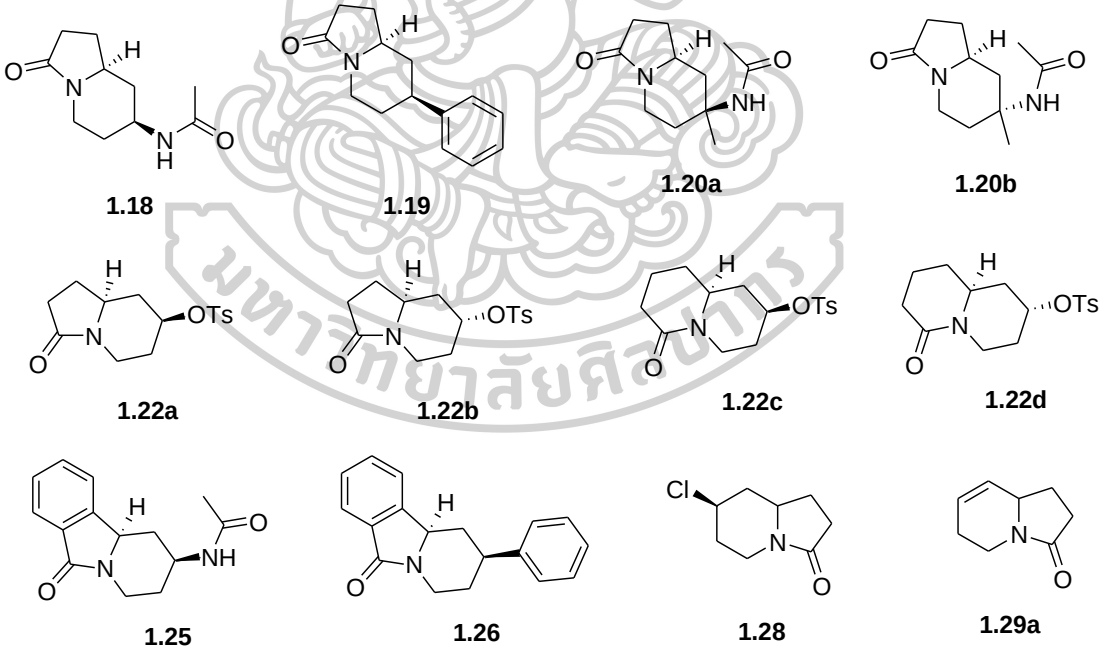

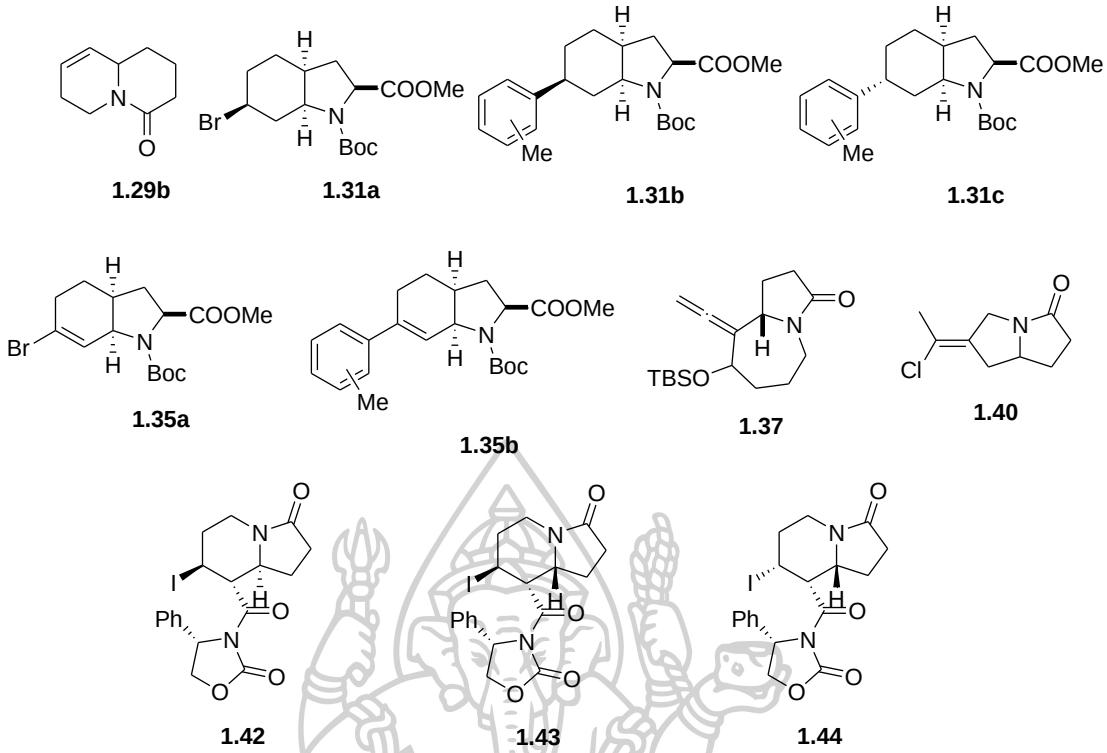

Figure 6 Structure synthesized bicyclic compounds from *N*-acyliminium cyclization by alkene nucleophiles

The endo-trig cyclization reaction of hydroxylactam compound **1.16** using boron trifluoride diethyl etherate ($BF_3 \cdot OEt_2$) to give azabicyclic carbocation intermediates **1.17** followed by tandem aza-Prins-Ritter reactions generate amido-substituted azabicyclic compounds **1.18** in 81% yield using nitriles. Another approach of Friedel-Crafts reactions of carbocation intermediates **1.17** in the presence of benzene gave phenyl-substituted compounds **1.19** in 73% yield. The aza-Prins-Ritter hydrolysis of hydroxylactam compound **1.16a** using boron trifluoride diethyl etherate ($BF_3 \cdot OEt_2$) and nitriles gave bicyclic **1.20a** and **1.20b** in 86% yield as 3:2 diastereomeric ratio (Scheme 9) (8).

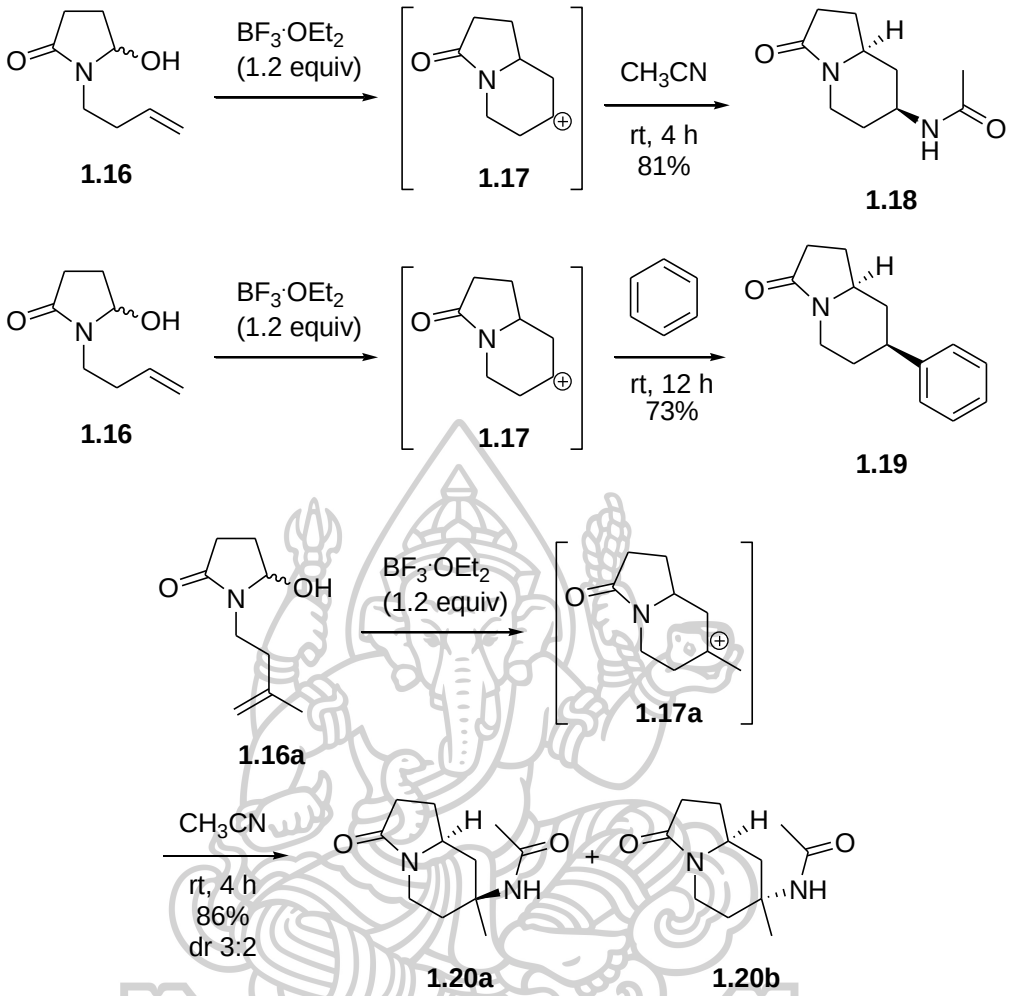

Scheme 9 Endo-trig cyclization reaction of hydroxylactam followed by aza-Prins-Ritter reaction and Friedel-Crafts reaction

Another example is the tandem aza-Prins-Ritter reaction of *N*-homoallyl hydroxylactam **1.21a** and **1.21b**, the structure leading to the formation of *N*-acyliminium ion using *p*-toluenesulfonic acid (TsOH) as both Bronsted acid catalyst and nucleophile gave bicyclic lactam **1.22a** and **1.22b** in 88% yield as 17:3 diastereomeric ratio of **1.22c** and **1.22d** in 80% yield as 9:1 diastereomeric ratio, respectively. Effect of diastereomeric ratio is a result of the steric effect at the carbocation position of intermediate. Ts-deprotection of the bicyclic lactam **1.22a**, **1.22b**, **1.22c** and **1.22d** using magnesium in methanol generated alcohol compound. From this structure can be enhanced to synthesize indolizidine alkaloids (Scheme 10) (9).

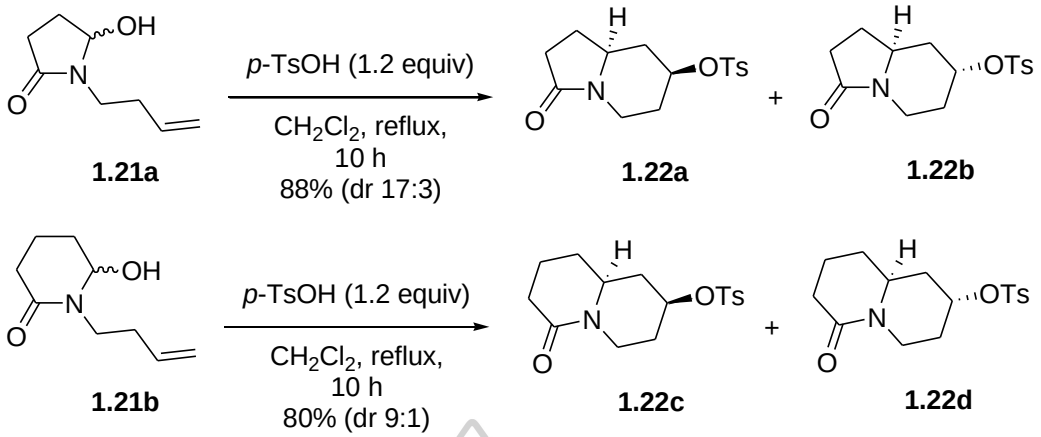

Scheme 10 The *N*-acyliminium ion cyclization via Tandem aza-Prins-Ritter reaction of *N*-homoallyl hydroxylactam

For example, the aza-Prins-Ritter reaction of bicyclic isoindolin-1-one compound **1.23** using boron trifluoride diethyl etherate ($BF_3 \cdot OEt_2$) and nitrile afford tricyclic amido compound **1.25** in 68% yield. Similarly, aza-Prins/Friedel-Crafts reaction by reacting with benzene instead of nitrile gave phenyl compound **1.26** in 78% yield. The diastereoselective for synthesis of tricycic compound was obtained from aza-Prins cyclization reaction of cyclic *N*-acyliminium ions intermediate using *p*-toluene sulphonic acid (*p*-TSA) under mild conditions. This aza-Prins-Ritter reaction aza-Prins/Friedel-Crafts reaction gave highly diastereoselective and excellent yields (Scheme 11) (9).

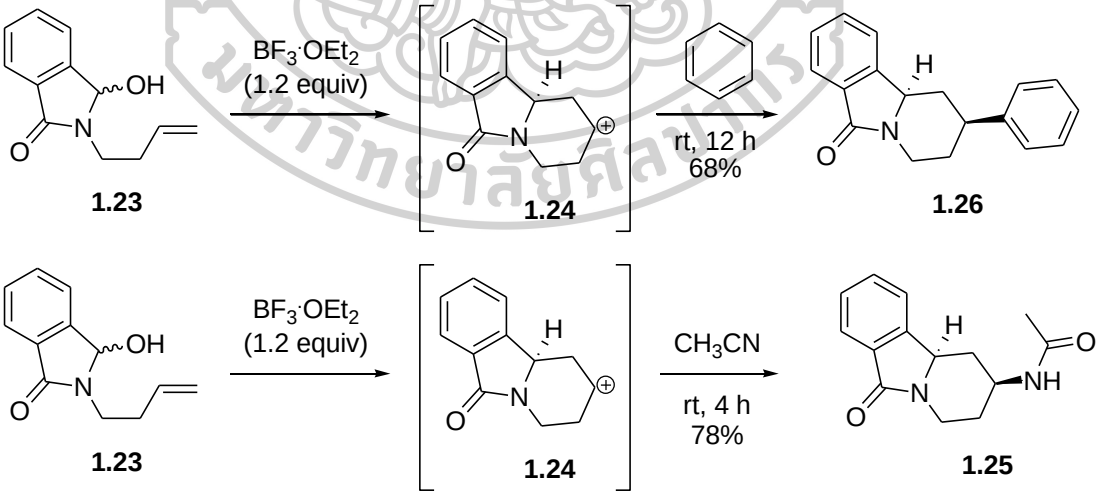

Scheme 11 The *N*-acyliminium ion cyclization via tandam aza-Prins-Ritter and tandem aza-Prins/Friedel-Crafts reaction of bicyclic isoindolin-1-one

The intramolecular aza-Prins and aza-silyl-Prins reactions have been ongoing from acyclic materials as the key reactant to form the core skeletons of various alkaloids. According to Dobbs and coworker research, intramolecular *N*-

acyliminium ion formation followed by aza-Prins cyclization of amide **1.27a** masked with an acetal protecting group using iron(III) chloride ($FeCl_3$) as Lewis acid gave lactam **1.28** in 94% yield as 9:1 diastereomeric ratio. Likewise, intramolecular *N*-acyliminium ion formation followed by aza-silyl-Prins cyclization of amide **1.27b** and **1.27c** using scandium(III) triflate ($Sc(OTf)_3$) as Lewis acid gave lactam **1.29a** and **1.29b** in 75% and 64% yield, respectively (Scheme 12) (10).

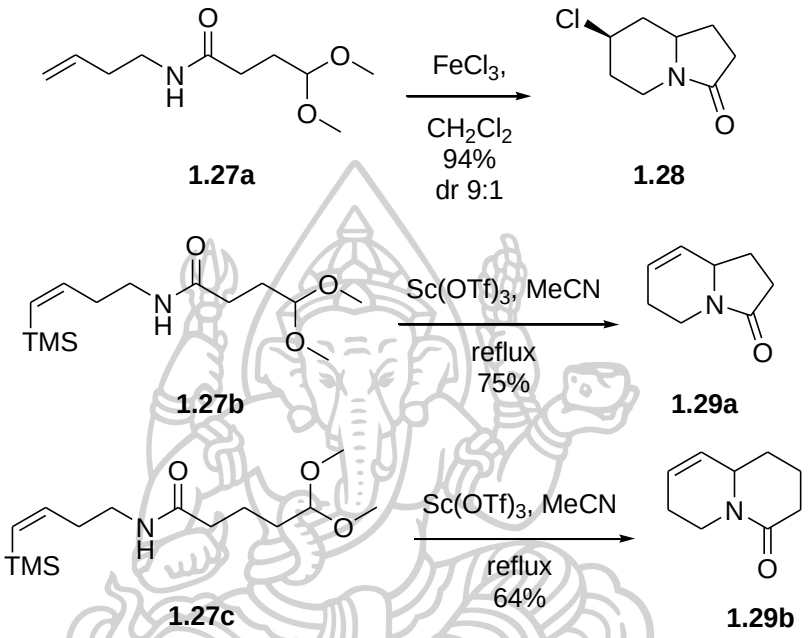

Scheme 12 The *N*-acyliminium ion formation via aza-Prins and aza-silyl-Prins cyclization of amide masked with an acetal protecting group

The five-membered ring *N*-Boc acyliminium ions derived from L-pyroglutamic acid undergo Lewis acid and tandem Friedel−Crafts carbocyclization to provide octahydroindole and hexahydroindole, respectively. According to research by Hanessian and coworker, terminal alkene **1.30** and **1.32** reacted with tin(II) halides and boron trifluoride diethyl etherate ($BF_3{\cdot}OEt_2$) as Lewis acid via intramolecular tandem Friedel-Crafts cyclization through *N*-Boc acyliminium ions intermediate produced octahydroindole **1.31a** in 78%, **1.31b** in 78% and **1.31c** in 74% yield, respectively. Similarly, intramolecular tandem Friedel-Crafts cyclization of alkyne precursor **1.34** was formed hexahydroidole **1.35a** in 80% and **1.35b** in 69% yield, respectively (Scheme 13) (11). The octahydroindole **1.31a** and hexahydroidole **1.35a** compound is a suitable precursor with halogen group can be decoration used to palladium catalyst of Suzuki-Miyaura, Heck and Stille reaction.

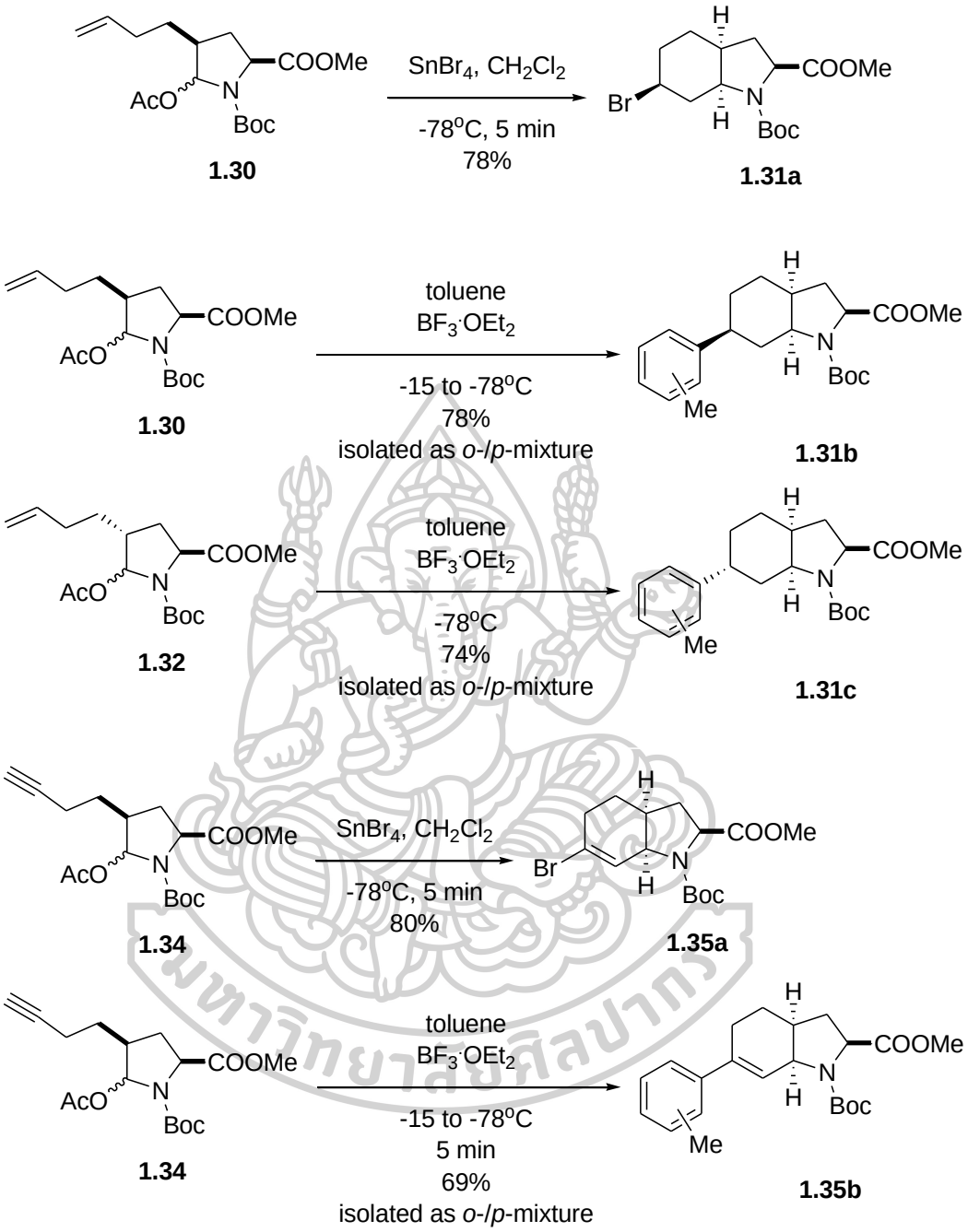

Scheme 13 The *N*-Boc acyliminium ions intermediate via intramolecular tandem Friedel-Crafts cyclization of terminal alkene and alkyne

Stemona alkaloids associated pyrrolo[1,2-*a*]azepine core with the polycyclic architecture, which interesting biological properties. Hong and coworker research based on the intramolecular *N*-acyliminium ions cyclization of propargylsilane **1.36** using iron(III) chloride ($FeCl_3$) as Lewis acid made it possible to synthesize bicyclic pyrrolo[1,2-a]azepine **1.37** in 86% yield, which from the structure can lead to the synthesis of stemoamide **1.38** as shown in scheme 14 (12).

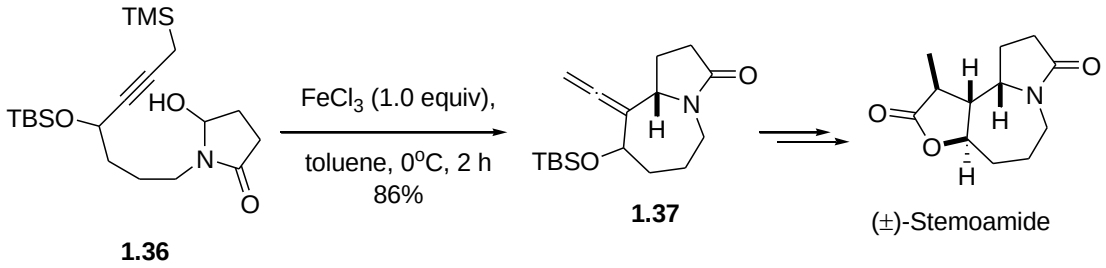

1.36 **1.37**

Scheme 14 Intramolecular *N*-acyliminium ions cyclization of propargylsilane lead to the synthesis of stemoamide

Preparation of substituted pyrrolizines through Schmidt reaction between acyl chlorides and alkyl azides was achieved in efficiency of the conversion to demonstrate in ring and bond construction. Publication of Gu and coworker used intramolecular Schmidt *N*-acyliminium ions cyclization of alkyne azide compound **1.39** with oxalyl chloride and Tin(IV) chloride ($SnCl_4$) synthesized bicyclic pyrrolizine **1.40** in 35% yield (Scheme 15) (13).

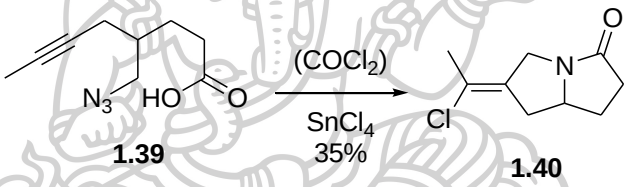

1.39 **1.40**

Scheme 15 Intramolecular Schmidt *N*-acyliminium ions cyclization of alkyne azide

Publication of nagasaka and coworker used intramolecular tandem Michael/Mannich reaction of *α,β*-unsaturated carbonyl compound **1.41** using titanium tetrachloride (TiCl) and tetrabutylammonium iodide (*n*-Bu_4NI) in the mixture of Ethyl acetate and dichloromethane afford the mixture of diastereomer of lactam **1.42**, **1.43** and **1.44** in 60% yield as 65:28:7 diastereomeric ratio (Scheme 16) (14).

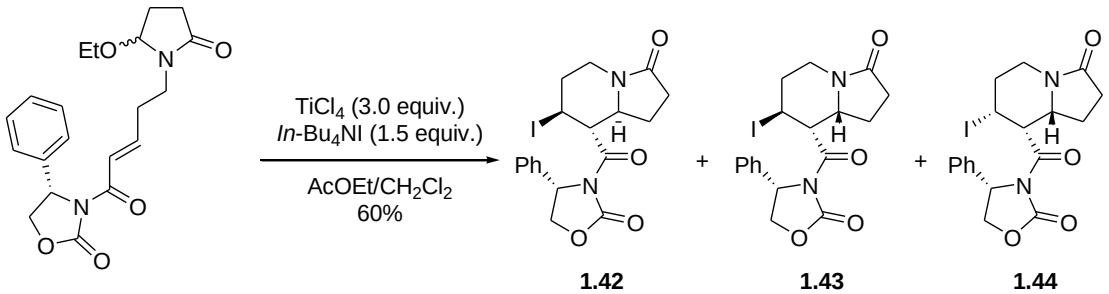

1.41 **1.42** **1.43** **1.44**

65 : 28 : 7

Scheme 16 The *N*-acyliminium ion cylization via intramolecular tandem Michael/Mannich reaction of *α,β*-unsaturated carbonyl compound

Bicyclic skeletons by aromatic nucleophiles

The Pictet-Spengler and aza-Nazarov cyclization have been used for the synthesis of bicyclic skeletons with fused rings or shared bonds by aromatic nucleophiles through *N*-acyliminium ion intermediate. An example of structurally diverse compounds produced bicyclic compound through cyclization of *N*-acyliminium ion by aromatic nucleophiles is shown in the figure 7.

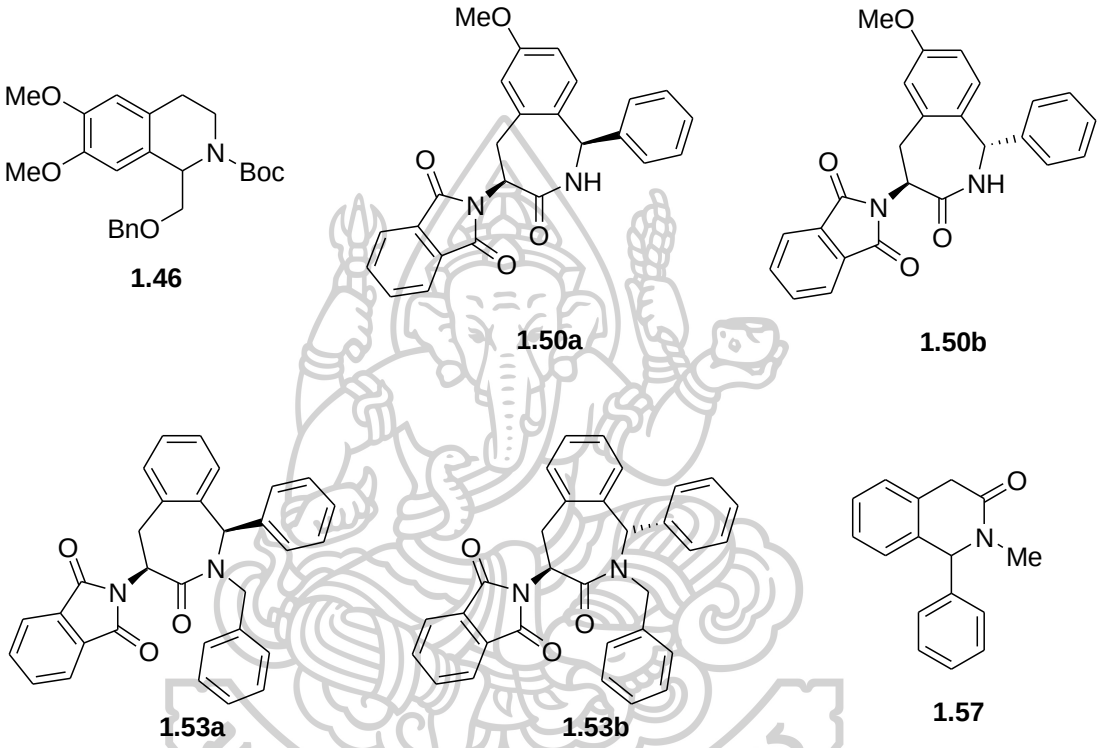

Figure 7 Structure synthesized bicyclic compounds from *N*-acyliminium cyclization by aromatic nucleophiles

Example of aromatic nucleophile in *N*-acyliminium ion cyclization using Pictet-Spengler cyclization via *N*-acyliminium ion of *N*,*O*-acetalic trimethylsilyl ethers **1.45** using boron trifluoride diethyl etherate ($BF_3 \cdot OEt_2$) as Lewis acid gave tetrahydroisoquinoline **1.46** in 85%. From this compound led to the synthesis of calycotomine as natural product (Scheme 17) (15).

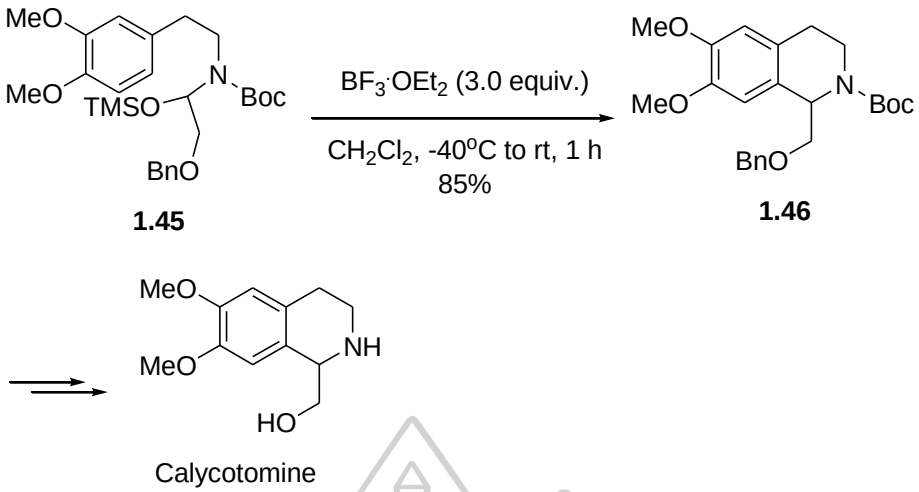

Scheme 17 The *N*-acyliminium ion cylization via Pictet-Spengler cyclization by aromatic nucleophile.

The 2-benzazepinone derivatives are used *N*-acyliminium ions as reactive intermediates, which are cyclized upon addition of aluminium chloride ($AlCl_3$). For instance for *N*-acyliminium ion cylization of benzotriazole compound **1.49** using aluminium chloride ($AlCl_3$) under reflux gave bicyclic **1.50** as seven-membered ring in 71% yield as 1:1 diastereomeric ratio. The benzotriazole (Bt) compound **1.49** synthesized from amide **1.48** reacting with aldehyde, benzotriazole and *p*-toluenesulfonic acid (*p*-TsOH) for overnight. In the second way, *N*-acylation of acid chloride compound **1.51** reacting with imine and antimony pentachloride ($SbCl_5$) undergo *N*-acyliminium intermediate **1.52** gave bicyclic compound **1.53** in 26% yield as 5:6 diastereomeric ratio (Scheme 18) (16).

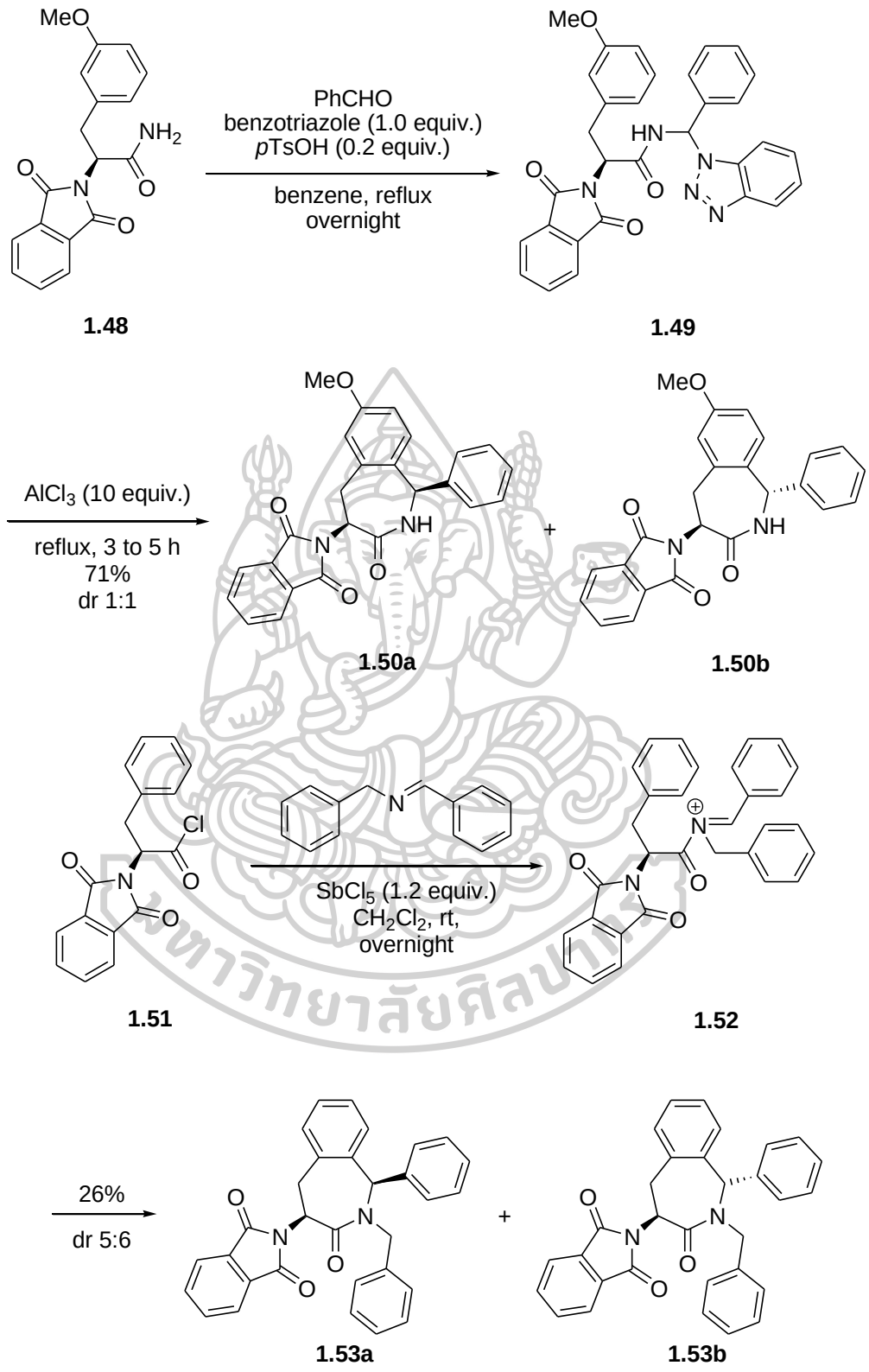

Scheme 18 The *N*-acyliminium ion cylization generated seven-membered ring compound

Intramolecular cyclizations involving *N*-acyliminium ions as the key reaction are used triflic acid (CF_3SO_3H). The tetrahydroisoquinolines have been transformed in high yields to tetrahydroisoquinoline derivatives. The aromatic nucleophile in *N*-acyliminium ion cylization published by Klumpp and coworker through aza-Nazarov cyclization, which is a reaction between imine **1.54** and arylacetyl chloride **1.55** using trifluoromethanesulfonic acid (CF_3SO_3H) gave bicyclic3-oxo-1,2,3,4-tetrahydroisoquinolines **1.57** in 95% yield (Scheme 19) (17).

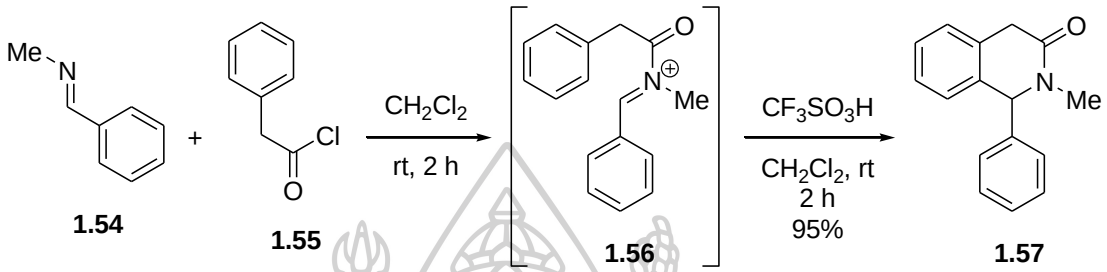

Scheme 19 Aromatic nucleophile in *N*-acyliminium ion cylization by Klumpp and coworker

Bicyclic skeletons with multiple shared bonds

The Lewis-acid-catalyzed *N*-acyliminium ion cyclization has been used for the synthesis of bicyclic skeletons with multiple shared bonds through *N*-acyliminium ion intermediate. An example of structurally diverse compounds produced through cyclization of *N*-acyliminium ion with multiple shared bonds is shown in the figure 8.

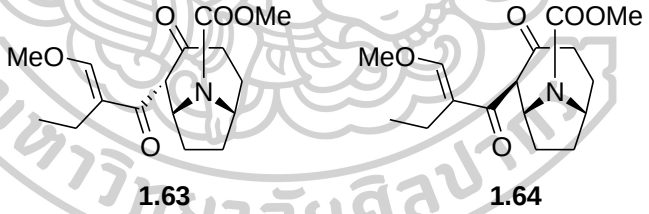

Figure 8 Structure synthesized bicyclic compounds from *N*-acyliminium cyclization with multiple shared bonds

The intramolecular reaction of an *N*-acyliminium ion cyclization was a key step in the synthesis of both pinnamine and anatoxin-a as natural product. The complete racemization was detected during the reaction of the *N*-acyliminium ion cyclization leading to pinnamine and anatoxin-a. Factors contributing to the stereochemistry of cyclization reactions included the kind of Lewis acid, solvent component, reaction time and the temperature. Publication of Tanner and coworker used Lewis-acid-catalyzed *N*-acyliminium ion cyclization of *β*-diketone compound **1.62** with tin(II) trifluoromethanesulfonate ($Sn(OTf)_2$) as Lewis acid and *N*-ethylpiperidine gave bicyclic compound **1.63** in 41% yield and **1.64** in 19% yield (Scheme 20) (18).

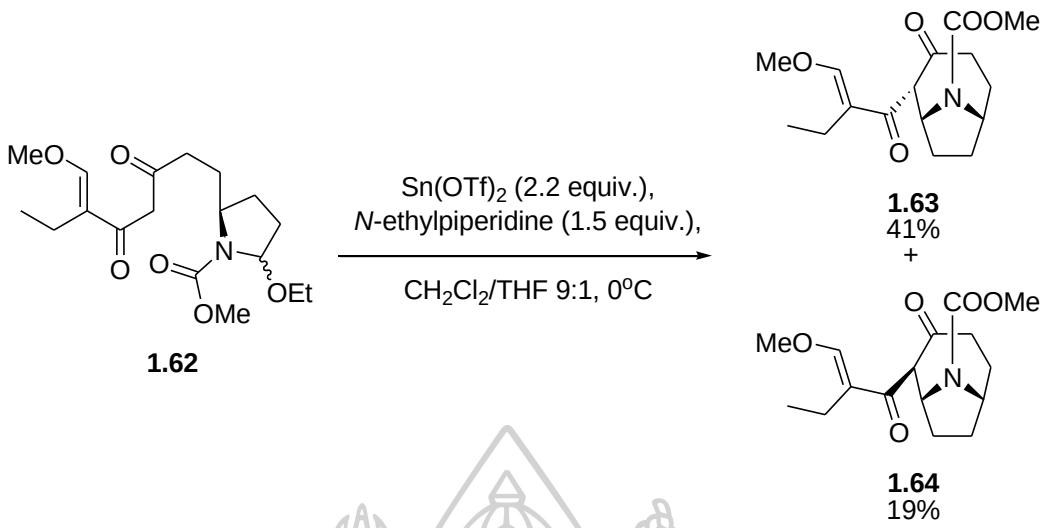

Scheme 20 Lewis-acid-catalyzed *N*-acyliminium ion cyclization of *β*-diketone compound by Tanner and coworker

Bicyclic skeletons with spiro atoms

The *N*-acyliminium ion spirocyclization and intramolecular aza-spirocyclization reaction have been used for the synthesis of bicyclic skeletons with spiro atoms through *N*-acyliminium ion intermediate. An example of structurally diverse compounds produced bicyclic compound through cyclization of *N*-acyliminium ion with multiple spiro atoms is shown in the figure 9.

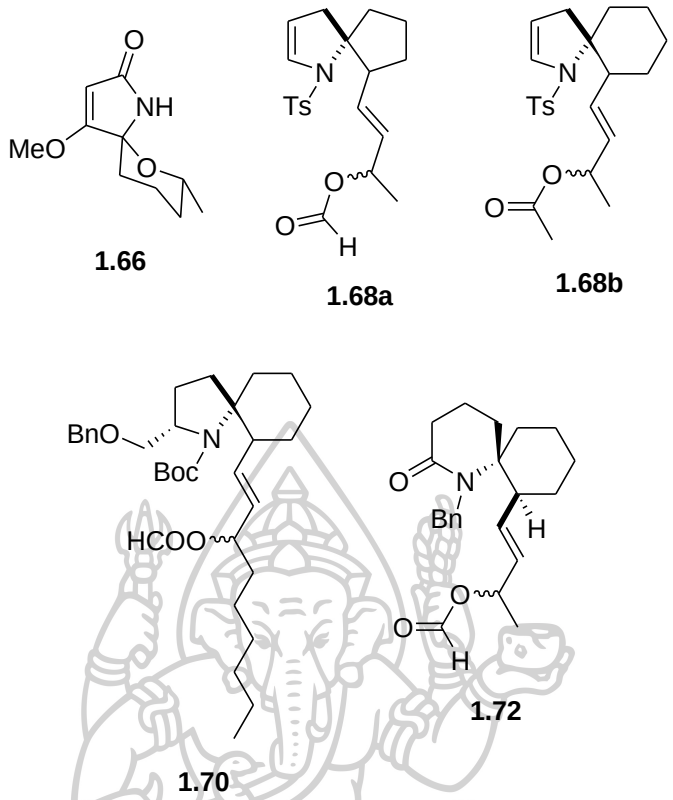

Figure 9 Structure synthesized bicyclic compounds from *N*-acyliminium cyclization with spiro atoms

The marineosins A and B were defined natural product to contain spiroiminal fragment. The key steps involve an acid-catalyzed *N*-acyliminium ion cyclization and Vilsmeier–Haack reaction with Trifluoromethanesulfonic anhydride (Tf_2O). For instance for *N*-acyliminium ion cyclization of lactam compound **1.65** as *N*-acyliminium ion precursor using *p*-toluenesulfonic acid (*p*-TsOH) in chloroform generated spiro compound **1.66** as single isomer in 54% yield by Shi and coworker (Scheme 21) (19).

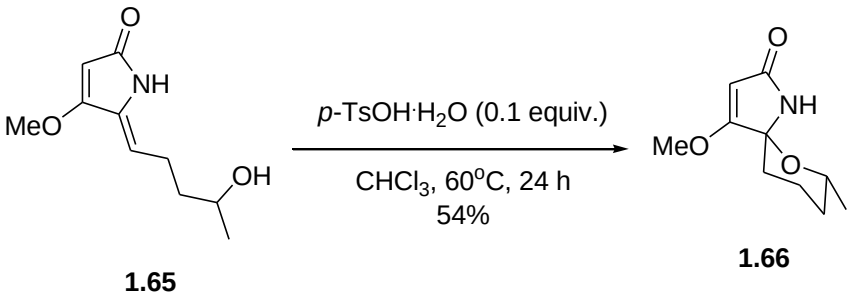

Scheme 21 The *N*-acyliminium ion cylization for synthesis spiro compound by Shi and coworker

The key strategic for the synthesis the tricyclic marine alkaloids such as (-)-lepadiformine, (+)-cylindricine C and (-)-fasicularin was the formic acid-induced intramolecular conjugate azaspirocyclization which to give highly efficient and stereoselective way. Publication of Kibayashi and coworker used *N*-acyliminium ion spirocyclization reactions has 3 examples. First, formic acid-induced intramolecular aza-spirocyclization reaction of *N*-Boc protecting compound **1.67a** using formic acid as Bronsted acids gave aza spiro compound **1.68a** as five membered ring in 43% yield. Similarly, intramolecular aza-spirocyclization reactions of *N*-Boc protecting compound **1.67b** was formed aza spiro compound **1.68b** as six membered ring in 55% yield. Third, the *N*-acyliminium ion spirocyclization of diene **1.69** used formic acid in mixture of toluene and tetrahydrofuran spirocyclic formate ester **1.70** in 88% yield (Scheme 22) (20).

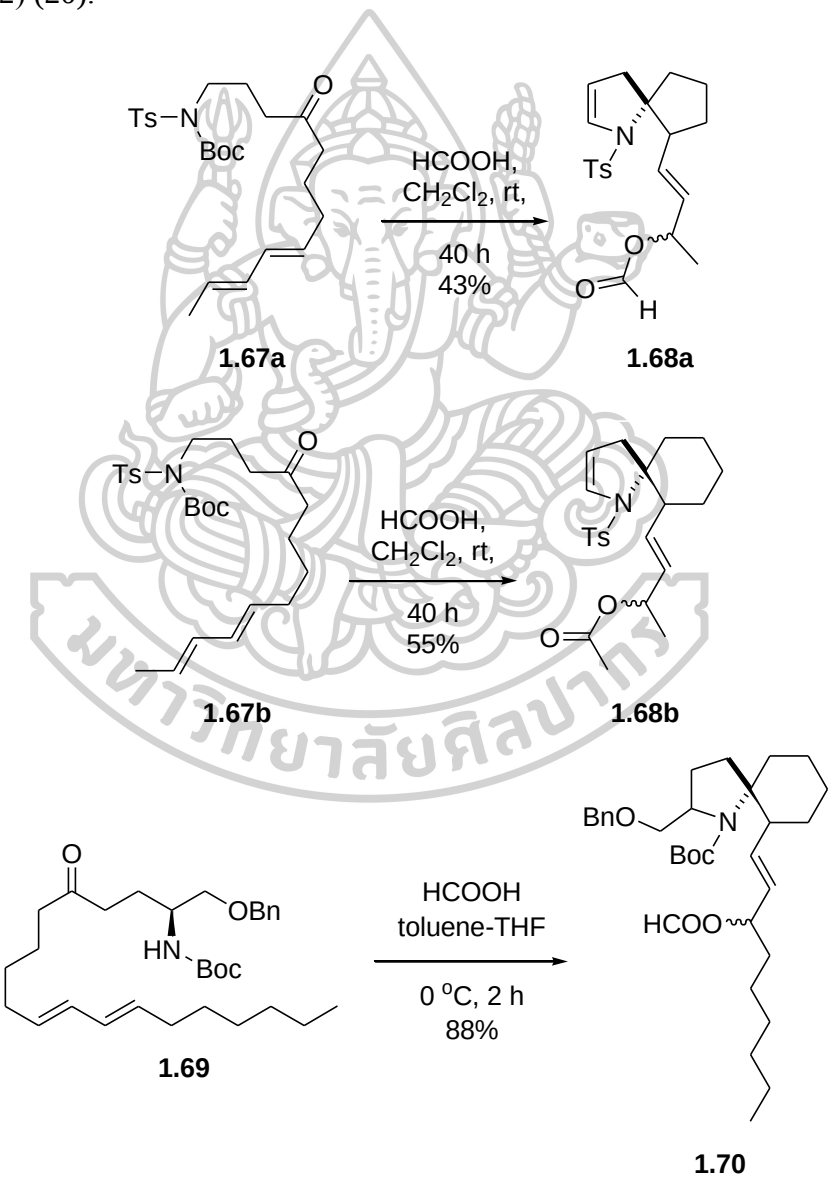

Scheme 22 The *N*-acyliminium ion spirocyclization reaction using Bronsted acids by Kibayashi and coworker

Synthesis of a spirocyclic product via six membered *N*-acyliminium ions of *N*-benzylamide ketone compound **1.71** with an endocyclic carbonyl group reacted with formic acid (HCOOH) gave bicyclic spiro compound **1.72** in 59% yield (Scheme 23) (21).

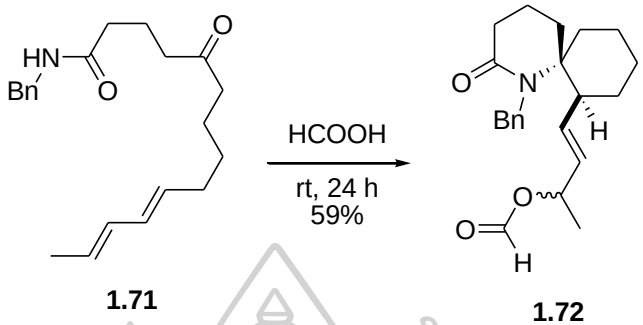

1.71 **1.72**

Scheme 23 The *N*-acyliminium ion spirocyclization reaction via six membered *N*-acyliminium ions of *N*-benzylamide ketone compound

Tricyclic skeletons by heteroatom nucleophiles

The *N*-acyliminium ion cyclization cascade has been used for the synthesis of tricyclic skeletons with heteroatom nuclephiles through *N*-acyliminium ion intermediate. An example of structurally diverse compounds produced tricyclic compound through cyclization of *N*-acyliminium ion by heteroatom nucleophile is shown in the figure 10.

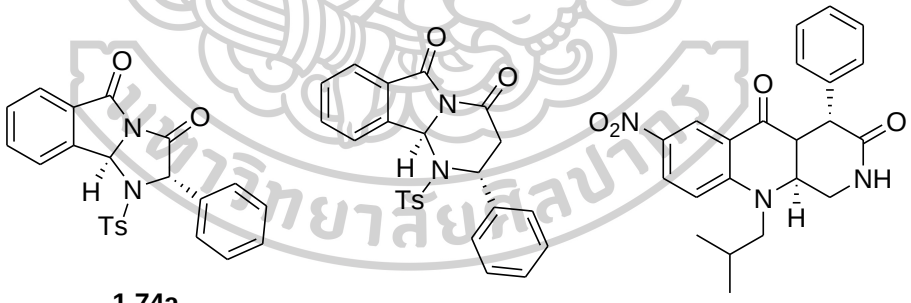

1.74a **1.74b** **1.77**

Figure 10 Structure synthesized tricyclic compounds from *N*-acyliminium cyclization by heteroatom nucleophiles

The stereoselective synthesis of five-membered bicyclic with *trans* conformation used *N*-acyliminium ion cyclization. The *N*-sulfonyl substituted compounds were cyclized to give acetals in high yields and stereoselectivities. The intramolecular interaction between the iminium and the sulfonyl group were key role in the cyclization. Heteroatom nuclephiles reacting with *N*-acyliminium ion, an example of reaction between *N*-substituted compound **1.73a** and **1.73b** with trimethylsilyl trifluoromethanesulfonate (TMSOTf) as Lewis acid provided tricyclic

compounds **1.74a** in 78% yield as 90:10 diastereomeric ratio and **1.74b** in 92% yield as more than 99% diastereomeric excess, respectively (Scheme 24) (22).

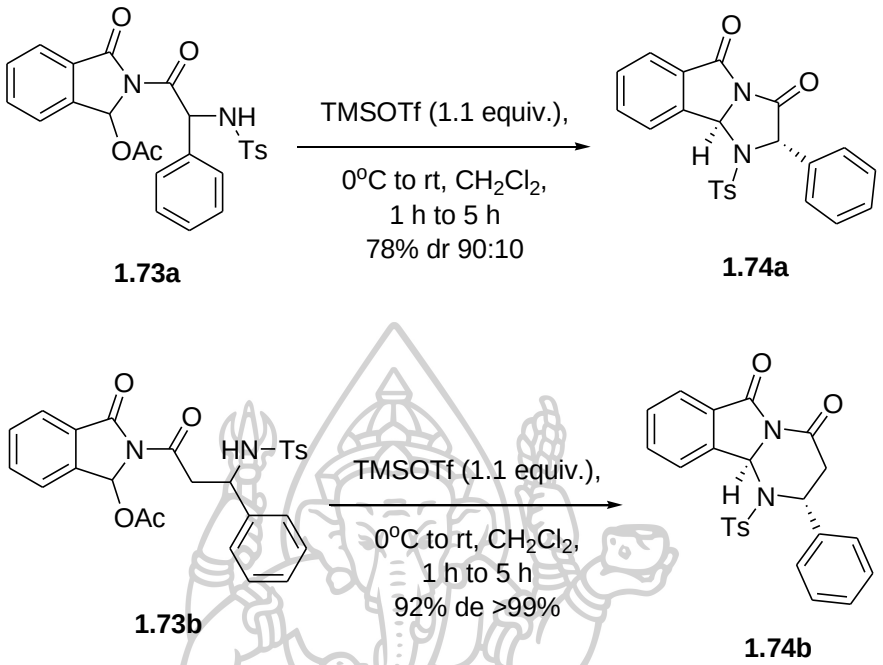

Scheme 24 The *N*-acyliminium ion cyclization with heteroatom nuclephiles obtained tricyclic compounds

The *N*-acyliminium ion cyclization cascade is an important reaction in the synthesis of more than one ring in a single step. First, substitution reaction between aryl fluoride **1.75** and 2-methylpropanamine in dichloromethane generated secondary amine compound **1.76**. Second, *N*-acyliminium ion cyclization cascade of diamide **1.76** using formic acid (HCOOH) under microwave irradiation with elimination of the 2,4-dimethoxybenzyl protecting group gave tricyclic compound **1.77** in 79% yield over 2 steps (Scheme 25) (23).

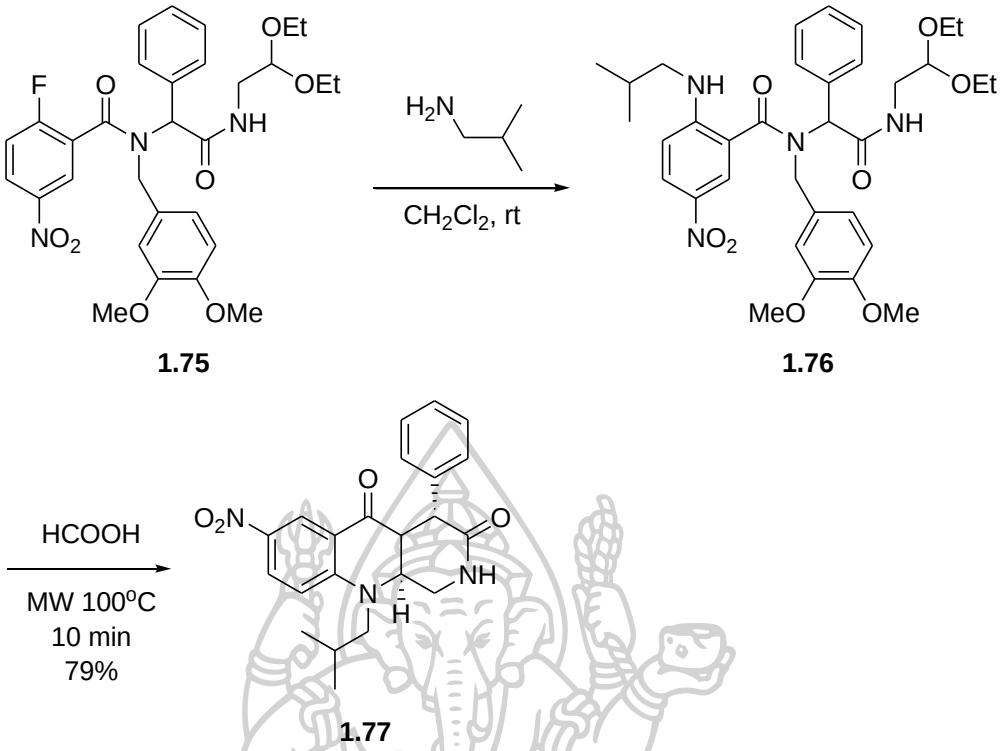

Scheme 25 The *N*-acyliminium ion cyclization cascade using Bronsted acids afforded tricyclic compounds

Tricyclic skeletons by alkene nucleophiles

The *N*-carbamoyliminium ion cyclization and intramolecular *N*-acyliminium ion cyclization have been used for the synthesis of tricyclic skeletons with alkene nucleophile through *N*-acyliminium ion intermediate. An example of structurally diverse compounds produced tricyclic compound through cyclization of *N*-acyliminium ion by alkene nucleophile is shown in the figure 11.

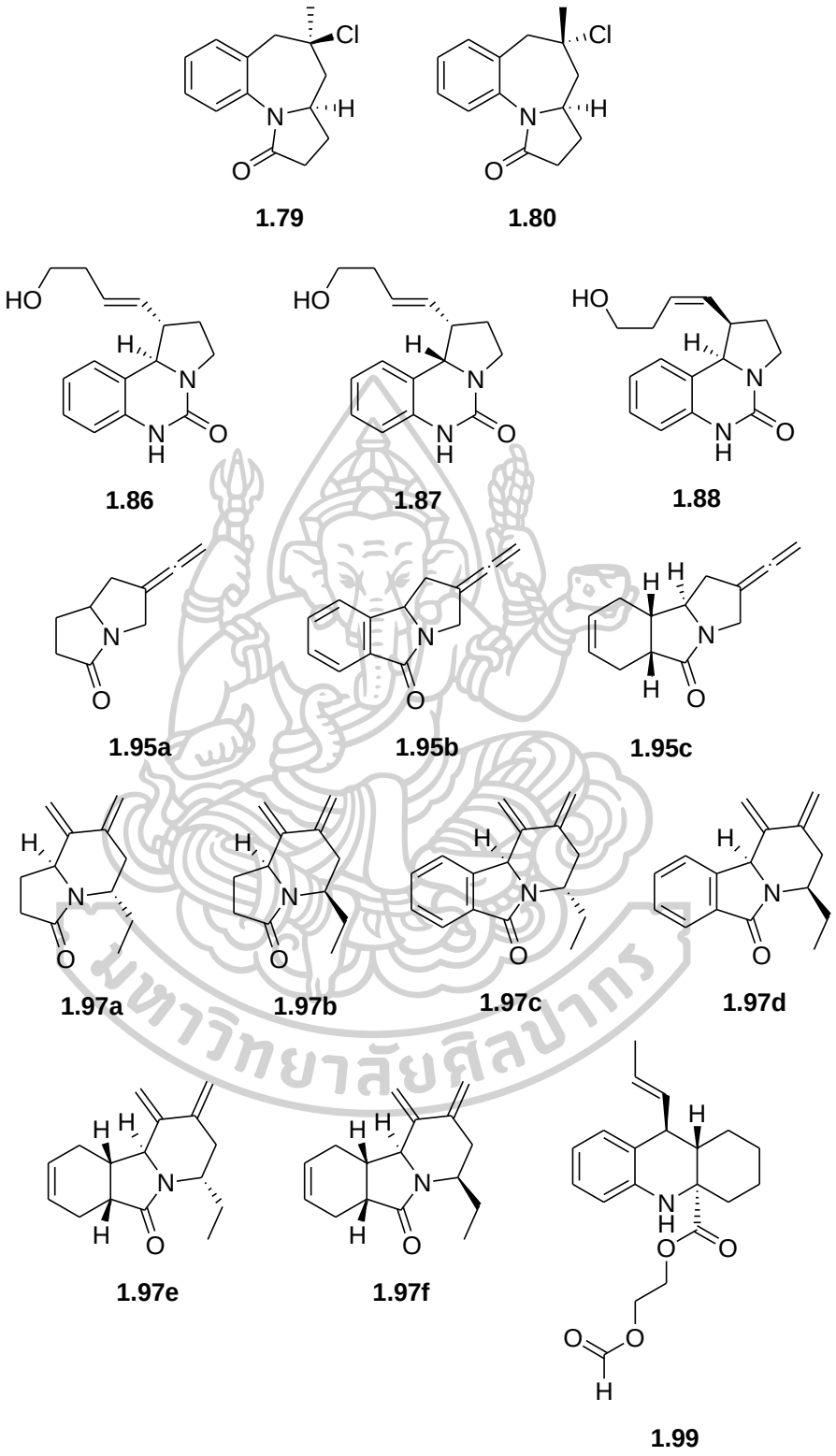

Figure 11 Structure synthesized tricyclic compounds from *N*-acyliminium cyclization by alkene nucleophiles

The synthesis of the tetracyclic core of complex tetrapetalones has been achieved from the intermediate *γ*-hydroxy amide, which can be accessed through the *N*-acyliminium ion cyclization to give high yield. Publication of Hong and coworker used *N*-acyliminium ion cyclization reaction of hydroxylactam **1.78** using iron(III) chloride ($FeCl_3$) and trimethylsilyl chloride (TMSCl) at room temperature through *N*-acyliminium ion intermediate provided 4:1 diastereomeric ratio of tricyclic compound **1.79** and **1.80** which seven membered ring in 80% yield. Influence that causes diastereoselective because of the *π*-bridged chairlike transition state of tertiary carbocation intermediate by intramolecular between alkene and *N*-acyliminium ion (Scheme 26) (24).

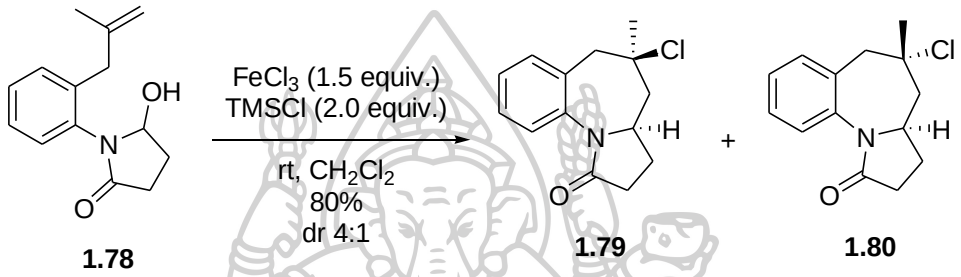

1.78 **1.79** **1.80**

Scheme 26 The *N*-acyliminium ion cyclization reaction to construct seven membered ring compounds by Hong and coworker

Publication of Aubé and coworker used *N*-carbamoyliminium ion cyclization reaction of allylsilanes **1.84** in the presence of titanium tetrachloride ($TiCl_4$) as Lewis acids through *N*-carbamoyliminium ion intermediates **1.85** generated 87:10:3 diastereomeric ratio of sequence of tricyclic compounds **1.86**, **1.87** and **1.88** in 80% yield, respectively. The occurrence of major tricyclic compounds **1.87** is due the benzyloxy substituent group leading to diastereoselective from the mechanism complicated a transient cationic five-membered oxonium ion species (Scheme 27) (25).

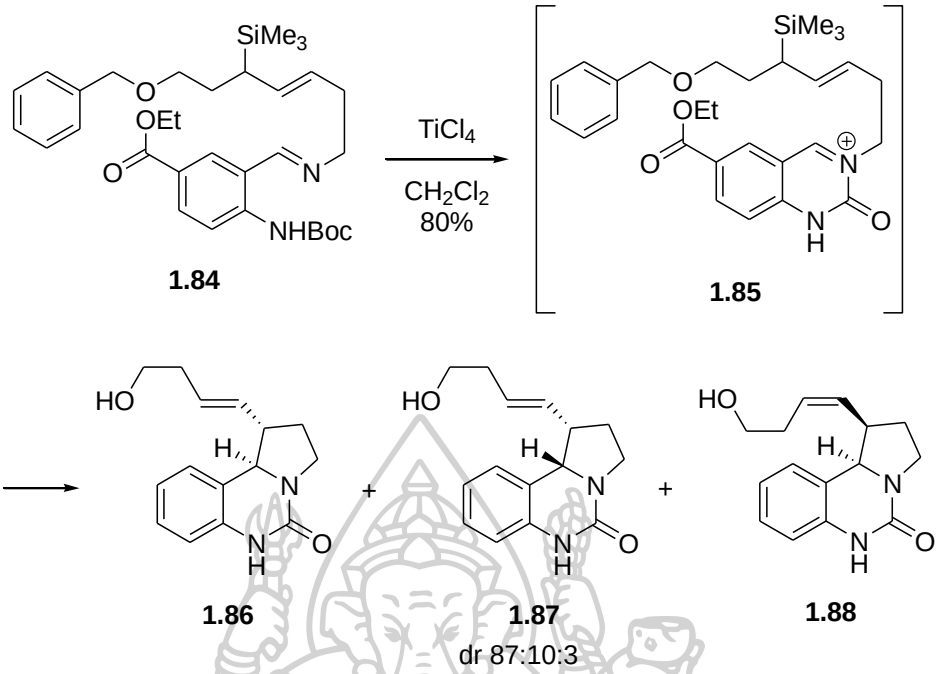

Scheme 27 The *N*-carbamoyliminium ion cyclization reaction to generate tricyclic compounds by Aubé and coworker

Publication of Cho and coworker used Prins cyclization as key reaction of trimethylsilylmethylallene compound. Intramolecular *N*-acyliminium ion cyclization reaction of succinimide and phthalimide allenylmethylsilane hydroxylactams **1.94a**, **1.94b** and **1.94c** using trimethylsilyl trifluoromethanesulfonate (TMSOTf) as Lewis acid generated five membered ring of pyrrolizidinone products **1.95a**, **1.95b** and **1.95c** in 70%, 40% and 39% yield, respectively.

Similarly, Intramolecular *N*-acyliminium ion cyclization reaction of succinimide and phthalimide allenylmethylsilane hydroxylactams **1.96a**, **1.96b** and **1.96c** afforded cyclic compound **1.97a** and **1.97b** in 87% yield as 2:1 diastereomeric ratio, **1.97c** and **1.97d** in 87% yield as 6:1 diastereomeric ratio, **1.97e** and **1.97f** in 88% yield as 1:1 diastereomeric ratio, respectively (Scheme 28) (26).

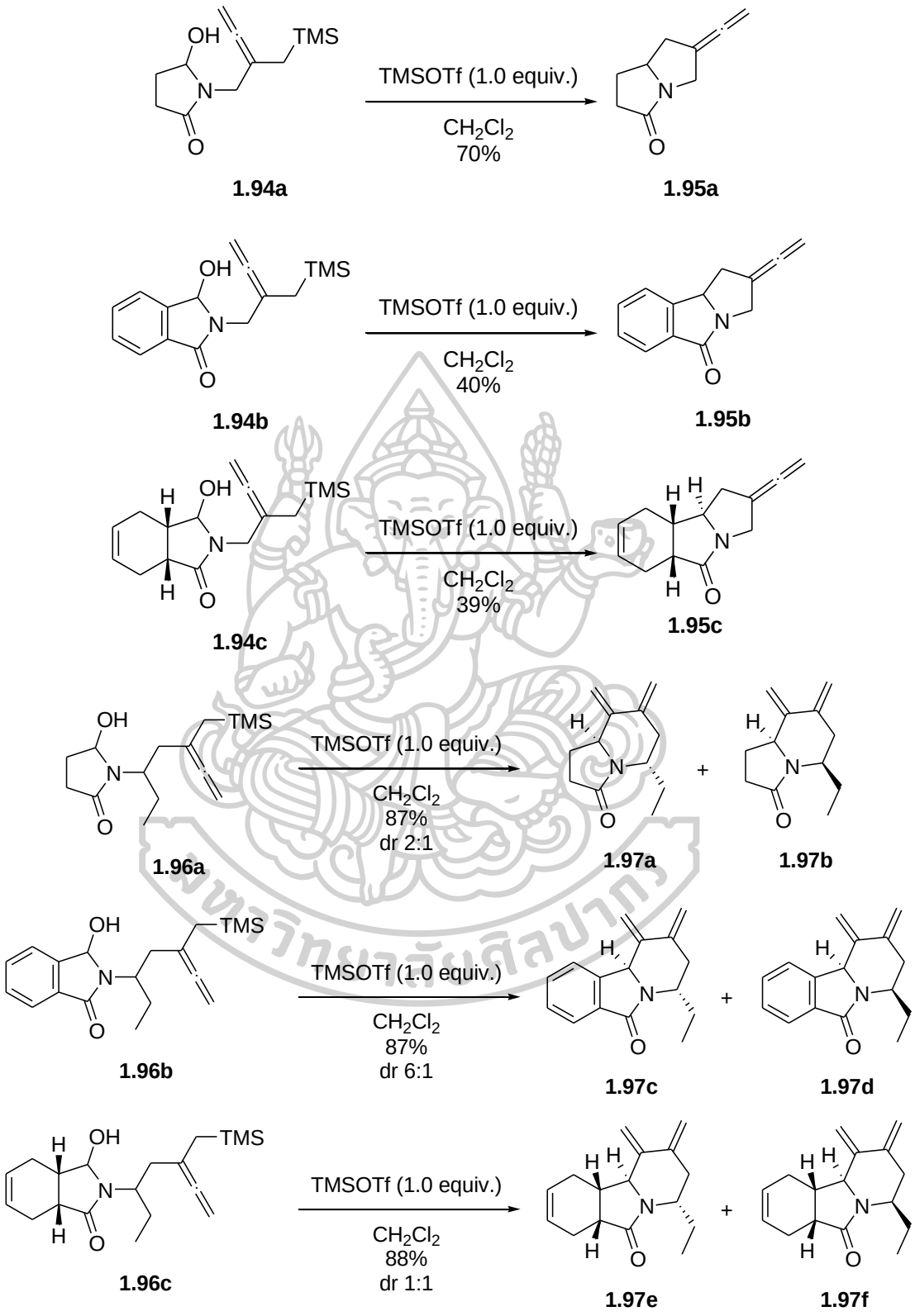

Scheme 28 Prins cyclization of trimethylsilylmethylallene compound via intramolecular *N*-acyliminium ion cyclization reaction by Cho and coworker

Another example from Kibayashi publication through *N*-acyliminium ion cyclization reaction of spiroindole compound **1.98** with formic acid (HCOOH) to construct linear tricyclic tricyclic compound **1.99** in 54% yield (Scheme 29) (27).

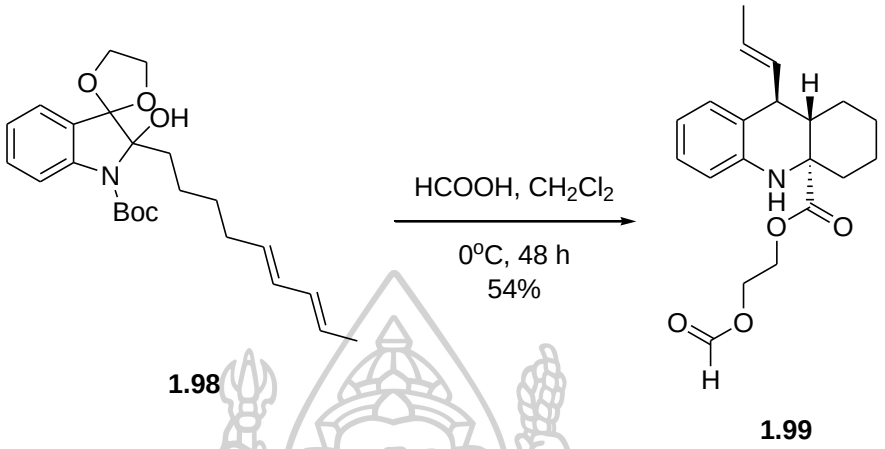

1.98 **1.99**

Scheme 29 The *N*-acyliminium ion cyclization reaction of spiro compound by Kibayashi and coworker

Tricyclic skeletons by indole and heteroaromatic nucleophiles

The enantioselective intermolecular Mannich reaction, Pictet-Spengler reaction, metal-catalyzed tandem isomerization/*N*-acyliminium ion cyclization and one-pot hemiaminal formation/*N*-acyliminium ion cyclization have been used for the synthesis of tricyclic skeletons with indole and heteroaromatic nucleophile through *N*-acyliminium ion intermediate. An example of structurally diverse compounds produced tricyclic compound through cyclization of *N*-acyliminium ion by indole and heteroaromatic nucleophile is shown in the figure 12. Indole compound display excellent nucleophiles for *N*-acyliminium cyclization in Pictet-Spengler reaction.

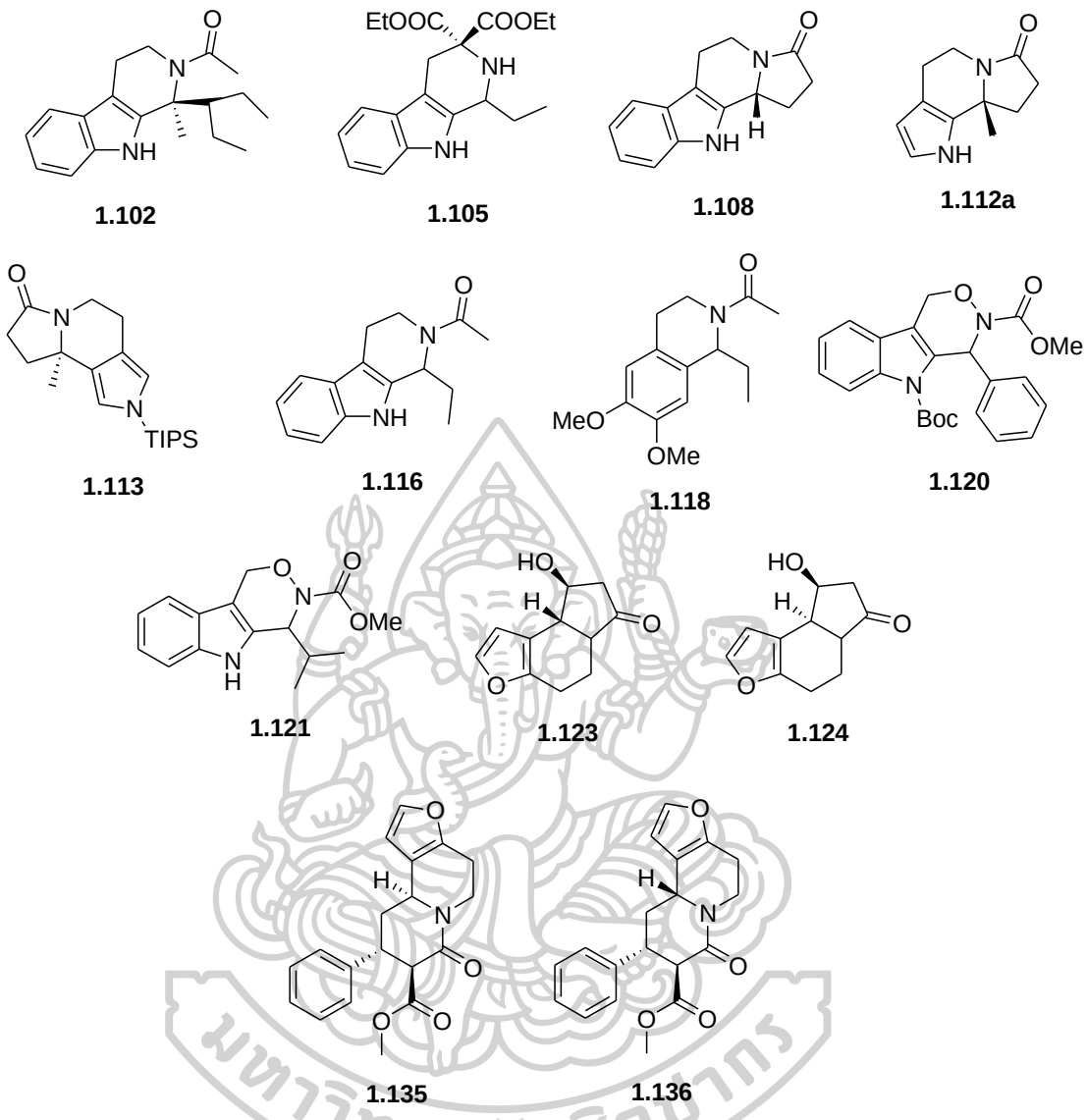

Figure 12 Structure synthesized tricyclic compounds from *N*-acyliminium cyclization by indole and heteroaromatic nucleophiles

The enantioselective intermolecular Mannich reaction of *N*-acylisoquinolinium ions intermediate produced between tryptamine-derived imine compound **1.100** and 3-ethylpentanal. The *N*-acylisoquinolinium ions intermediate reacting with acetyl chloride, 2,6-lutidine and thiourea catalyst **1.101** gave *N*-acetyl tetrahydro-*β*-carboline **1.102** in 65% yield and 93%ee by Jacobsen and coworker (Scheme 30) (28).

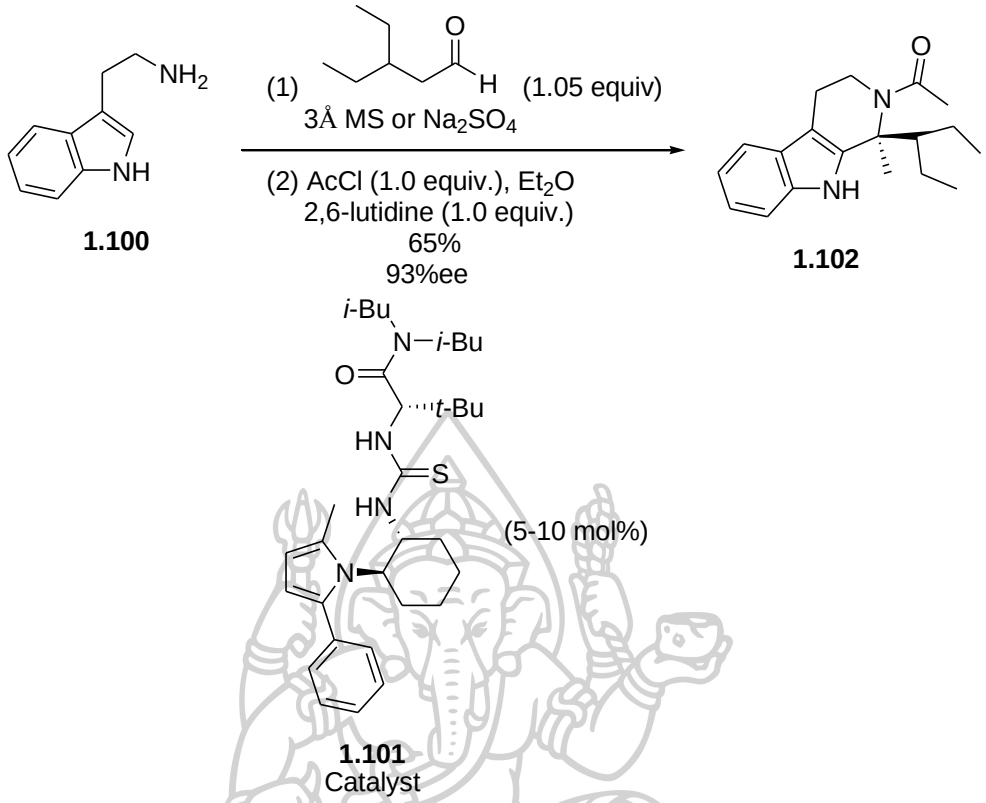

Scheme 30 The enantioselective intermolecular Mannich reaction of *N*-acylisoquinolinium ions intermediate by Jacobsen and coworker

A similar approach of *N*-acyliminium ion cyclization reaction of bicarbonyl tryptamine compound **1.103** using propionaldehyde and chiral phosphoric acid **1.104** as catalyst afforded tetrahydro-*β*-carboline compound **1.102** in 76% yield and 88%ee (Scheme 31) (29).

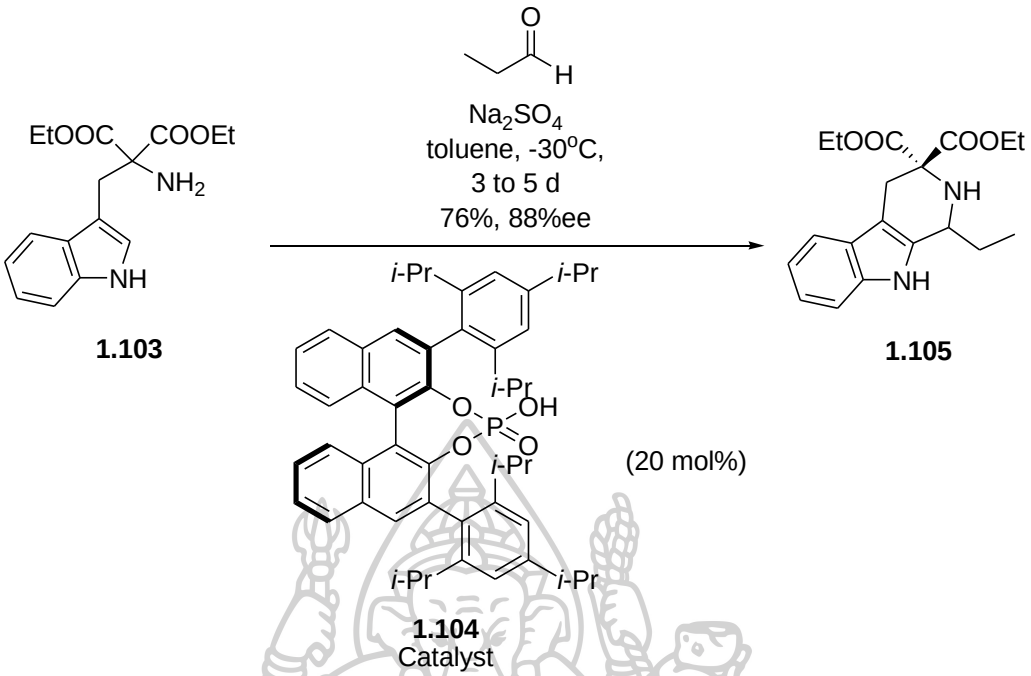

Scheme 31 The *N*-acyliminium cyclization reaction of bicarbonyl tryptamine compound using chiral phosphoric acid as catalyst

Another example from the publication of Jacobsen and coworker is synthesized tetracyclic compound **1.108** via Pictet-Spengler reactions which occurs through the unimolecular nucleophilic substitution (S_N1) mechanism containing anion binding between intermediate and thiourea catalyst **1.107**. The hydroxylactams **1.106** reacted with chiral thiourea catalyst **1.107** and trimethylsilyl chloride (TMSCl) provided product in 90% yield and 97%ee (Scheme 32) (30).

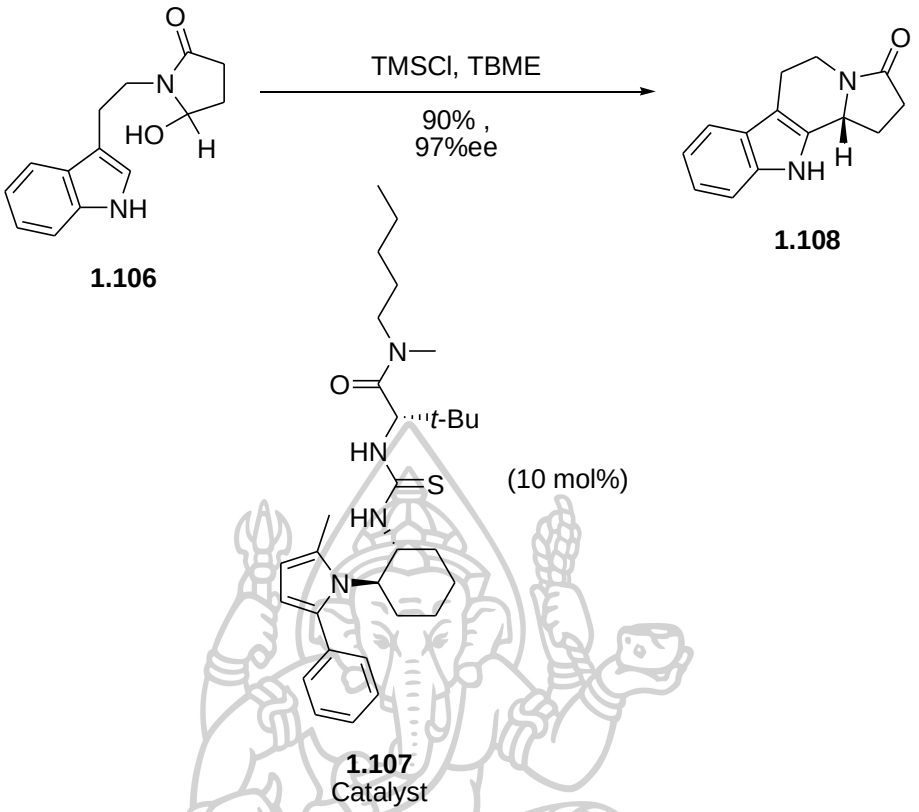

Scheme 32 Pictet-Spengler reaction through the unimolecular nucleophilic substitution (S_N1) mechanism by Jacobsen and coworker

Publication of Jacobsen and coworker used *N*-acyliminium ion cyclization part of Pictet-Spengler reactions as key reactions. Regioselective cyclization of pyrrole compound **1.111a** in the presence of acetyl chloride and chiral thiourea catalyst **1.107** obtained through C2-cyclization to give tricyclic compound **1.112a** in 70% yield and 90%ee.

Likewise, *N*-acyliminium ion cyclization reaction through C4-cyclization of triisoproylsilyl (TIPS) protecting compound **1.111b** using trimethylsilyl chloride (TMSCl) and chiral thiourea catalyst **1.107** gave tricyclic compound **1.113** in 77% yield and 92%ee (Scheme 33) (31).

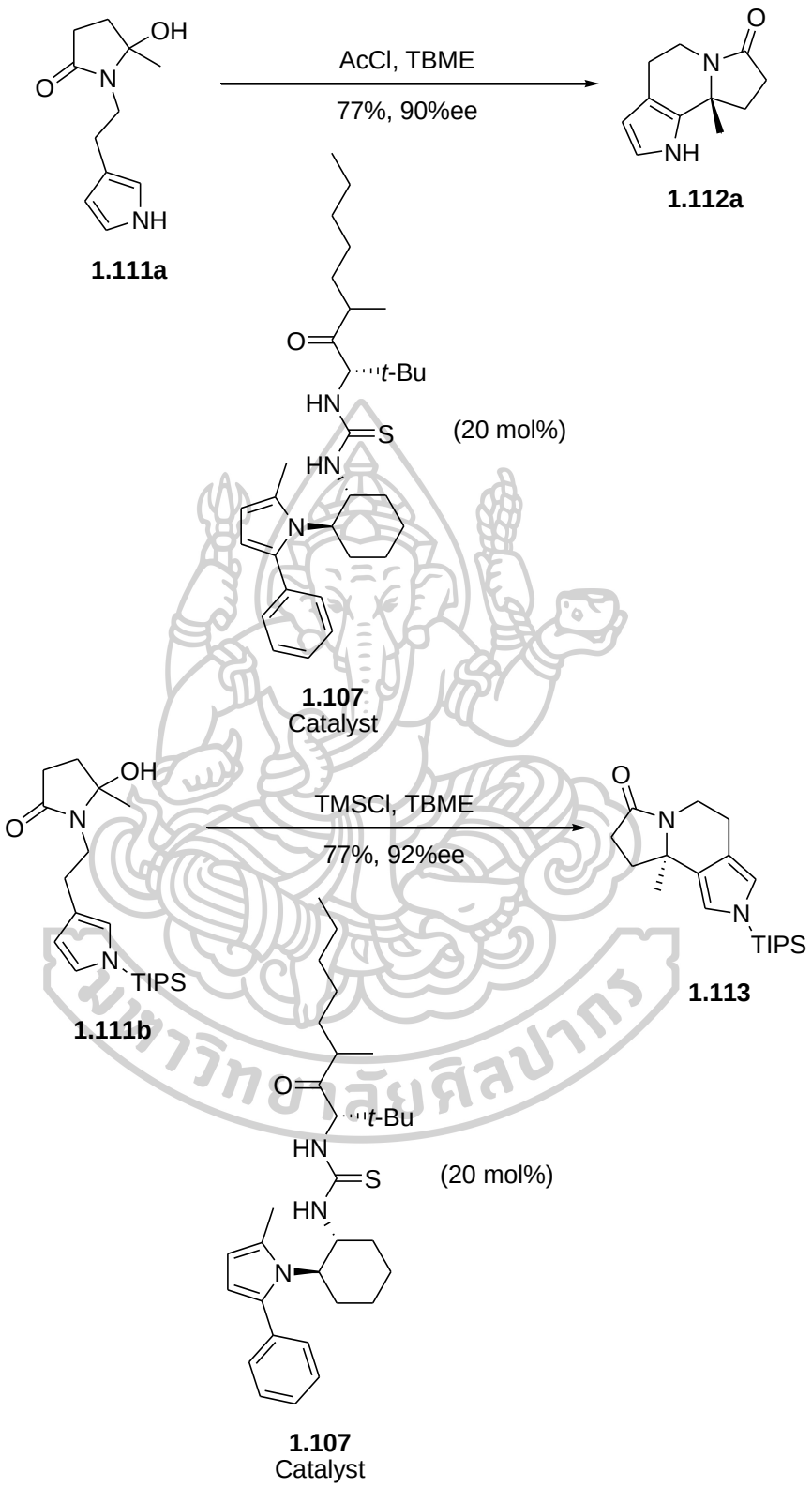

Scheme 33 The *N*-acyliminium ion cyclization through C2-cyclization and C4-cyclization by Jacobsen and coworker

The metal-catalyzed tandem isomerization/*N*-acyliminium ion cyclization of *N*-allylic tryptamine compound **1.114** in the presence of ruthenium hydride catalyst ($RuCl(PPh_3)_3$) through acetamide **1.115** to react with dibenzyl phosphate ($(PhO)_2POOH$) generated tetrahydro *β*-carbolines **116** in 76% yield.

Similar reaction conditions, metal-catalyzed tandem isomerization/*N*-acyliminium ion cyclization of amides **1.117** using ruthenium hydride catalyst ($RuCl(PPh_3)_3$) and dibenzyl phosphate ($(PhO)_2POOH$) generated dihydroisoquinoline **1.118** in 67% yield (Scheme 34) (32).

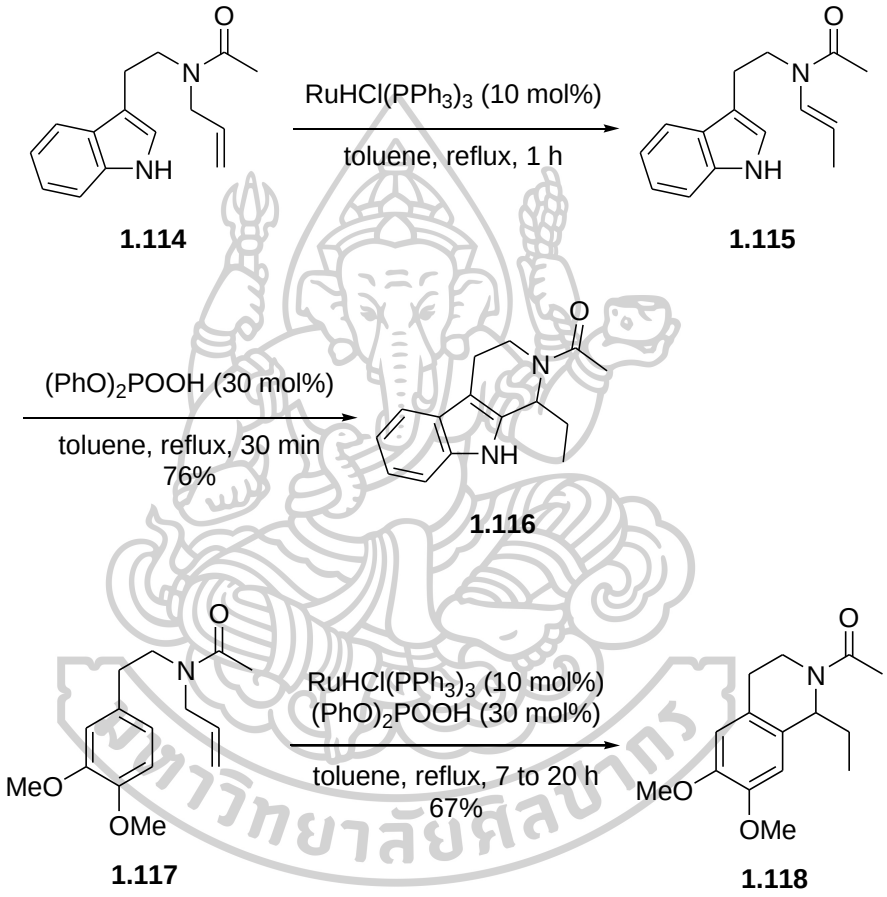

Scheme 34 The metal-catalyzed tandem isomerization/*N*-acyliminium ion cyclization using ruthenium hydride catalyst ($RuCl(PPh_3)_3$) and dibenzyl phosphate ($(PhO)_2POOH$)

The oxo-*N*-acyliminium ion cyclization of hydroxamate compound **1.119** reacting with benzaldehyde using trimethylsilyl chloride (TMSCl) and sodium iodide provided tricyclic compound **1.120** in 94% yield.

Similarly, the reaction between **1.119** and isobutyraldehyde in the presence of boron trifluoride diethyl etherate ($BF_3{\cdot}OEt_2$) as Lewis acid gave tricyclic compound **1.121** in 79% yield (Scheme 35) (33).

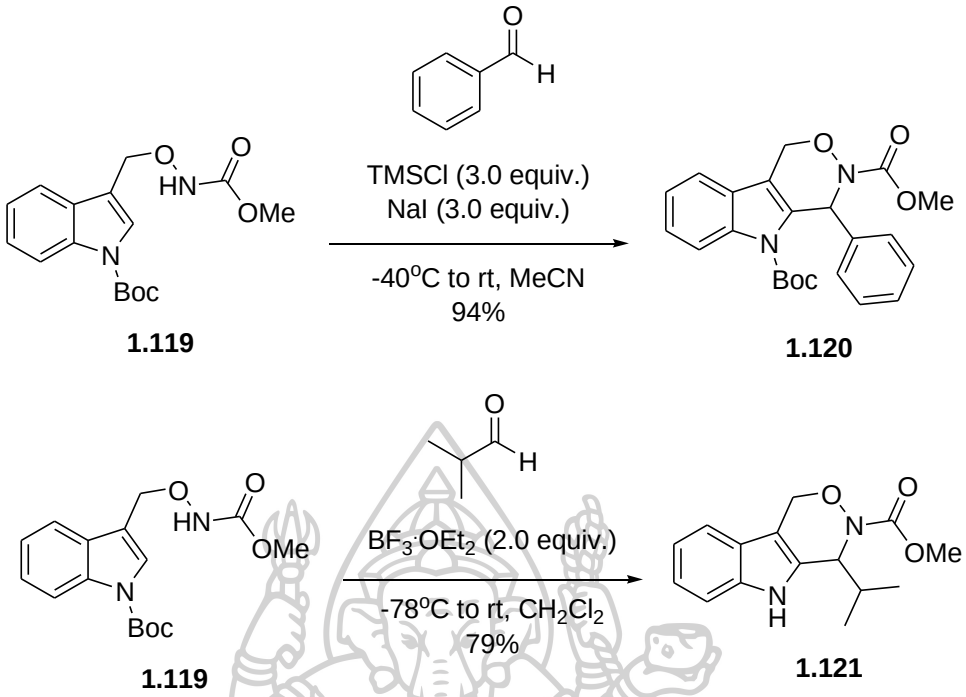

Scheme 35 The oxo-*N*-acyliminium ion cyclization of hydroxamate compound

Publication of Pyne and coworker used acid-promoted cyclization of *N*-acyliminium ion intermediate of lactam **1.122** in the presence of trifluoroacetic acid (TFA) give 11:39 as diastereomeric ratio of both trans- and cis-diastereoisomeric tricyclic compound **1.123** in 19% yield and **1.124** in 67% yield (Scheme 36) (34).

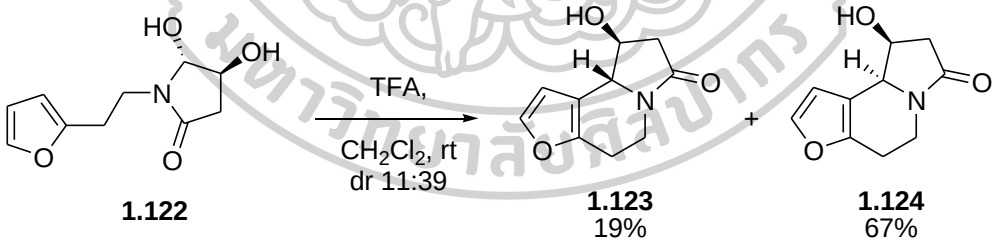

Scheme 36 Acid-promoted cyclization of *N*-acyliminium ion intermediate by Pyne and coworker

Publication of Franzen and coworker described one-pot hemiaminal formation/*N*-acyliminium ion cyclization. Enantioselective conjugate addition of aldehyde **1.131** with nucleophile amide **1.132** using chiral pyrrolidine compound **1.133** generated hemiaminal compound **1.134** in 62% yield as 78:22 diastereomeric ratio. (Scheme 37) (35).

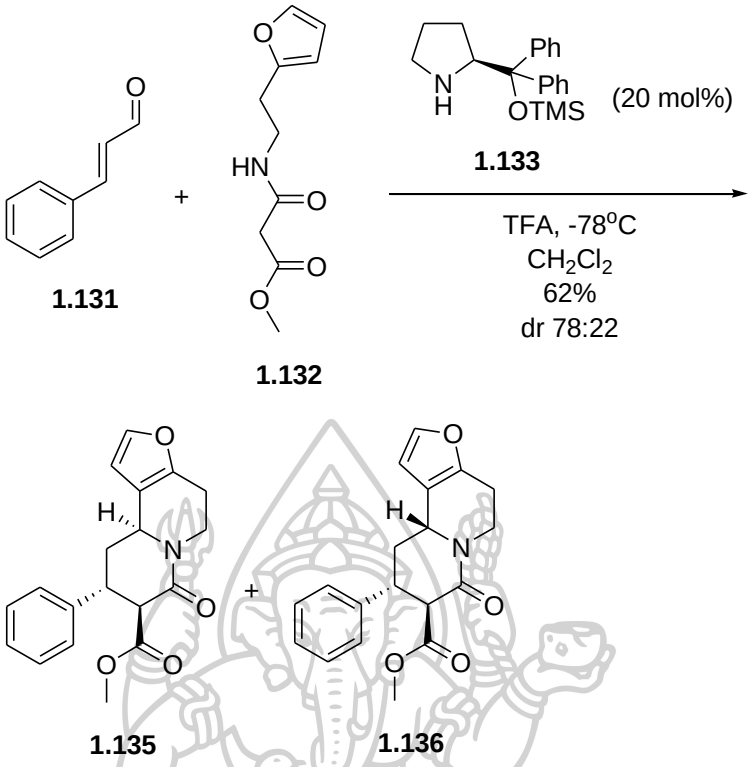

Scheme 37 One-pot hemiaminal formation/*N*-acyliminium ion cyclization using chiral pyrrolidine compound by Franzen and coworker

Tricyclic skeletons with spiro compound by alkene nucleophiles

The sequential 1,4- and 1,2-addition has been used for the synthesis of tricyclic skeletons with spiro compound by alkene nucleophiles through *N*-acyliminium ion intermediate. An example of two structurally compounds produced tricyclic compound with spiro compound through cyclization of *N*-acyliminium ion by alkene nucleophile is shown in the figure 13.

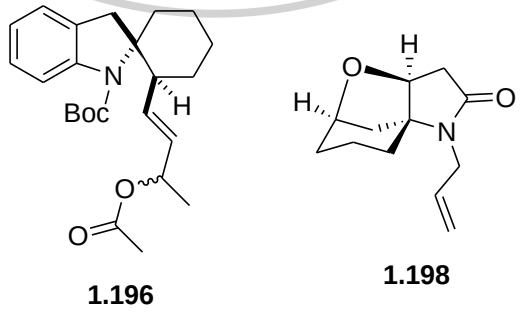

Figure 13 Structure synthesized tricyclic compounds with spiro compound from *N*-acyliminium cyclization by alkene nucleophiles

Publication of Abe and coworker used indole compound **1.195** reacting with formic acid (HCOOH) at the carbon 3-position through *N*-acyliminium ion

intermediate followed by addition of formic acid with conjugated diene gave tricyclic spiro compounds **1.196** in 36% yield (Scheme 38) (36).

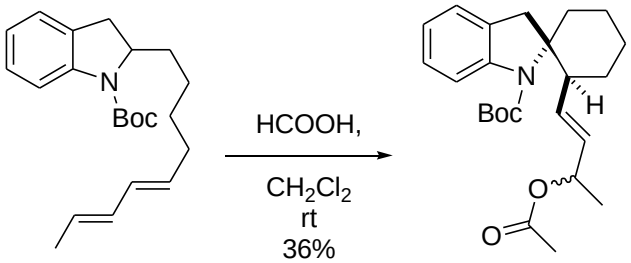

1.195 **1.196**

Scheme 38 The *N*-acyliminium ion conjugated diene spiro cyclization gave tricyclic spiro compound by Abe and coworker

Publication of Yazici and Pyne, sequential 1,4- and 1,2-addition of (E)-enamide compound **1.197** in the presence of boron trifluoride diethyl etherate ($BF_3 \cdot OEt_2$) as Lewis acid through *α,β*-unsaturated *N*-acyliminium ion converted tricyclic spiro compound **1.198** in 66% yield with high diastereomeric selectivity (Scheme 39) (37).

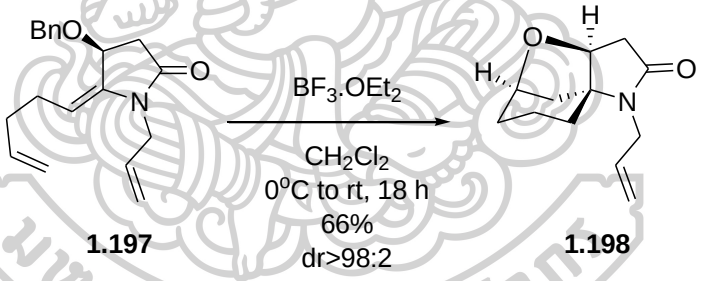

1.197 **1.198**

Scheme 39 Consecutive 1,4- and 1,2-addition of (E)-enamide compound through *α,β*-unsaturated *N*-acyliminium ion by Yazici and Pyne

Tricyclic skeletons with spiro compound by aromatic and heteroaromatic nucleophiles

The *N*-acyliminium ion cyclization via pyridine nucleophile has been used for the synthesis of tricyclic skeletons with spiro compound by aromatic and heteroaromatic nucleophile through *N*-acyliminium ion intermediate. An example of structurally diverse compounds produced tetracyclic compound with spiro compound through cyclization of *N*-acyliminium ion by aromatic and heteroaromatic nucleophiles is shown in the figure 14.

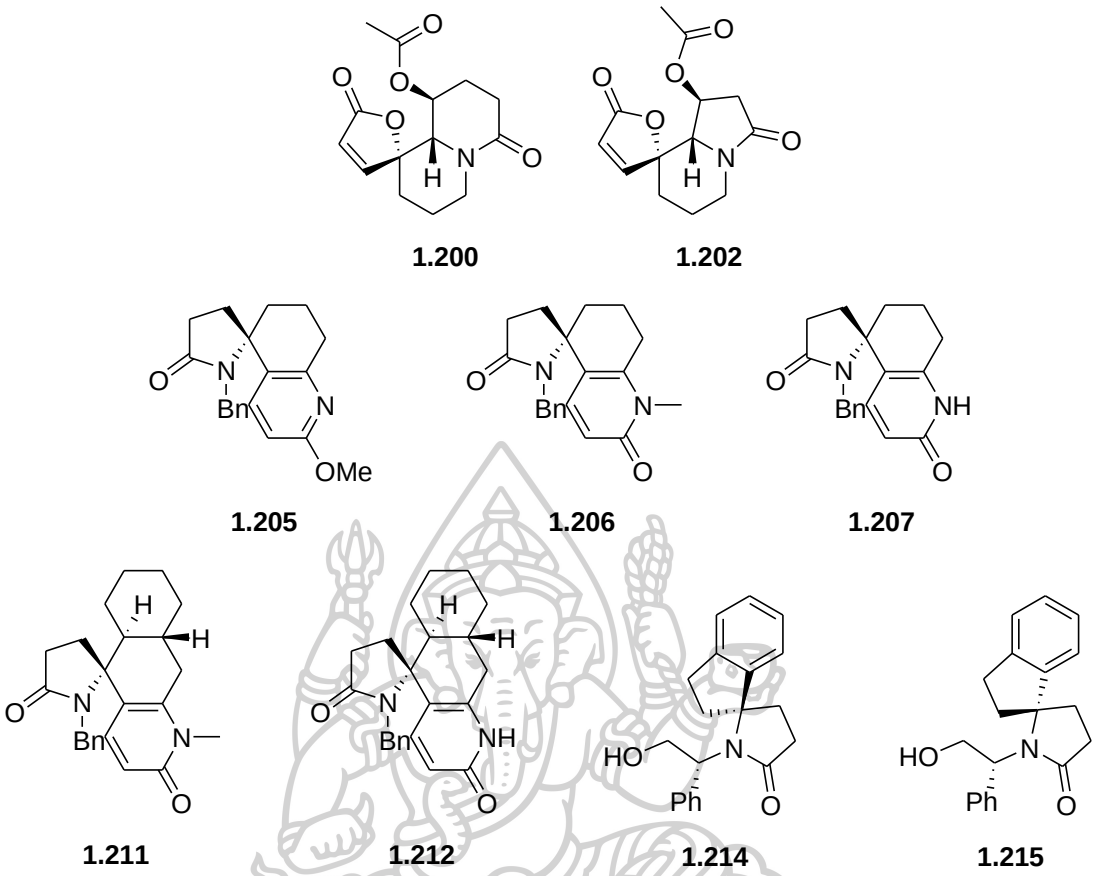

Figure 14 Structure synthesized tricyclic compounds with spiro compound from *N*-acyliminium ion cyclization by aromatic and heteroaromatic nucleophiles

Publication of Pyne and coworker from two different acid conditions in which the *N*-acyliminium ion cyclization of 5-bromo furan **1.199** and **1.201** using scandium trifluoromethanesulfonate ($Sc(OTf)_3$) and trifluoroacetic acid (TFA) obtained spirotricyclic compound **1.200** in 71% and **1.202** in 59% yield as single diastereomer, respectively (Scheme 40) (38).

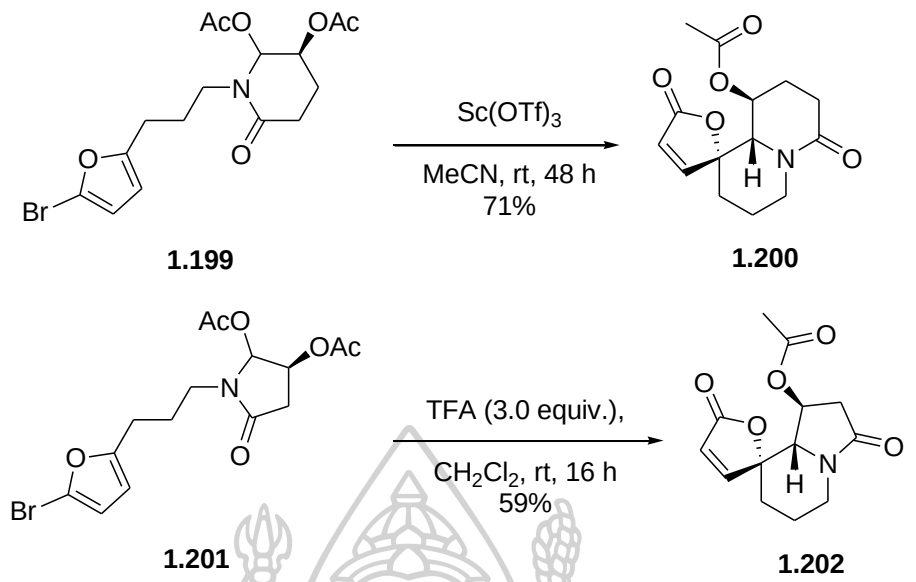

Scheme 40 The *N*-acyliminium ion cyclization generated spirotricyclic compound by Pyne and coworker

The *N*-acyliminium ion cyclization by pyridine nucleophile of amido ketone compound **1.203** using *p*-toluenesulfonic acid (TsOH) as Brønsted acid through *N*-acyliminium ion **1.204** and rearrangement gave three product of tricyclic spiro lactam compound **1.205** in 16%, **1.206** in 47% and **1.207** in 25% yield (Scheme 41) (39).

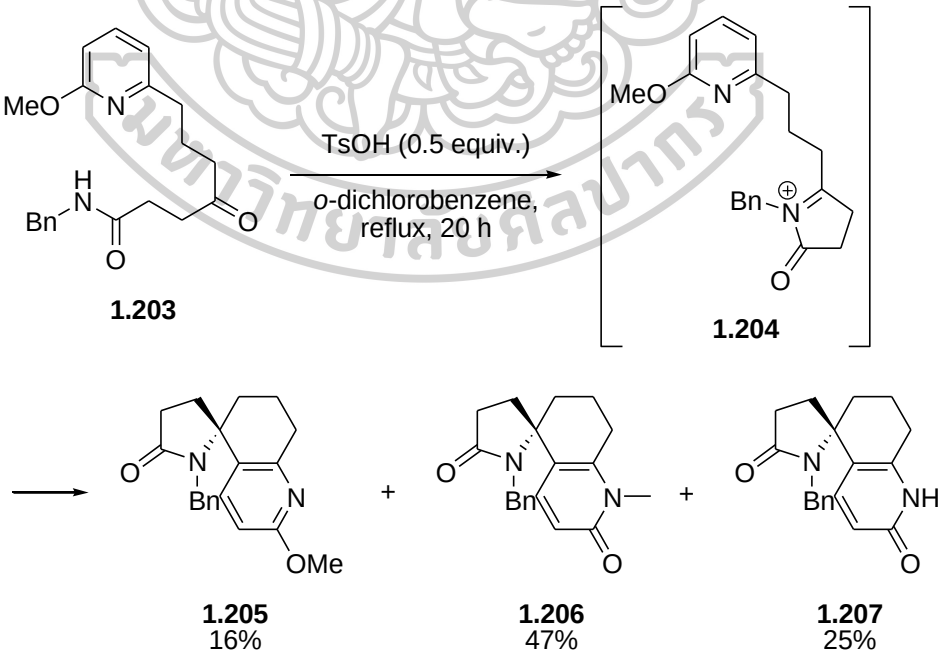

Scheme 41 The *N*-acyliminium ion cyclization by pyridine nucleophile in the formation of tricyclic spiro lactam compound

Another example of *N*-acyliminium ion cyclization by pyridine nucleophile of amido ketone compound **1.208** in the presence of camphorsulfonic acid (CSA) through *N*-acyliminium ion intermediate **1.209** to give tricyclic spiro lactam compound **1.210** followed by thermally induced rearrangement generated spiro lactam compound **1.211** in 44% and **1.212** in 27% yield (Scheme 42) (40).

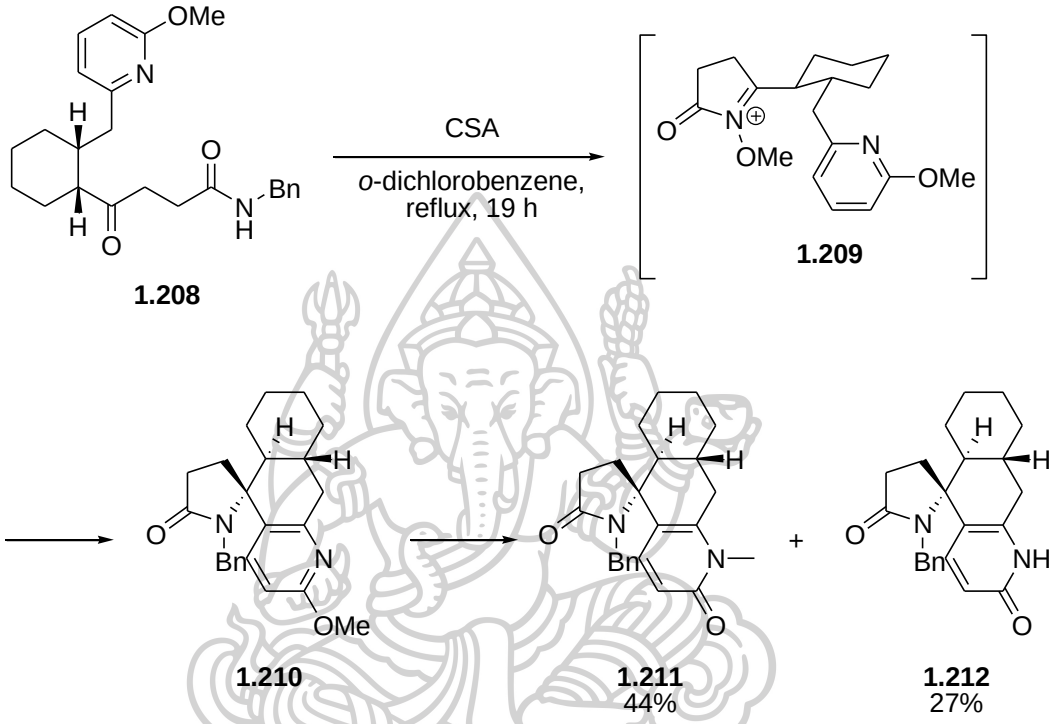

Scheme 42 The *N*-acyliminium ion cyclization by pyridine nucleophile using camphorsulfonic acid (CSA) in the formation of tricyclic spiro lactam compound

Publication of Vernon and coworker, asymmetric synthesis of bicyclic oxylactam pyrrolidines **1.213** reacting with trifluoroacetic acid (TFA) gave 78:22 diastereomeric ratio of spiro compound **1.214** and **1.215** in 93% yield (Scheme 43) (41).

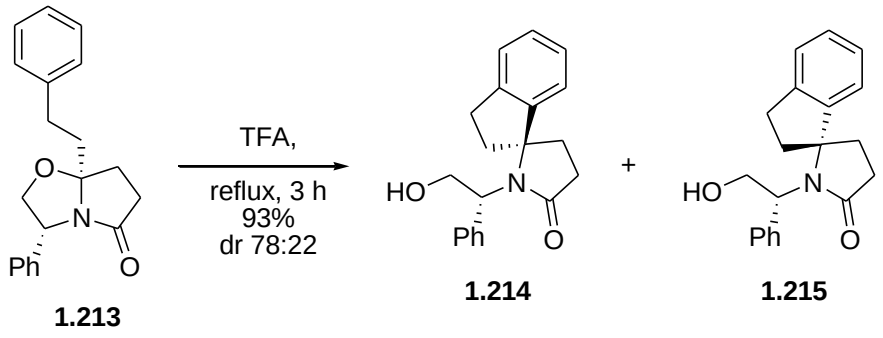

Scheme 43 Asymmetric synthesis through *N*-acyliminium ion cyclization generated spirotricyclic compound by Vernon and coworker

Tetracyclic skeletons by indole and heteroaromatic nucleophiles

The ruthenium-catalyzed tandem ring-closing metathesis (RCM)/isomerization, ruthenium hydride/Brønsted acid-catalyzed isomerization and Sonogashira/ *N*-acyliminium ion cyclization reaction have been used for the synthesis of tetracyclic skeletons by indole and heteroaromatic nucleophile through *N*-acyliminium ion intermediate. An example of structurally diverse compounds produced tetracyclic compound through cyclization of *N*-acyliminium ion by indole and heteroaromatic nucleophiles is shown in the figure 15.

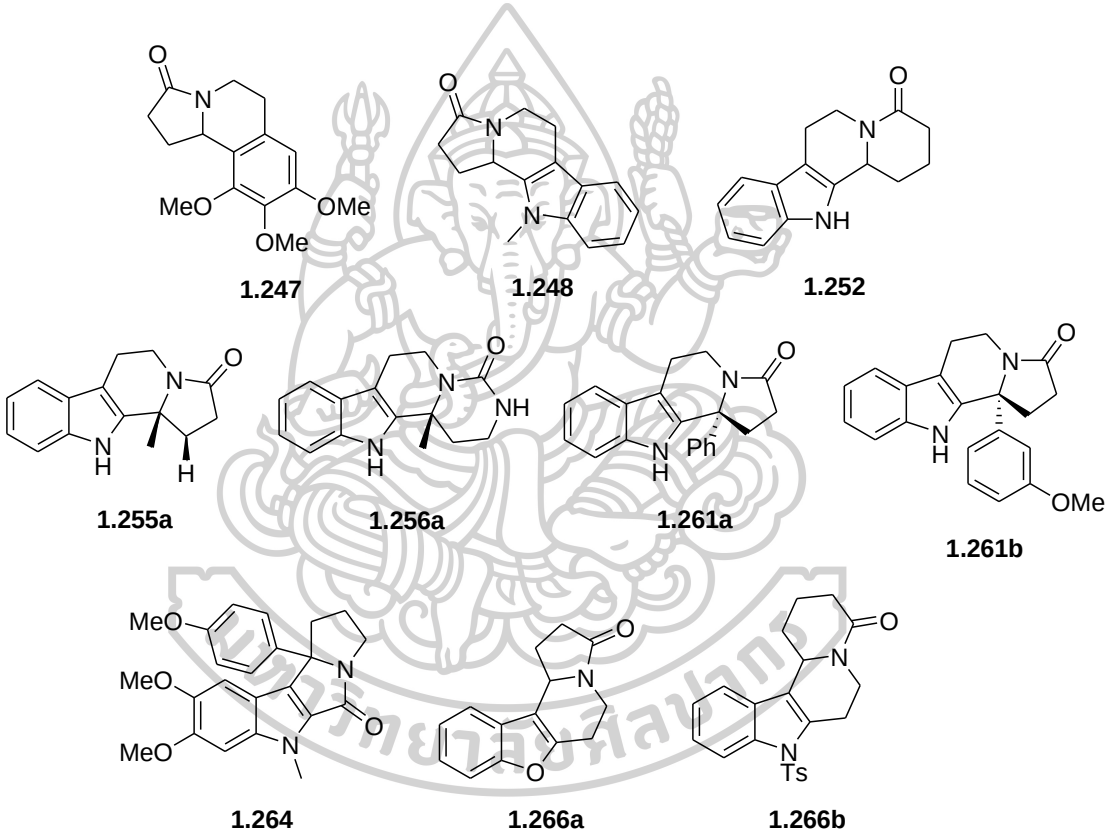

Figure 15 Structure synthesized tetracyclic compounds from *N*-acyliminium ion cyclization by indole and heteroaromatic nucleophiles

Ruthenium-catalyzed tandem ring-closing metathesis (RCM)/isomerization of enamide compound **1.237a** in the existence of Hoveyda-Grubb I catalyst to give *α,β*-unsaturated lactam compound **1.238a** followed by isomerization generated lactam compound **1.239a**. The *N*-acyliminium ion intermediate **1.240a** synthesized from lactam compound **239a**. Intramolecular cyclization of *N*-acyliminium ion intermediate **1.240a** with carbon nucleophile gave tricyclic lactam **1.247** in 64% yield.

Similarly condition, Ruthenium-catalyzed tandem ring-closing metathesis (RCM)/isomerization of enamide indole compound **1.237b** in the presence of Hoveyda-Grubb I catalyst to provide *α,β*-unsaturated lactam indole compound **1.238b**

followed by isomerization produced lactam indole compound **1.239b**. The *N*-acyliminium ion intermediate **1.240b** synthesized from lactam indole compound **1.239b**. Intramolecular cyclization of *N*-acyliminium ion intermediate **1.240b** with carbon nucleophile gave tetracyclic lactam indole **1.248** in 86% yield (Scheme 44) (42).

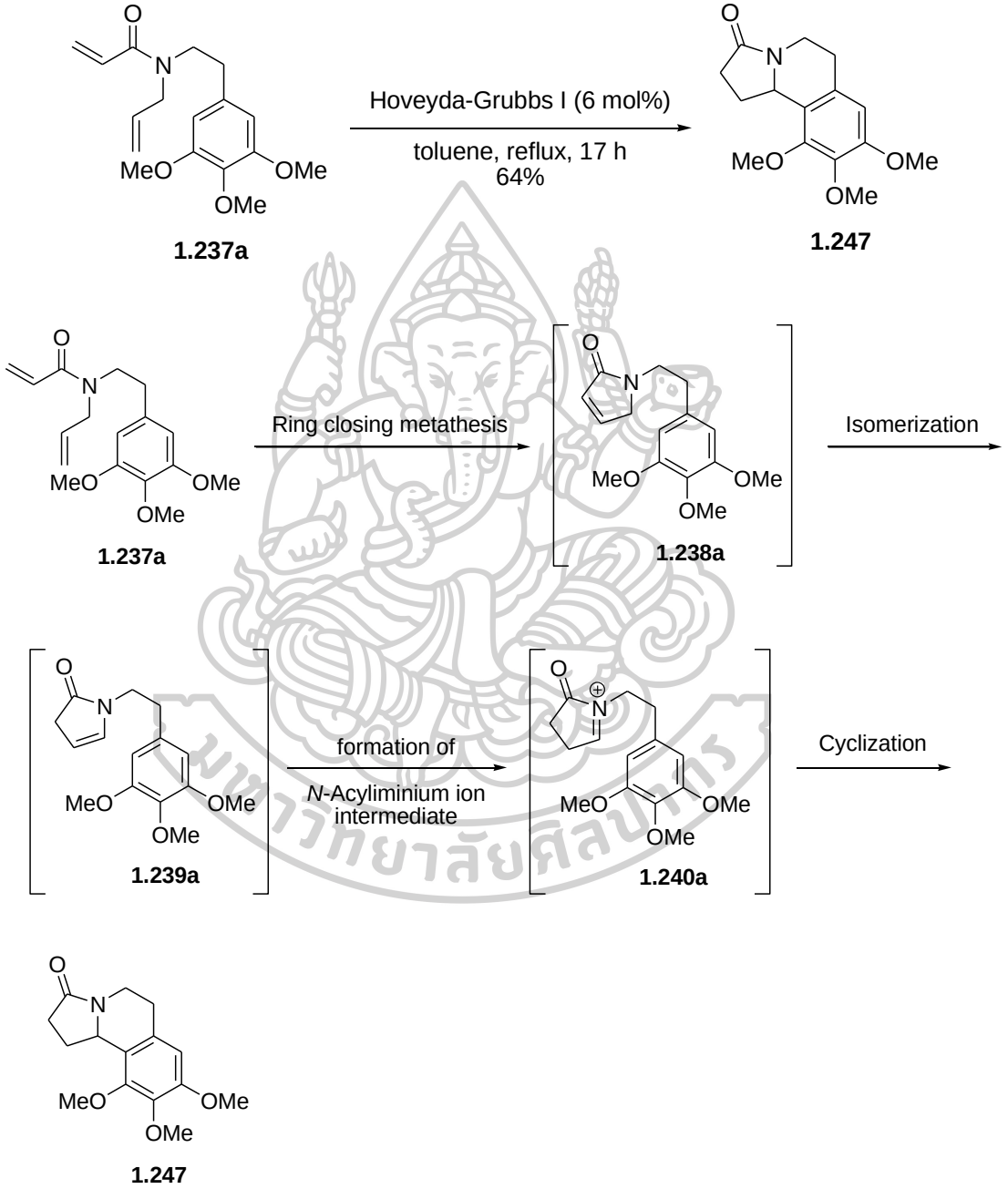

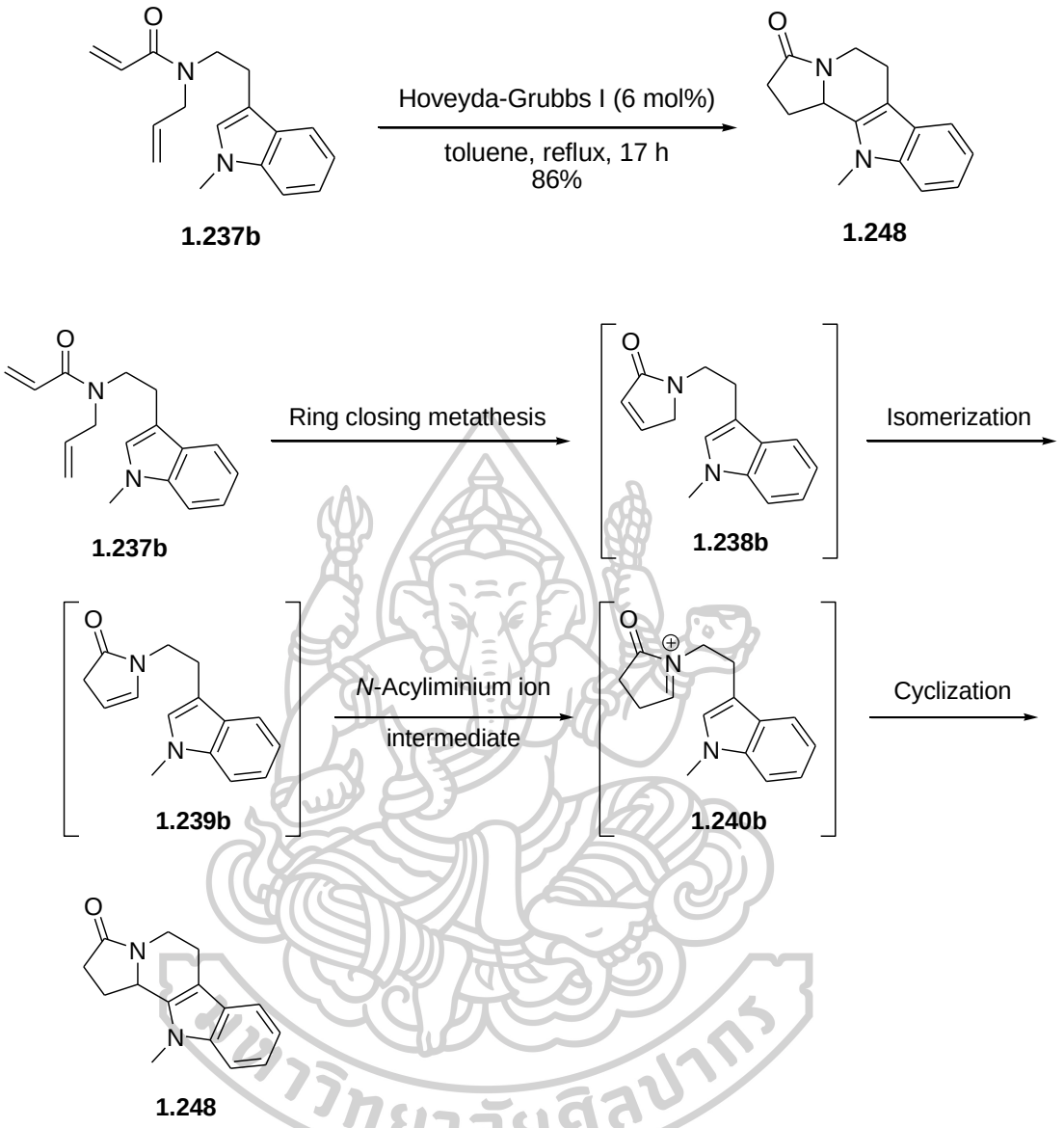

Scheme 44 Ruthenium-catalyzed tandem ring-closing metathesis (RCM)/isomerization using Hoveyda-Grubb I catalyst through *N*-acyliminium ion intermediate gave polycyclic compound

Publication of Nielsen and coworker, ruthenium hydride/Brønsted acid-catalyzed isomerization of allylic amides **1.251** reacting with carbonylchlorohydridotris(triphenylphosphine)ruthenium(II) ($RuHCl(CO)(PPh_3)_3$) and dibenzyl phosphate ($(PhO)_2POOH$) isomerized to *N*-acyliminium ion intermediate. Intramolecular cyclization of *N*-acyliminium ion intermediate with indole nucleophile afforded tetracyclic lactam compound **1.252** in 92% yield (Scheme 45) (32).

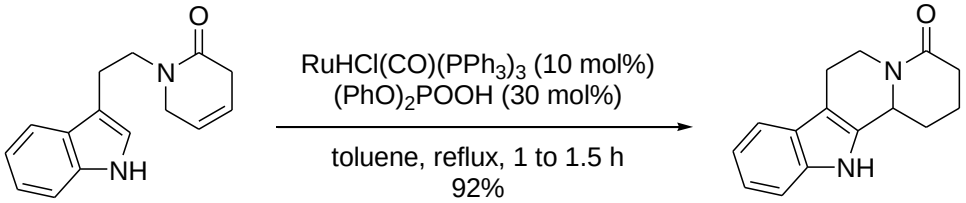

1.251 **1.252**

Scheme 45 Ruthenium hydride/Brønsted acid-catalyzed isomerization through *N*-acyliminium ion intermediate by Nielsen and coworker

Dixon and coworker used enantioselective BINOL phosphoric acid- (BPA-) catalyzed cascade reaction of tryptamine compound **1.253a** and **1.253b** with lactone to give *N*-acyliminium ion intermediate which reacted with indole nucleophile in an enantioselective character by chiral conjugate base of BINOL phosphoric acid generated tricyclic compound **1.255a** in 99% yield, 84%ee and **1.256a** in 76% yield, 73%ee, respectively (Scheme 46) (43) (44).

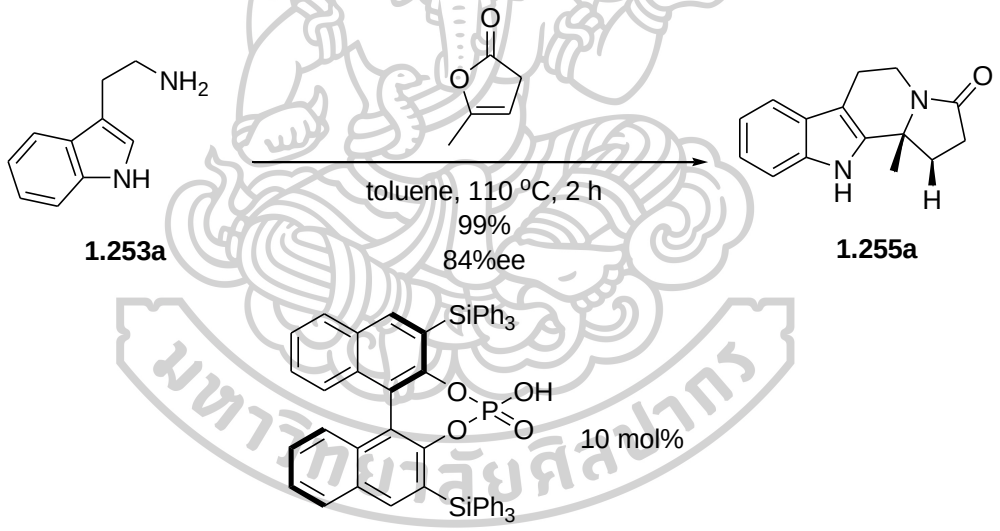

1.253a **1.255a**

1.254

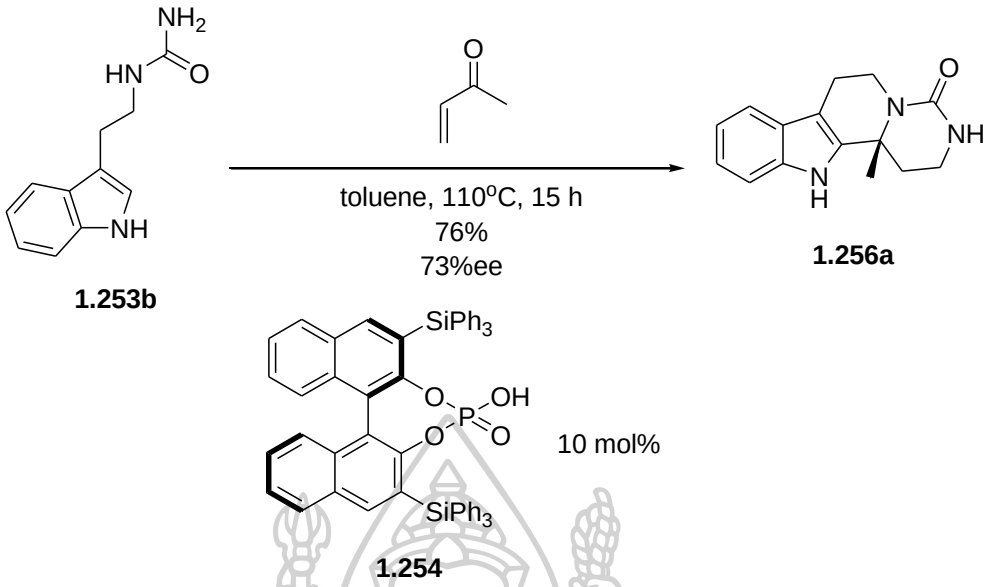

Scheme 46 The enantioselective BINOL phosphoric acid- (BPA-) catalyzed cascade reaction through *N*-acyliminium ion intermediate by Dixon and coworker

Nielsen and coworker, ruthenium catalyzed tandem ring-closing metathesis (RCM)/isomerization of allyl amine derivative compound **1.260a** and **1.260b** using Hoveyda-Grubb II catalyst and enantioselective BINOL phosphoric acid- (BPA-) catalyst **1.254** generated tetrahydro-*β*-carbolines **1.261a** in 95% yield, 85% ee and **1.261b** in 93% yield, 80%ee, respectively (Scheme 47) (45).

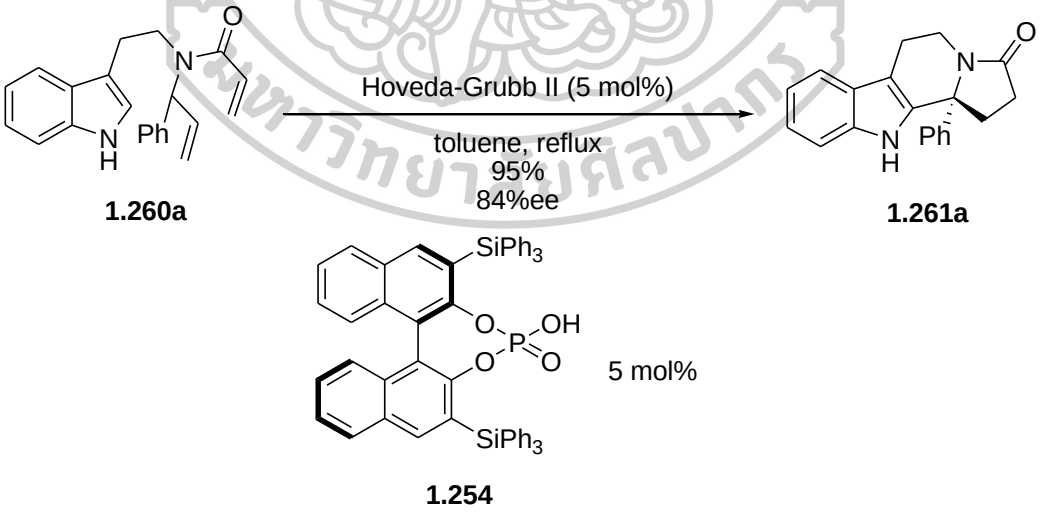

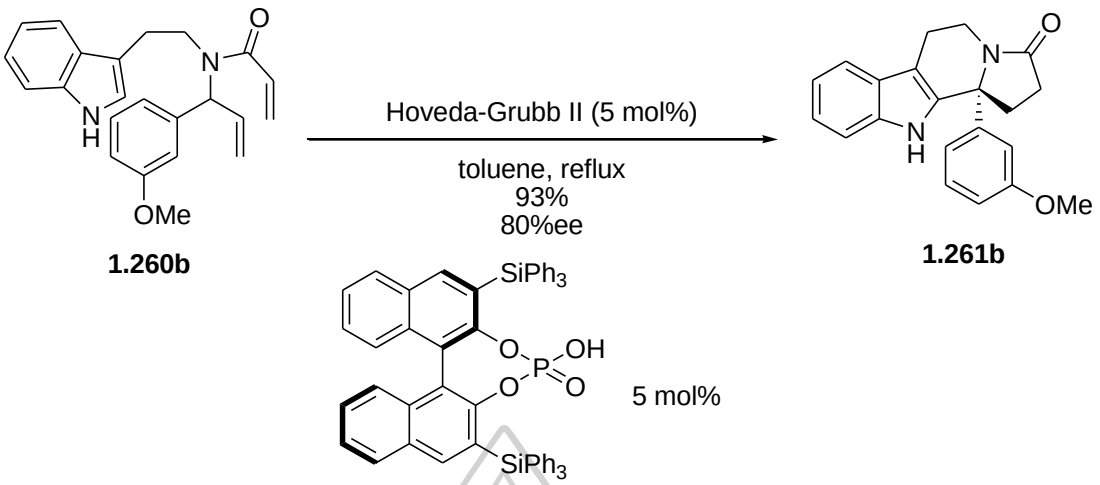

1.260b **1.261b** **1.254**

Scheme 47 The ruthenium -catalyzed tandem ring-closing metathesis (RCM)/isomerization through *N*-acyliminium ion intermediate by Nielsen and coworker

Publication of Cincinelli and coworker, TFA-catalyzed cyclization reaction of amide compound **1.262** using trifluoroacetic acid (TFA) through *N*-acyliminium ion precursor **1.263** synthesized tetracyclic compound **1.264** in 93% yield (Scheme 48) (46).

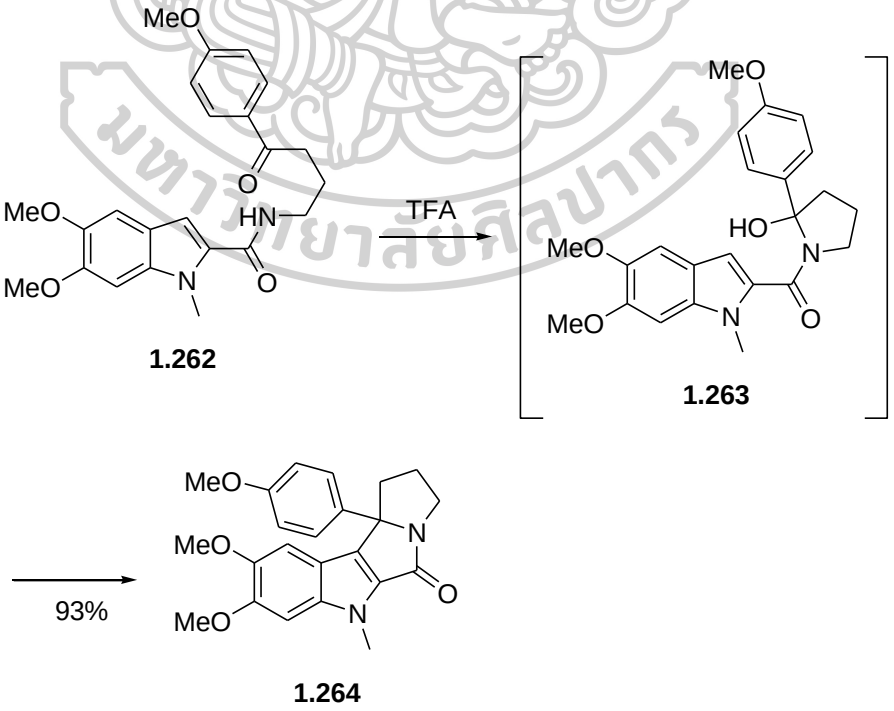

1.262 **1.263** **1.264**

Scheme 48 The TFA-catalyzed cyclization reaction through *N*-acyliminium ion intermediate by Cincinelli and coworker

Consecutive Sonogashira/ *N*-acyliminium ion cyclization reaction of succinimide compound **1.265a** and glutarimide compound **1.265b** by selective partial reduction using lithium triethylborohydride ($LiEt_3BH$) gave *N*-acyliminium ion precursor. The *N*-acyliminium ion cyclization of hydroxylactam intermediate using *p*-toluenesulfonic acid (*p*-TsOH) obtained tetracyclic lactams **1.266a** in 64% yield and **1.266b** in 74% yield, respectively (Scheme 49) (47).

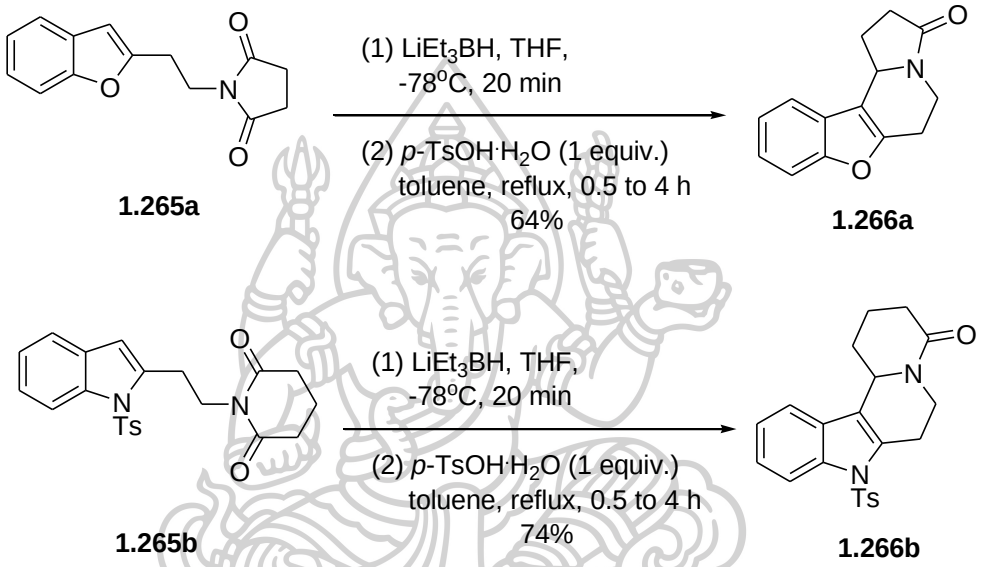

Scheme 49 Consecutive Sonogashira/ *N*-acyliminium ion cyclization reaction through *N*-acyliminium ion intermediate gave tetracyclic compound

Tetracyclic skeletons with spiro compound by indole and heteroaromatic nucleophiles

The Pummerer/Pictet-Spengler cyclization and *N*-tosylation have been used for the synthesis of tetracyclic skeletons with spiro compound by indole and heteroaromatic nucleophile through *N*-acyliminium ion intermediate. An example of structurally diverse compounds produced tetracyclic compound with spiro compound through cyclization of *N*-acyliminium ion by indole and heteroaromatic nucleophiles is shown in the figure 16.

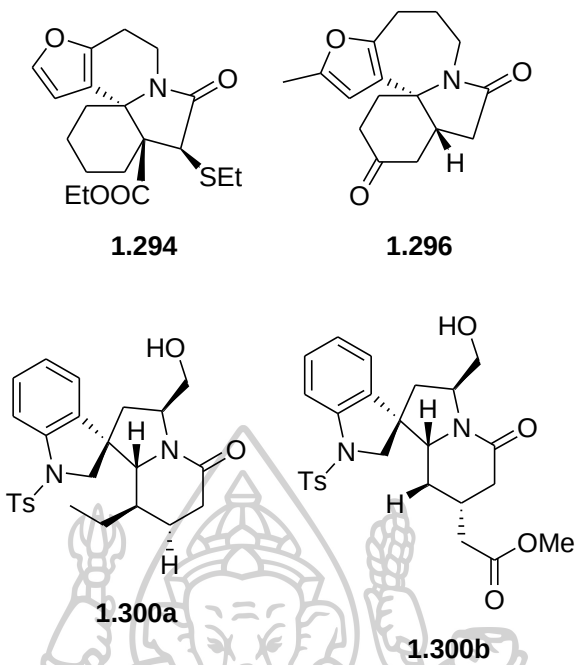

Figure 16 Structure synthesized tetracyclic compounds with spiro compound from *N*-acyliminium ion cyclization by indole and heteroaromatic nucleophiles

Pummerer/Pictet-Spengler cyclization of sulfoxide amide compound **1.293** treatment with trifluoroacetic anhydride (TFAA) and trifluoroacetic acid (TFA) generated racemic mixture of tetracyclic lactam compound **1.294** in 76% yield.

Similarly, *N*-acyliminium ion cyclization of hydroxylactam **1.295** reacting with trifluoroacetic acid (TFA) gave seven-membered ring of racemic compound **1.296** in 75% yield (Scheme 50) (48).

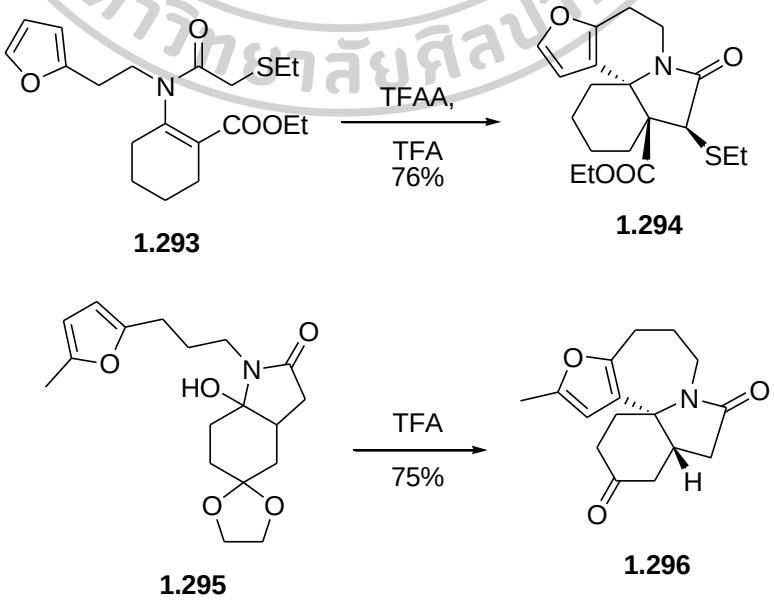

Scheme 50 Pummerer/Pictet-Spengler cyclization through *N*-acyliminium ion intermediate gave tetracyclic lactam compound

The *N*-tosylation of lactam compound **1.297a** treatment with *p*-toluenesulfonyl chloride (TsCl) gave *N*-tosyl lactam **1.299a**. *N*-acyliminium ion cyclization of *N*-tosyl lactam **1.299a** reacting with titanium tetrachloride ($TiCl_4$) as lewis acid through spiroindoleninium cation intermediate generated tetracyclic spiroindole-3,3´-indolizidine compound **1.300** in 73% yield.

Similarly, *N*-tosylation of lactam compound **1.297b** using *p*-toluenesulfonyl chloride (TsCl) generated *N*-tosyl lactam **1.299b**. *N*-acyliminium ion cyclization of *N*-tosyl lactam **1.299b** reacting with boron trifluoride diethyl etherate ($BF_3{\cdot}OEt_2$) as lewis acid through spiroindoleninium cation intermediate generated tetracyclic spiroindole-3,3´-indolizidine compound **1.300b** in 93% yield (Scheme 51) (49).

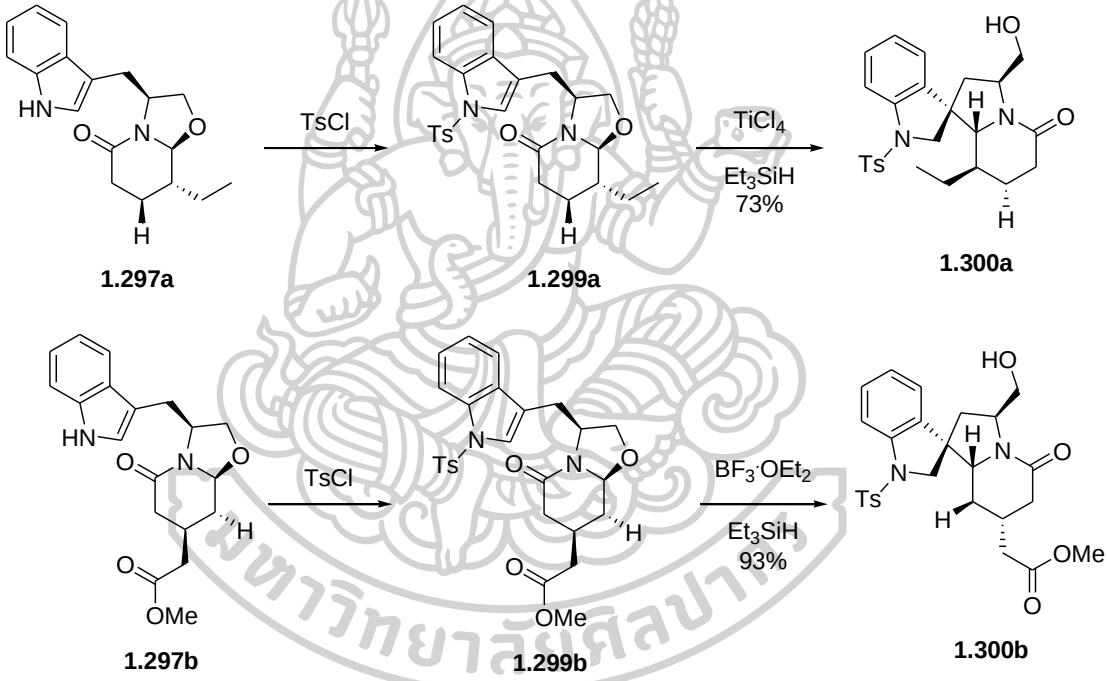

Scheme 51 The *N*-acyliminium ion cyclization of *N*-tosyl lactam using Lewis acid gave tetracyclic spiroindole-3,3´-indolizidine compound

Reactions for synthesis spiro cyclic compound

The spirooxindole core structures are oxindole with spiro-fused to other cyclic frameworks. Spirooxindole compound have attracted great interest from researchers in synthetic organic chemistry and medical chemistry all over the world. Spirooxindole core structure occurs in many natural products such as rhynchophylline, isorhynchophylline, Pteropodine, Spirotryprostatin A, Spirotryprostatin B, Mitraphylline, Elacomine, (±)-Horsfiline, (±)-Coerulescine, Marcfortine A, Surugatoxin, Alstonisine and Formosanine (Figure 17) (50).

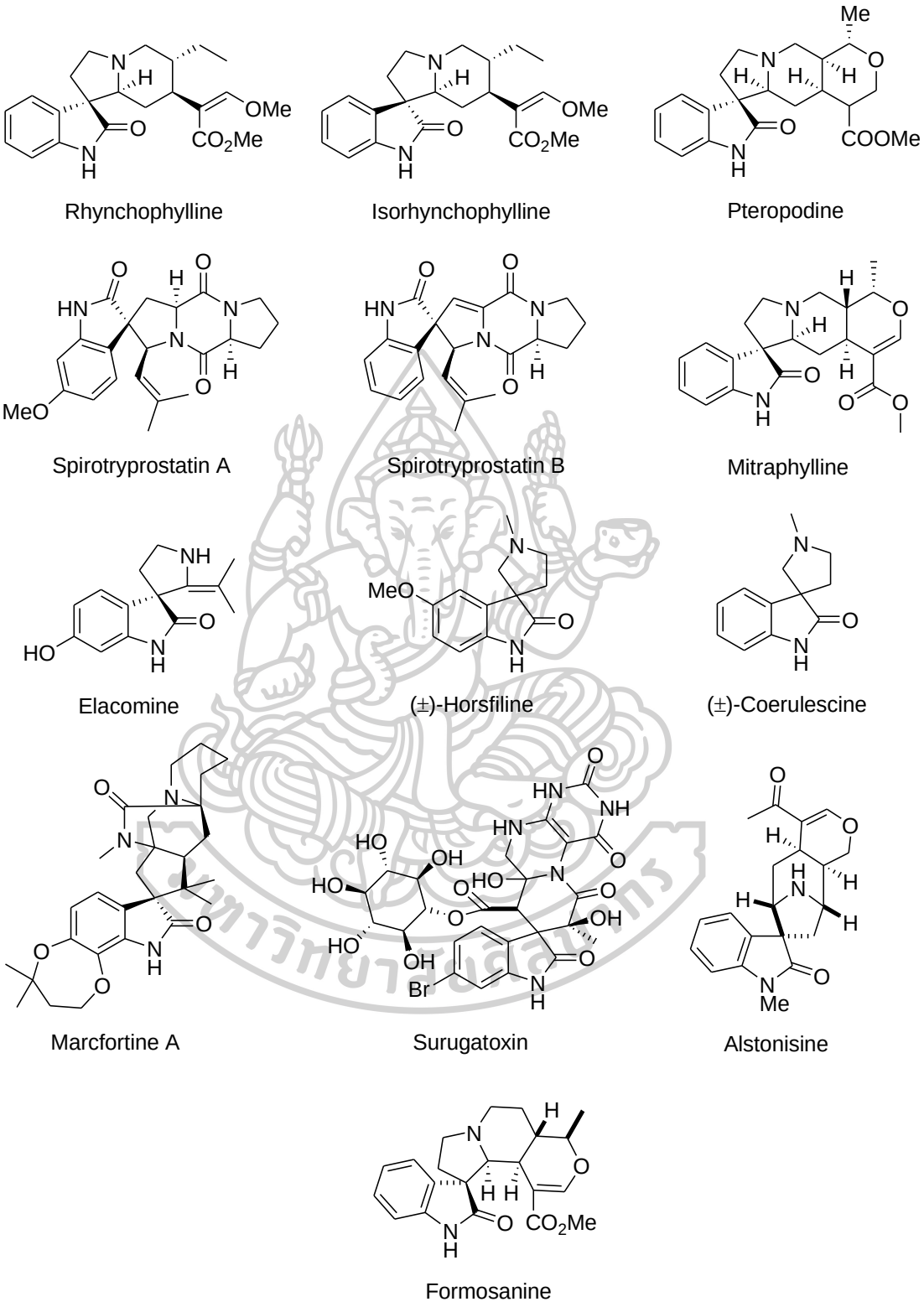

Figure 17 Structure of natural product with spiro oxindole compound

Structurally diverse compounds of spirooxindole are useful in the treatment of diseases that are used in a variety of medical. Spirooxindole compound have been modified to provide high bioactivity which suitable for treatment with diseases such as such as progesterone receptor agonist, MDM2-p53 interaction inhibitor, Inhibitor at the vanilloid receptor1, antimalarial, CR TH2 receptor antagonist, Satavaptan and MI-63 MDM2 inhibitor (Figure 18).

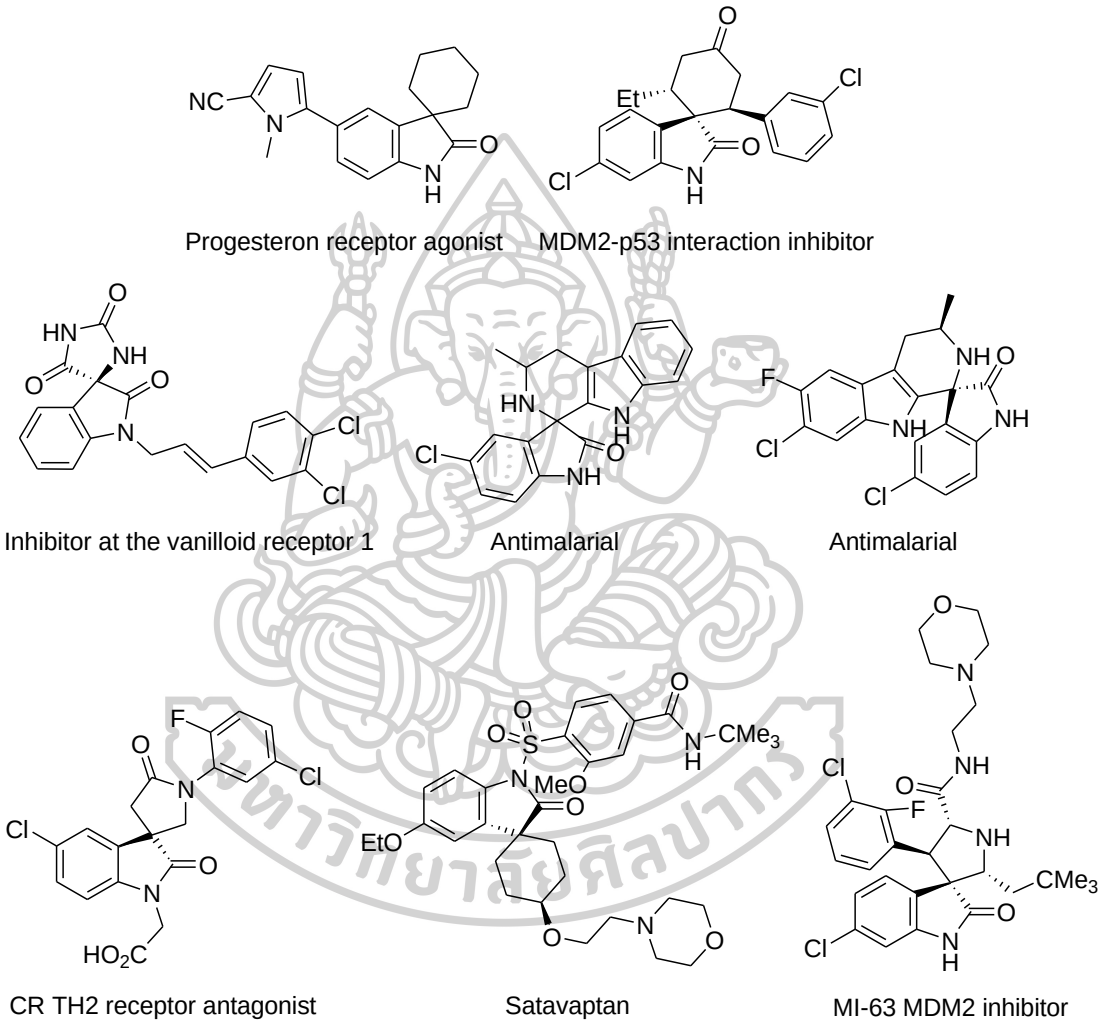

Figure 18 Important biologically activity of spirooxindole core structure compounds

Cyclocondensation reaction for synthesis spirooxindole derivative

Key reaction exist synthesis spirooxindole core structure. The cyclocondensation reaction of isatin **2.1** with a diaminofurazane **2.47** to dissolve acetonitrile gave spirooxindole **2.48** in 77% yield (Scheme 52) (51).

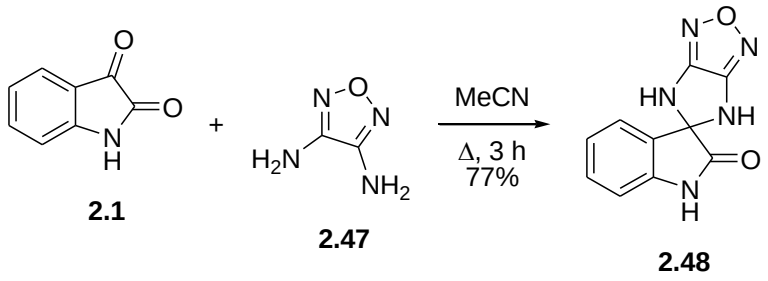

2.1 **2.47** **2.48**

Scheme 52 Cyclocondensation reaction between isatin and diaminofurazane for synthesis spirooxindole

For another example of cyclocondensation reaction of isatins **2.1** with 2-nitrobenzamides compound **2.49** using tin(II) chloride as both reducing agent and oxidized tin (IV) generated spirooxindole compound **2.50** in 83% yield (Scheme 53) (52).

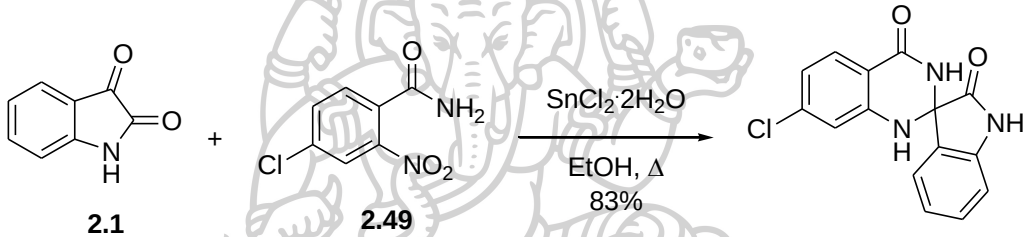

2.1 **2.49** **2.50**

Scheme 53 Cyclocondensation reaction using stannous chloride for synthesis spiroquinazolinone-oxindoles compound

The cyclocondensation reaction of isatins **2.1** with 2-hydroxynaphthalene-1,4-dione **2.59** in 1:2 equivalent in the presence of *p*-toluenesulfonic acid (*p*-TsOH) to afford intermediate **2.61**. Intermediate **2.61** reating with 2-hydroxynaphthalene-1,4-dione **2.59** in the loss of water gave polycyclic compound **2.62** followed by cyclization to give spirooxindole **2.60** in 80% yield (Scheme 54) (53).

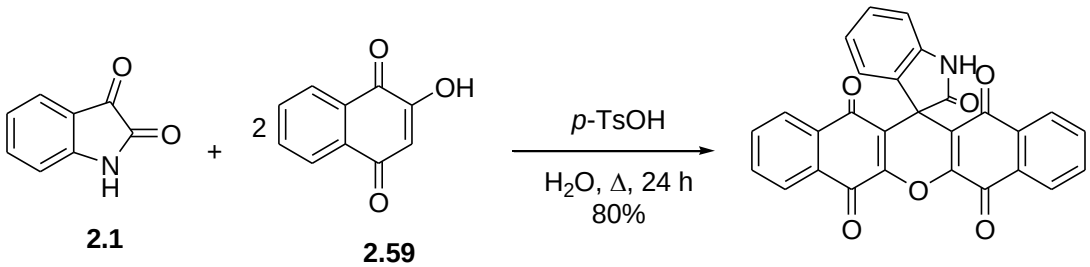

2.1 **2.59** **2.60**

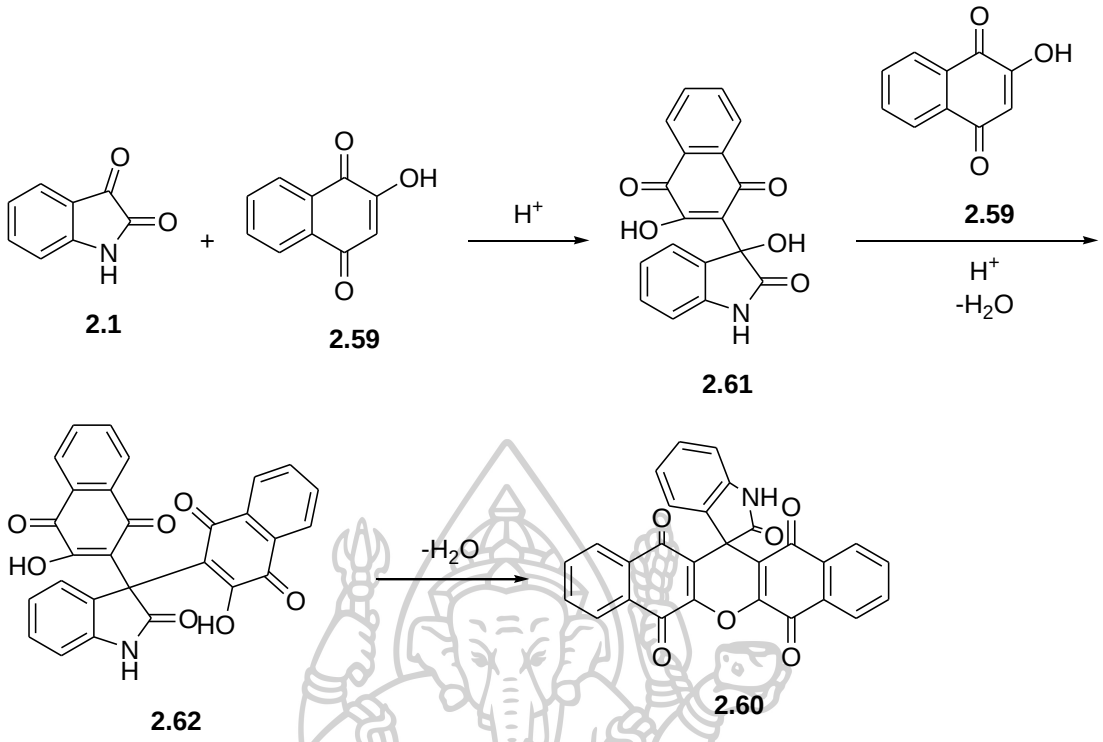

Scheme 54 Cyclocondensation reaction using Brønsted acids for synthesis spiroquinazolinone-oxindoles compound

The cyclocondensation reaction of isatin derivatives **2.1a** with 4-indol-(3yl)-1-butanamine **2.63** in the presence of *p*-toluenesulfonic acid (p-TsOH) as Brønsted acids provided eight membered ring of spirooxindole compound **2.64** in 8% yield (Scheme 55) (54).

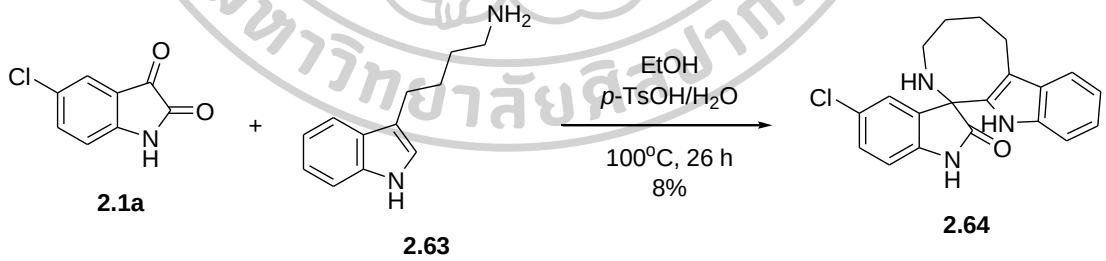

Scheme 55 Cyclocondensation reaction using Brønsted acids generated spirooxindole

Cycloaddition and cyclization reaction for synthesis spirooxindole derivative

The nitrile ylides compound **2.73** synthesized via base-catalyzed reaction of imidoyl chloride **2.72** in the presence of triethylamine. The [2+3]-cycloaddtion as key reaction occurs synthesis spirooxindole core structure of nitrile ylide **2.73** with *N*-methyl isatin **2.1b** gave spirooxindole **2.74** in 81% yield (Scheme 56) (55).

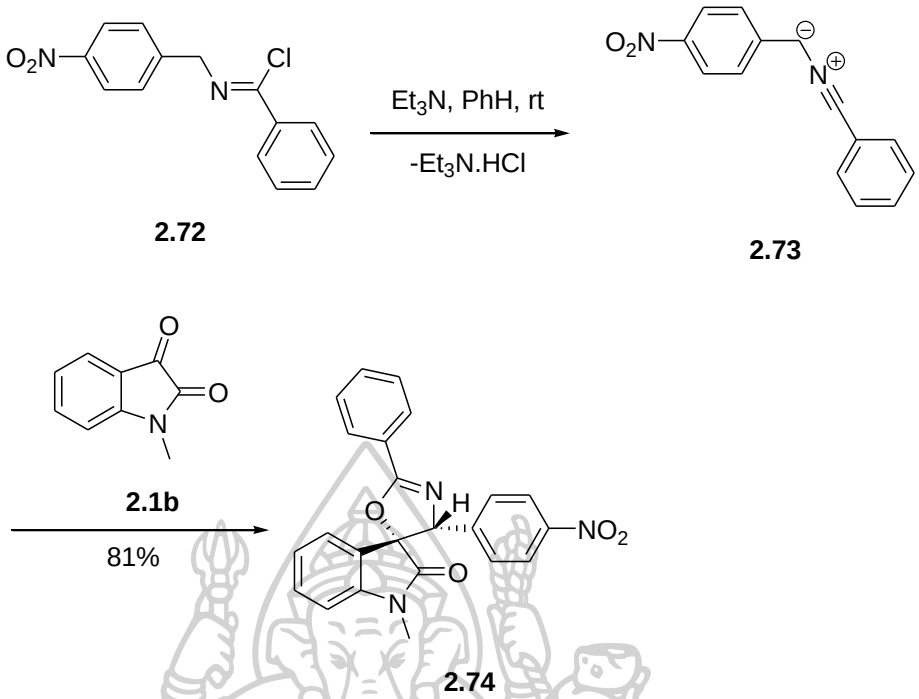

Scheme 56 The [2+3]-cycloaddtion through nitrile ylides for synthesis spirooxindole compound

The [2+3]-cycloaddtion of 5-diazo-1-arylpentane-1,4-dione **2.75** using Rhodium(II) acetate ($Rh_2(OAc)_4$) as Rh(II)-catalyzed decomposition through cyclic carbonyl ylide **2.76** in the presence of isatin **2.1c** generated spirooxindoles **2.77** in 75% yield (Scheme 57) (56).

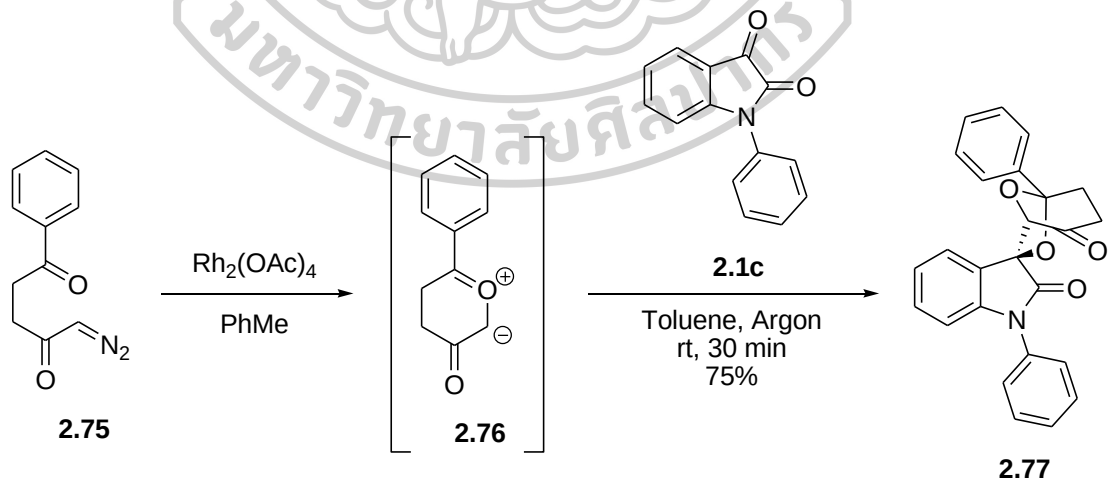

Scheme 57 The [2+3]-cycloaddtion in the presence Rhodium (II) acetate through cyclic carbonyl ylide for synthesis spirooxindole compound

Publication of Hosomi and coworker, the reaction between *N*-benzyl isatin **2.1d** and chloromethyl trimethylsilyl sulfide **2.81** using cesium fluoride (CsF) synthesized spirooxindole **2.82** in 86% yield (Scheme 58) (57).

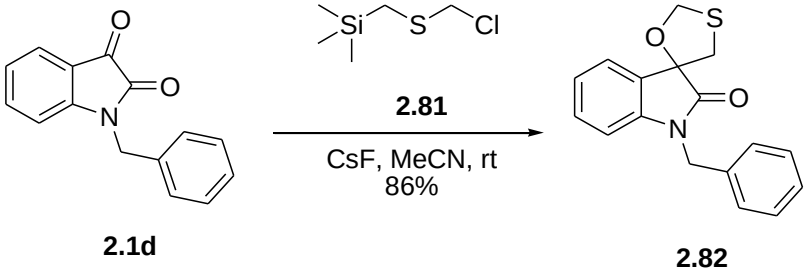

Scheme 58 Reaction of a thiocarbonyl ylide with carbonyl compounds by Hosomi and coworker

The [4+2]-annulations of *N*-benzyl isatin **2.1d** with but-3-yn-2-one **2.83** in the occurrence of a 100 mol-% stoichiometric amount of 1,4-diazabicyclo[2.2.2]octane (DABCO) as Brønsted base in tetrahydrofuran through nucleophilic attack of enolates on the C-3 carbonyl group of *N*-benzyl isatins **2.1d** and intramolecular cyclization of the oxy anion (O^-) in alkyne intermediate **2.85** followed by protonation of spirooxindole intermediate **2.86** gave spirooxindole **2.84** (Scheme 59) (58).

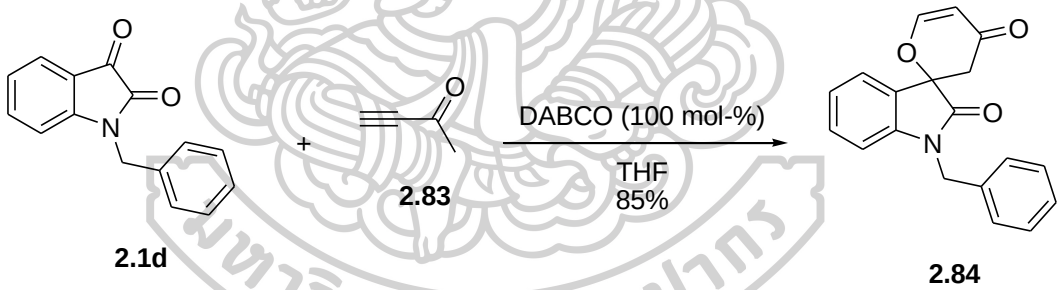

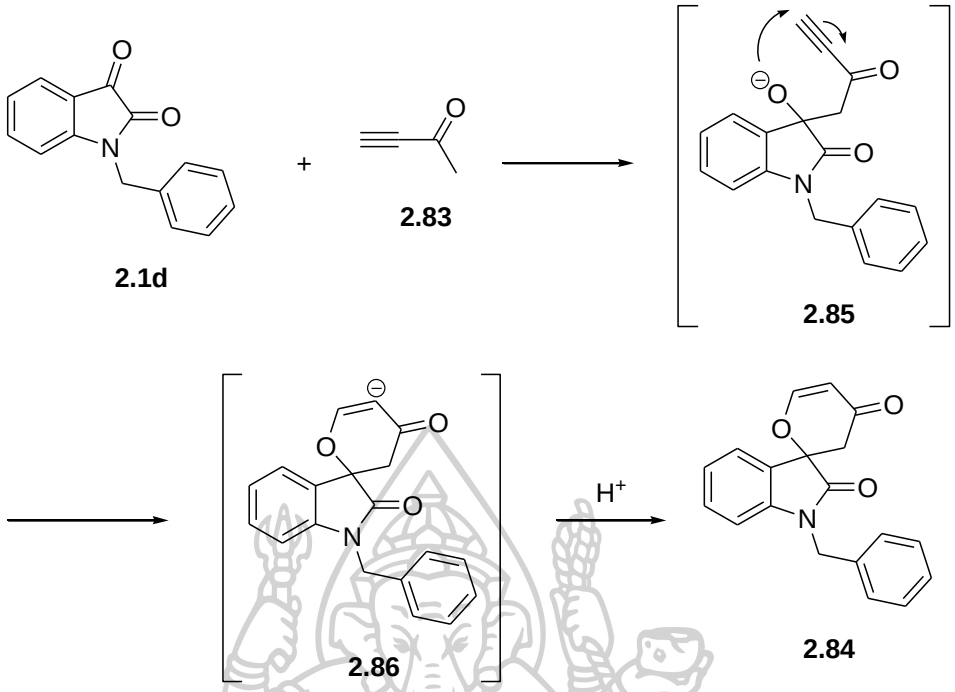

Scheme 59 The [4+2]-annulation of *N*-benzyl isatins with but-3-yn-2-one for synthesis spirooxindole.

Similar reaction has a catalyst conversion from nitrogen catalyst as 1,4-diazabicyclo[2.2.2]octane (DABCO) to phosphorus catalyst (PPh_2Me) from [4+2]-annulations of *N*-benzyl isatin **2.1d** with but-3-yn-2-one **2.83**. The reaction of interest after replacing the catalyst, [3+2]-annulation between *N*-benzyl isatin **2.1d** and phosphorus catalyst (PPh_2Me) through [1,3]-Hydrogen shift of zwitterionic intermediate **2.88** to give enolate **2.89** followed by nucleophilic attack of enolate **2.89** with *N*-benzyl isatin **2.1d** gave oxy anion intermediate **2.90**. Cyclization oxy anion intermediate 90 to generate ylide intermediate **2.91** which undergo 1,2-hydrogen shift to form spirooxindole intermediate **2.92** followed by elimination of phosphorus catalyst catalyst generated spirooxindole **2.87** in 86% yield (Scheme 60) (58).

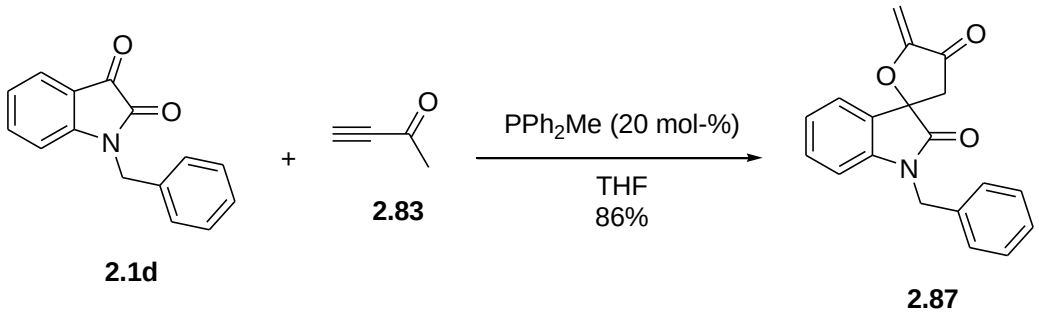

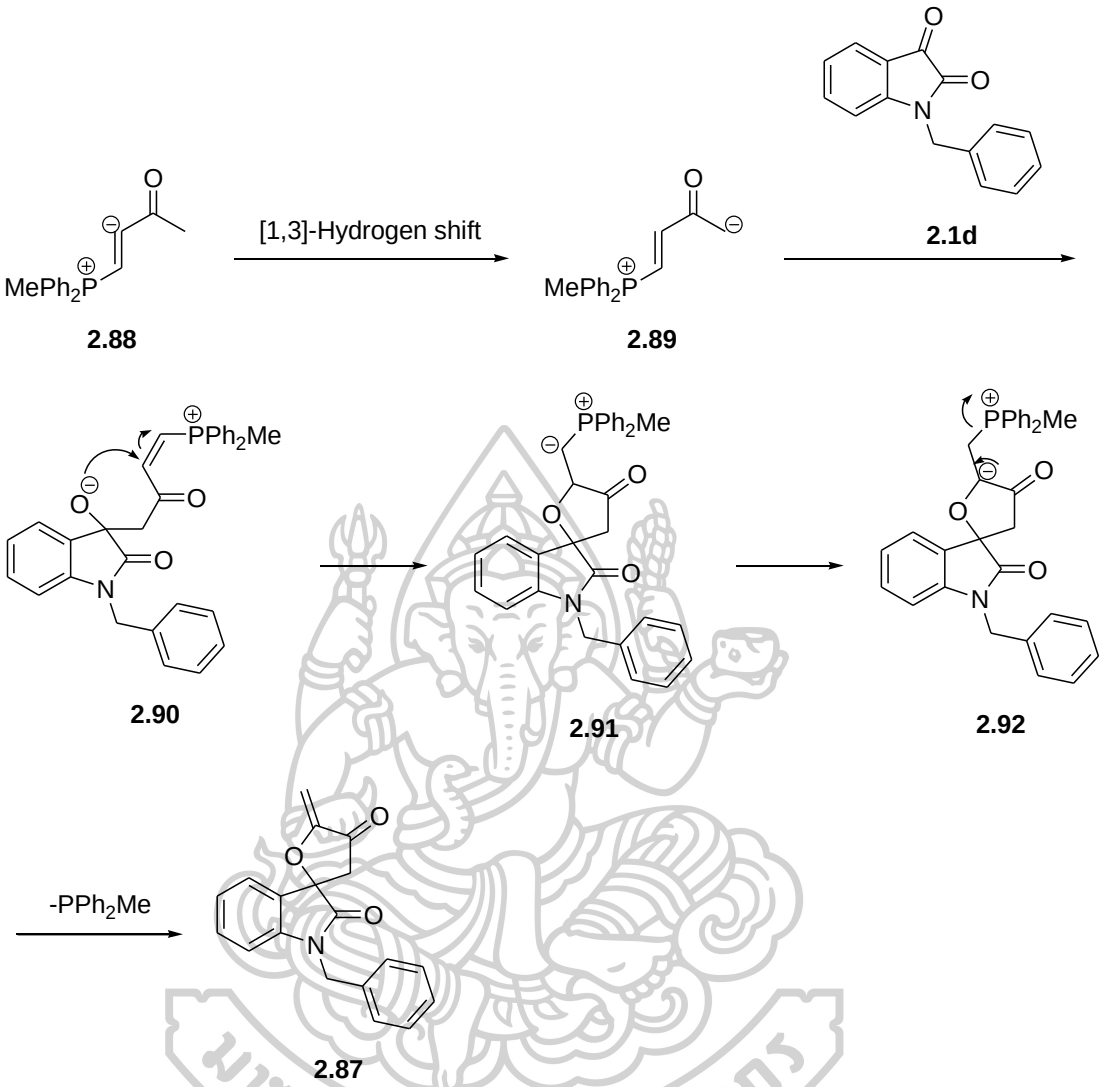

Scheme 60 The [3+2]-annulation in the presence of phosphorus catalyst for synthesis spirooxindole

Stereoselective reaction for synthesis spirooxindole derivative

The [2+2]-cycloaddition between *N*-methyl isatin **2.1** and ketene **2.93** using *N*-heterocyclic carbenes (NHCs) at -40 °C to room temperature gave *trans*-spiro-*β*-lactone-oxindole **2.95a** and *cis*-spiro-*β*-lactone-oxindole **2.95a** as ratio 3:1 in 92% and 99%ee (Scheme 61) (59).

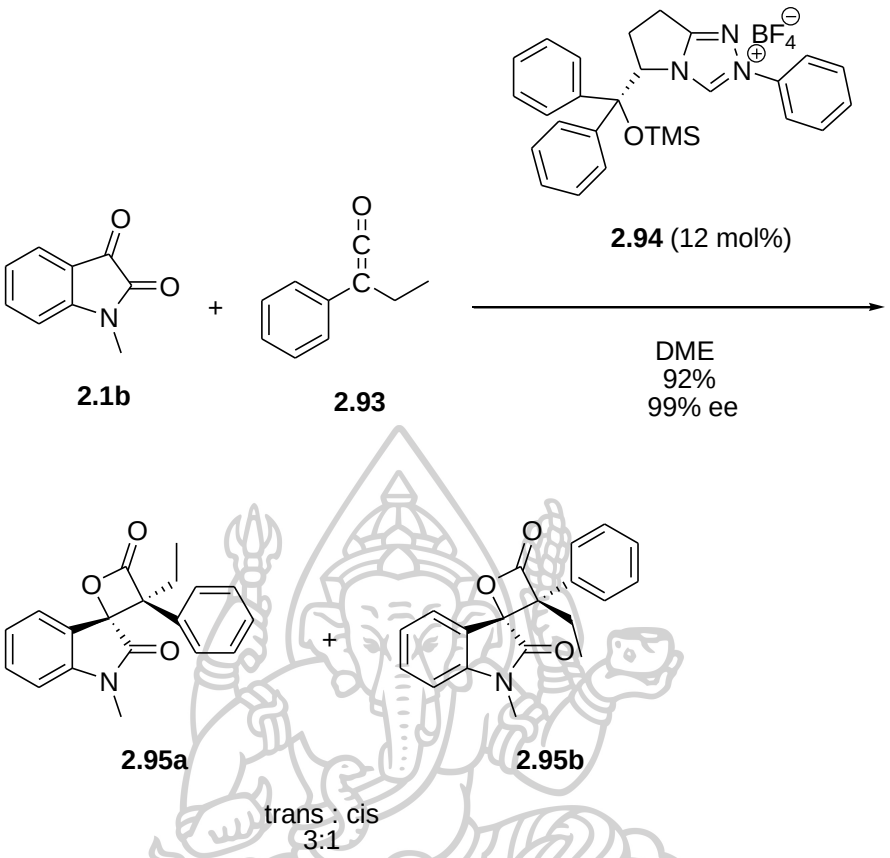

Scheme 61 The [2+2]-cycloaddition catalyzed by the *N*-heterocyclic carbenes (NHCs) for synthesis spirooxindole.

Publication of Ye and coworker, the reaction of between *N*-benzylisatin **2.1** with *α,β*-unsaturated aldehyde **2.96** using L-pyroglutamic acids derived *N*-heterocyclic carbene **2.97** in tetrahydrofuran at room temperature through transition state **2.99** synthesized 17:1 ratio of spiro *γ*-lactone-oxindoles **2.98** in 86% yield and 93%ee (Scheme 62) (60).

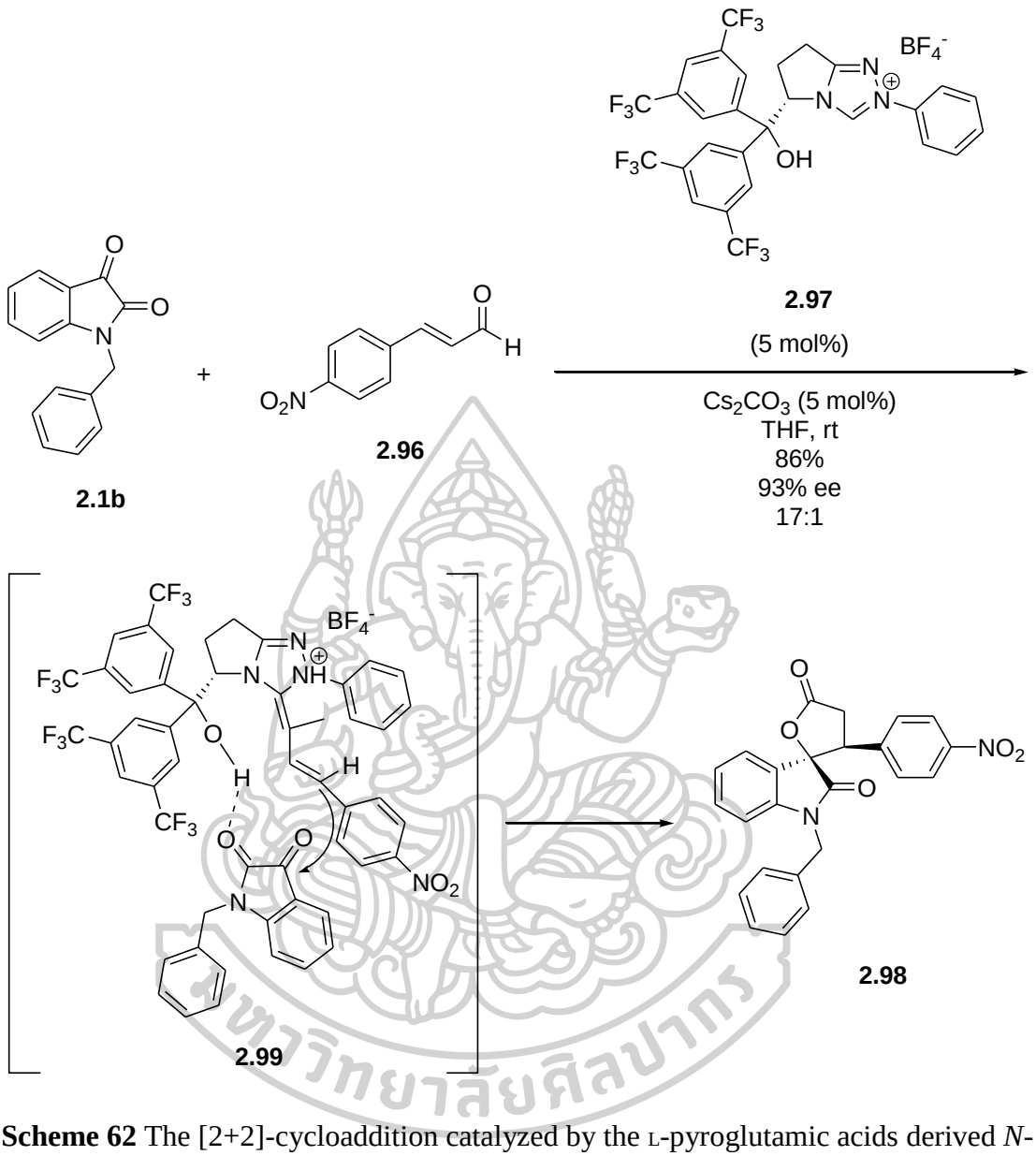

Scheme 62 The [2+2]-cycloaddition catalyzed by the L-pyroglutamic acids derived *N*-heterocyclic carbene for synthesis spirooxindole by Ye and coworker

Tandem C-C and C-O bonds formations in the presence of titanium tetrachloride ($TiCl_4$) catalyzed coupling of pyran compound **2.100** with isatin **2.1** in present a simple methodology for the stereoselective to generate spirooxindole **2.101** in 74% yield (Scheme 63) (61).

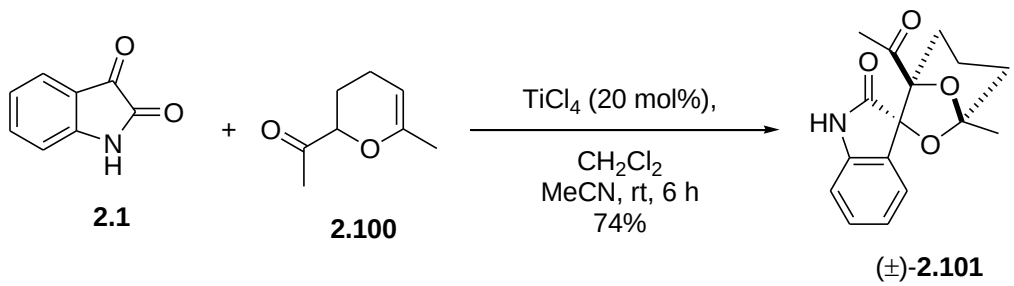

Scheme 63 Reaction of $TiCl_4$-catalyzed coupling reaction for synthesis spirooxindole

The reaction of isatin **2.1** and pyran compound **2.100** in the presence of 20 mol% of titanium catalyst at room temperature through initial coordination of pyran with titanium catalyst generated titanium intermediate. The titanium intermediate reacting with isatin **2.1** gave transition state **2.102** which can selectively to give spirooxindole precursor **2.103** followed by cyclization affored spirooxindole compound **2.101** (Scheme 64) (61).

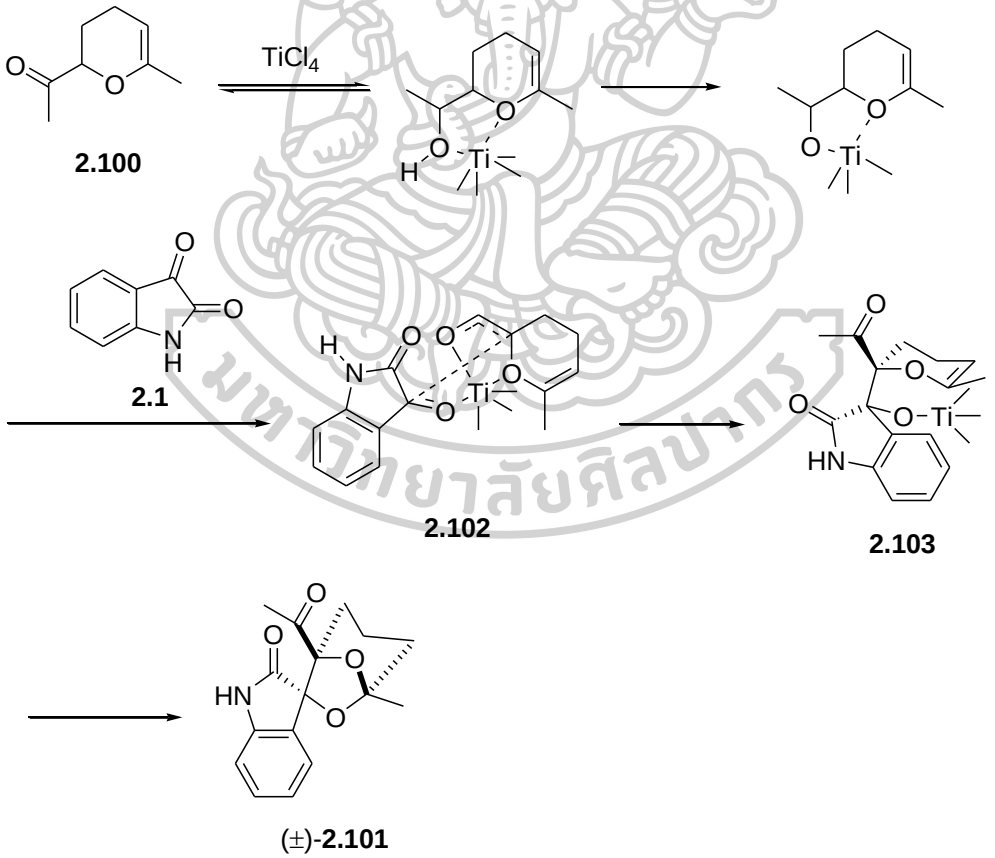

Scheme 64 Proposed mechanisms for $TiCl_4$-catalyzed coupling reaction for synthesis spirooxindole.

Publication of Franz and coworker, titanium-catalyzed regio- and stereoselective spiroannulation of *N*-methyl isatin **2.1d** with 2-aryl-5-methoxyoxazoles **2.104a** in the presence of titanium tetrachloride ($TiCl_4$) catalyzed through intermediate **2.107** generted spiro-oxazolineoxindole **2.105** in 99% yield and high diastereomer.

Similarly condition of titanium-catalyzed regio- and stereoselective spiroannulation of *N*-methyl isatin **2.1b** with 2-aryl-5-methoxyoxazole **2.104b** using titanium tetrachloride ($TiCl_4$) catalyzed through intermediate **2.108** synthesized 92:8 diastereomeric ratio of spirooxindole **2.106** in 91% yield. (Scheme 65) (62).

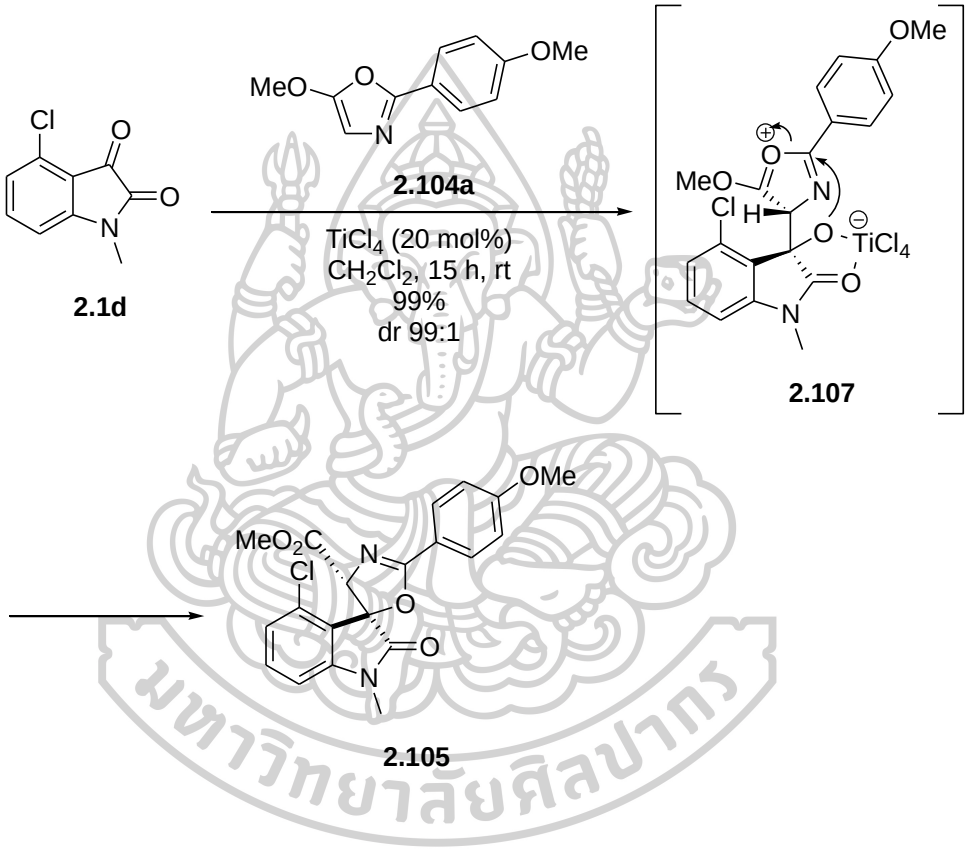

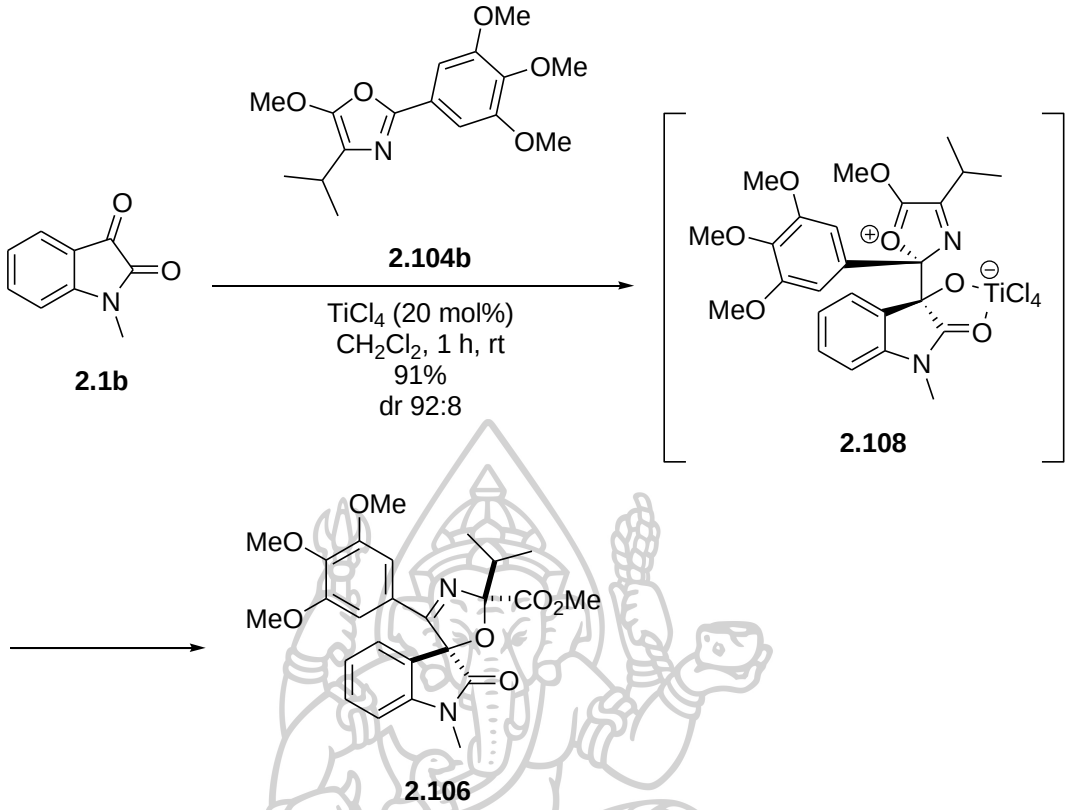

Scheme 65 Titanium-catalyzed stereoselective synthesis of spirooxindole by Franz and coworker

Catalytic asymmetric [3+2]-spiroannulation of isatin **2.1a** with allylsilane in the presence of chiral cationic $ScCl_2(SbF_6)$-pybox **2.109** complex and trimethylsilyl chloride gave spirooxindole **2.110** in 81% yield and 97% ee (Scheme 66) (63).

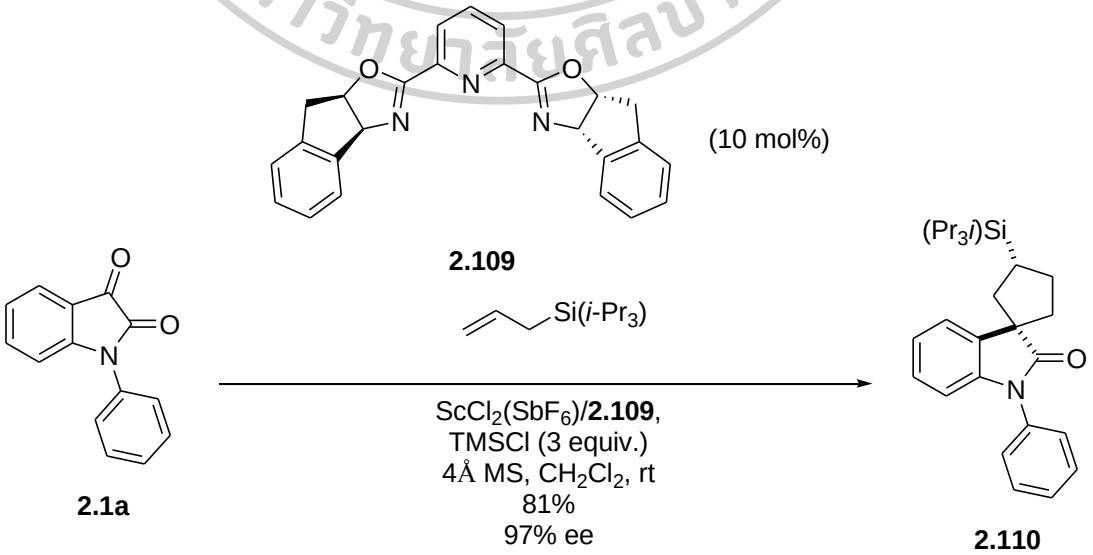

Scheme 66 Catalytic asymmetric [3+2] spiroannulation of allylsilanes with isatins for synthesis spirooxindole

Publication of Hayashi and coworker used palladium-catalyzed decarboxylative cyclization of *N*-methyl isatin **2.1b** with *γ*-methylidene-*δ*-valerolactone **2.116** in the presence of chiral phosphoramidite ligand **2.117** gave 88:12 diastereomeric ratio of spirooxindole compound **2.118** in 87% yield (Scheme 67) (64).

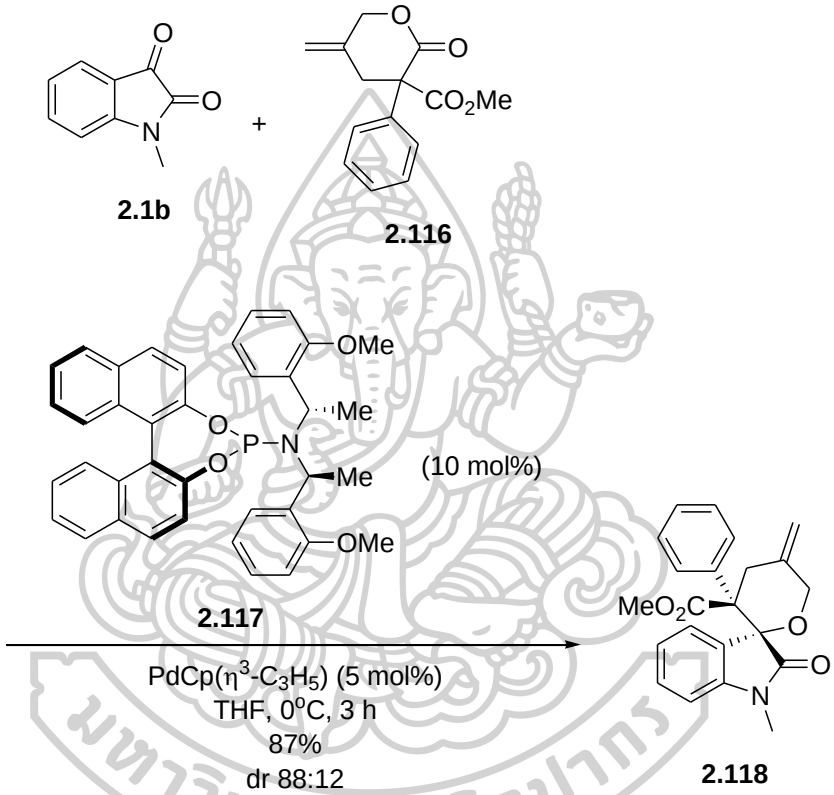

Scheme 67 Palladium-catalyzed decarboxylative cyclization of *γ*-Methylidene-*δ*-valerolactones with isatin for synthesis spirooxindole by Hayashi and coworker

Publication of Hayashi and coworker carried out cationic rhodium-catalyzed intermolecular [4+2]annulation of *N*-methyl isatin **2.1a** with 2-alkynylbenzaldehyde **2.119** using rhodium-catalyst ([Rh((*R*,*R*)-**2.120**)]BF_4) complex gave spirooxindole **2.121** in 96% yield and excellent enantioselectivity (Scheme 68) (65).

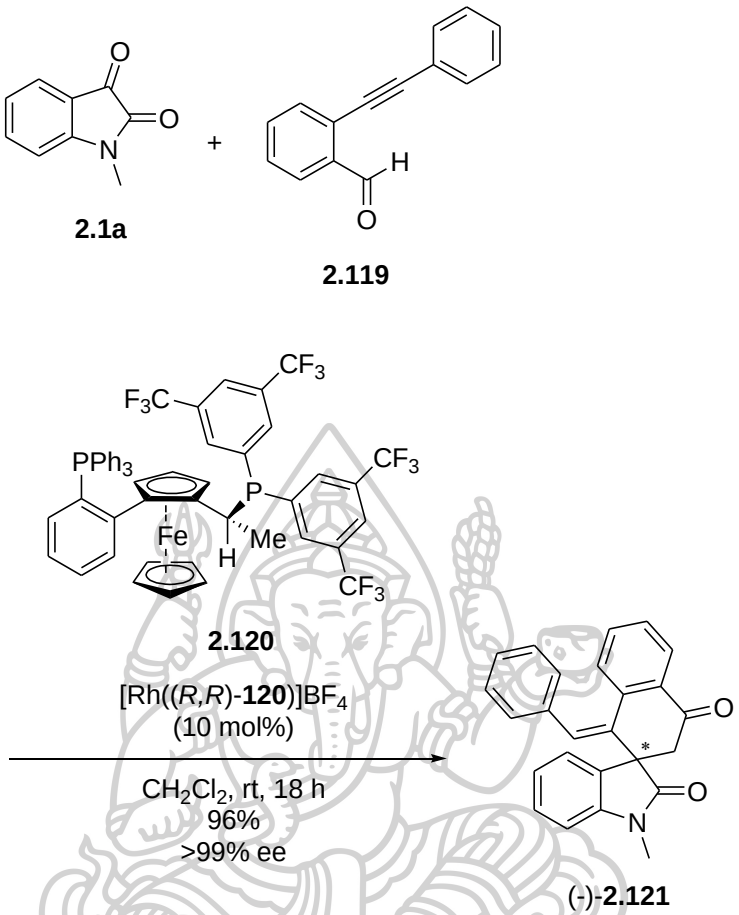

Scheme 68 Rhodium-catalyzed intermolecular [4+2] annulation for enantioselective synthesis of spirooxindole by Hayashi and coworker

Publication of List and coworker, Brønsted acid catalyzed reaction of isatin **2.1** with 2-aminobenzamide **2.122** in the presence of catalyst **1.114** in toluene generated spirooxindole compound **1.123** in 85% yield and 84% ee (Scheme 69) (66).

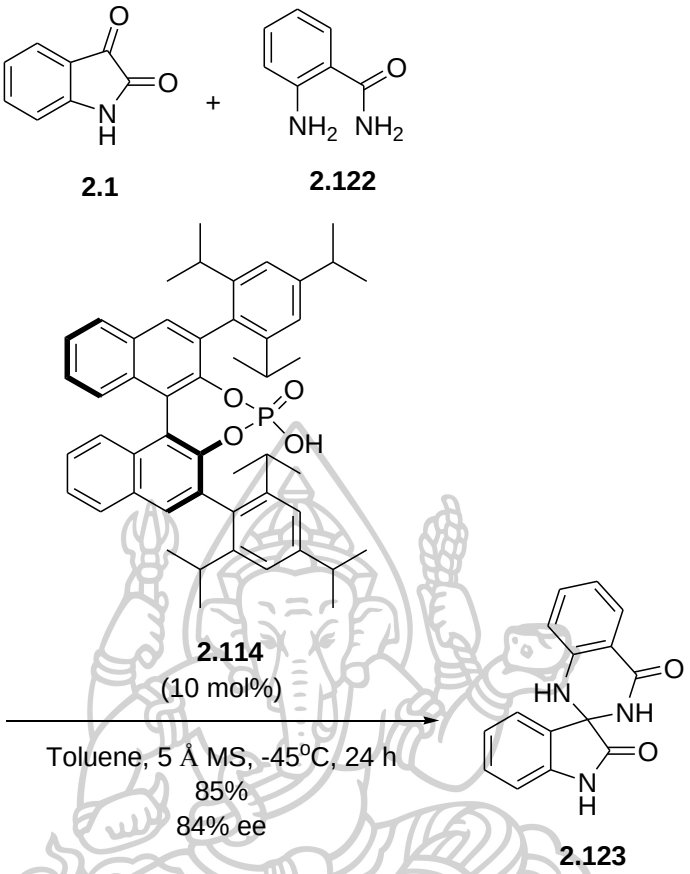

Scheme 69 Catalytic asymmetric synthesis of spirooxindole by List and coworker

Asymmetric aldol reaction between *N*-methyl isatin **2.1a** and acyclic isothiocyanate **2.124** using chiral thiourea catalyst **2.125** at room temperature outcomed in the formation of spirooxindole compound **2.126** in 81% yield and excellent enantioselective (Scheme 70) (67).

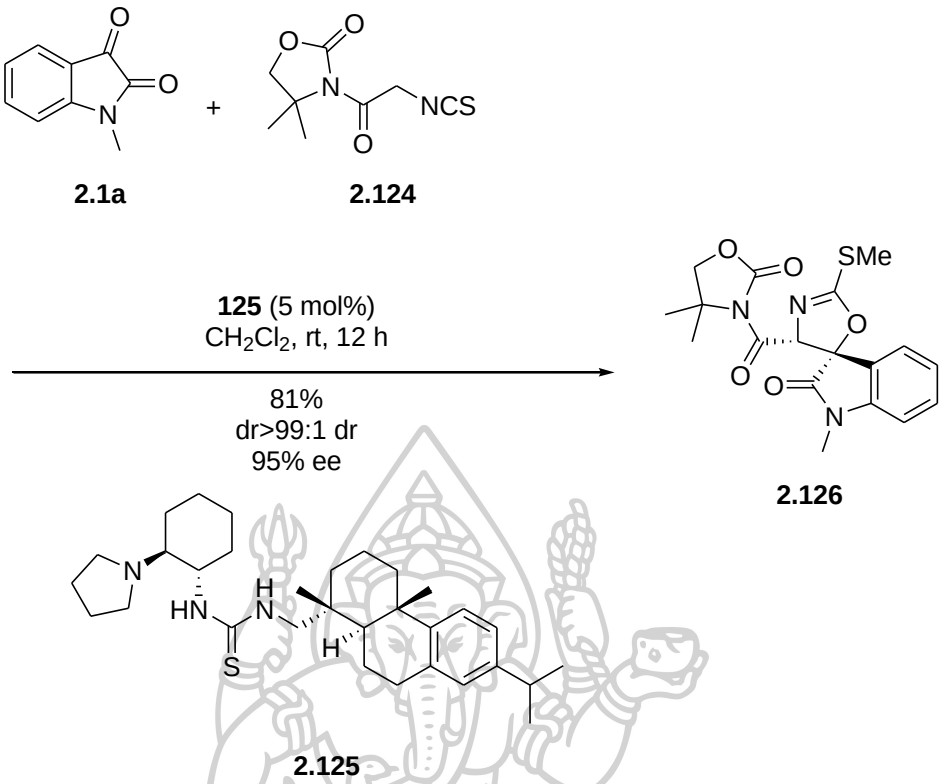

Scheme 70 Asymmetric aldol reaction using chiral thiourea catalyst for synthesis of spiro-oxazolineoxindole compound

Modify asymmetric aldol reaction between *N*-methyl isatin **2.1a** and cyclic isothiocyanate **2.127** in the presence of chiral thiourea catalyst **2.125** in dichloromethane generated spirooxindole compound **2.128** in 81% yield and excellent enantioselective (Scheme 71) (67).

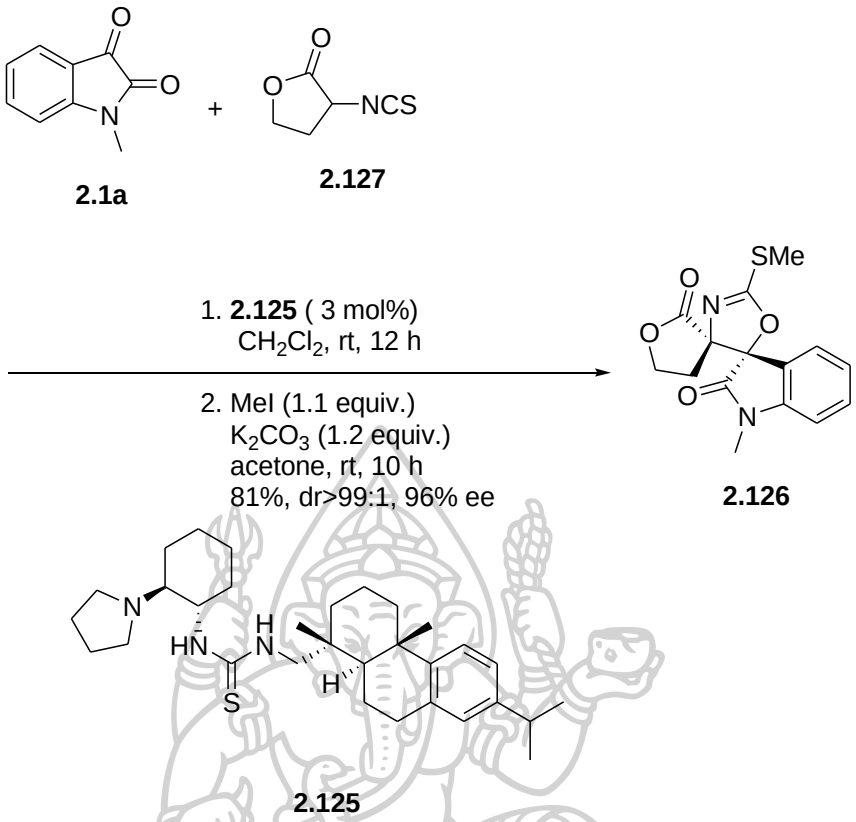

Scheme 71 Modify asymmetric aldol reaction using chiral thiourea catalyst for synthesis of spirooxindole compound

Reaction for synthesis spirooxindole derivative from three components

The reaction of isatin **2.1** and picolic acid **2.130** generated azomethine ylide **2.131** followed by stereospecific 1,3-dipolar cycloaddition of fumeronitrile **2.132** with azomethine ylide **2.131** to give spirooxindole **2.133** in 76% yield (Scheme 72) (68).

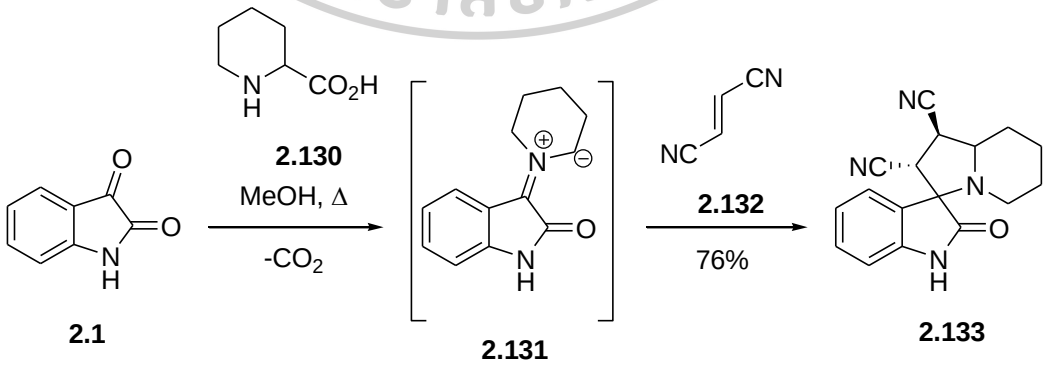

Scheme 72 The stereospecific 1,3-dipolar cycloaddition for synthesis spirooxindole

The reaction between *N*-methylisatin **2.1a** and sarcosine in mixture of methanol and water formed ylide in termediate **2.137**. Dipolar cycloaddition of ylide

2.137 with 3,4-diphenylcyclobutene-1,2-dione **2.138** gave spirooxindole **2.139** in 58% yield (Scheme 73) (69).

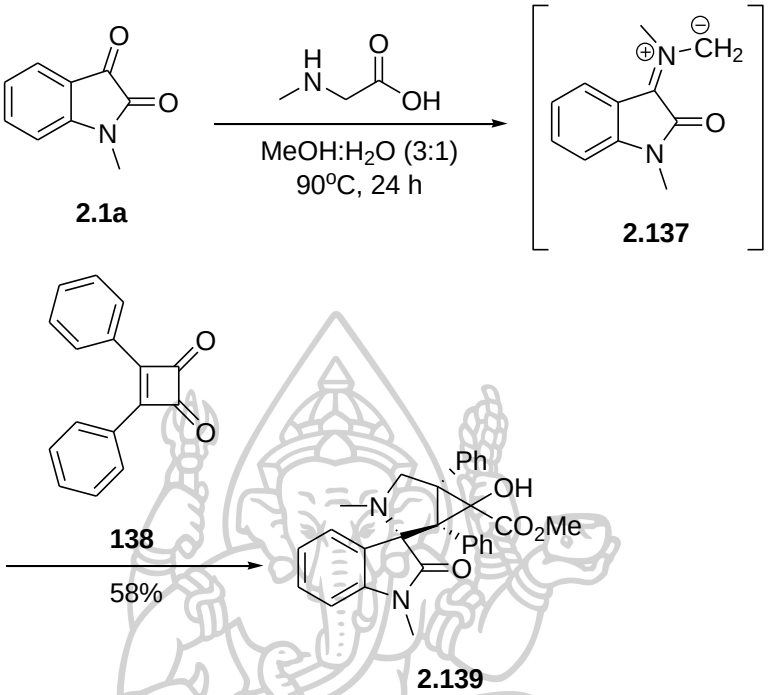

Scheme 73 Dipolar cycloaddition reactions of azomethine ylide with 3,4-diphenylcyclobutene-1,2-dione for synthesis spirooxindole

Publication of Hu and Feng, the reaction between *N*-methyl isatin **2.1a** and sarcosine gave azomethine ylide compound **2.168**. The [2+3]-cycloaddition of azomethine ylide compound **2.168** with pyrimidine-3-one **2.169** affored spirooxindole **2.170** in 85% yield (Scheme 74) (70).

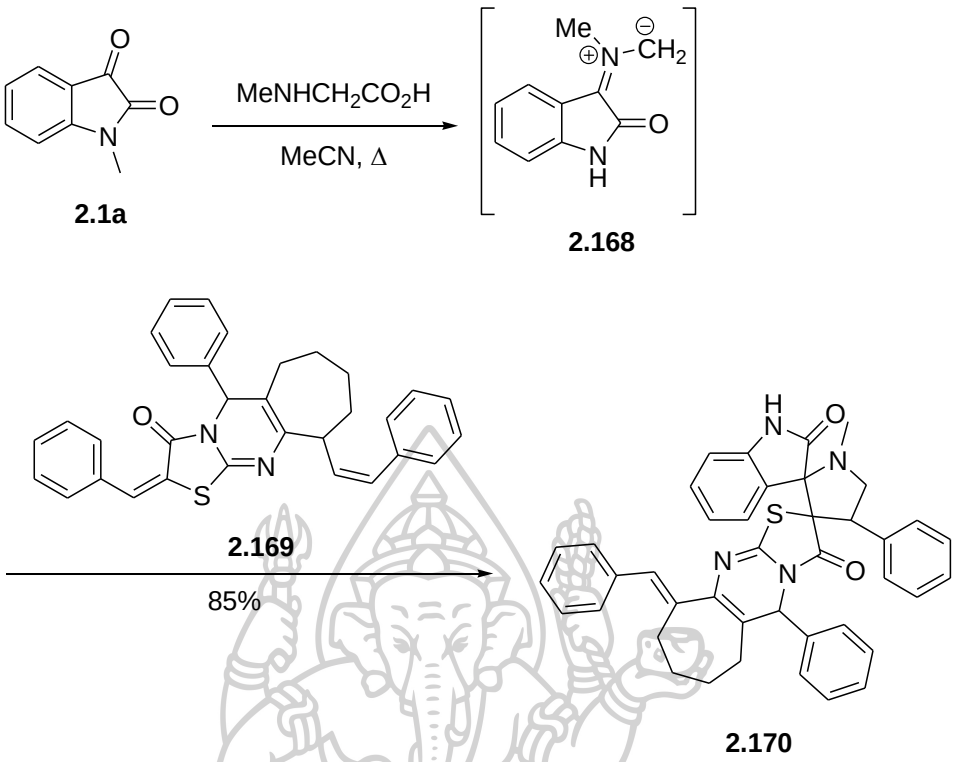

Scheme 74 The [2+3]-cycloaddtion for synthesis spirooxindole

One pot reaction between three-component which Knoevenagel reaction between isatin **2.1** and cyanoacetic ester **2.175** using nickel(II) chloride ($NiCl_2$) as Lewis acid to activate nitrile transformed into amine of Knoevenagel intermediate. The aza-Michael addition of phthalhydrazide **2.174** to the Knoevenagel intermediate followed by cycloaddition and isomerization gave spirooxindole **2.176** in 82% yield (Scheme 75) (71).

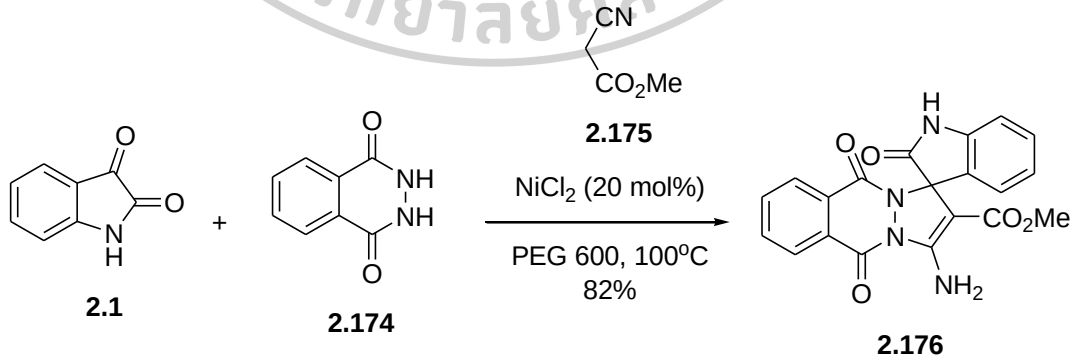

Scheme 75 Nickel chloride catalyzed of three compound synthesis of spirooxindole

One pot reaction of three component between isatin **2.1**, malononitrile and pentane-2,4-dione **2.196** using (-)-(*S*)-brevicolline as an organocatalyst generated spirooxindole compound **2.199** in 62% yield and 94% ee (Scheme 76) (72).

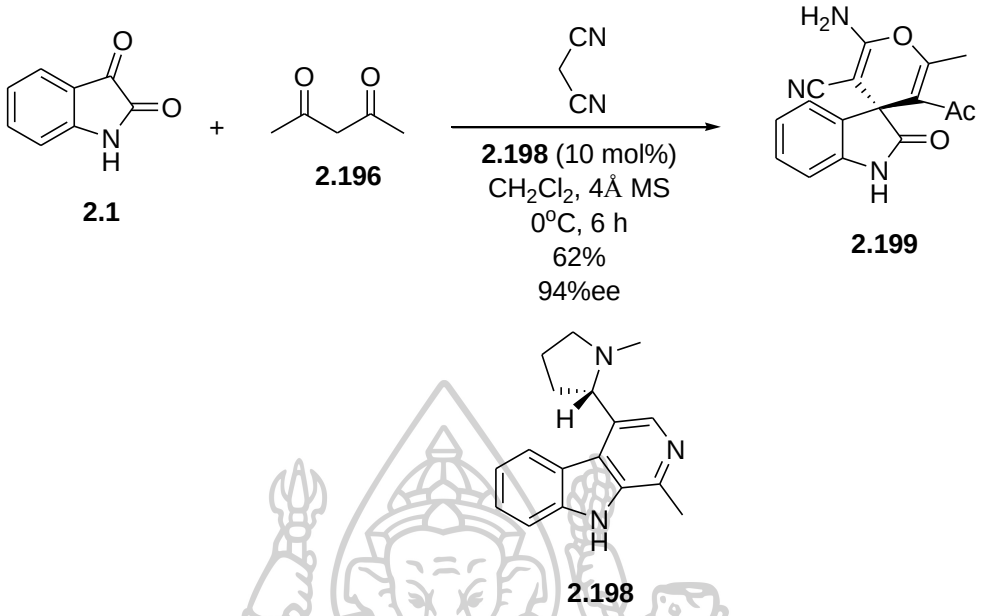

Scheme 76 One pot reaction for the synthesis spirooxindole using (-)-(*S*)-brevicolline

Publication of Stephenson and coworker, multicomponent reaction of three components between isatin **2.1,** 4-hydroxy-6-methyl-2-pyrone **2.200** and cyclic 1,3-diketone **2.185** in the presence of Lewis acid catalyst tin(IV) chloride ($SnCl_4$) gave spirooxindole compound **2.201** in 63% yield.

Similarly condition of tin(IV) chloride ($SnCl_4$) catalyzed irradiated by microwave between isatin **2.1**, 4-hydroxy-6-methyl-2-pyrone **2.200** and cyclic 1,3-diketone **2.185** gave spirooxindole compound **2.201** in 78% yield (Scheme 77) (73).

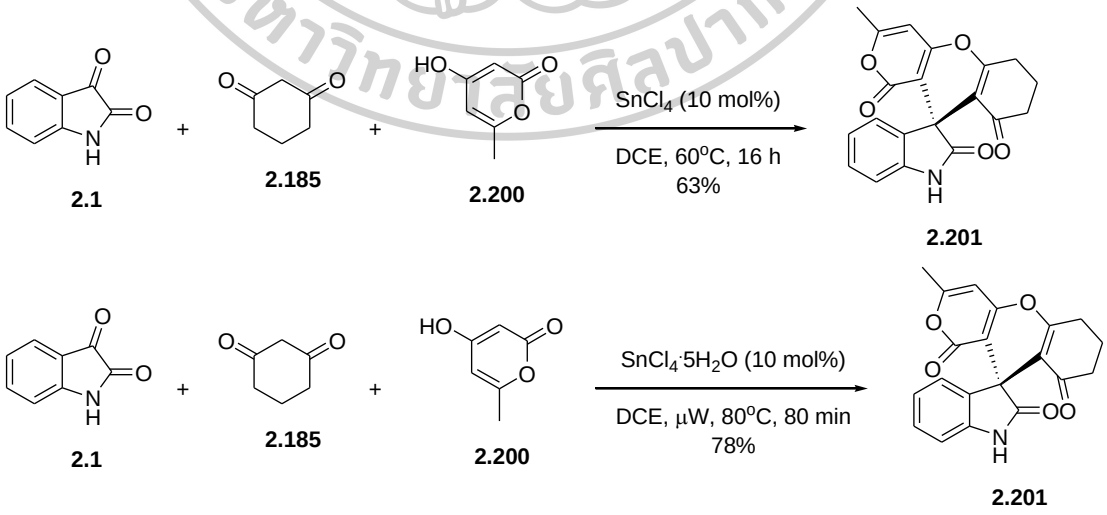

Scheme 77 Multicomponent reaction of three components for the synthesis of spirooxindole

Stephenson proposed two route of the mechanism of formation of spirooxindole. The first route begins with aldol condensation of isatin **2.1** with cyclic 1,3-diketone **2.185** gave indolenium ion intermediate. The reaction of indolenium ion intermediate with pyrone **2.200** afforded spirooxindole intermediate **2.203** followed by dehydration to give spirooxindole compound **2.201**.

Route 2 for synthesis spirooxindole compound of three components synthesized spirooxindole. The reaction of isatin **2.1** with pyrone **2.200** generated indolenium ion intermediate. The reaction of indolenium ion intermediate with cyclic 1,3-diketone **2.185** gave spirooxindole intermediate **2.203** followed by dehydration to give spirooxindole compound **2.201** (Scheme 78) (73).

Route 1 Mechanism of Multicomponent reaction for the synthesis of spirooxindole

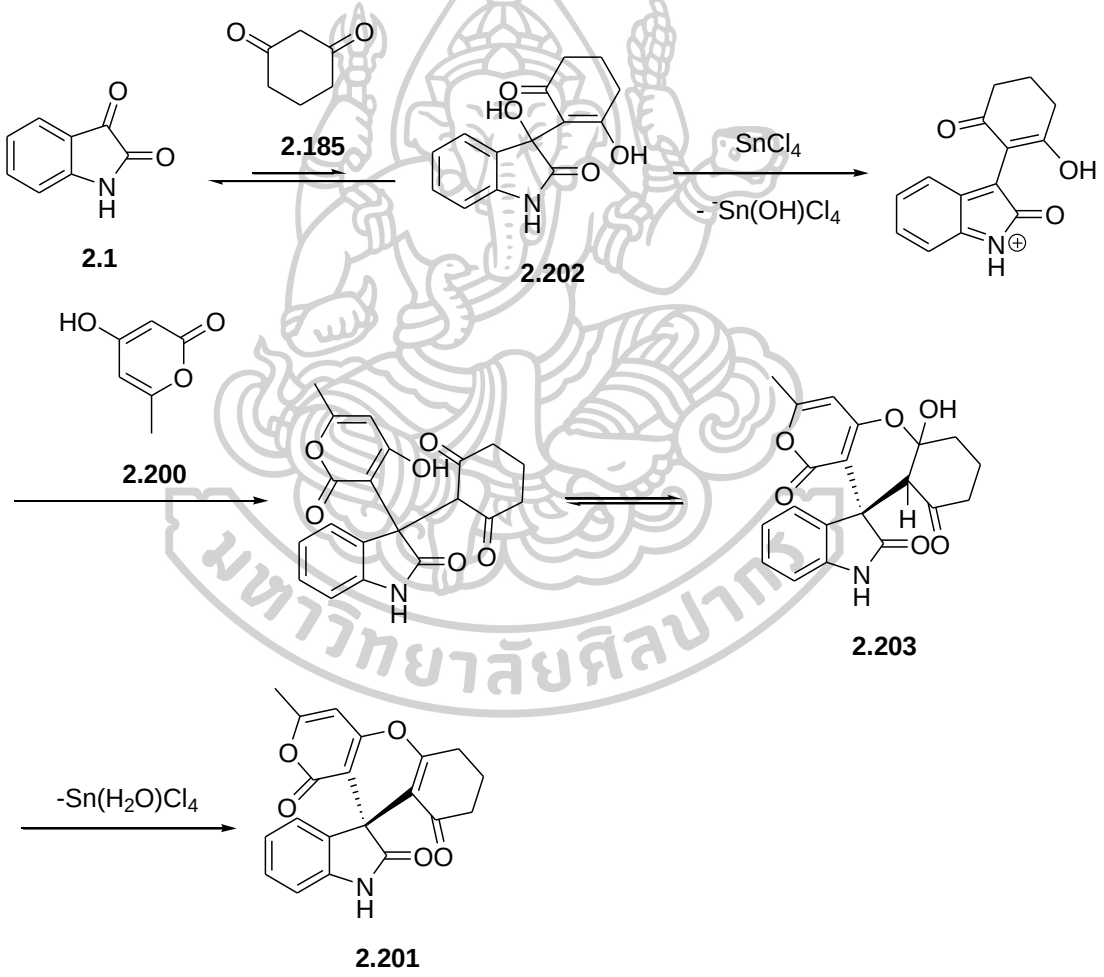

Route 2 Mechanism of Multicomponent reaction for the synthesis of spirooxindole

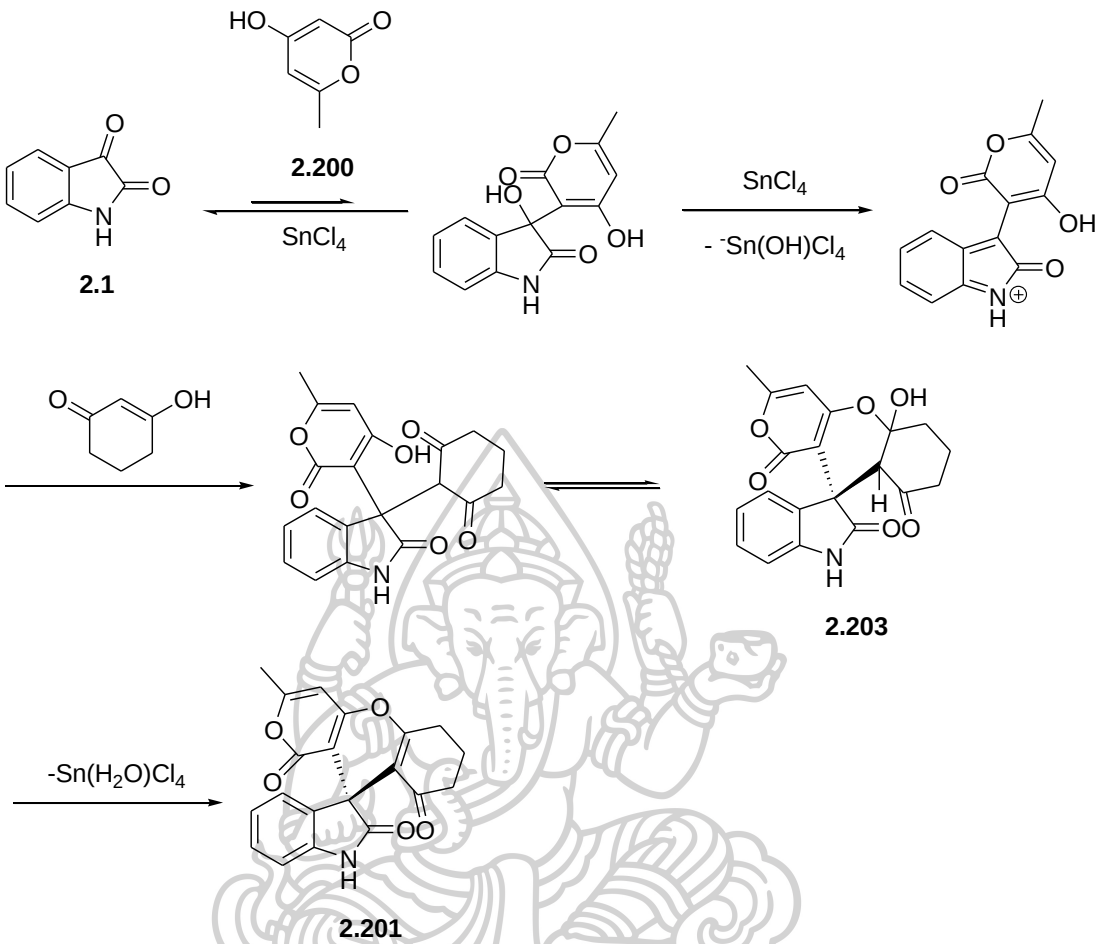

Scheme 78 Proposed mechanism of multicomponent reaction of three components for the synthesis of spirooxindole

A four-component reaction of isatin **2.1**, 3-aminocrotononitrile **2.207** and cyclic β-diketone compound **2.208** soluble in water in the presence of (±)-camphor-10-sulfonic acid on heating at 100°C for 2 h generated spirooxindole **2.209** in 92% yield (Scheme 79) (74).

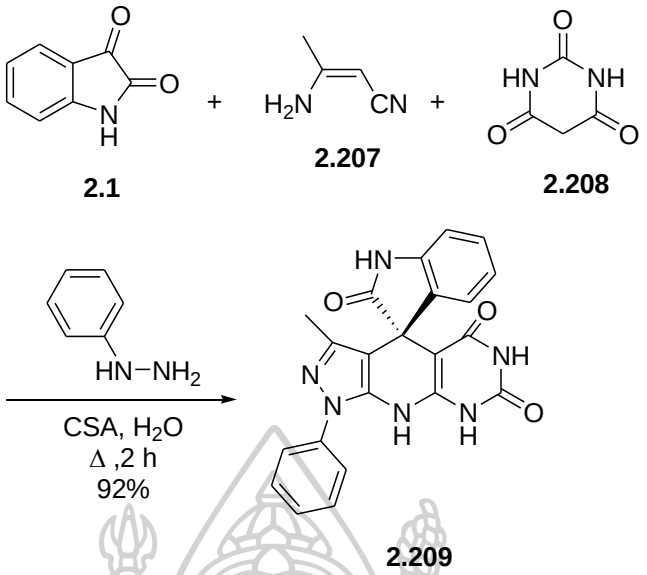

Scheme 79 Four component reactions approach the metal-free synthesis of spirooxindole

Proposed mechanism for acid catalyzed reaction of phenylhydrazine with nitrile **2.207** gave pyrazole **2.187**. The reaction between isatin **2.1** and pyrazole compound **2.187** under acid condition produced oxindole derivative 210 followed by reacting with cyclic *β*-diketone compound **2.208** to give intermediate compound **2.211**. Cyclodehydration and subsequent dehydration of intermediate compound **2.211** to eliminate of water produced spirooxindole **2.209** (Scheme 80) (74).

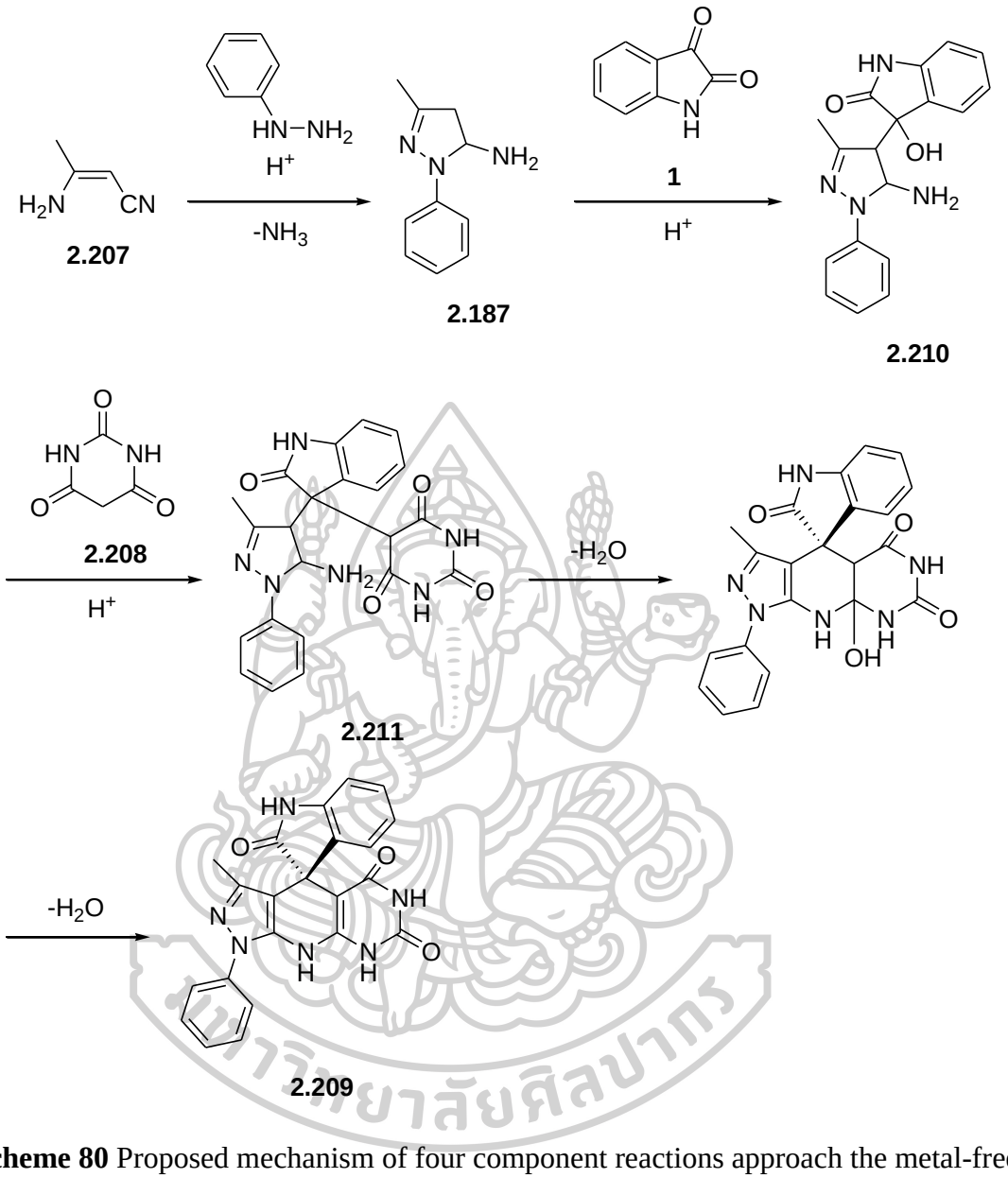

Scheme 80 Proposed mechanism of four component reactions approach the metal-free synthesis of spirooxindole

The one pot reaction of three compound between isatin **2.1**, aminopyrazole **2.187** and mercaptoacetic acid **2.212** using *p*-toluenesulfonic acid (*p*-TsOH) as Brønsted acid gave seven membered ring of spirooxindole **2.213** in 86% yield (Scheme 81) (75).

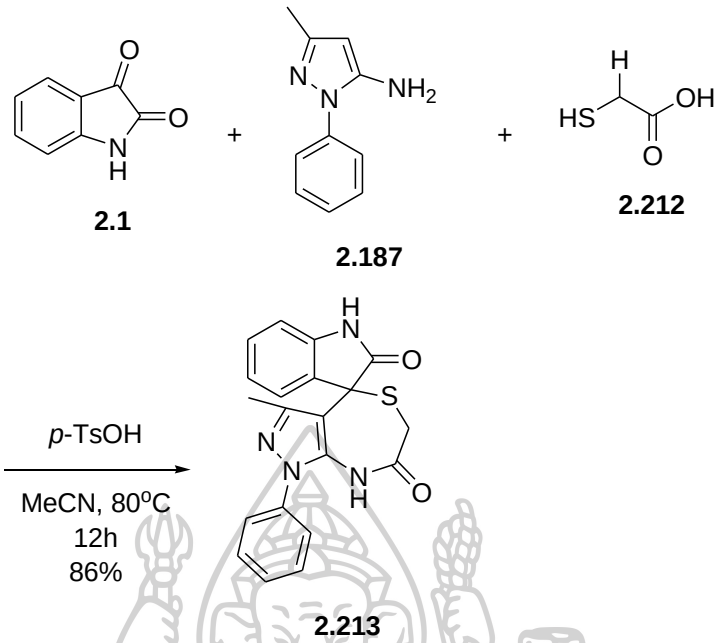

Scheme 81 One-pot synthesis of spirooxindole via three-component reaction

One-pot reaction is suggested through the nucleophilic addition of pyrazole **2.187** with isatin **2.1** to form hydroxyl oxindole **2.214** which undergoes protonation of the hydroxyl group. Dehydration of hydroxyl oxindole **2.214** gave intermediate **2.215**. Michael addition of mercaptoacetic acids with intermediate **2.215** created an intermediate product **2.216** followed by cyclization to give spiro-fused heterocycle **2.217** Dehydration of spiro-fused heterocycle **2.217** gave seven membered ring of spirooxindole **2.213** (Scheme 82) (75).

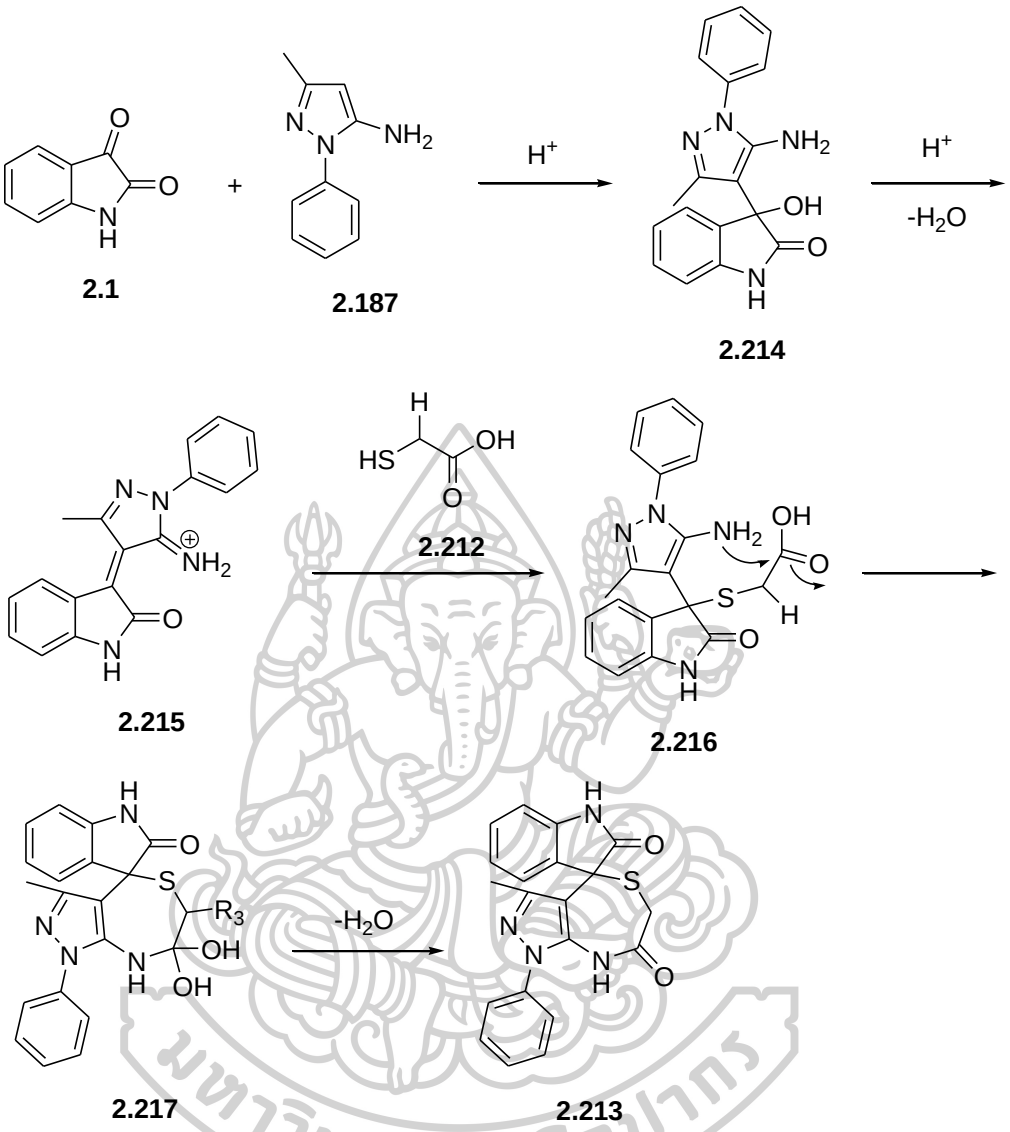

Scheme 82 Proposed mechanisms one pot synthesis of spirooxindole via three-component reaction

The Wadsworth-Emmons reaction of *N*-benzyl isatin **2.1c** with tetraethyl methylenebis(phosphonate) **2.221** gave 3-(phosphoromethylene)-2-oxindole **2.222**. The epoxidation of oxindole **2.222** in the presence of hydrogen peroxide afforded 83:17 as diastereomeric ratio of spirooxindole **2.223** in 80% yield (Scheme 83) (76).

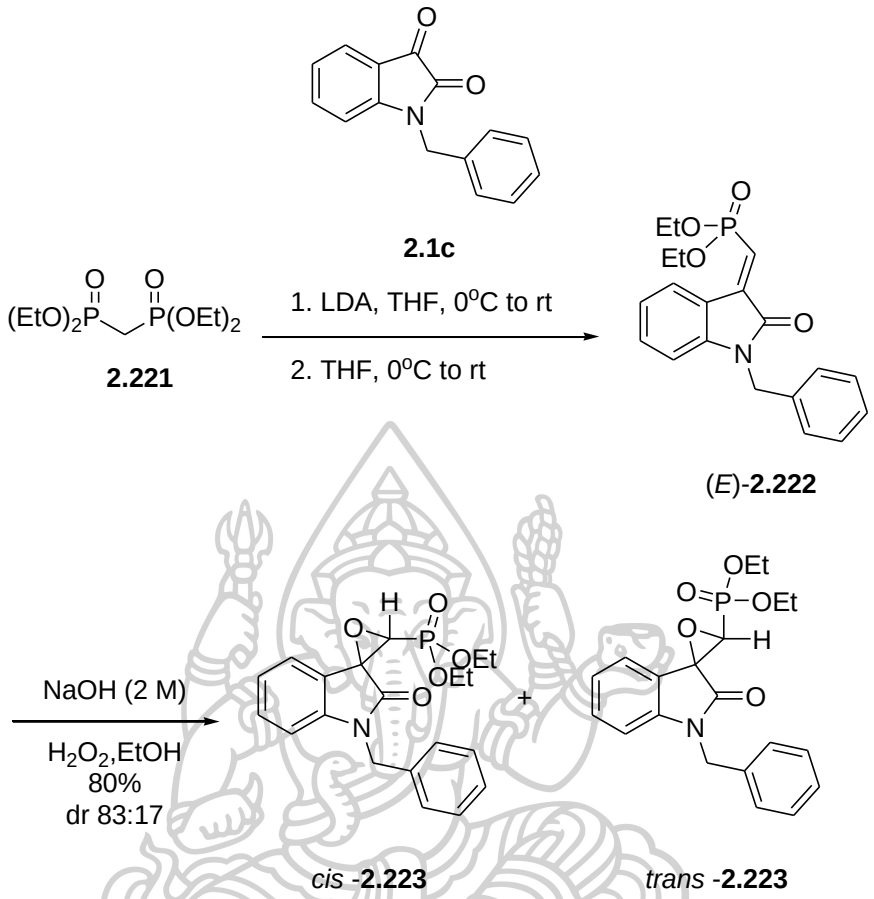

Scheme 83 Wadsworth-Emmons reaction and epoxidation for synthesis spirooxindole

The reactions of diarylketene **2.225** generated from diarylethanone **2.224**. The Staudinger ketene-imine cycloaddition of 3-alkylimino-*N*-methylindolin-2-one **2.7** with diarylketene **2.225** for 6 h gave four membered ring of spirooxindole compound **2.226** in 66% yield (Scheme 84) (77).

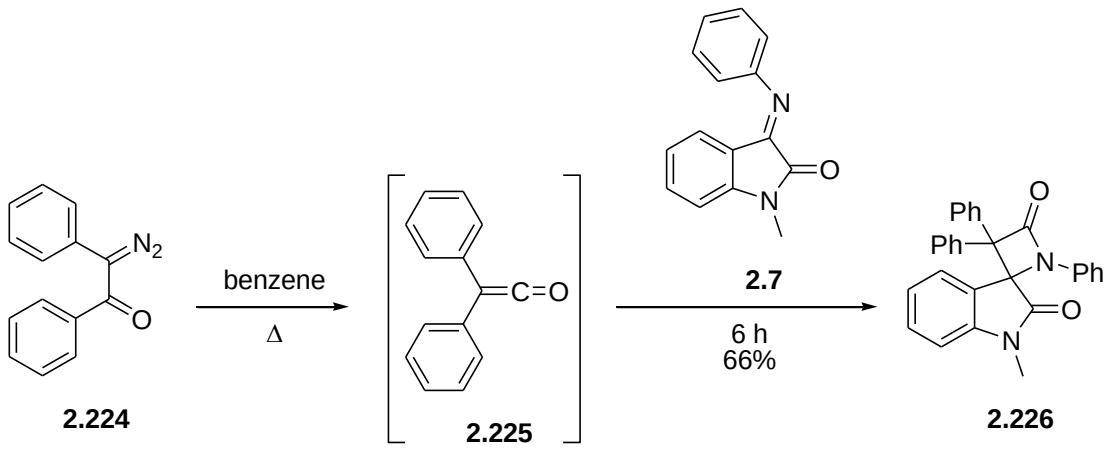

Scheme 84 Staudinger ketene-imine cycloaddition for synthesis four membered ring of spirooxindole

The reactions of *N*-benzyl isatin **2.1c** with 2,4-dimethoxybenzenamine generated 1-benzylindolin-2-one compound **2.229**. The Staudinger ketene-imine cycloaddition of 1-benzylindolin-2-one compound **2.229** with 2-phenoxyacetyl chloride in dichloromethane for 15 h gave four membered ring of spirooxindole **2.230** in 71% yield (Scheme 85) (78).

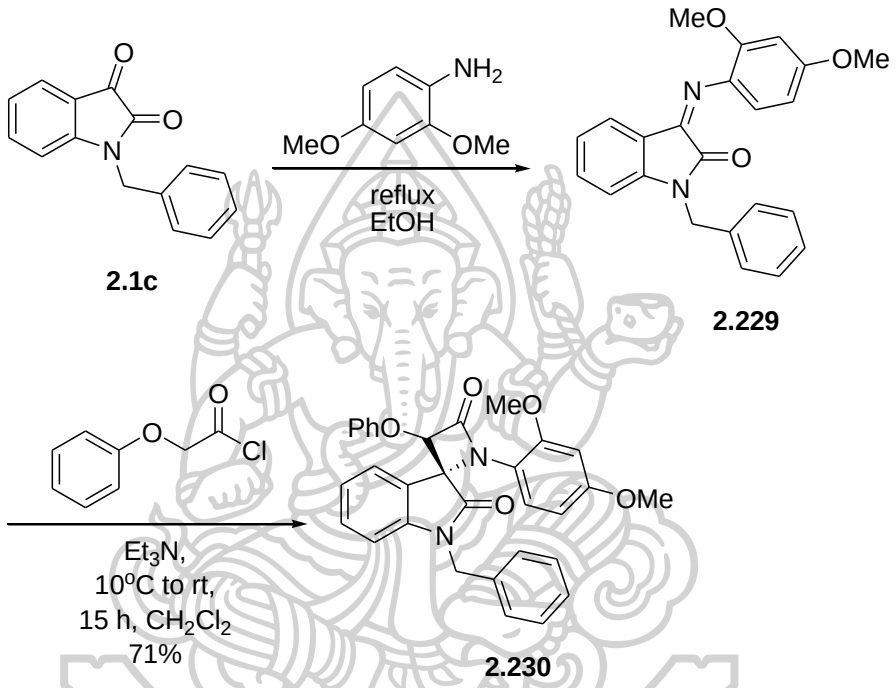

Scheme 85 Staudinger ketene-imine cycloaddition for synthesis four membered ring of spirooxindole

The Staudinger ketene-imine cycloaddition of isatin-3-semicarbazone **2.231** with chloroacetyl chloride in the presence of triethylamine gave four membered ring of spirooxindole **2.232** in 62% yield (Scheme 86) (79).

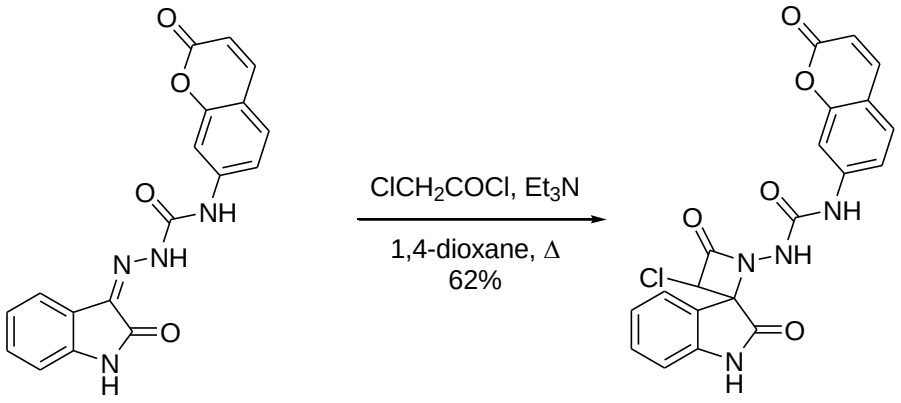

Scheme 86 Staudinger ketene-imine cycloaddition for synthesis four membered ring of spiroazetidinone-oxindole

Reactions for the synthesis of the spiro[pyrrolidine-3,3´-oxindole]

Intramolecular Mannich reaction

In environment, Rhynchophylline occur pairs of interconvertible isomer as Isorhynchophylline which explained by isomerization mechanism, where both natural product can be equilibrated through ring-opened intermediate **3.7** via retro-Mannich reaction (Scheme 87) (80).

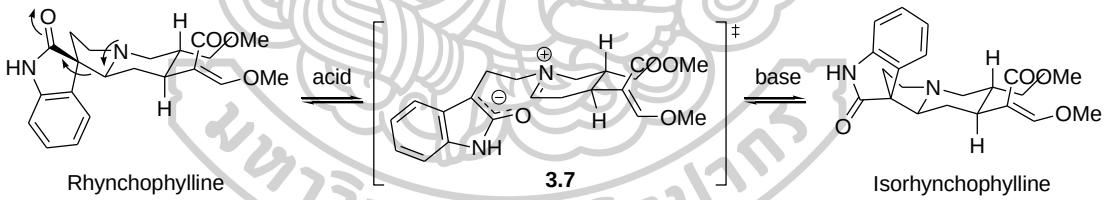

Scheme 87 Isomerization of Rhynchophylline and Isorhynchophylline via intramolecular Mannich reaction

In synthetic (±)-salacin is natural products which spirooxindole core structure **3.11** can be synthesized through intramolecular Mannich reaction as key reaction. Condensation of oxytryptamine hydrochloride **3.9** with acetal **3.10** followed by intramolecular Mannich reaction afforded spiro[pyrrolidine-3,3´-oxindole] **3.11** (Scheme 88) (81).

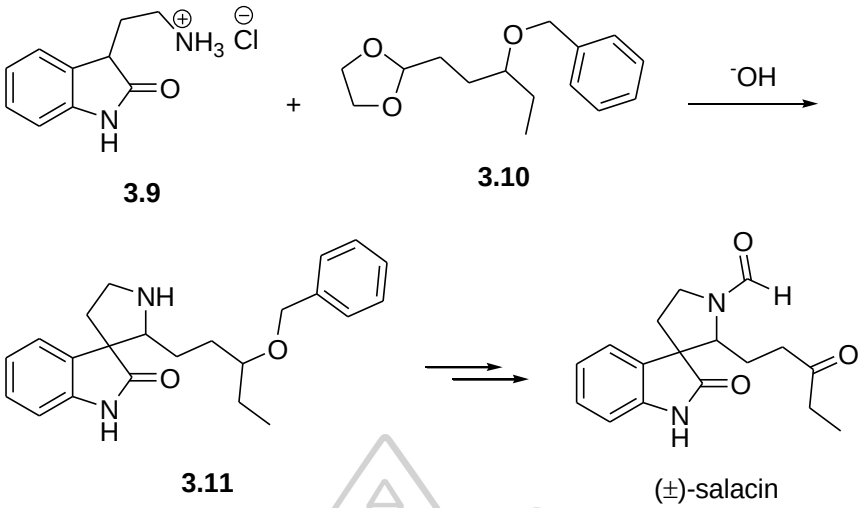

Scheme 88 Intramolecular Mannich reaction for synthesis spiro[pyrrolidine-3,3′-oxindoles] core structure of (±)-Salacin

Publication of Laronze and coworker, tryptamine-oxindole **3.13** synthesized from tryptamine derivative **3.12** via oxidation reaction. The spirocyclization of tryptamine-oxindole **3.13** with formaldehyde in acetic acid through an intramolecular Mannich reaction of intermediate **3.13a** generated (±)-horsfiline which is a natural product in 35% yield over 2 steps (Scheme 89) (82).

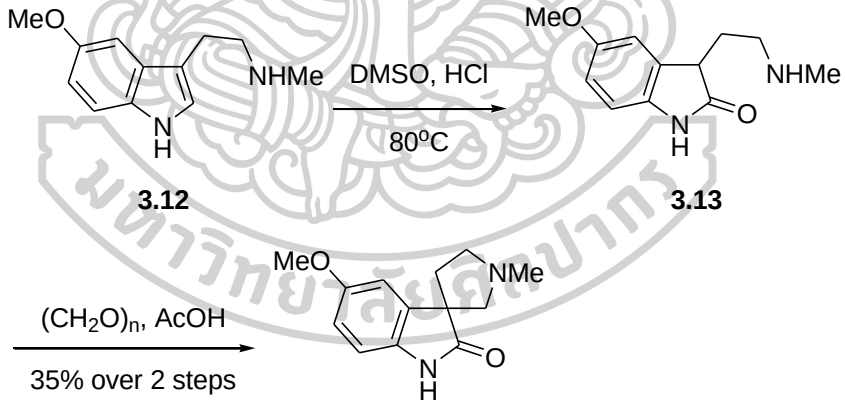

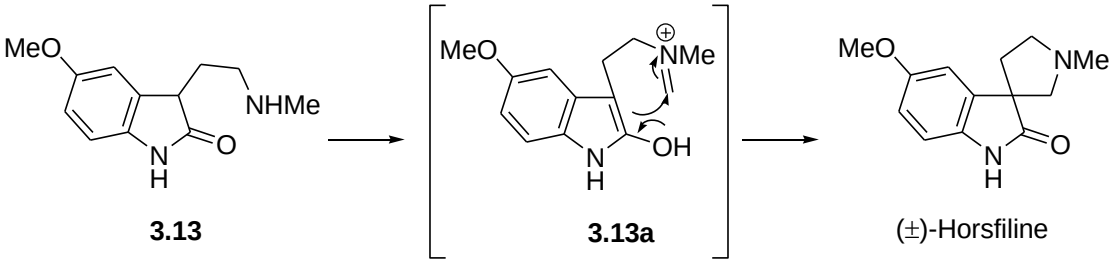

Scheme 89 Intramolecular Mannich reaction for the synthesis of the oxindole alkaloid: (±)-Horsfiline

Publication of Danishefsky and coworker, intramolecular Mannich reaction of oxindole **3.14** with 3-methylbut-2-enal **3.15** using triethylamine in pyridine synthesized a mixture of diastereoisomeric spiro[pyrrolidine3,3´-oxindole] compound **3.16** in 73% yield to separate in late stage for the synthesis Spirotryprostatin B (Scheme 90) (83).

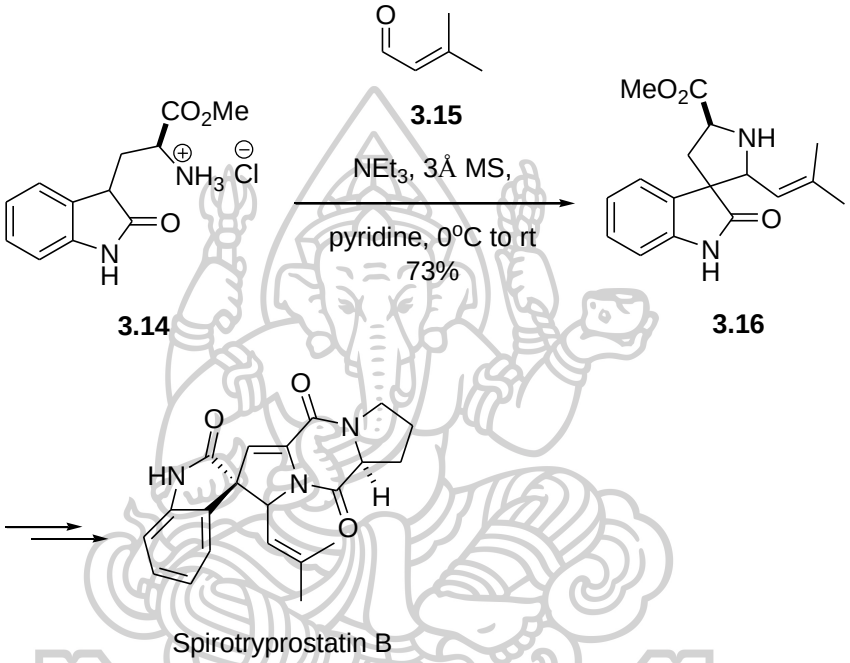

Scheme 90 Intramolecular Mannich reaction for the synthesis of the oxindole alkaloid: Spirotryprostatin B

Oxidative rearrangement sequences

The most widely used method for construction the spiroindolizidine-oxindole ring system using the oxidative rearrangement of tetrahydro-*β*-carboline. Tetrahydro-*β*-carbolines are suitably available from tryptamine derivatives by Pictet Spengler reaction. Reaction of tetrahydro-*β*-carbolin with suitable oxidant followed by a hydroxide source results in oxidative rearrangement of the spiroindolizidine-oxindole as shown in scheme 91 (84).

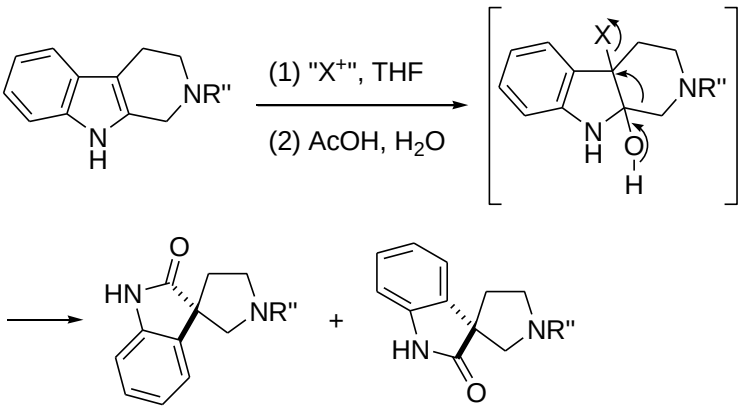

Scheme 91 Oxidative rearrangement of tetrahydro-*β*-carboline

Halogenating agents as oxidants for oxidative rearrangement sequences

Publication of John Shavel and Harold, Zinnes, oxidative rearrangement of indoloquinoizidinone **4.1** in the presence of *tert*-butyl hypochloride as oxidant followed by addition of silver perchlorate to rearrangement of the chloroindolenine synthesized spiro[pyrrolidine-3,3´-oxindole] compound **4.2** in 87% yield and led to Pteropodine (Scheme 92) (85).

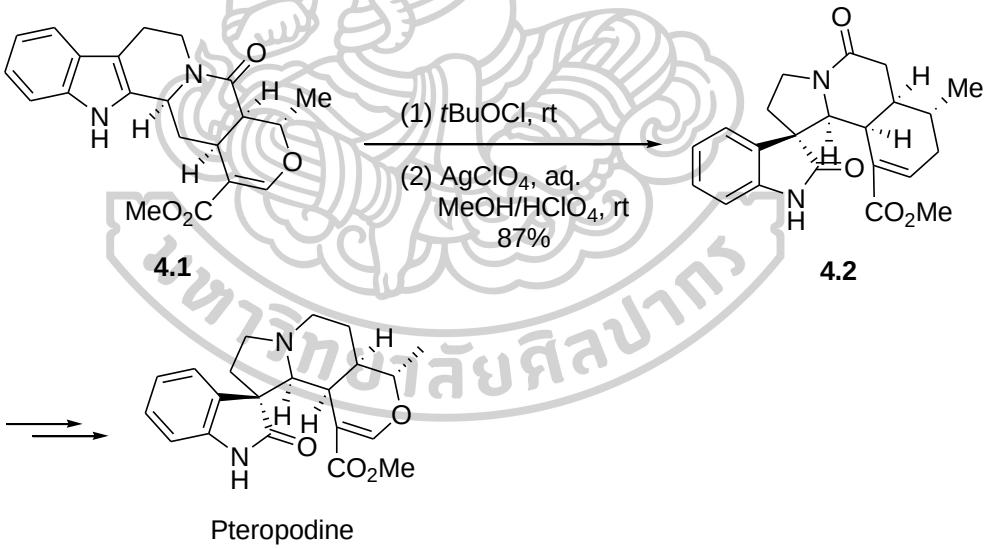

Scheme 92 Oxidative rearrangement using *tert*-butyl hypochloride for synthesis Pteropodine

For the synthesis of *N*-Boc tetrahydro-*β*-carboline **4.4** and *N*-methyl tetrahydro-*β*-carboline **4.6** are derived from indole compound **4.3**. Oxidative rearrangement of *N*-Boc tetrahydro-*β*-carboline **4.4** and *N*-methyl tetrahydro-*β*-carboline **4.6** using *N*-bromosuccinimide (NBS) as oxidant and acetic acid in mixture of tetrahydrofuran with water afforded spiro[pyrrolidine-3,3´-oxindole] compound **4.5** in 77% yield from *N*-Boc derivative **4.4**, and spiro[pyrrolidine-3,3´-oxindole]

compound **4.7** in 50% yield from the *N*-methyl derivative **4.6**. In the late step, (-)-Horsfiline synthesized from spiro[pyrrolidine-3,3´-oxindole] compound **4.5**. (+)-Horsfiline produced from spiro[pyrrolidine-3,3´-oxindole] compound **4.7** (Scheme 93) (86).

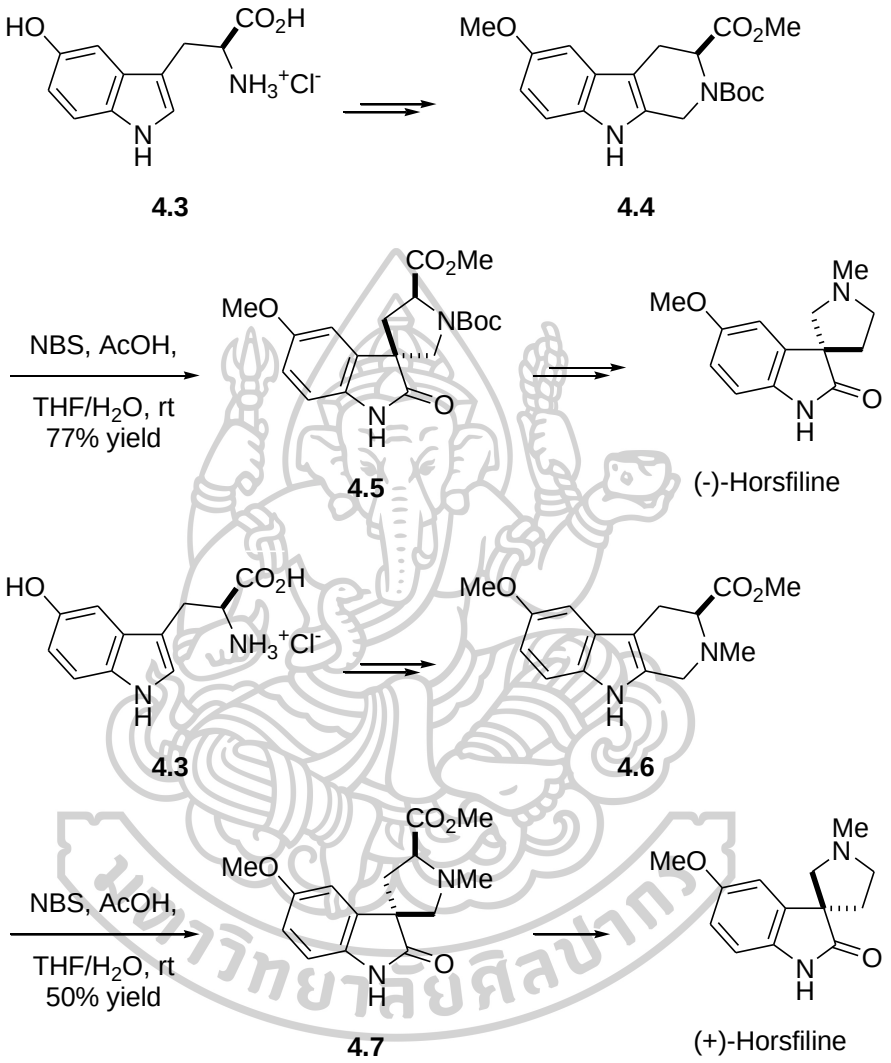

Scheme 93 Oxidative rearrangement reaction using *N*-bromosuccinimide (NBS) for synthesis of (-)-Horsfiline and (+)-Horsfiline

Publication of Danishefsky and coworker, oxidative rearrangement reaction of *N*-Boc tetrahydro-*β*-carboline **4.8** using *N*-bromosuccinimide (NBS) as oxidant and acetic acid in mixture of tetrahydrofuran with water synthesized spiro[pyrrolidine-3,3´-oxindole] compound **4.9** in 46% yield. Spirotryprostatin A was obtained by deprotection and coupling raction with *N*-Troc-L-proline of spiro[pyrrolidine-3,3´-oxindole] compound **4.9** (Scheme 94) (87).

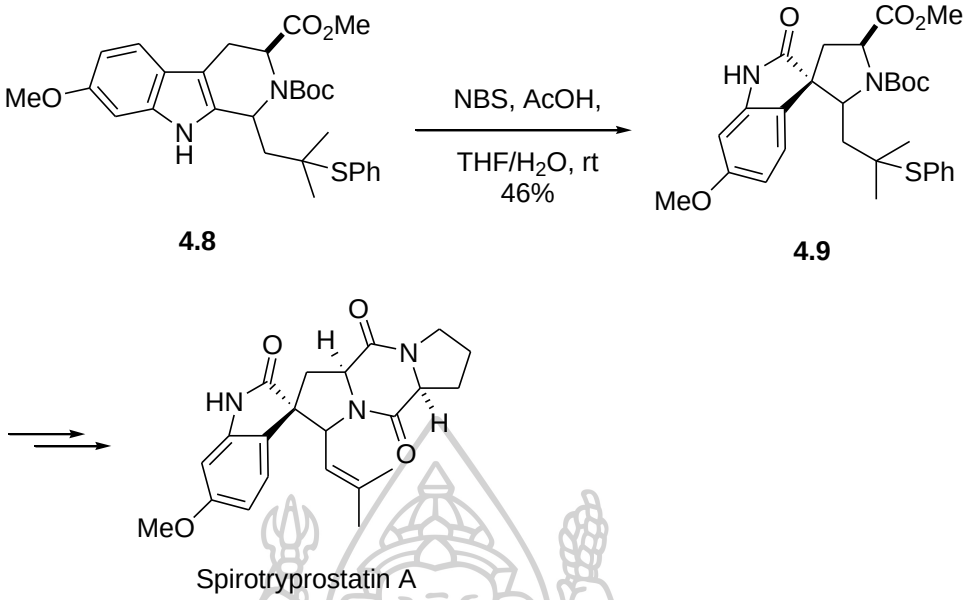

Scheme 94 Oxidative rearrangement reaction using *N*-bromosuccinimide (NBS) for synthesis of Spirotryprostatin A

Publication of Ganesan and coworker, oxidative rearrangement reaction of *N*-Fmoc-L-proline tetrahydro-*β*-carboline compound **4.10** using *N*-bromosuccinimide (NBS) as oxidant and acetic acid in mixture of tetrahydrofuran with water generated spiro[pyrrolidine-3,3′-oxindole] compound **4.11** in 68% yield. Spirotryprostatin B was obtained by deprotection and cyclization of spiro[pyrrolidine-3,3′-oxindole] compound **4.11** (Scheme 95) (88).

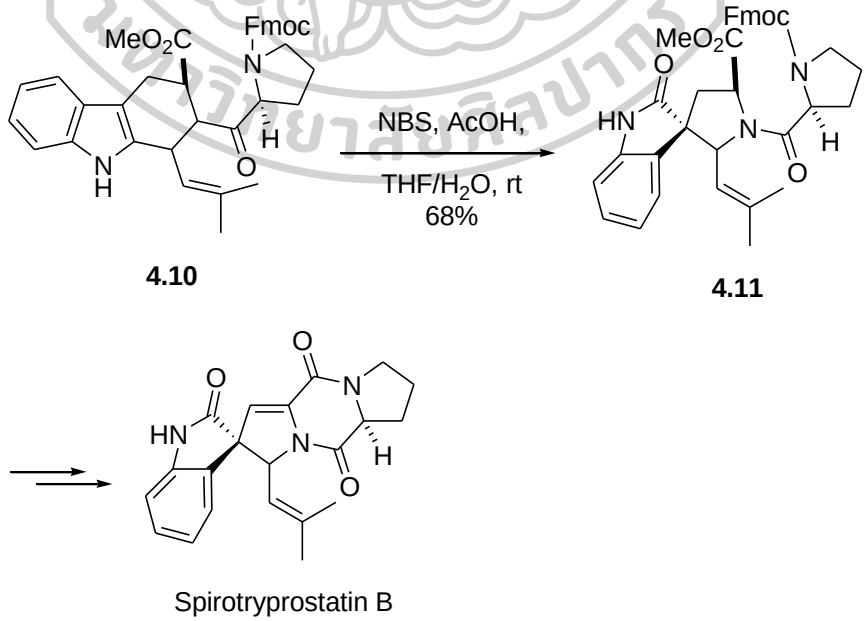

Scheme 95 Oxidative rearrangement reaction using *N*-bromosuccinimide (NBS) for synthesis of Spirotryprostatin B

Sodium tungstate as oxidants for oxidative rearrangement sequences

Oxidation reaction of hexahydro-*β*-carboline compound **4.12** in the presence of sodium tungstate and urea/hydrogen peroxide as oxidant gave *N*-hydroxy-tetrahydro-*β*-carboline compound **4.13** in 69% yield. The reaction of *N*-hydroxy-tetrahydro-*β*-carboline compound **4.13** using aqueous HCl in methanol through chloroindolenine, which rearrangement to give spiro[pyrrolidine-3,3´-oxindoles] compound **4.14** in 91% yield (Scheme 96) (89).

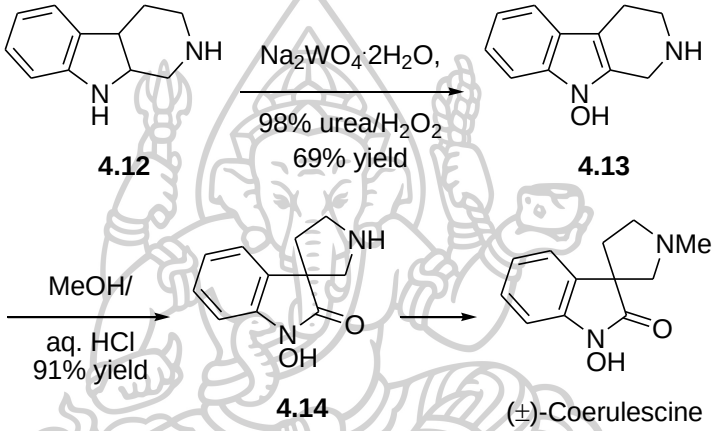

Scheme 96 The two step oxidative rearrangement reaction using sodium tungstate for synthesis of (±)-Coerulescine

Lead tetraacetate as oxidants for oxidative rearrangement sequences

Oxidative rearrangement reaction of tetrahydro-*β*-carbolines compound **4.15** in the presence of lead tetraacetate and methanol/water/acetic acid gave (±)-Horsfiline in 30% yield (Scheme 97) (90) (91).

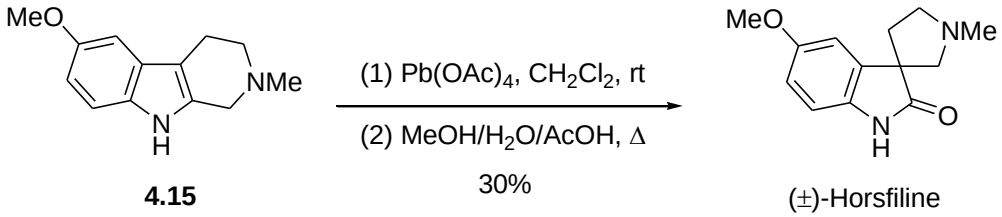

Scheme 97 Oxidative rearrangement reaction using lead tetraacetate for synthesis of (±)-Horsfiline

Osmium tetroxide as oxidants for oxidative rearrangement sequences

Publication of Cook and coworker, the keto acetal compound **4.17** achieved from olefin compound **4.16**. Oxidative rearrangement of hexahydro-*β*-carboline compound **4.17** in the presence of osmium tetroxide as oxidant and pyridine in tetrahydrofuran which osmium atom complexed to nitrogen atom of pyridine and then dihydroxylation followed intramolecular from one face to give spiro[pyrrolidine-3,3´-oxindole] compound **4.18** in 81% yield. Deprotection of the nitrogen atom followed by base-induced elimination of methanol of spiro[pyrrolidine-3,3´-oxindole] compound **4.18** synthesized Alstonisine (Scheme 98) (92).

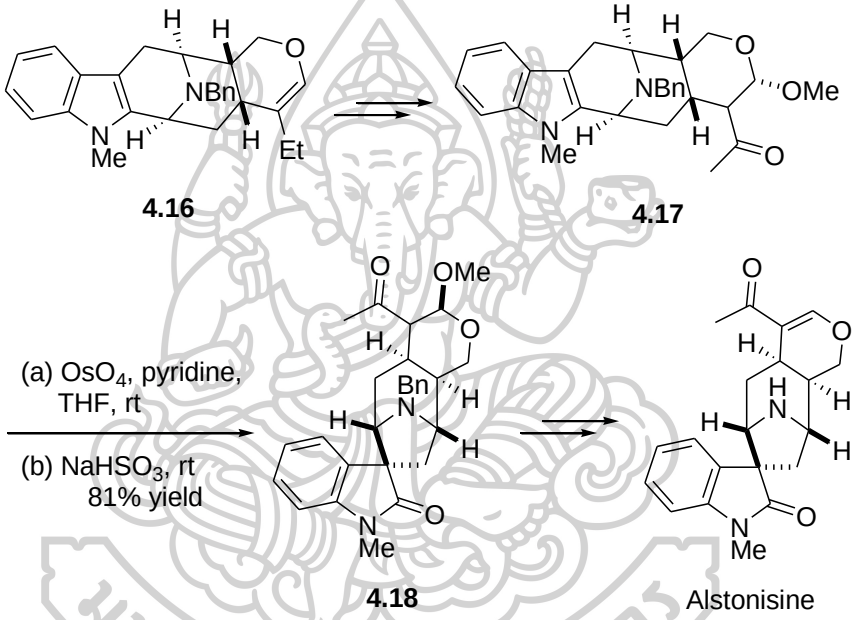

Scheme 98 Oxidative rearrangement reaction using osmium tetroxide for synthesis of Alstonisine

Dipolar cycloaddition reaction

Publication of Palmisano and coworker, the *N*-methylazomethine yilde compound was obtained from formaldehyde and sarcosine **4.39**. Dipolar cycloaddition reaction of dipolarophile **4.38** bearing a chiral auxiliary [R'=(-)-menthyl) with *N*-methylazomethine yilde compound generated spiro[pyrrolidine-3,3´-oxindole] compound **4.40** in 41% yield. Hydrolysis of the ester followed by formal decarboxylation afforded (-)-horsfiline.

Similarly condition, the *N*-methylazomethine yilde compound was obtained from formaldehyde and sarcosine **4.39**. The [2+3] cycloaddition of chiral auxiliaries aromatic acrylate **4.41** with *N*-methylazomethine yilde compound produced spiro[pyrrolidine-3,3´-oxindole] presursor **4.42** in 78% yield and 86% de. Cyclization of ester compound **4.42** synthesized (-)-horsfiline (Scheme 99) (93).

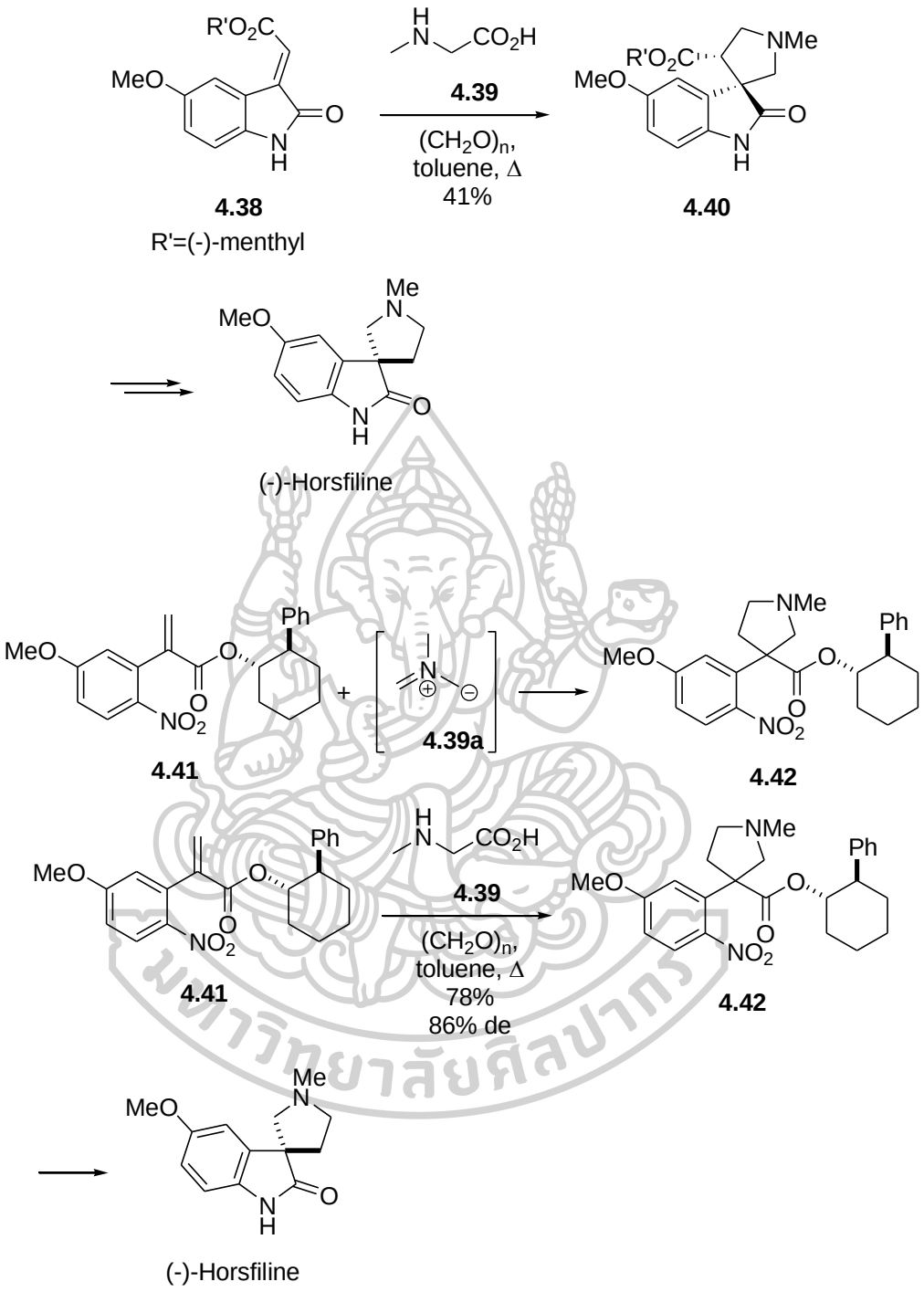

Scheme 99 Dipolar cycloaddition reaction for synthesis of (-)-Horsfiline

Publication of Williams and coworker, 1,3-dipolar cycloaddition reaction of chiral azomethine ylide **4.44** with oxindole compound **4.43** generated spiro[pyrrolidine-3,3′-oxindole] compound **4.45** in 82% yield. Spirotryprostatin B was obtained from spiro[pyrrolidine-3,3′-oxindole] compound **4.45** (Scheme 100) (94).

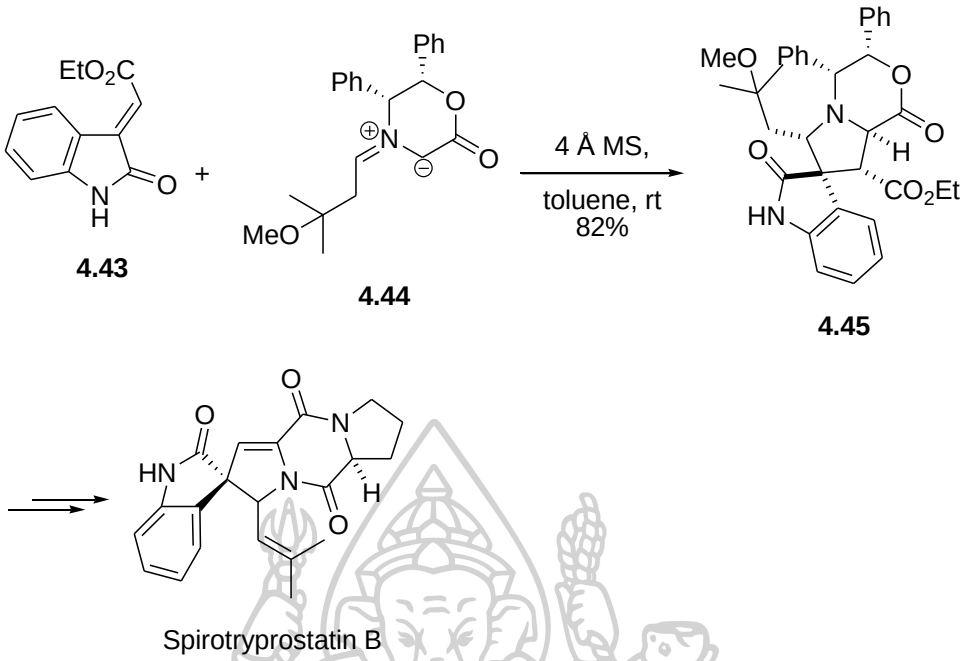

Scheme 100 The 1, 3-dipolar cycloaddition reaction for synthesis of Spirotryprostatin B

Radical cyclization reaction

Publication of Jones and Wilkinson, radical cyclization reaction of amide compound **4.46** in the presence of tributyltin hydride (Bu_3SnH) and azobisisobutyronitrile (AIBN) in toluene generated spiro[pyrrolidine-3,3´-oxindole] compound **4.47** in 70% yield. Deprotection of spiro[pyrrolidine-3,3´-oxindole] compound **4.47** followed by methylation afforded (±)-Horsfiline (Scheme 101) (95).

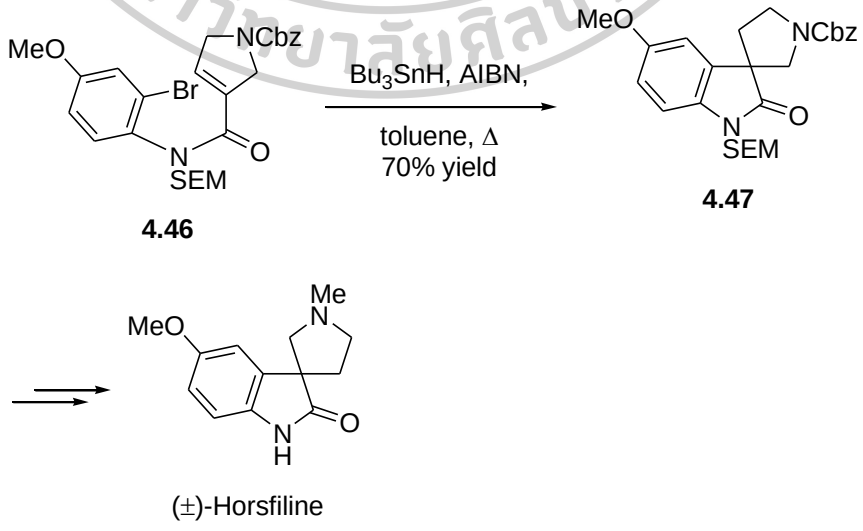

Scheme 101 Radical cyclization reaction for synthesis of (±)-Horsfiline

Publication of Murphy and coworker, aryl iodoazide tandem radical cyclization of azide compound **4.48** in the presence of tris(trimethylsilyl)silane (TTMSS) and azobisisobutyronitrile (AIBN) in benzene gave spiro[pyrrolidine-3,3´-oxindole] compound **4.49** followed by methylation and deprotection of the indole nitrogen atom synthesized (±)-Horsfiline in 60% yield over 2 steps (Scheme 102) (96).

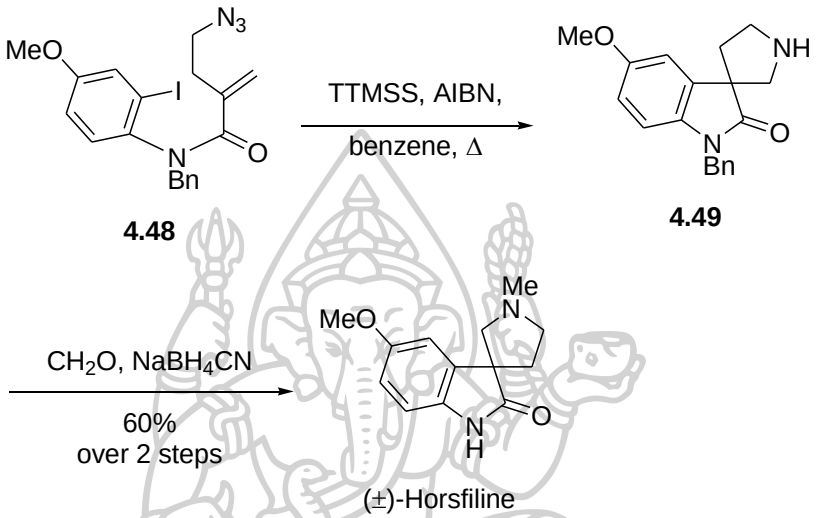

Scheme 102 Radical cyclization reaction using tris(trimethylsilyl)silane for synthesis of (±)-Horsfiline

Intramolecular Heck reaction

One-pot Heck reaction/η^3-allylpalladium trapping of triene cyclization substrate **4.50** using Tris(dibenzylideneacetone)dipalladium(0)-chloroform adduct ($[Pd_2(dba)_3]\cdot CHCl_3$), tri-*o*-tolylphosphane and excess potassium acetate in THF at 70°C through η^3-allylpalladium intermediate gave spiro[pyrrolidine-3,3´-oxindole] compound **4.51** in 36% yield. Deprotection of the indole nitrogen atom synthesized Spirotryprostatin B (Scheme 103) (97).

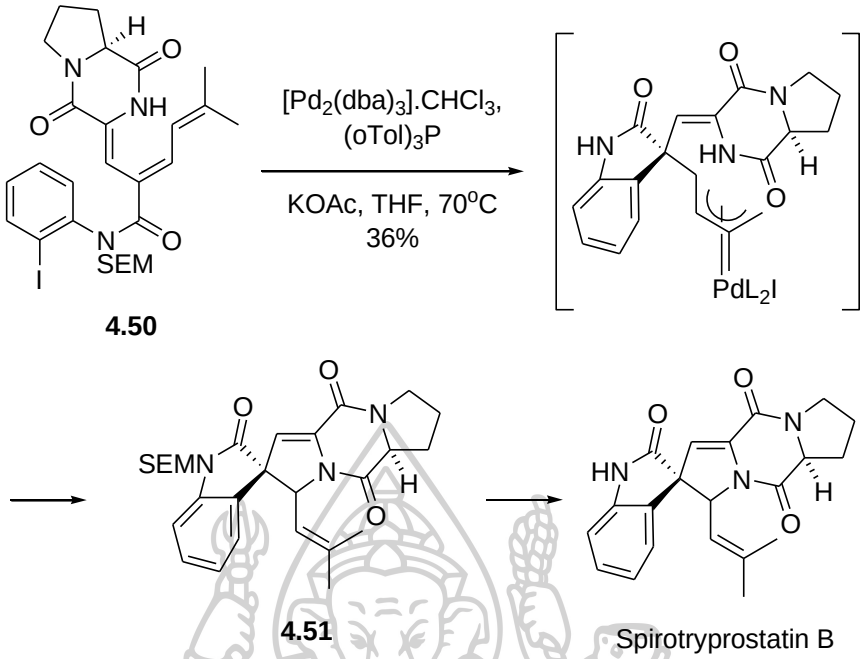

Scheme 103 Intramolecular Heck reaction for synthesis of Spirotryprostatin B

Magnesium iodide catalysed ring-expansion reaction

Magnesium iodide catalysed ring-expansion reaction of cyclopropane compound **4.66** with aldimine **4.62** in the presence of a catalytic amount (10 mol%) of magnesium iodide (MgI_2) acts as a bifunctional catalyst which both the Lewis metal center (Mg^{2+}) and the nucleophilic counter ion (I^-) gave 79:21 as diastereomeric ratio of spiro[pyrrolidine-3,3′-oxindole] compound **4.67a** and **4.67b** in 99% yield (Scheme 104) (98).

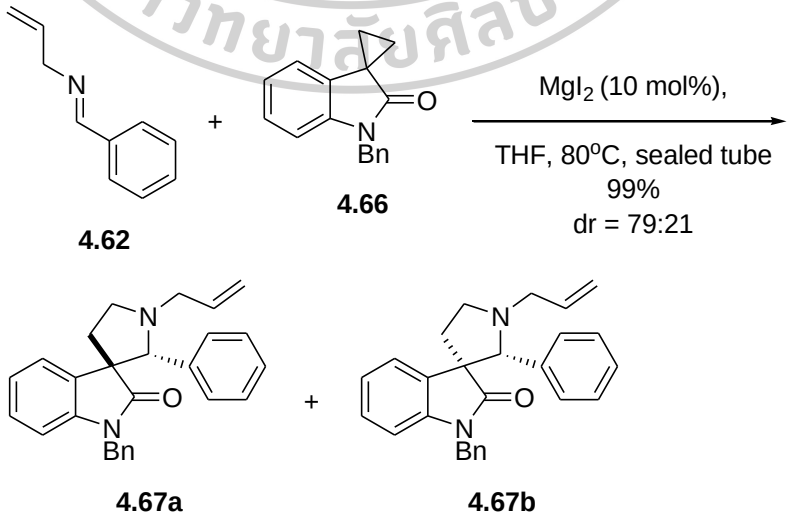

Scheme 104 The magnesium iodide catalysed ring-expansion reaction for synthesis of spiro[pyrrolidine-3,3´-oxindole]

The two possible pathway mechanism for magnesium iodide catalysed ring-expansion reaction of synthesis spiro[pyrrolidine-3,3´-oxindole] compound. Cyclopropane compound **4.61** opened by iodide anion to give enolate ion **4.63** followed by nucleophilic imine attack enolate intermediate **4.63** generated enolate intermediate **4.64**. The spiro[pyrrolidine-3,3´-oxindole] **4.60** was obtained by cyclization of iminium intermediate of enolate intermediate **4.64** to show in pathway 1.

The imine compound **4.62** was more electrophilic. The reaction between enolate intermediate **4.63** and imine compound **4.62** gave nitrogen anion intermediate **4.65**. *N*-alkylation of nitrogen anion intermediate **4.65** synthesized spiro[pyrrolidine-3,3´-oxindole] **4.60** to show in pathway 2 (Scheme 105) [98].

Pathway 1 for magnesium iodide catalysed ring-expansion reaction

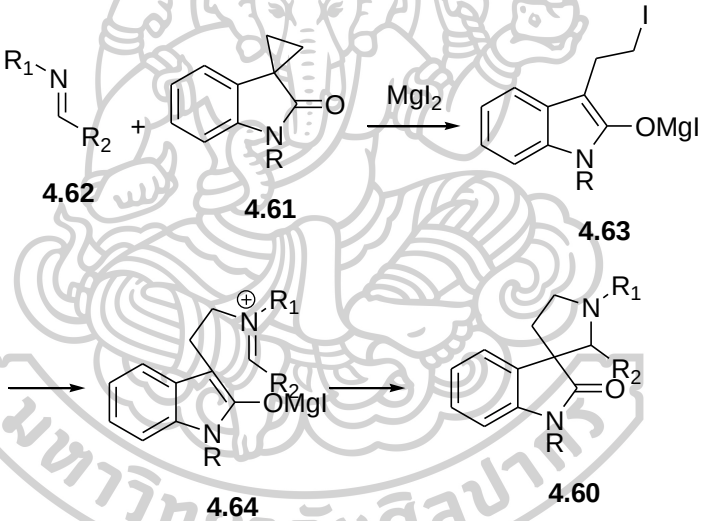

Pathway 2 for magnesium iodide catalysed ring-expansion reaction

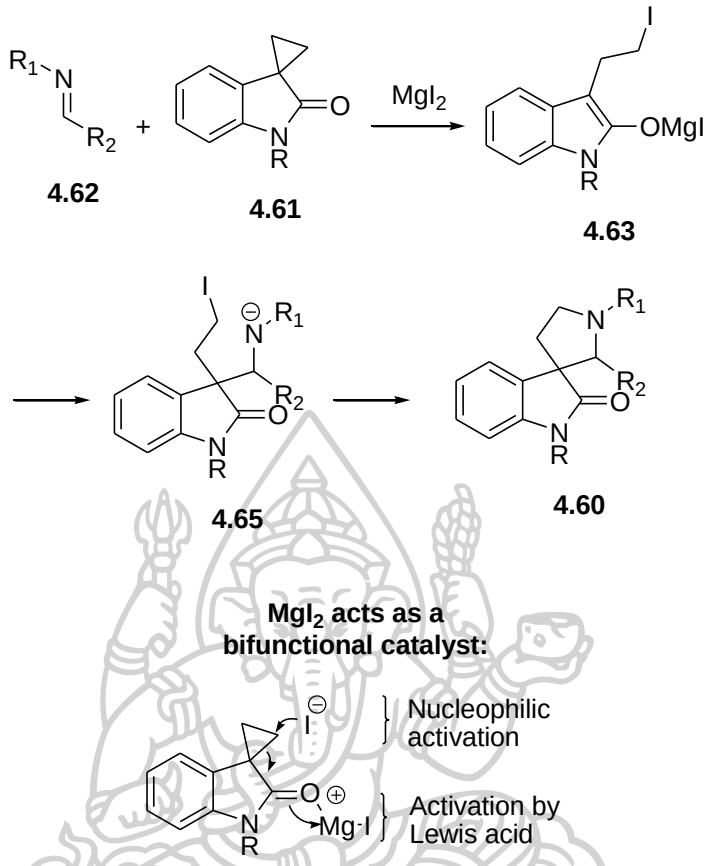

Scheme 105 Proposed mechanism of magnesium iodide catalysed ring-expansion reaction for synthesis of spiro[pyrrolidine-3,3´-oxindole]

The spiroindolizidine-oxindole and indoloquinolizidine in nature and their biological activities

The spirooxindole core structures are oxindole with spiro-fused to other cyclic frameworks. Spirooxindole compound have attracted great interest from researchers in synthetic organic chemistry and medical chemistry all over the world. Spirooxindole core structure occurs in many natural products such as rhynchophylline, isorhynchophylline, Pteropodine, Spirotryprostatin A, Spirotryprostatin B, Mitraphylline, Elacomine, (±)-Horsfiline, (±)-Coerulescine, Marcfortine A, Surugatoxin, Alstonisine and Formosanine (Figure 19).

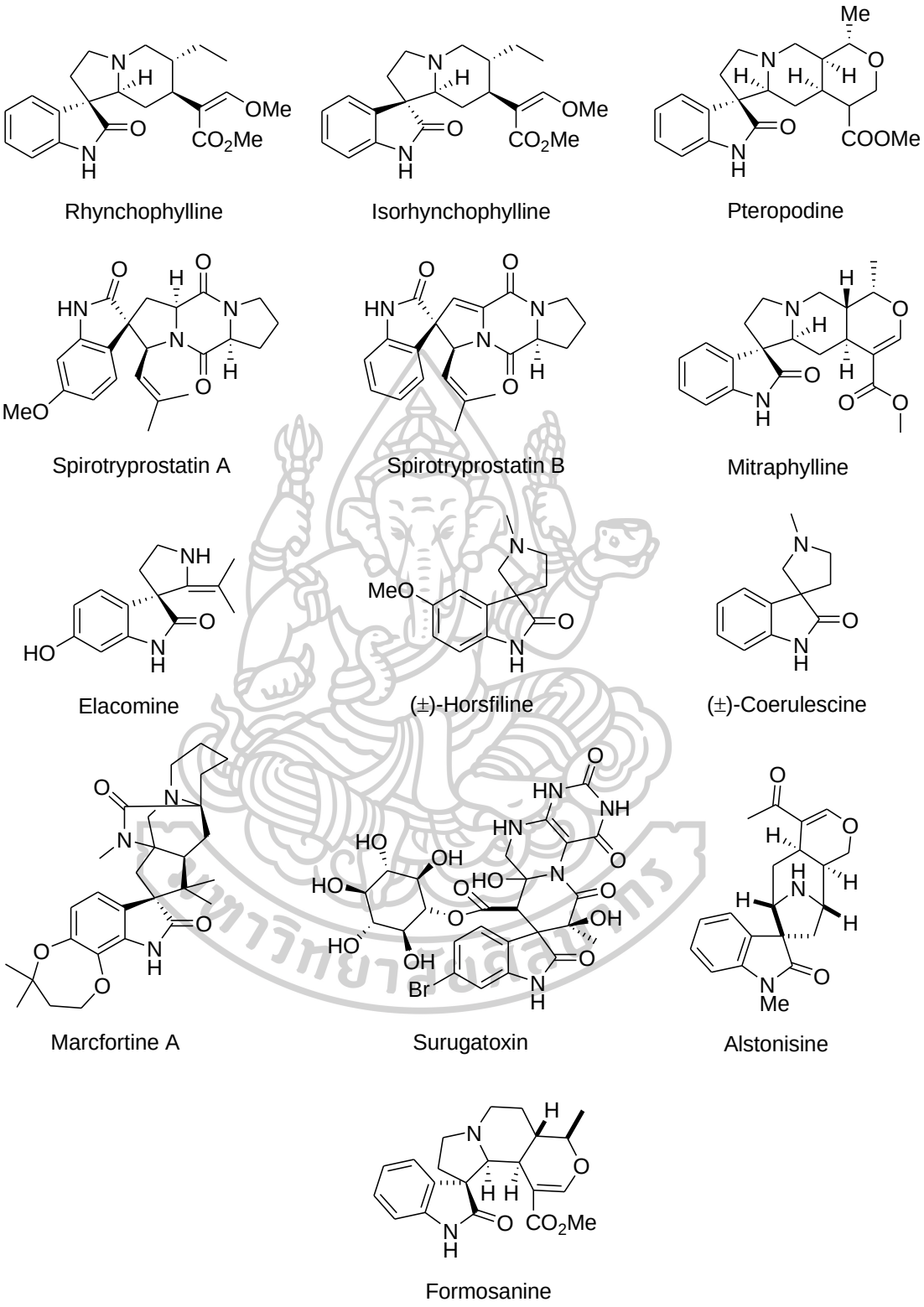

Figure 19 Structure of natural product with spirooxindole compound

Structurally diverse compounds of spirooxindole are useful in the treatment of diseases that are used in a variety of medical. Spirooxindole compound have been modified to provide high bioactivity which suitable for treatment with diseases such as such as progesterone receptor agonist, MDM2-p53 interaction inhibitor, M. tuberculosis inhibitor, Inhibitor at the vanilloid receptor1, antimalarial, CR TH2 receptor antagonist, Satavaptan and MI-63 MDM2 inhibitor (Figure 20) (99), (100).

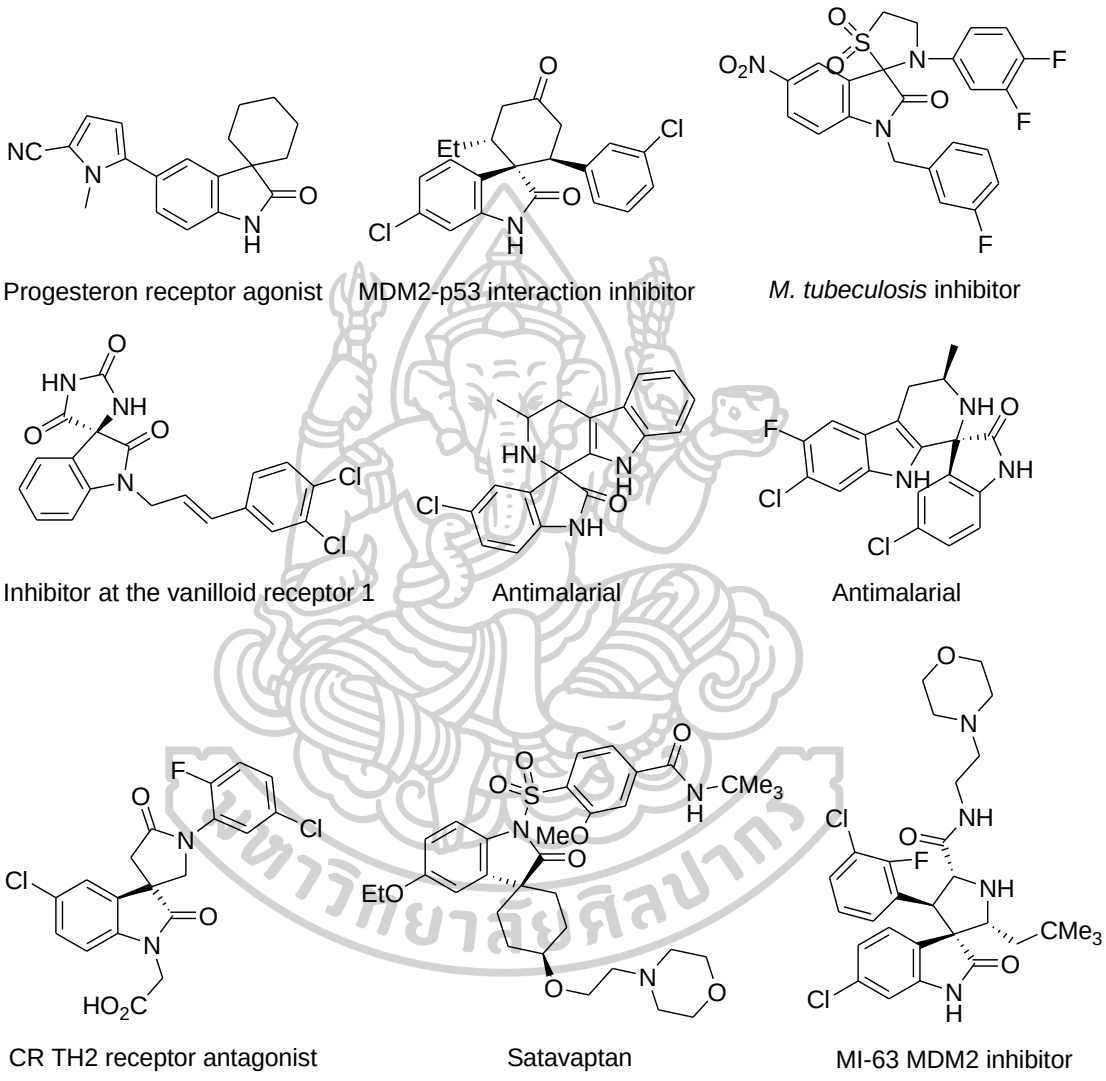

Figure 20 Important biologically activity of spirooxindole core structure compounds

The Rhynchophylline, Isorhynchophylline and Hirsutine are found in *Mitragyna speciosa* (kratom) (Figure 21) which is a plant that has been used in traditional medicine in southeastern Asia, Africa and South America. The purification of rhynchophylline from *Mitragyna speciosa* (kratom) has significantly helped the investigation into the therapeutic applications. Rhynchophylline used for the treatment of acts on cardiovascular and central nervous system diseases, including hypertension, bradycardia, arrhythmia, sedation, vascular dementia, epileptic seizures, drug addiction, and cerebralischemia. Moreover, this alkaloid has been found to protect

against glutamate-induced death in cultured cerebellar granule cell. Rhynchophylline has properties on anticoagulation, inhibits vasculars mooth muscle cell proliferation. Rhynchophylline has shown anti-endotoxemic. Rhynchophylline is a candidate drug for several cardiovascular and central nervous system diseases. Rhynchophylline will interest organic chemist to pursue the potential pharmacological effects and mechanisms with medical benefits. Thus, more information in vivo validations and investigations of antihypertensive and neuroprotective mechanisms of Rhynchophylline are necessary. The Rhynchophylline consist of four chiral center of spiroindolizidine-oxindole compound. The isorhynchophylline is diastereomer of Rhynchophylline (Figure 21) (101).

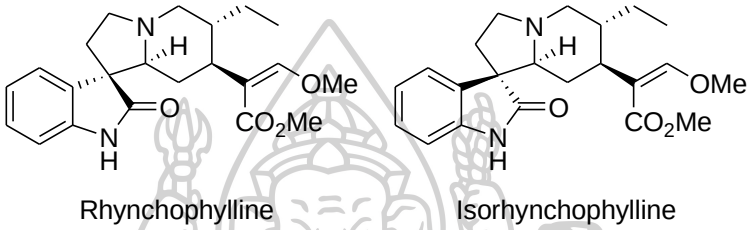

Figure 21 The structures of Rhynchophylline and Isorhynchophylline

Figure 22 *Mitragyna speciosa* (kratom)

An alkaloid compound extracted from the *Mitragyna speciosa* (kratom) (Figure 22) contains Rhynchophylline, Isorhynchophylline, Hirsutine, Hirsuteine, Corynantheine, Dihydrocorynantheine, Isocorynoxeine, Akuammigine and Geissoschizine methyl ether (Figure 23). Extracted from *Mitragyna speciosa* (kratom)

contains the main alkaloid compounds such as Rhynchophylline and Isorhynchophylline.

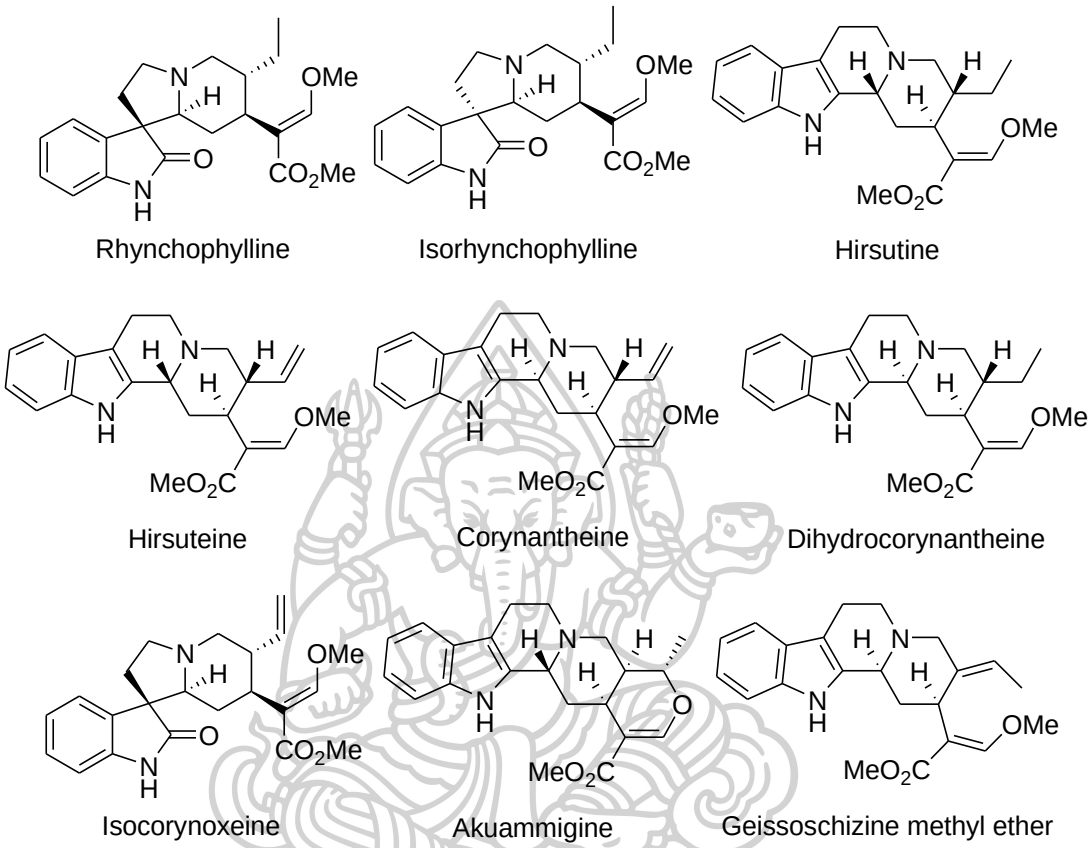

Figure 23 shows the structure of the natural product of Rhynchophylline, Isorhynchophylline, Hirsutine, Hirsuteine, Corynantheine, Dihydrocorynantheine, Isocorynoxeine, Akuammigine and Geissoschizine methyl ether

Diabetes is a chronic disease that is considered a serious disease caused by pancreas does not produce enough insulin (hormones that control blood glucose levels) or as a result of the body's inability to work properly with insulin. Glucose absorption disorders are common causes of diabetes. Diabetes is recognized as a severe global health problem characterized by high blood sugar levels. According to the Diabetes Association of Thailand were more than 4.4 million people living with diabetes disease in 2017. The Thai population aged 60-69 years is the most diabetic. Diabetes leads to serious consequences for the development of coronary heart disease, liver damage, retinal disease, kidney disease, cerebrovascular disease and peripheral kidney disease. Type II diabetes is more common among people with diabetes. Inhibition of α-glucosidase during the digestion of starch is helps control post-prandial hyperglycemia. The α-glucosidase are key enzymes involve in the breakdown and intestinal absorption of carbohydrates, respectively. The α-glucosidase inhibition blocks increased blood sugar levels after carbohydrate intake, an important strategy in the management of non-insulin-dependent diabetes mellitus

(NIDDM). Numerous chemical structures for antidiabetic drugs consisted Acarbose, Voglibose and Miglitol (Figure 24).

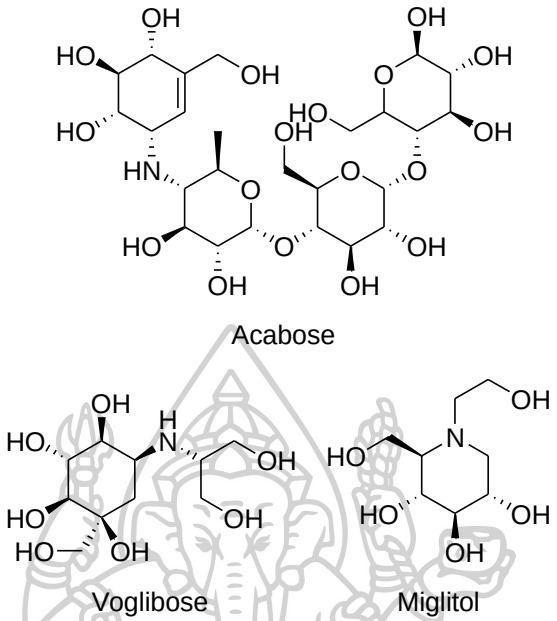

Figure 24 Chemical structures for antidiabetics drugs (Acarbose, Voglibose and Miglitol).

CHAPTER 2
LITERATURE REVIEW

Prior Synthetic Strategies for the Rhynchophylline and Isorhynchophylline

Ban's Total Synthesis of Alkaloids (±)-Rhynchophylline and (±)-Isorhynchophylline (1975)

Retrosynthetic analysis of Rhynchophylline was published by Yoshio Ban and coworker. Rhynchophylline was obtained by acid catalyzed isomerization from Isorhynchophylline. Isorhynchophylline was synthesized by methylation from enol compound **5.11**. The enol compound **5.11** could be synthesized from diester compound **5.7**. The diester compound **5.7** could be constructed from oxindole compound **5.3** with ethyl sodium formyl acetate **5.4** (Scheme 106) (102).

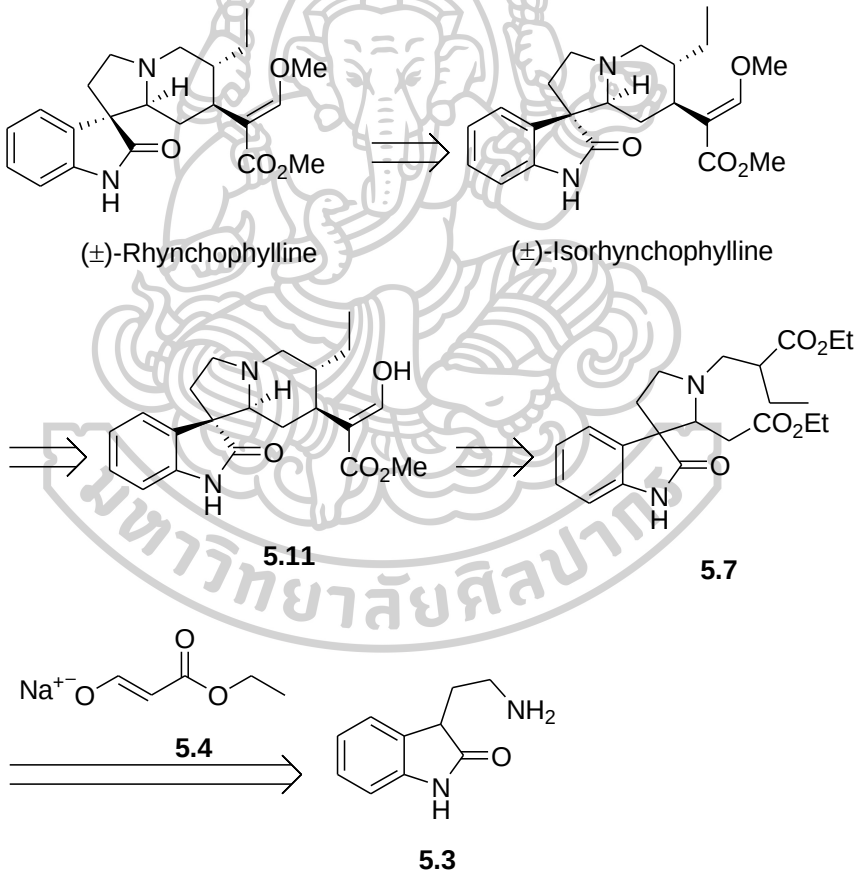

Scheme 106 Retrosynthetic analysis of Rhynchophylline by Yoshio Ban and coworker

Total synthesis of Rhynchophylline by Yoshio Ban and coworker which condensation of oxindole compound **5.3** with ethyl sodium formyl acetate **5.4** gave spiro compound **5.5** in 63% yield. Condensation followed by hydrogenation of spiro compound **5.5** generated diester compound **5.7** in 77% yield over two steps.

Dieckmann condensation of diester compound **5.7** synthesized ketone compound **5.8** in 60% yield. Horner–Wadsworth–Emmons olefination of ketone compound **5.8** gave ester compound **5.9** in 61% yield. Hydrogenation of ester compound **5.9** constructed diastereomer of ester compound **5.10b** and **5.10a** in 28% and 38% yield respectively. Condensation reaction of ester compound **5.10b** with ethyl formate gave enol compound **5.11** in 14% yield. Methylation reaction of formyl compound **5.11** generated Isorhynchophylline in 26% yield. Acid catalyzed isomerization of Isorhynchophylline afforded Rhynchophylline in 36% yield. Key reaction for the synthesis of Rhynchophylline was obtained by Horner–Wadsworth–Emmons olefination, Dieckmann condensation and acid catalyzed isomerization. The total synthesis of Rhynchophylline was achieved in 9 total steps, 9 steps in longest linear sequence, 0.065% overall yield of Rhynchophylline (Scheme 107).

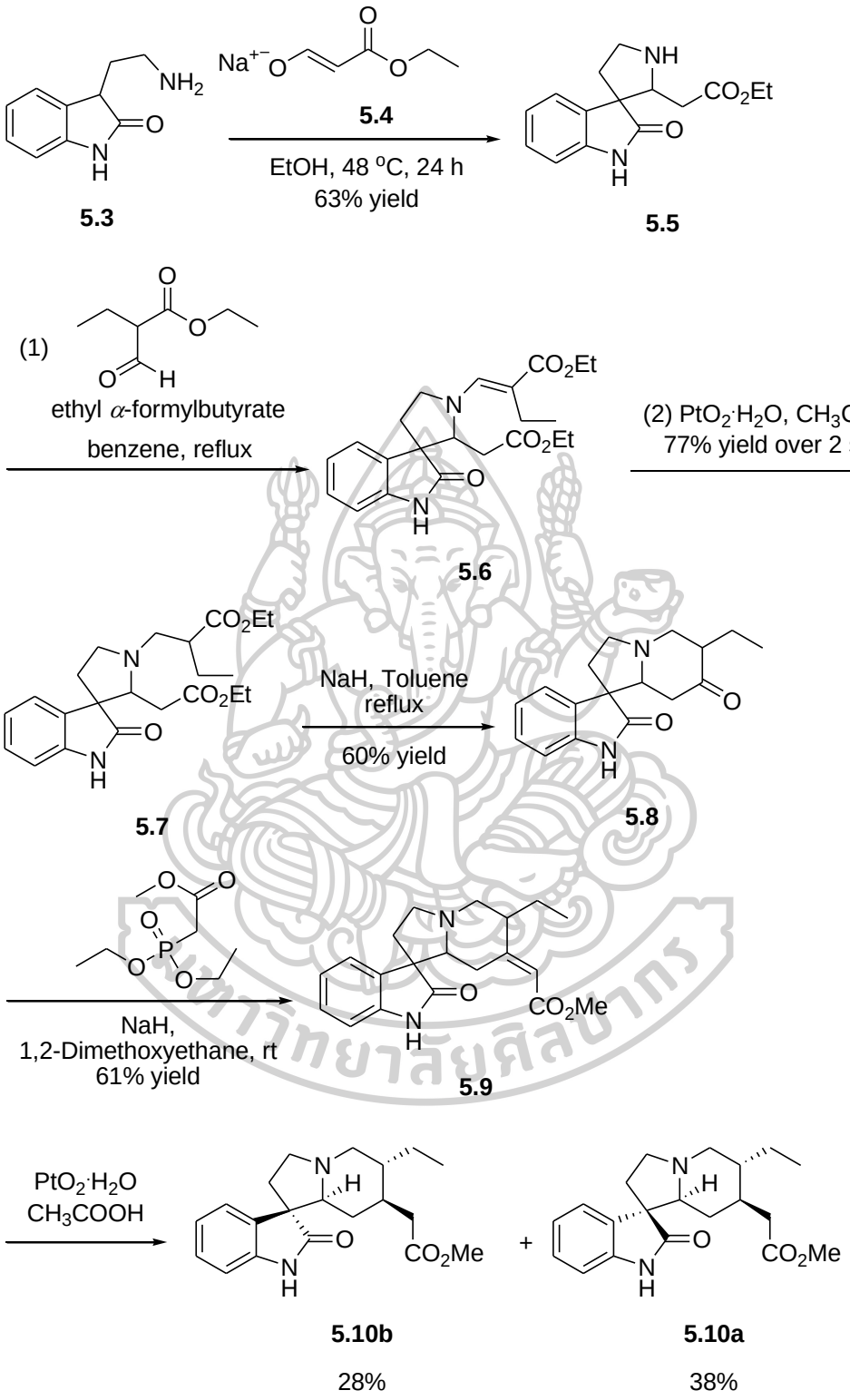
5.3
5.4
EtOH, 48 °C, 24 h
63% yield
5.5
(1)
ethyl α-formylbutyrate
benzene, reflux
5.6
(2) PtO2·H2O, CH3COOH
77% yield over 2 steps
5.7
NaH, Toluene
reflux
60% yield
5.8
NaH,
1,2-Dimethoxyethane, rt
61% yield
5.9
PtO2·H2O
CH3COOH
5.10b
28%
5.10a
38%

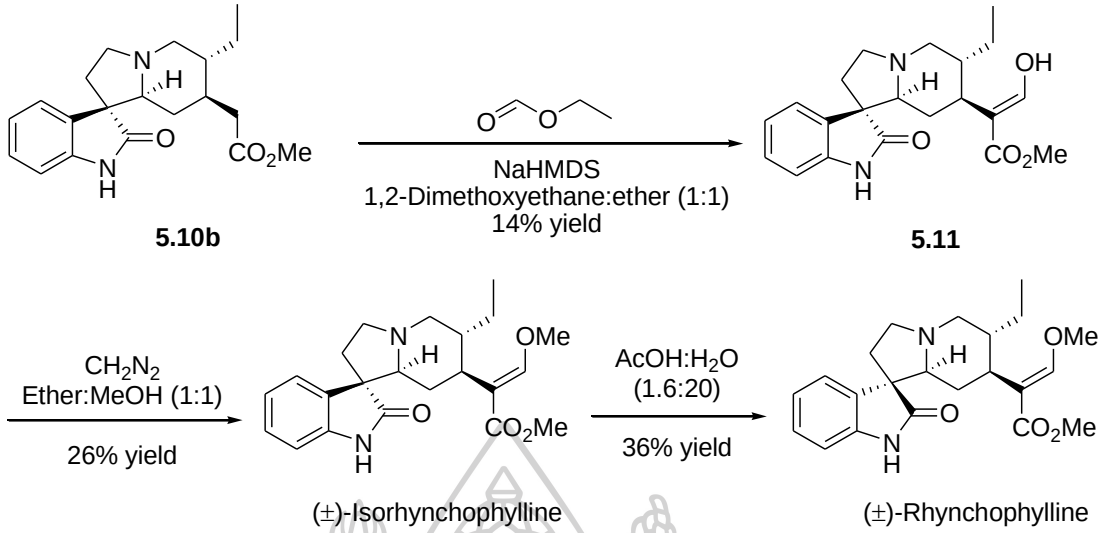

Scheme 107 Total synthesis of Rhynchophylline by Yoshio Ban and coworker

Martin's General Strategy for the Syntheses of Rhynchophylline (2006)

Retrosynthetic analysis of Rhynchophylline was published by Stephen F. Martin and coworker. Rhynchophylline was obtained by Bischler-Napieralski reaction from lactam **6.4**. The lactam **6.4** was obtained by ring-closing metathesis from diene **6.5**. The diene **6.5** could be synthesized from diallylamine **6.8** (Scheme 108) (103).

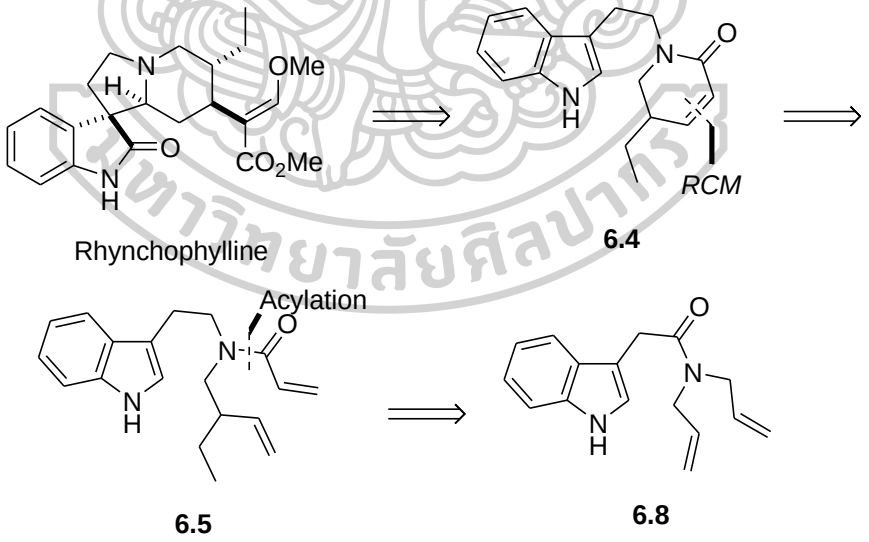

Scheme **108** Retrosynthetic analysis of Rhynchophylline by Stephen F. Martin and coworker

Total synthesis of Rhynchophylline by Stephen F. Martin and coworker which amide coupling reaction of indole-3-acetic acid **6.9** gave diallylamine **6.8** in 88% yield. Ring-closing metathesis followed by Grignard reaction of diallylamine **6.8** gave terminal alkene **6.7** in 71% yield over two steps. Reduction of amide **6.7** gave amine

6.6 in 87% yield. Acylation of amine **6.6** with acid chloride gave amide **6.5** in 73% yield. Ring-closing metathesis of diene **6.5** gave lactam **6.4** in 91% yield. Conjugate addition of lactam **6.4** gave ester **6.22** in 71% yield. Bischler-Napieralski reaction of ester **6.22** gave tetracyclic compound **6.23** in 92% yield. Reduction of dithiolane **6.23** gave ester **6.24** in 95% yield. Chlorination of indole compound **6.24** gave intermediate **6.25**. Hydrolysis of intermediate **6.25** gave 56:44 diastereomeric ratio of spiro compound **6.26** in 75% yield over three steps. Condensation reaction of ester **6.26** with ethyl formate gave enol **6.15** in 14 % yield. Methylation reaction of formyl compound **6.15** gave Isorhynchophylline in 26% yield. Acid catalyzed isomerization of Isorhynchophylline gave Rhynchophylline in 36% yield. Key reaction for the synthesis of Rhynchophylline was obtained by Bischler-Napieralski reaction, Hydrolysis and acid catalyzed isomerization. The total synthesis of Rhynchophylline was achieved in 15 total steps, 15 steps in longest linear sequence, 0.0022% overall yield of Rhynchophylline (Scheme 109).

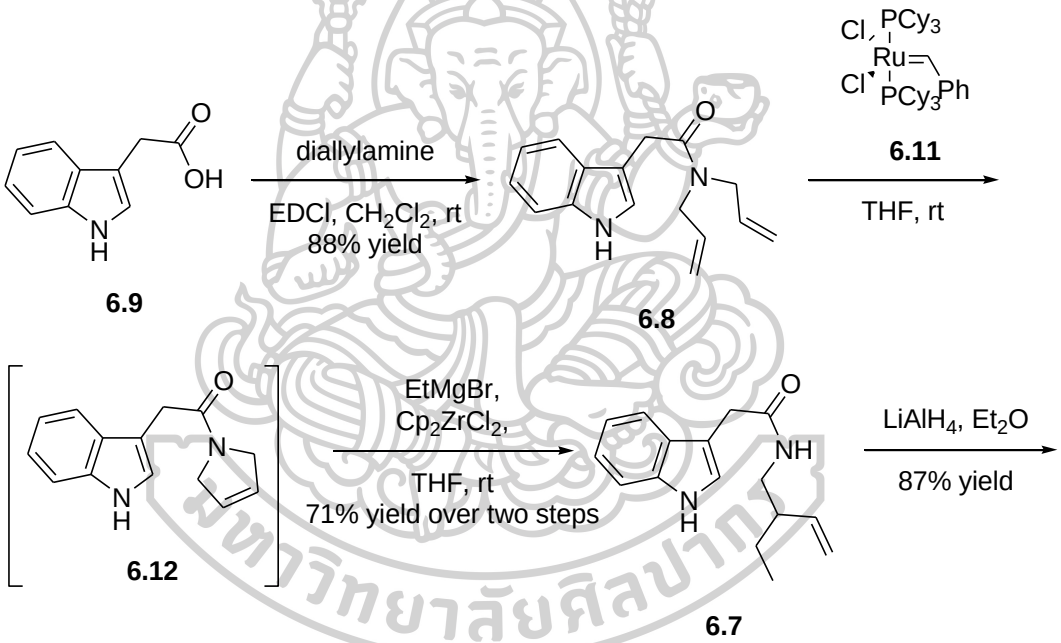

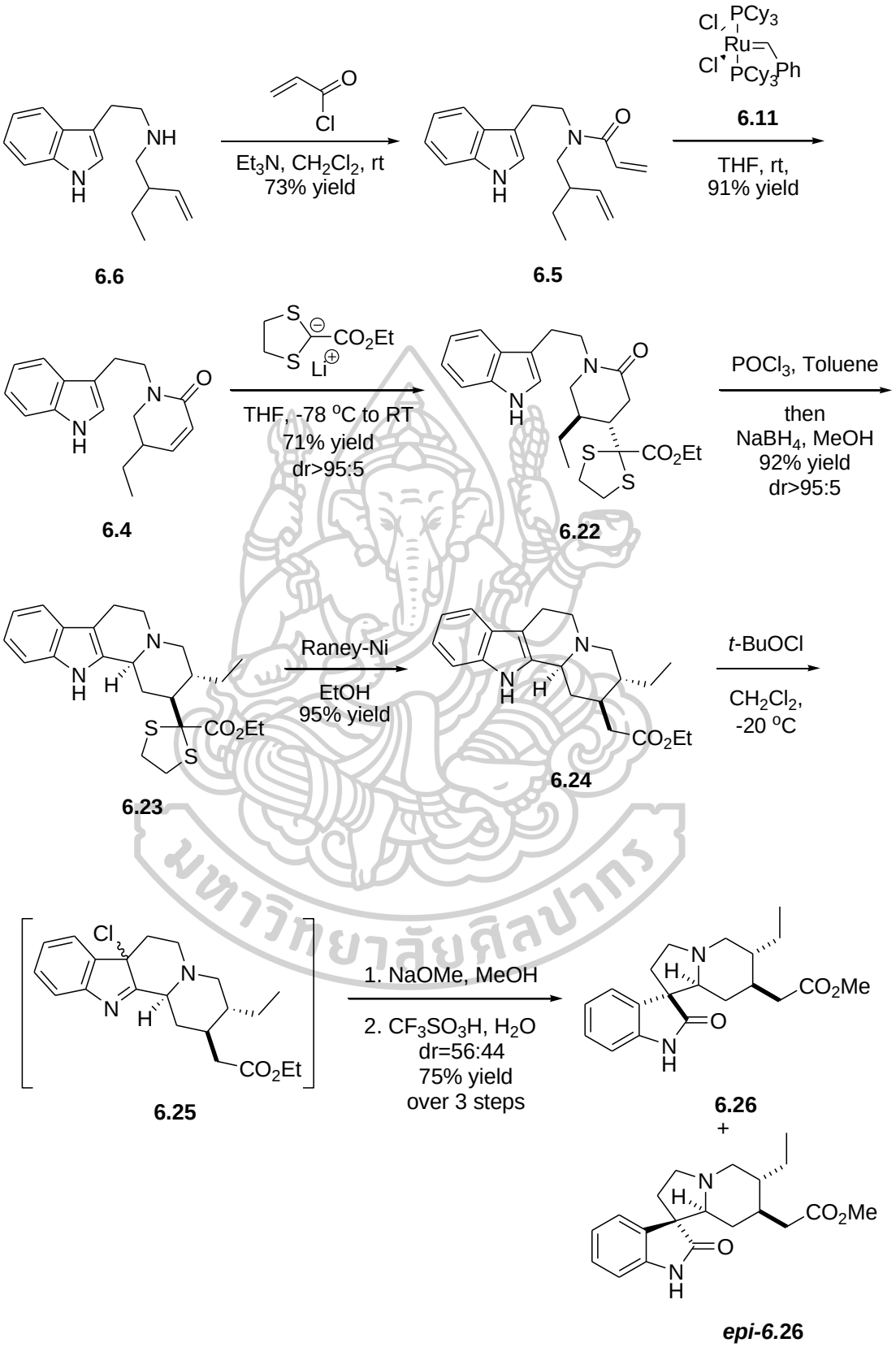
Cl
PCy3
Ru=
Cl
PCy3
Ph
6.11
Et3N, CH2Cl2, rt
73% yield
THF, rt,
91% yield
6.6
6.5
CO2Et
Li
THF, -78 °C to RT
71% yield
dr>95:5
POCl3, Toluene
then
NaBH4, MeOH
92% yield
dr>95:5
6.4
6.22
Raney-Ni
EtOH
95% yield
t-BuOCl
CH2Cl2,
-20 °C
6.23
6.24
1. NaOMe, MeOH
2. CF3SO3H, H2O
dr=56:44
75% yield
over 3 steps
6.25
6.26
+
epi-6.26

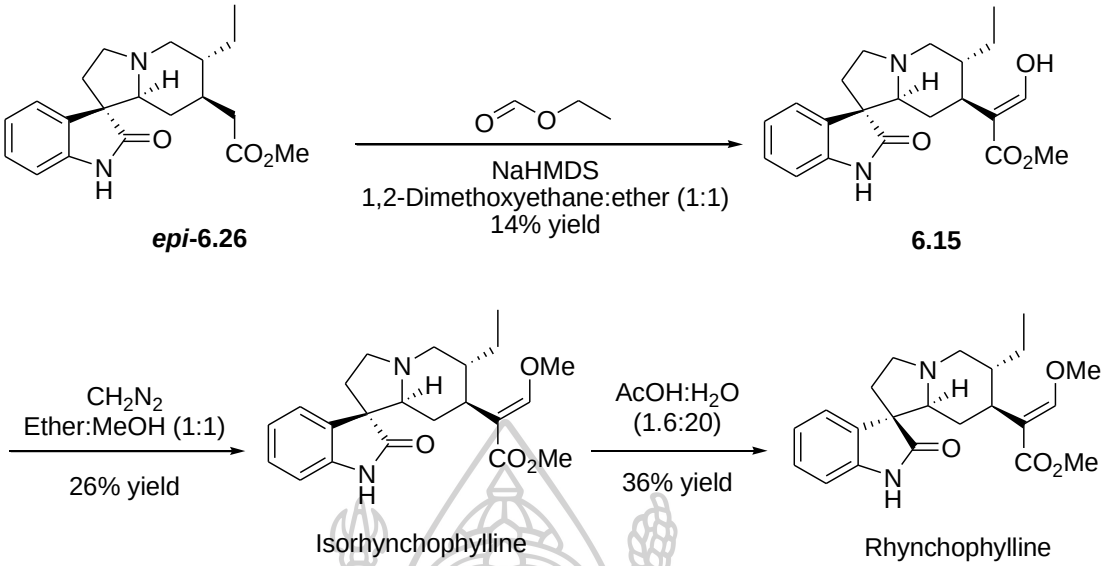

Scheme 109 Total synthesis of Rhynchophylline by Stephen F. Martin and coworker

Itoh's Formal Synthesis of Rhynchophylline and Isorhynchophylline (2010)

Retrosynthetic analysis of Rhynchophylline was published by Takashi Itoh and coworker. Rhynchophylline could be obtained from spirooxindole compound **7.9**. The spirooxindole compound **7.9** was obtained by oxidative rearrangement from hexahydro-*β*-carboline compound **7.6**. The hexahydro-*β*-carboline compound **7.6** was synthesized by Hornor-Wadsworth-Emmons reaction from hexahydro-*β*-carboline compound **7.5**. The hexahydro-*β*-carboline compound **7.5** was obtained by Mannich Michael reaction between dihydrocorynantheine compound **7.1** and 3-methylenepentan-2-one (Scheme 110) (104).

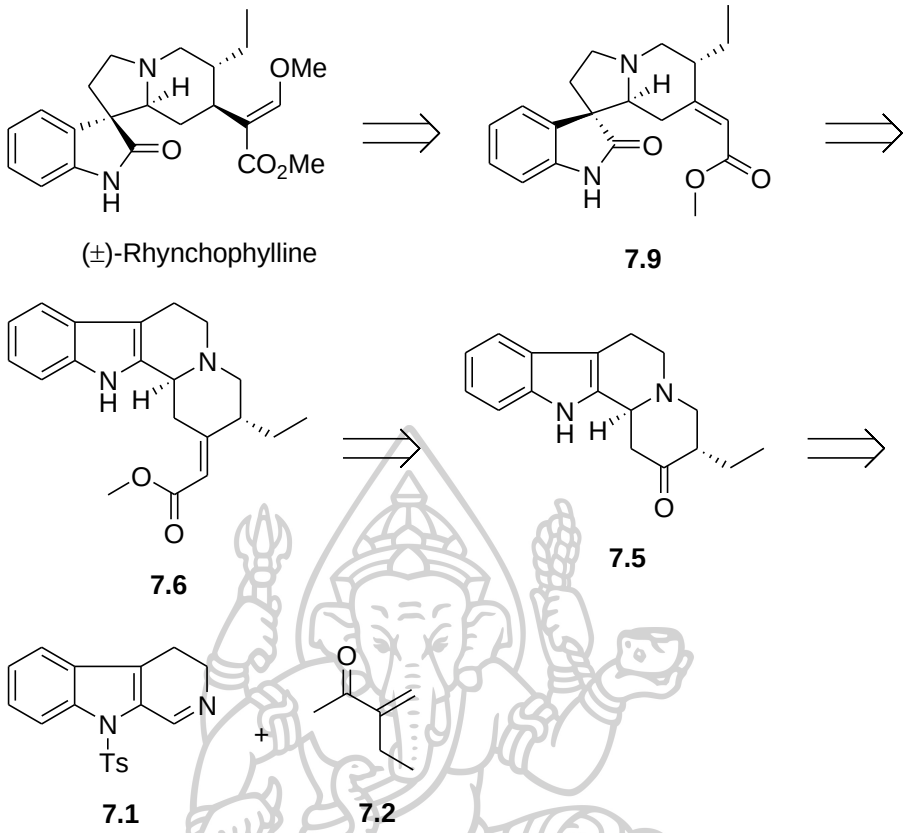

Scheme 110 Retrosynthetic analysis of Rhynchophylline by Takashi Itoh and coworker

Total synthesis of Rhynchophylline was published by Takashi Itoh and coworker. The enantioselective Mannich-Michael reaction of dihydrocorynantheine compound **7.1** with 3-methylenepentan-2-one catalyzed by (*R*)-proline gave hexahydro-*β*-carboline compound **7.3** in 85% yield and 99% ee. Protection of tetracyclic compound **7.3** with 1,3-propanediol using toluenesulfonic acid (TsOH) gave protected compound **7.4** in 90% yield. Removal of tosyl group of protected compound **7.4** was performed in the presence of sodium bis(2-methoxyethoxy)aluminum dihydride (Red-Al) followed by deprotection of acetal group synthesized hexahydro-*β*-carboline compound **7.5** in 77% yield. Hornor-Wadsworth-Emmons reaction of ketone compound **7.5** in the basic conditions generated *α,β*–unsaturated ester compound **7.6** in 84% yield. Oxidative rearrangement of hexahydro-*β*-carboline compound **7.6** using *N*-bromosuccinimide in the mixture of tetrahydrofuran, water and acetic acid at 0^{o}C constructed spiro[pyrrolidine-3,3'-oxindole] compound **7.9** in 57% yield. Reduction of *α,β*–unsaturated ester compound **7.9** in the presence of Platinum(IV) oxide hydrate gave spiro[pyrrolidine-3,3'-oxindole] compound **7.14b** in 28% yield and spiro[pyrrolidine-3,3'-oxindole] compound **7.14a** in 38% yield. Condensation reaction of ester **7.14b** with ethyl formate gave enol **7.15** in 14% yield. Methylation reaction of formyl compound **7.15** gave Isorhynchophylline in 26% yield. Acid catalyzed isomerization of Isorhynchophylline gave Rhynchophylline in 36% yield. Key reaction for the

synthesis of Rhynchophylline and Isorhynchophylline were obtained by oxidative rearrangement, Hornor-Wadsworth-Emmons reaction and Mannich Michael reaction. The formal synthesis of Rhynchophylline was achieved in 10 total steps, 10 steps in longest linear sequence, 0.103% overall yield of Rhynchophylline (Scheme 111).

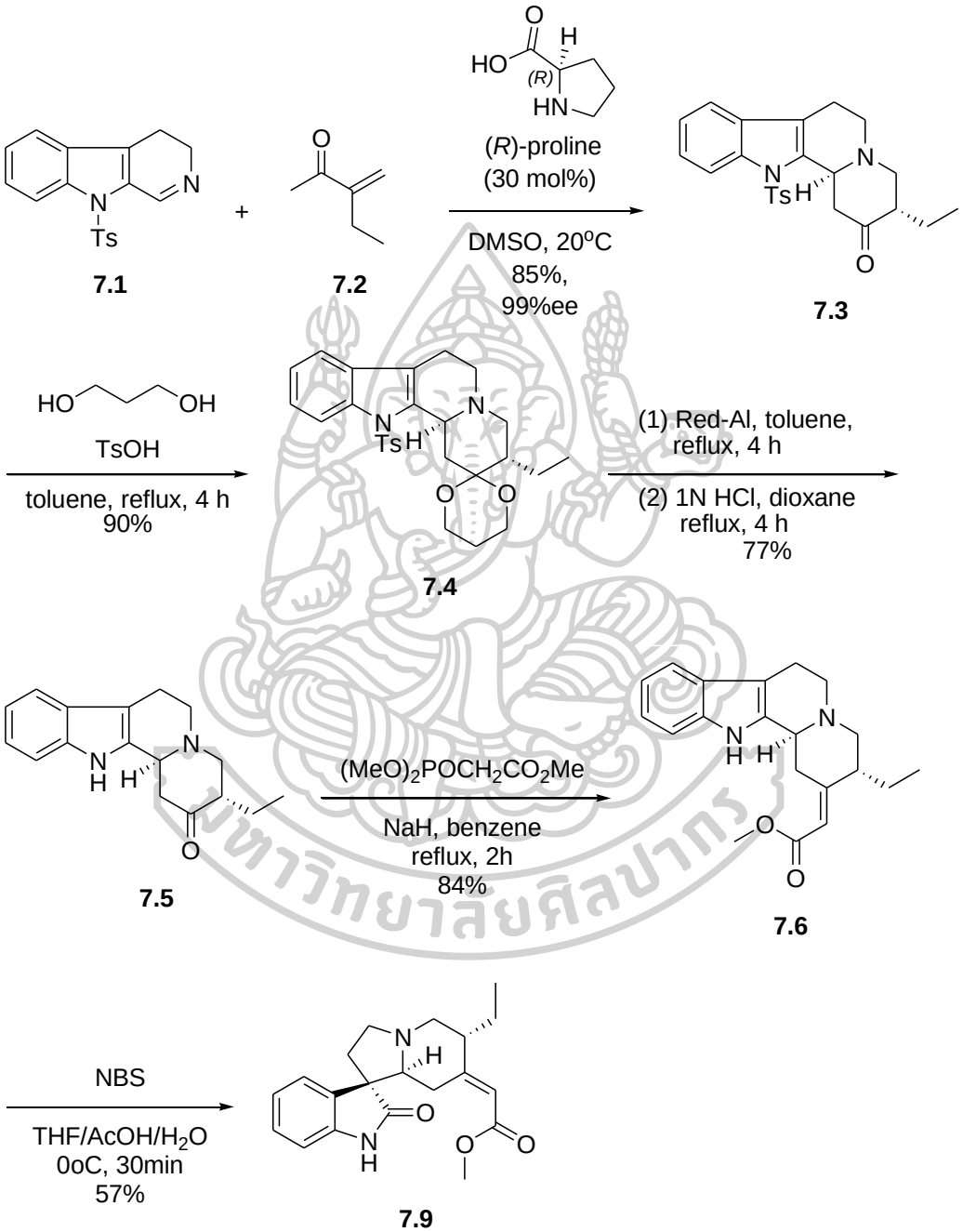

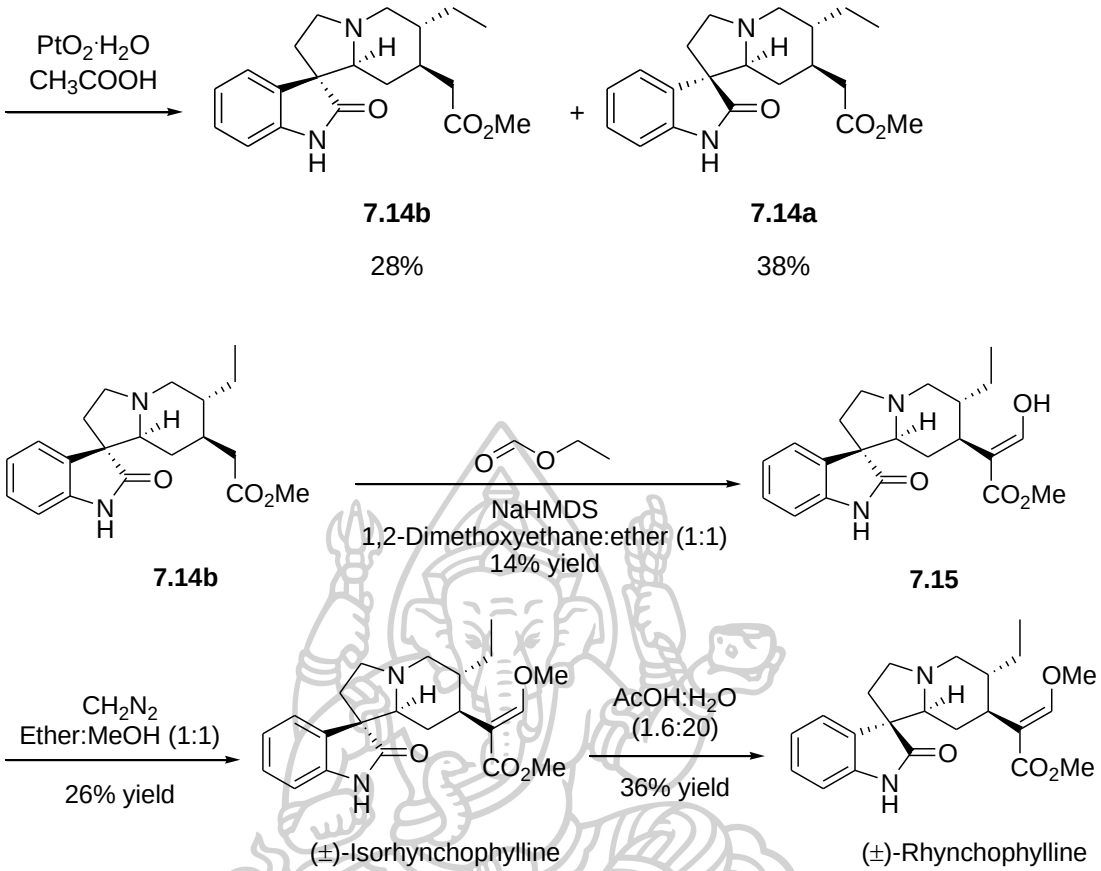

Scheme **111** Total synthesis of Rhynchophylline by Takashi Itoh and coworker

Wang's Enantioselective Formal Synthesis of Rhynchophylline and Isorhynchophylline (2012)

Retrosynthetic analysis of Rhynchophylline was published by Rui Wang and coworker. Rhynchophylline could be obtained from spiro tetracyclic compound **8.13**. The spiro tetracyclic compound **8.13** was obtained by cyclization from 2-halotryptamine **8.10** with aldehyde **8.11**. The aldehyde **8.11** was synthesized by asymmetric Michael addition from aldehyde **8.9** with methylmalonate **8.8** (Scheme 112) (105).

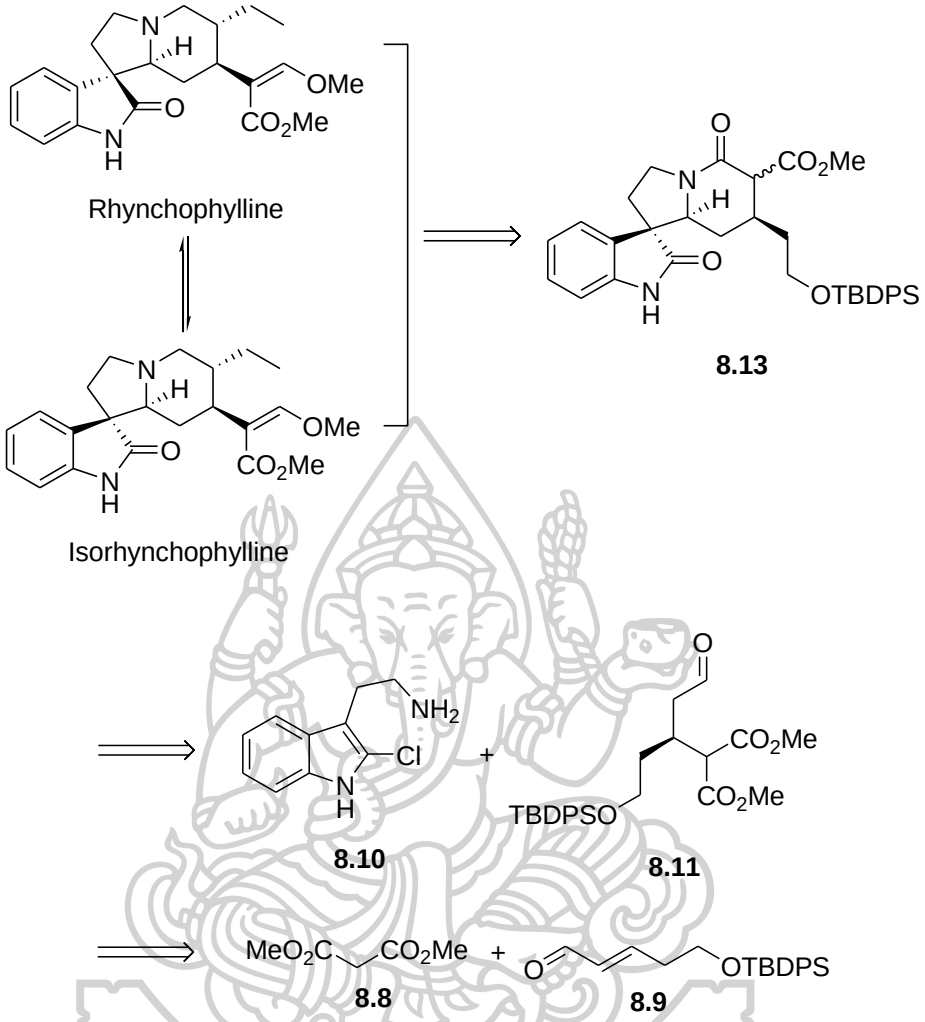

Scheme 112 Retrosynthetic analysis of Rhynchophylline by Rui Wang and coworker

Total synthesis of Rhynchophylline was published by Rui Wang and coworker. Cross-metathesis of 3-butenol **8.3** with acroleine **8.4** gave primary alcohol **8.5** in 99% yield. Protection of primary alcohol **8.5** gave unsaturated aldehyde **8.9** in 97% yield. Asymmetric Michael addition of aldehyde **8.9** with methylmalonate **8.8** gave adehyde **8.11**. Cyclization of aldehyde **8.11** with 2-halotryptamine **8.10** produced Schiff base to give diastereomeric ratio 3:1 of spiro tetracyclic core **8.13** in 78% yield over 2 steps. Protection reaction followed by Lawesson's reaction of spiro tetracyclic core **8.13** gave thiolactam **8.14** in 74% yield over 2 steps. Reduction reaction of thiolactam **8.14** gave alkene **8.15** in 80% yield. Reduction reaction of alkene **8.15** gave diastereomeric ratio 1:3.5 of ester **8.16** in 79% yield. Deprotection of protected compound **8.16** gave oxindole **8.17** in 90% yield. Isomerization of ester **8.17a** gave ester **8.17b** in 70% yield. Reduction, oxidation followed by Wittig reaction of ester **8.17b** gave terminal alkene **8.18** in 59% yield over 3 steps. Deprotection of protected compound **8.18** gave primary alcohol **8.19** in 96% yield. Oxidation, Pinnick oxidation and esterification of primary alcohol **8.19** gave ester **8.20** in 61% yield. Hydrogenation reaction of ester **8.20** gave spiro compound **8.21** in 98% yield.

Condensation reaction of ester **8.21** with ethyl formate gave enol **8.22** in 14 % yield. Methylation reaction of formyl compound **8.22** gave Isorhynchophylline in 26% yield. Acid catalyzed isomerization of Isorhynchophylline gave Rhynchophylline in 36% yield. Key reaction for the synthesis of Rhynchophylline was obtained by asymmetric Michael addition and cyclization. The total synthesis of Rhynchophylline was achieved in 21 total steps, 21 steps in longest linear sequence, 0.00098% overall yield of Rhynchophylline (Scheme 113).

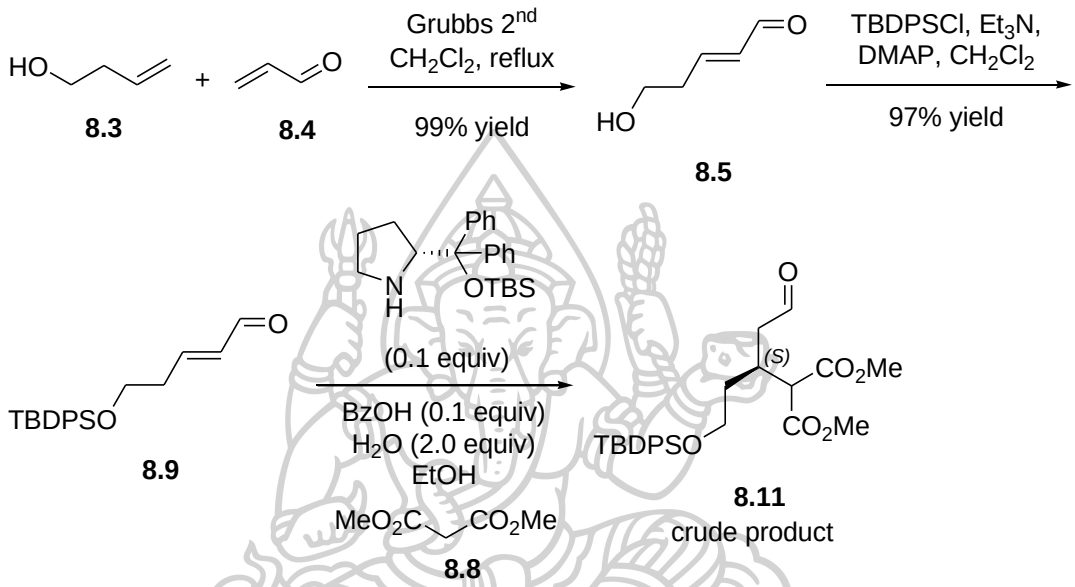

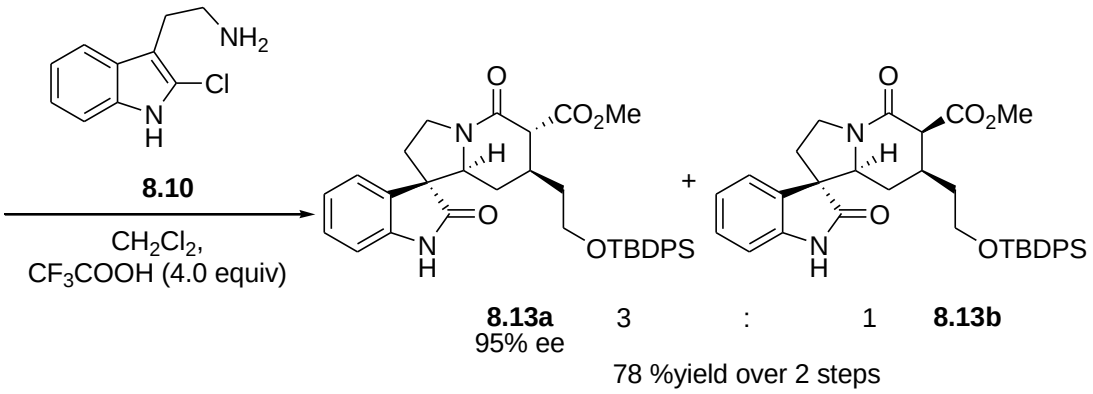

8.13a 3 : 1 **8.13b**

95% ee

78 %yield over 2 steps

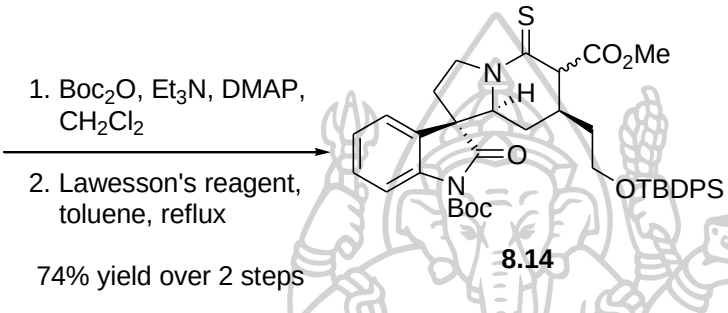

8.14

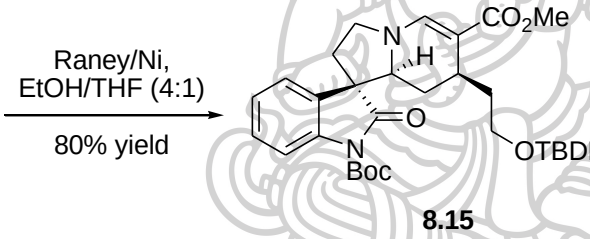

8.15

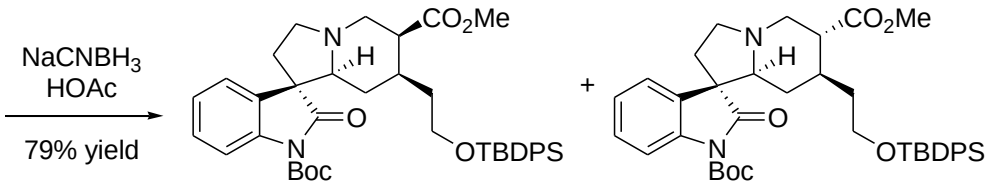

8.16a 1 : 3.5 **8.16b**

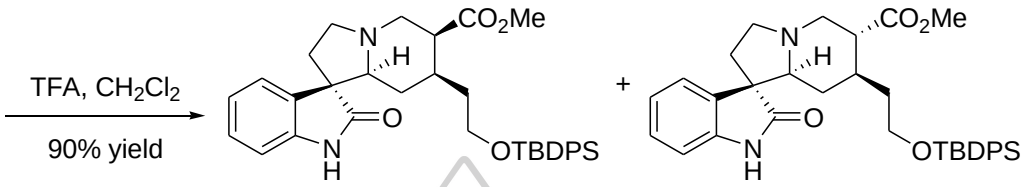

8.17a 1 : 3.5 **8.17b**

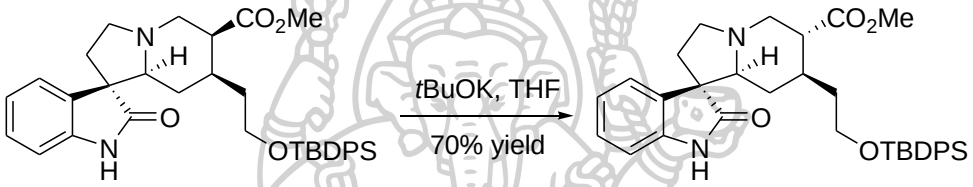

8.17a **8.17b**

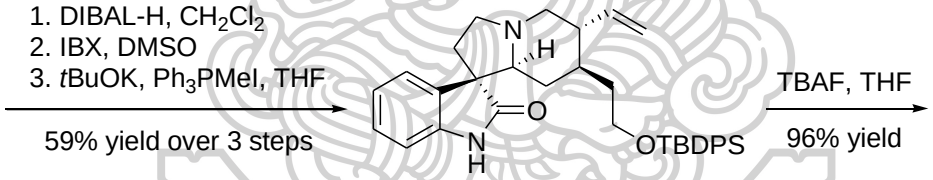

8.18

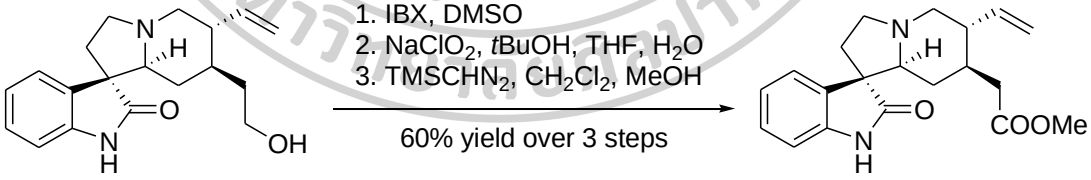

8.19 **8.20**

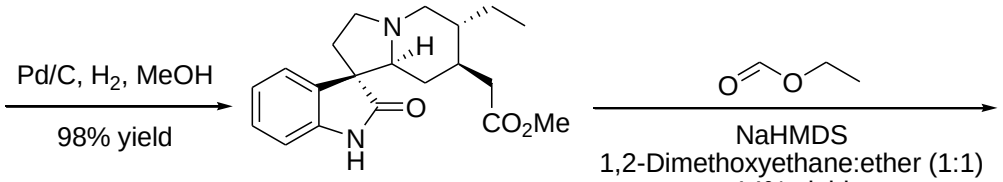

8.21

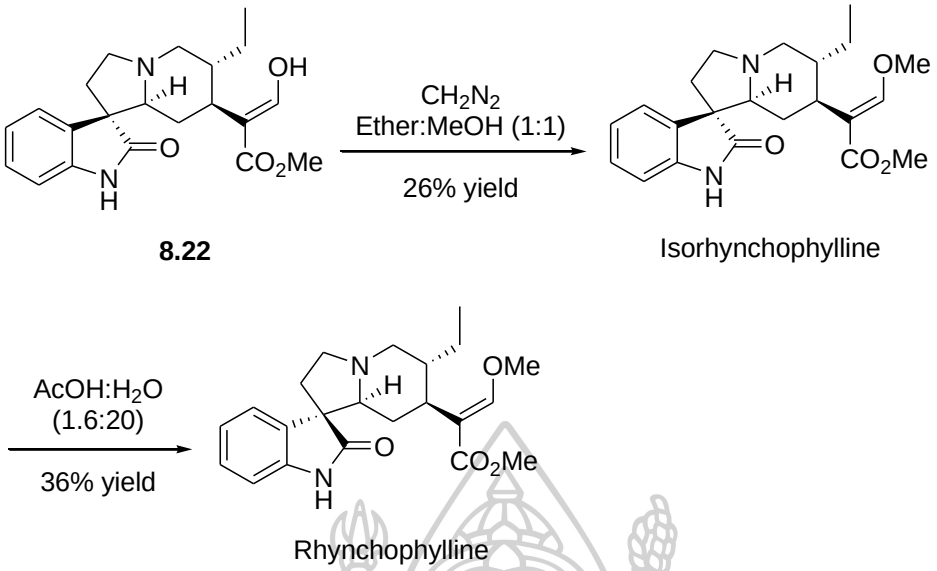

8.22

Isorhynchophylline

Rhynchophylline

Scheme 113 Total synthesis of Rhynchophylline by Rui Wang and coworker

Amat's Enantioselective Formal Synthesis of *ent*-Rhynchophylline and *ent*-Isorhynchophylline (2013)

Retrosynthetic analysis of *ent*-Rhynchophylline was published by Mercedes Amat and coworker. The *ent*-Rhynchophylline **9.11** was obtained by reduction from oxindole **9.10**. The oxindole **9.10** was obtained by oxidation from spiro compound **9.9**. The spiro compound **9.9** was synthesized by cyclization from lactam **9.3**. The lactam **9.3** was constructed by cyclocondensation from tryptophanol with aldehyde **9.1** (Scheme 114) (106).

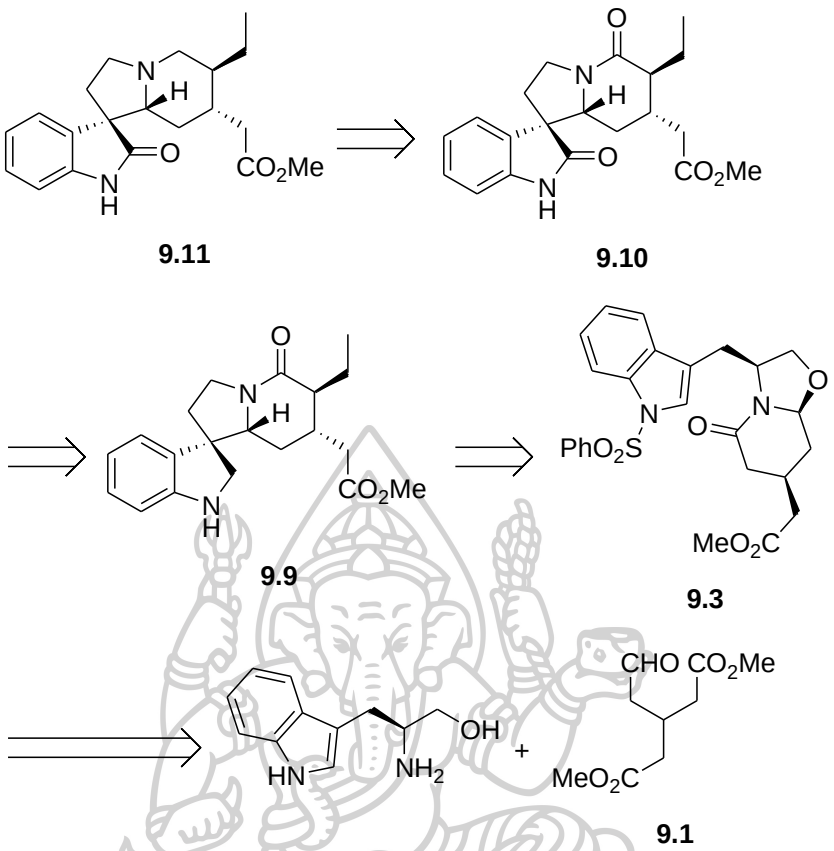

Scheme 114 Retrosynthetic analysis of *ent*-Rhynchophylline by Mercedes Amat and coworker

Cyclocondensation of tryptophanol with aldehyde **9.1** gave lactam **9.2** in 65% yield. Protection of lactam **9.2** gave cycloalkene **9.3** in 90% yield. Cyclization reaction of lactam **9.3** gave spiro compound **9.4** in 93% yield. Oxidation of primary alcohol **9.4** gave aldehyde intermediate in 79% yield. Pinnick oxidation of aldehyde intermediate gave carboxylic acid intermediate in 64% yield. Radical reductive decarbonylation reaction of carboxylic acid intermediate gave lactam **9.5** in 65% yield. Reduction reaction of ester **9.5** gave primary alcohol intermediate in 83% yield. Protection of primary alcohol intermediate gave protected alcohol **9.6** in 87% yield. Alkylation reaction of lactam **9.6** gave lactam **9.7** in 72% yield. Deprotection reaction of protecting compound **9.7** gave primary alcohol intermediate in 93% yield. Oxidation followed by esterification of alcohol intermediate gave ester **9.8** in 66% yield over 2 steps. Deprotection reaction of protecting compound **9.8** gave spiro compound **9.9** in 88% yield. Oxidation reaction of spiro compound **9.9** gave oxindole **9.10** in 70% yield. Selective reduction reaction of oxindole **9.10** gave *ent*-Rhynchophylline **9.11** in 47% yield. Key reaction for the synthesis of *ent*-Rhynchophylline was obtained by cyclocondensation and cyclization. The total synthesis of *ent*-Rhynchophylline was achieved in 16 total steps, 16 steps in longest linear sequence, 0.017% overall yield of *ent*-Rhynchophylline (Scheme 115).

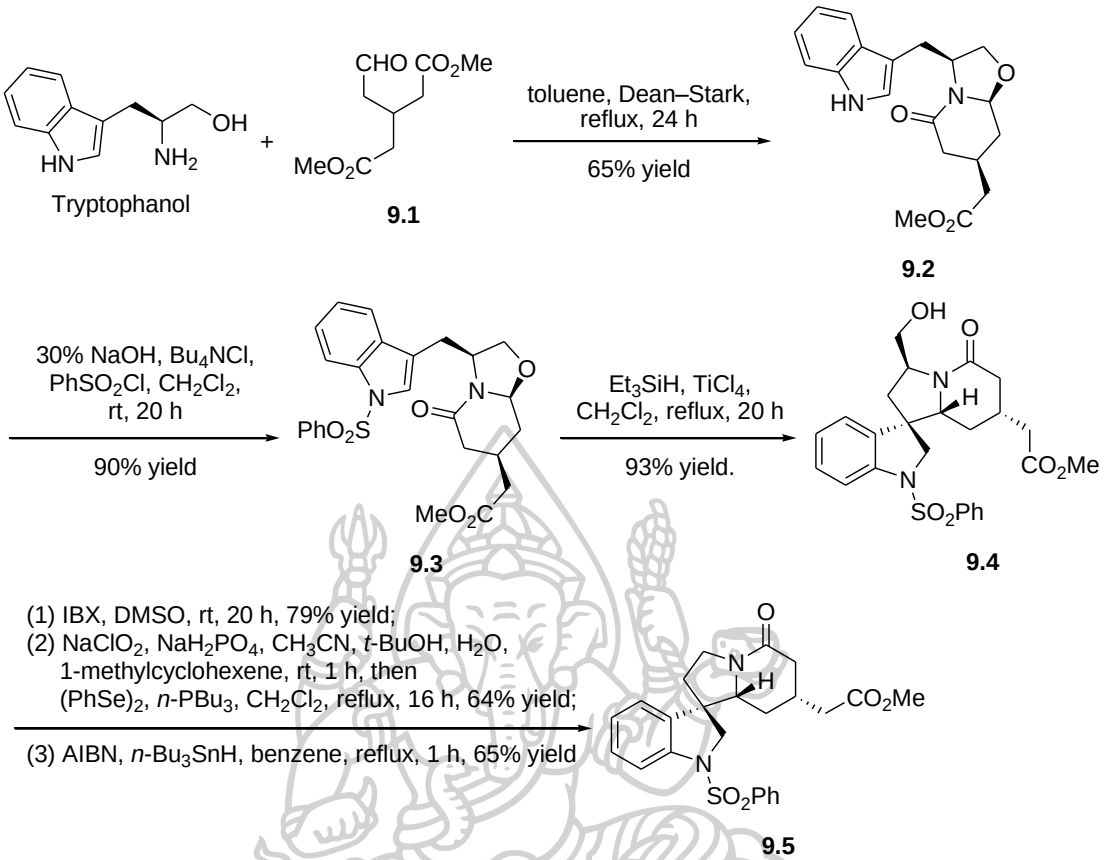
Tryptophanol
9.1
toluene, Dean–Stark, reflux, 24 h
65% yield
9.2
30% NaOH, Bu4NCl, PhSO2Cl, CH2Cl2, rt, 20 h
90% yield
9.3
Et3SiH, TiCl4, CH2Cl2, reflux, 20 h
93% yield.
9.4
(1) IBX, DMSO, rt, 20 h, 79% yield;
(2) NaClO2, NaH2PO4, CH3CN, t-BuOH, H2O, 1-methylcyclohexene, rt, 1 h, then (PhSe)2, n-PBu3, CH2Cl2, reflux, 16 h, 64% yield;
(3) AIBN, n-Bu3SnH, benzene, reflux, 1 h, 65% yield
9.5

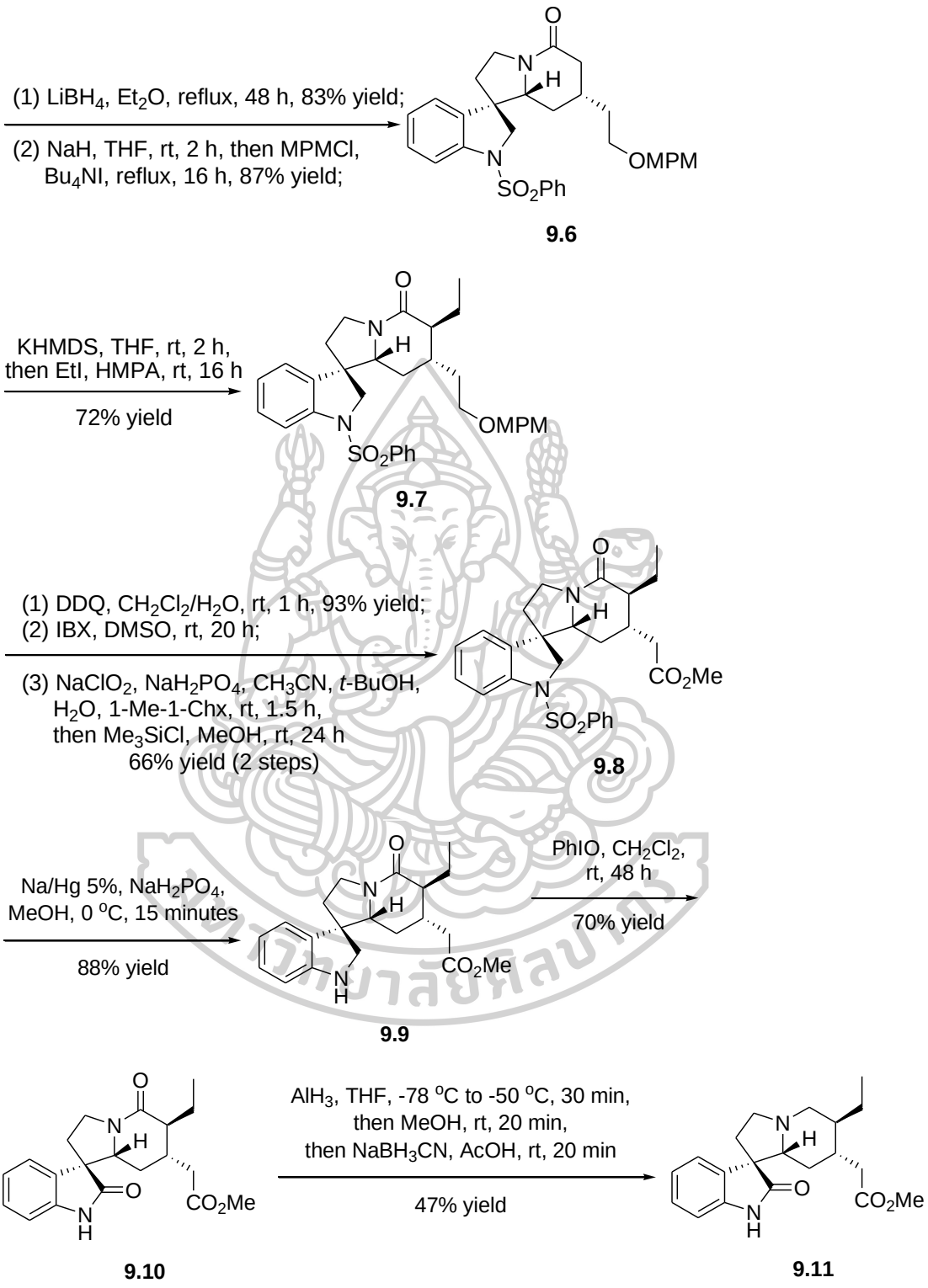

Scheme 115 Total synthesis of *ent*-Rhynchophylline by Mercedes Amat and coworker

Hiemstra's Total Synthesis of the Spirocyclic Oxindole Alkaloids Rhynchophylline (2013)

Retrosynthetic analysis of Rhynchophylline was published by Henk Hiemstra and coworker. Rhynchophylline was obtained by Wittig reaction and hydrogenation from spiro[pyrrolidine-3,3´-oxindole] compound **10.25**. The spirotetracyclycic compound **10.25** was synthesized by palladium catalyzed Tsuji-Trost allylic alkylation from spirotricyclic compound **10.19**. The spirotricyclic compound **10.19** was obtained by cyclization from spirotricyclic compound **10.19**. The spirotricyclic compound **10.19** was constructed by Mannich condensation reaction between amine compound **10.9** and aldehyde **10.16**. The secondary amine compound **10.9** was synthesized by alkylation reaction by tryptamine **10.1** with allylic bromide compound **10.10** (Scheme 116) (107).

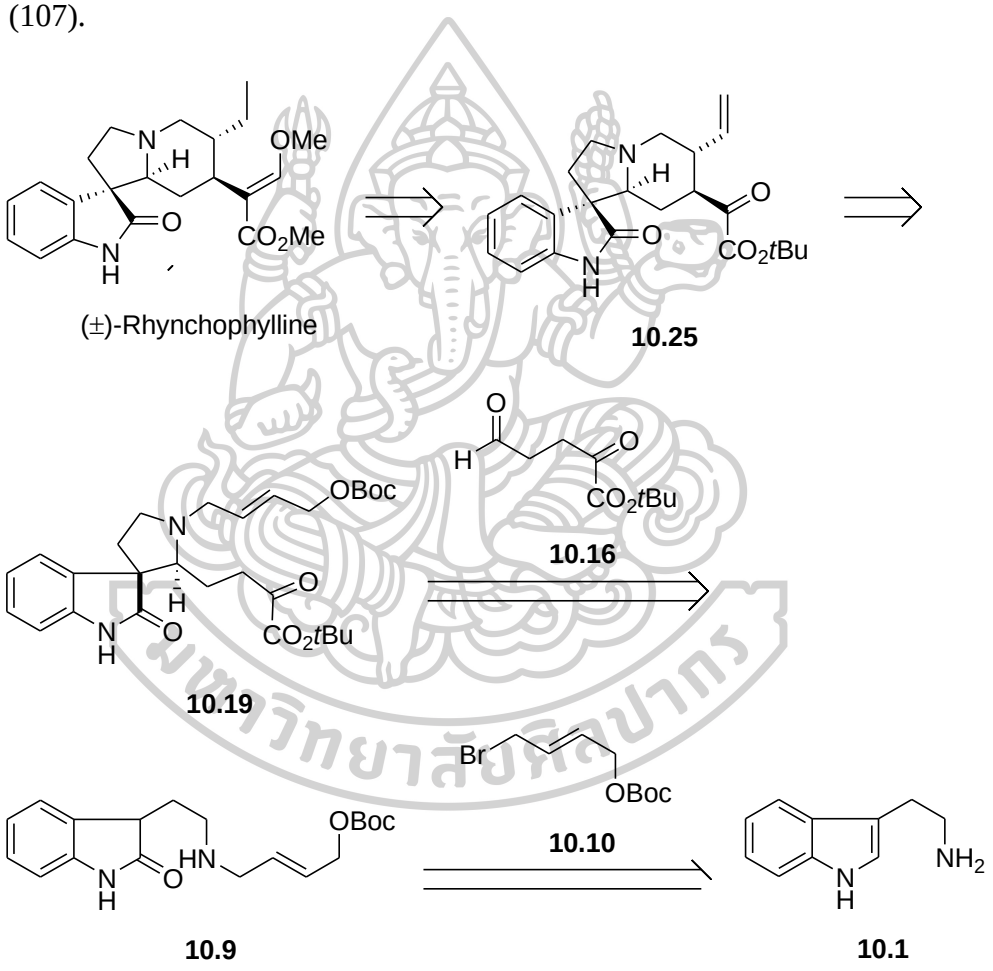

Scheme **116** Retrosynthetic analysis of Rhynchophylline by Henk Hiemstra and coworker

Protection of tryptamine **10.1** with 4-Nitrobenzenesulfonyl chloride in the presence of triethylamine followed by alkylation of *N*-protected tryptamine with *tert*-butyl (*E*)-4-bromobut-2-enyl carbonate **10.10** gave sulfonamide compound **10.11** in 92% yield. The reaction between sulfonamide compound **10.11** and *N*-chlorosuccinimide in aqueous tetrahydrofuran generated oxindole compound **10.12** in 93% yield. Removal of the sulfonyl group of *N*-protected oxindole compound **10.12**

using thiophenol (PhSH) and potassium carbonate synthesized secondary allylic amine compound **10.9** in 96% yield. Mannich condensation reaction of secondary allylic amine compound **10.9** with aldehyde **10.16** in the presence of triethyl amine through spirocyclization generated 1:2 as diastereomeric ratio of spirotricyclic compound **10.18** and **10.19** in 75% yield. Palladium catalyzed Tsuji-Trost allylic alkylation of spirotricyclic compound **10.19** in mixture of base cesium carbonate and diethylisopropylamine in the presence of palladium catalyst synthesized spiro[pyrrolidine-3,3´-oxindole] compound **10.24** and **10.25** in isolated yields in 56% and 14% yield, respectively. Transesterification reaction of *tert*-butylester spirooxindole compound **10.25** which unreactive towards the Wittig reagent using potassium carbonate in methanol generated methylester spirooxindole compound **10.26** in 90% yield. Wittig reaction of methyl ester compound **10.26** produced *Z*-alkene spirooxindole compound **10.27** followed by isomerization of *Z*-alkene spirooxindole compound **10.27** under the influence of trifluoroacetic acid and Trifluoroacetic anhydride synthesized (±)-Corynoxeine as natural product in 55% yield over 2 steps. Hydrogenation reaction of (±)-Corynoxeine using palladium on activated charcoalunder hydrogen gas gave (±)-Rhynchophylline in 97% yield. Key reaction for the synthesis of (±)-Rhynchophylline was obtained by Mannich condensation reaction, palladium catalyzed Tsuji-Trost allylic alkylation and Wittig reaction. The total synthesis of (±)-Rhynchophylline was achieved in 10 total steps, 10 steps in longest linear sequence, 4.18% overall yield of (±)-Rhynchophylline (Scheme 117).

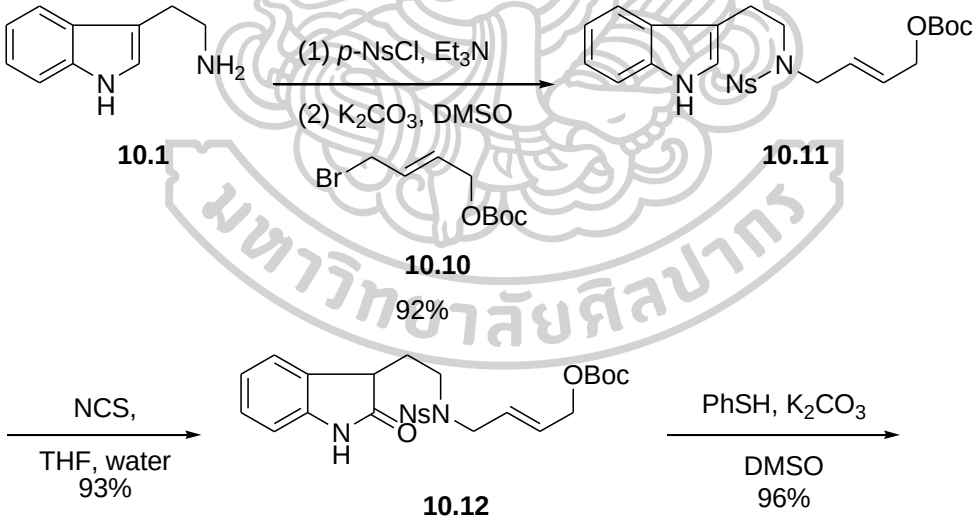

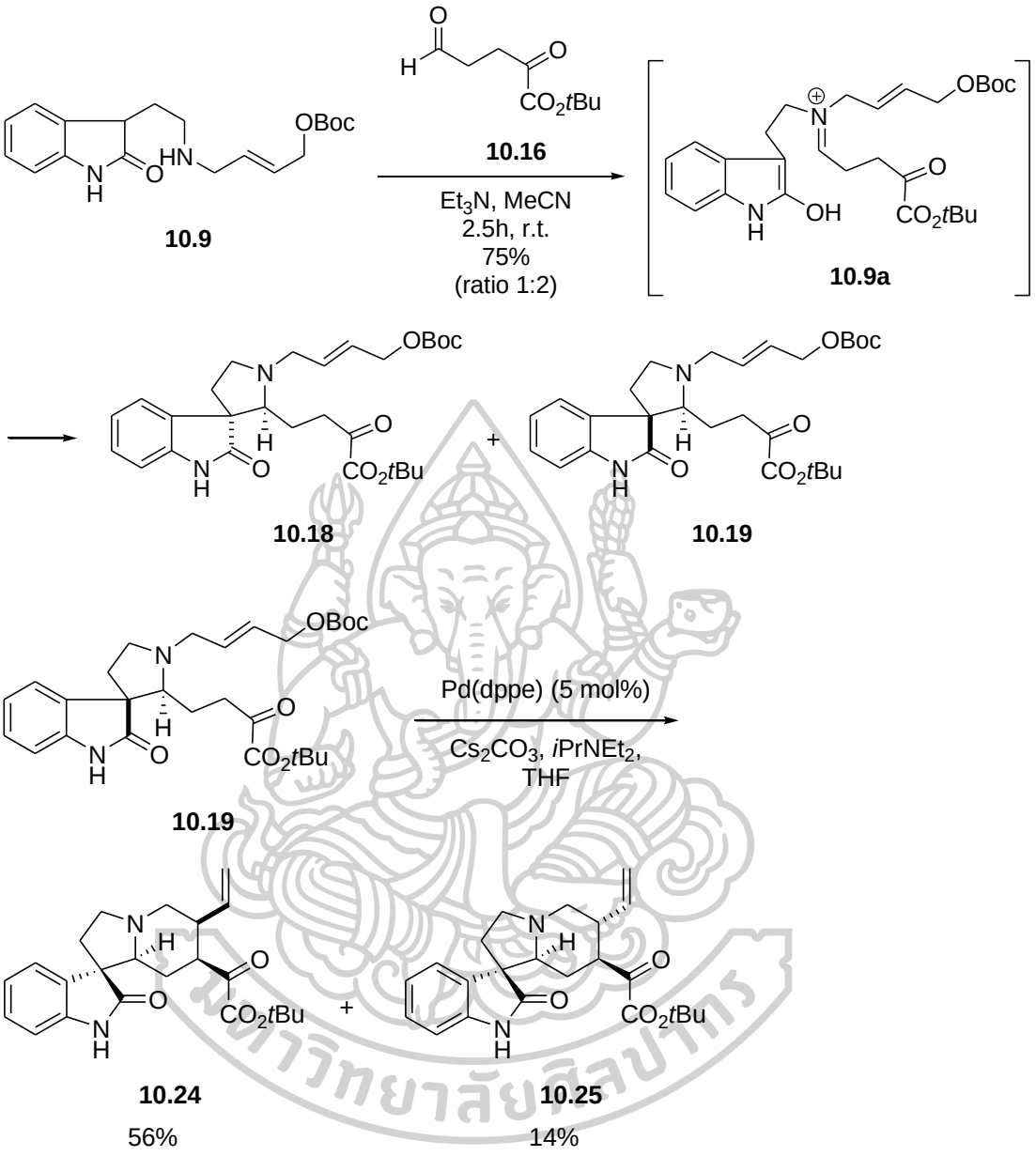
OBoc
HN
N
H
O
10.9
O
H
O
CO2tBu
10.16
Et3N, MeCN
2.5h, r.t.
75%
(ratio 1:2)
OBoc
N
OH
O
CO2tBu
10.9a
OBoc
N
H
O
CO2tBu
10.18
+
10.19
Pd(dppe) (5 mol%)
Cs2CO3, iPrNEt2,
THF
10.19
10.24
56%
+
10.25
14%

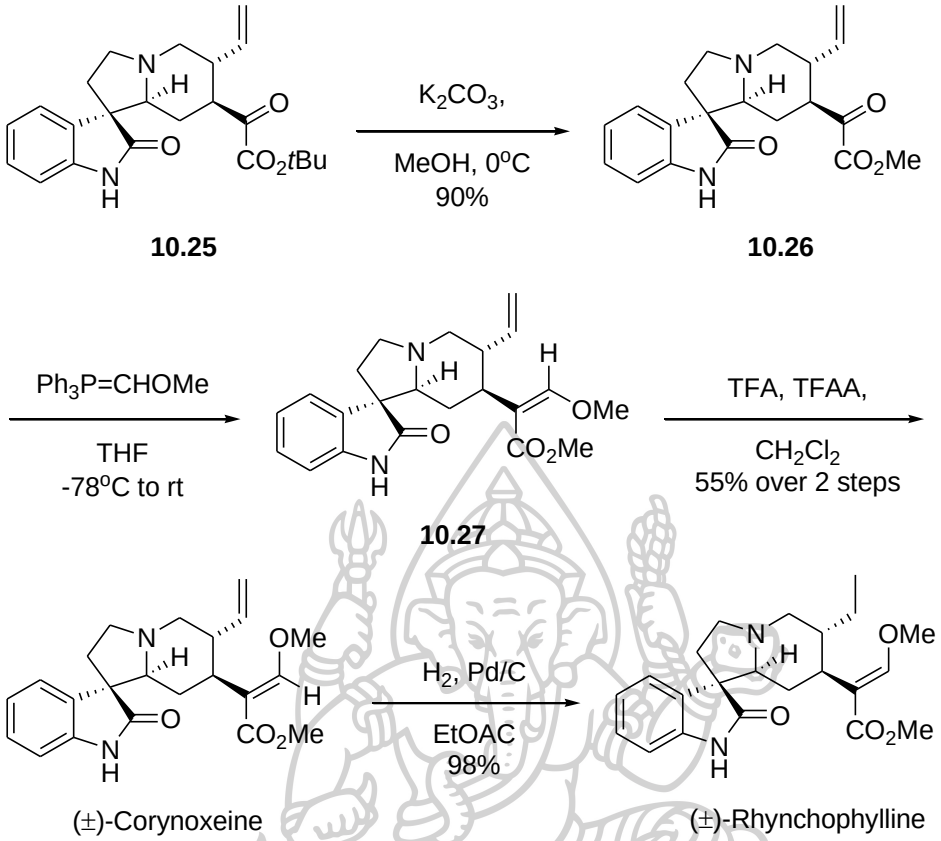

Scheme 117 Total synthesis of Rhynchophylline by Henk Hiemstra and coworker

Zhao's Formal Synthesis of (±)-Rhynchophylline (2016)

The idea was based on research by Qin-Shi Zhao and coworker who reported on the synthesis of bioactive oxindole alkaloid compounds consisting of (±)-Rhynchophylline, (±)-Isorhynchophylline, (±)-Mitraphylline, (±)-Formosanine, (±)-Isomitraphylline and (±)-Isoformosanine. The synthesis approach does not use protection reactions and key reaction involving one-pot reactions include one-pot *N*-alkylation/cross-dehydrogenative coupling and one-pot Michael/Karpocho reaction. The goal of research is minimize to use of chemicals and purify the compounds at each step of the reaction. Retrosynthetic analysis of Rhynchophylline Qin-Shi Zhao and coworkers which Rhynchophylline was obtained by acid catalyzed isomerization from Isorhynchophylline. Isorhynchophylline was obtained by methylation from enol compound **11.10**. The enol compound **11.10** was synthesized by Michael addition from cycloalkane compound **11.6**. The cycloalkane compound **11.6** was constructed by *N*-alkylation and cross-dehydrogenative coupling reaction from alkyl bromide **11.2** and pyidine **11.3** (Scheme 118) (108).

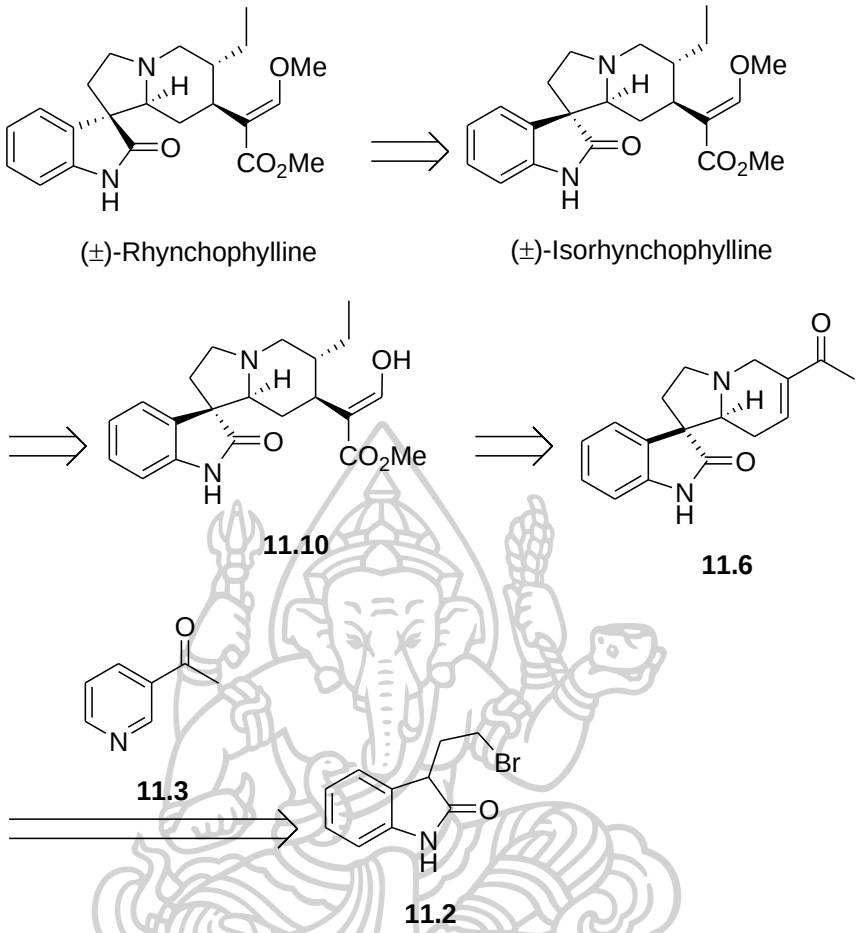

Scheme 118 Retrosynthetic analysis of Rhynchophylline Qin-Shi Zhao and coworker

Total synthesis of Rhynchophylline was published by Qin-Shi Zhao and coworker. One-pot *N*-alkylation cross-dehydrogenative coupling reaction of alkyl bromide **11.2** with pyidine **11.3** generated pyridinium salt **11.4** in 56% yield. Dearomatization of pyridinium salt **11.4** gave cycloalkane compound **11.5** in 79% yield. Dess–Martin periodinane oxidation reaction of allylic alcohol **11.5** synthesized cycloalkane compound **11.6** in 80% yield. Michael addition of cycloalkane compound **11.6** gave keto-monoester compound **11.7** in 53% yield. Protection reaction of ketone compound **11.7** using 1,2-ethanedithiol afforded dithioether compound **11.8** in 86% yield. Desulfuration reaction of dithioether compound **11.8** generated terminal alkane compound **11.9** in 81% yield. Condensation reaction of ester compound **11.9** with ethyl formate gave enol compound **11.10** in 14 % yield. Methylation reaction of formyl compound **11.10** constructed Isorhynchophylline in 26% yield. Acid catalyzed isomerization of Isorhynchophylline gave Rhynchophylline in 36% yield. Key reaction for the synthesis of Rhynchophylline was obtained by *N*-alkylation/cross-dehydrogenative coupling reaction and reduction. The total synthesis of Rhynchophylline was achieved in 9 total steps, 9 steps in longest linear sequence, 0.17% overall yield of Rhynchophylline (Scheme 119).

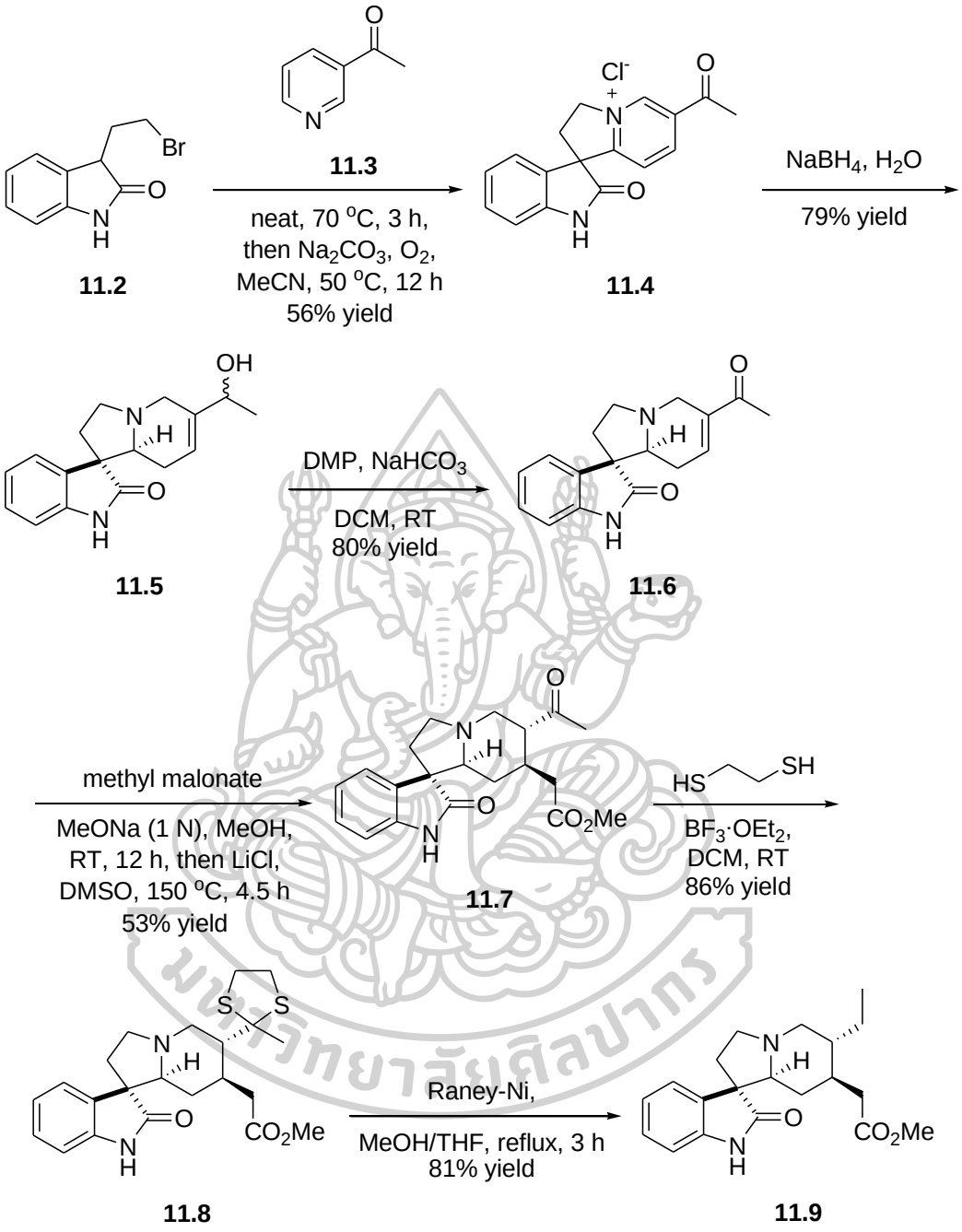
11.2
11.3
neat, 70 °C, 3 h,
then Na2CO3, O2,
MeCN, 50 °C, 12 h
56% yield
11.4
NaBH4, H2O
79% yield
11.5
DMP, NaHCO3
DCM, RT
80% yield
11.6
methyl malonate
MeONa (1 N), MeOH,
RT, 12 h, then LiCl,
DMSO, 150 °C, 4.5 h
53% yield
11.7
BF3·OEt2,
DCM, RT
86% yield
11.8
Raney-Ni,
MeOH/THF, reflux, 3 h
81% yield
11.9

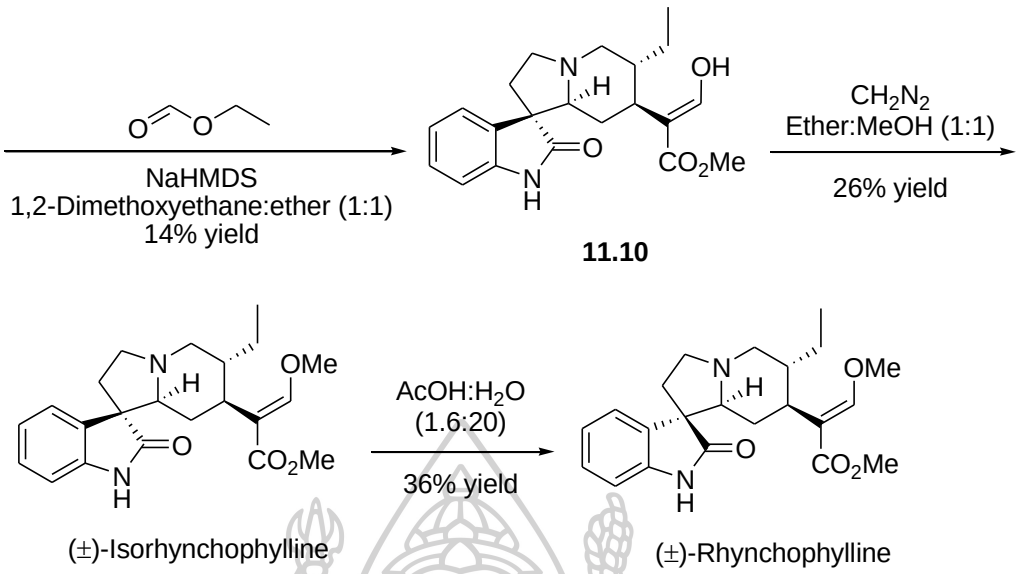

Scheme 119 Total synthesis of Rhynchophylline Qin-Shi Zhao and coworker

Tong's Asymmetric Total Syntheses of Rhynchophylline and Isorhynchophylline (2019)

Retrosynthetic analysis of Rhynchophylline and Isorhynchophylline were published by Rongbiao Tong and coworker. The core structure of Rhynchophylline and Isorhynchophylline was obtained by Claisen condensation and methyl esterification from carboxylic acid **12.2**. Carboxylic acid **12.2** was achieved by hydroboration/oxidation, IBX oxidation and Pinnick oxidation from tetracyclic spirooxindole **12.6** respectively. The tetracyclic spirooxindole **12.6** was synthesized by Carreira's [3+2] ring-expansion reaction from cyclopropyl spirooxindole **12.7** with cyclic imine **12.8**. The cyclic imine **12.8** was obtained by cyclocondensation from butanal **12.10** with ethyl acrylate **12.11** (Scheme 120) (109).

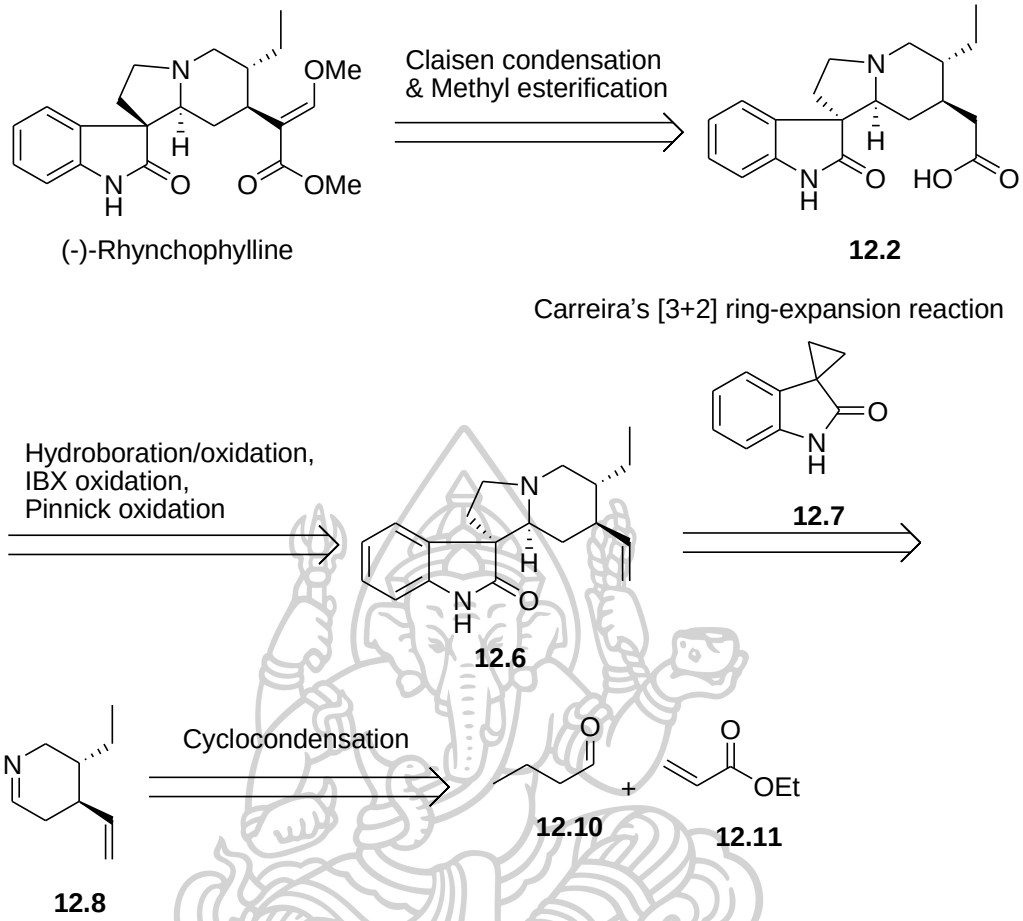

Scheme 120 Retrosynthetic analysis of Rhynchophylline and Isorhynchophylline by Rongbiao Tong and coworker

Michael addition of butanal **12.10** with ethyl acrylate **12.11** gave aldehyde compound **12.12** in 90% yield. Cyclocondensation of aldehyde compound **12.12** gave Bosch chiral lactam **12.9** in 55% yield. Reductive removal of chiral lactam **12.9** using titanium (IV) chloride/ triethylsilane gave product in 81% yield subsequent reacted with sodium/ammonia to afford *δ*-lactam compound **12.13** in 71% yield. Boc-protection of *δ*-lactam gave protected compound **12.14** in 87% yield. Sharpless *α,β*-unsaturation of *δ*-lactam **12.14** gave *α,β*-unsaturated *δ*-lactam **12.15** in 76% yield. Michael addition of *α,β*-unsaturated *δ*-lactam **12.15** using vinyl Grignard reagent and copper (I) cyanide gave *trans*-substituted compound **12.16** in 75% yield. Reduction of lactam **12.16** gave cyclic enamine **12.17** in 75% yield. Tautomerization of cyclic enamine **12.17** gave cyclic imine **12.8**. Carreira's [3+2] ring-expansion reaction of imine **12.8** with cyclopropyl spirooxindole gave cyclic spirooxindole **12.6** in 68% yield over 2 steps. Hydroboration/oxidation of cyclic spirooxindole **12.6** gave primary alcohol **12.18** in 50% yield. IBX oxidation of primary alcohol **12.18** gave aldehyde **12.1** in 64% yield. Pinnick oxidation followed by esterification of aldehyde **12.1** gave intermediate **12.19** in 70% yield over 2 steps. Claisen condensation followed by methyl esterification of intermediate **12.19** gave (+)-Isorhynchophylline in 15% yield. Isomerization of (+)-Isorhynchophylline gave (-)-Rhynchophylline in 55% yield.

Key reaction for asymmetric total syntheses of Rhynchophylline and Isorhynchophylline were obtained by [3+2] ring-expansion reaction, cyclocondensation, Claisen condensation, methyl esterification, Hydroboration/oxidation, IBX oxidation and Pinnick oxidation. The asymmetric total syntheses of Rhynchophylline and Isorhynchophylline were achieved in 17 and 16 total steps respectively. The asymmetric total synthesis of (-)-Rhynchophylline was achieved in 17 steps in longest linear sequence, 0.0013% overall yield. The asymmetric total synthesis of (+)-Isorhynchophylline was achieved in 16 steps in longest linear sequence, 0.0024% overall yield (Scheme 121).

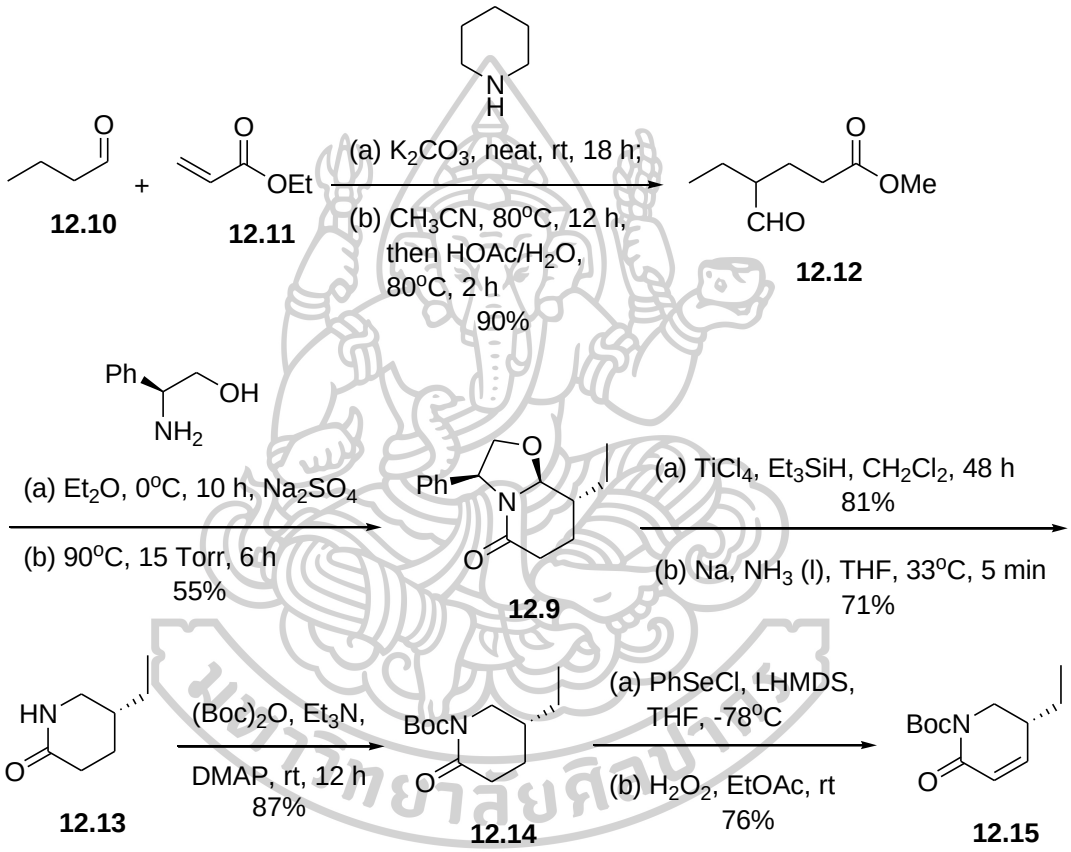

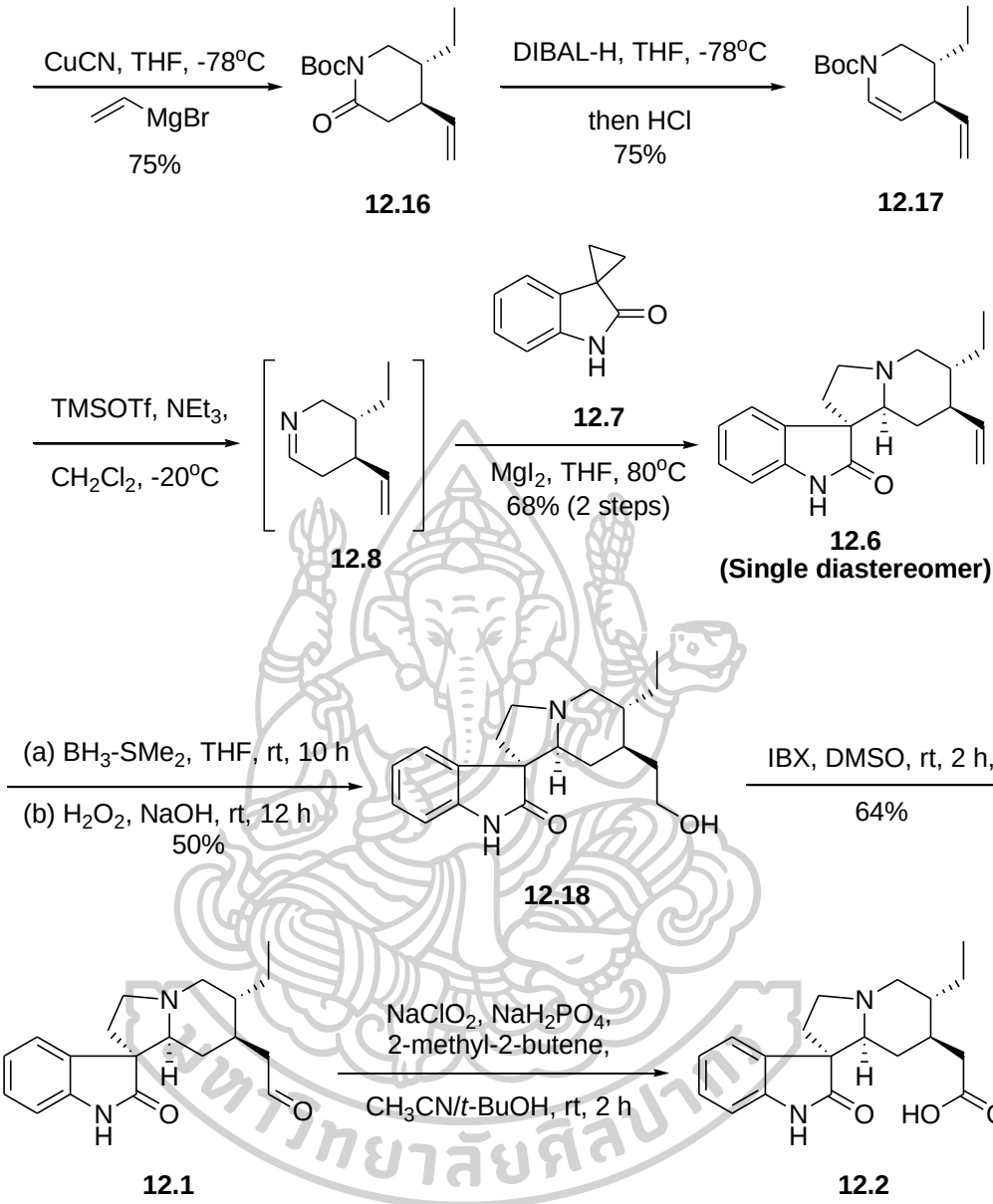
CuCN, THF, -78°C
MgBr
75%
BocN
O
12.16
DIBAL-H, THF, -78°C
then HCl
75%
BocN
12.17
TMSOTf, NEt3,
CH2Cl2, -20°C
N
12.8
O
N
H
12.7
MgI2, THF, 80°C
68% (2 steps)
N
H
O
12.6
(Single diastereomer)
(a) BH3-SMe2, THF, rt, 10 h
(b) H2O2, NaOH, rt, 12 h
50%
N
H
OH
12.18
IBX, DMSO, rt, 2 h,
64%
N
H
O
12.1
NaClO2, NaH2PO4,
2-methyl-2-butene,
CH3CN/t-BuOH, rt, 2 h
HO
12.2

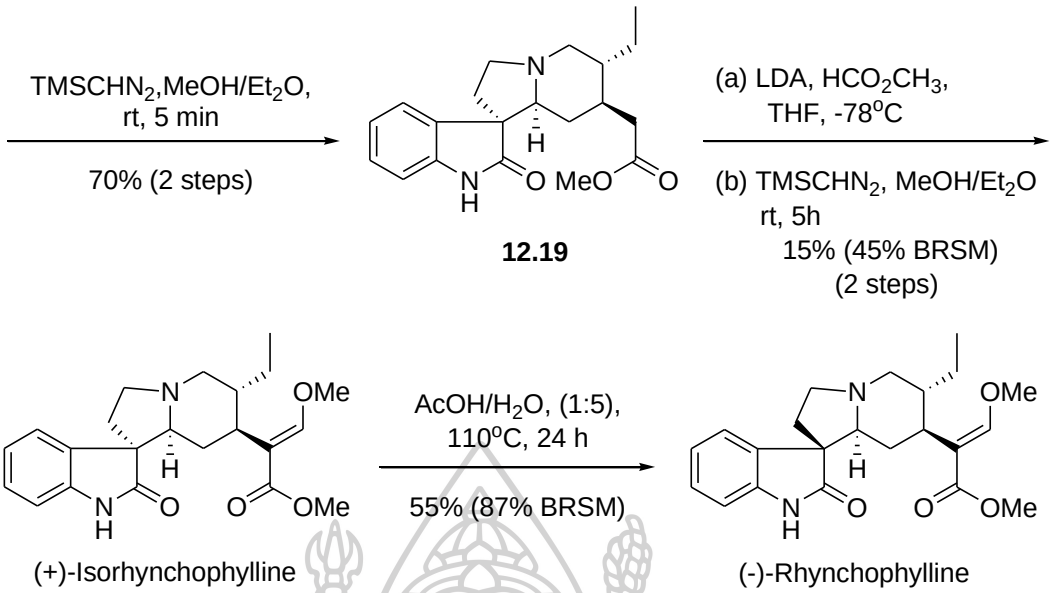

Scheme 121 Asymmetric total syntheses of Rhynchophylline and Isorhynchophylline by Rongbiao Tong and coworker

History for synthesis of Hirsutine

Lounasmaa's Racemic Synthesis of Hirsutine (1998)

The publication of Mauri Lounasmaa and co-workers described development toward the synthesis of Hirsutine in 1998. The accomplishment of the synthetic path rested on the use of alkylation, cyclization, 1,4-addition and Claisen rearrangement. In the retrosynthetic analysis of Hirsutine would arise from diene compound **13.7** by Claisen rearrangement. Diene compound **13.7** was obtained from *α,β*–unsaturated alcohol compound **13.6** by 1,4-addition. The *α,β*–unsaturated alcohol compound **13.6** was synthesized from *α,β*–unsaturated ketone compound **13.4** via reduction. The indoloquinolizidine compound **13.4** was obtained from pyridinium bromide compound **13.3** by cyclization. The pyridinium bromide compound **13.3** would be formed from the components of tryptophyl bromide compound **13.2** and 3-ethylpyridine compound **13.1** by alkylation (Scheme 122) (110).

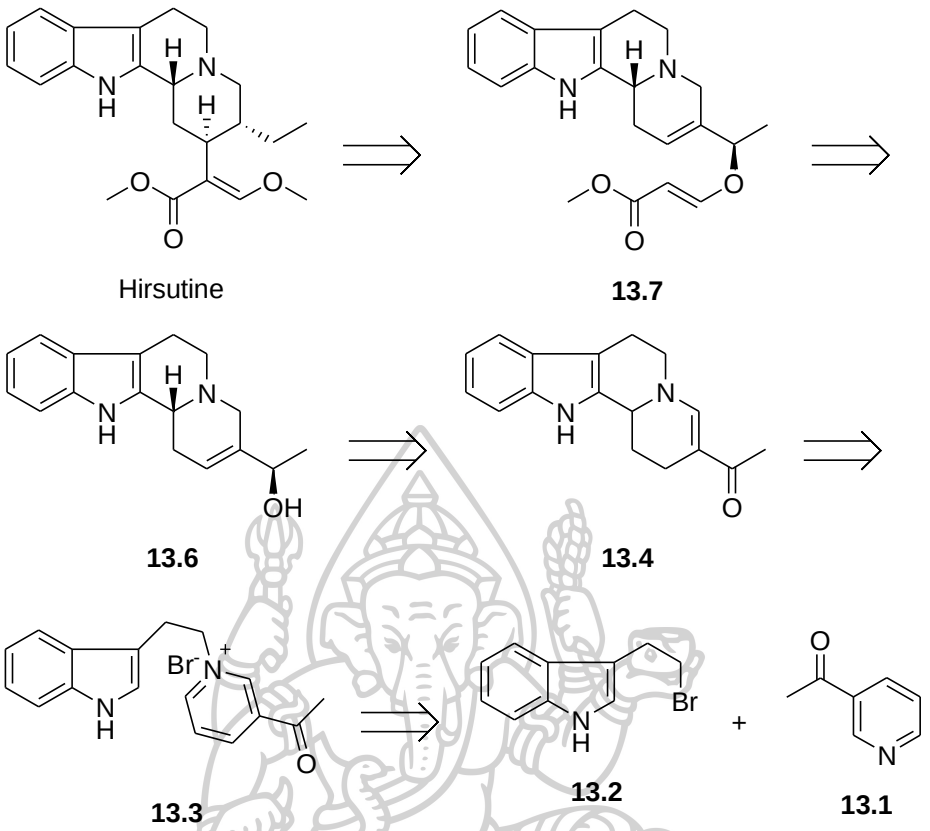

Scheme 122 Retrosynthetic analysis of Hirsutine by Mauri Lounasmaa and coworker

Total synthesis of Hirsutine was published by Mauri Lounasmaa and coworkers. Alkylation between 3-ethylpyridine compound **13.1** and tryptophyl bromide compound **13.2** generated pyridinium bromide compound **13.3** in 95% yield. Cyclization of pyridinium bromide compound **13.3** using sodium dithionite in methanol and water provided indoloquinolizidine compound **13.4** in 45% yield. The reaction of indoloquinolizidine compound **13.4** with palladium on activated charcoal and maleic acid followed by sodium perchlorate generated pyridinium perchlorate compound **13.5** in 60% yield. Reduction of pyridinium perchlorate compound **13.5** in the presence of sodium borohydride afforded 1:1 diastereomeric ratio of indoloquinolizidine compound **13.6** in 90% yield. The 1,4-addition of *α*,*β*–unsaturated alcohol compound **13.6** with methyl prop-2-ynoate using *N*-methylmorpholine gave diene compound **13.7** in 92% yield. Claisen rearrangement of diene compound **13.7** produced 5:4 diastereomeric ratio of indoloquinolizidine compound **13.8** and **13.9** in 32% yield. It is difficult to separate of the diasereomer of indoloquinolizidine compound **13.8** and **13.9**. The mixture of indoloquinolizidine compound **13.8** and **13.9** was treated with di-*tert*-butyl dicarbonate (Boc_2O) generated pure stereoisomer of Boc protected compound **13.10** in 40% yield. The reaction of Boc protected compound **13.10** with trimethoxymethane gave core structure of Hirsutine in 25% yield. Hydrogenation of the ethylidine group constructed 1:1 diastereomeric ratio of Hirsutine in 72% yield (Scheme 123).

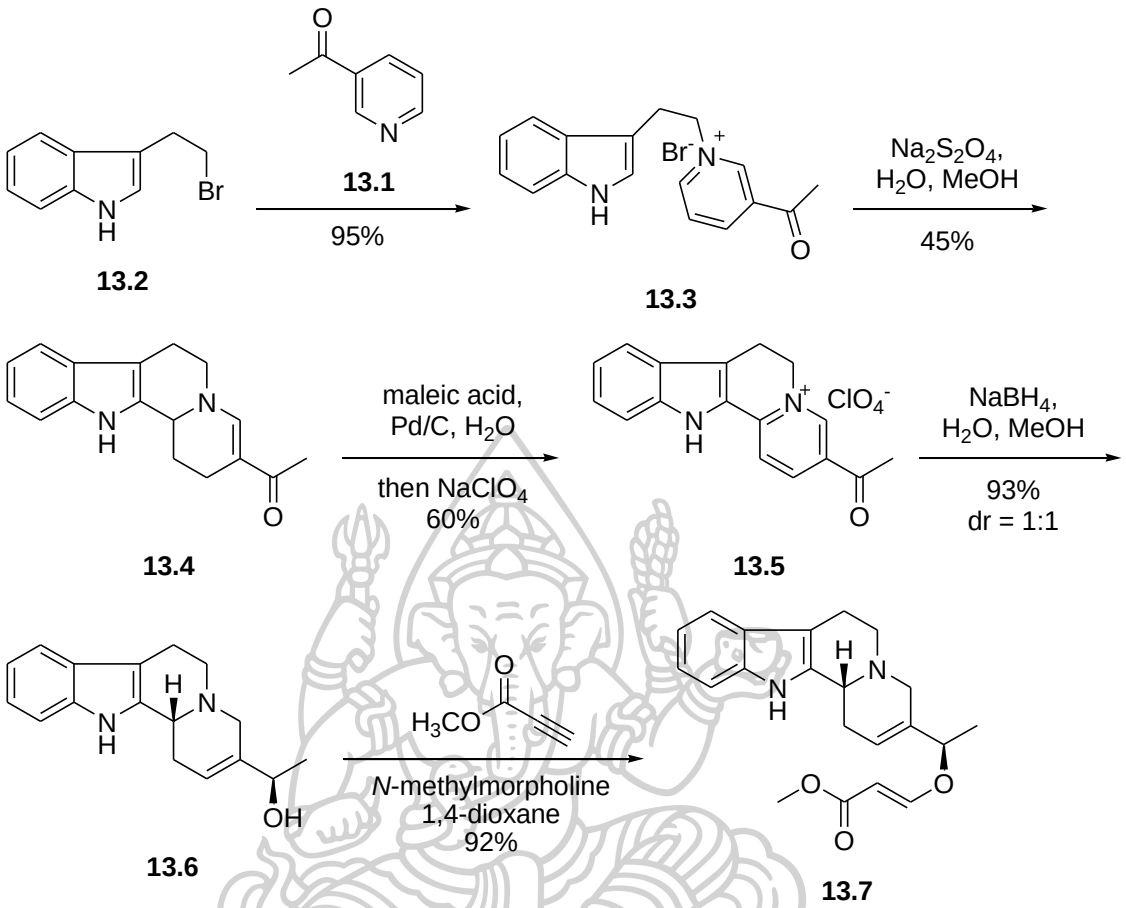
13.1
95%
13.2
13.3
Na2S2O4,
H2O, MeOH
45%
maleic acid,
Pd/C, H2O
then NaClO4
60%
13.4
13.5
NaBH4,
H2O, MeOH
93%
dr = 1:1
13.6
H3CO
N-methylmorpholine
1,4-dioxane
92%
13.7

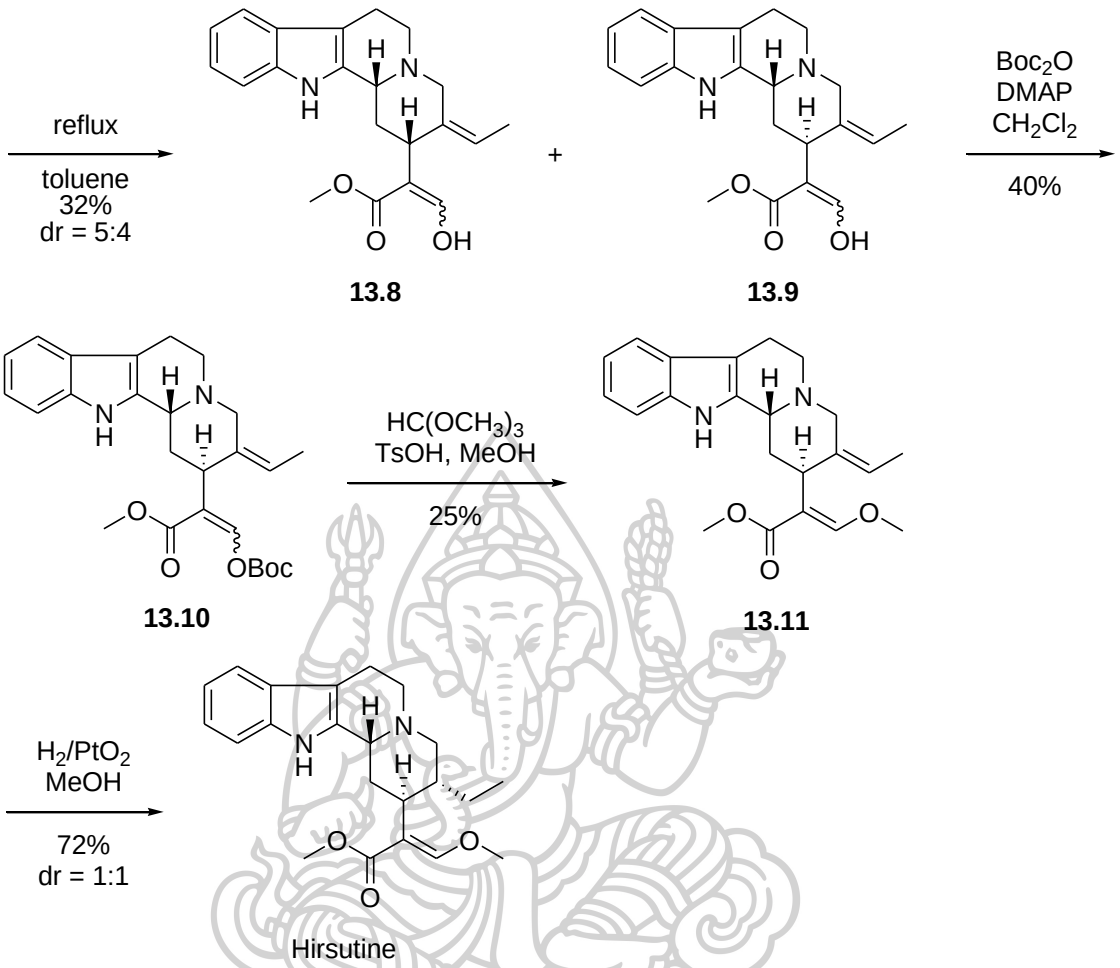

Scheme 123 Total synthesis of Hirsutine by Mauri Lounasmaa and coworker

Ohyun Kwon's Total synthesis of (±)-Hirsutine: Application of Phosphine-Catalyzed Imine–Allene [4+2] Annulation (2012)

Another indole alkaloid natural product Hirsutine is indoloquinolizidine alkaloid isolated from the plant family *Hirsutus* and *Uncaria*. Hirsutine demonstrated to utilize central depressive and vasodilatory effects as protective effects against neuronal death in cultured rat cerebellar granule cells. Hirsutine showed antihypertensive, negative chronotropic and antiarrhythmic activity. Hirsutine involved the attention of the medical community for its ability to inhibit the growth of influenza A virus (subtype H3N2) with an EC_{50} value of 0.40-0.57 μg/mL. Hirsutine is 10-20 times more powerful than the clinically used drug ribavirin.

The publication of Qhyun Kwon and co-worker reported evolution toward the synthesis of Hirsutine in 2012. The success of the synthetic route rested on the use of phosphine-catalyzed [4+2] annulation as key reaction, Michael addition and selective reduction. In the retrosynthetic analysis of Hirsutine would arise from diester compound **14.4** by selective reduction and enol methylation. Alkene compound **14.4** was obtained from trimester compound **14.5** by selective reduction and methylation.

Triester compound **14.5** was synthesized from tricyclic compound **14.7** via conjugate addition and C ring formation. Tricyclic compound **14.7** would be formed from the components of ethyl α-methylallenoate compound **14.8** and indolylimine compound **14.9** by phosphine-catalyzed [4+2] annulation as the key reaction (Scheme 124) (111).

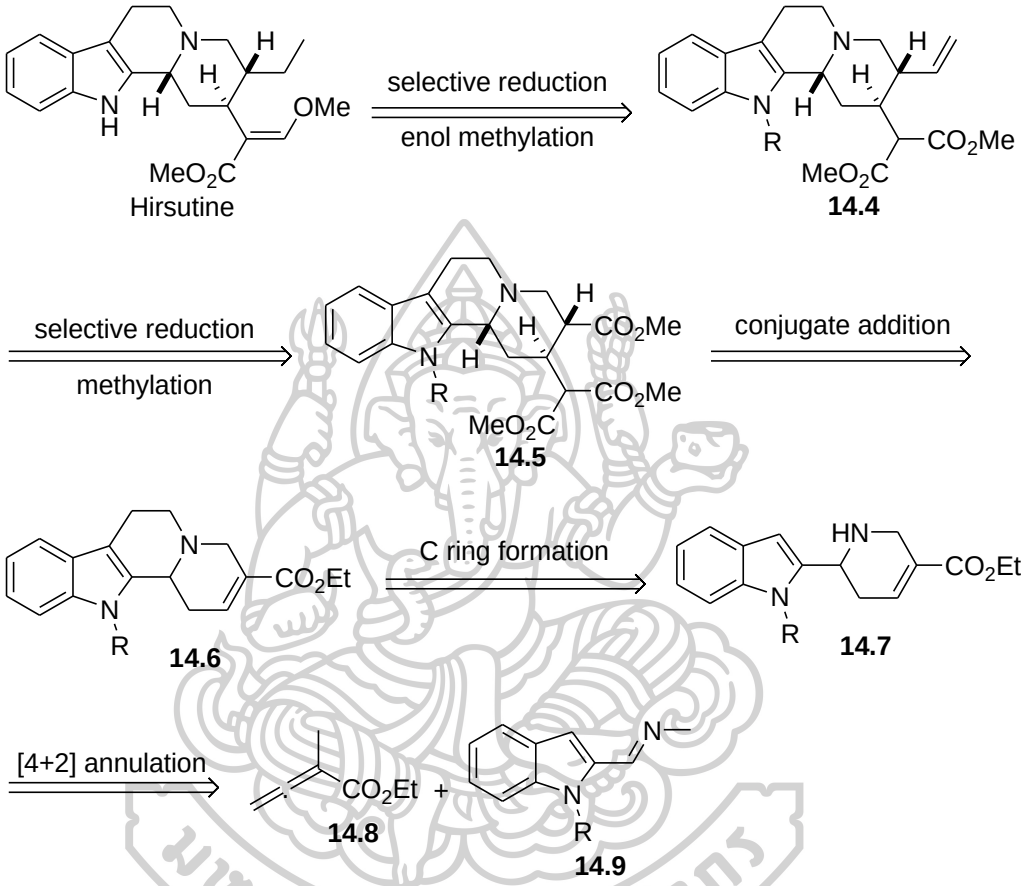

Scheme 124 Retrosynthetic analysis of Hirsutine by Ohyun Kwon and coworker

Total synthesis of Hirsutine was published by Ohyun Kwon and coworker. First, Boc protoection of indole 2-carboxaldehyde compound **14.10** gave *N*-Boc protected aldehyde compound **14.11** in 98% yield. Next, reaction of *N*-Boc-protected aldehyde compound **14.11** with *o*-nitrobenzenesulfonamide ($NsNH_2$) in the presence of triethyl amine (Et_3N) and catalytic titanium tetrachloride ($TiCl_4$) generated *N*-(*o*-nosyl)imine compound **14.12** followed by phosphine-catalyzed annulation of *N*-(*o*-nosyl)imine compound **14.12** with ethyl α-methylallenoate compound **14.8** using tributylphosphine catalyst (PBu_3) to produce tricyclic compound **14.13** in 73% yield over two steps. Deprotection of *N*-Boc protected compound **14.13** in the presence of silicon dioxide (SiO_2) reflux with toluene produced tricyclic compound **14.14** in 90%yield. Acylation at the C3 position of tricyclic compound **14.14** with oxalyl chloride followed by reduction of the resulting keto acid chloride with borane provided the required tryptophol compound **14.15** in 96% yield over 2 steps. The nosyl group of tryptophol compound **14.15** removed in the presence of thiophenol

(PhSH) and potassium carbonate (K_2CO_3) in acetonitrile (MeCN) at 50^oC produced tetracyclic compound **14.16** in quantitative yield. Formation of the C-ring through intramolecular *N*-alkylation reaction proceeded under the influence of iodine (I_2) and triphenylphosphine (PPh_3) to produce the tetracyclic compound **14.17** in 96% yield. Michael addition between tetracyclic compound **14.17** and dimethyl malonate anion generated triester compound **14.18** in 89% yield. Selective reduction of triester compound **14.18** using diisobutylaluminum hydride (DIBALH) followed by Wittig olefination reaction to give terminal alkene compound **14.20** in 41%yield. Hydrogenation of terminal alkene compound **14.20** gave core structure of Hirsutine **14.21** in 99% yield. Selective reduction of tetracyclic compound **14.21** followed by methylation generated Hirsutine in 31%yield over 2 steps. The total synthesis of Hirsutine was achieved in 14 total steps, 14 steps in longest linear sequence, 6.64% overall yield of Hirsutine (Scheme 125).

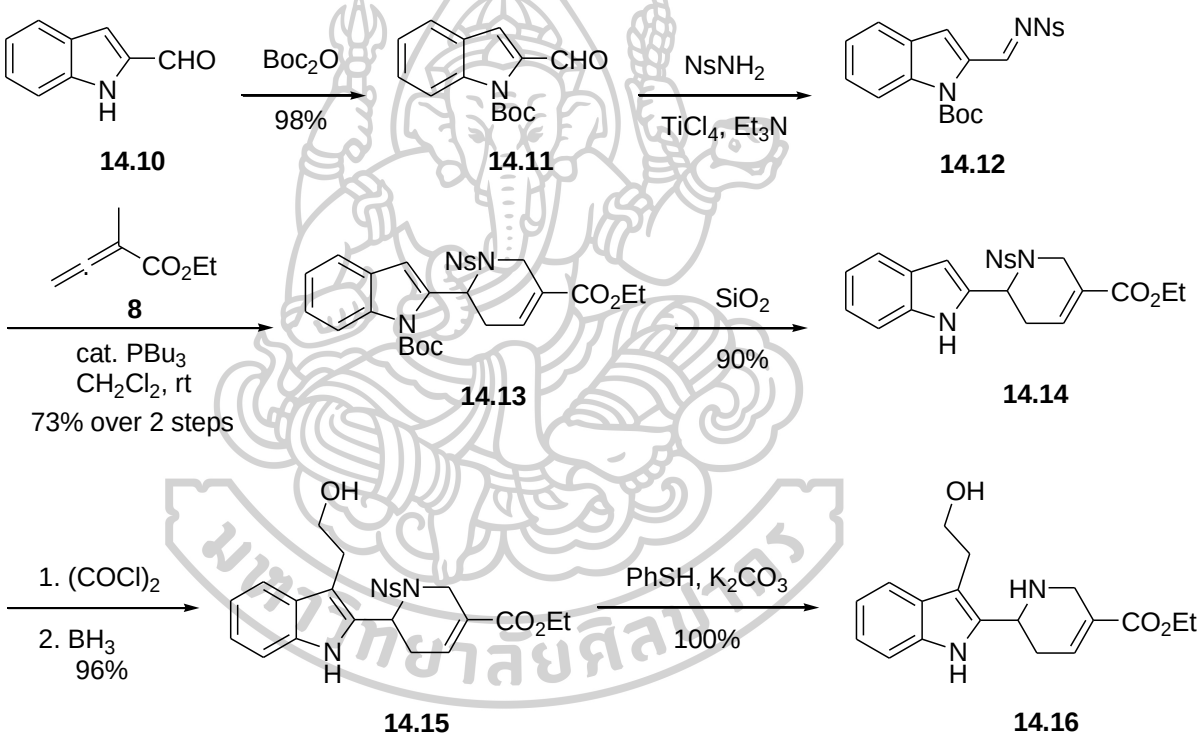

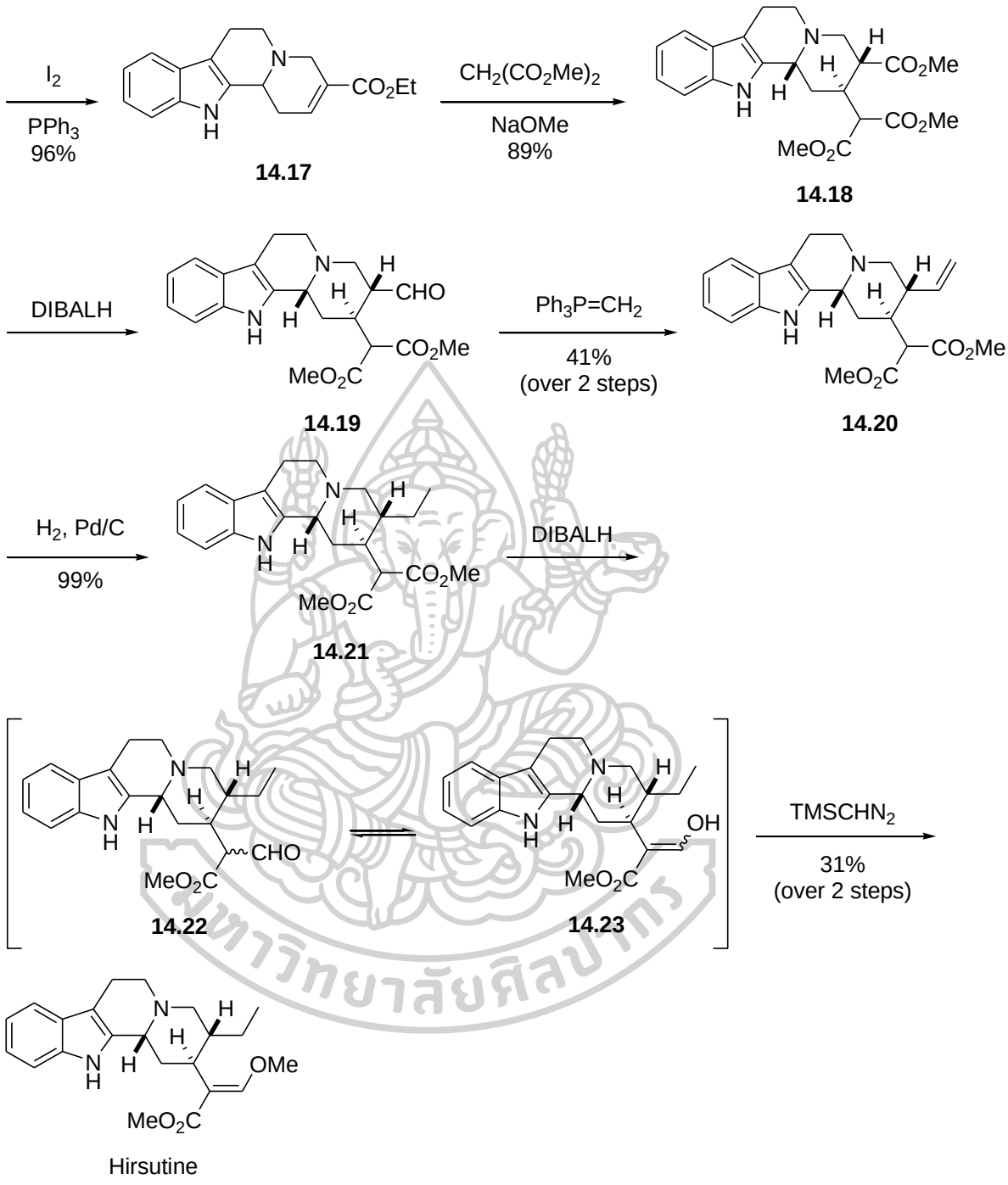

Scheme 125 Total synthesis of Hirsutine by Ohyun Kwon and coworker

Biological activity for spiroindolizidine-oxindole structure

Meshram's 1,3-Dipolar cycloaddition reactions for the synthesis of novel oxindole derivatives and their cytotoxic properties (2017)

Combinatorial chemistry is a chemical synthesis method that allows the synthesis of a large number of compounds (tens to thousands or even millions) in a single process. The compound libraries can be mixed. It groups of single compounds

or chemical structures created by computer software. Combinatorial chemistry can synthesize small molecules in organic chemistry (Figure 25) (112).

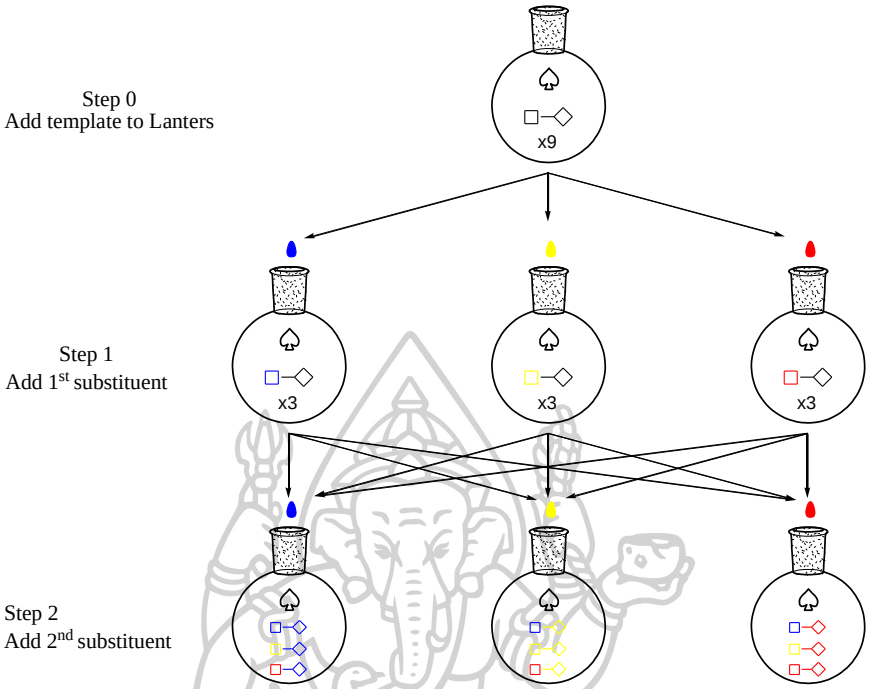

Figure 25 Flow diagram of the combinatorial chemistry synthesis in organic chemistry

Cancer is a major health concern increasing in the number of patients throughout the world over the past decade. According to statistics, cancer is the second important cause of death in human more than cardiovascular disease. The multicomponent reaction between isatin, amino acid, but-2-ynedioates and phenacyl bromide was developed in the presence of microwave irradiation in aqueous medium. The 1,3-dipolar cycloaddition reaction synthesized spirooxindole derivative compounds were estimated for their anticancer activity against three human cancer cell lines such as MCF-7 (breast), A549 (lung) and HeLa cervical. There are several spirooxindoles core structure are found in natural product which showed better biological activity. The reaction for the synthesis of isatin based spiro compounds using microwave. The spirooxindole compounds were directed toward examining the feasibility of procedures and the optimization of the reaction conditions. The systematically varying key reaction conditions for synthesis of spirooxindole to effect the multicomponent reaction between various isatins **15.1**, but-2-ynedioates **15.2** and amino acids **15.3** as typical substrates (Figure 26).

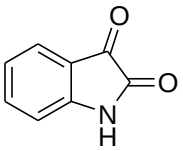

15.1{1}

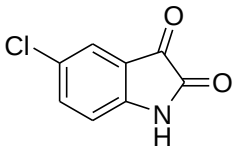

15.1{2}

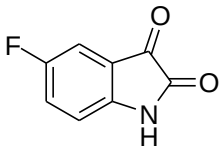

15.1{3}

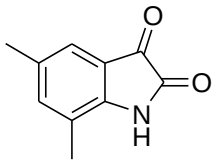

15.1{4}

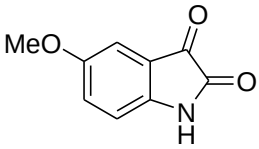

15.1{5}

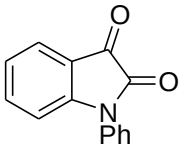

15.1{6}

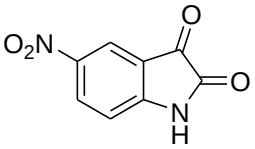

15.1{7}

Chemical set 15.1 Diversity reagents **{1-7}**

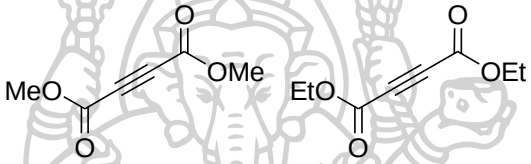

15.2{1} **15.2{2}**

Chemmical set 15.2 Diversity reagents **{1-2}**

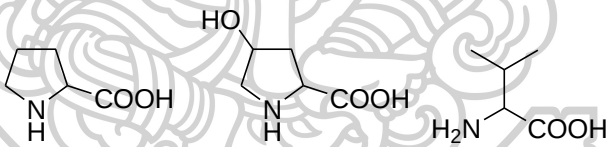

15.3{1} **15.3{2}** **15.3{3}**

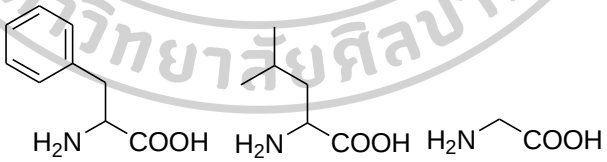

15.3{4} **15.3{5}** **15.3{6}**

Chemical set 15.3 Diversity reagents **{1-6}**

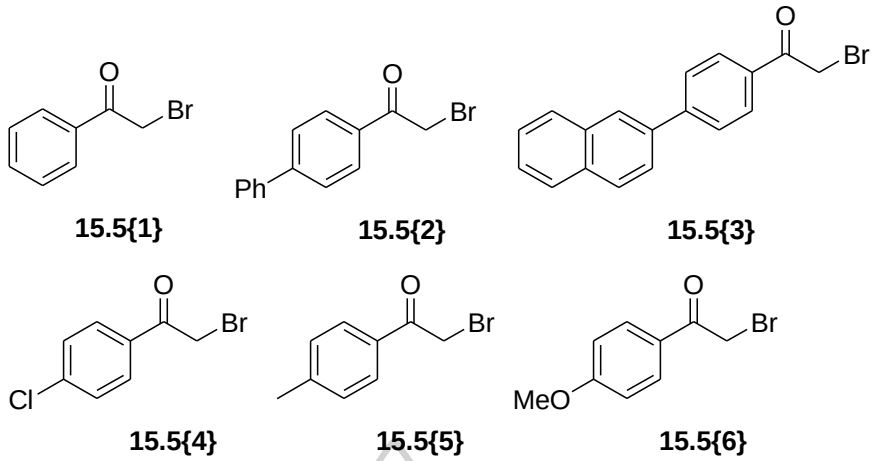

Chemical set 5 Diversity reagents **{1-6}**

Figure 26 Chemical sets: Isatin Chemical set **15.1**, but-2-ynedioate Chemical set **15.2**, amino acid Chemical set **15.3** and phenacyl bromide Chemical set **15.5**.

The 1,3-dipolar cycloaddition of multicomponent of isatin, amino acid, but-2-ynedioates and phenacyl bromide has been developed. The reaction used microwave irradiation in aqueou solution. The multicomponent reaction shows a broad substrate scope gave spirooxindole compound with excellent yields and shorter reaction time. The reaction was examined in water, methanol, ethanol, dichloromethane, tetrahydrofuran, dimethylformamide, acetonitrile, dimethyl sulfoxide, toluene and 1,4-dioxane at various temperatures and times. Water was found to be best solvent for the synthesis of spirooxindole derivatives compound **15.4** and **15.6**. The optimal temperature and reaction time for the 1,3-dipolar cycloaddition of multicomponent reaction was found to be 100°C for 15 minutes and 80°C for 10 minutes to synthesis spirooxindole derivatives compound **15.4** and **15.6**, respectively (Scheme 126).

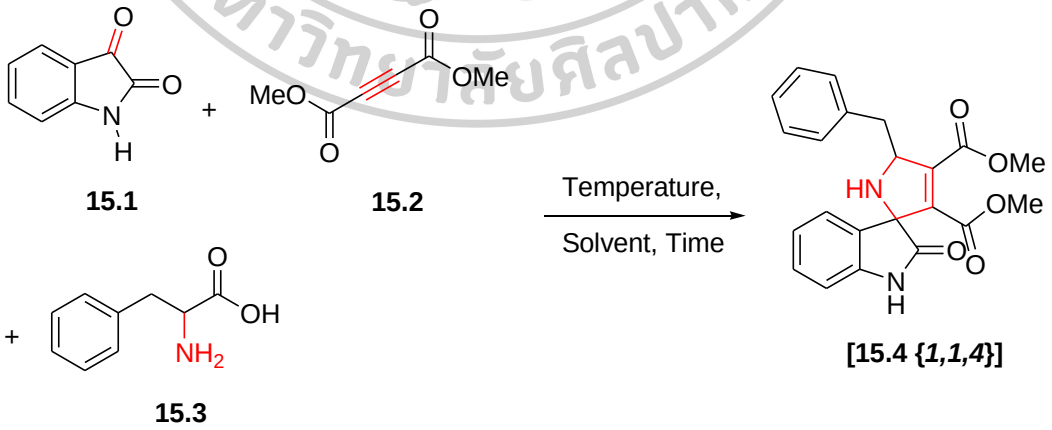

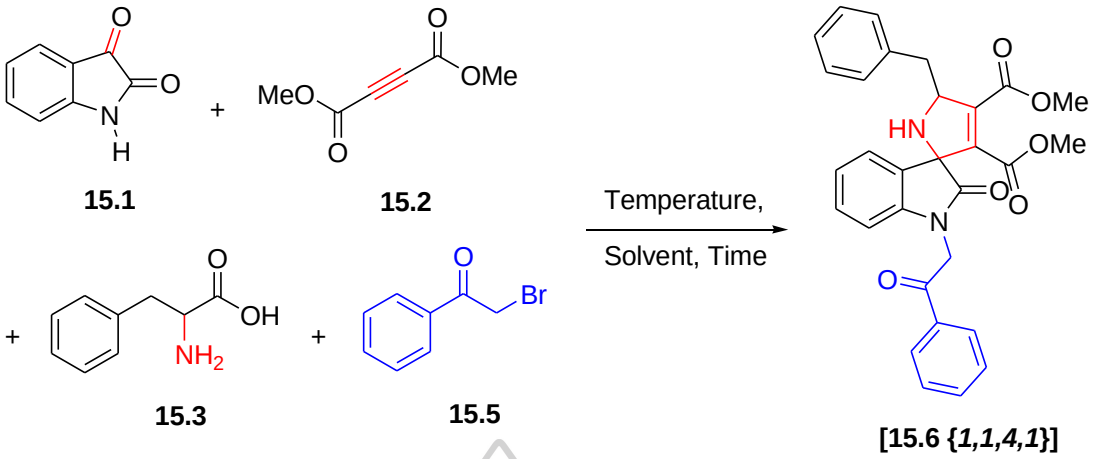

15.1 **15.2** **15.3** **15.5** **[15.6 {*1,1,4,1*}]**

entry	solvent		temp (°C)		time (min)		yield (%)	
	comp 15.4 {1,1,4}	comp 15.6 {1,1,4,1}	comp 15.4 {1,1,4}	comp 15.6 {1,1,4,1}	comp 15.4 {1,1,4}	comp 15.6 {1,1,4,1}	comp 15.4 {1,1,4}	comp 15.6 {1,1,4,1}
1	1,4-dioxane	water	80	70	20	20		27
2	toluene	water	100	90	15	15		40
3	dimethylformamide	water	110	100	15	15	20	91
4	tetrahydrofuran	water	80	110	20	15	15	85
5	ethanol	methanol	90	100	20	15	30	60
6	dimethyl sulfoxide	ethanol	110	90	18	15	20	20
7	dichloromethane	1,4-dioxane	60	60	10	15	28	
8	methanol	dimethylformamide	80	70	15	15	55	
9	water	dimethyl sulfoxide	110	90	15	15	70	
10	water	dichloromethane	100	100	10	10	80	
11	water	toluene	80	110	10	10	89	
12	water		80		15		75	
13	water		70		20		40	
14	water		50		15		26	

Scheme 126 Optimization of reaction conditions for three- and four-component for spirooxindole synthesis

The 1,3-dipolar cycloaddition of multicomponent reaction mechanism for the spirooxindole synthesis from four-component compound. At first, the condensation reaction of *α*-amino acid compound **15.3** with isatin compound **15.1** gave the imine intermediate by eliminating carbondioxide. Next, the 1,3-dipolar cycloaddition reaction takes place between the imine intermediate and but-2-ynedioate compound **15.2** to generate spirooxindole core structure compound **15.4**. Last, the spirooxindole compound **15.4** reacted with phenacyl bromide compound **15.5** to provide spirooxindole compound derivative compound **15.6** (Scheme 127).

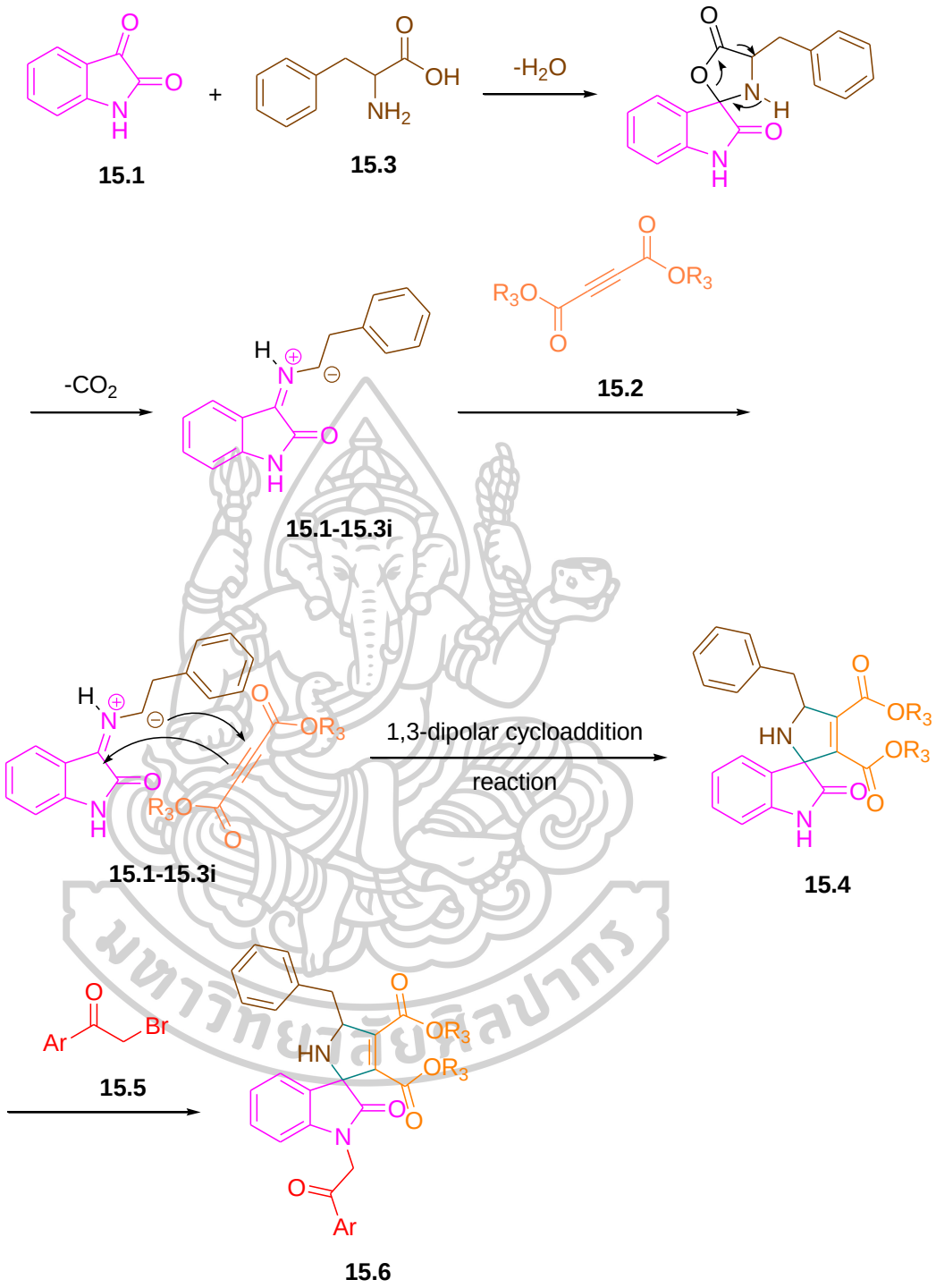

Scheme 127 Mechanism for the 1,3-dipolar cycloaddition reaction of multicomponent component for synthesis spirooxindole compound derivative

The optimized conditions for the 1,3-dipolar cycloaddition reaction of multicomponent for synthesis spirooxindole compound derivative. The effect of the different substituents on the aromatic ring of isatin was verified. The electron-donating substrates compound such as 5,7-dimethyl isatin, 5-methoxy isatin generated

spirooxindole compound derivative in high yields (Scheme 128, compound **15.4**(20) and **15.4**(20). The isatin derivative containing halogen group gave spirooxindole compound derivative in moderate yields (Scheme 128, compound **15.4**(20), **15.4**{3,1,1}, **15.4**{2,2,1}, **15.4**{3,2,1}, **15.4**{2,1,3}, **15.4**{3,1,3}, **15.4**{3,2,3}, **15.4**{2,1,4}, **15.4**{3,2,4}, **15.4**{2,2,4}, **15.4**{3,1,4}, **15.4**{3,1,5}, **15.4**{2,1,5}, **15.4**{2,2,5}, **15.4**{3,2,5}, **15.4**{1,1,5}, and **15.4**{1,1,6}). The 1,3-dipolar cycloaddition reaction of multicomponent which isatin containing halogen group generated spirooxindole compound **15.4**{2,1,1}, **15.4**{3,1,1}, **15.4**{2,2,1}, **15.4**{3,2,1}, **15.4**{2,1,3}, **15.4**{3,1,3}, **15.4**{3,2,3}, **15.4**{2,1,4}, **15.4**{3,2,4}, **15.4**{2,2,4}, **15.4**{3,1,4}, **15.4**{3,1,5}, **15.4**{2,1,5}, **15.4**{2,2,5}, **15.4**{3,2,5}, **15.4**{1,1,5} and **15.4**{1,1,6} in moderate yields. The reaction of *N*-protected isatin gave the spirooxindole compound derivative compound **15.4**{6,2,3} and **15.4**{6,2,4} in high yield as compared to isatin having free N-H group. The reaction of isatin with phenyl alanine and but-2-ynedioates provided a enhanced yield compared to other amino acids such as proline, isoleucine, valine and glycine (Scheme 128).

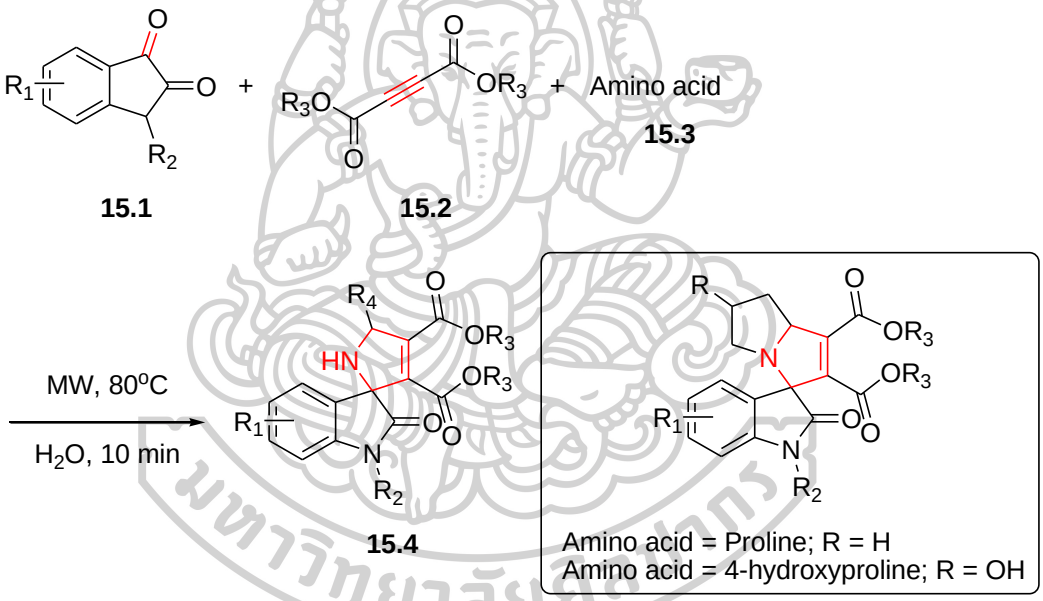

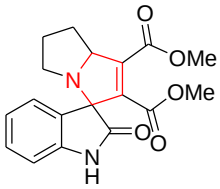

15.4{*1,1,1*}; 84%

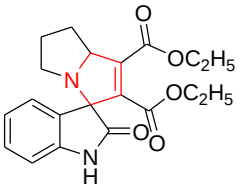

15.4{*1,2,1*}; 82%

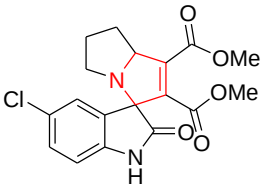

15.4{*2,1,1*}; 73%

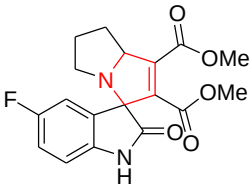

15.4{*3,1,1*}; 75%

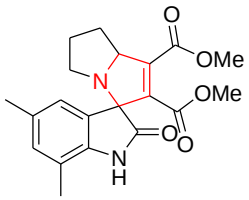

15.4{*4,1,1*}; 90%

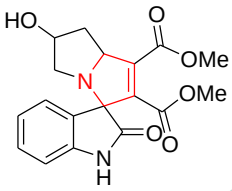

15.4{*1,1,2*}; 80%

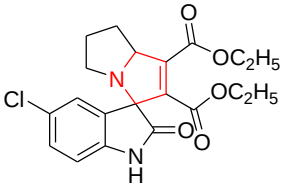

15.4{*2,2,1*}; 85%

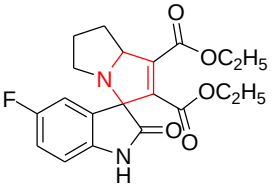

15.4{*3,2,1*}; 71%

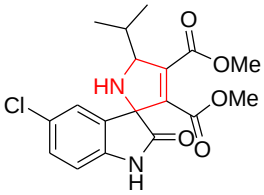

15.4{*2,1,3*}; 83%

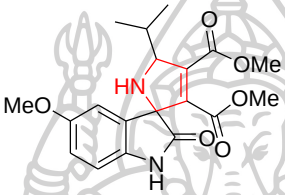

15.4{*5,1,3*}; 93%

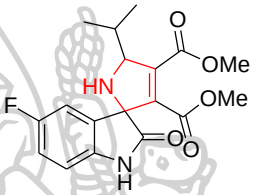

15.4{*3,1,3*}; 76%

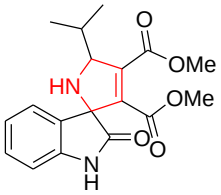

15.4{*1,1,3*}; 80%

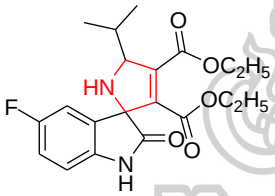

15.4{*3,2,3*}; 70%

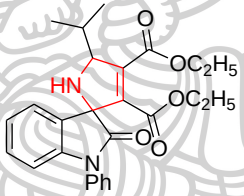

15.4{*6,2,3*}; 82%

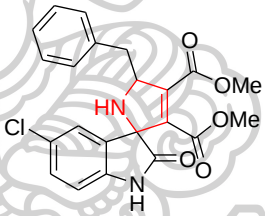

15.4{*2,1,4*}; 77%

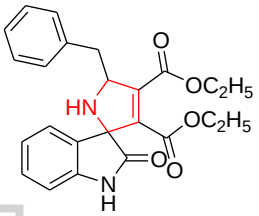

15.4{*1,2,4*}; 84%

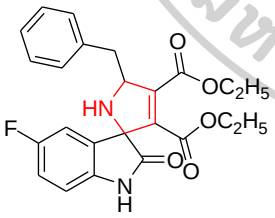

15.4{*3,2,4*}; 81%

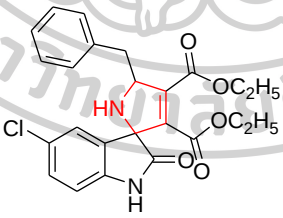

15.4{*2,2,4*}; 83%

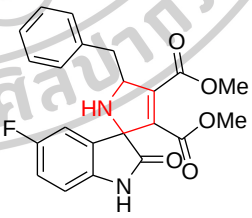

15.4{*3,1,4*}; 78%

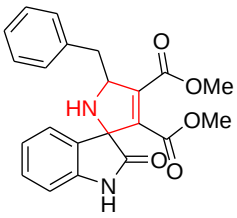

15.4{*1,1,4*}; 88%

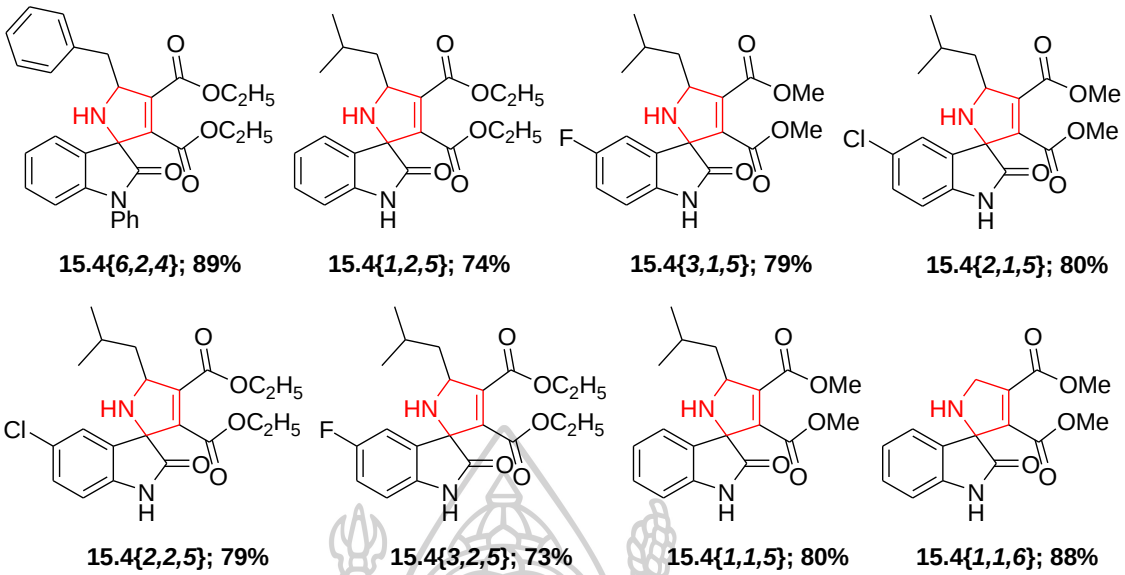

Scheme 128 Substrate scope of isatins, amino acids and but-2-ynedioates amines for the 1,3-dipolar cycloaddition of multicomponent synthesis of spirooxindole compound derivative

The 1,3-dipolar cycloaddition reaction of multicomponent which isatin derivatives having both electron-donating and electron-withdrawing groups. The spirooxindole derivative compounds **15.6**{3,1,4,2} and **15.6**{7,1,5,4}) related isatin bearing electron-withdrawing substituent's gave higher yields. Phenacyl bromide containing aryl group with electron-withdrawing substituent's gave spirooxindole derivative compounds **15.6**{1,1,5,6}, **15.6**{1,1,3,5} and **15.6**{1,1,1,5} in higher yields than electron-donating groups in spirooxindole derivative compounds **15.6**{1,1,5,6}, **15.6**{1,1,3,5} and **15.6**{1,1,1,5}). The 1,3-dipolar cycloaddition reaction of multicomponent was accomplished using *N*-alkylated isatin derivative compound, it did not provide any desired spirooxindole derivative compound. The 1,3-dipolar cycloaddition reaction of multicomponent resulted from different amino acids, proline generated the highest yield as compare to other amino acids of spirooxindole derivative compounds **15.6**{1,1,1,1}, **15.6**{1,1,1,3}, **15.6**{1,1,1,4}, **15.6**{1,1,1,5} and **15.6**{1,1,1,2} (Scheme 129).

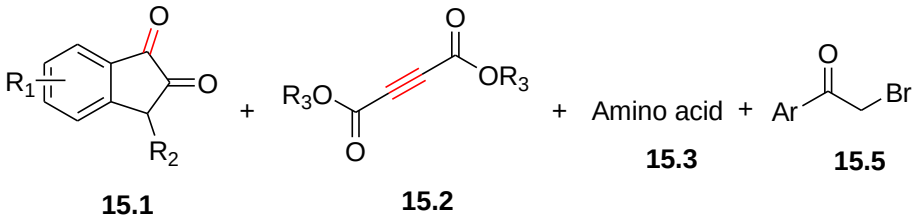

15.1 **15.2** **15.3** **15.5**

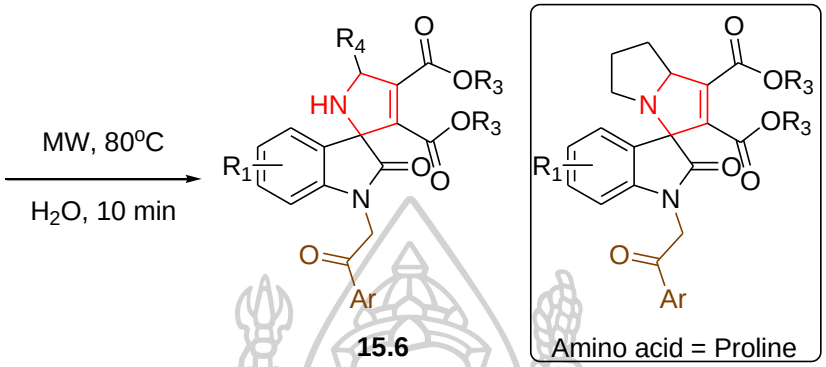

15.6

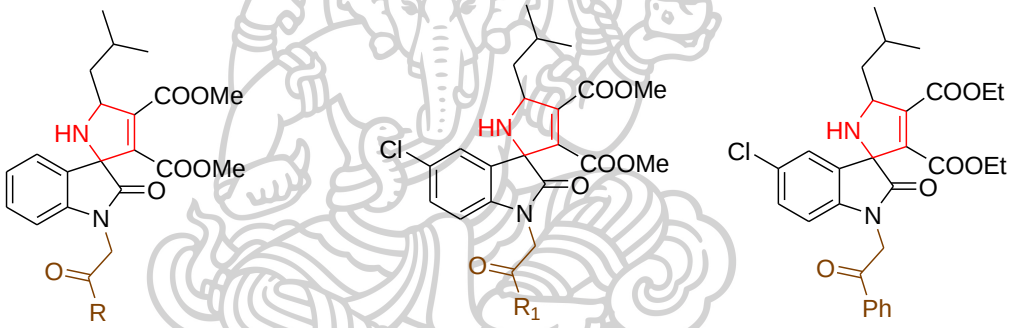

R = 4-Ph C_6H_4, 15.6{*1,1,5,2*}, 83%
R = C_6H_5, 15.6{*1,1,5,1*}, 85%
R = Napthyl, 15.6{*1,1,5,3*}, 88%
R = 4-Cl C_6H_4, 15.6{*1,1,5,4*}, 76%
R = 4-Me C_6H_4, 15.6{*1,1,5,5*}, 78%
R = 4-OMe C_6H_4, 15.6{*1,1,5,6*}, 70%

R_1 = 4-Cl C_6H_4, 15.6{*2,1,5,4*}, 80%
R_1 = C_6H_5, 15.6{*2,1,5,1*}, 80%

15.6{2,2,5,1}, 76%

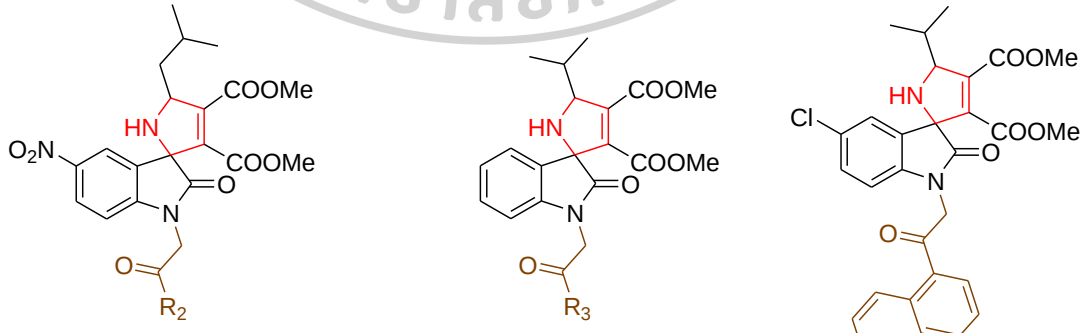

R_2 = 4-Cl C_6H_4, 15.6{*7,1,5,4*}, 81%
R_2 = 4-Ph C_6H_4, 15.6{*7,1,5,2*}, 86%
R_2 = Napthyl, 15.6{*7,1,5,3*}, 82%

R_3 = C_6H_5, 15.6{*1,1,3,1*}, 75%
R_3 = 4-Ph C_6H_4, 15.6{*1,1,3,2*}, 82%
R_3 = 4-Me C_6H_4, 15.6{*1,1,3,5*}, 73%
R_3 = Napthyl, 15.6{*1,1,3,1*}, 78%

15.6{2,1,3,3}, 78%

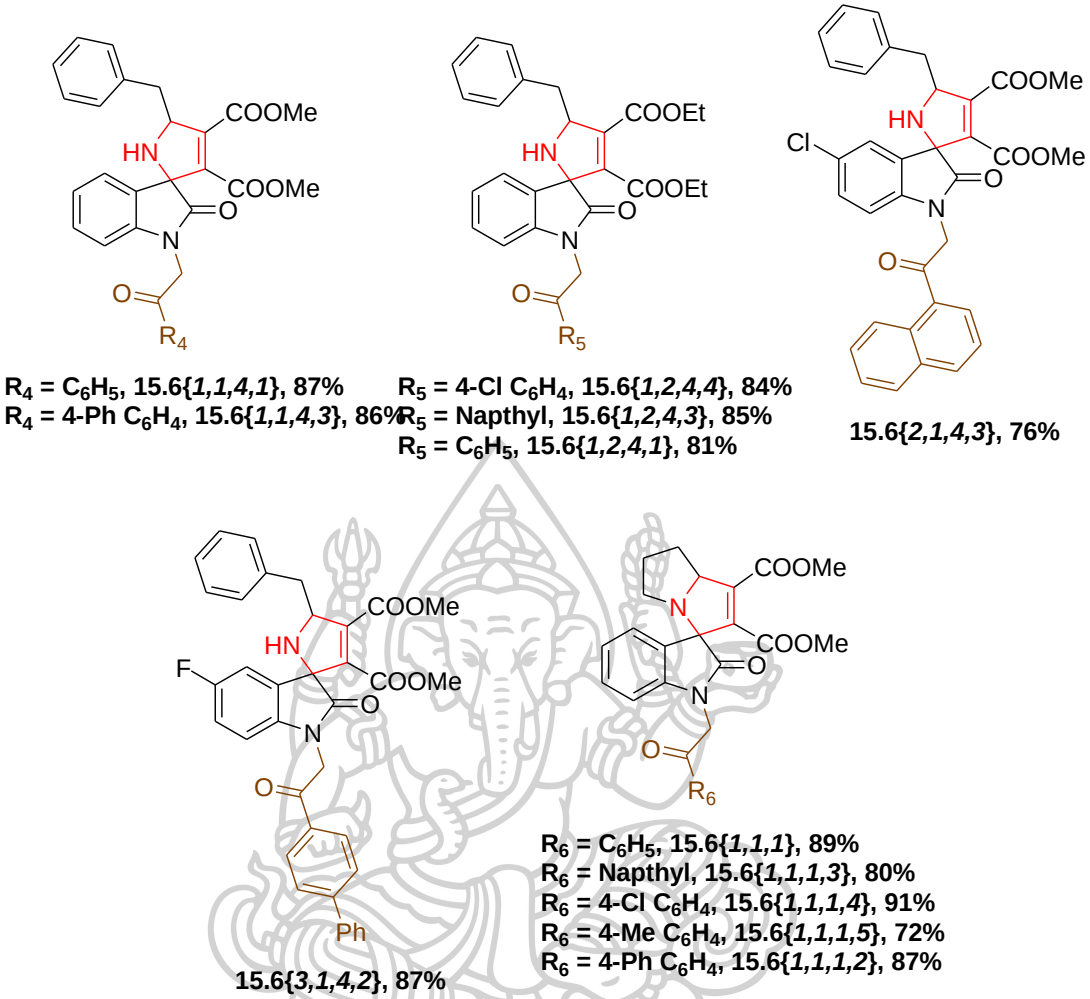

Scheme 129 Substrate scope for 1,3-dipolar cycloaddition reaction of multicomponent synthesis of *n*-substituted spirooxindole derivative

The relative configuration of spirooxindole compound **15.4**{2,1,1} and **15.6**{2,2,5,1} was clearly confirmed by X-ray diffraction, and those of the other spirooxindole compounds were realized on the basis of these consequences.

All the spirooxindole derivative compounds **15.4**{1,1,1}−**15.4**{6,2,4} were estimated for their anticancer activity in three human cancer cell lines, A549 (lung), HeLa (cervical) and MCF-7 (breast). All the spirooxindole derivative compounds exhibited good to potent activity against cancer cell lines. The spirooxindole derivative compounds **15.4**{1,2,1} and **15.4**{1,2,5} displayed significant activity against human lung cancer cell line, A549 with IC_{50} values 2.03 and 4.52 μM, respectively. The spirooxindole compound **15.4**{1,2,5} was found more potent against MCF-7 cancer cell line having IC_{50} 5.00 μM. The spirooxindole compound **15.4**{1,2,1} exhibited good activity against Hela cancer cell line IC_{50} values 8.3 μM. The reaction generated spirooxindole derivative compound in efficient from catalyst-free and base-free reaction using microwave irradiation in aqueous medium. This reaction has several advantages comprised: (i) water is used as the reaction solvent; (ii) high atom economy; (iii) catalyst free and (iv) broad substrate scope (Figure 27).

compound	IC_{50} (μ M)		
	MCF-7	A549	HeLa
15.4{1,1,1}	19.3	18.6	>50
15.4{1,1,2}	9.4	4.8	16.6
15.4{1,1,3}	25.3	19.5	38.6
15.4{1,1,4}	>50	31.4	43.0
15.4{1,1,5}	9.5	8.7	19.9
15.4{1,1,6}	31.2	34.6	40.7
15.4{1,2,1}	3.3	2.0	8.3
15.4{1,2,4}	17.0	10.0	12.5
15.4{1,2,5}	5.0	4.5	>50
15.4{2,1,1}	16.2	8.6	15.9
15.4{2,1,3}	>50	>50	>50
15.4{2,1,4}	>50	>50	>50
15.4{2,1,5}	24.5	18.7	30.3
15.4{2,2,1}	>50	36.1	>50
15,4{2,2,4}	22.0	15.8	>50
15.4{2,2,5}	>50	40.6	>50
15.4{3,1,1}	14.5	16.9	17.0
15.4{3,1,3}	25.4	21.3	26.3
15.4{3,1,4}	24.9	18.3	27.8
15.4{3,1,5}	26.6	10.3	29.1
15.4{3,2,1}	>50	54.1	>50
15.4{3,2,3}	>50	42.2	47.3
15.4{3,2,4}	16.3	10.7	39.9
15.4{3,2,5}	>50	>50	>50
15.4{4,1,1}	19.3	18.6	>50
15.4{5,1,3}	20.6	29.2	20.1
15.4{6,2,3}	>50	>50	>50
15.4{6,2,4}	>50	27.7	>50
doxorubicin	1.6	1.8	1.9
sunitinib	25.4	7.9	>30

Figure 27 The IC_{50} values (in μM) for spirooxindole derivative compounds in selected human cancer cell lines

Shailja Singh & Subhabrata Sen's Spiro[pyrrolidine-3,3´-oxindole] as potent anti-breast cancer compounds: Their design, synthesis, biological evaluation and cellular target identification (2016)

The spiro[pyrrolidine-3,3´-oxindole] compound is core structure in number of alkaloids with biological activities. The publication of Shailja Singh and Subhabrata Sen design and synthesis of a library of spiro[pyrrolidine-3, 3´-oxindole] compound

derivative compound which proved excellent inhibitory activity against the proliferation of MCF-7 breast cancer cells. There are several medical treatments for breast cancer included mono and combination drug therapies, radiation techniques and surgical, cancer vaccines and novel targeted therapies. Many breast cancer drugs contained amoxifen™, Letrozole™, Docetaxyl™ and etc. A variety of natural product skeletons the spiro[pyrrolidine-3,3´-oxindole] skeleton forms as well as non-natural compounds that exhibits evident anticancer activities which family of natural products were first isolated from plants *Rubiacae* and *Apocynaceae* family. Interesting therapeutic characteristics of spiro[pyrolidine-3,3´-oxindole] skeleton creates it an attractive synthetic by Pictet Spengler reaction of tryptamine and an aldehyde and oxidative ring contraction of tetrahydro-*β*–carbolines in early work. The publication of Shailja Singh and Subhabrata Sen used one pot reaction of Pictet-Spengler and oxidative ring contraction reaction for the synthesis spiro[pyrolidine-3,3´-oxindole] skeleton in high yield (Scheme 130) (113).

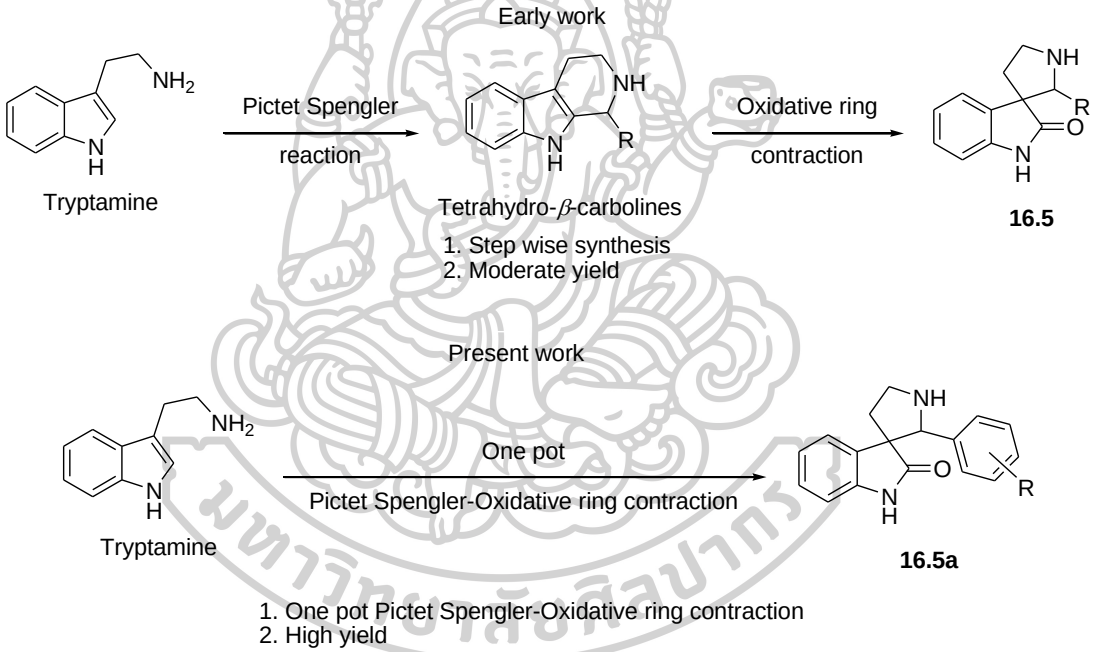

Scheme 130 Comparison of one pot scheme against linear sequence of Pictet-Spengler and oxidative ring contraction reaction of tryptamine with suitable aldehydes

The stepwise reaction involved Pictet Spengler reaction of tryptamine with suitable aldehydes to generate tetrahydro-*β*-carboline subsequent undergo oxidative ring contraction in presence of water, suitable acid and an oxidant to afford the spiro[pyrrolidine-3,3´-oxindole] skeleton. The one pot reaction involved Pictet-Spengler and oxidative ring contraction reaction, which the intermediate tetrahydro-*β*-carboline not isolated. Tryptamine and *p*-tolualdehyde were used as main commercial reactant which variety of solvents such as tetrahydrofuran (THF), acetonitrile (ACN), 1, 4-dioxane, toluene, dichloromethane (DCM), ethylene glycol were used (Table 1, entry 1–7), respectively. All the reactions were started at 0 °C and warmed to several temperatures ranging from rt to 100 °C synthesized tetrahydro-*β*-carboline

intermediate **16.4a** was isolated with the spiro[pyrolidine-3,3´-oxindole] skeleton compound **16.5a**. Finally the well optimization included one equivalent of tryptamine, one equivalent of *p*-tolualdehyde and 1.1 equivalent of *N*-bromosuccinimide in 1:1 tetrahydrofuran (THF) and water with catalytic trifluoroacetic acid at 0 °C to rt afforded the spiro[pyrolidine-3,3´-oxindole] skeleton compound **16.5a** 81% yield (Entry 7, Scheme 131).

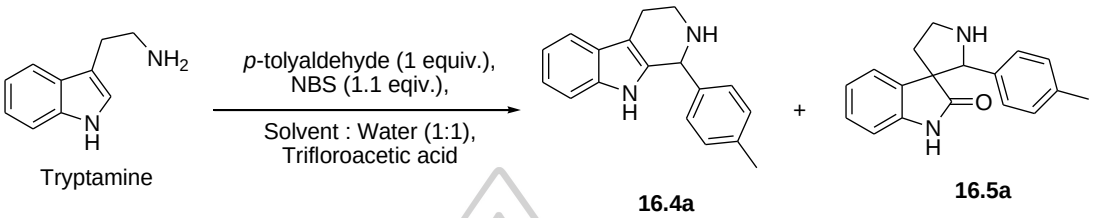

Entry	Solvent	Temperature (0 to T°C)	Percent yield	
			Compound **16.4a**	Compound **16.5a**
1	Tetrahydrofuran	40	5	72
2	Acetonitrile	70	21	64
3	1,4-dioxane	90	34	43
4	Toluene	110	46	no reaction
5	Dichloromethane	35	62	15
6	Ethylene glycol	85	54	32
7	Tetrahydrofuran	room temperature	-	81

Scheme 131 Optimization reaction of one pot Pictet Spengler-Oxidative ring contraction of tryptamine for the synthesis spiro[pyrrolidine-3,3´-oxindole] skeleton

The one pot Pictet Spengler-oxidative ring contraction of tryptamine with electron rich and electron poor aromatic aldehydes generated spiro[pyrrolidine-3,3´-oxindole] derivative compound **16.5b-16.5m** in 45–94% yield. The reaction condition was manageable to electron poor aromatic aldehydes to generate the spiro[pyrrolidine-3,3´-oxindole] derivative compounds **16.5b, 16.5d-16.5e** in 45–60% yield compared to electron rich aromatic aldehydes to give the spiro[pyrrolidine-3,3´-oxindole] derivative compounds **16.5a**/**16.5c** and **16.5f-16.5l** in 73–94% yield. The heteroaromatic aldehydes afforded the spiro[pyrrolidine-3,3´-oxindole] derivative compounds **16.5n** and **16.5o** in 59% and 64% yield, respectively (Scheme 132).

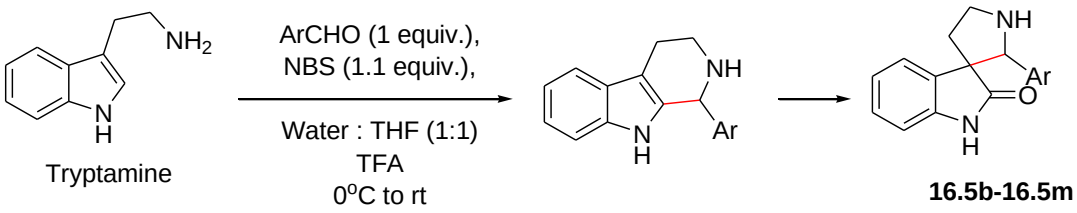

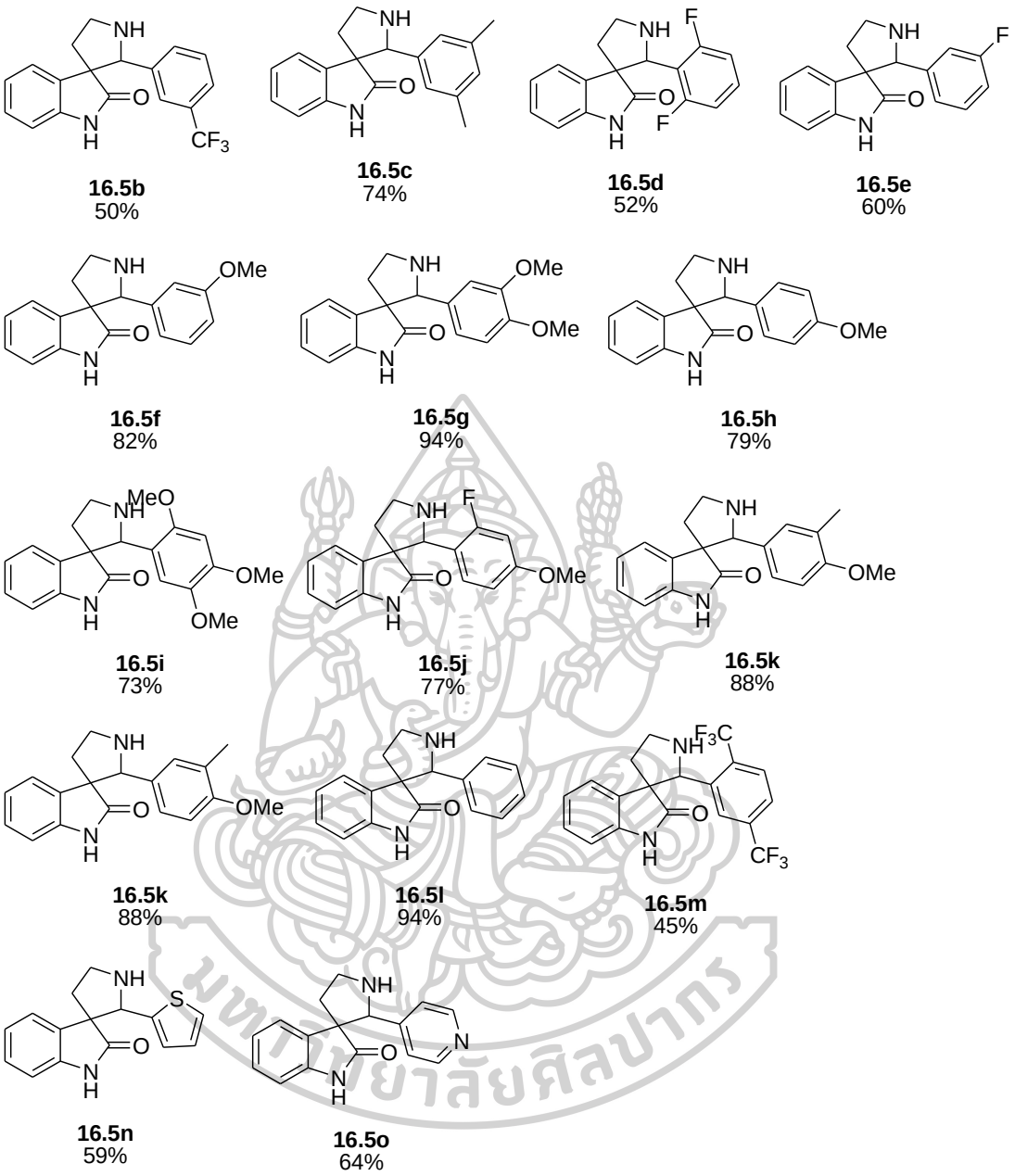

Scheme 132 Synthesis of a library of spiro[pyrrolidine-3,3´-oxindole] derivative compounds **16.5b–16.5o** via one pot Pictet Spengler-oxidative ring contraction of tryptamine with variation aromatic aldehydes at room temperature

Methods used to assess the antibreast cancer potential of spiro[pyrrolidine-3,3´-oxindole] derivative compounds library to screen them at 50 μM concentration against MCF-7 breast cancer cells using MTT colorimetric cell viability assay with EC_{50} values. Etoposide used as the standard breast cancer drug as a positive control. The structure-activity relationships (SAR) validate that electron withdrawing groups are accepted at meta position and electron donating groups at ortho and para positions. The spiro[pyrrolidine-3,3´-oxindole] derivative compound **16.5e**, **16.5i** and **16.5l** are not inhibit the proliferation of healthy mammalian COS-7 and MCF10A cell lines.

The unsubstituted spiro[pyrrolidine-3,3´-oxindole] derivative compound **16.5l** showed best potency with an EC_{50} in 3.53 μM (Figure 28).

Entry	Compound	Percentage inhibition			EC_{50} (μM)
		MCF-7	COS-7	MCF10A	MCF-7
1	**16.5a**	35.06±0.09	11.73±0.09	-	-
2	**16.5b**	33.10±0.12	20.73±0.11	-	-
3	**16.5c**	34.46±0.11	28.80±0.13	-	-
4	**16.5d**	44.25±0.17	9.22±0.12	-	-
5	**16.5e**	54.67±0.08	3.56±0.19	4.48	6.00
6	**16.5f**	38.48±0.18	34.87±0.17	-	-
7	**16.5g**	25.29±0.24	2.39±0.23	-	-
8	**16.5h**	50.62±0.24	25.20±0.06	-	-
9	**16.5i**	53.66±0.06	15.60±0.09	0.80	4.01
10	**16.5j**	38.72±0.15	7.52±0.15	-	-
11	**16.5k**	44.40±0.09	7.14±0.19	-	-
12	**16.5l**	60.96±0.09	15.42±0.18	0.08	3.53
13	**16.5m**	31.81±0.11	-0.51±0.29	-	-
14	Etoposide	71.95±0.11	77.65±0.10	-	-

Figure 28 In vitro phenotypic activity of the library of spiro[pyrrolidine-3,3´-oxindole] compound against MCF-7 and COS-7 cells

Cheng Peng's Design, synthesis, and biological evaluation of nitroisoxazole containing spiro[pyrrolidin-oxindole] derivatives as novel glutathione peroxidase 4/mouse double minute 2 dual inhibitors that inhibit breast adenocarcinoma cell proliferation (2021)

The sequences of CF_3-containing 3´-(nitroisoxazole)spiro[pyrrolidin-3,2´-oxindoles] derivative compound were synthesized and highly active dual inhibitors to be novel glutathione peroxidase 4 (GPX4)/mouse double minute 2 (MDM2). Ferroptosis is an iron-dependent form of programmed cell death. Ferroptosis is a important feature of drug-resistant cancer cells. Several pathways can cause ferroptosis. This is mainly done directly through the mechanism of using covalent inhibitors to bind glutathione peroxidase 4 (GPX4). It is a unique selenoprotein that can reduce lipid hydroperoxides and neutralize their toxicity (Figure 29) (114).

(a) Mechanism of ferroptosis induced by covalent inhibition of GPX4.

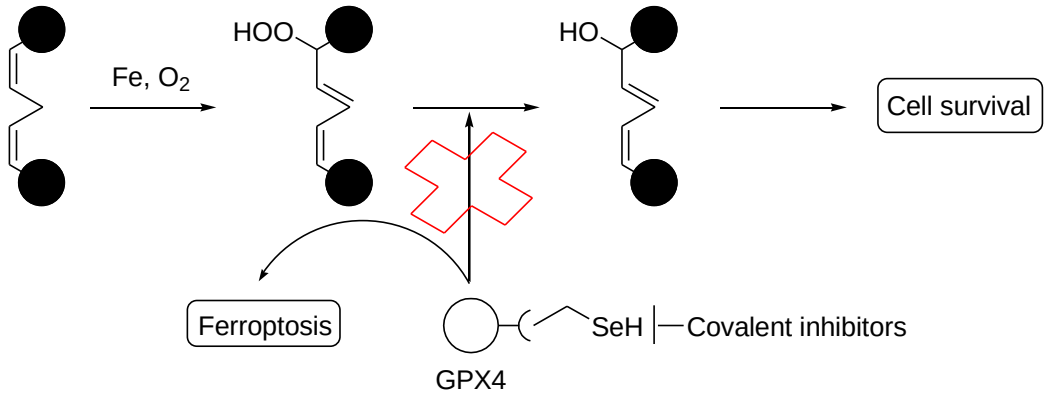

(b) Mechanism of ML210 as covalent inhibitors with GPX4

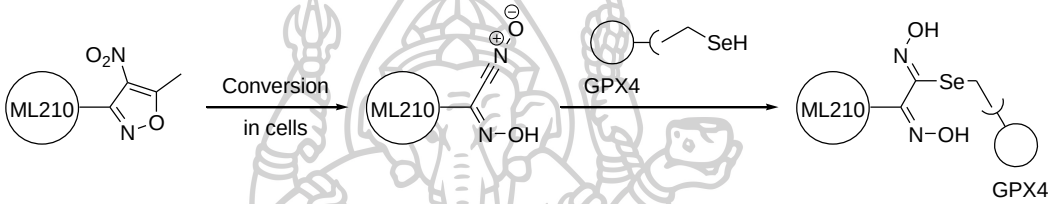

Figure 29 (a) Mechanism of ferroptosis induced by covalent inhibition of glutathione peroxidase 4 (GPX4). (b) Mechanism of ML210 for selective covalent targeting of glutathione peroxidase 4 (GPX4)

The transcription factor p53 is encoded by one of the most frequently mutated genes in cancer, and approximately 50% of human cancers are associated with a mutation or deletion. The p53 can intermediate the regulation of ferroptosis through the accumulation of lipid hydroperoxides or toxic iron. The activity of p53 can be controlled by the overexpression of mouse double minute 2 (MDM2) to bring a tendency with regard to tumor formation. The spiro[pyrrolidin-3,2´-oxindoles] derivative compound such as DS-3032b/Milademetan, SAR405838 and APG-115 demonstrative MDM2-p53 inhibitor. The insertion of fluorine-containing groups in core structure are enhanced the efficacy of drugs such as drug's molecular properties and influence its target selectivity by modulating its conformation, permeability, hydrophobicity, metabolism and lipophilicity (Figure 30).

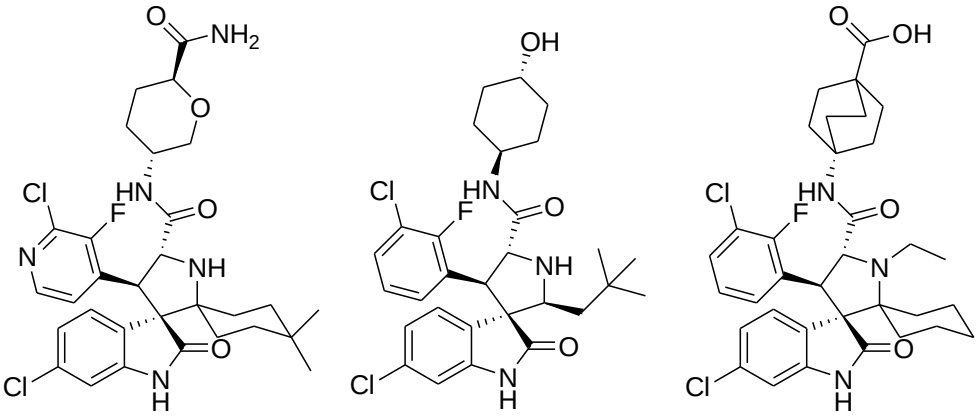

Figure 30 The MDM2 inhibitors with spiro[pyrrolidin-3,2′-oxindoles] compound

The 1,3-dipolar cycloaddition of alkenes to azomethine ylides is green chemistry concepts by its total atom economy. The 1,3-dipolar cycloaddition reaction of the 1,3-dipole compound **17.1** and electron-poor alkene compound **17.2** to attach CF_3-containing spirooxindole and nitro-containing isoxazole skeletons (Scheme 133).

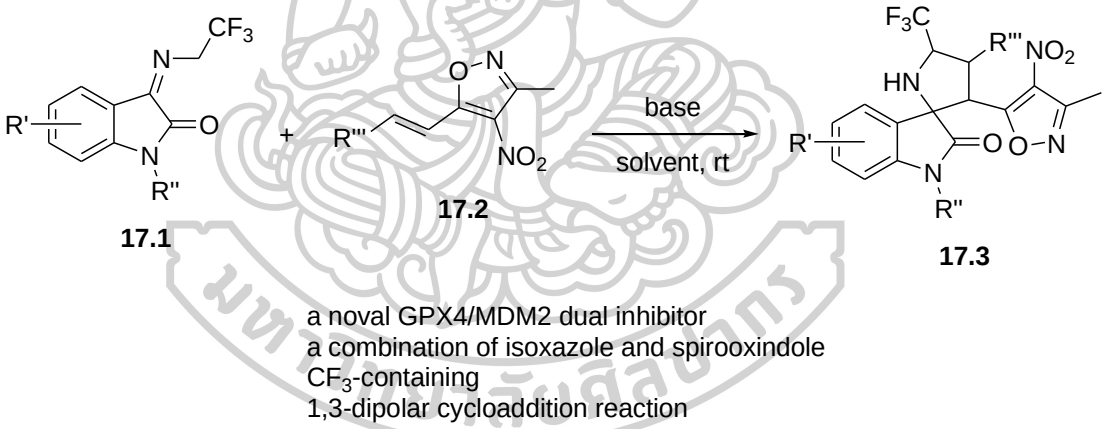

Scheme 133 The 1,3-dipolar cycloaddition reaction for synthesis CF_3-containing spirooxindole and nitro-containing isoxazole skeletons

The reaction between *N*-2,2,2-trifluoroethylsubstituted isatin imine compound **17.1a** and 3-methyl-4-nitro-5-styrylisoxazole compound **17.2a** gave CF_3-containing spirooxindole and nitro-containing isoxazole skeleton compound **17.3a** with best diastereoselectivity in the presence of triethylamine in dichloromethane at room temperature. Various solvents such as dichloromethane, ethanol, toluene, 1,4-dioxane, acetonitrile, dimethylformamide and tetrahydrofuran were in order to improve the yield and shorten the reaction time. The acetonitrile gave CF_3-containing spirooxindole and nitro-containing isoxazole skeleton compound **17.3a** in the best result of the reaction (entry 5). The reaction was optimized to use the various Brønsted bases. Both organic base such as *N*,*N*-diisopropylethylamine (DIPEA), 1,8-

diazabicyclo[5.4.0]undec-7-ene (DBU), 4-dimethylaminopyridine (DMAP) and 1,4-diazabicyclo[2.2.2]octane (DABCO) and inorganic base such as potassium carbonate were catalyzed the reaction to give good yields with high efficiency. The optimal reaction conditions between *N*-2,2,2-trifluoroethylsubstituted isatin imine compound **17.1a** and 3-methyl-4-nitro-5-styrylisoxazole compound **17.2a** using 1,8-Diazabicyclo(5.4.0)undec-7-ene (DBU) in acetonitrile at room temperature for 5 minutes generated CF_3-containing spirooxindole and nitro-containing isoxazole skeleton compound **17.3a** in the excellent result in the reaction (entry 9) (Scheme 134).

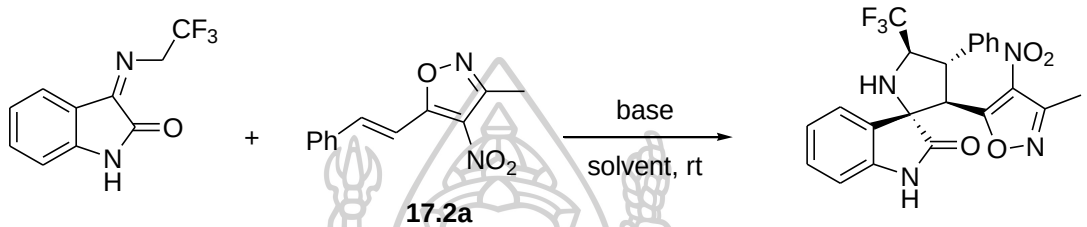

17.1a **17.2a** **17.3a**

Entry	Solvent	Base	Time (minute)	% yield	Diastereomeric ratio
1	Dichloromethane	Triethylamine	40	85	>20:1
2	Ethanol	Triethylamine	20	79	>20:1
3	Toluene	Triethylamine	>12 h	<5	>20:1
4	1,4-dioxane	Triethylamine	>12 h	<5	>20:1
5	Acetonitrile	Triethylamine	5	88	>20:1
6	Dimethylformamide	Triethylamine	15	80	>20:1
7	Tetrahydrofuran	Triethylamine	>12 h	64	>20:1
8	Acetonitrile	*N*,*N*-Diisopropylethylamine	10	86	>20:1
9	Acetonitrile	1,8-Diazabicyclo[5.4.0]undec-7-ene	5	93	>20:1
10	Acetonitrile	4-Dimethylaminopyridine	15	87	>20:1
11	Acetonitrile	1,4-diazabicyclo[2.2.2]octane	15	83	>20:1
12	Acetonitrile	Potassium carbonate	25	86	>20:1

Scheme 134 Optimization of the 1,3-dipolar cycloaddition reaction conditions

The various substituents and substitution positions on the *N*-protecting-group-free *N*-2,2,2-trifluoroethylsubstituted isatin imine derivative compound **17.1** with 3-methyl-4-nitro-5-styrylisoxazole compound **17.2** generated the corresponding spirooxindole compounds **17.3a-17.3h** in 75-93% yields. Reactions of electron-withdrawing group as nitro substituent bearing *N*-protecting-group-free *N*-2,2,2-trifluoroethylsubstituted isatin imine compound **17.1** afforded spirooxindole compound **17.3g** in low yield. Reactions of 3-methyl-4-nitro-5-styrylisoxazole derivative compound **17.2** examined with both electron-withdrawing and electron-donating substituents proceeded spirooxindole compounds (**17.3i-17.3w**).in high yields and excellent diastereoselectivity. The 2-furyl, 2-thienyl and a-naphthyl replaced the aryl ring at position R'''' of 1,3-dipolar cycloaddition reaction between isatin imine compound **17.1** and 3-methyl-4-nitro-5-styrylisoxazole compound **17.2** generated spirooxindole compounds (**17.3x-17.3z**) in high yield. The various

substituents on *N*-protecting groups such as methyl, allyl and acetyl of isatin imine compound **17.1** gave spirooxindole compounds (**17.3aa**-**17.3ac**) in high yield (Scheme 135).

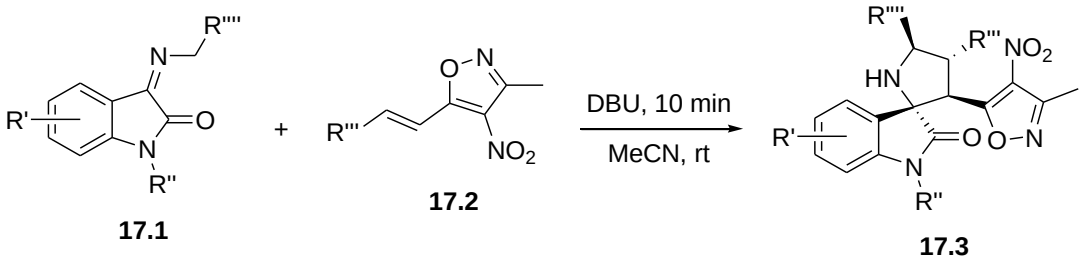

17.1 **17.2** **17.3**

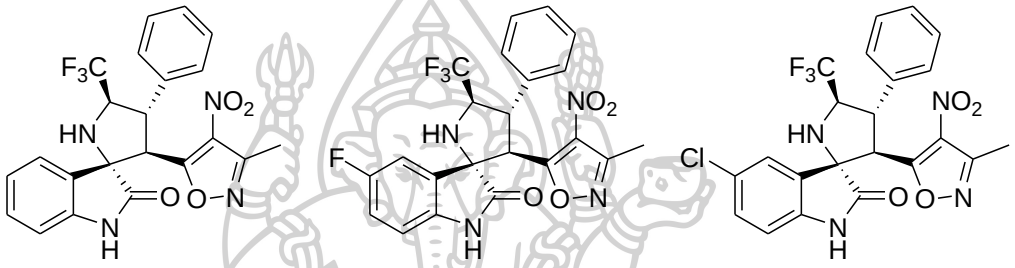

17.3a 93% **17.3b** 82% **17.3c** 80%

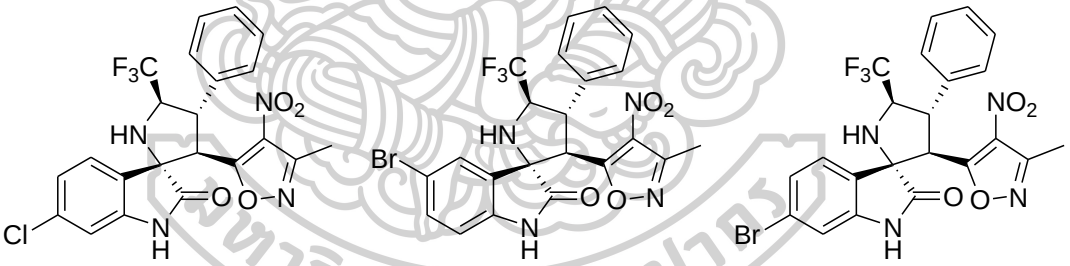

17.3d 86% **17.3e** 86% **17.3f** 90%

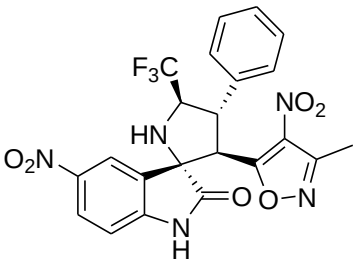

17.3g
75%

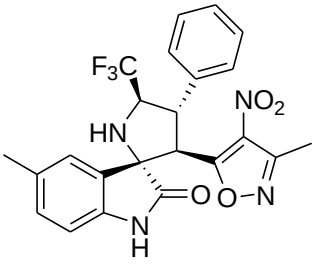

17.3h
81%

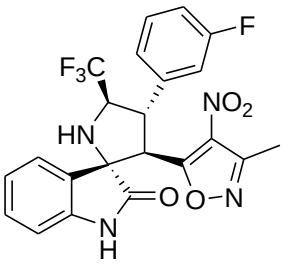

17.3i
88%

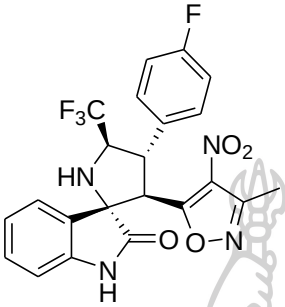

17.3j
86%

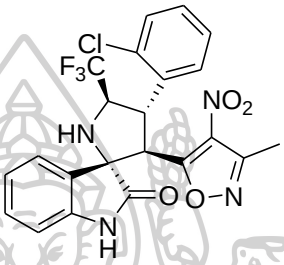

17.3k
79%

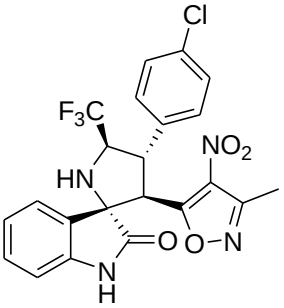

17.3l
86%

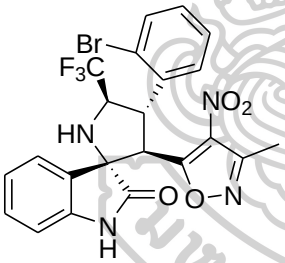

17.3m
82%

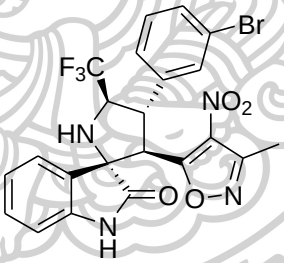

17.3n
85%

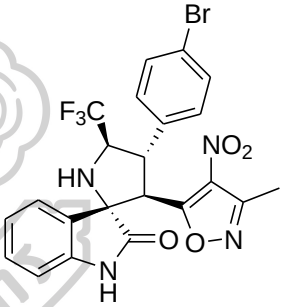

17.3o
90%

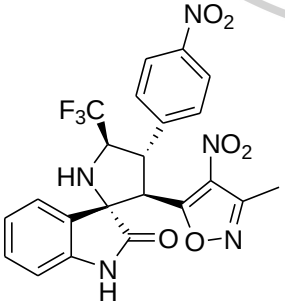

17.3p
72%

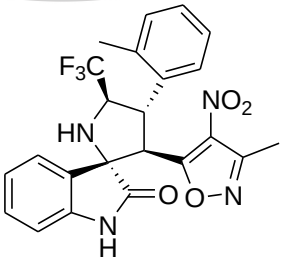

17.3q
81%

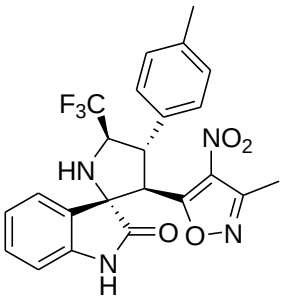

17.3r
84%

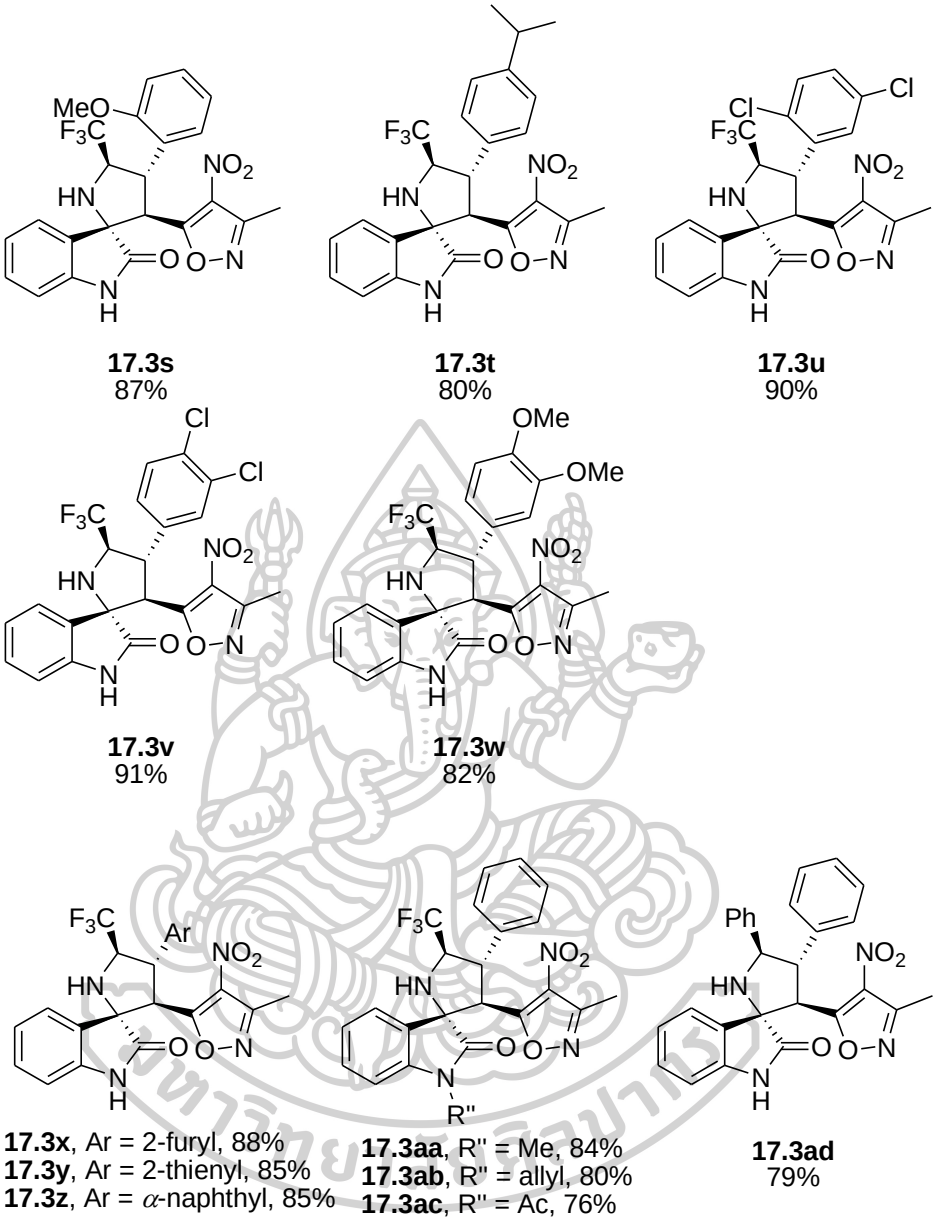

Scheme 135 Substrate scope of the 1,3-dipolar cycloaddition reaction of various substituents and substitution positions

The relative configuration of 5-methyl-3′-(3-methyl-4-nitroisoxazol-5-yl)-4′-phenyl-5′-(trifluoromethyl)spiro[indoline-3,2′-pyrrolidin]-2-one comound **17.3h** was clearly confirmed by X-ray diffraction, and those of the other spirooxindole compounds were realized on the basis of these consequences.

The series of CF_3-containing 3′-(nitroisoxazole)spiro[pyrrolidin-3,2′-oxindoles] derivative compounds were evaluated as MDM2 and GPX4 inhibitors using nutlin-3 and ML210, respectively, as reference drugs. The 3′-(nitroisoxazole)spiro[pyrrolidin-3,2′-oxindoles] derivative compounds are accomplished of inducing ferroptosis, which treated cells with 3′-(nitroisoxazole)spiro[pyrrolidin-3,2′-oxindoles] derivative compounds to lead to

ferroptosis, which could be prohibited by adding ferrostatin-1 (Fer-1). The 3′-(nitroisoxazole)spiro[pyrrolidin-3,2′-oxindoles] compounds (**17.3d**, **17.3f**) with a halogen substituent at the 6-position of isatin imine compound **17.1** showed apparent inhibitory activity against MDM2 and the highest selectivity for GPX4. The 3-methyl-4-nitro-5-styrylisoxazole derivative compound **17.2** were substituted at position R′′′ gave 3′-(nitroisoxazole)spiro[pyrrolidin-3,2′-oxindoles] compounds (**17.3i-17.3w**) exhibited average activity toward GPX4. The influence of mono-substituents of 3-methyl-4-nitro-5-styrylisoxazole derivative compound **17.2** at R′′′ with different steric and electronic properties were showed distinctly different activities to exhibit among various electronwithdraw (**17.3i-17.3p**) and electron-donating groups (**17.3o-17.3t**), which *para*-fluorine-substituted 3′-(nitroisoxazole)spiro[pyrrolidin-3,2′-oxindoles] compound (**17.3j**) provided the comparatively best inhibitory activity against GPX4. Disubstituted of 3-methyl-4-nitro-5-styrylisoxazole derivative compound **17.2** at R′′′ at position R′′′ compounds were included electron-withdrawing halogen groups (**17.3u** and **17.3v**) and electron-donating methoxy group (**17.3w**) to show lower activities than mono-substituted compounds, probably because of their larger steric hindrance. The 3-methyl-4-nitro-5-styrylisoxazole derivative compound **17.2** were substituted heteroaryl and a-naphthyl groups at R′′′ ensued in mediocre activities against both MDM2 and GPX4 (**17.3x-17.3z**). The isatin imine compound **17.1** replaced trifluoromethyl with phenyl, which decreased activities on both MDM2 and GPX4 were observed in 3′-(nitroisoxazole)spiro[pyrrolidin-3,2′-oxindoles] compounds **17.3ad**, demonstrating that the trifluoromethyl be beneficial to improve activities. *N*-protecting groups such as methyl (**17.3aa**), allyl (**17.3ab**), and acetyl (**17.3ac**) at position R′′ of isatin imine compound **17.1** inhibited the effects of MDM2 and GPX4. The 3′-(nitroisoxazole)spiro[pyrrolidin-3,2′-oxindoles] compound **17.3d** presented better MDM2 inhibition than Nutlin-3 and showed the best activities against GPX4 among all compounds, although slightly less than ML210 (Scheme 136).

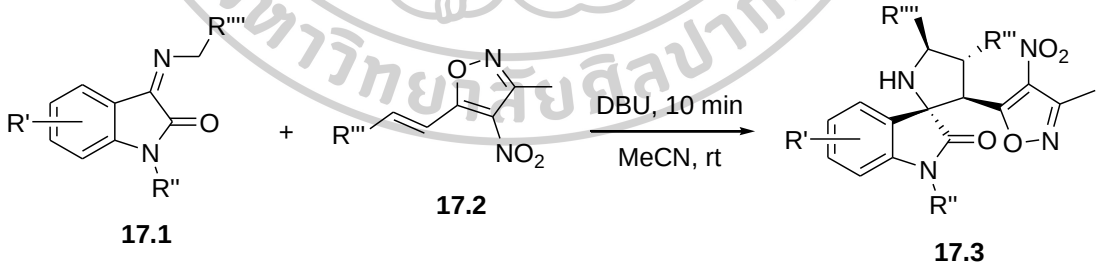

17.1 **17.2** **17.3**

Compound	R'	R"	R"'	R""	MDM2 *Ki* (μM)	Cytotoxicity IC_{50} (μM)		Selectivity
						-	+ Fer-1	
17.3a	H	H	Ph	CF_3	1.28±0.23	0.38	17.6	46.3
17.3b	5-F	H	Ph	CF_3	0.49±0.08	0.21	15.6	74.2
17.3c	5-Cl	H	Ph	CF_3	0.68±0.13	0.37	19.8	53.5
17.3d	6-Cl	H	Ph	CF_3	0.24±0.06	0.12	13.5	112.5
17.3e	5-Br	H	Ph	CF_3	1.02±0.23	0.55	16.3	29.6
17.3f	6-Br	H	Ph	CF_3	0.26±0.05	0.17	13.7	80.5
17.3g	5-NO_2	H	Ph	CF_3	3.68±0.57	4.75	>20	>4.21
17.3h	5-Me	H	Ph	CF_3	1.42±0.21	4.91	18.1	3.68
17.3i	H	H	3-F-C_6H_4	CF_3	1.14±0.20	0.87	15.6	17.9
17.3j	H	H	4-F-C_6H_4	CF_3	1.03±0.14	0.55	17.4	31.6
17.3k	H	H	2-Cl-C_6H_4	CF_3	>10	3.77	>20	>5.30
17.3l	H	H	4-Cl-C_6H_4	CF_3	2.77±0.31	1.14	>20	>17.5
17.3m	H	H	2-Br-C_6H_4	CF_3	>10	4.71	>20	>4.24
17.3n	H	H	3-Br-C_6H_4	CF_3	2.78±0.37	2.31	>20	>8.65
17.3o	H	H	4-Br-C_6H_4	CF_3	1.87±0.20	3.01	17.0	5.64
17.3p	H	H	4-NO_2-C_6H_4	CF_3	6.74±0.96	5.36	>20	>3.73
17.3q	H	H	2-Me-C_6H_4	CF_3	>10	3.50	>20	>5.71
17.3r	H	H	4-Me-C_6H_4	CF_3	1.49±0.36	2.81	18.8	6.69
17.3s	H	H	2-OMe-C_6H_4	CF_3	>10	4.59	>20	>4.35
17.3t	H	H	4-*i* Pr-C_6H_4	CF_3	2.26±0.37	2.83	>20	>7.06
17.3u	H	H	2,5-Cl_2-C_6H_3	CF_3	>10	3.98	>20	>5.02
17.3v	H	H	3,4-Cl_2-C_6H_3	CF_3	2.36±0.17	3.22	>20	>6.21
17.3w	H	H	3,4-$(OMe)_2$-C_6H_3	CF_3	3.68±0.29	4.13	>20	>4.84
17.3x	H	H	2-furyl	CF_3	1.19±0.21	1.46	14.3	9.79
17.3y	H	H	2-thienyl	CF_3	1.36±0.24	1.53	19.0	12.4
17.3z	H	H	α-naphthyl	CF_3	8.35±1.04	7.17	>20	>2.78
17.3aa	H	Me	Ph	CF_3	>10	3.52	>20	>5.68
17.3ab	H	Allyl	Ph	CF_3	>10	3.42	>20	>5.84
17.3ac	H	Ac	Ph	CF_3	>10	3.23	>20	>6.19
17.3ad	H	H	Ph	Ph	6.33±0.95	5.24	>20	>3.81
Nutlin-3	-	-	-	-	0.28±0.0	14.63	15.72	1.07
ML210	-	-	-	-	N.D.	0.076	>20	>263

Scheme 136 The *Ki* values (μM) of compounds **17.3a-17.3ad** on MDM2 and their selective cytotoxicity

Assem Barakat's Spiroindolone analogues as potential hypoglycemic with dual inhibitory activity on *α*-amylase and *α*-glucosidase (2019)

Diabetes is a chronic disease that is considered a serious disease caused by pancreas does not produce enough insulin (hormones that control blood glucose levels) or as a result of the body's inability to work properly with insulin. According to the Diabetes Association of Thailand were more than 4.4 million people living with diabetes disease in 2017. The Thai population aged 60-69 years is the most diabetic. Diabetes leads to serious consequences for the development of coronary heart disease, liver damage, retinal disease, kidney disease, cerebrovascular disease and peripheral kidney disease. The *α*-glucosidase are key enzymes involve in the breakdown and intestinal absorption of carbohydrates, respectively. The *α*-glucosidase inhibition blocks increased blood sugar levels after carbohydrate intake, an important strategy in the management of non-insulin-dependent diabetes mellitus (NIDDM).

The spirooxindole compounds demonstration pharmaceutical activity to lead spirooxindole compounds for drug discovery. Numerous biological activities have been reported for spirooxindole compounds, including anti-inflammatory, anti-cancer, antiviral, antibacterial, MDM2-p53 protein interaction inhibitory and local anaesthetic activities (Figure 31) (99).

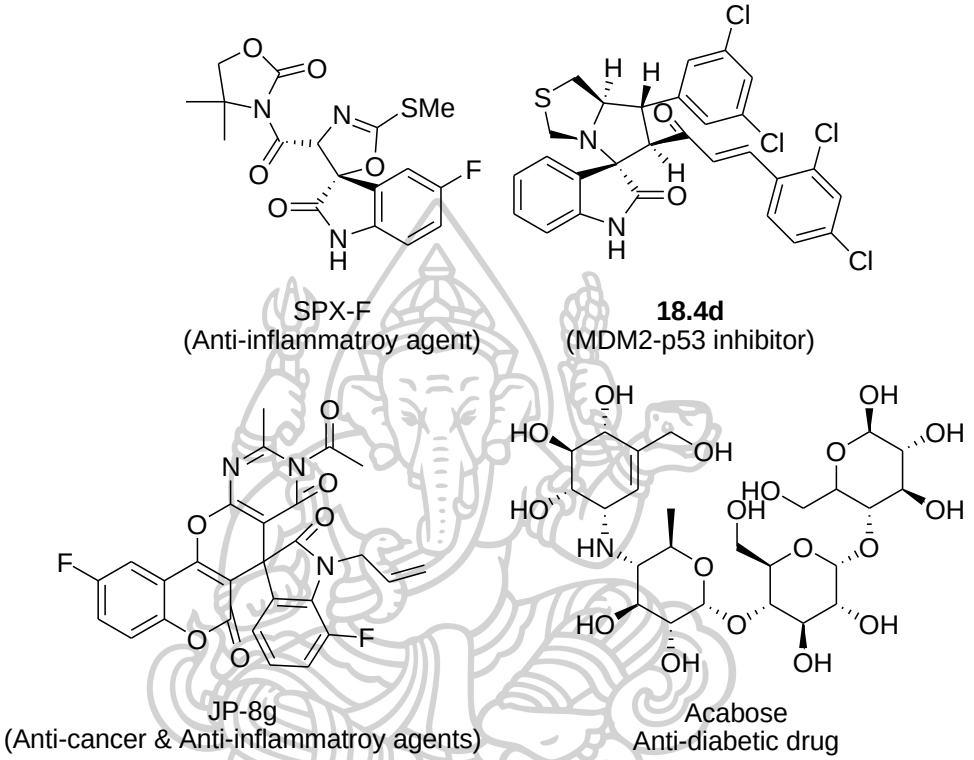

Figure 31 Biological activity for example of the spiroxindole compound, acarbose as standard drug

The aldol condensation of 4-substituted 1-phenylethan-1-one with 2-benzofurancarboxaldehyde using sodium hydroxide generated benzofuran-based chalcone compounds **18.2a**-**18.2f**. One pot reaction of benzofuran-based chalcone compounds **18.2a**-**18.2f** were reacted with substituted isatin compounds **18.3a**-**18.3c** and heterocyclic amino acids **18.4a**, **18.4b** in the presence of methanol to construct spirooxindole derivative compounds **18.5a**-**18.5r** (Scheme 137).

The different spirooxindoles fused benzo[*b*]furan scaffold compounds **18.5a**–**18.5r** established for α-glucosidase inhibitory activity. The spirooxindoles fused benzo[*b*]furan scaffold compounds **18.5j**, **18.5k**, **18.5q** and **18.5r** inhibit the enzyme α-glucosidase with IC_{50} values of 29.20, 39.10, 26.29 and 14.05 μM, respectively which is most effective from a variety of synthetic structures. The spirooxindoles fused benzo[*b*]furan scaffold compound **18.5r** exhibited better α-glucosidase inhibitory activity with IC_{50} values of 14.05 μM and selectivity indexes of 1.60. This result was compared with Acarbose which the IC_{50} value of 2.35 μM and the selectivity index of 0.31 (Scheme 137).

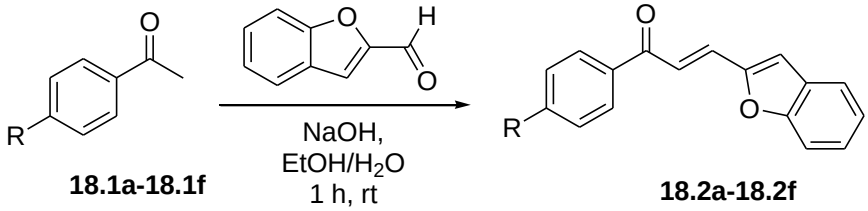

18.1a-18.1f **18.2a-18.2f**

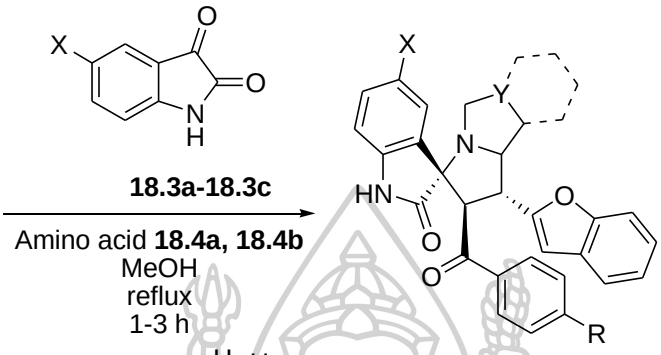

14.5a-14.5r

18.4a **18.4b**

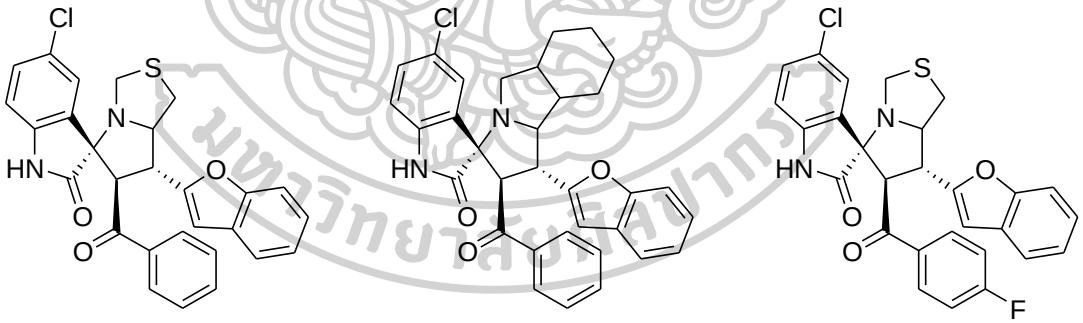

18.5a **18.5b** **18.5c**

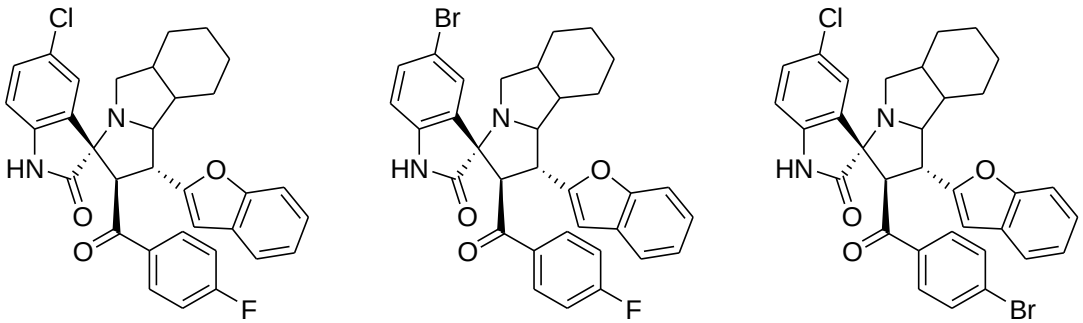

18.5d **18.5e** **18.5f**

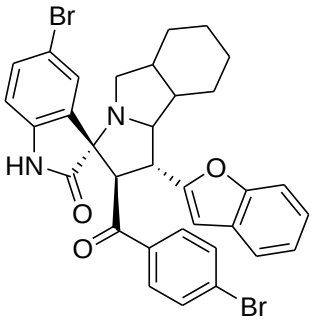

18.5g

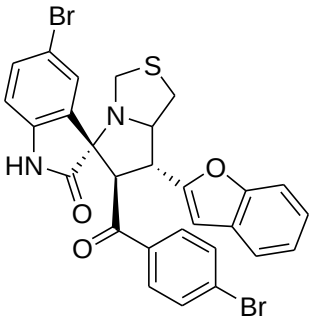

18.5h

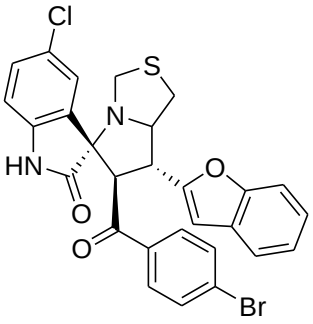

18.5i

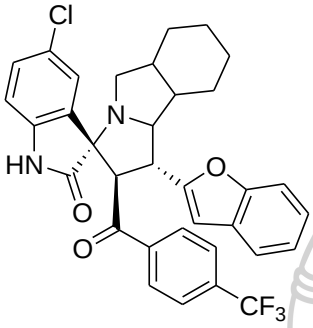

18.5j

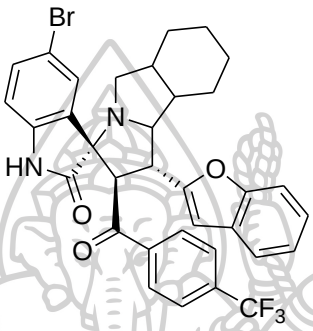

18.5k

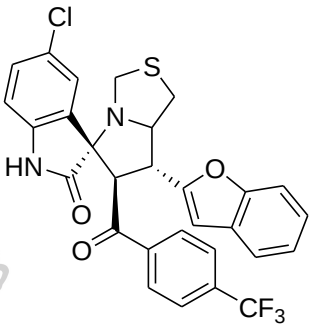

18.5l

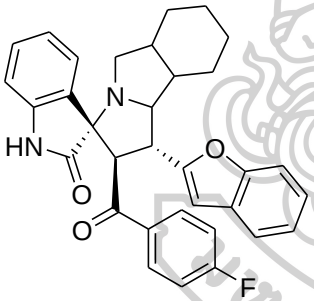

18.5m

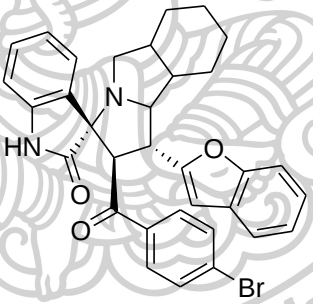

18.5n

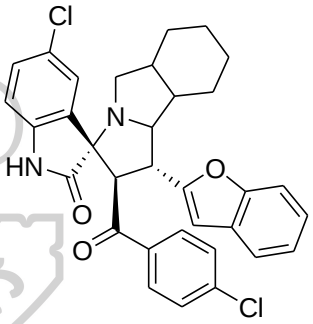

18.5o

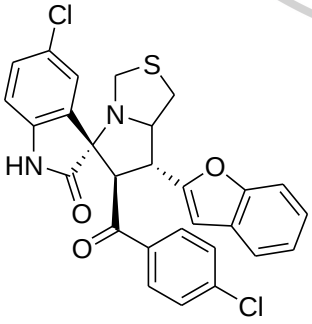

18.5p

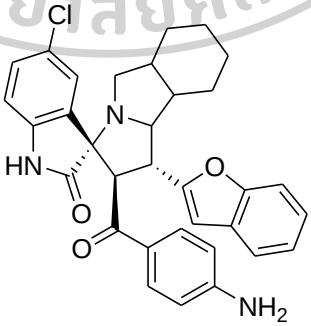

18.5q

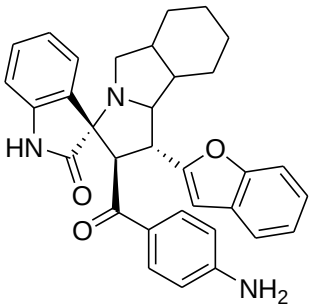

18.5r

Compound	R	X	Amino acid	α-glucosidase	
				IC_{50} (μM±SD)	Selectivity
18.5a	H	Cl	**18.4a**	465.12±0.12	1.49
18.5b	H	Cl	**18.4b**	545.01±1.09	1.37
18.5c	F	Cl	**18.4a**	585.11±0.02	1.22
18.5d	F	Cl	**18.4b**	549.17±1.06	1.32
18.5e	F	Br	**18.4b**	554.12±1.42	1.28
18.5f	Br	Cl	**18.4b**	534.04±1.09	1.25
18.5g	Br	Br	**18.4b**	554.12±1.42	1.24
18.5h	Br	Br	**18.4a**	494.10±0.04	1.19
18.5i	Br	Cl	**18.4a**	684.12±0.35	1.13
18.5j	CF_3	Cl	**18.4b**	29.20±0.33	1.33
18.5k	CF_3	Br	**18.4b**	39.10±0.54	1.26
18.5l	CF_3	Cl	**18.4a**	414.12±0.52	1.37
18.5m	F	H	**18.4b**	69.11±0.34	1.37
18.5n	Br	H	**18.4b**	98.23±1.24	1.88
18.5o	Cl	Cl	**18.4b**	68.18±1.54	1.69
18.5p	Cl	Cl	**18.4a**	392.13±1.07	1.24
18.5q	NH_2	Cl	**18.4b**	26.29±0.45	1.41
18.5r	NH_2	H	**18.4b**	14.05±1.03	1.60
Acarbose (μM)	-	-	-	2.35±0.13	0.31

Scheme 137 Synthesized spirooxindoles fused benzo[*b*]furan scaffold compounds **18.5a–18.5r** and α-glucosidase inhibitory activity

The spirooxindoles fused benzo[*b*]furan scaffold compounds **18.5a–18.5r** from regio- and diastereoselectivity were previously established by X-ray crystallography which explained by the mechanism represented in Scheme I. Initially, the reaction of isatin derivative compounds with heterocyclic amino acid generated spirooxindole intermediate followed by elimination of carbondioxide to give azomethine ylide. The approach of the chalcone derivative compound towards azomethine ylide intermediate (Path A and B) and the double bond geometry of the azomethine (Path D and C) determine the regioselectivity and diastereoselectivity of the reaction, respectively. Possible reactions will occur through the regioselectivity path A and diastereoselectivity path C (Scheme 138).

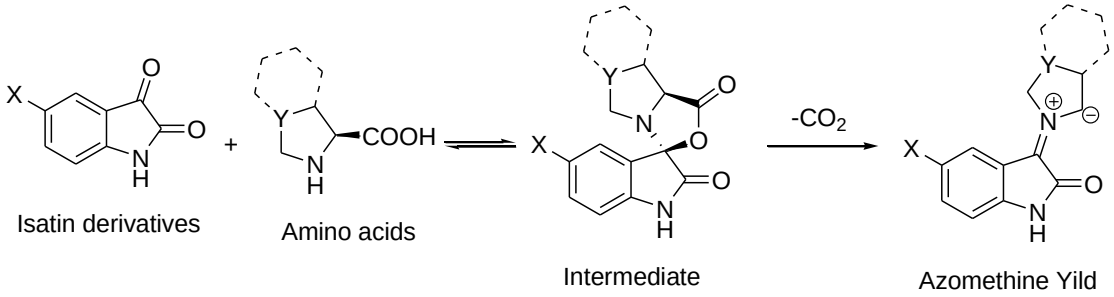
Isatin derivatives
Amino acids
Intermediate
Azomethine Yild
-CO2

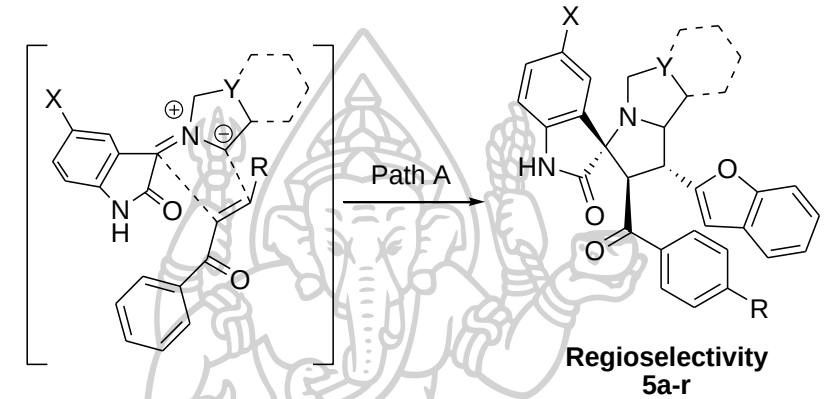
Path A
Regioselectivity
5a-r

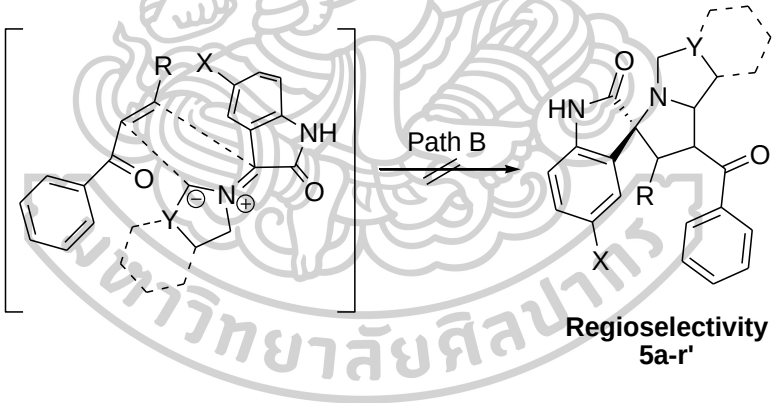
Path B
Regioselectivity
5a-r'

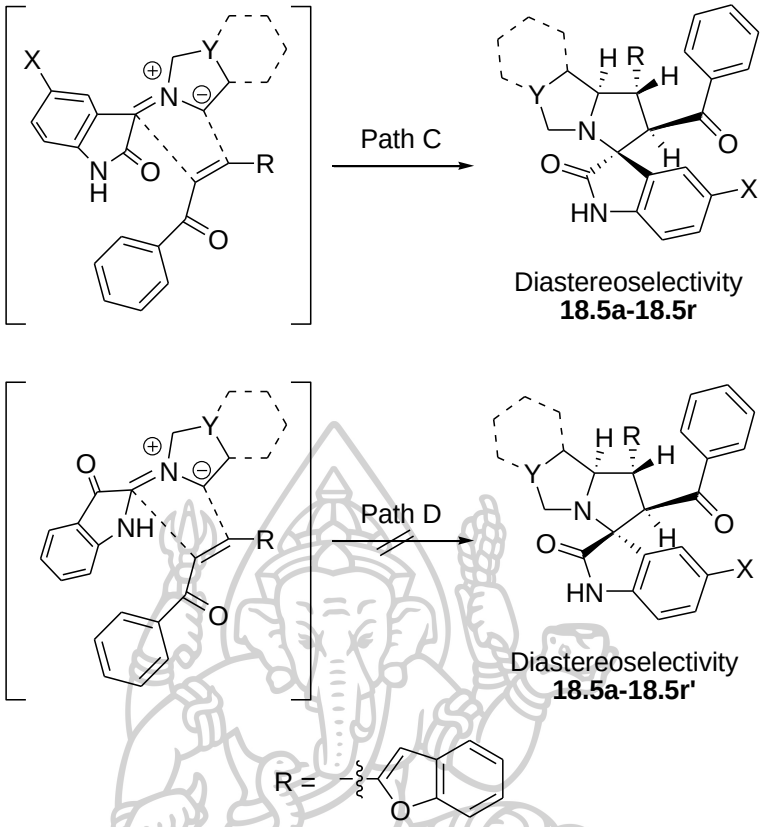

Scheme 138 Plausible mechanism of formation of the spirooxindoles fused benzo[*b*]furan scaffold compounds **18.5a–18.5r**

CHAPTER 3
SYNTHETIC STUDY

A synthetic study of spiroindolizidine-oxindole and indolizidine in this laboratory used a commercially available starting materials such as L-glutamic acid and tryptamine. All spiroindolizidine-oxindole and indolizidine began with a benzylation, *O*-methylation and condensation to generated a chiral *N*-alkylglutarimide which was a key intermediate that can converted to core structure of Rhynchophylline and Hirsutine alkaloids respectively (115). This key intermediate was synthesized by a commercially available amino acid and alkyl-primary amine. We used L-glutamate which was prepared from L-glutamic acid, to generate chiral *N*-indolylethylglutarimide with *N*-atom of imide created from primary amine. The spiroindolizidine-oxindole and indolizidine system were synthesized in a chiral form using cyclization of chiral *N*-acyliminium ions as key intermediate. The stereocenter bearing a dibenzylamino group was used for stereocontrol and resulted in diastereomeric products. The key oxidative ring contraction of chiral *N*-indolylethylglutarimide was achieved by treatment with *N*-bromosuccinimide (NBS) in tetrahydrofuran (THF)/water in the presence of catalytic trifluoroacetic acid. The dibenzylamino moiety was subsequently transformed via Cope elimination to the corresponding cyclic enamide which suitable as a synthetic precursor for a spiroindolizidine-oxindole and indolizidine derivative in enantiomerically pure form. The spiroindolizidine-oxindole and indolizidine derivative are core structure of Rhynchophylline and Hirsutine as natural product, respectively. The spiroindolizidine-oxindole and indolizidine derivative isolated from *Uncaria rhynchophylla* which is a plant that has been used in traditional medicine. These spiroindolizidine-oxindole and indolizidine derivative were exhibited potent activity against *α*-glucosidase, an enzyme, which plays critical roles in carbohydrate metabolism and cell cycle. This interesting biological activity renders them potential leads for medicinal investigation for treatment of diabetes diseases.

Synthesis of chiral *N*-indolylethylglutarimide

This synthesis methodology synthesized a chiral *N*-indolylethylglutarimide as a chiral substrate. First, chiral dimethyl *N*,*N*-dibenzylglutamate **19.3** was obtained from commercial L-glutamic acid via benzylation and subsequent methylation. The synthesis of indoloquinolizidine (scheme 1) began with condensation of tryptamine and dimethyl *N*,*N*-dibenzylglutamate **19.3** to give chiral *N*-indolylethylglutarimide **19.4** using lithium diisopropylamide with tetrahydrofuran as the solvent in 92% yield. Boc protection of *N*-atom in trypimide chiral *N*-indolylethylglutarimide **19.4** using Di-*tert*-butyl dicarbonate (Boc_2O) in basic condition provided *N*-Boc-tryp-imide **19.19** in 98% yield (Scheme 139).

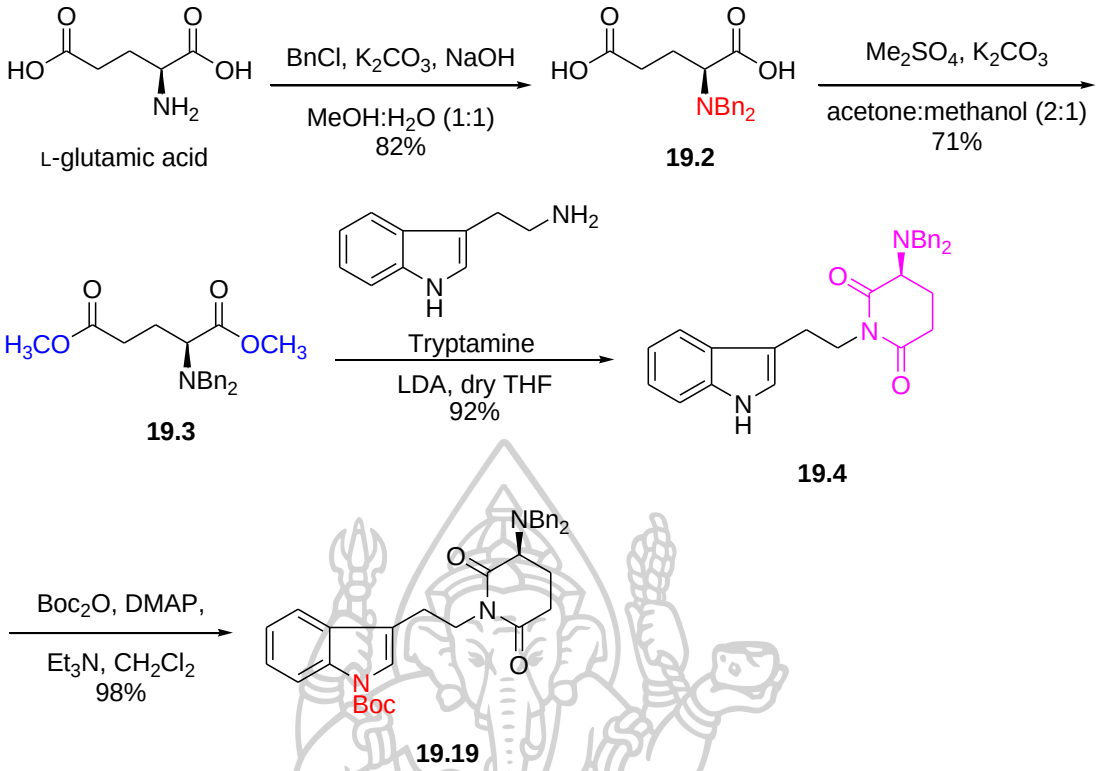

Scheme 139 Synthesis of chiral *N*-indolylethylglutarimide

Synthesis of indoloquinolizidine derivative

The diisobutylaluminium hydride reduction of the glutarimide **19.4** was completely regioselective at the less hindered carbonyl group when toluene was used as solvent and the temperature was controlled at -78°C to give hydroxylactam **19.5** as a single product. The *N*-acyliminium ion cyclization of hydroxylactam **19.5** treatment with trimethylsilyl trifluoromethanesulfonate (TMSOTf) in dichloromethane produced two diastereomeric indoloquinolizidines **19.6a** and **19.6b** to separate by column chromatography in 1:2.3 as diastereomeric ratio (Scheme 140).

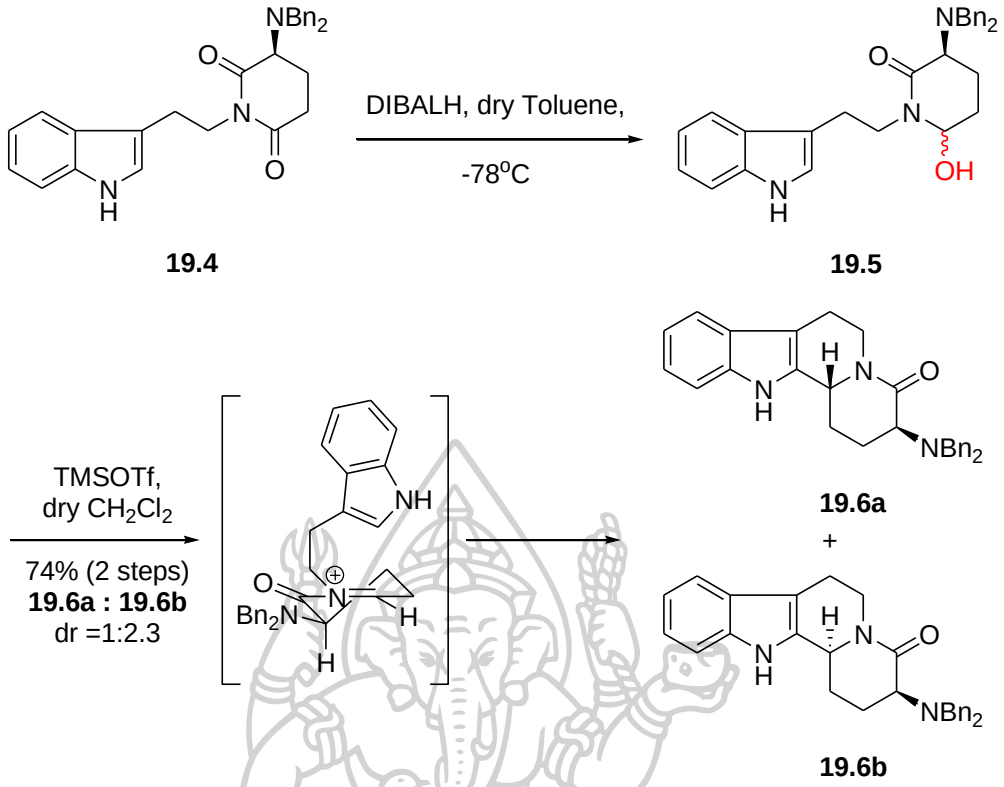

Scheme 140 Synthesis of indoloquinolizidines **19.6a** and **19.6b**

The two diastereomers of indoloquinolizidines **19.6a** and **19.6b** were converted to a couple of enantiomers indoloquinolizidine derivatives **19.13** and **19.26**. First, the Boc carbamate protection of the indole nitrogen position of indoloquinolizidine **19.6a** using di-*tert*-butyl dicarbonate (Boc_2O), 4-dimethylaminopyridine (DMAP) and triethylamine to dissolve dichloromethane generated *N*-Boc indoloquinolizidine **19.11** in 87% yield. Cope elimination of the dibenzylamino group of *N*-Boc indoloquinolizidine **19.11** in the presence of meta-chloroperoxybenzoic acid (*m*CPBA) provided *α,β*-unsaturated lactam **19.12** in 74%. Elimination of the Boc protecting group of *N*-Boc indoloquinolizidine **19.12** using trifluoroacetic acid (TFA) to dissolve in tetrahydrofuran (THF) generated indoloquinolizidine-enamide **19.13** in 71% yield (Scheme 141).

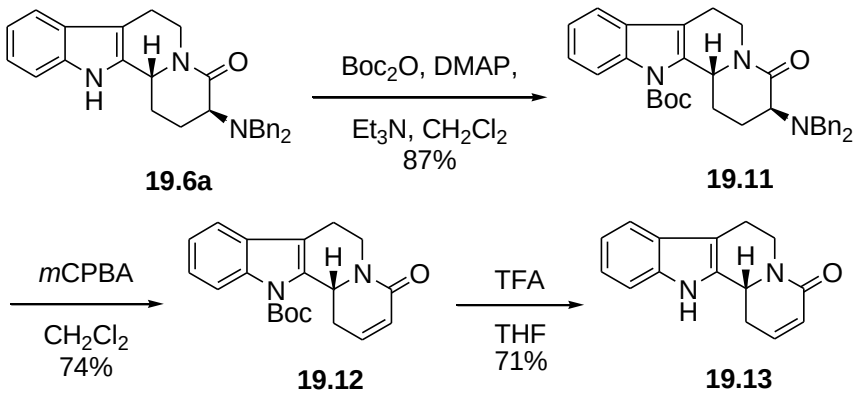

Scheme 141 Synthesis of indoloquinolizidines derivative **19.12** and **19.13**

Similarly, the Boc carbamate protection of the indole nitrogen position of indoloquinolizidine **19.6b** in the presence of di-*tert*-butyl dicarbonate (Boc_2O), 4-dimethylaminopyridine (DMAP) and triethylamine to dissolve dichloromethane generated *N*-Boc indoloquinolizidine **19.9** in 98% yield. Cope elimination of the dibenzylamino group of *N*-Boc indoloquinolizidine **19.9** using meta-chloroperoxybenzoic acid (*m*CPBA) gave *α,β*-unsaturated lactam **19.10** in 66%. Elimination of the Boc protecting group of *N*-Boc indoloquinolizidine **19.10** under acid condition generated indoloquinolizidine-enamide **19.26** in 69% yield (Scheme 142).

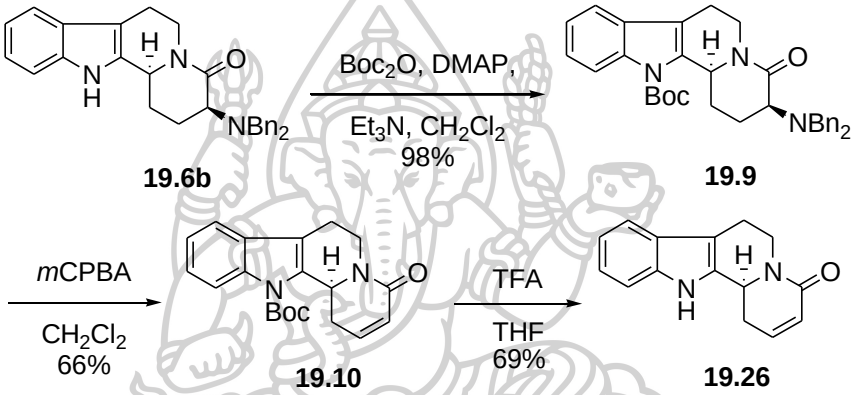

Scheme 142 Synthesis of indoloquinolizidine derivatives **19.10** and **19.26**

Synthesis of spiroindolizidine-oxindole derivative

Oxidative rearrangement of tetracyclic indoloquinolizidine compound **19.6a** with *N*-bromosuccinimide as oxidant in the mixture of tetrahydrofuran (THF) and water at 0 ^{o}C in the presence of catalytic amount of trifluoroacetic acid (TFA) constructed spiro[indolizidine-1,3′-oxindole] compound **19.7** in 46% yield. Cope elimination reaction of spiro[indolizidine-1,3′-oxindole] compound **19.7** in the presence of meta-chloroperoxybenzoic acid (*m*CPBA) to eliminate of the dibenzylamino group generated *α,β*–unsaturated spiroindolizidine-oxindole **19.8** in 48% yield (Scheme 143).

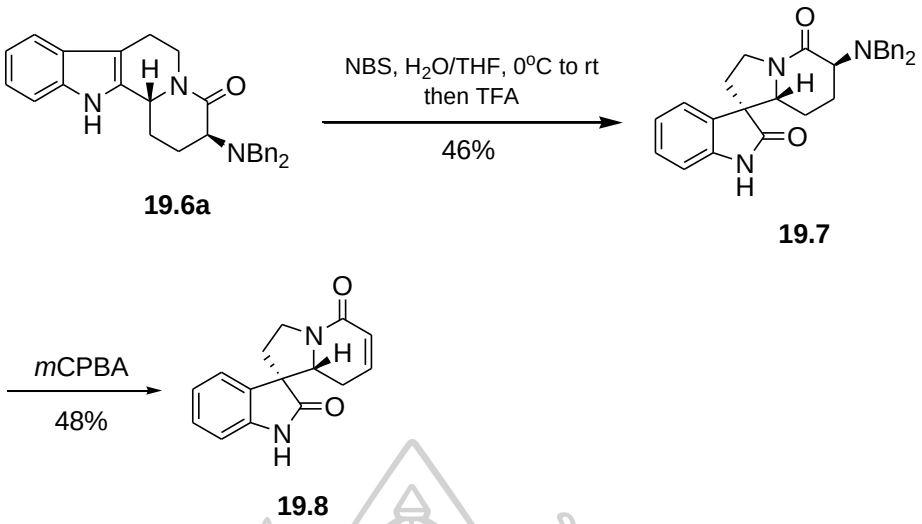

19.6a **19.7** **19.8**

Scheme 143 Synthesis of spiro[indolizidine-1,3′-oxindole] derivative **19.8**

The stereochemical of oxidative rearrangement was considered the conformation of tetracyclic indoloquinolizidine **19.6a** as starting materials. The syndiastereomer **19.6a** has a molecular structure that is rather flat and steric bias between the two diastereotopic faces of this molecule. The initial bromination of the indole ring from either face of the molecule followed by rearrangement to give spiro[indolizidine-1,3′-oxindole] **19.7** (Scheme 144).

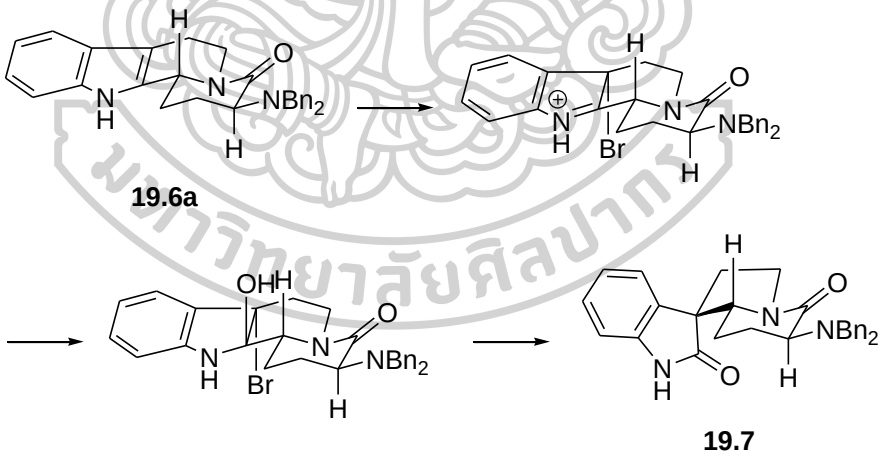

19.6a **19.7**

Scheme 144 Stereochemistry of oxidative rearrangement of tetracyclic indoloquinolizidine **19.6a**

Oxidative rearrangement of tetracyclic indoloquinolizidinone compound **19.6b** using *N*-bromosuccinimide as oxidant in aqueous tetrahydrofuran (THF) at 0 ^{o}C in the presence of catalytic amount of trifluoroacetic acid (TFA) generated single diastereomer of spiro[indolizidine-1,3′-oxindole] compound **19.15** in 49% yield. Cope elimination reaction of the dibenzylamino group of spiro[indolizidine-1,3′-oxindole] compound **19.15** treatment with meta-chloroperoxybenzoic acid (*m*CPBA)

produced *α,β*–unsaturated spiroindolizidine-oxindole **19.16** in 40% yield (Scheme 145).

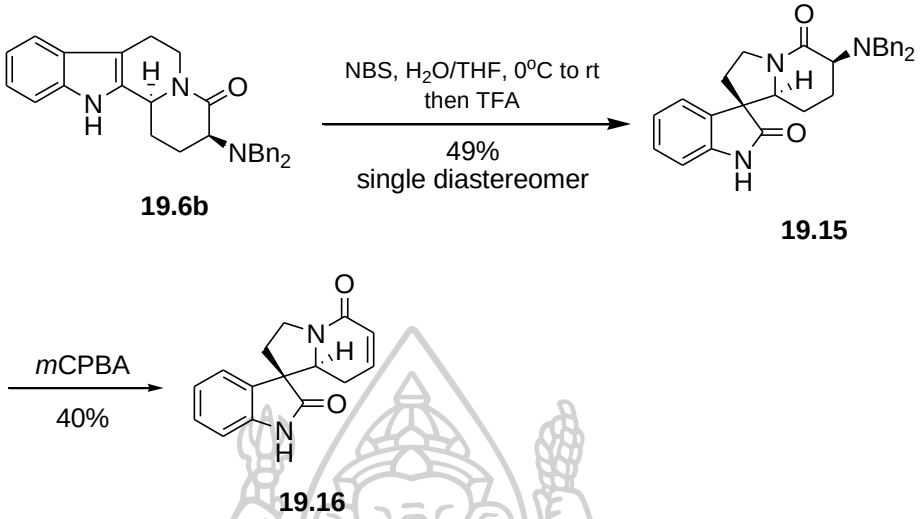

Scheme 145 Synthesis of spiro[indolizidine-1,3′-oxindole] derivative **19.16**

On the other hand, the oxidative ring contraction of diastereomer tetracyclic indoloquinolizidine **19.6b** gave a single product as a single diastereomer. The mechanism of oxidative ring contraction was explained by the molecular shape of the molecule. The initial bromination step happened only on the convex side of the molecule followed by rearrangement leading to a single diastereomer of spirooxindole **19.15** (Scheme 146).

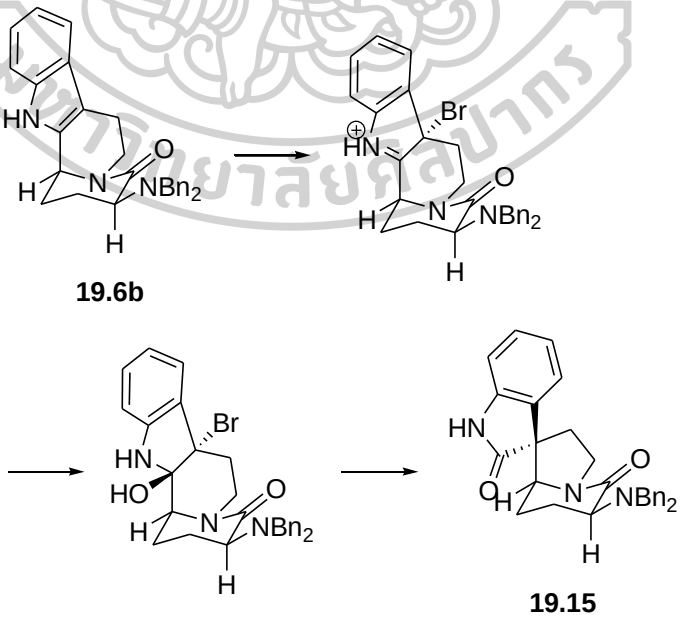

Scheme 146 Stereochemistry of oxidative rearrangement of tetracyclic indoloquinolizidine **19.6b**

The Boc carbamate protection of the indole nitrogen position of spiro[indolizidine-1,3′-oxindole] **19.8** and **19.16** using di-*tert*-butyl dicarbonate (Boc_2O), 4-dimethylaminopyridine (DMAP) and triethylamine to dissolve dichloromethane at room temperature generated *N*-Boc unsaturated spiro[indolizidine-1,3′-oxindole] **19.25** and **19.24** in 99% yield, respectively (Scheme 147).

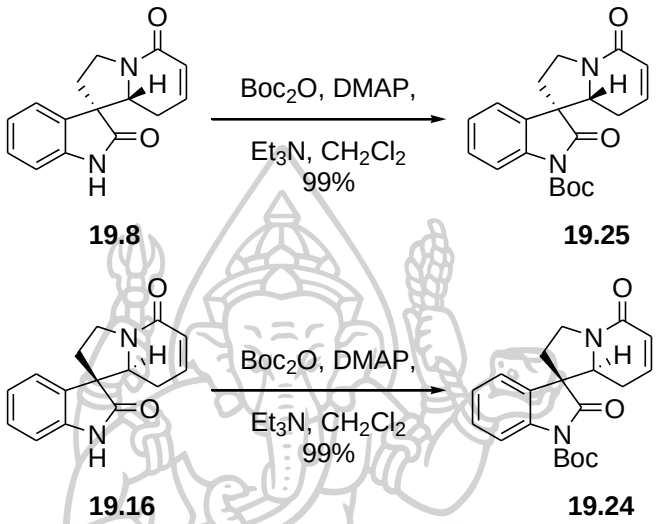

19.8 **19.25**

19.16 **19.24**

Scheme 147 Synthesis of *N*-Boc unsaturated spiro[indolizidine-1,3′-oxindole] derivative **19.24** and **19.25**

Hydrogenation of spiro[indolizidine-1,3′-oxindole] **19.7** and **19.15** under hydrogen atmosphere in the presence of palladium on activated charcoal (Pd/C) followed by Boc carbamate protection of the indole nitrogen using di-*tert*-butyl dicarbonate (Boc_2O), 4-dimethylaminopyridine (DMAP) and triethylamine at room temperature generated *N*-Boc spiro[indolizidine-1,3′-oxindole] **19.23** and **19.22** in 82% yield and 79% yield, respectively (Scheme 148).

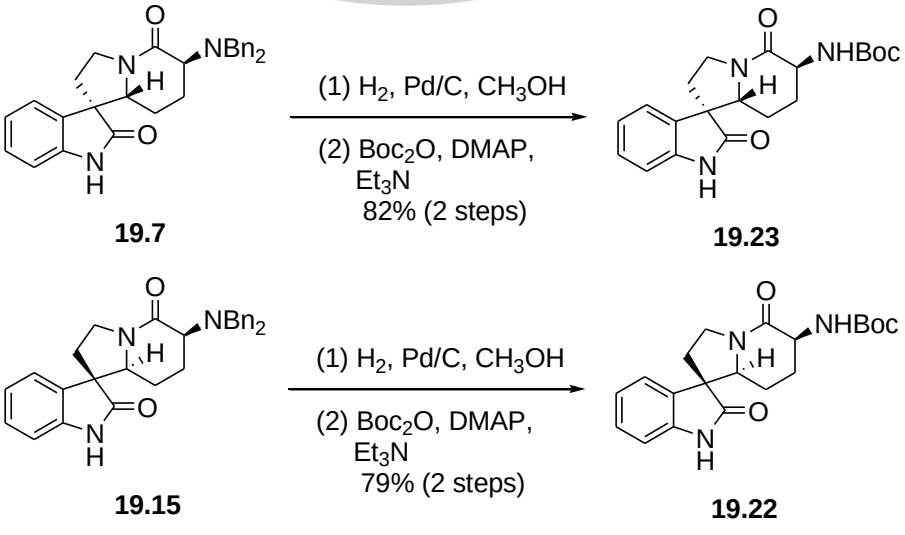

19.7 **19.23**

19.15 **19.22**

Scheme 148 Synthesis of *N*-Boc spiro[indolizidine-1,3´-oxindole] derivative **19.22** and **19.23**

The oxidative rearrangement of indoloquinolizidine-enamide **19.13** with *N*-bromosuccinimide as oxidant in the mixture of tetrahydrofuran (THF) and water at 0 ^{o}C in the presence of catalytic amount of trifluoroacetic acid (TFA) gave brominated spiroindolizidine-oxindole **19.14** as a single product and single diastereomer in 72% yield (Scheme 149).

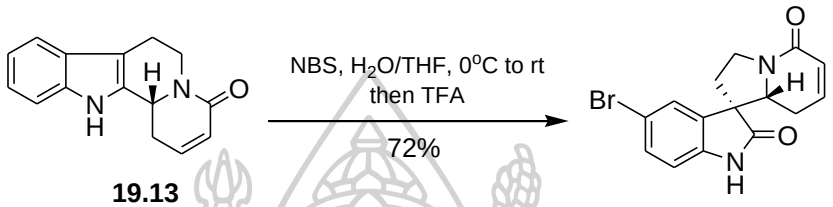

Scheme 149 Synthesis of spiro[indolizidine-1,3´-bromooxindole] **19.14**

Conformation investigation of indoloquinolizidine-enamide **19.13** reveals that the molecule is flat. Additional steric bias arises from the C1 allylic *β*-proton of the unsaturated lactam. Bromination of the indole ring happened from the bottom and subsequent addition of water and rearrangement generated spiroindolizidine-oxindole as a single diastereomer. Electrophilic aromatic bromination then occurred at the available C5 to provide the spiro[indolizidine-1,3´-bromooxindole] **19.14** (Scheme 150).

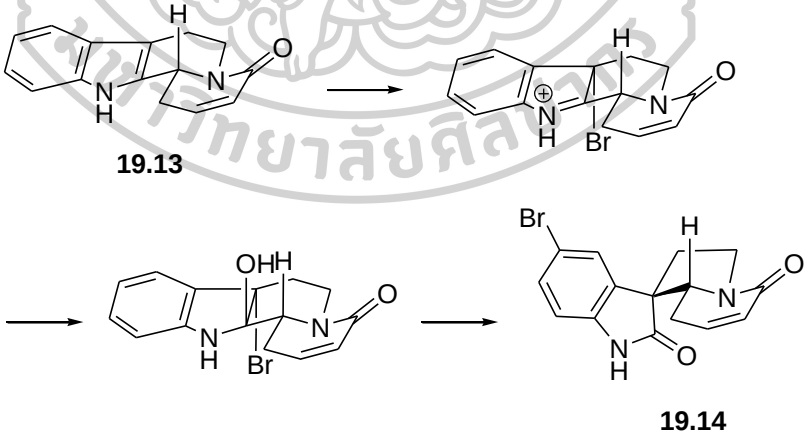

Scheme 150 Stereochemistry of oxidative rearrangement of indoloquinolizidine-enamide **19.13**

Conjugate addition of spiro[indolizidine-1,3´-bromooxindole] **19.14** using sodium to dissolve in methanol to generate methoxide install methyl ether substituent on C2 provided spiro[7-methoxyindolizidine-1,3´-bromooxindole] **19.27** in 65% yield (Scheme 148).

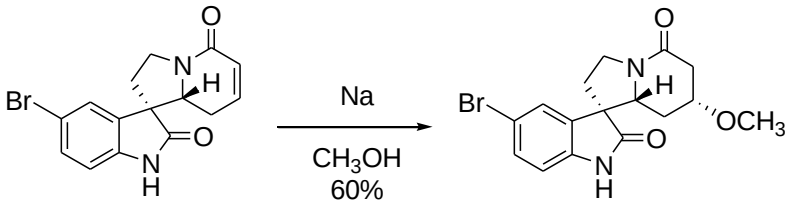

19.14 **19.27**

Scheme 151 Synthesis of spiro[7-methoxyindolizidine-1,3′-bromooxindole] **19.27**

The unsaturated lactam functionality of spiro[indolizidine-1,3′-bromooxindole] **19.14** is suitable for installation of substituents at the *β*-carbon via nucleophilic conjugate addition and possibly at the *α*-carbon via either tandem *α*-alkylation of the resulting enolate or subsequent C-alkylation of the lactam. The unsaturated spirolactam **19.14** was treated with sodium metal in methanol to generate methoxide to install methyl ether substituent on C2 to generate spiro[7-methoxyindolizidine-1,3′-bromooxindole] **19.27** as a single diastereomer. The stereochemistry was explained from the R-configuration due to methoxide attack from the *re* face of the enamide, while the *si* face was blocked by the oxindole ring (Scheme 152).

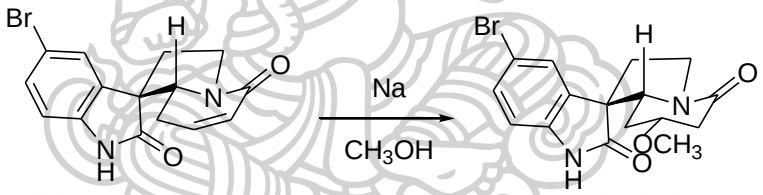

19.14 **19.27**

Scheme 152 Stereochemistry of conjugate addition of spiro[indolizidine-1,3′-bromooxindole] **19.14**

Conjugate addition of *α,β*–unsaturated spirolactam **19.8** was used with sodium in methanol to install methyl ether substituent on C2 to generate spiro[7-methoxyindolizidine-1,3′-bromooxindole] **19.17** in 65%. Likewise, if using sodium in ethanol reacted with *α,β*–unsaturated spirolactam **19.8** to give spiro[7-ethoxyindolizidine-1,3′-bromooxindole] **19.18** in 60% yield. The stereochemistry was explained from the R-configuration due to alkoxide attack from the re face of the enamide, while the si face was blocked by the oxindole ring (Scheme 153).

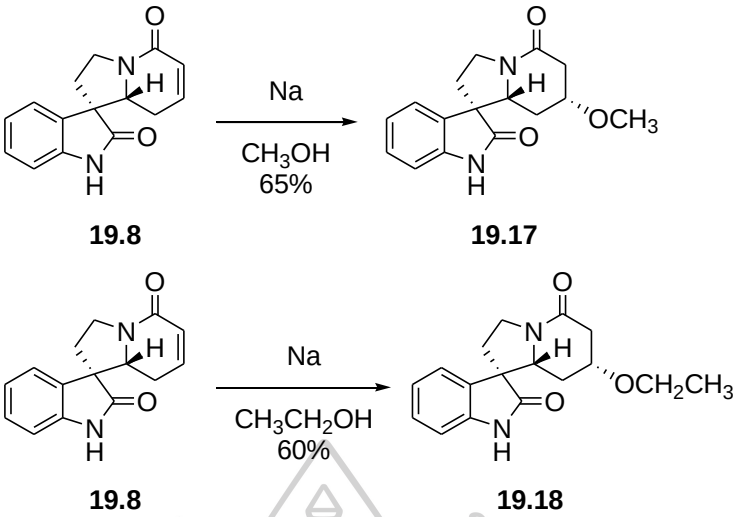

Scheme 153 Synthesis of spiro[7-methoxyindolizidine-1,3′-oxindole] **19.17** and spiro[7-ethoxyindolizidine-1,3′-oxindole] **19.18**

The synthesis of Rhynchophylline from spiroindolizidine-oxindole

The spiroindolizidine-oxindole **19.16** and indoloquinolizidine **19.13** are the core structure of Rhynchophylline and Hirsutine, respectively. In the future, this core structure could be synthesis the natural product. Concept used in the synthesis of Rhynchophylline in this research of the researcher. Rhynchophylline can be synthesized using a key reaction consisting of oxidative ring contraction, *N*-acyliminium ion cyclization, Cope elimination and Prins reaction. The structure of Rhynchophylline was obtained by Prins reaction from spiroindolizidine-oxindole **19.16**. The core structure of spiroindolizidine-oxindole **19.16** was achieved by oxidative ring contraction from indoloquinolizidinone **19.6b** (Scheme 154).

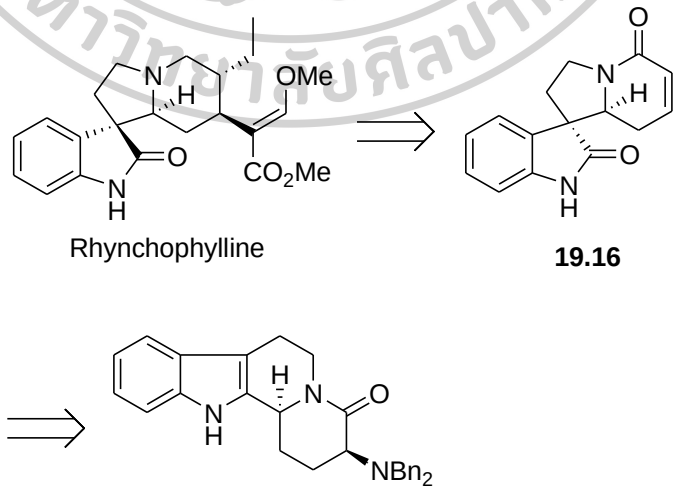

Scheme 154 Retrosynthetic analysis of Rhynchophylline as natural product

Concept used in the synthesis of Rhynchophylline. The spiroindolizidine-oxindole compound **19.16** is a suitable precursor compound for the formation of functional groups at different position leading to the total synthesis of Rhynchophylline. In the Future, the researcher is able to achieve a reduction reaction for synthesis followed by Prins reaction leads to the synthesis of unsaturated alcohol compound **19.29**, which is the core structure of Rhynchophylline which completed synthesis according to the research of Qin-Shi Zhao in the Journal of the Royal Society of Chemistry Advances 2016 (Scheme 155) (108).

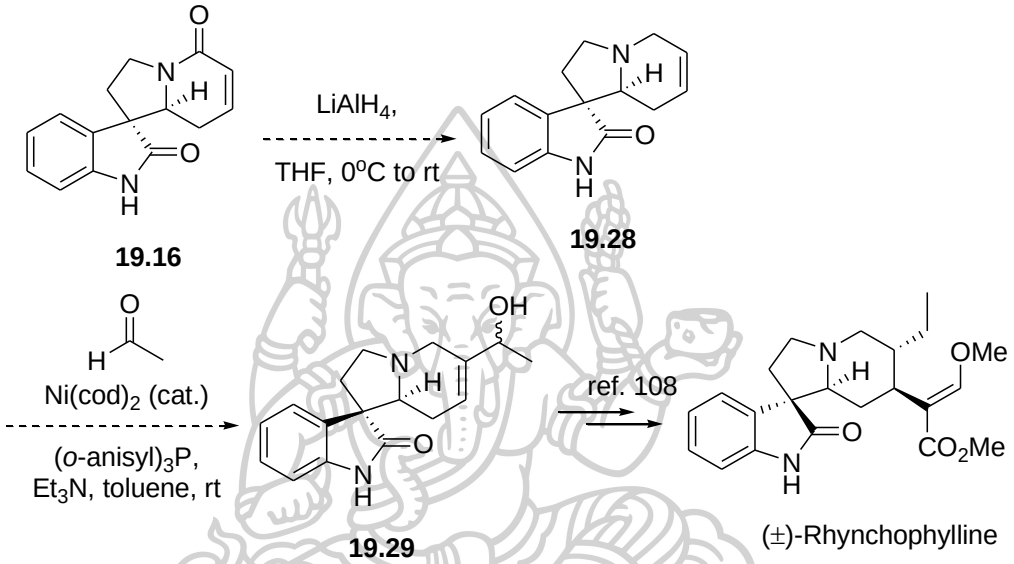

Scheme 155 The total synthesis of Rhynchophylline

Screening of *α*-glucosidase inhibitory activity from spiroindolizidine-oxindole and indolizidine derivaive

Diabetes mellitus is serious global health problem. Type 2 diabetes mellitus is public in diabetic populations. In Type 2 diabetes mellitus, inhibition of *α*-glucosidase is treatment to delay the absorption of glucose. The *α*-glucosidase is show a role in the conversion of carbohydrates into glucose. The glucose levels in the blood can be returned within normal limit by inhibiting α-glucosidase.

In this test, the *α*-glucosidase enzyme disintegrated with *p*-nitrophenyl *α*–D-glucopyranoside as a substrate by breaking the bonds in the structure to give *α*–D-glucopyranose and 4-nitrophenol. The 4-nitrophenol at pH 7.4 can absorb light at a wavelength of 405 nm. The intensity of light measured the quantity of *p*-nitrophenol released from *p*-nitrophenyl *α*–D-glucopyranoside. Acarbose was used as positive control of *α*-glucosidase inhibitor. The concentration of spiroindolizidine-oxindole and indolizidine derivaive required to inhibit 50% of *α*-glucosidase activity under the assay conditions was defined as the IC_{50} value (Scheme 156).

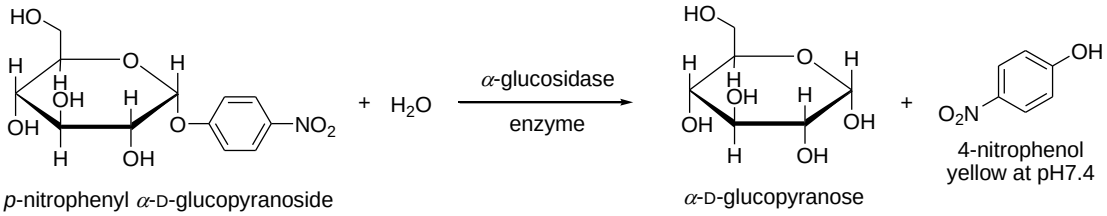

Scheme 156 Reaction between *p*-nitrophenyl α–D-glucopyranoside and α-glucosidase

The different of indoloquinolizidine and spiro[indolizidine-1,3′-oxindole] derivatives established for α-glucosidase inhibitory activity. The indoloquinolizidines (**19.10**, **19.6b**) and spiro[indolizidine-1,3′-oxindole] (**19.7**, **19.20**, **19.24**) inhibit the enzyme α-glucosidase with IC_{50} values of 18.06±0.01, 111.26±0.01, 107.14±0.02, 131.19±0.01 and 13.83±0.01 μM±SD, respectively which is most effective from a variety of synthetic structures. The spiro[indolizidine-1,3′-oxindole] (**19.24**) exhibited better α-glucosidase inhibitory activity with IC_{50} values of 13.83±0.01 μM±SD. This result was compared with acarbose as positive control which the IC_{50} value of 106.09±0.03 μM (Figure 32).

Figure 32 The α-glucosidase activity of indoloquinolizidine and spiro[indolizidine-1,3′-oxindole] derivatives.

No.	Compound	IC_{50} (μM) ± SD
1	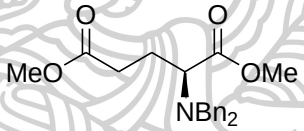 **19.2**	294.82±0.01
2	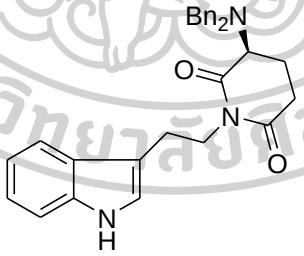 **19.4**	256.70±0.00
3	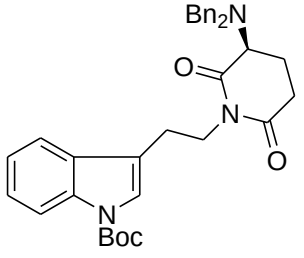 **19.19**	515.76±0.01

4	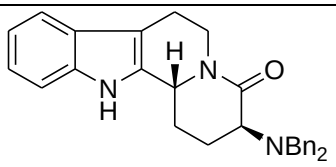 **19.6a**	145.32±0.01
5	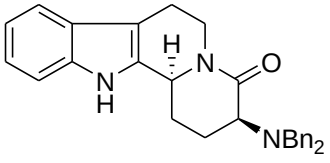 **19.6b**	111.26±0.01
6	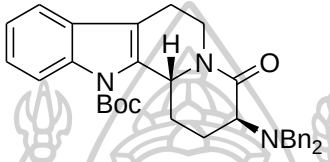 **19.11**	343.43±0.01
7	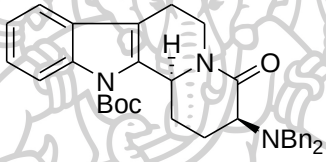 **19.9**	702.69±0.01
8	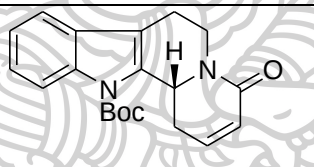 **19.12**	900.44±0.01
9	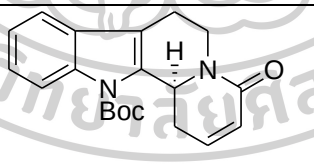 **19.10**	18.06±0.01
10	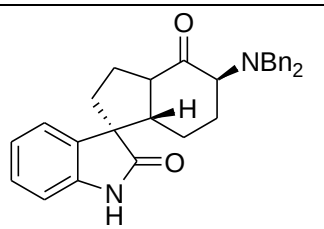 **19.7**	107.14±0.02

11	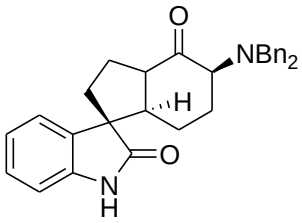 **19.15**	422.10±0.02
12	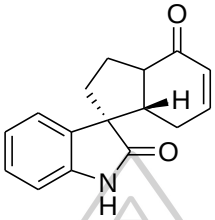 **19.8**	384.23±0.01
13	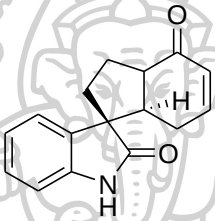 **19.16**	224.72±0.02
14	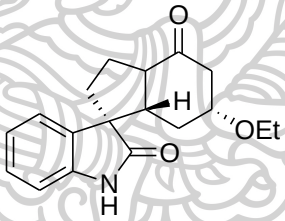 **19.18**	131.19±0.01
15	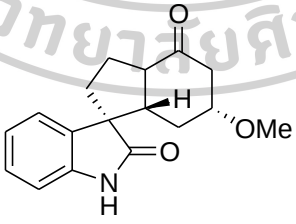 **19.17**	122.53±0.01
16	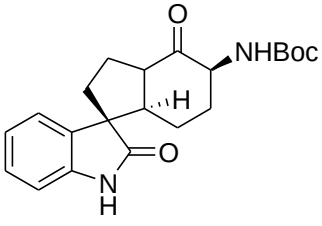 **19.22**	216.33±0.01

17	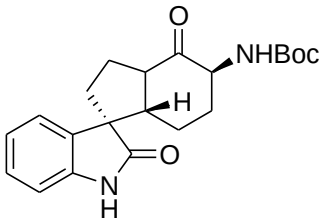 **19.23**	220.48±0.01
18	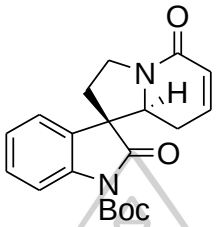 **19.24**	13.83±0.01
19	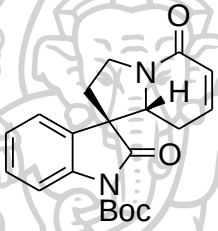 **19.25**	293.18±0.02
STD	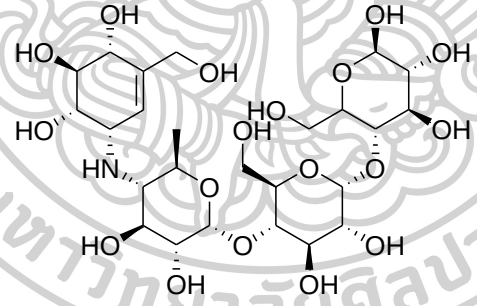 Acarbose	106.09±0.03

Nitric oxide synthesis inhibition assay: The Griess Test

Nitric oxide can be used as a signal for inflammation which can be induced by lipopolysaccharide (LPS). Nitric oxide synthesis is catalyzed in cells by nitric oxide synthase (NOS). Inhibition of this enzyme can be assayed using Griess test. Our experiments consisted of 3 modes. First the Raw264.7 (mouse) cells were treated with only the synthetic spiroindolizidine-oxindole and indolizidine derivaive for 48 h. Second experiments involved treatment with the chemical for 2 h followed by addition of LPS to induce inflammation. In the third set of experiments cells were treated with LPS first for 2 h prior to treatment with spiroindolizidine-oxindole and indolizidine derivaive. The results of nitric oxide (NO) assessment using Griess Test are shown below (Scheme 157).

Griess test	Day 0	Day 1		Day 2
Only sample	Plate cells →	Treat sample	→	NO assessment
Pretreat sample	Plate cells →	Treat sample	2h → LPS →	NO assessment
Pretreat LPS	Plate cells →	Treat LPS	2h → Sample →	NO assessment

Scheme 157 Experiment of nitric oxide synthesis inhibition assay: The Griess Test

The chart shows nitric oxide (NO) concentration (in μM) for spiroindolizidine-oxindole and indolizidine derivaives at the concentrations where cells had 90% survival, ranging from 0.5-20 *m*M. All spiroindolizidine-oxindole and indolizidine derivaives showed certain level of NOS inhibition. However, indoloquinolizidinone **19.6a** and amino-spiroindolizidine-oxindole **19.30** showed the most significant activity against nitric oxide (NO) production in LPS-pretreated cells. The spiroindolizidine-oxindole **19.15** was found to be more potent against nitric oxide (NO) production when it was used to pretreat the cells prior to LPS addition (Figure 33).

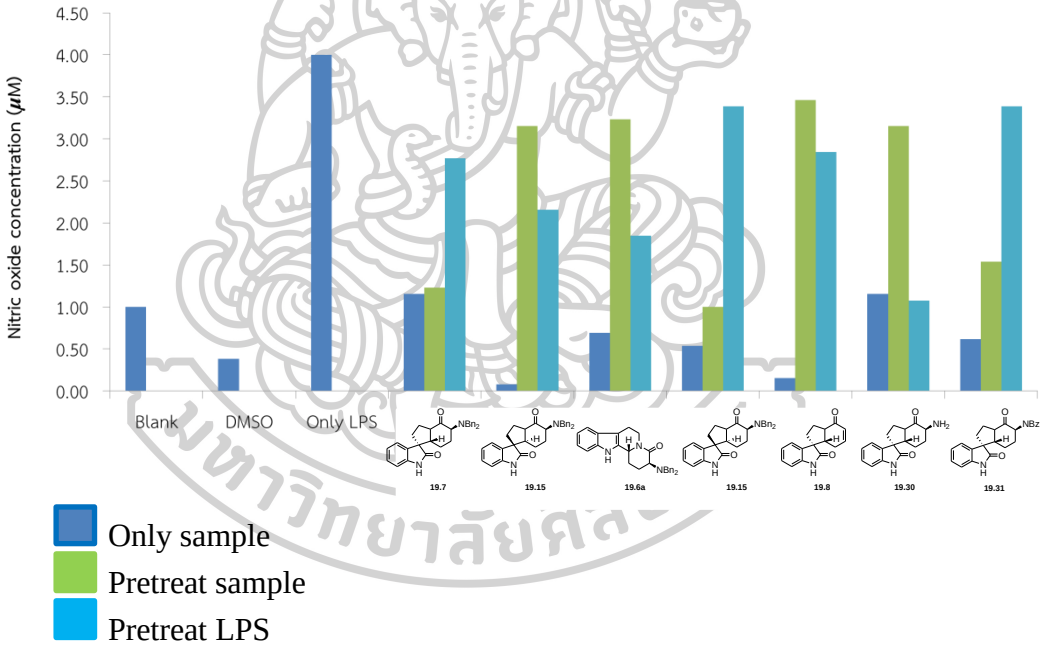

Figure 33 Chart of nitric oxide (NO) concentration (in μM) for spiroindolizidine-oxindole and indolizidine derivaive

Induced nitric oxide synthase (iNOS) protein expression: Western blot

In Western blot method, nitric oxide can be used as inflammatory signal which can be induce by lipopolysaccharide (LPS). Nitric oxide synthesis is catalyzed in cells by nitric oxide synthase (NOS). Thus, the protein expression of this enzyme can be assayed by Western blot. Our experiments consisted of 3 modes. First, the Raw264.7 (mouse) macrophage cells were treated with only the synthetic spiroindolizidine-oxindole and indolizidine derivaive for 48 h. Second experiments involved treatment with the spiroindolizidine-oxindole and indolizidine derivaive for 2 h followed by

addition of LPS to induce inflammation. In the third set of experiments, cells were treated with LPS for 2 h prior to treatment with spiroindolizidine-oxindole and indolizidine derivaive. The results of iNOS expression were examined by western blot as shown below (Scheme 158).

Western blot	**Day 0**	**Day 1**		**Day 2**
Only sample	Plate cells →	Treat sample	→	iNOS assessment
Pretreat sample	Plate cells →	Treat sample	2h → LPS →	iNOS assessment
Pretreat LPS	Plate cells →	Treat LPS	2h → Sample →	iNOS assessment

Scheme 158 Experiment of Induced nitric oxide synthase (iNOS) protein expression : Western blot

At day 2 of the experiments, cells were collected and examined the protein expression by western blot. It was found that LPS significantly increased iNOS expression when compared with control, LPS-induced inflammation. In part of LPS pretreatment (blue bar), spiroindolizidine-oxindole **19.8** and indoloquinolizidinone **19.6a** significantly decreased this protein level when compared with LPS. It might be suggested that these spiroindolizidine-oxindole and indolizidine have a preventive effect. Additionally, in part of chemical pretreatment (green bar), which spiroindolizidine-oxindole **19.31** significantly reduced iNOS expression. It seemed like that this spiroindolizidine-oxindole and indolizidine could protect inflammation. Taken together, these synthetic spiroindolizidine-oxindole and indolizidine might be having both preventive and protective effects on LPS-induced condition (Figure 34).

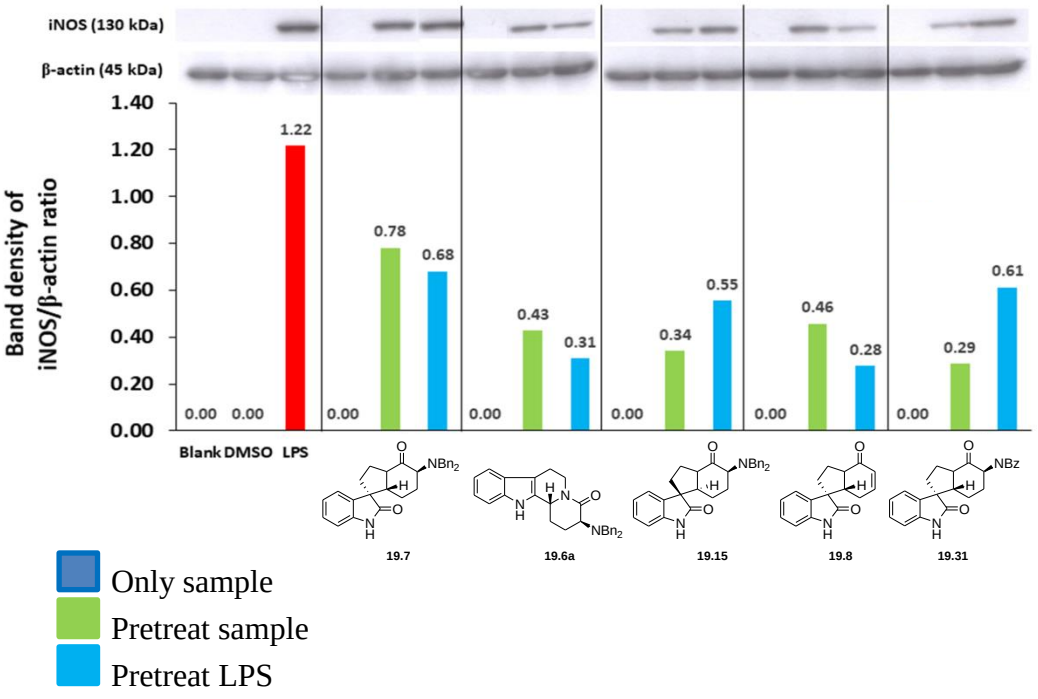

Figure 34 Chart of spiroindolizidine-oxindole and indolizidine derivaive against iNOS protein expression by Western blot with *β*–actin as a loading control

CHAPTER 4
EXPERIMENTAL PROCEDURE

Protocols for the *α*-glucosidase Inhibition
Reagents

1. Phosphate buffer saline (PBS), pH 7.4, 1000 mL

Disodium hydrogen phosphate (Na_2HPO_4) 1.4196 g., potassium dihydrogen phosphate (KH_2PO_4) 0.24496 g., sodium chloride (NaCl) 8.00669 g. and potassium chloride 0.20129 g dissolved with distilled water 1000 mL. The pH was then adjusted with 0.1 M HCl or 0.1 M NaOH to pH 7.4 with pH meter.

2. *p*-nitrophenyl *α*–D-glucopyranoside (MW = 301.25 g/mol) 5 mM, 100 mL

p-nitrophenyl *α*–D-glucopyranoside (Sigma-Aldrich) 0.151 g. dissolved with distilled water 100 mL for substrate.

3. Sodium carbonate (Na_2CO_3) (MW = 106.0 g/mol) 200 mM, 100 mL

Sodium carbonate 2.12 g. dissolved with distilled water 100 mL for stop reaction.

4. *α*-glucosidase enzyme 0.15 U/mL 1000 *μ*L

α-glucosidase enzyme (Sigma-Aldrich) (81 U/mg) 0.3 mg. dissolved with phosphate buffer saline (PBS) 1000 *μ*L. Take 6 *μ*L of the *α*-glucosidase enzyme solution from the above stock dissolved with phosphate buffer saline (PBS) 994 μL for assay.

5. Acarbose (MW = 645.6 g/mol) 1 mM 1000 *μ*L

Acarbose (Sigma-Aldrich) 0.6 mg. dissolved with phosphate buffer saline (PBS) 1000 *μ*L.for positive control.

Equipment

1. Auto pipette 1-20 *μ*L, 20-200 *μ*L and 100-1000 *μ*L
2. Tips 1-20 and 200-1000 *μ*L
3. Eppendorf tube 1 mL
4. Microplate
5. Vertex
6. pH meter
7. EZ Read 2000 Microplate Reader

Experiment

Blank reaction = Solvent + PBS Buffer + Enzyme + Substrate → 0% inhibition
Blank control = Solvent + PBS Buffer + Substrate → 100% inhibition

Sample reaction = Test sample + PBS Buffer + Enzyme + Substrate
Sample control = Test sample + PBS Buffer + Substrate

1. Divide the experiment into 4 sets and pipet the substance each concentration into a 96well-plate to the following volumes.

Series	PBS Buffer (μL)	Test sample (μL)	Enzyme (μL)	Solvent (μL)
Blank reaction	100	-	20	20
Blank control	120	-	-	20
Sample reaction	100	20	20	-
Sample control	120	20	-	-

2. The reaction mixture of sample at varying concentrations (0 to 640 μmol/L) was premixed with phosphate buffer pH 7.4. All solutions were mixed well and incubated at 25°C for 15 minutes.
3. The reaction mixture was added 20 μL of *p*-nitrophenyl α–D-glucopyranoside solution to each well, mix all the solutions together and incubate at 25°C for 15 minutes.
4. The reaction was terminated by the addition of 20 μL of sodium carbonate solution (Na_2CO_3) to each well for stop the reaction.
5. The α-glucosidase activity was determined spectrophotometrically at 405 nm on EZ Read 2000 Microplate Reader by measuring the quantity of *p*-nitrophenol released from *p*-nitrophenyl α–D-glucopyranoside. Acarbose was used as positive control of α-glucosidase inhibitor. The concentration of spiroindolizidine-oxindole and indolizidine derivaive required to inhibit 50% of α-glucosidase activity under the assay conditions was defined as the IC_{50} value.

Formula for calculated percent inhibition

$$\%\text{Inhibition} = [(A_{blank} - A_{sample})/A_{blank}] \times 100$$

$A_{blank} = A_{blank\ reaction} - A_{blank\ control}$
$A_{sample} = A_{sample\ reaction} - A_{sample\ control}$

General information

All ^1H and ^{13}C NMR spectra were recorded with a Bruker Avance-300 spectrometer (^1H at 300 and ^{13}C at 75 MHz) at room temperature in deuterated chloroform ($CDCl_3$). Chemical shifts are δ (ppm) with tetramethylsilane as an internal standard. Coupling constants (*J*) are given in Hertz (Hz). Analytical thin-layer chromatography (TLC) was performed using a Fluka precoated TLC plates of silica gel 60 F-254 plates with 0.2 mm layer thickness. Column chromatography was performed using silica gel 60, 230-400 mesh. Commercially available reagents and solvents were purchased from Sigma–Aldrich, Fluka and RCI Labscan. Starting materials and reagent were used without futher purification. Moisture-sensitive and air-sensitive reactions were carried out under an argon atmosphere. Tetrahydrofunran

(THF) was purified from sodium metal (Na) and benzophenone under argon atmosphere. Dichloromethane, toluene and triethylamine were freshly distilled from calcium hydride (CaH_2) under argon atmosphere. All round bottom flask and laboratory glassware were oven dried at 105 degree of Celsius prior to use. Unless otherwise stated, concentrated product was accomplished under reduced pressure. Ultraviolet (UV) active compounds were visualized with UV a light at 254 nm and heating the TLC plate after sinking in a 1% solution of vanillin in 0.1 M sulfuric acid in distilled ethanol.

General procedure

Synthesis of dimethyl *N*,*N*-dibenzyl-L-glutamate **19.3**

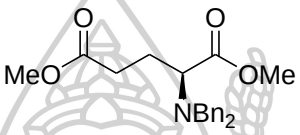

19.3

The *N*,*N*-dibenzyl-L-glutamic acid **19.2** (2.5 g, 7.64 mmol) was dissolved in acetone (100 mL) and methanol (50 mL). To this solution was added dimethyl sulfate (Me_2SO_4) (1.5 mL, 15.28 mmol) and potassium carbonate (K_2CO_3) (2.13 g, 15.28 mmol). The reaction was stirred at room temperature for 24 h. Upon completion was monitored by thin-layer chromatography (TLC). The reaction was quenched with drop-wise addition of saturated ammonium chloride solution (150 mL). The aqueous phase was extracted with dichloromethane (6x50 mL). The organic phase was washed with 5% sodium hydroxide (NaOH) (4x50 mL). The combined organic layers were dried over anhydrous sodium sulfate, filtered and concentrated under reduced pressure to give crude yellow oil. The crude product was purified by flash chromatography (silica gel, 4:1 hexane/ethyl acetate) to provide dimethyl *N*,*N*-dibenzyl-L-glutamate **19.3** as light yellow oil (1.9 g, 71%). R_f (4:1 hexane/EtOAc) 0.60; ^{1}H NMR (300 MHz, $CDCl_3$) δ 7.45-7.20 (m, 10H); 5.20 (dd, J = 12.0 Hz, 1H); 3.90 (m, 2H); 3.84 (s, 3H), 3.53 (s, 3H); 3.52 (m, 2H); 2.50 (t, 2H), 2.05 (m, 2H); ^{13}C NMR (75 MHz, $CDCl_3$) δ 172.7, 172.1, 139.2, 139.1, 135.9, 128.9, 128.6, 128.4, 128.3, 128.2, 127.0, 66.1, 59.5, 59.5, 54.4, 54.3, 51.4, 51.1, 30.3, 24.2, 24.1.ν_{max} (film) 1730, 1675, 1497, 1455, 1440, 1295, 1215, 1176 cm^{-1}

Synthesis of chiral *N*-indolylethylglutarimide **19.4**

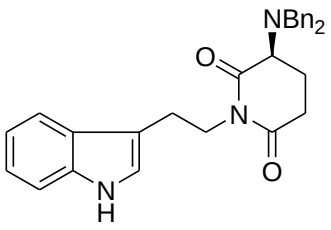

19.4

To a solution of tryptamine (0.503 g, 3.14 mmol) was dissolved in tetrahydrofuran (THF) (5 mL) under an argon atmosphere at 0 °C. To this solution was added lithium diisopropylamide (LDA) (3.14 mL, 6.28 mmol) for 10 min The mixture was added chiral dimethyl *N*,*N*-dibenzylglutamate **19.3** (0.5578 g, 1.57 mmol) to stir vigorously at 0 °C. Upon completion was monitored by thin-layer chromatography (TLC). The reaction was quenched with drop-wise addition of saturated sodium bicarbonate solution (10 mL). The aqueous phase was extracted with dichloromethane (5x10 mL). The combined organic layers were dried over anhydrous sodium sulfate, filtered and concentrated under reduced pressure to give crude yellow oil. The crude product was purified by flash chromatography (silica gel, 4:1 hexane/ethyl acetate) to provide chiral *N*-indolylethylglutarimide **19.4** as light yellow oil (0.651 g, 92%). R_f (4:1 hexane/EtOAc) 0.25; ^{1}H NMR (300 MHz, $CDCl_3$) δ 8.10 (brs, 1H); 7.80 (d, J = 7.2 Hz, 1H); 7.48-7.19 (m, 11H); 7.14 (td, J = 7.0 Hz, 1.4 Hz, 1H); 7.10 (td, J = 7.0, 1.4 Hz, 1H); 7.02 (d, J = 2.1 Hz, 1H); 4.13 (ddd, J = 12.0, 9.0, 7.5 Hz, 1H); 3.99 (ddd, J = 12.0, 8.7, 5.5, 1H); 3.84 (d, J = 14.0 Hz, 2H); 3.54 (d, J = 14.0 Hz, 2H); 3.39 (dd, J = 12.0, 5.4, 1H); 3.11-2.91 (m, 2H); 2.73 (ddd, J = 17.2, 4.0, 2.9 Hz, 1H); 2.35 (ddd, J = 17.2, 13.2, 5.8 Hz, 1H); 2.10 (m, 2H); ^{13}C NMR (75 MHz, $CDCl_3$) δ 173.2, 171.8, 139.7, 139.4, 136.1, 128.8, 128.5, 128.3, 127.7, 127.5, 127.1, 122.2, 122.0, 119.4, 119.0, 114.4, 112.8, 111.0, 66.1, 60.6, 59.2, 54.8, 54.6, 48.1, 40.5, 33.5, 33.0, 32.2, 29.6; ν_{max} (film) 3057, 3030, 2925, 2890, 1711, 1669, 1459, 1441, 1143, 1017, 736, 697 cm^{-1}; $[\alpha]^{D}_{25}$ -45.9 (c 1.2, $CHCl_3$).

Synthesis of chiral *N*-Boc indolylethylglutarimide **19.19**

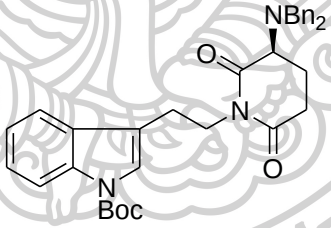

19.19

To a solution of chiral *N*-indolylethylglutarimide **19.4** (0.3574 g, 0.794 mmol) in dichloromethane (CH_2Cl_2) (15 mL) was added di-*tert*-butyldicarbonate (Boc_2O) (0.867 g, 3.97 mmol), triethylamine (Et_3N) (0.04 mL, 0.28 mmol) and 4-dimethylaminopyridine (DMAP) (0.556 mL, 0.867 mmol) and the mixture was stirred for 24 h. The reaction was quenched with water (15 mL) and dichloromethane (CH_2Cl_2) (15 mL). The phases were separated and extracted with dichloromethane (6x10 mL). The combined organic layers were dried over anhydrous sodium sulfate, filtered and concentrated under reduced pressure to give crude yellow oil. The crude product was purified by flash chromatography (silica gel, 4:1 hexane/EtOAc) to give chiral *N*-Boc-indolylethylglutarimide **19.19** (0.4279 g, 98%) as a yellow oil; R_f (4:1 hexane/EtOAc) 0.55; ^{1}H NMR (300 MHz, $CDCl_3$) δ 7.70 (d, 1H); 7.44-7.25 (m, 14H); 4.11 (m, 1H); 4.07 (m, 1H); 3.97 (d, 2H); 3.86 (d, 2H); 3.46 (dd, 1H); 2.95-2.91 (m, 2H); 2.89 (dt, 1H); 2.49 (dt, 1H); 1.90 (m, 2H); 1.62(s, 9H); ^{13}C NMR (75 MHz, $CDCl_3$) δ 173.2, 171.8, 149.6, 139.5, 139.5, 139.5, 135.4, 135.4, 130.5, 128.6, 128.6, 128.6, 128.6, 127.2, 127.2, 124.4, 123.5, 122.5, 119.1, 117.3, 115.2, 83.4, 59.2, 59.2,

54.9, 39.7, 32.2, 29.7, 28.1, 28.1, 28.1, 23.5, 23.5, 22.6; ν_{max} (film) 3025, 2928, 1727, 1650, 1481, 1230, 777, 679 cm^{-1}; $[\alpha]^{D}_{25}$ -35.7 (c 1.0, $CHCl_3$).

Synthesis of indoloquinolizidinone **19.6a**

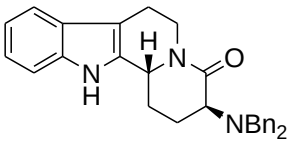

19.6a

Hydroxylactam **19.5** (141.80 mg, 0.31 mmol) was dissolved in dry dichloromethane (20 mL) under an argon atmosphere at 0 °C. To this solution was added trimethylsilyl trifluoromethanesulfonate (TMSOTf) (0.10 mL, 0.63 mmol) via syringe. The mixture was stirred at 0 °C for 3 h. The reaction was quenched with drop-wise addition of saturated sodium bicarbonate solution (20 mL). The mixture was extracted with dichloromethane (5x10 mL). The combined organic layers were dried over anhydrous sodium sulfate, filtered and concentrated under reduced pressure to give crude yellow oil. The crude product was purified by flash chromatography (silica gel, 4:1 hexane/ethyl acetate) to give 2 diastereomers of the indoloquinolizidinone product **19.6a** and diastereomer **19.6b** (99.70 mg, 1:2.3, 74% combined yield). R_f (4:1 hexane/EtOAc) 0.48; ^{1}H NMR (300 MHz, $CDCl_3$) δ 7.80 (brs, 1H); 7.45 (d, 1H); 7.40-7.02 (m, 13H); 5.22 (dd, J = 16.0, 8.0 Hz, 1H); 4.70 (d, J = 8.0 Hz, 1H); 4.15 (d, J = 14.0 Hz, 2H); 3.80 (d, J = 14.0 Hz, 2H); 3.39 (dd, J = 12.1, 6.4 Hz, 1H); 2.94-2.70 (m, 3H); 2.40 (dq, J = 13.2, 3.5 Hz, 1H); 2.30 (m, 1H); 2.06-1.91 (m, 1H); 1.60 (m, 1H). ^{13}C NMR (75 MHz, $CDCl_3$) δ 170.5, 140.4, 140.0, 136.2, 133.2, 129.2, 128.9, 128.8, 128.7, 128.7, 128.6, 128.5, 127.9, 127.5, 127.0, 126.8, 126.7, 125.8, 122.0, 119.7, 110.9, 109.3, 58.5, 55.6, 54.4, 54.1, 29.6, 28.4, 25.9. ν_{max} (film) 3228, 2923, 1618, 1453, 1431, 1263, 1155 cm^{-1}; $[\alpha]^{D}_{25}$ +44.0 (c 1.3, $CHCl_3$).

Indoloquinolizidinone **19.6b**

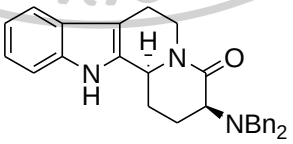

19.6b

R_f (4:1 hexane/EtOAc) 0.30; ^{1}H NMR (300 MHz, $CDCl_3$) δ 7.80 (brs, 1H); 7.50 (d, J = 7.20 Hz, 1H); 7.42 (m, 13H); 5.03 (dd, J = 12.0 Hz, J = 3.2 Hz, 1H); 4.75 (brs, 1H); 4.04 (d, J = 13.9 Hz, 2H); 3.65 (d, J = 13.9 Hz, 2H); 3.41 (dd, J = 10.0 Hz, J = 6.9 Hz, 1H); 3.07-2.82 (m, 2H); 2.73 (d, J = 12.0 Hz, 1H); 2.30-2.10 (m, 2H); 2.00-1.77 (m, 2H). ^{13}C NMR (75 MHz, $CDCl_3$) δ 171.5, 140.4, 136.0, 133.0, 128.9, 128.6, 128.5, 128.3, 128.3, 128.2, 128.1, 127.2, 126.7, 119.6, 118.1, 111.0, 110.5, 111.0, 58.3, 55.5, 53.8, 42.0, 25.8, 23.7, 21.2; ν_{max} (film) 3283, 3027, 2921, 1619, 1444, 1420, 1374, 1300 cm^{-1}; $[\alpha]^{D}_{25}$ -50.1 (c 1.5, $CHCl_3$).

Synthesis of *N*-Boc indoloquinolizidine **19.11**

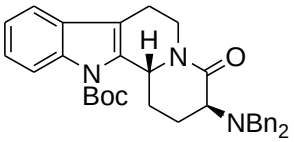

19.11

To a solution of indoloquinolizidine **19.6a** (29.7 mg, 0.0680 mmol) in dichloromethane (CH_2Cl_2) (10 mL) was added di-*tert*-butyldicarbonate (Boc_2O) (72.2 mg, 0.34 mmol), triethylamine (Et_3N) (0.05 mL, 0.34 mmol) and 4-dimethylaminopyridine (DMAP) (0.84 mg, 0.0068 mmol) and the mixture was stirred for 24 h. The reaction was quenched with water (10 mL) and dichloromethane (CH_2Cl_2) (10 mL). The phases were separated and extracted with dichloromethane (5x10 mL). The combined organic layers were dried over anhydrous sodium sulfate, filtered and concentrated under reduced pressure to give crude yellow oil. The crude product was purified by flash chromatography (silica gel, 4:1 hexane/EtOAc) to give *N*-Boc indoloquinolizidine **19.11** (31.8 mg, 87%) as a yellow oil; R_f (4:1 hexane/EtOAc) 0.55; ^{1}H NMR (300 MHz, $CDCl_3$) δ 8.00 (d, J = 8.0 Hz, 1H); 7.50 (m, 3H); 7.35-7.15 (m, 10H); 5.15 (d, J = 12.0 Hz, 1H); 5.05 (d, J = 10.2 Hz, 1H); 4.10 (d, J = 14.0 Hz, 2H); 3.80 (d, J = 13.9 Hz, 2H); 3.35 (dd, J = 11.6, 7.3 Hz, 1H); 2.85-2.70 (m, 3H); 2.60 (d, J = 13.0 Hz, 1H); 2.00 (m, 3H); 1.70 (s, 9H). ^{13}C NMR (75 MHz, $CDCl_3$) δ 170.8, 150.2, 140.5, 136.7, 135.2, 133.0, 132.2, 129.2, 129.0, 128.8, 128.7, 128.5, 128.1, 127.7, 126.8, 126.0, 124.6, 123.0, 118.2, 115.5, 84.3, 80.0, 58.7, 56.1, 55.4, 42.7, 38.7, 31.9, 30.0, 29.7, 29.5, 29.4, 28.5, 28.2; ν_{max} (film) 3420, 2930, 2854, 1720, 1625, 1470, 1337, 1229, 759, 677 cm^{-1}; $[\alpha]^{D}_{25}$ +70.2 (c 1.6, $CHCl_3$).

Synthesis of *N*-Boc indoloquinolizidine **19.9**

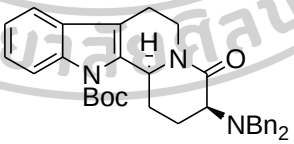

19.9

To a solution of indoloquinolizidine **19.6b** (24.4 mg, 0.0552 mmol) in dichloromethane (CH_2Cl_2) (10 mL) was added di-*tert*-butyldicarbonate (Boc_2O) (60.3 mg, 0.28 mmol), triethylamine (Et_3N) (0.04 mL, 0.28 mmol) and 4-dimethylaminopyridine (DMAP) (0.67 mg, 0.0055 mmol) and the mixture was stirred for 24 h. The reaction was quenched with water (10 mL) and dichloromethane (CH_2Cl_2) (10 mL). The phases were separated and extracted with dichloromethane (5x10 mL). The combined organic layers were dried over anhydrous sodium sulfate, filtered and concentrated under reduced pressure to give crude yellow oil. The crude product was purified by flash chromatography (silica gel, 4:1 hexane/EtOAc) to give *N*-Boc indoloquinolizidine **19.9** (29.4 mg, 98%) as a yellow oil; R_f (4:1

hexane/EtOAc) 0.75; ^{1}H NMR (300 MHz, $CDCl_3$) δ 8.00 (dd, J = 12.6, 7.6 Hz, 1H); 7.50 (m, 4H); 7.40-7.15 (m, 10H); 5.05 (d, J = 7.5 Hz, 2H); 4.20 (d, J = 14.0 Hz, 2H); 3.80 (d, J = 14.0 Hz, 2H); 3.5 (dd, J = 11.4, 7.0 Hz, 1H); 2.85-2.70 (m, 3H); 2.40 (m, 1H); 2.10 (m, 1H); 1.90 (m, 1H); 1.60 (s, 9H). ^{13}C NMR (75 MHz, $CDCl_3$) δ 172.4, 172.4, 149.9, 140.7, 140.7, 136.6, 136.1, 134.5, 128.5, 128.2, 126.7, 124.8, 124.6, 123.4, 123.0, 118.6, 118.4, 118.2, 117.7, 115.8, 115.7, 84.3, 57.0, 56.9, 55.3, 55.2, 53.8, 52.7, 52.5, 38.8, 38.6, 29.7, 29.6, 28.1, 24.0; ν_{max} (film) 3320, 2935, 2859, 1701, 1680, 1480, 1347, 1230, 765, 675 cm^{-1}; $[\alpha]^{D}_{25}$ -65.9 (c 1.2, $CHCl_3$).

Synthesis of *N*-Boc-indoloquinolizidine-enamide **19.12**

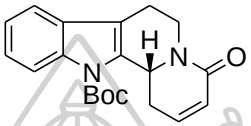

19.12

To a solution of *N*-Boc indoloquinolizidine **19.11** (16.9 mg, 0.032 mmol) in dichloromethane (CH_2Cl_2) (10 mL) at 0 ^{o}C was added *m*CPBA (70%w/w, 11.6 mg, 0.047 mmol) and the mixture was stirred for 15 min. The reaction was quenched saturated aqueous sodium hydrogencarbonate ($NaHCO_3$) (10 mL). The phases were separated and extracted with dichloromethane (5x10 mL). The combined organic layers were dried over anhydrous sodium sulfate, filtered and concentrated under reduced pressure to give crude yellow oil. The crude product was purified by flash chromatography (silica gel, 1:1 hexane/EtOAc) to give *N*-Boc-indoloquinolizidine-enamide **19.12** (7.9 mg, 74%) as a yellow oil; R_f (1:1 hexane/EtOAc) 0.55; ^{1}H NMR (300 MHz, $CDCl_3$) δ 8.20 (d, J = 7.5 Hz, 1H); 8.10 (d, J = 7.5 Hz, 1H); 7.50 (dd, J =7.5, 1.6 Hz, 1H); 7.60-7.25 (m, 2H); 6.70 (ddd, J = 9.1, 6.7, 2.0, 1H); 6.10 (dd, J = 9.7, 3.0 Hz, 1H); 5.20 (d, J = 12.0 Hz, 1H); 5.00 (dd, J = 13.0, 3.0 Hz, 1H); 3.10 (ddd, J = 17.0, 6.9, 3.5, 1H); 2.85-2.70 (m, 1H); 2.20 (m, 1H); 1.90 (m , 1H); 1.70 (s, 9H); ^{13}C NMR (75 MHz, $CDCl_3$) δ 162.4, 147.6, 136.6, 134.2, 128.0, 127.3, 126.8, 126.2, 125.8, 123.0, 122.3, 116.0, 115.6, 113.4, 68.8, 50.9, 35.1, 29.2, 27.2, 25.8; ν_{max} (film) 3420, 2922, 2854, 1730, 1615, 1605, 1350, 1273, 770, 679 cm^{-1}; $[\alpha]^{D}_{25}$ +85.0 (c 1.0, $CHCl_3$).

Synthesis of *N*-Boc-indoloquinolizidine-enamide **19.10**

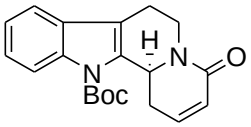

19.10

To a solution of *N*-Boc indoloquinolizidine **19.9** (12.4 mg, 0.023 mmol) in dichloromethane (CH_2Cl_2) (10 mL) at 0 ^{o}C was added *m*CPBA (70%w/w, 8.6 mg, 0.035 mmol) and the mixture was stirred for 15 min. The reaction was quenched saturated aqueous sodium hydrogencarbonate ($NaHCO_3$) (10 mL). The phases were separated and extracted with dichloromethane (5x10 mL). The combined organic

layers were dried over anhydrous sodium sulfate, filtered and concentrated under reduced pressure to give crude yellow oil. The crude product was purified by flash chromatography (silica gel, 1:1 hexane/EtOAc) to give *N*-Boc-indoloquinolizidine-enamide **19.10** (5.2 mg, 66%) as a yellow oil; R_f (1:1 hexane/EtOAc) 0.57; ^{1}H NMR (300 MHz, $CDCl_3$) δ 8.20 (d, J = 7.5 Hz, 1H); 8.10 (d, 1H); 7.45 (dd, J =7.5, 1.6 Hz, 1H); 7.40-7.20 (m, 2H); 6.70 (ddd, J = 9.1, 6.7, 2.0, 1H); 6.10 (dd, J = 9.5, 2.9 Hz, 1H); 5.20 (d, J = 12.0 Hz, 1H); 5.00 (dd, J = 13.0, 3.0 Hz, 1H); 3.10 (ddd, 16.9, 6.8, 3.1, 1H); 2.85-2.70 (m, 1H); 2.20 (m, 1H); 1.90 (m, 1H); 1.70 (s, 9H). ^{13}C NMR (75 MHz, $CDCl_3$) δ 164.8, 150.0, 139.1, 136.6, 134.3, 134.1, 133.2, 130.5, 130.4, 129.2, 128.9, 128.6, 128.5, 128.4, 84.5, 71.2, 53.3, 37.5, 31.6, 29.7; ν_{max} (film) 3415, 3022, 2755, 1710, 1604, 1595, 1357, 1278, 786, 678 cm^{-1}; $[\alpha]^D_{25}$ -70.4 (c 0.9, $CHCl_3$).

Synthesis of indoloquinolizidine-enamide **19.13**

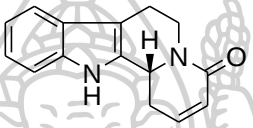

19.13

To a solution of *N*-Boc-indoloquinolizidine-enamide **19.12** (28.4 mg, 0.084 mmol) in tetrahydrofuran (THF) (5 mL) at 0 ^{o}C was added trifluoroacetic acid (TFA) (0.01 mL, 0.16 mmol) and the mixture was stirred for 4 h. The reaction was quenched saturated aqueous sodium carbonate (Na_2CO_3) (10 mL). The phases were separated and extracted with dichloromethane (5x10 mL). The combined organic layers were dried over anhydrous sodium sulfate, filtered and concentrated under reduced pressure to give crude yellow oil. The crude product was purified by flash chromatography (silica gel, 1:1 hexane/EtOAc) to give indoloquinolizidine-enamide **19.13** (14.2 mg, 71%) as a colorless oil; R_f (1:1 hexane/EtOAc) 0.25; ^{1}H NMR (300 MHz, $CDCl_3$) δ 8.10 (brs, 1H); 7.60 (d, J = 7.5 Hz, 1H); 7.25-7.40 (m, 3H); 6.70 (ddd, J = 10.0, 7.1, 2.9 Hz, 1H); 6.10 (dd, J = 9.8, 3.0 Hz, 1H); 5.25 (ddd, J = 12.9, 5.0, 3.2 Hz, 1H); 5.05 (dd, J = 13.6, 4.4, 1H); 3.10 (dt, 1H); 2.85-2.70 (m, 3H); 2.20 (t, 1H). ^{13}C NMR (75 MHz, $CDCl_3$) δ 170.9, 140.5, 139.9, 129.8, 126.8, 124.1, 124.0, 118.3, 111.0, 67.9, 63.3, 58.4, 25.6, 25.6, 18.4; ν_{max} (film) 3215, 2821, 1644, 1595, 1352, 1303, 1137, 986, 878 cm^{-1} $[\alpha]^D_{25}$ +51.4 (c 1.1, $CHCl_3$).

Synthesis of indoloquinolizidine-enamide **19.26**

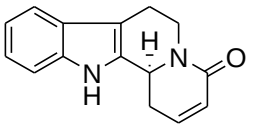

19.26

To a solution of *N*-Boc-indoloquinolizidine-enamide **19.10** (33.5 mg, 0.099 mmol) in tetrahydrofuran (THF) (5 mL) at 0 ^{o}C was added trifluoroacetic acid (TFA) (0.02 mL, 0.20 mmol) and the mixture was stirred for 4 h. The reaction was quenched saturated aqueous sodium carbonate (Na_2CO_3) (10 mL). The phases were separated

and extracted with dichloromethane (5x10 mL). The combined organic layers were dried over anhydrous sodium sulfate, filtered and concentrated under reduced pressure to give crude yellow oil. The crude product was purified by flash chromatography (silica gel, 1:1 hexane/EtOAc) to give indoloquinolizidine-enamide **19.26** (16.3 mg, 69%) as a colorless oil; R_f (1:1 hexane/EtOAc) 0.25; ^{1}H NMR (300 MHz, $CDCl_3$) δ 8.10 (brs, 1H); 7.60 (d, J = 7.6 Hz, 1H); 7.25-7.40 (m, 3H); 6.70 (ddd, J = 10.5, 7.0, 3.0 Hz, 1H); 6.10 (dd, J = 10.3, 3.0 Hz, 1H); 5.25 (ddd, J = 12.7, 5.0, 3.2 Hz, 1H); 5.05 (dd, J = 13.1, 4.4, 1H); 3.10 (dt, 1H); 2.85-2.70 (m, 3H); 2.20 (t, 1H). ^{13}C NMR (75 MHz, $CDCl_3$) δ 163.0, 136.5, 122.8, 122.5, 121.0, 116.1, 113.4, 51.4, 50.7, 35.1, 29.0, 27.2, 19.1; ν_{max} (film) 3298, 2906, 1689, 1590, 1351, 1299, 1147, 990, 867 cm^{-1} $[\alpha]^{D}_{25}$ -44..7 (c 0.9, $CHCl_3$).

Synthesis of spiro[indolizidine-1,3′-oxindole] **19.7**

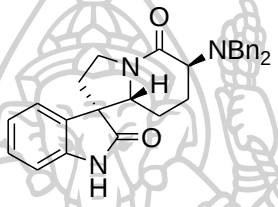

19.7

To a solution of indoloquinolizidine **19.6a** (0.021 g, 0.049 mmol) was dissolved in a 1:1 mixture tetrahydrofuran (3 mL) with water (3 mL). The mixture was added *N*-bromosuccinimide (NBS) (10.41 mg, 0.059 mmol) for 10 min at room temperature. The reaction was added trifluoroacetic acid (TFA) (0.30 μL, 0.49 mmol) at 0 ^{o}C. The mixture was stirred vigorously at 0 °C to room temperature. Upon completion monitored by thin layer chromatography (TLC) for overnight. The reaction was quenched with drop-wise addition of saturated sodium hydrogencarbonate solution ($NaHCO_3$) (5 mL). The mixture was extracted with dichloromethane (CH_2Cl_2) (5x5 mL). The combined organic layers were dried over anhydrous sodium sulfate, filtered and concentrated under reduced pressure by evaporator to give crude pale yellow oil. The crude product was purified by column chromatography (silica gel, a 1:1 mixture of hexane and ethyl acetate) to provide spiro[indolizidine-1,3′-oxindole] **19.7** as a colorless oil (0.010 g, 46%); R_f (1:1 hexane/EtOAc) 0.57; ^{1}H NMR (300 MHz, $CDCl_3$) δ 8.30 (s, 1H); 7.40 (d, J = 7.0 Hz, 4H); 7.17-7.35 (m, 7H); 7.00 (m, 3H); 6.90 (m, 3H); 4.10 (m, 1H); 4.00 (d, J = 14.0 Hz, 2H); 3.90 (m, 2H); 3.70 (d, J = 14.0 Hz, 2H); 3.3-3.4 (t, J = 7.1 Hz, 1H); 2.50 (dd, J = 12.7, 10.1, 1H); 2.10 (ddd, J = 8.0, 7.0, 1.2, 1H); 1.80-1.90 (m, 2H); 1.50 (dd, J = 14.0, 6.0 Hz, 1H); 1.22 (dd, J = 14.0, 7.9 Hz, 1H); ^{13}C NMR (75 MHz, $CDCl_3$) δ 178.5, 178.2, 171.0, 140.1, 129.8, 129.6, 128.7, 128.6, 128.5, 128.4, 128.3, 128.2, 127.7, 127.1, 126.8, 124.2, 123.9, 123.0, 122.0, 110.5, 64.9, 58.1, 56.0, 55.3, 44.0, 33.4, 29.5, 24.9, 23.1; ν_{max} (film) 3205, 2930, 2880, 1701, 1615, 1476, 1353, 1180, 750, 700 cm^{-1}; $[\alpha]^{D}_{25}$ -36.7 (c 0.8, $CHCl_3$).

Synthesis of spiro[indolizidine-1,3′-oxindole] **19.15**

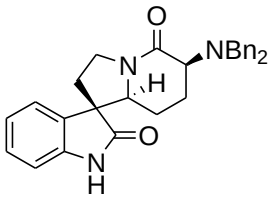

19.15

To a solution of indoloquinolizidine **19.6b** (0.020 g, 0.046 mmol) was dissolved in a 1:1 mixture tetrahydrofuran (3 mL) with water (3 mL). The mixture was added *N*-bromosuccinimide (NBS) (9.77 mg, 0.055 mmol) for 10 min at room temperature. The reaction was added trifluoroacetic acid (TFA) (0.28 μL, 0.46 mmol) at 0 ^{o}C. The mixture was stirred vigorously at 0 °C to room temperature. Upon completion monitored by thin layer chromatography (TLC) for overnight. The reaction was quenched with drop-wise addition of saturated sodium hydrogencarbonate solution ($NaHCO_3$) (5 mL). The mixture was extracted with dichloromethane (CH_2Cl_2) (5x5 mL). The combined organic layers were dried over anhydrous sodium sulfate, filtered and concentrated under reduced pressure by evaporator to give crude pale yellow oil. The crude product was purified by column chromatography (silica gel, a 1:1 mixture of hexane and ethyl acetate) to provide spiro[indolizidine-1,3′-oxindole] **19.15** as a colorless oil (0.010 g, 49%); R_f (1:1 hexane/EtOAc) 0.40; ^{1}H NMR (300 MHz, $CDCl_3$) δ 8.50 (s, 1H); 7.40 (d, J = 7.1 Hz, 4H); 7.15-7.32 (m, 7H); 7.08 (m, 3H); 6.90 (m, 3H); 4.13 (m, 1H); 4.08 (d, J = 14.0 Hz, 2H); 3.89 (m, 2H); 3.70 (d, J = 14.0 Hz, 2H); 3.2-3.4 (t, J = 7.0 Hz, 1H); 2.50 (dd, J = 13.0, 10.2 Hz, 1H); 2.10 (ddd, J = 8.1, 6.9, 1.2, 1H); 1.80-1.90 (m, 2H); 1.50 (dd, J =14.0, 5.7 Hz, 1H); 1.20 (dd, J = 14.0, 8.0 Hz, 1H); ^{13}C NMR (75 MHz, $CDCl_3$) δ 177.7, 177.4 171.0, 140.2, 129.8, 128.7, 128.5, 128.5, 128.5, 128.5, 128.2, 128.2, 128.2, 128.2, 126.8, 126.8, 124.0, 122.9, 110.3, 63.2, 57.4, 56.0, 55.3, 43.9, 33.3, 29.5, 25.1, 22.2; ν_{max} (film) 3207, 2927, 2890, 1714, 1619, 1477, 1333, 1310, 750 cm^{-1}; $[\alpha]^{D}_{25}$ +40.5 (c 0.9, $CHCl_3$).

Synthesis of *α,β*–unsaturated spiroindolizidine-oxindole **19.8**

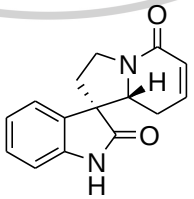

19.8

To a solution of spiro[indolizidine-1,3′-oxindole] **19.7** (20.9 mg, 0.046 mmol) in dichloromethane (CH_2Cl_2) (10 mL) at 0 ^{o}C was added *m*CPBA (70%w/w, 17.0 mg, 0.069 mmol) and the mixture was stirred for 15 minutes. The reaction was quenched saturated aqueous sodium hydrogencarbonate ($NaHCO_3$) (10 mL). The phases were separated and extracted with dichloromethane (5x10 mL). The combined organic layers were dried over anhydrous sodium sulfate, filtered and concentrated under reduced pressure to give crude yellow oil. The crude product was purified by flash

chromatography (silica gel, 1:1 hexane/EtOAc) to give *α,β*–unsaturated spiroindolizidine-oxindole **19.8** (5.7 mg, 48%) as a colorless oil; R_f (1:2 hexane/EtOac) 0.20; ^{1}H (300 MHz, $CDCl_3$) δ 8.40 (brs, 1H), 7.30 (td, *J* = 7.7, 1.1 Hz, 1H), 7.14 (d, *J* = 7.0 Hz, 1H), 7.10 (t, *J* = 7.7 Hz, 1H), 6.97 (d, *J* = 7.7 Hz, 1H), 6.45 (ddd, *J* = 9.8, 6.2, 2.0 Hz, 1H), 5.95 (dd, *J* = 9.8, 2.9 Hz, 1H), 4.28 (dd, *J* = 13.9, 5.7 Hz, 1H) 4.05 (dd, *J* = 11.2, 10.5 Hz, 1H), 3.99 (ddd, *J* = 10.7, 7.6, 7.6 Hz, 1H), 2.53 (dt, *J* = 12.7, 10.5 Hz, 1H), 2.12 (ddd, *J* = 12.5, 7.4, 1.3 Hz, 1H, 2.04 (dt, *J* = 17.5, 6.0 Hz, 1H), 1.84 (ddt, *J* = 17.1, 14.2, 2.7 Hz, 1H); ^{13}C (75 MHz, $CDCl_3$) δ 177.9, 168.7, 139.8, 138.9, 129.6, 128.8, 124.9, 124.4, 123.2, 110.4, 62.2, 57.3, 43.5, 33.5, 25.1; ν_{max} (film) 3219, 2934, 1716, 1663, 1470, 1340, 1229, 1145, 812, 795 cm^{-1}; $[\alpha]^{D}_{25}$ +18.5 (c 0.8, $CHCl_3$).

Synthesis of *α,β*–unsaturated spiroindolizidine-oxindole **19.16**

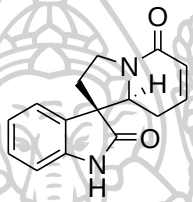

19.16

To a solution of spiro[indolizidine-1,3´-oxindole] **19.15** (20.0 mg, 0.044 mmol) in dichloromethane (CH_2Cl_2) (10 mL) at 0 ^{o}C was added *m*CPBA (70%w/w, 16.2 mg, 0.066 mmol) and the mixture was stirred for 15 min. The reaction was quenched saturated aqueous sodium hydrogencarbonate ($NaHCO_3$) (10 mL). The phases were separated and extracted with dichloromethane (5x10 mL). The combined organic layers were dried over anhydrous sodium sulfate, filtered and concentrated under reduced pressure to give crude yellow oil. The crude product was purified by flash chromatography (silica gel, 1:1 hexane/EtOAc) to give *α,β*–unsaturated spiroindolizidine-oxindole **19.16** (4.5 mg, 40%) as a colorless oil; R_f (1:2 hexane/EtOac) 0.20; ^{1}H (300 MHz, $CDCl_3$) δ 9.35 (brs, 1H), 7.32 (td, *J* = 7.5, 1.2 Hz, 1H), 7.20 (d, *J* = 7.0 Hz, 1H), 7.10 (t, *J* = 7.7 Hz, 1H), 6.97 (d, *J* = 7.7 Hz, 1H), 6.43 (ddd, *J* = 9.7, 6.2, 2.0 Hz, 1H), 5.95 (dd, *J* = 9.7, 3.0 Hz, 1H), 4.28 (dd, *J* = 14.0, 6.0 Hz, 1H) 4.05 (dd, *J* = 12.0, 10.7 Hz, 1H), 3.99 (ddd, *J* = 10.7, 7.6, 7.6 Hz, 1H), 2.53 (dt, *J* = 12.5, 10.7 Hz, 1H), 2.12 (ddd, *J* = 12.5, 7.4, 1.3 Hz, 1H, 2.04 (dt, *J* = 17.3, 6.0 Hz, 1H), 1.84 (ddt, *J* = 17.3, 14.2, 2.7 Hz, 1H); ^{13}C (75 MHz, $CDCl_3$) δ 177.9, 167.4, 140.4, 138.5, 129.8, 128.8, 124.9, 124.4, 123.0, 110.6, 62.3, 57.4, 43.6, 33.6, 25.3; ν_{max} (film) 3189, 2904, 1756, 1673, 1439, 1335, 1240, 1141, 866, 789 cm^{-1}; $[\alpha]^{D}_{25}$ -14.1 (c 0.5, $CHCl_3$).

Synthesis of *N*-Boc unsaturated spiroindolizidine-oxindole **19.25**

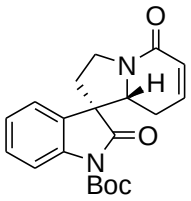

19.25

To a solution of *α,β*–unsaturated spiroindolizidine-oxindole **19.8** (24.3 mg, 0.0956 mmol) in dichloromethane (CH_2Cl_2) (10 mL) was added di-*tert*-butyldicarbonate (Boc_2O) (104.4 mg, 0.478 mmol), triethylamine (Et_3N) (0.07 mL, 0.478 mmol) and 4-dimethylaminopyridine (DMAP) (1.2 mg, 0.0096 mmol) and the mixture was stirred for 24 h. The reaction was quenched with water (10 mL) and dichloromethane (CH_2Cl_2) (10 mL). The phases were separated and extracted with dichloromethane (5x10 mL). The combined organic layers were dried over anhydrous sodium sulfate, filtered and concentrated under reduced pressure to give crude yellow oil. The crude product was purified by flash chromatography (silica gel, 1:1 hexane/EtOAc) to give *N*-Boc unsaturated spiroindolizidine-oxindole **19.25** (33.9 mg, 99%) as a colorless oil; R_f (1:1 hexane/EtOAc) 0.4; ^{1}H NMR (300 MHz, $CDCl_3$) δ 7.90 (d, 1H), 7.40 (td, J = 7.5, 1.2 Hz, 1H), 7.20 (m, J = 7.4, 1.2 Hz, 3H), 6.45 (ddd, J = 9.7, 6.1, 2.0 Hz, 1H), 5.95 (dd, J = 9.7, 2.9 Hz, 1H); 4.30 (dd, J = 14.0, 5.7 Hz, 1H), 3.85 (ddd, J = 10.7, 7.6, 7.6 Hz, 1H), 2.55 (dt, J = 13.0, 10.7 Hz, 1H), 2.12 (ddd, J = 13.0, 7.4, 1.3 Hz, 1H), 2.04 (dt, J = 17.5, 6.0 Hz, 1H), 1.84 (ddt, J = 17.5, 14.2, 2.7 Hz, 1H), 1.60 (s, 9H); ^{13}C (75 MHz, $CDCl_3$) δ 174.4, 163.8, 148.8, 138.9, 138.2, 129.0, 128.3, 125.0, 124.9, 123.9, 115.4, 85.0, 63.1, 57.1, 43.5, 34.8, 29.6, 28.0, 27.8, 25.3; ν_{max} (film) 3100, 2911, 1770, 1702, 1690, 1447, 1339, 1235, 1111, 869 cm^{-1}; $[\alpha]^{D}_{25}$ +24.5 (c 0.4, $CHCl_3$).

Synthesis of *N*-Boc unsaturated spiroindolizidine-oxindole **19.24**

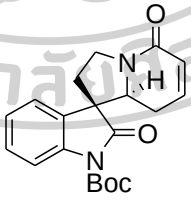

19.24

To a solution of *α,β*–unsaturated spiroindolizidine-oxindole **19.16** (15.5 mg, 0.0609 mmol) in dichloromethane (CH_2Cl_2) (10 mL) was added di-*tert*-butyldicarbonate (Boc_2O) (66.6 mg, 0.305 mmol), triethylamine (Et_3N) (0.05 mL, 0.305 mmol) and 4-dimethylaminopyridine (DMAP) (0.8 mg, 0.0061 mmol) and the mixture was stirred for 24 h. The reaction was quenched with water (10 mL) and dichloromethane (CH_2Cl_2) (10 mL). The phases were separated and extracted with dichloromethane (5x10 mL). The combined organic layers were dried over anhydrous sodium sulfate, filtered and concentrated under reduced pressure to give crude yellow oil. The crude product was purified by flash chromatography (silica gel, 1:1 hexane/EtOAc) to give *N*-Boc unsaturated spiroindolizidine-oxindole **19.24** (21.4 mg,

99%) as a colorless oil; R_f (1:1 hexane/EtOAc) 0.4; ^{1}H NMR (300 MHz, $CDCl_3$) δ 7.60 (brs, 1H), 7.40 (td, J = 7.6, 1.2 Hz, 2H), 7.20 (dt, J = 7.5, 1.2 Hz, 2H), 6.45 (ddd, J = 9.7, 6.1, 2.0 Hz, 1H), 5.95 (dd, J = 9.7, 2.9 Hz, 1H); 4.30 (dd, J = 13.7, 5.7 Hz, 1H), 4.05 (dd, J = 10.5, 7.6 Hz, 1H), 2.55 (m, 1H), 2.10 (m, 1H), 2.04 (m, 1H), 1.84 (m, 1H), 1.60 (s, 9H); $[\alpha]^D_{25}$ -19.7 (c 0.3, $CHCl_3$).

Synthesis of *N*-Boc spiro[indolizidine-1,3′-oxindole] **19.23**

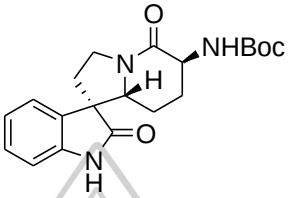

19.23

To a solution of spiro[indolizidine-1,3′-oxindole] **19.7** (8.3 mg, 0.0184 mmol) in methanol (MeOH) (10 mL) was added palladium on activated charcoal (Pd/C) (9.7 mg, 0.092 mmol) under hydrogen atmosphere. The reaction mixture was stirred for 24 h at room temperature. This solution was added di-*tert*-butyldicarbonate (Boc_2O) (20.1 mg, 0.092 mmol) for 24 h at room temperature. This solution was filtered to remove palladium on activated charcoal (Pd/C). The reaction was quenched with water (10 mL) and dichloromethane (CH_2Cl_2) (10 mL). The phases were separated and extracted with dichloromethane (5x10 mL). The combined organic layers were dried over anhydrous sodium sulfate, filtered and concentrated under reduced pressure to give crude yellow oil. The crude product was purified by flash chromatography (silica gel, 4:1 hexane/EtOAc) to give *N*-Boc spiro[indolizidine-1,3′-oxindole] **19.23** (5.6 mg, 82%) as a yellow oil; R_f (1:1 hexane/EtOAc) 0.20; ^{1}H NMR (300 MHz, $CDCl_3$) δ 8.25 (s, 2H); 7.05 (t, 2H); 6.95 (d, 2H); 5.25 (m , 1H); 4.0 (m, 3H); 3.85 (m, 2H); 2.50 (m, 1H); 2.10 (m, 1H); 1.85-1.90 (m, 1H); 1.50 (s, 9H); 1.22 (m, 1H).

Synthesis of *N*-Boc spiro[indolizidine-1,3′-oxindole] **19.22**

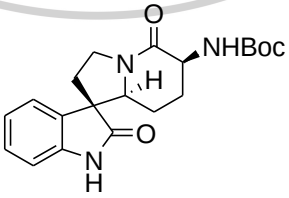

19.22

To a solution of spiro[indolizidine-1,3′-oxindole] **19.15** (10.0 mg, 0.0222 mmol) in methanol (MeOH) (10 mL) was added palladium on activated charcoal (Pd/C) (11.7 mg, 0.110 mmol) under hydrogen atmosphere. The reaction mixture was stirred for 24 h at room temperature. This solution was added di-*tert*-butyldicarbonate (Boc_2O) (24.0 mg, 0.110 mmol) for 24 h at room temperature. This solution was filtered to remove palladium on activated charcoal (Pd/C). The reaction was quenched with water (10 mL) and dichloromethane (CH_2Cl_2) (10 mL). The phases were

separated and extracted with dichloromethane (5x10 mL). The combined organic layers were dried over anhydrous sodium sulfate, filtered and concentrated under reduced pressure to give crude yellow oil. The crude product was purified by flash chromatography (silica gel, 4:1 hexane/EtOAc) to give *N*-Boc spiro[indolizidine-1,3′-oxindole] **19.22** (6.5 mg, 79%) as a yellow oil; R_f (1:1 hexane/EtOAc) 0.20; ^{1}H NMR (300 MHz, $CDCl_3$) δ 8.25 (s, 2H); 7.05 (t, 2H); 6.95 (d, 2H); 4.55-4.75 (m , 1H); 4.05 (m, 2H); 3.85 (t, 3H); 2.55 (q, 1H); 2.10 (m, 1H); 1.85-1.90 (m, 1H); 1.50 (s, 9H); 1.22 (m, 1H); ^{13}C (75 MHz, $CDCl_3$) δ 177.1, 168.4, 140.0, 129.8, 128.7, 123.9, 123.2, 100.3, 100.0, 65.4, 57.1, 56.9, 33.4, 28.4, 28.3.

Synthesis of spiro[indolizidine-1,3′-bromooxindole] **19.14**

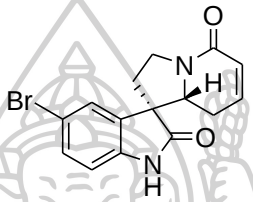

19.14

To a solution of indoloquinolizidine **19.13** (10 mg, 0.042 mmol) in tetrahydrofuran (THF) (5 mL) and water (5 mL) was added *N*-Bromosuccinimide (22 mg, 0.126 mmol) for 10 min. To this mixture was added trifluoroacetic acid (TFA) (0.1 mL) at 0 ^{o}C. The mixture was stirred for 24 h. Saturated aqueous solution of sodium hydrogencarbonate ($NaHCO_3$) (10 mL) and dichloromethane (10 mL) were added and the phases were separated. The aqueous phase was extracted with dichloromethane (5x10 mL). The combined organic layers were dried with anhydrous sodium sulfate (anh. Na_2SO_4), filtered and concentrated under reduced pressure. The crude product was purified by flash chromatography (silica gel, 1:2 hexane/ ethyl acetate) to give the spiro[indolizidine-1,3′-bromooxindole] **19.14** as a colorless oil (10 mg, 72%); R_f (1:2 hexane/EtOAc) 0.20; ^{1}H (300 MHz, $CDCl_3$) δ 8.1 (brs, 1H), 7.43 (dd, J = 8.2, 1.9 Hz, 1H), 7.27 (d, J = 2.0 Hz, 1H), 6.85 (d, J = 8.3 Hz, 1H), 6.45 (ddd, J = 9.9, 6.0, 2.1, 1H), 5.99 (dd, J = 9.8, 2.7, 1H), 4.25 (dd, J = 14.0, 5.6 Hz, 1H), 4.07 (t, J = 10.5 Hz, 1H), 3.80-3.90 (m, 1H), 2.50 (dt, J = 12.7, 10.1 Hz, 1H), 2.13 (ddd, J = 12.5, 7.5, 1.7, 1H), 2.05 (dt, J = 17.1, 6.0, 1H), 1.85 (dddd, J = 18.0, 14.1, 3.0, 3.0, 1H); ^{13}C (75 MHz, $CDCl_3$) δ 176.5, 163.9, 138.9, 138.2, 131.9, 131.8, 127.6, 125.2, 115.9, 111.6, 62.4, 57.5, 43.4, 33.6, 29.7, 25.3; ν_{max} (film) 3215, 3019, 2821, 1727, 1644, 1595, 1352, 1303, 1137, 986, 878 cm^{-1}; $[\alpha]^D_{25}$ +33.5 (c 0.8, $CHCl_3$).

Synthesis of spiro[7-methoxyindolizidine-1,3′-bromooxindole] **19.27**

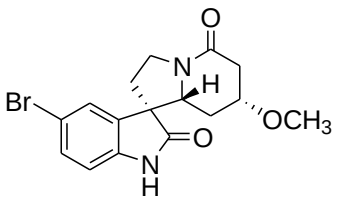

19.27

To a solution of sodium metal (Na) (4.2 mg, 0.18 mmol) in methanol (MeOH) (10 mL) was generated sodium methoxide (NaOMe). This solution was added spiro[indolizidine-1,3′-bromooxindole] **19.14** (10 mg, 0.030 mmol) at 0 ^{o}C. The mixture was stirred for 24 h. The reaction was quenched 1N hydrochloric acid (HCl) and dichloromethane (10 mL). The phases were separated. The aqueous phase was extracted with dichloromethane (5x10 mL). The combined organic layers were dried with anhydrous sodium sulfate (anh. Na_2SO_4), filtered and concentrated under reduced pressure. The crude product was purified by flash chromatography (silica gel, 1:2 hexane/ ethyl acetate) to give the spiro[7-methoxyindolizidine-1,3′-bromooxindole] **19.27** as a colorless oil (6.6 mg, 60%); R_f (1:2 hexane/EtOAc) 0.20; 1H (300 MHz, $CDCl_3$) δ 8.20 (brs, 1H), 7.41 (dd, J = 8.1, 2.0 Hz, 1H), 7.05 (d, J =1.9 Hz, 1H), 6.85 (d, J = 8.2 Hz, 1H), 4.20 (dd, J = 11.5, 3.5 Hz, 1H), 4.06-3.78 (m, 2H), 3.75-3.70 (m, 1H), 3.30 (s, 3H), 2.75-2.20 (m, 3H), 2.09 (ddd, J = 13.0, 8.5, 2.0 Hz, 1H), 1.89 (ddd, J = 13.8, 6.2, 3.6 Hz, 1H), 1.00 (td, J = 13.8, 2.0 Hz, 1H); ^{13}C (75 MHz, $CDCl_3$) δ 176.0, 167.0, 138.5, 131.5, 131.1, 126.2, 115.3, 111.1, 59.5, 56.5, 55.6, 43.3, 35.6, 32.5, 29.1, 26.8; ν_{max} (film) 3450, 2965, 2920, 2855, 1745, 1730, 1610, 1374, 1230, 1227, 1202, 1261, 768, 747 cm^{-1}; $[\alpha]^{D}_{25}$ -44.5 (c 0.3, $CHCl_3$).

Synthesis of spiro[7-methoxyindolizidine-1,3′-oxindole] **19.17**

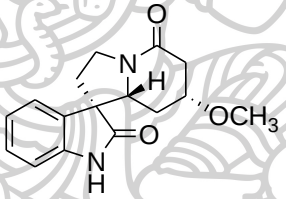

19.17

To a solution of sodium metal (Na) (2.0 mg, 0.096 mmol) in methanol (MeOH) (10 mL) was generated sodium methoxide (NaOMe). This solution was added *α,β*–unsaturated spiroindolizidine-oxindole **19.8** (5.0 mg, 0.016 mmol) at 0 ^{o}C. The mixture was stirred for 24 h. The reaction was quenched 1N hydrochloric acid (HCl) and dichloromethane (10 mL). The phases were separated. The aqueous phase was extracted with dichloromethane (5x10 mL). The combined organic layers were dried with anhydrous sodium sulfate (anh. Na_2SO_4), filtered and concentrated under reduced pressure. The crude product was purified by flash chromatography (silica gel, 1:2 hexane/ ethyl acetate) to give the spiro[7-methoxyindolizidine-1,3′-oxindole] **19.17** as a colorless oil (3.7 mg, 65%); R_f (1:2 hexane/EtOAc) 0.25; ^{1}H (300 MHz, $CDCl_3$) δ 8.30 (brs, 1H), 7.05 (t, J = 7.5 Hz, 1H), 6.99 (t, J = 7.5 Hz, 1H), 6.95 (d, J = 7.7 Hz, 2H), 4.20 (dd, J = 12.5, 5.7 Hz, 1H), 4.05 (dd, J = 12.0, 10.5, 2H), 3.85 (dt, J = 10.7, 7.5 Hz, 1H), 3.30 (s, 3H), 2.60 (t, 1H), 2.50 (t, 1H); 2.35 (m, 2H), 2.10 (ddd, J = 12.5, 7.5, 1.4 Hz, 1H); 1.89 (m, 1H), 1.00; ^{13}C (75 MHz, $CDCl_3$) δ 177.2, 167.5, 140.1, 129.8, 128.6, 123.8, 110.2, 100.0, 60.0, 56.7, 56.1, 43.9, 37.1, 36.3, 33.0, 31.9; ν_{max} (film) 3440, 2967, 2921, 2857, 1760, 1734, 1617, 1344, 1236, 1222, 1205, 1201, 769, 757 cm^{-1}.

Synthesis of spiro[7-ethoxyindolizidine-1,3′-oxindole] **19.18**

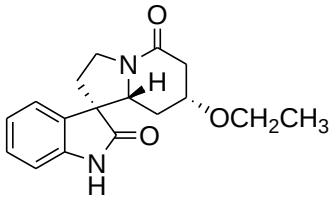

19.18

To a solution of sodium metal (Na) (9.0 mg, 0.370 mmol) in ethanol (EtOH) (10 mL) was generated sodium ethoxide (NaOEt). This solution was added to the *α,β*–unsaturated spiroindolizidine-oxindole **19.8** (15.7 mg, 0.062 mmol) at 0 ^{o}C. The mixture was stirred for 24 h. The reaction was quenched 1N hydrochloric acid (HCl) and dichloromethane (10 mL). The phases were separated. The aqueous phase was extracted with dichloromethane (5x10 mL). The combined organic layers were dried with anhydrous sodium sulfate (anh. Na_2SO_4), filtered and concentrated under reduced pressure. The crude product was purified by flash chromatography (silica gel, 1:2 hexane/ ethyl acetate) to give the spiro[7-ethoxyindolizidine-1,3´-oxindole] **19.18** as a colorless oil (11.1 mg, 60%); R_f (1:2 hexane/EtOAc) 0.25; ^{1}H (300 MHz, $CDCl_3$) δ 7.50 (brs, 1H), 7.05 (t, J = 7.5 Hz, 1H), 6.95 (m, 3H), 4.20 (dd, J = 12.6, 5.7 Hz, 1H), 4.05 (dd, J = 12.0, 10.5, 2H), 3.85 (dt, J = 10.5, 7.5 Hz, 1H), 3.40 (t, 3H), 2.70 (q, 2H); 2.55 (t, 1H), 2.35 (m, 2H); 2.10 (m, 2H); 1.85 (m, 1H); ν_{max} (film) 3433, 2966, 2925, 2867, 1764, 1730, 1619, 1355, 1237, 1221, 1210, 1200, 770, 765 cm^{-1}.

CHAPTER 5
CONCLUSION

A series of indoloquinolizidine and spiro[indolizidine-1,3′-oxindole] derivatives were prepared in enantiomerically pure form and good to excellent yield via oxidative ring contraction and *N*-acyliminium ion cyclization from commercial reagent. The indoloquinolizidine **19.9**, **19.11** and spiro[indolizidine-1,3′-oxindole] derivatives **19.7**, **19.15** has the amino substituent that can eliminate of this group by Cope elimination led to *α,β*–unsaturated indoloquinolizidines **19.10**, **19.12** and *α,β*–unsaturated spirolactam **19.8**, **19.16**. The functionalities of *α,β*–unsaturated indoloquinolizidines and *α,β*–unsaturated spirolactam were provided points for further functionalization with better pharmacological potency. The indoloquinolizidine and spiro[indolizidine-1,3′-oxindole] derivatives were assayed for their in vitro *α*-glucosidase inhibitory activities. The indoloquinolizidines **19.10** and spiro[indolizidine-1,3′-oxindole] **19.24** displayed the highest inhibition potency for *α*-glucosidase enzyme, with an IC_{50} value of 18.06±0.01 and 13.83±0.01 μM±SD, respectively. Some indoloquinolizidine and spiro[indolizidine-1,3′-oxindole] derivatives compounds exhibit nitric oxide synthesis inhibition and induced nitric oxide synthase (iNOS) protein expression. In part of chemical pretreatment spiroindolizidine-oxindole and indoloquinolizidine significantly reduced iNOS expression as evidered by the Western blot method. It showed the most significant activity against nitric oxide (NO) production by the Griess Test. The spiroindolizidine-oxindole **19.16** and indoloquinolizidine **19.13** are the core structure of Rhynchophylline and Hirsutine, respectively. In the future, this core structure could be synthesized the natural product via functionalities of *α,β*–unsaturated indoloquinolizidines and *α,β*–unsaturated spirolactam as core structure of Rhynchophylline and Hirsutine, respectively.

APPENDIX

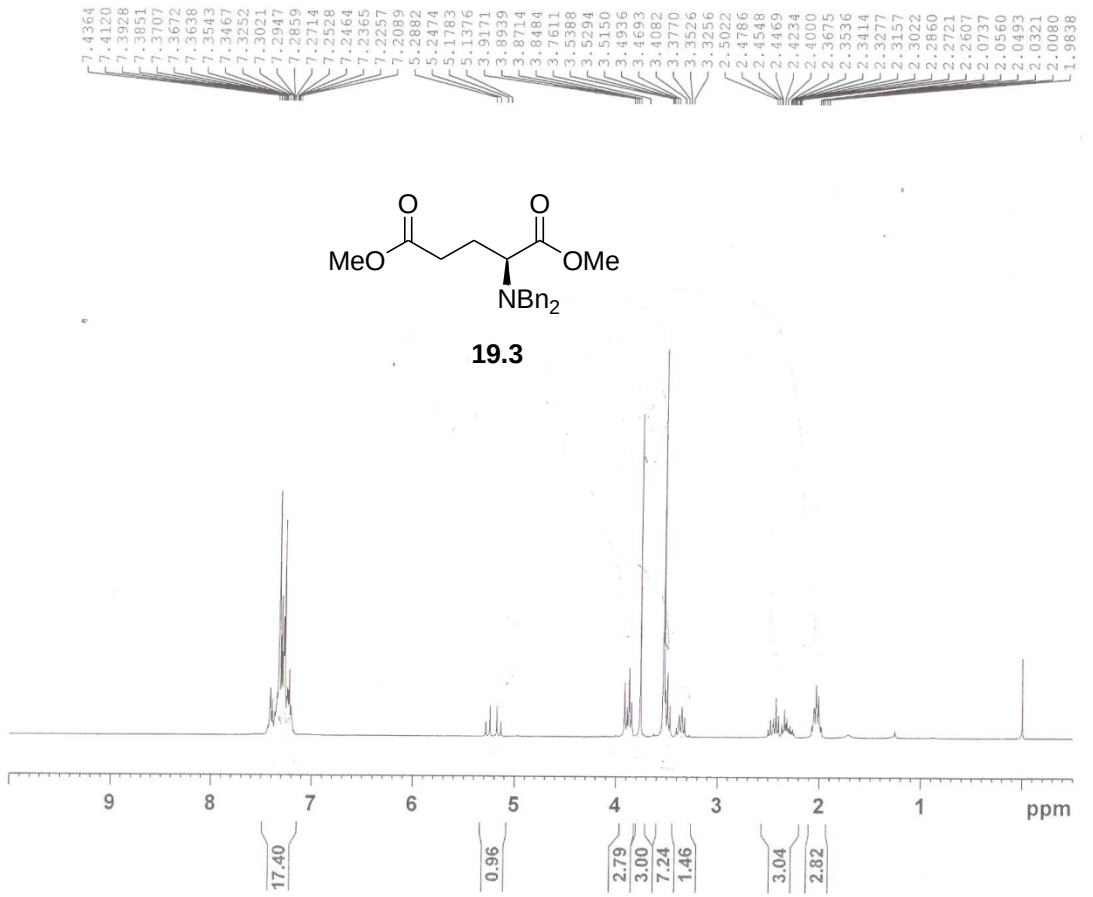

Figure 35 The ^{1}H NMR of dimethyl *N*,*N*-dibenzyl-L-glutamate **19.3** in $CDCl_3$

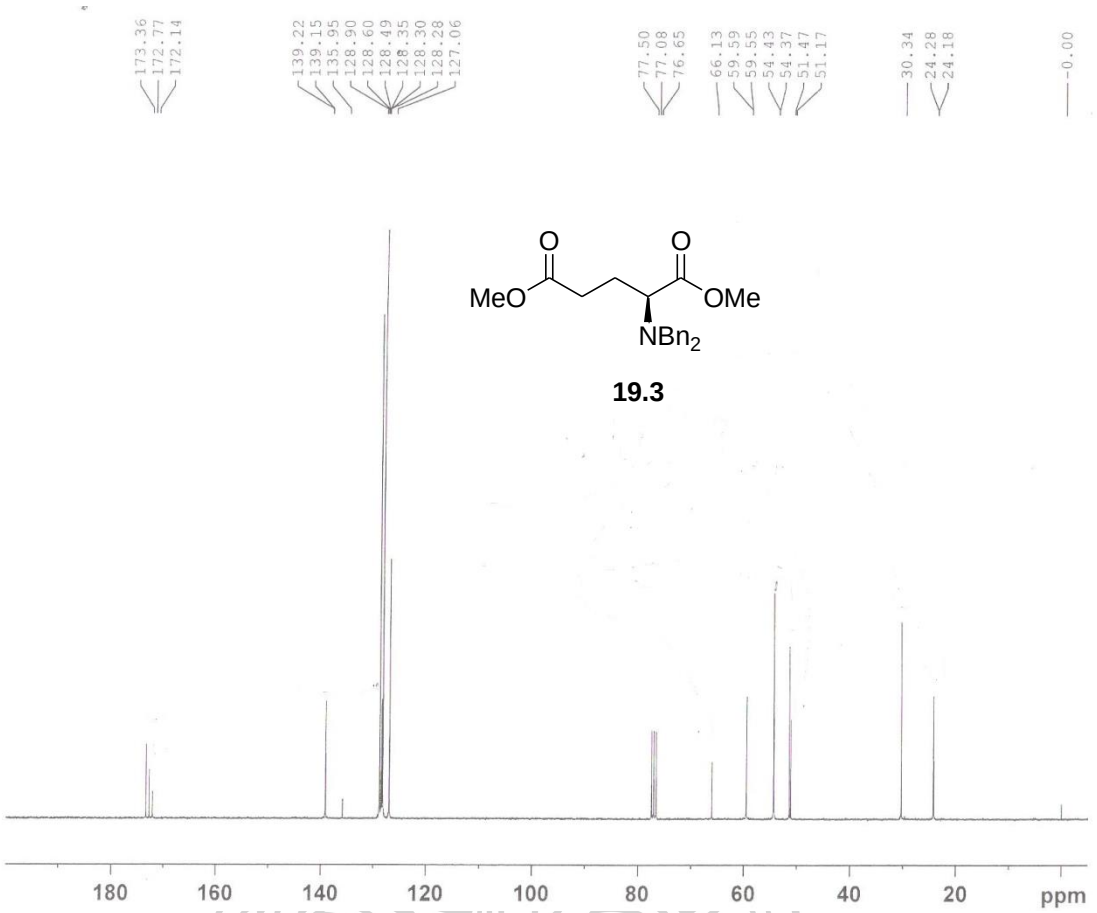

Figure 36 The ^{13}C NMR of dimethyl *N*,*N*-dibenzyl-L-glutamate **19.3** in $CDCl_3$

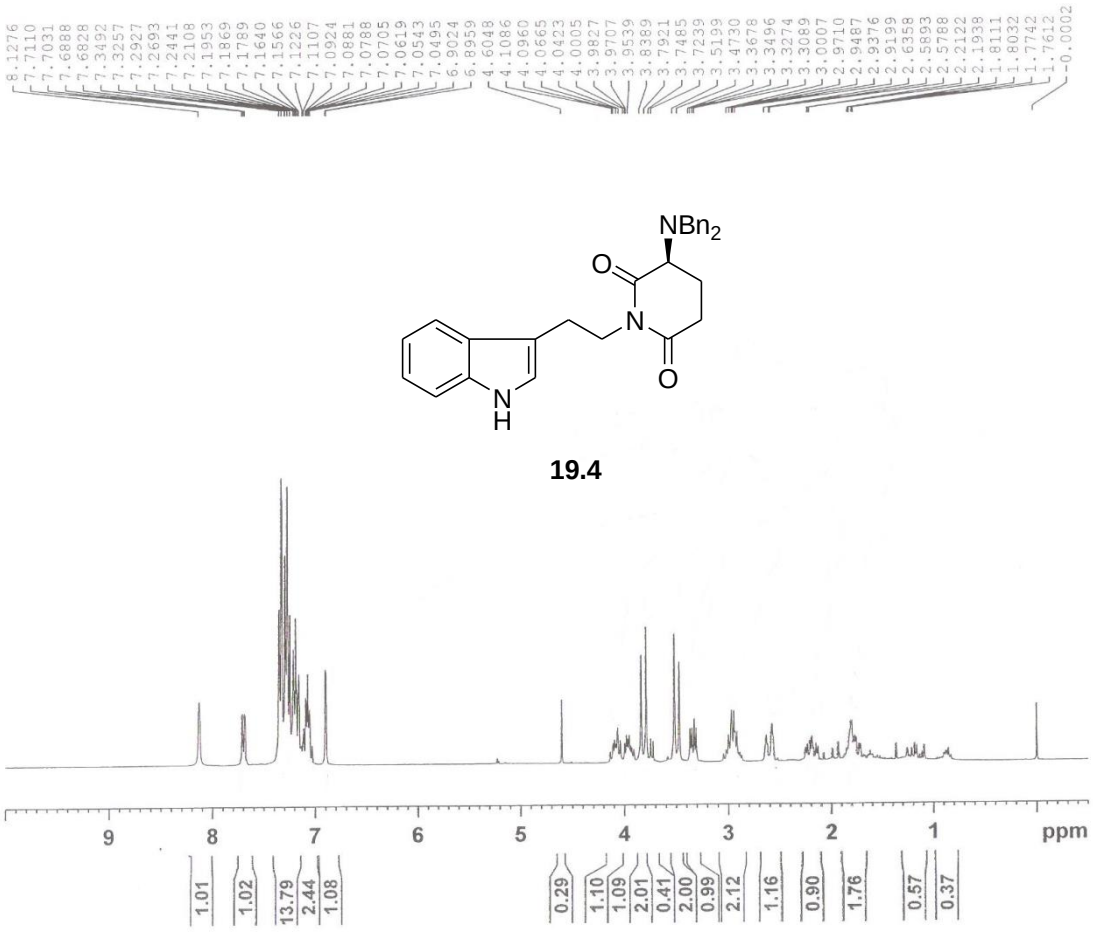

Figure 37 The ^{1}H NMR of chiral *N*-indolylethylglutarimide **19.4** in $CDCl_3$

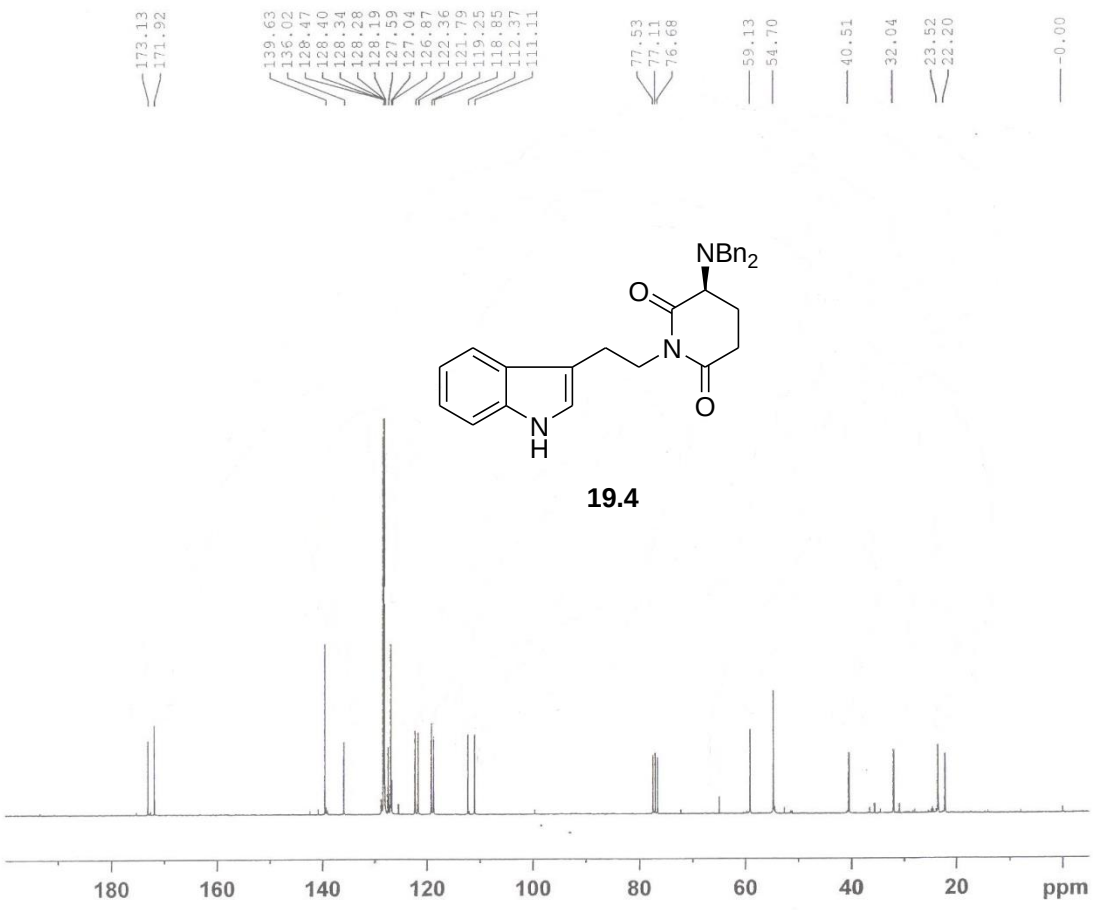

Figure 38 The ^{13}C NMR of chiral *N*-indolylethylglutarimide **19.4** in $CDCl_3$

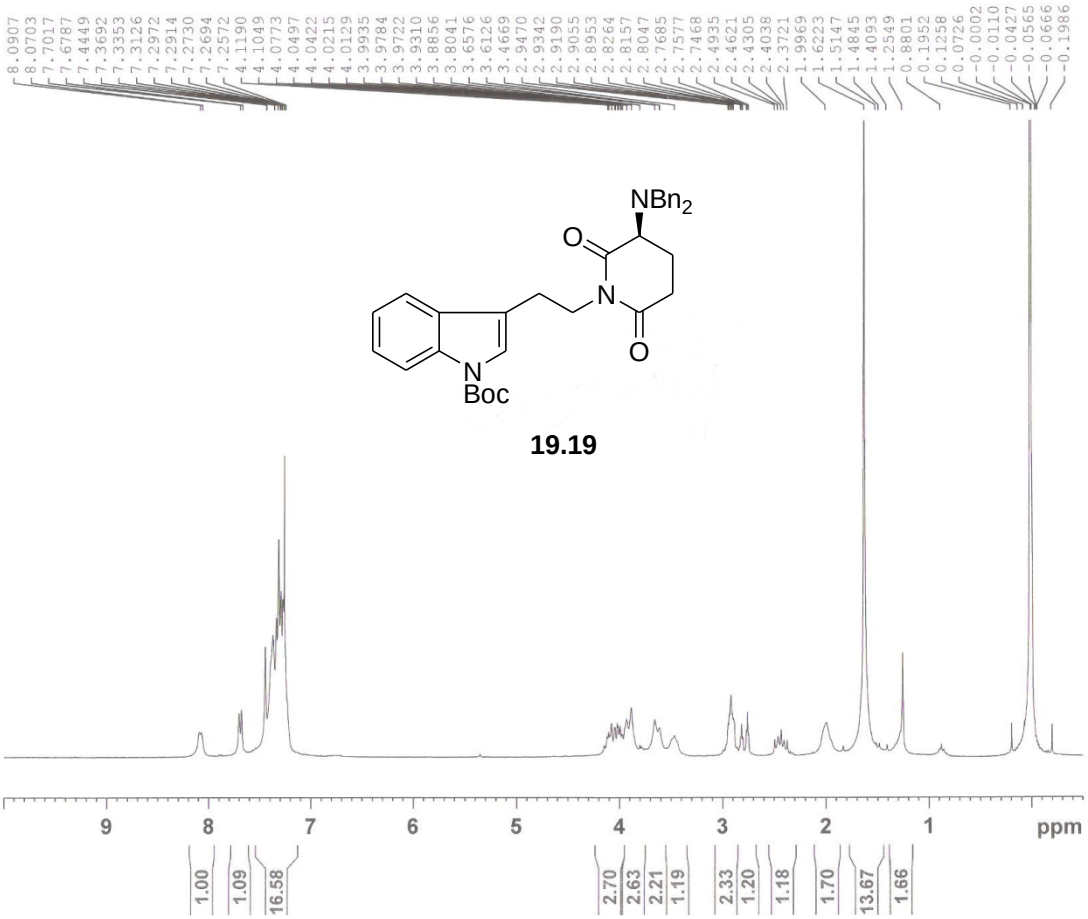

Figure 39 The ^{1}H NMR of chiral *N*-Boc indolylethylglutarimide **19.19** in $CDCl_3$

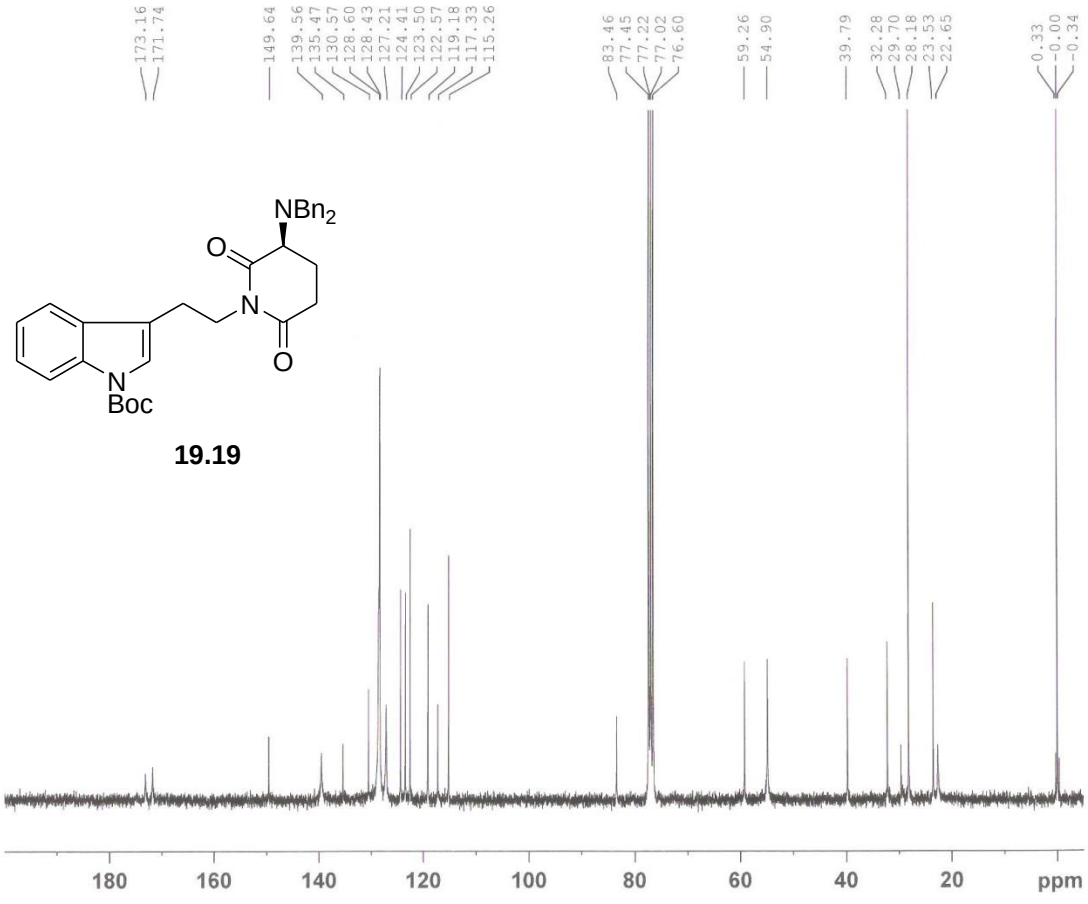

Figure 40 The ^{13}C NMR of chiral *N*-Boc indolylethylglutarimide **19.19** in $CDCl_3$

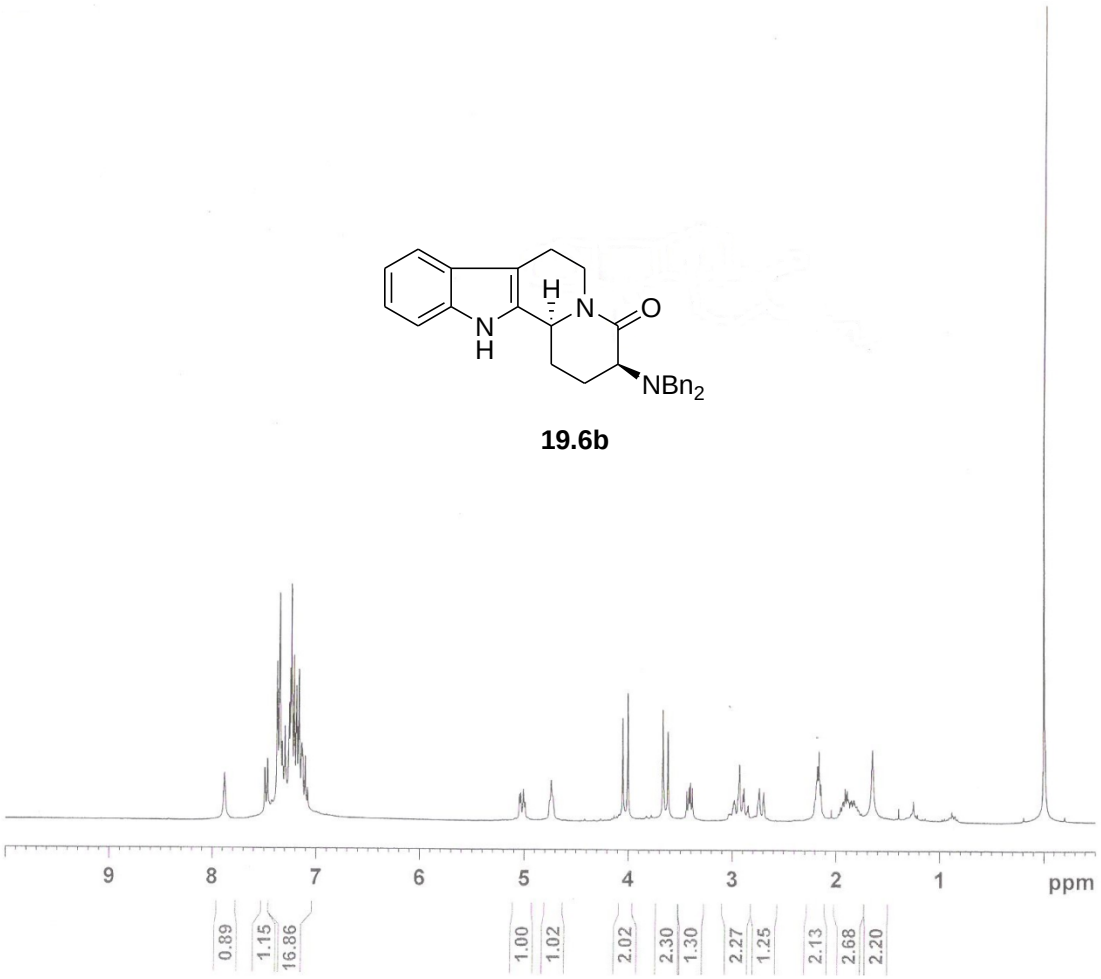

19.6b

Figure 41 The ^{1}H NMR of indoloquinolizidine **19.6b** in $CDCl_3$

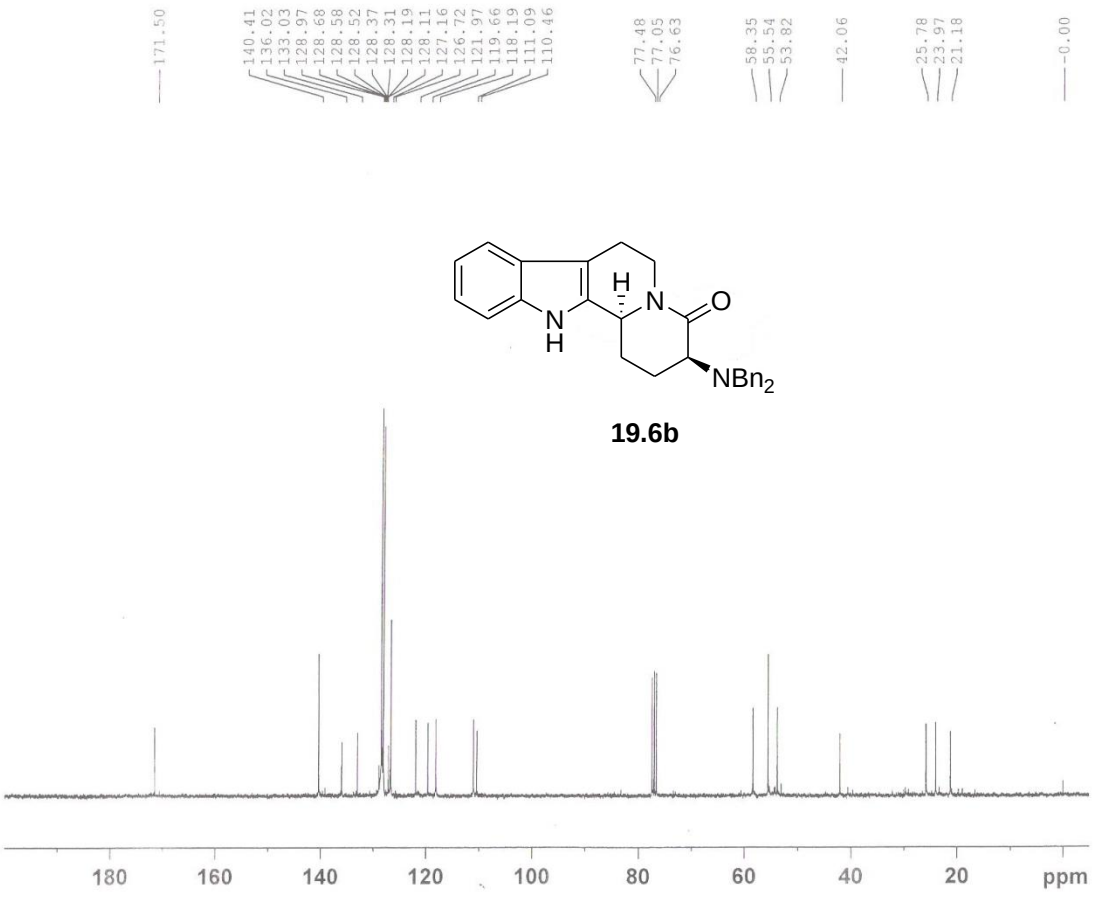

19.6b

Figure 42 The ^{13}C NMR of indoloquinolizidine **19.6b** in $CDCl_3$

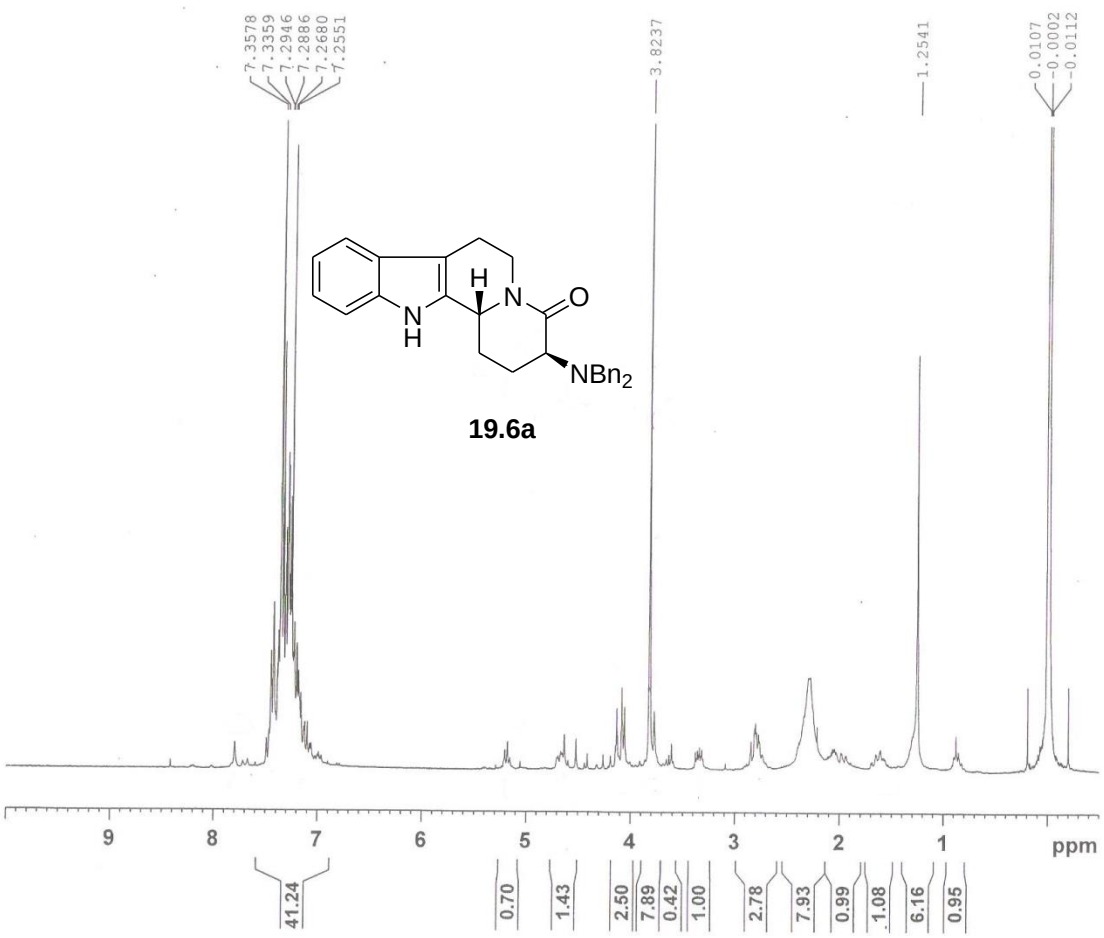

Figure 43 The ^{1}H NMR of indoloquinolizidine **19.6a** in $CDCl_3$

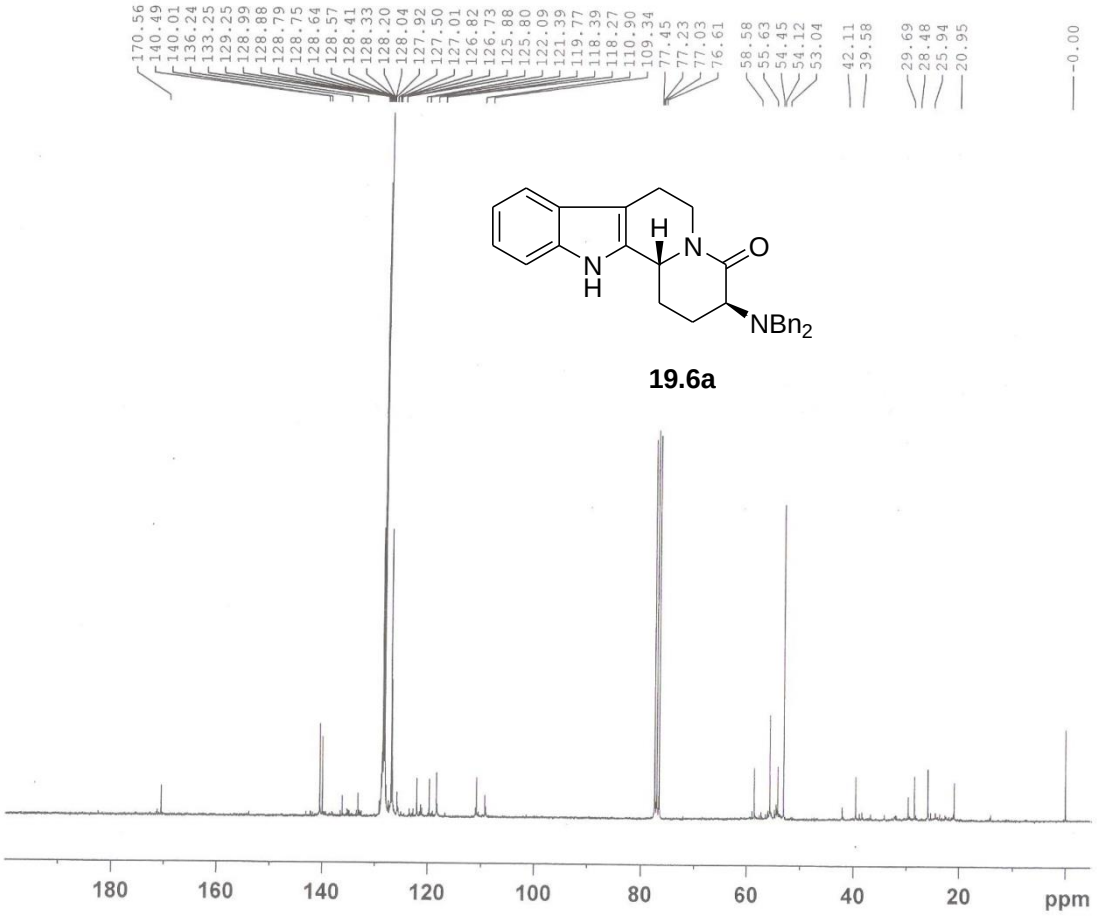

Figure 44 The ^{13}C NMR of indoloquinolizidine **19.6a** in $CDCl_3$

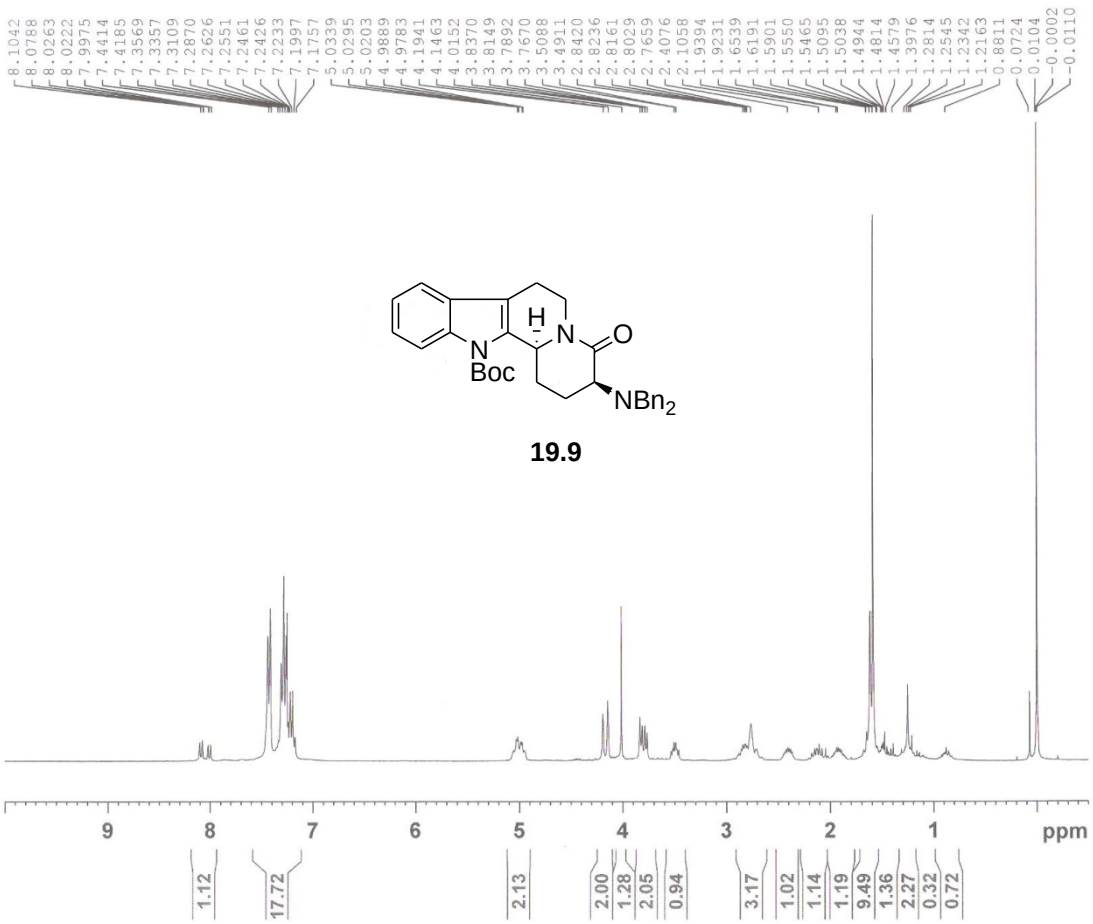

Figure 45 The ^{1}H NMR of *N*-Boc indoloquinolizidine **19.9** in $CDCl_3$

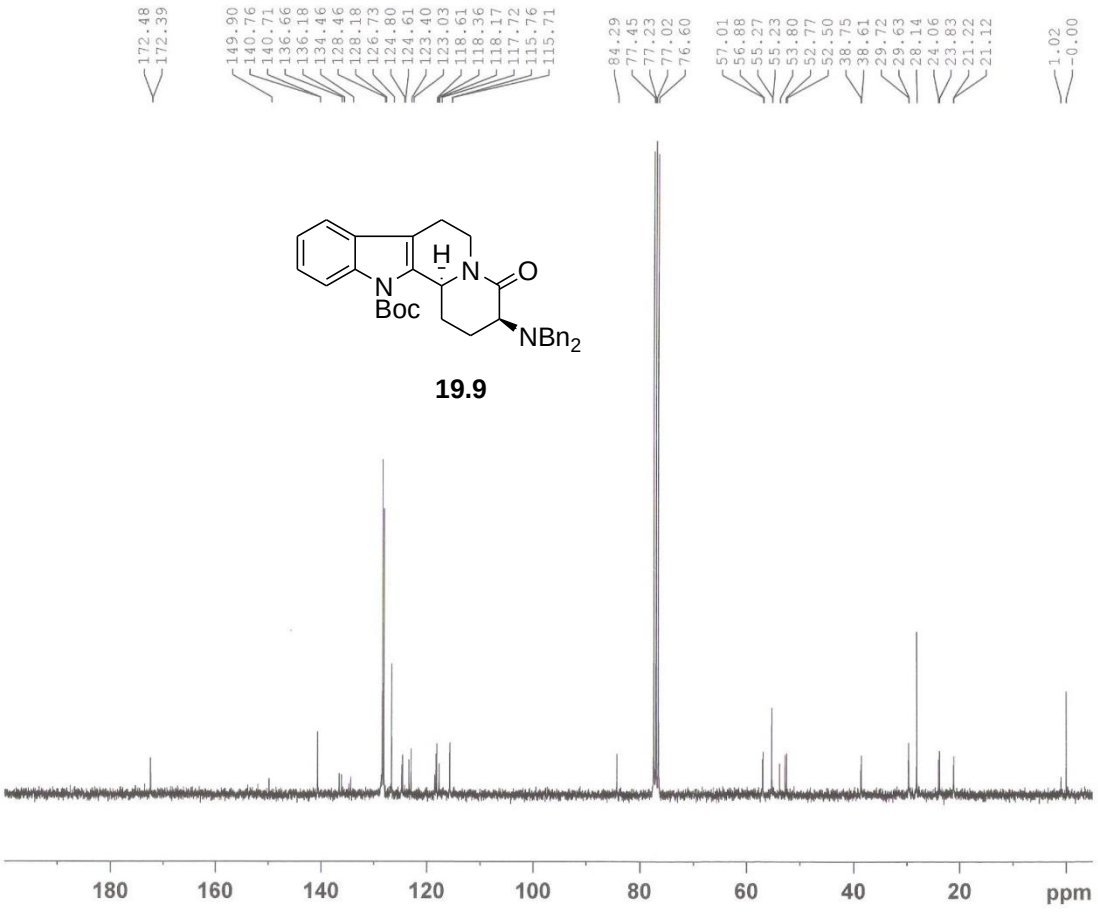

Figure 46 The ^{13}C NMR of *N*-Boc indoloquinolizidine **19.9** in $CDCl_3$

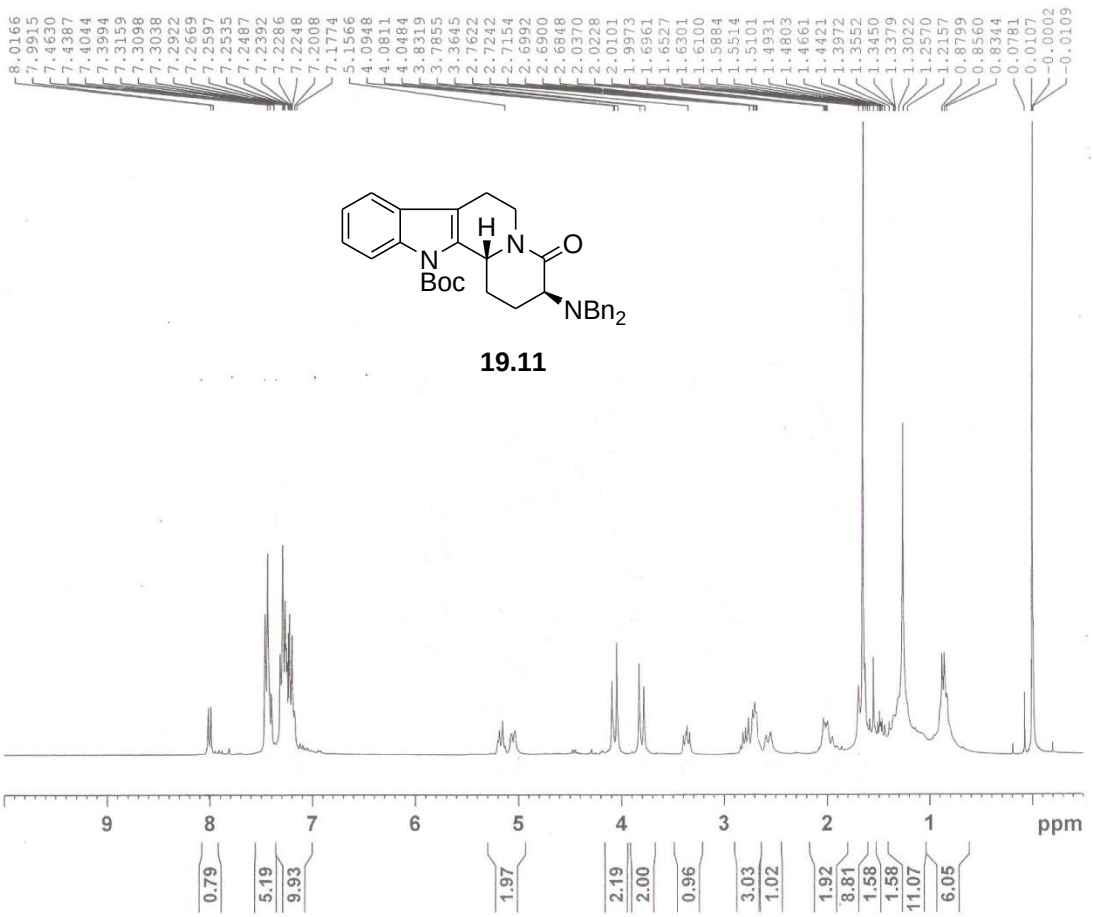

Figure 47 The ^{1}H NMR of of *N*-Boc indoloquinolizidine **19.11** in $CDCl_3$

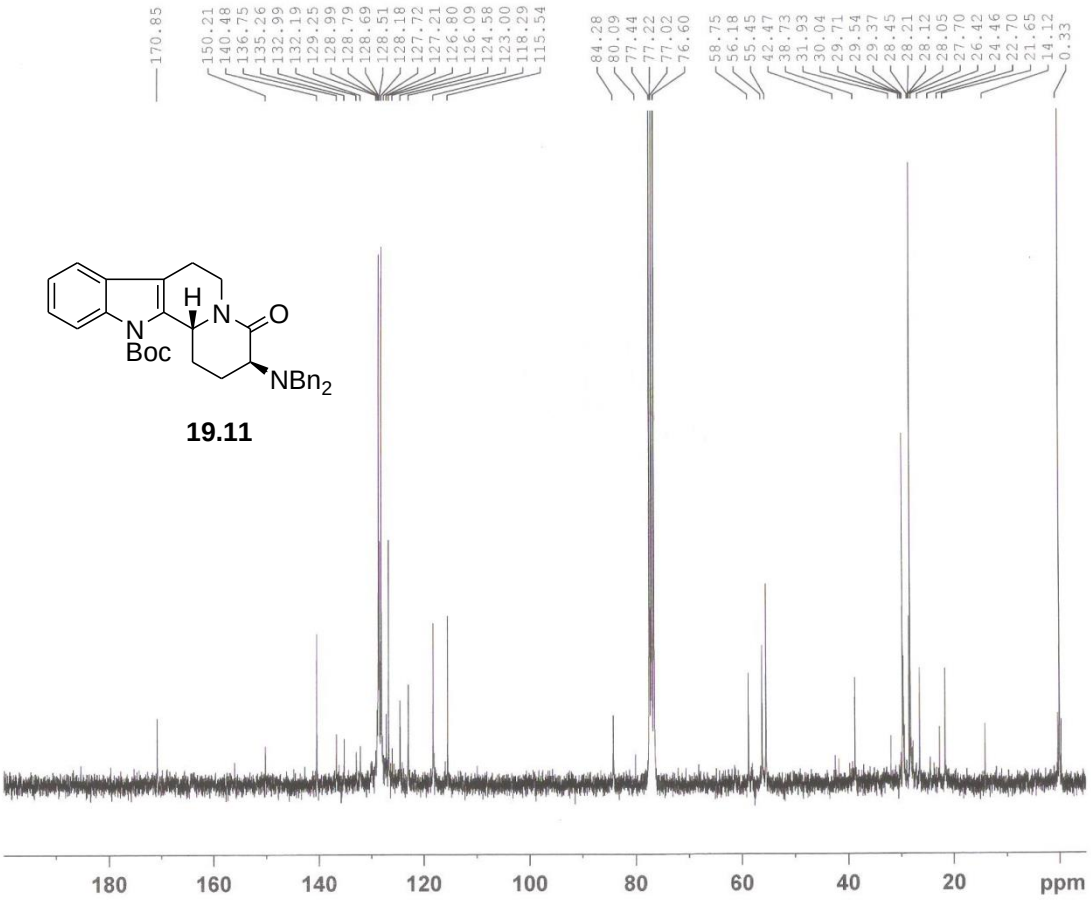

19.11

Figure 48 The ^{13}C NMR of *N*-Boc indoloquinolizidine **19.11** in $CDCl_3$

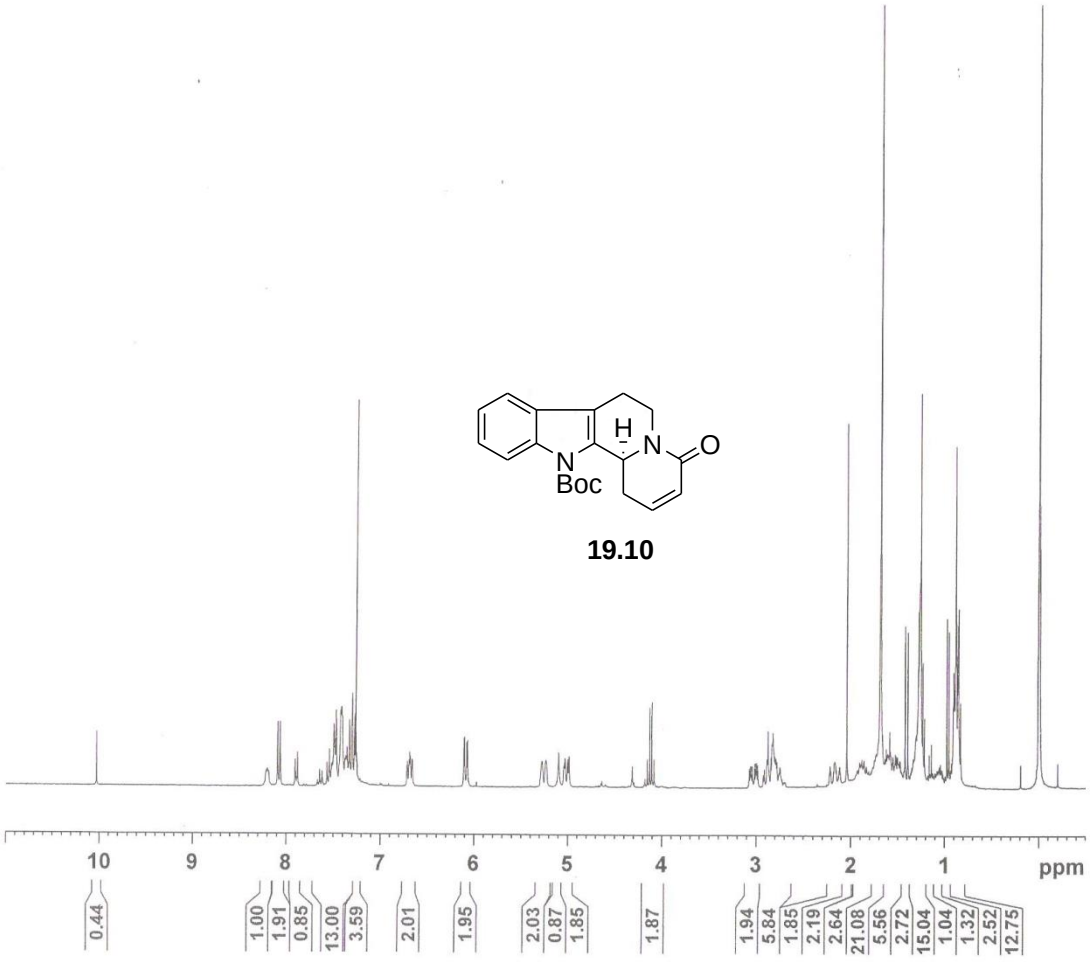

Figure 49 The ^{1}H NMR of *N*-Boc-indoloquinolizidine-enamide **19.10** in $CDCl_3$

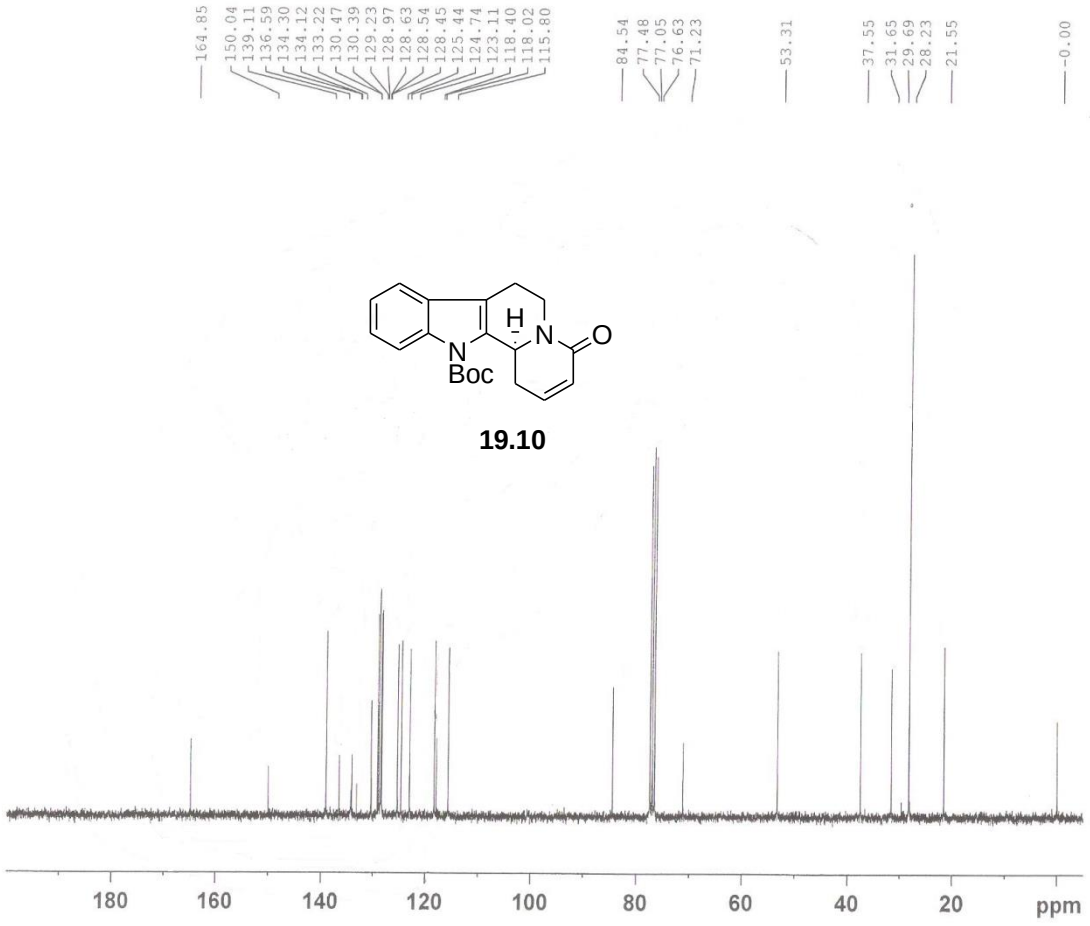

19.10

Figure 50 The ^{13}C NMR of *N*-Boc-indoloquinolizidine-enamide **19.10** in $CDCl_3$

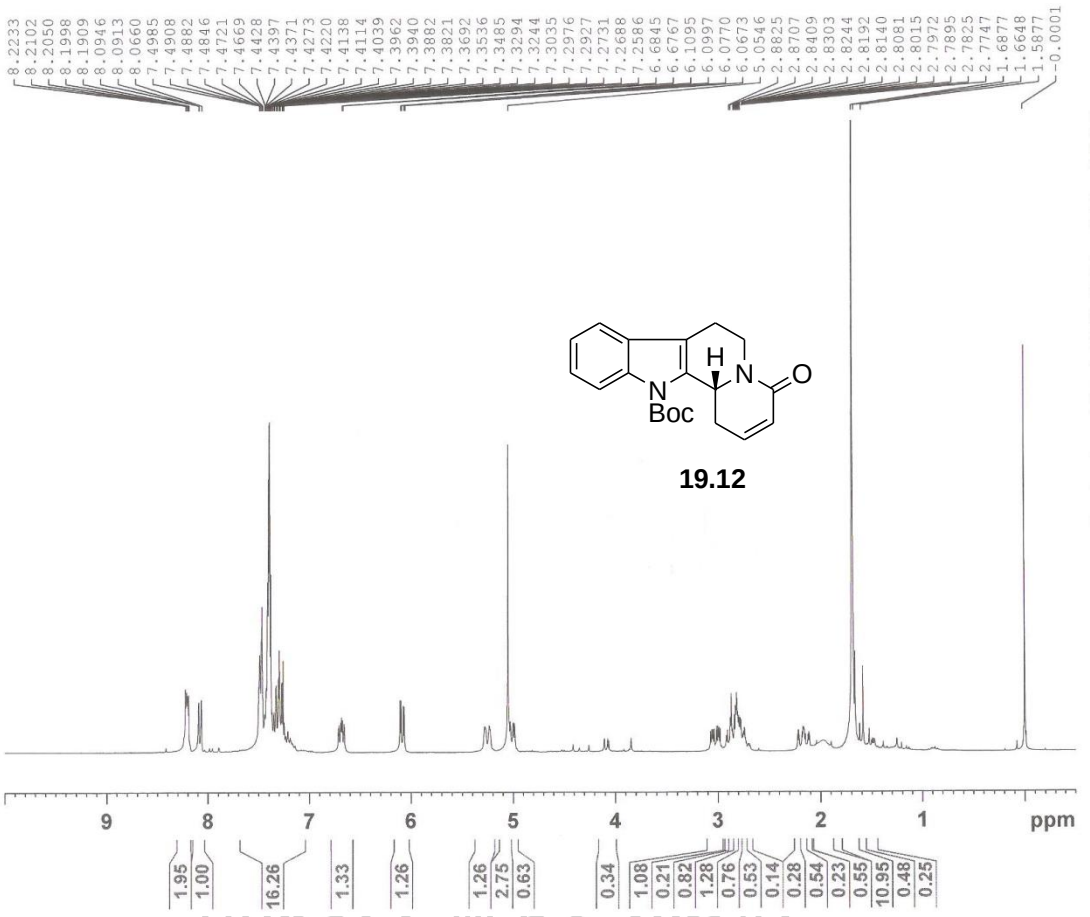

Figure 51 The ^{1}H NMR of *N*-Boc-indoloquinolizidine-enamide **19.12** in $CDCl_3$

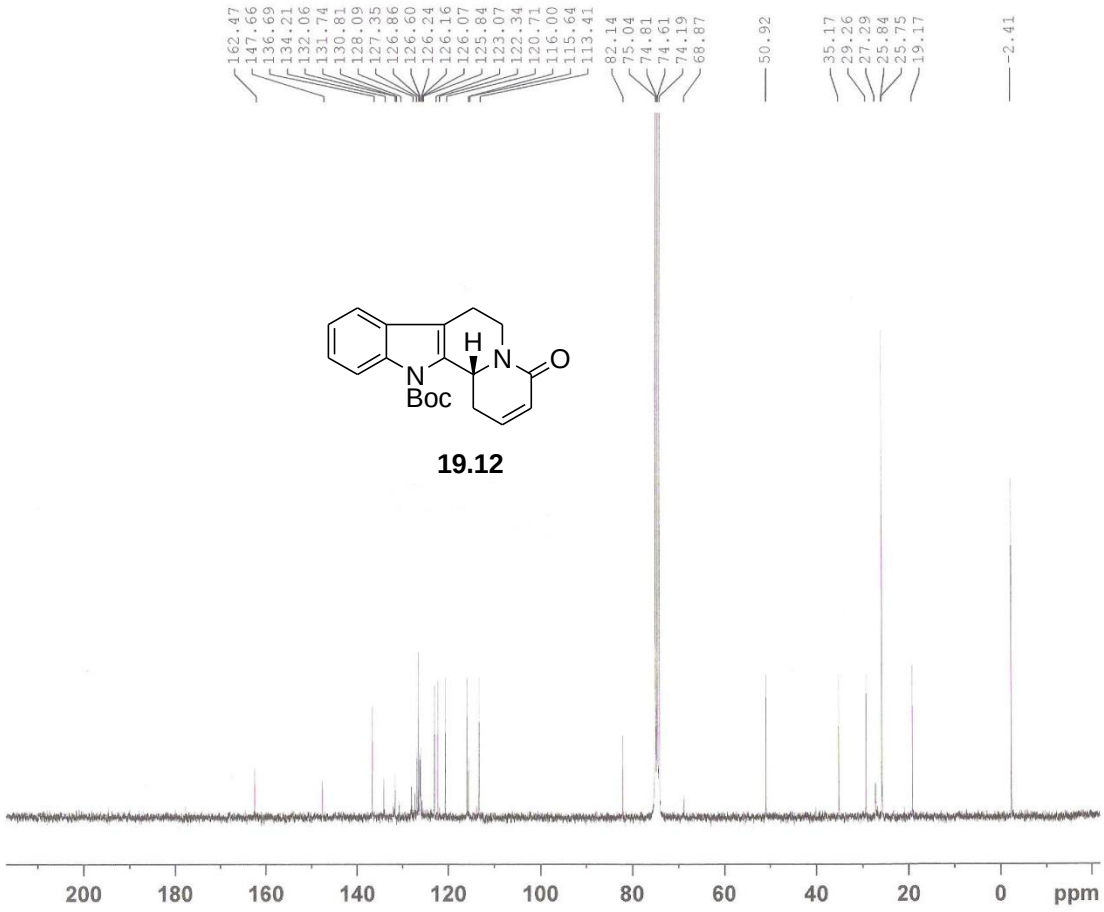

19.12

Figure 52 The ^{13}C NMR of *N*-Boc-indoloquinolizidine-enamide **19.12** in $CDCl_3$

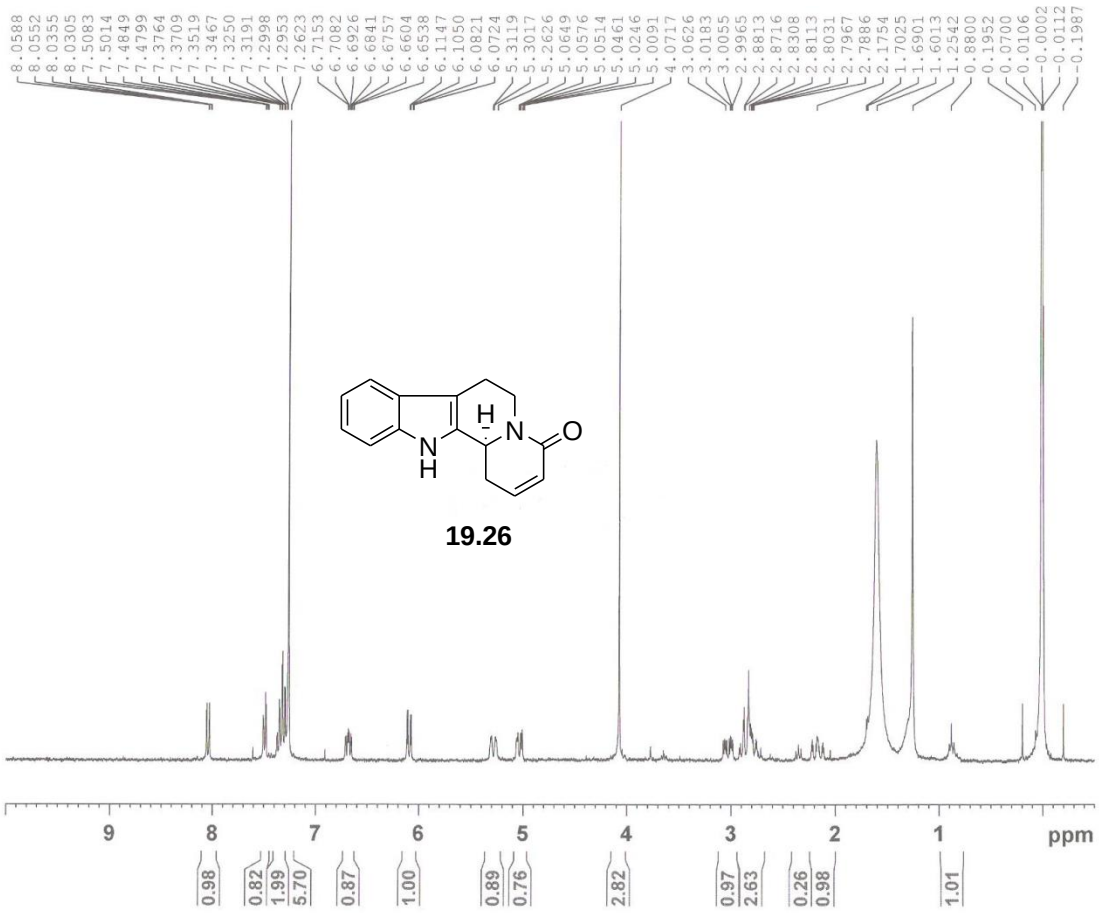

Figure 53 The ^{1}H NMR of indoloquinolizidine-enamide **19.26** in $CDCl_3$

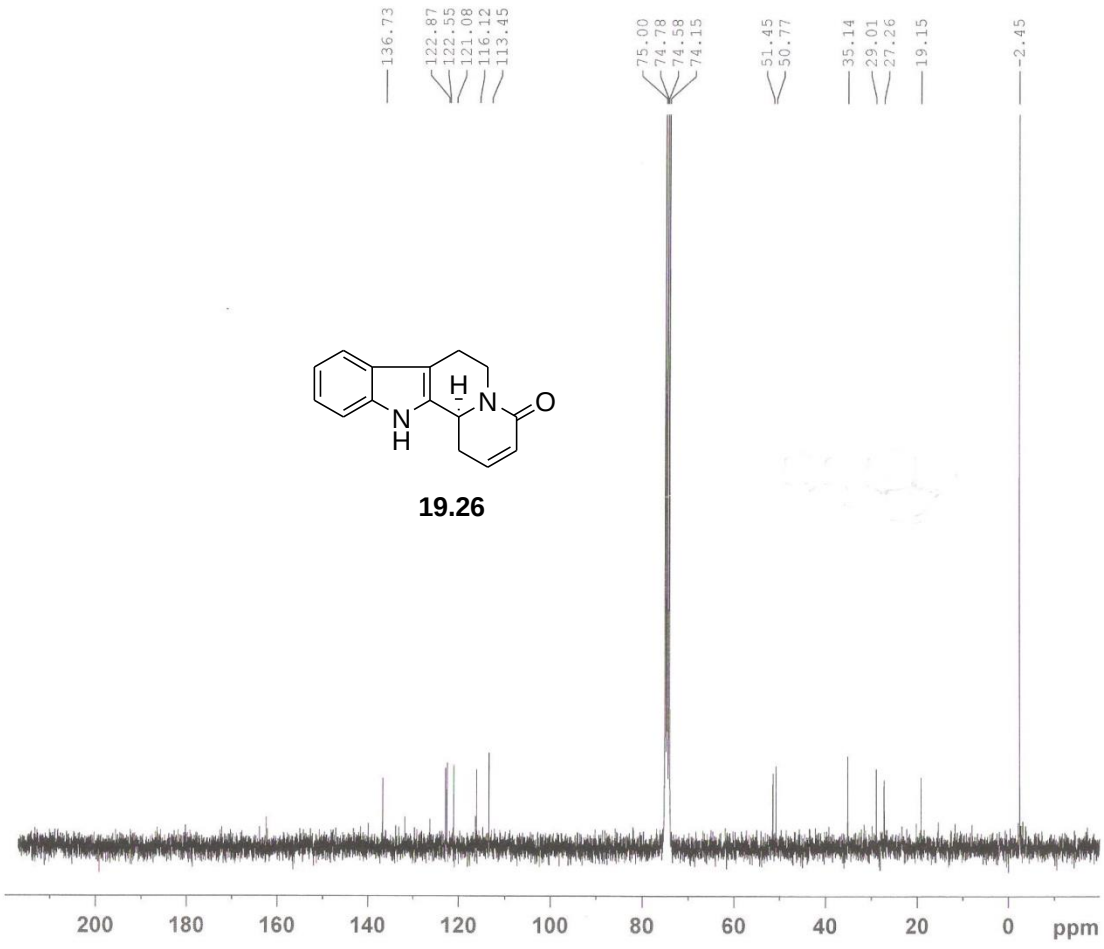

19.26

Figure 54 The ^{13}C NMR of indoloquinolizidine-enamide **19.26** in $CDCl_3$

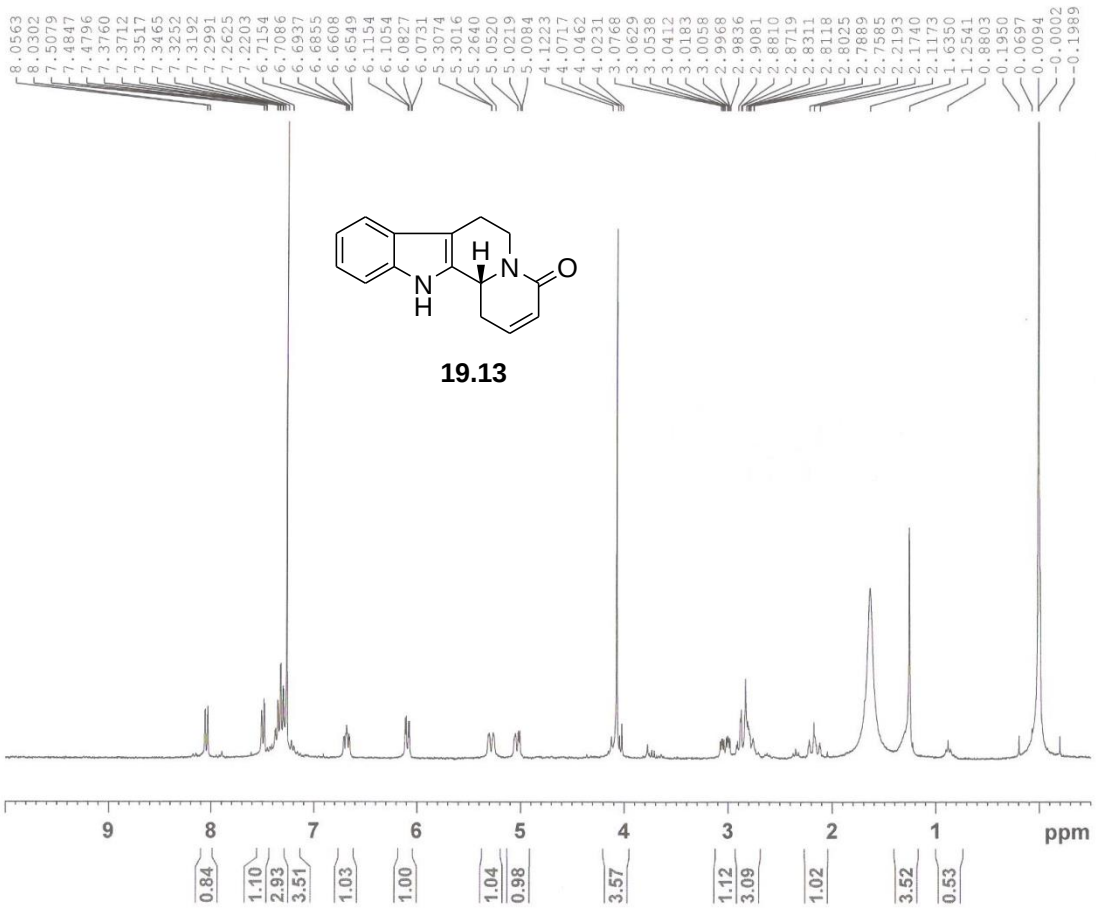

Figure 55 The ^{1}H NMR of indoloquinolizidine-enamide **19.13** in $CDCl_3$

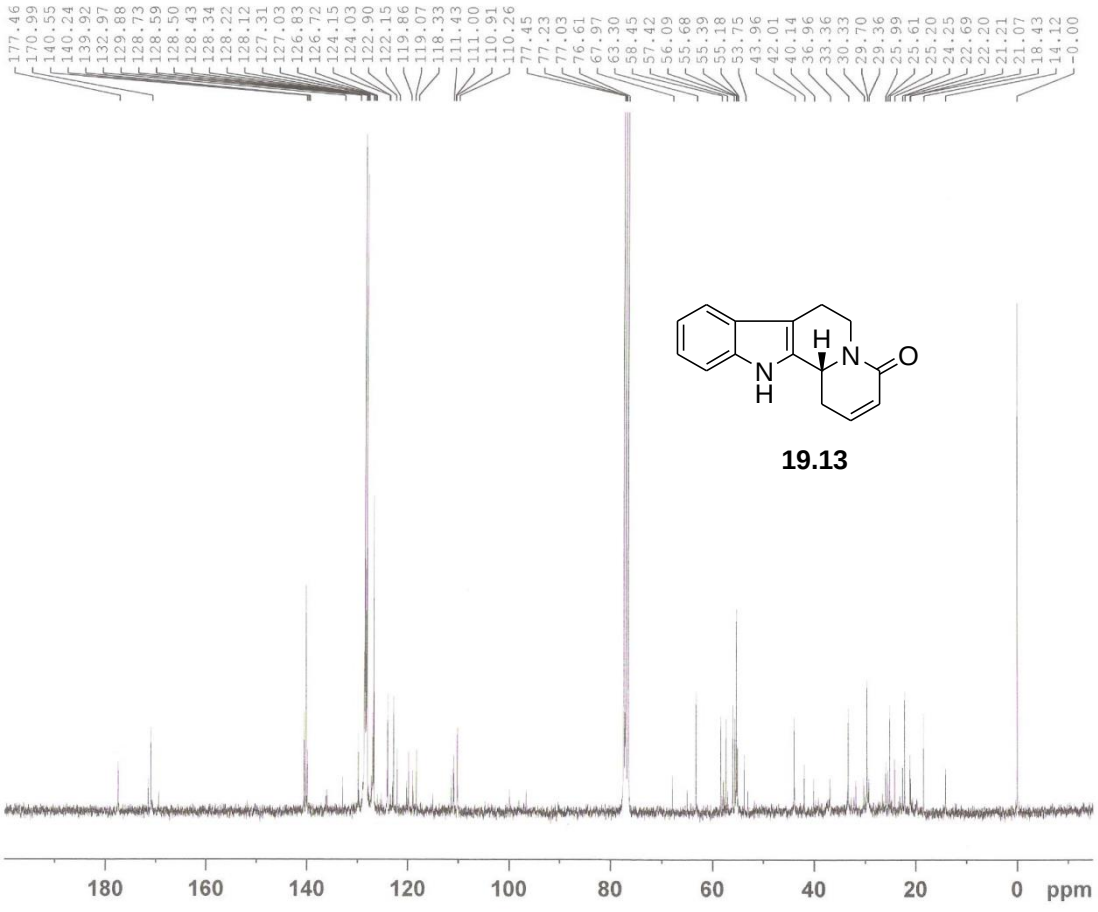

Figure 56 The ^{13}C NMR of indoloquinolizidine-enamide **19.13** in $CDCl_3$

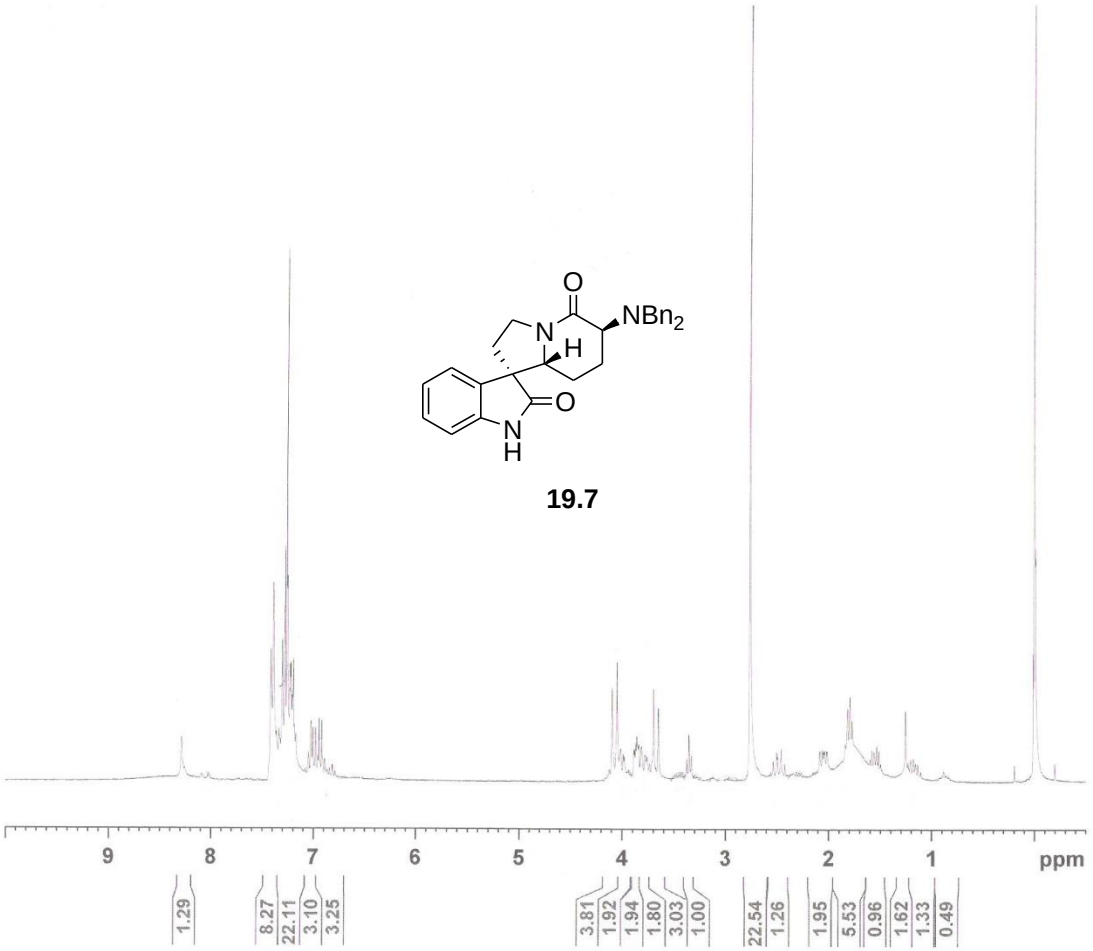

Figure 57 The ^{1}H NMR of spiro[indolizidine-1,3′-oxindole] **19.7** in $CDCl_3$

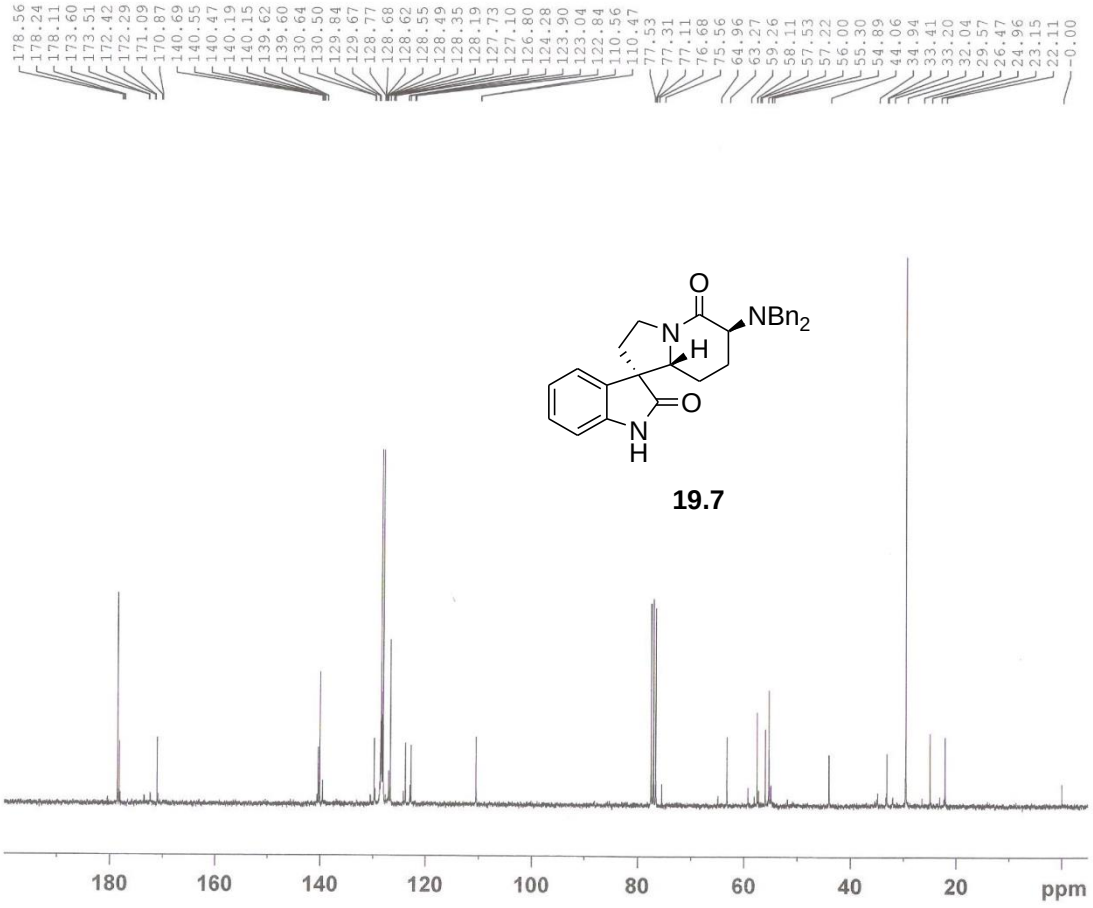

Figure 58 The ^{13}C NMR of spiro[indolizidine-1,3′-oxindole] **19.7** in $CDCl_3$

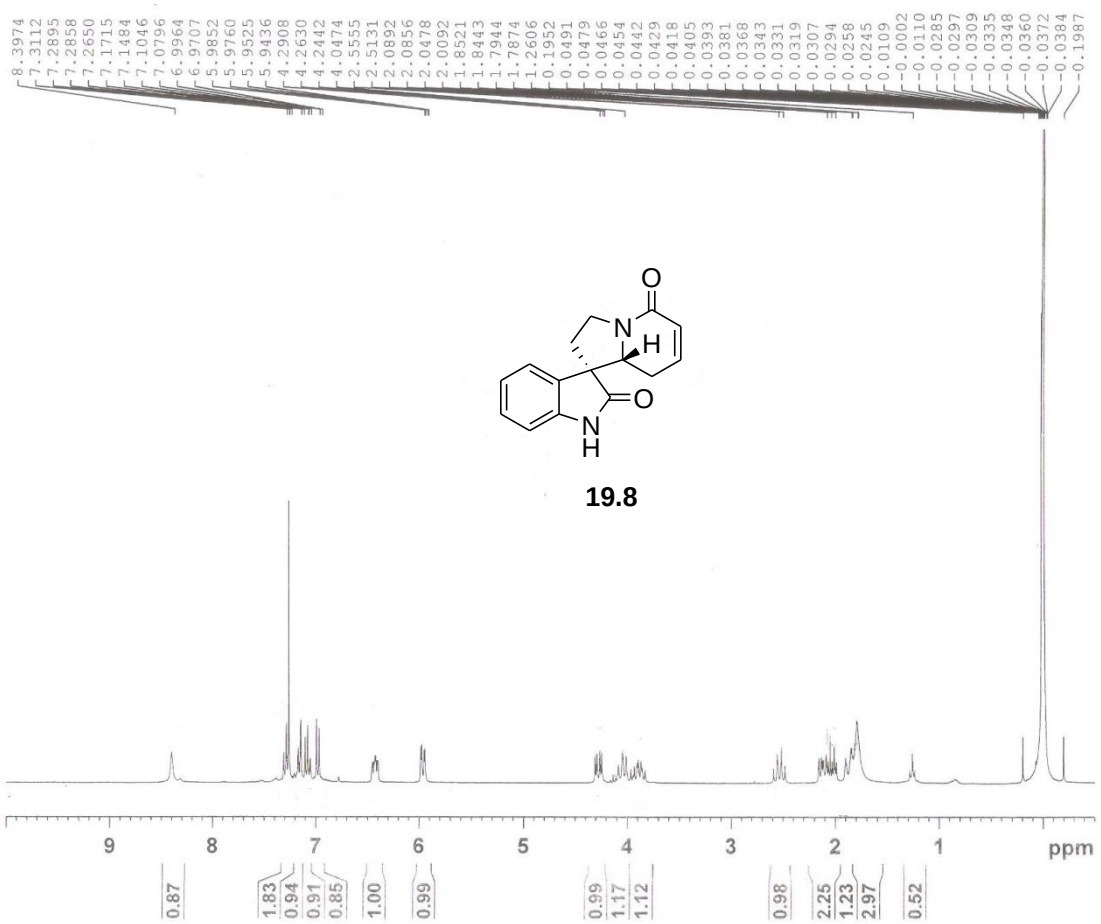

Figure 59 The ^{1}H NMR of *α,β*–unsaturated spiroindolizidine-oxindole **19.8** in $CDCl_3$

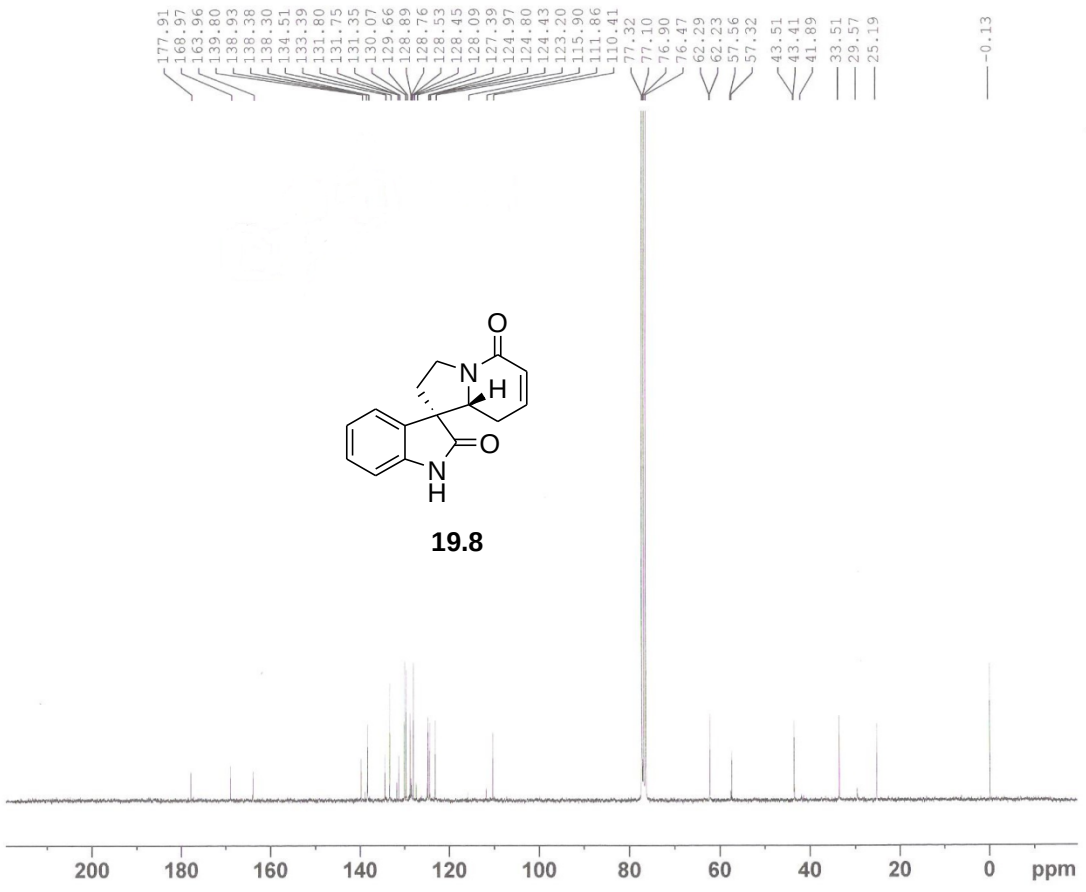

19.8

Figure 60 The ^{13}C NMR of α,β–unsaturated spiroindolizidine-oxindole **19.8** in $CDCl_3$

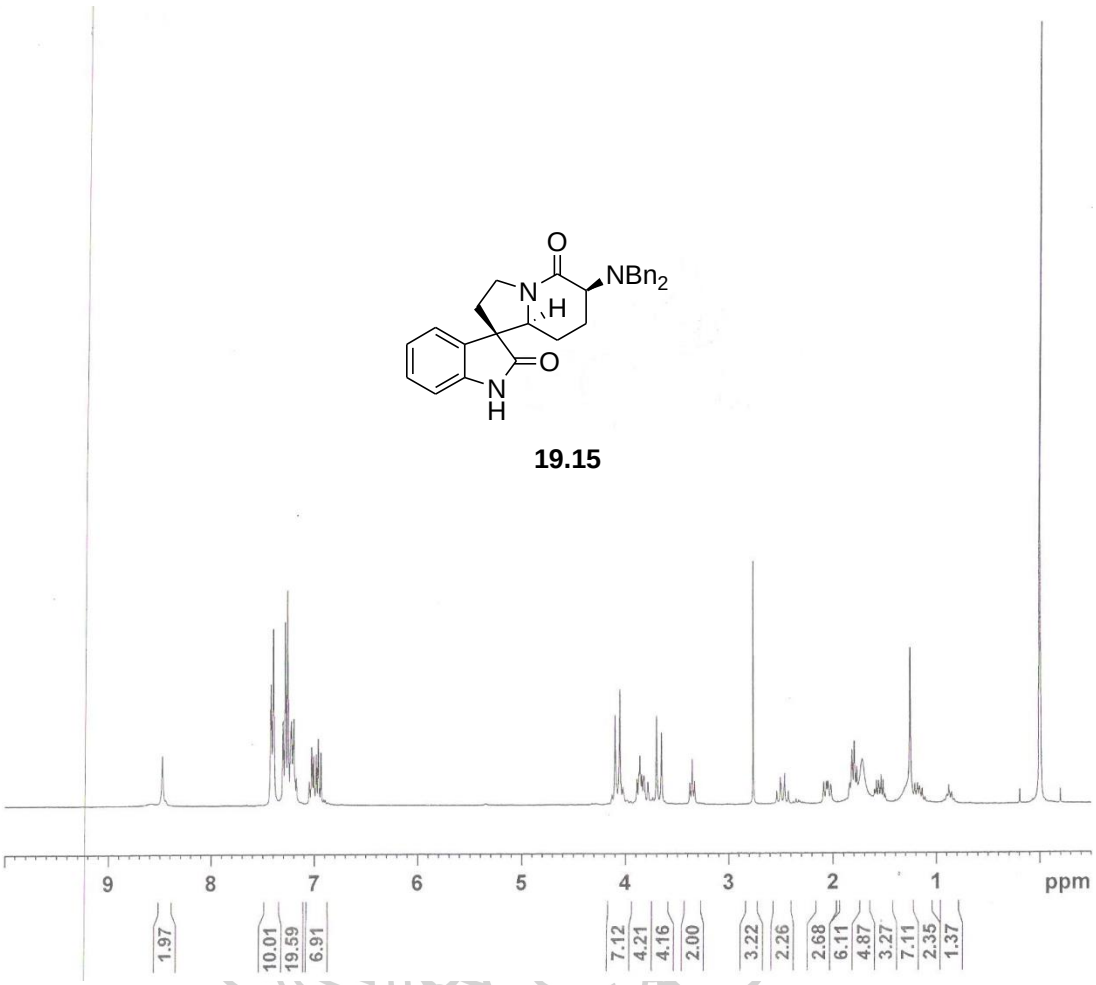

19.15

Figure 61 The ^{1}H NMR of spiro[indolizidine-1,3′-oxindole] **19.15** in $CDCl_3$

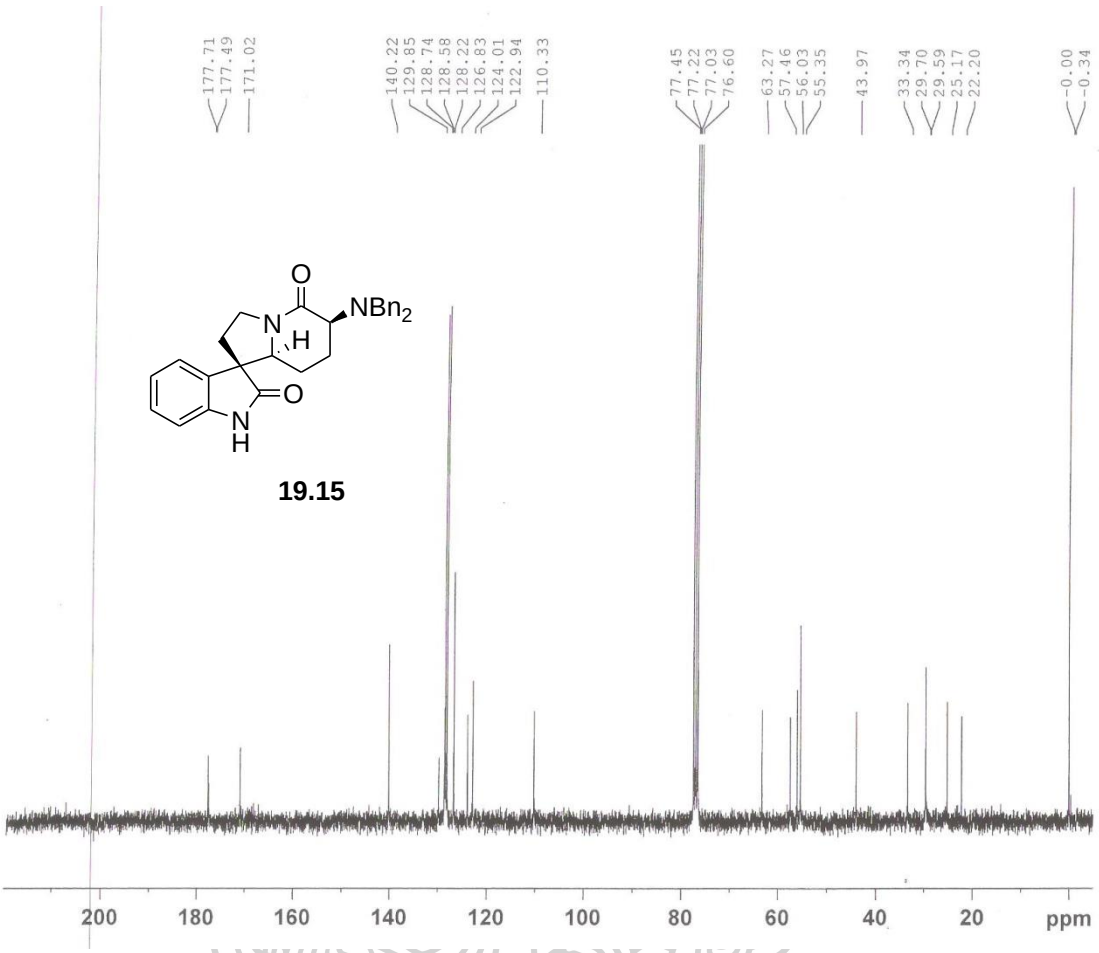

Figure 62 The ^{13}C NMR of spiro[indolizidine-1,3′-oxindole] **19.15** in $CDCl_3$

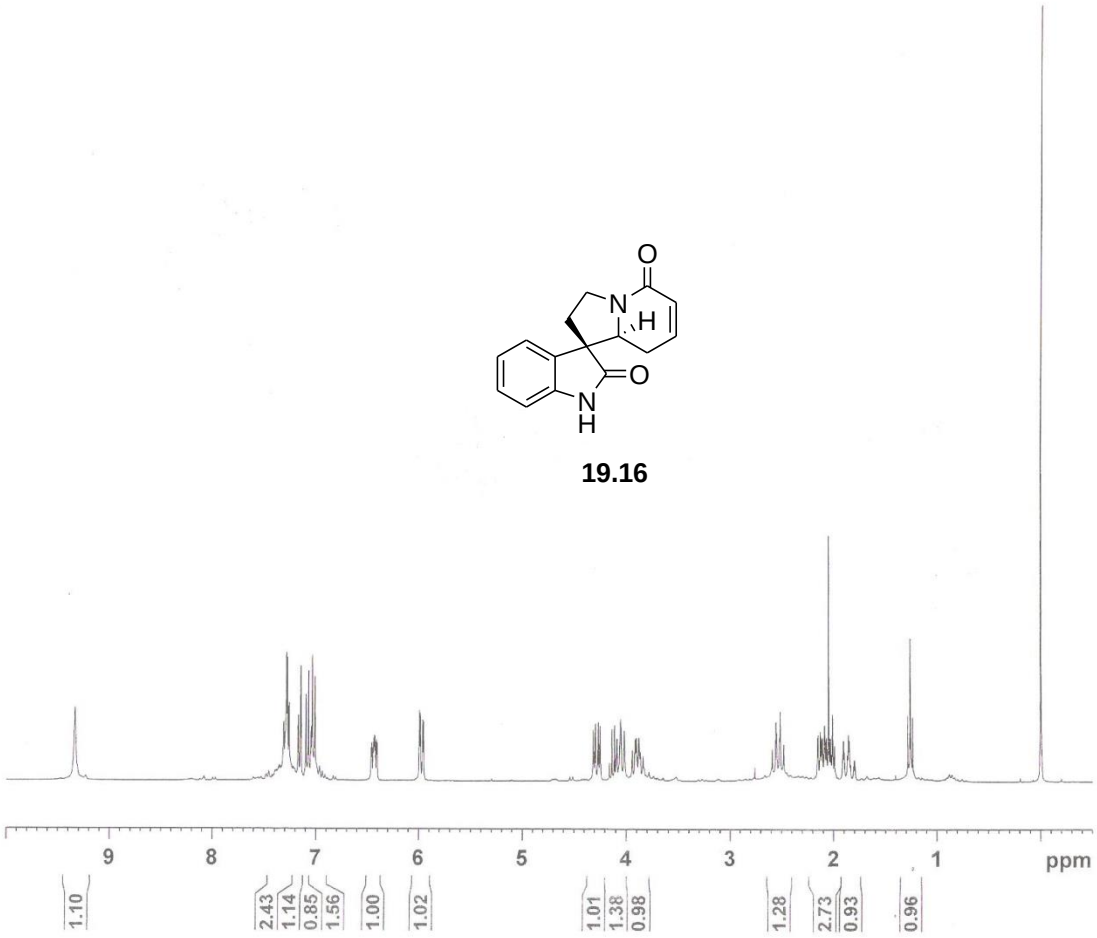

Figure 63 The ^{1}H NMR of α,β–unsaturated spiroindolizidine-oxindole **19.16** in $CDCl_3$

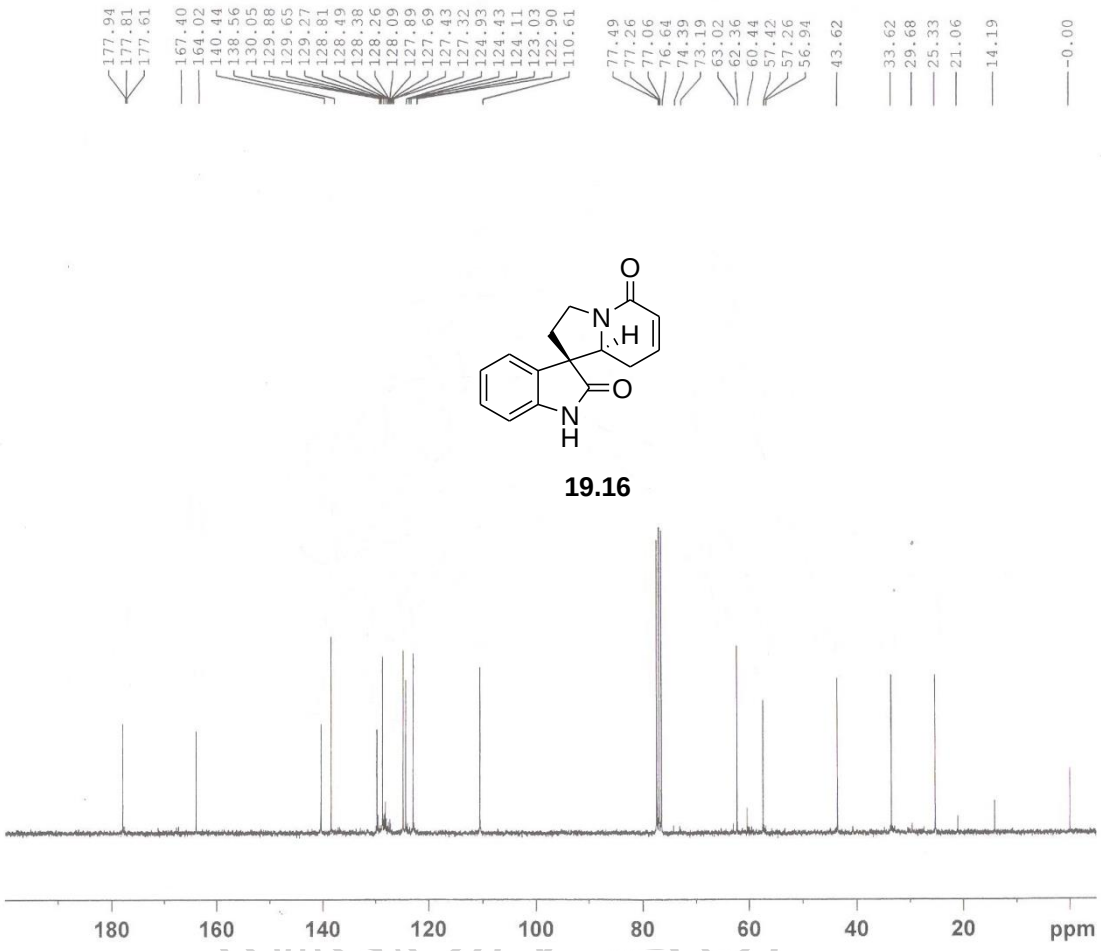

19.16

Figure 64 The ^{13}C NMR of α,β–unsaturated spiroindolizidine-oxindole **19.16** in $CDCl_3$

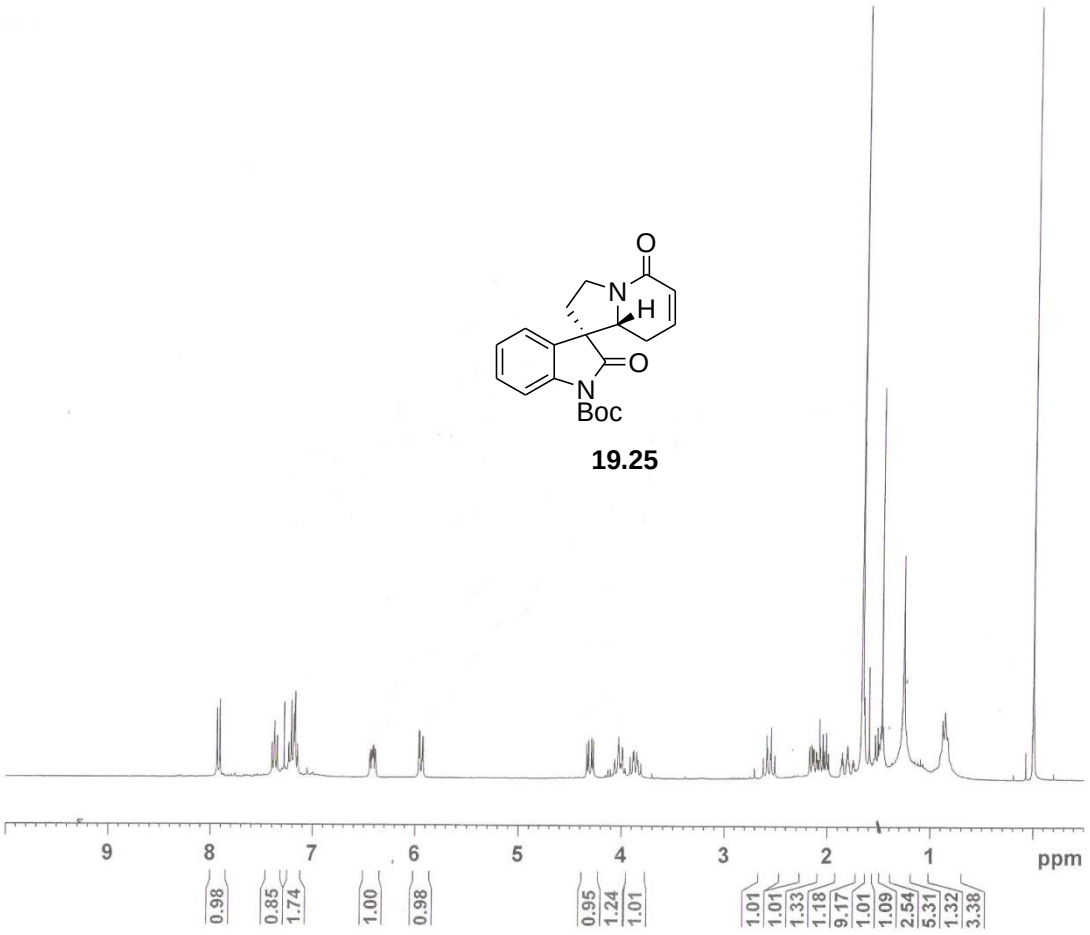

Figure 65 The ^{1}H NMR of *N*-Boc unsaturated spiroindolizidine-oxindole **19.25** in $CDCl_3$

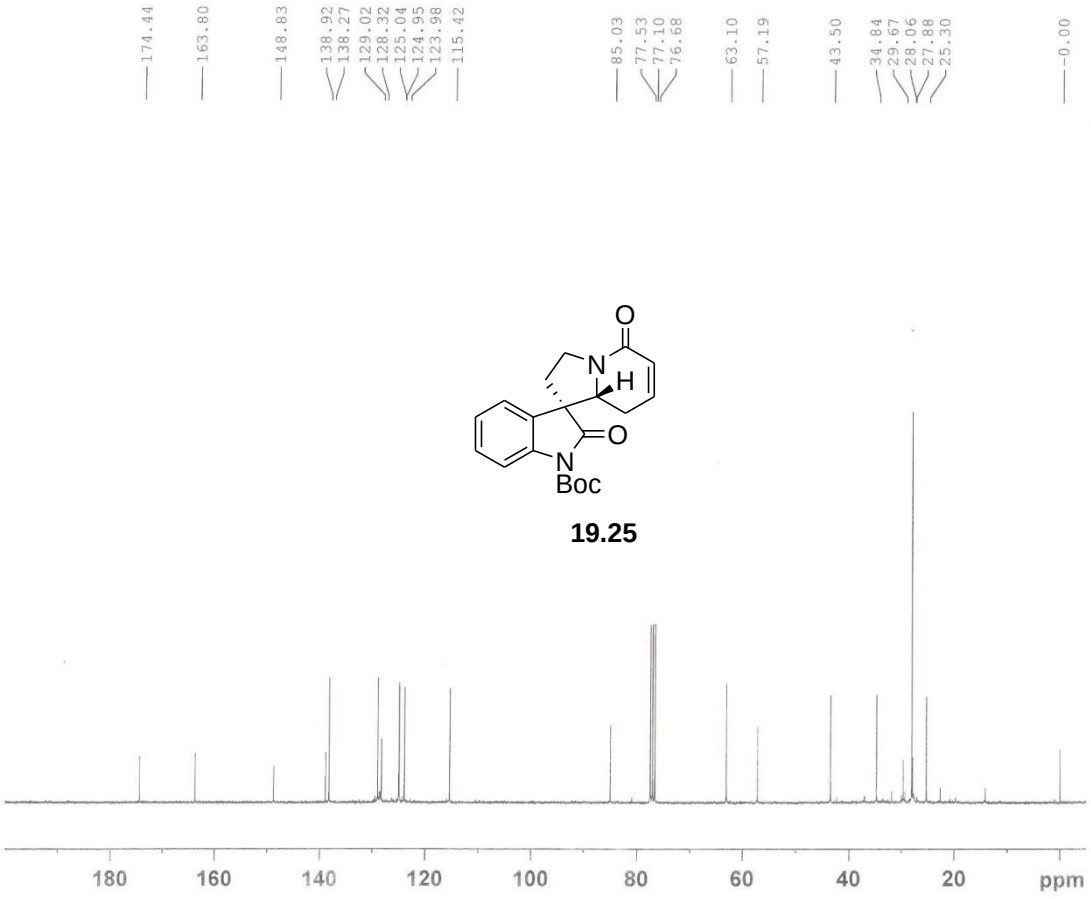

19.25

Figure 66 The ^{13}C NMR of *N*-Boc unsaturated spiroindolizidine-oxindole **19.25** in $CDCl_3$

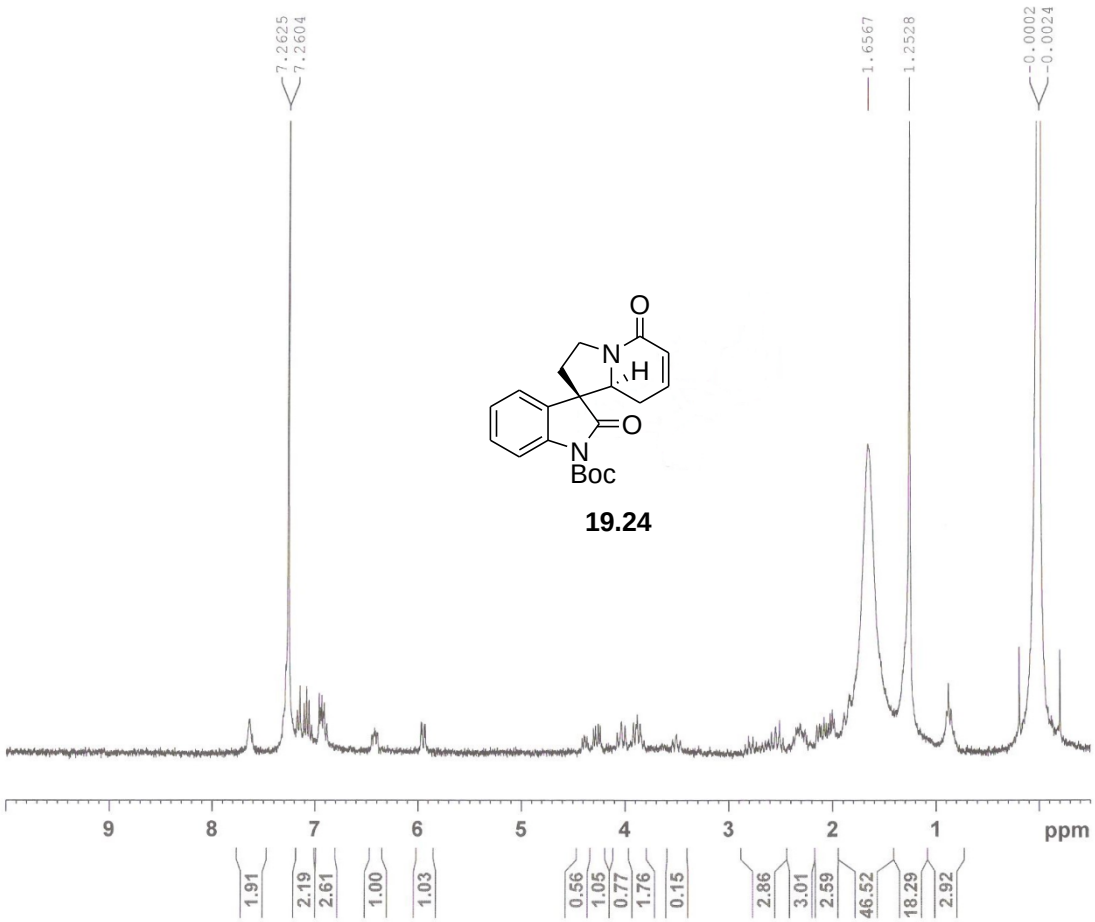

Figure 67 The ^{1}H NMR of *N*-Boc unsaturated spiroindolizidine-oxindole **19.24** in $CDCl_3$

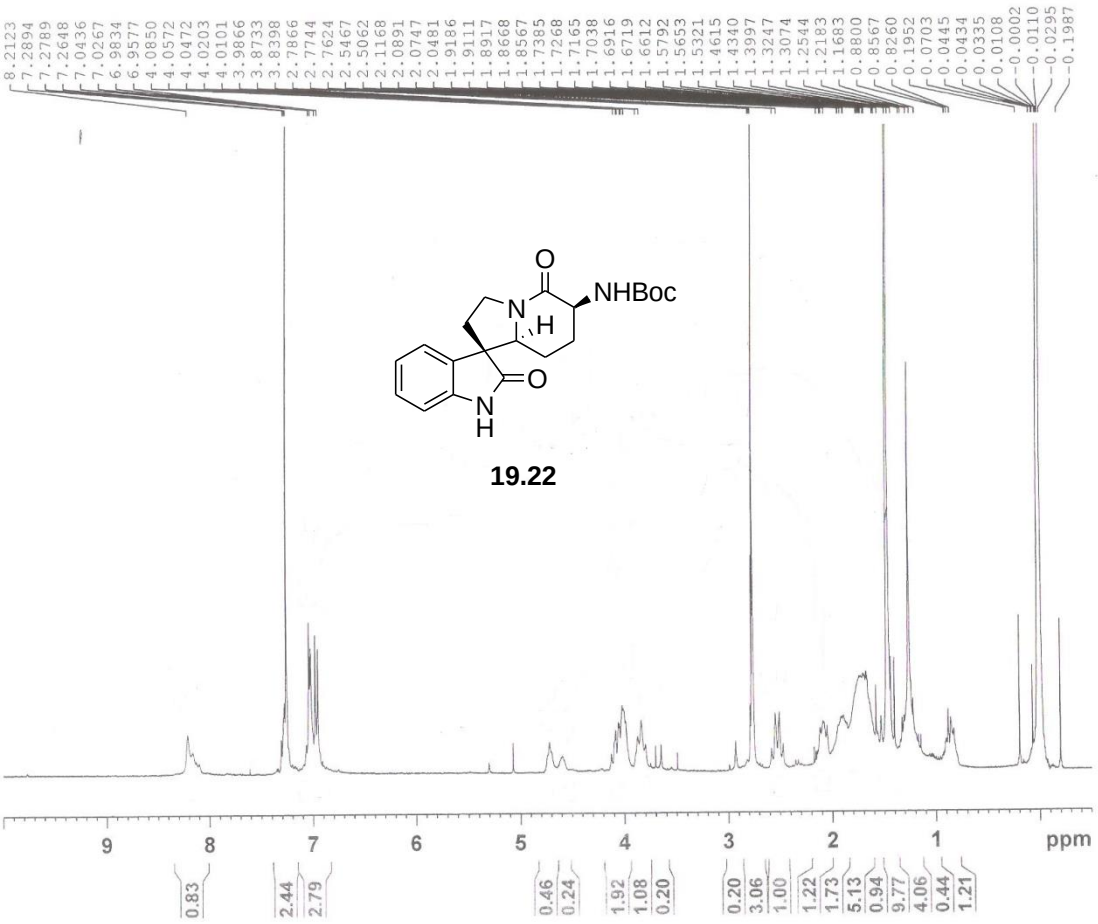

Figure 68 The ^{1}H NMR of *N*-Boc spiro[indolizidine-1,3´-oxindole] **19.22** in $CDCl_3$

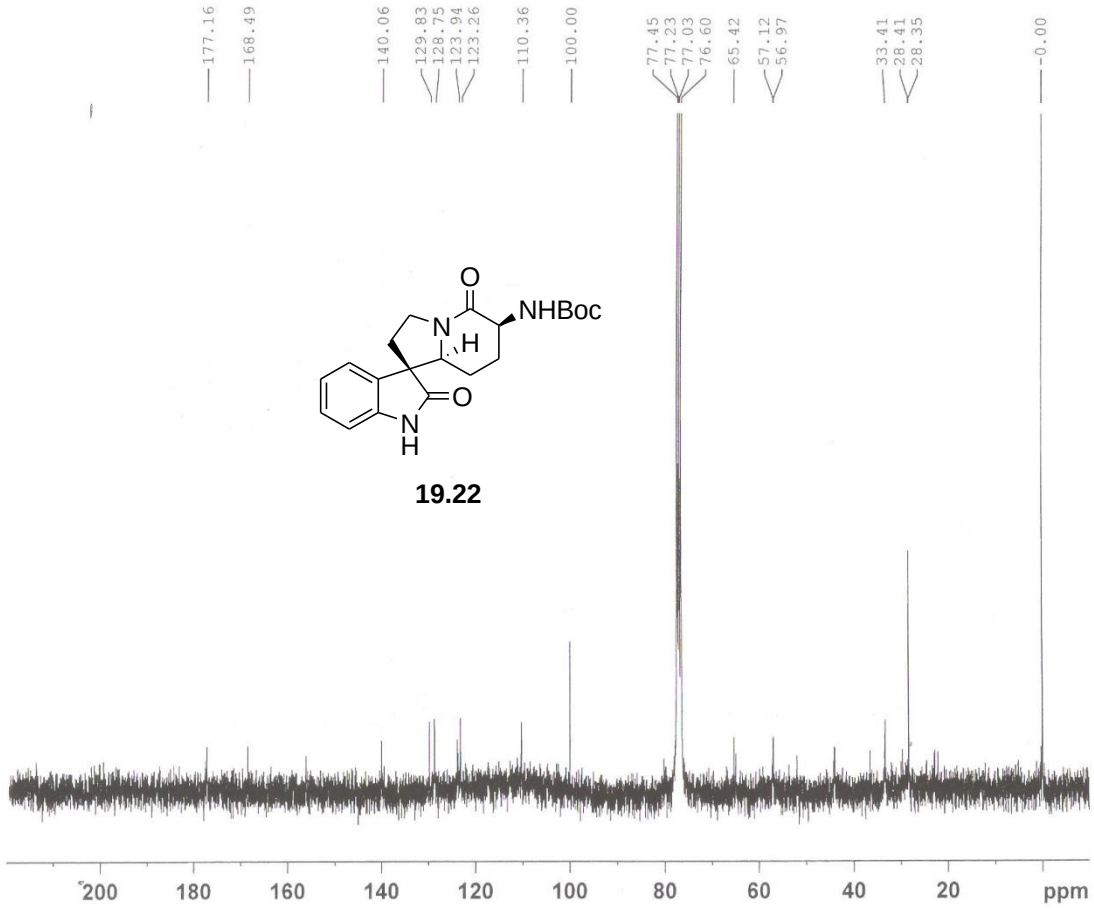

Figure 69 The ^{13}C NMR of *N*-Boc spiro[indolizidine-1,3′-oxindole] **19.22** in $CDCl_3$

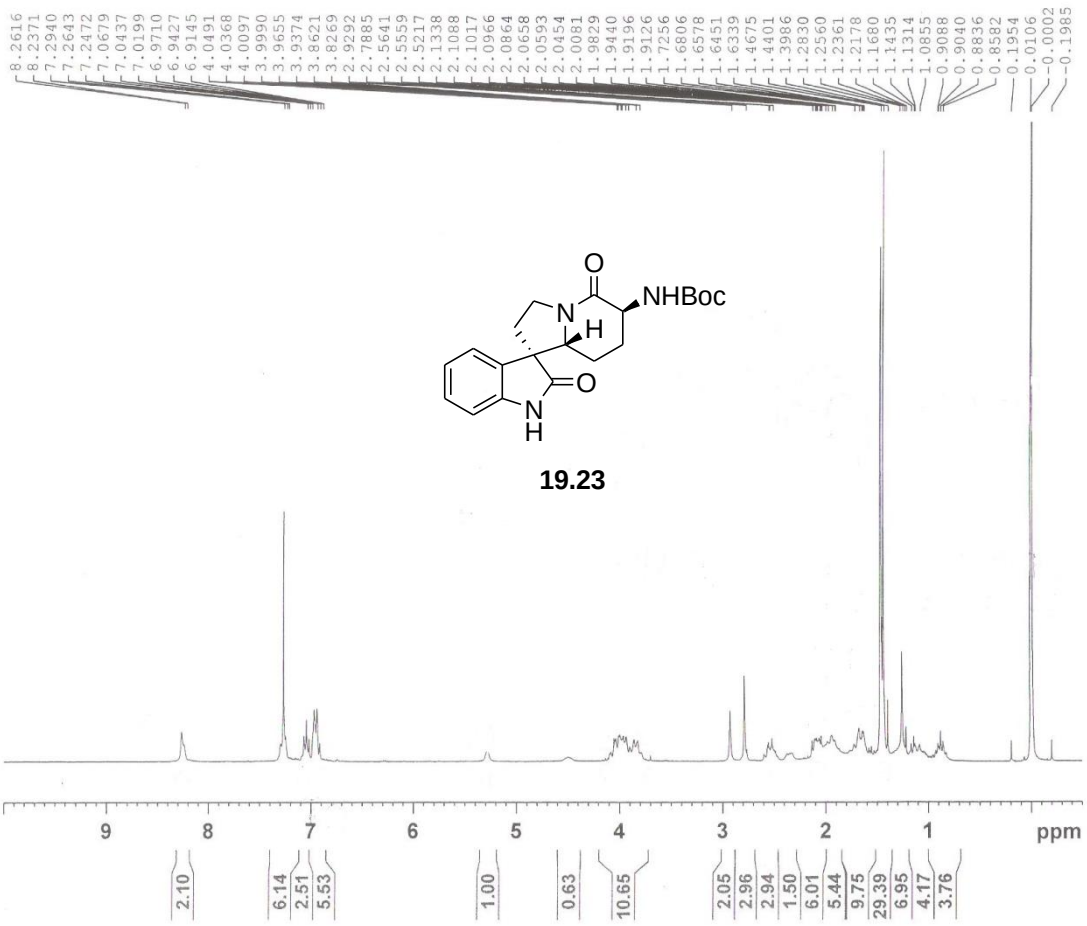

Figure 70 The ^{1}H NMR of *N*-Boc spiro[indolizidine-1,3´-oxindole] **19.23** in $CDCl_3$

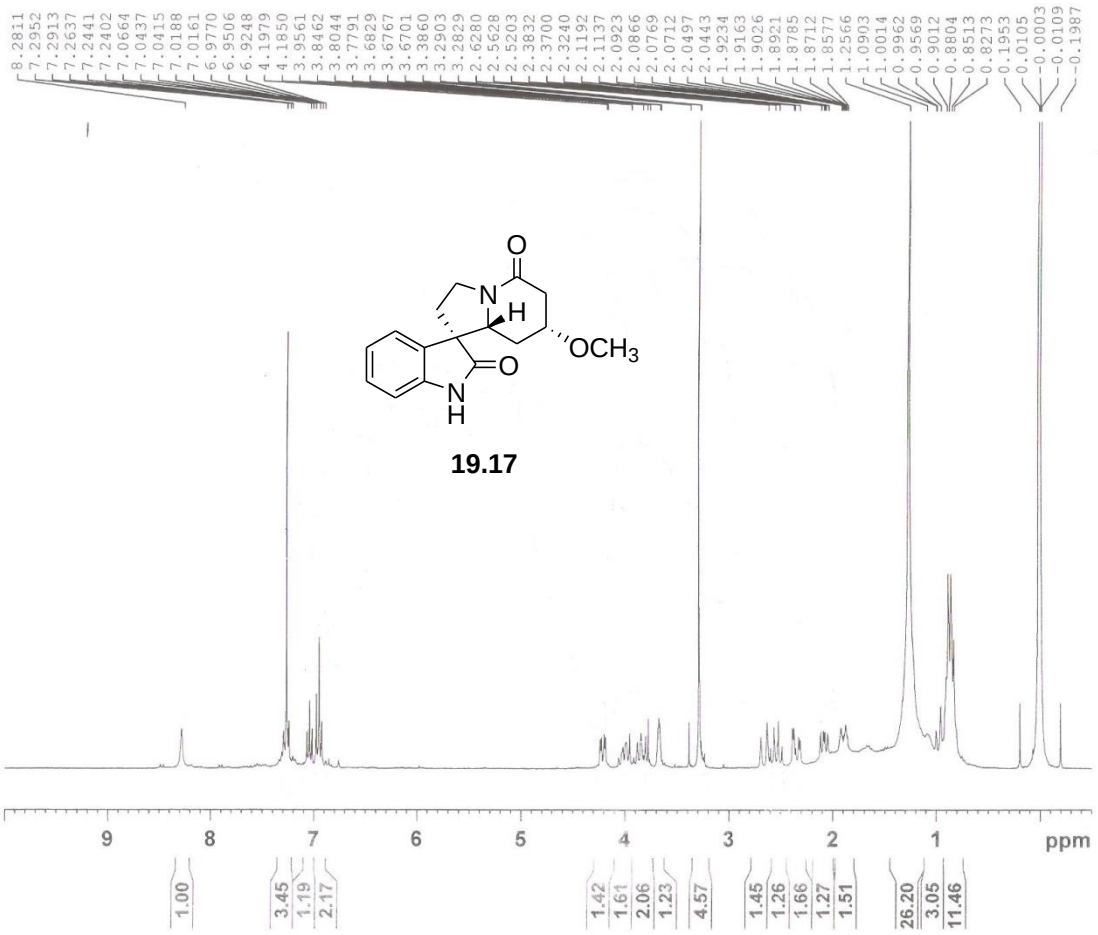

Figure 71 The ^{1}H NMR of spiro[7-methoxyindolizidine-1,3´-oxindole] **19.17** in $CDCl_3$

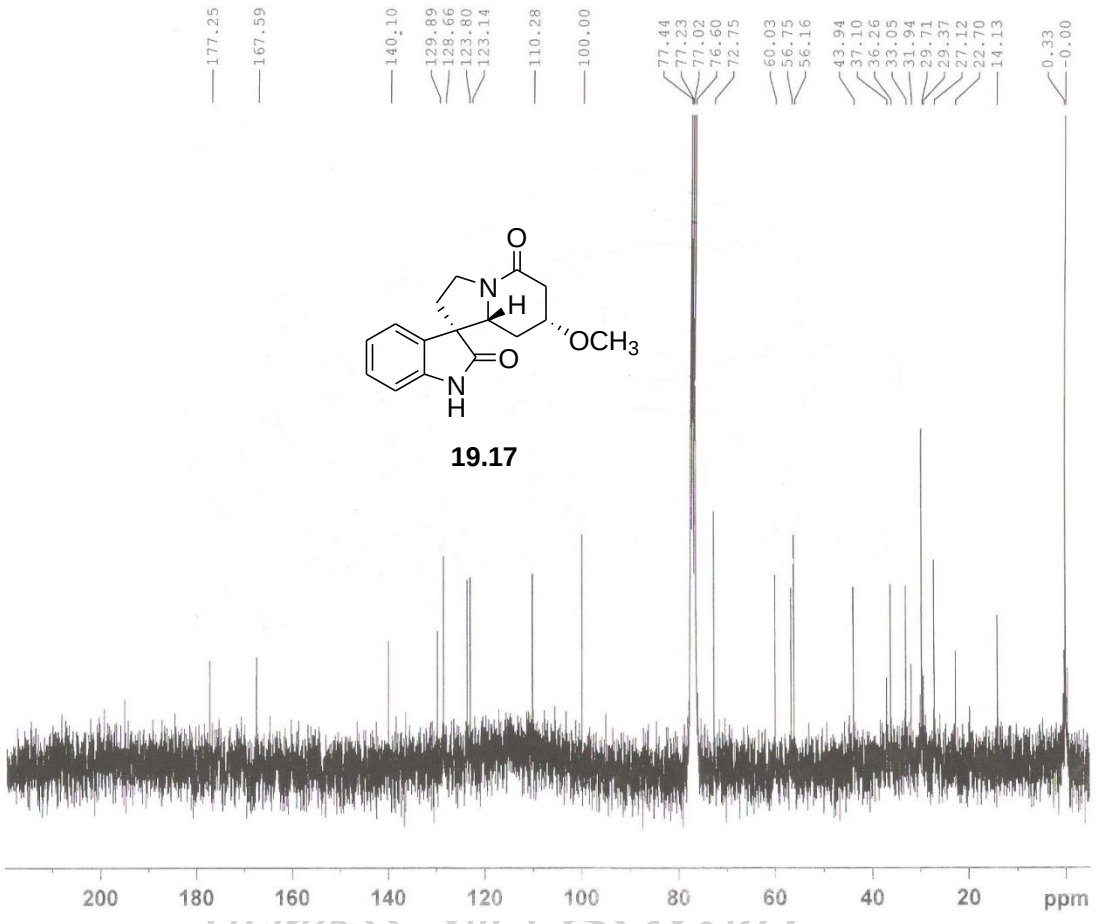

Figure 72 The ^{13}C NMR of spiro[7-methoxyindolizidine-1,3′-oxindole] **19.17** in $CDCl_3$

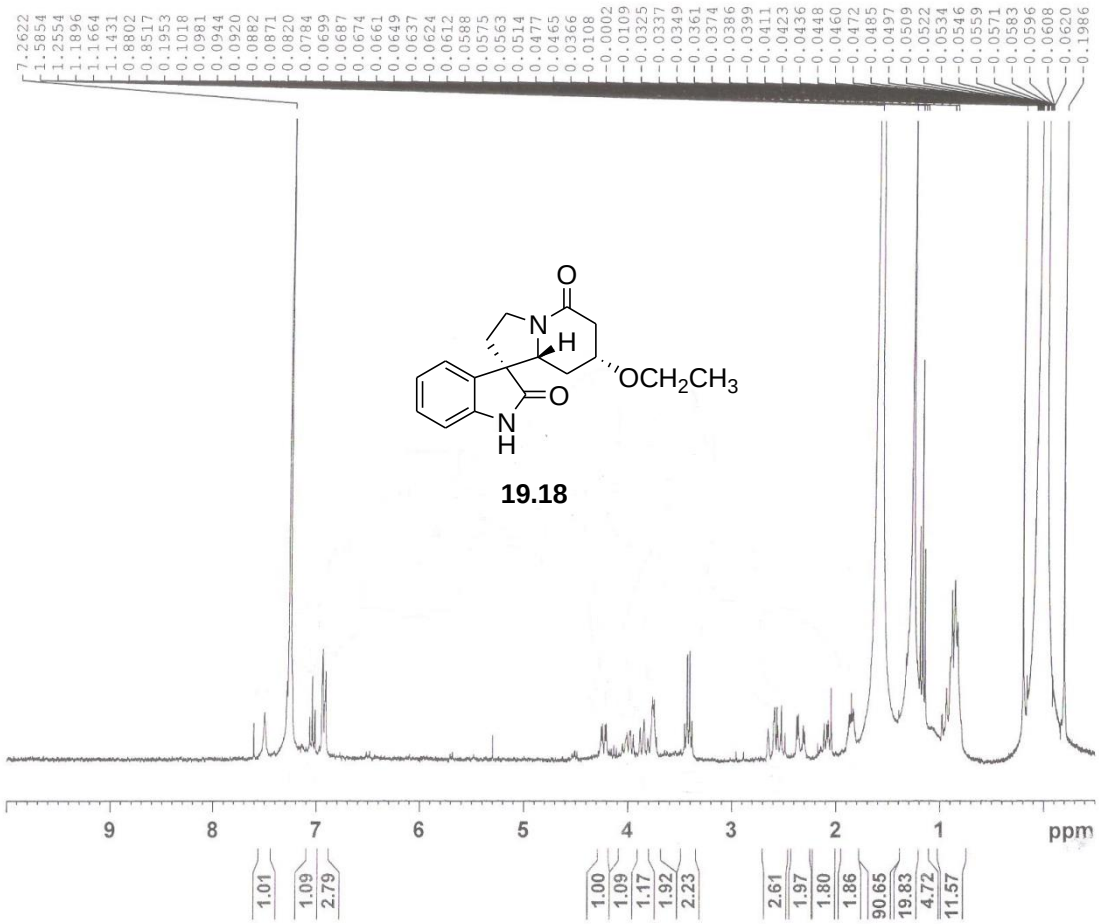

Figure 73 The ^{1}H NMR of spiro[7-ethoxyindolizidine-1,3′-oxindole] **19.18** in $CDCl_3$

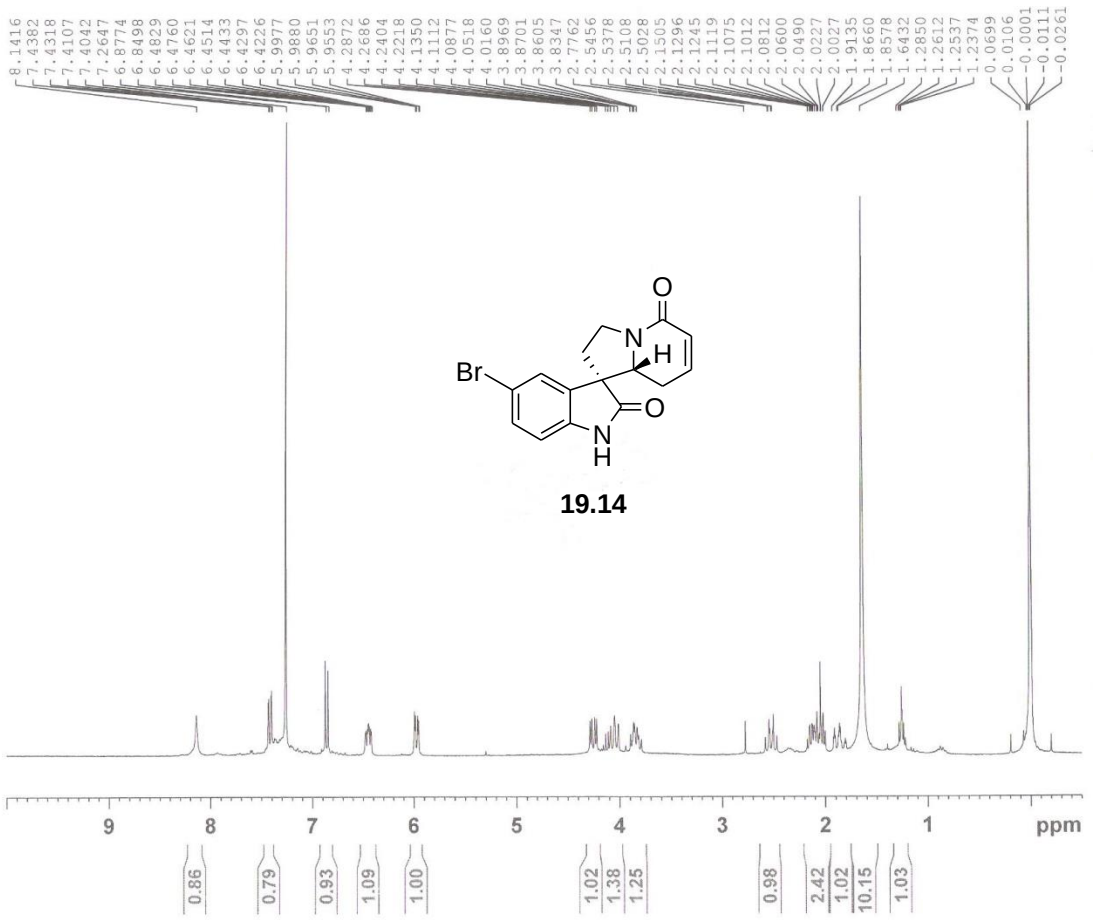

Figure 74 The ^{1}H NMR of spiro[indolizidine-1,3′-bromooxindole] **19.14** in $CDCl_3$

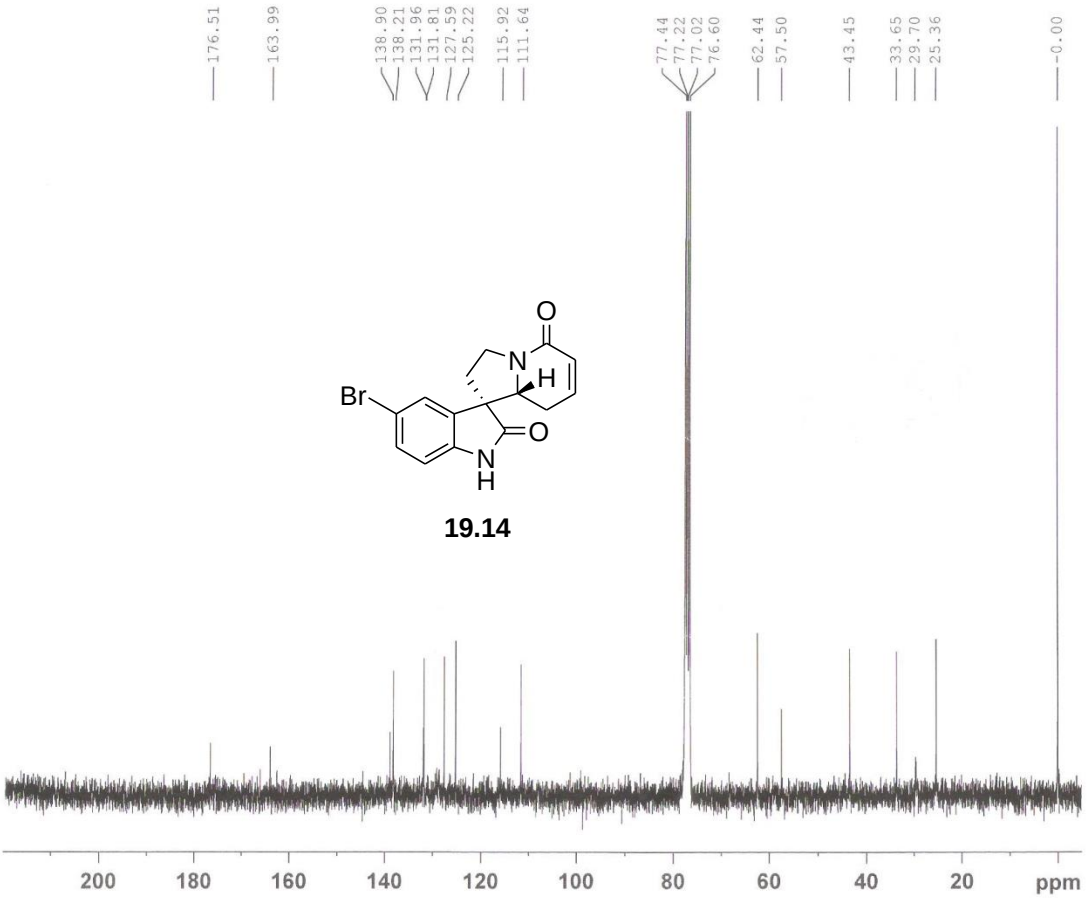

Figure 75 The ^{13}C NMR of spiro[indolizidine-1,3´-bromooxindole] **19.14** in $CDCl_3$

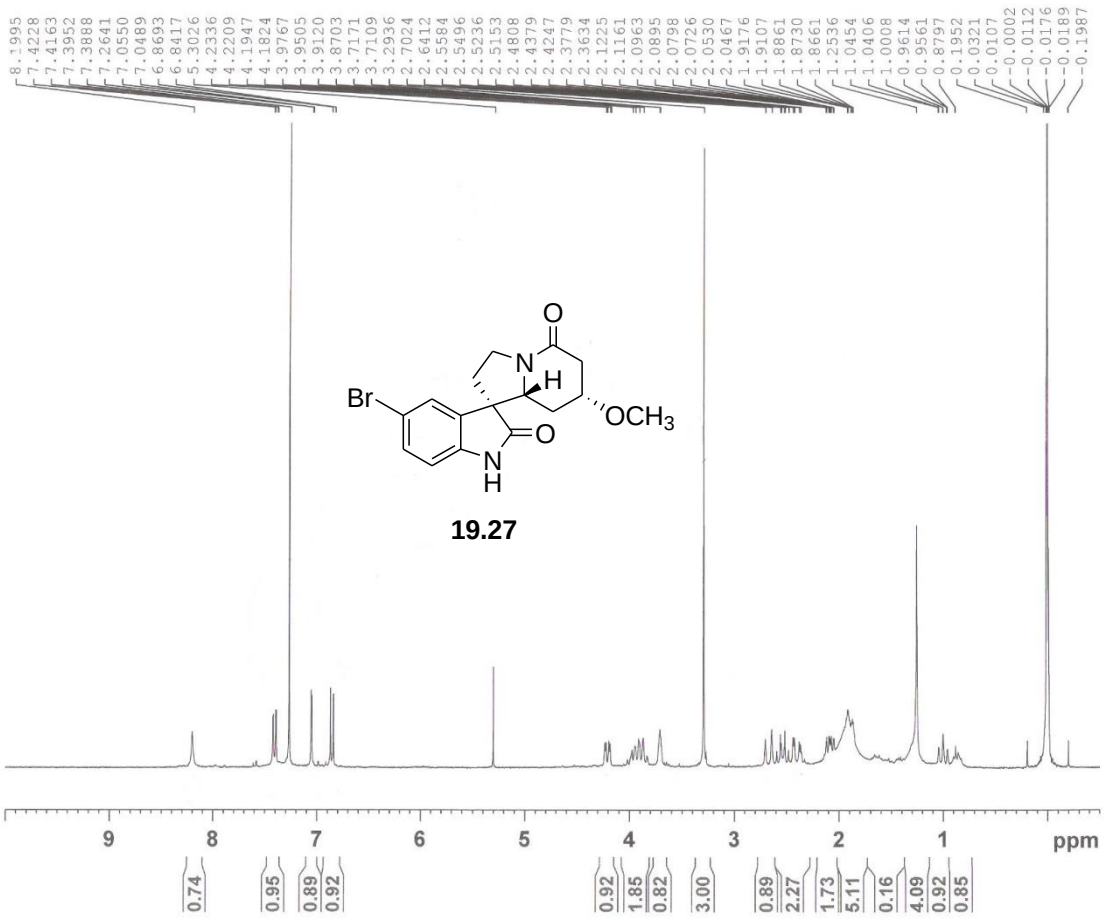

Figure 76 The ^{1}H NMR of spiro[7-methoxyindolizidine-1,3′-bromooxindole] **19.27** in $CDCl_3$

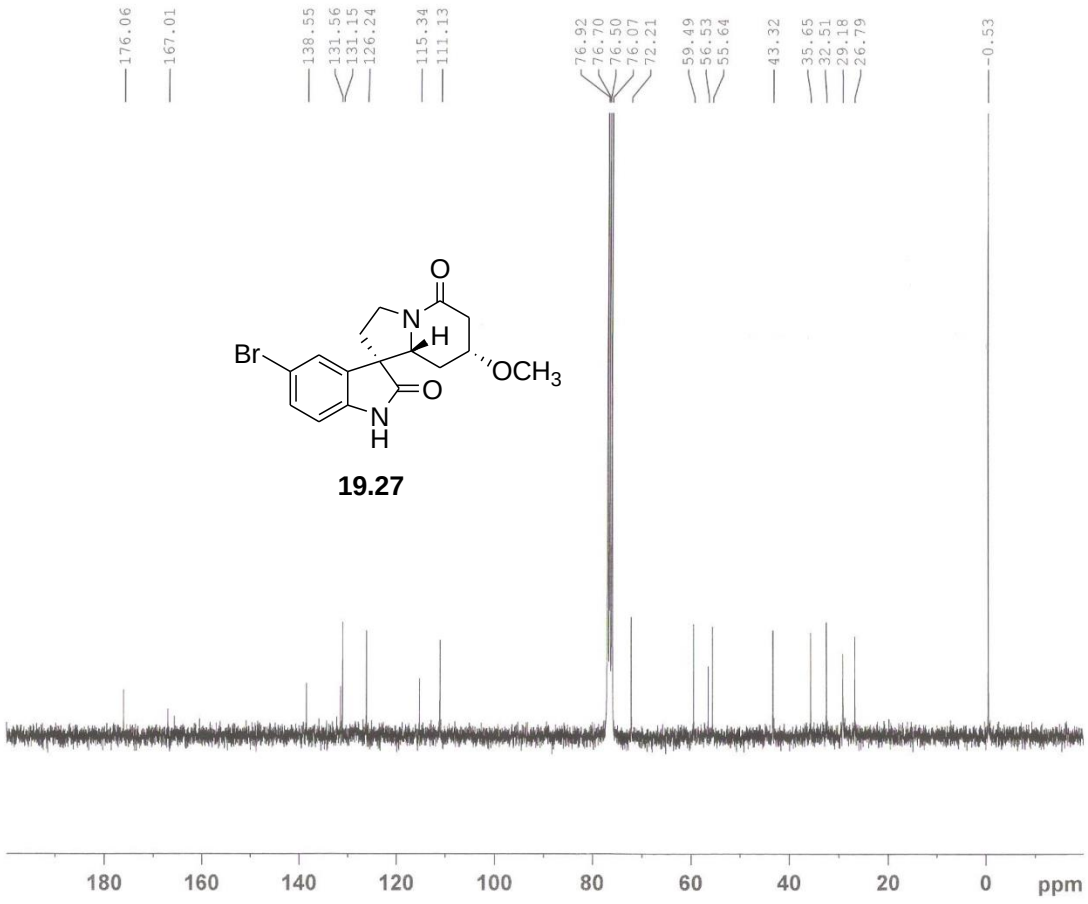

Figure 77 The ^{13}C NMR of spiro[7-methoxyindolizidine-1,3′-bromooxindole] **19.27** in $CDCl_3$

REFERENCES

1. Beiser A, McMurry J, Fay R, Erdődi F, Bailar J. LIST OF TEXTBOOKS.
2. Dey P, Kundu A, Kumar A, Gupta M, Lee BM, Bhakta T, et al. Analysis of alkaloids (indole alkaloids, isoquinoline alkaloids, tropane alkaloids). Recent advances in natural products analysis: Elsevier; 2020. p. 505-67.
3. Wu P, Nielsen TE. Scaffold diversity from N-acyliminium ions. Chemical reviews. 2017;117(12):7811-56.
4. IJzendoorn DR, Botman PN, Blaauw RH. Diastereoselective Cationic Tandem Cyclizations to N-Heterocyclic Scaffolds: Total Synthesis of (−)-Dysibetaine PP. Organic Letters. 2006;8(2):239-42.
5. Sakai R, Suzuki K, Shimamoto K, Kamiya H. Novel Betaines from a Micronesian Sponge Dysidea h erbacea. The Journal of organic chemistry. 2004;69(4):1180-5.
6. Dekeukeleire S, D'hooghe M, De Kimpe N. Diastereoselective synthesis of bicyclic γ-lactams via ring expansion of monocyclic β-lactams. The Journal of Organic Chemistry. 2009;74(4):1644-9.
7. Min BJ, Gu X, Yamamoto T, Petrov RR, Qu H, Lee YS, et al. Synthesis of a novel benzyl-octahydropyrazino [1, 2-a] pyrimidin-6-one derivative as a convenient internal bicyclic peptidomimetic. Tetrahedron letters. 2008;49(14):2316-9.
8. Indukuri K, Unnava R, Deka MJ, Saikia AK. Stereoselective synthesis of amido and phenyl azabicyclic derivatives via a tandem aza Prins-Ritter/Friedel–Crafts type reaction of endocyclic n-acyliminium ions. The Journal of Organic Chemistry. 2013;78(21):10629-41.
9. Saikia AK, Indukuri K, Das J. Stereoselective synthesis of O-tosyl azabicyclic derivatives via aza Prins reaction of endocyclic N-acyliminium ions: application to the total synthesis of (±)-epi-indolizidine 167B and 209D. Organic & Biomolecular Chemistry. 2014;12(36):7026-35.
10. Chio FK, Guesne SJ, Hassall L, McGuire T, Dobbs AP. Synthesis of azabicycles via cascade aza-Prins reactions: accessing the indolizidine and quinolizidine cores. The Journal of organic chemistry. 2015;80(20):9868-80.
11. Hanessian S, Tremblay M. Tandem functionalization of nonactivated alkenes and alkynes in intramolecular N-acyloxyiminium ion carbocyclization. Synthesis of 6-substituted hydroindole 2-carboxylic acids. Organic Letters. 2004;6(25):4683-6.
12. Wang Y, Zhu L, Zhang Y, Hong R. Bioinspired and Concise Synthesis of (±)-Stemoamide. Angewandte Chemie. 2011;123(12):2839-42.
13. Wang B-J, Xue P, Gu P. Intramolecular Schmidt reaction of acyl chlorides with alkyl azides: preparation of pyrrolizine by intramolecular capture of intermediates with alkenes or alkynes. Chemical Communications. 2015;51(12):2277-9.
14. Koseki Y, Fujino K, Takeshita A, Sato H, Nagasaka T. The intramolecular tandem Michael/Mannich-type reaction of α, β-unsaturated carbonyl compounds with acyliminium ions provides access to chiral indolizidines. Tetrahedron: Asymmetry. 2007;18(13):1533-9.
15. Yang J-E, In J-K, Lee M-S, Kwak J-H, Lee H-S, Lee S-J, et al. Synthesis of calycotomine via pictet-spengler type reaction of N, O-Acetal TMS ethers as N-acyliminium ion equivalents. Bulletin of the Korean Chemical Society. 2007;28(8):1401-4.

16. Ballet S, Urbanczyk-Lipkowska Z, Tourwe D. Synthesis of substituted 4-amino-2-benzazepin-3-ones via N-acyliminium ion cyclizations. Synlett. 2005;2005(18):2791-5.
17. Zhang Y, Kindelin PJ, DeSchepper DJ, Zheng C, Klumpp DA. Superacid-Promoted Reactions of N-Acyliminium Ions: An effective route to substituted 3-Oxo-1, 2, 3, 4-tetrahydroisoquinolines and related products. Synthesis. 2006;2006(11):1775-80.
18. Hjelmgaard T, Søtofte I, Tanner D. Total synthesis of pinnamine and anatoxin-a via a common intermediate. A caveat on the anatoxin-a endgame. The Journal of Organic Chemistry. 2005;70(14):5688-97.
19. Li G, Zhang X, Li Q, Feng P, Shi Y. A concise approach to the spiroiminal fragment of marineosins. Organic & Biomolecular Chemistry. 2013;11(18):2936-8.
20. Abe H, Aoyagi S, Kibayashi C. Total synthesis of the tricyclic marine alkaloids (−)-lepadiformine,(+)-cylindricine C, and (−)-fasicularin via a common intermediate formed by formic acid-induced intramolecular conjugate azaspirocyclization. Journal of the American Chemical Society. 2005;127(5):1473-80.
21. Abe H, Muramatsu Y, Watanabe K, Aoyagi S, Kibayashi C, Katoh T. Spirocyclization of Six-Membered Cyclic N-Acyliminium Ions with a Conjugated Diene. Heterocycles. 2009;79:1087-91.
22. Yamada S, Takahashi Y. Stereoselective synthesis of N, N-acetals by cyclization of an N-acyliminium ion through interaction with an N-sulfonyl group. Tetrahedron Letters. 2009;50(38):5395-8.
23. Gunawan S, Hulme C. Construction of functionalized tricyclic dihydropyrazino-quinazolinedione chemotypes via an Ugi/N-acyliminium ion cyclization cascade. Tetrahedron letters. 2013;54(33):4467-70.
24. Li C, Li X, Hong R. Synthetic Study on Tetrapetalones: Stereoselective Cyclization of N-Acyliminium Ion To Construct Substituted 1-Benzazepines. Organic letters. 2009;11(18):4036-9.
25. Judd WR, Ban S, Aubé J. Remote control of diastereoselectivity in intramolecular reactions of chiral allylsilanes. Journal of the American Chemical Society. 2006;128(42):13736-41.
26. Kim SH, Kim HG, Choo H, Cha JH, Pae AN, Koh HY, et al. N-Acyliminium ion cyclizations of trimethylsilylmethylallenes. Tetrahedron letters. 2006;47(36):6353-6.
27. Abe H, Sato Y, Watanabe K. Stereoselective synthesis of a 4a, 9-disubstituted octahydroachdine from isatin. Heterocycles. 2009;77(1):533-8.
28. Taylor MS, Tokunaga N, Jacobsen EN. Enantioselective thiourea-catalyzed acyl-Mannich reactions of isoquinolines. Angewandte Chemie. 2005;117(41):6858-62.
29. Seayad J, Seayad AM, List B. Catalytic Asymmetric Pictet− Spengler Reaction. Journal of the American Chemical Society. 2006;128(4):1086-7.
30. Raheem IT, Thiara PS, Peterson EA, Jacobsen EN. Enantioselective Pictet− Spengler-type cyclizations of hydroxylactams: H-bond donor catalysis by anion binding. Journal of the American Chemical Society. 2007;129(44):13404-5.
31. Raheem IT, Thiara PS, Jacobsen EN. Regio-and enantioselective catalytic cyclization of pyrroles onto N-acyliminium ions. Organic letters. 2008;10(8):1577-80.
32. Hansen CL, Clausen JW, Ohm RG, Ascic E, Le Quement ST, Tanner D, et al. Ruthenium hydride/Brønsted Acid-catalyzed tandem isomerization/N-acyliminium cyclization sequence for the synthesis of tetrahydro-β-carbolines. The Journal of Organic Chemistry. 2013;78(24):12545-65.

33. Zheng X, Chang J, Zhao K. Synthesis of Indole Derivatives by Cyclization of Oxo N-Acyliminium Ions. Synthesis. 2008;2008(09):1345-50.
34. Shengule SR, Ryder G, Willis AC, Pyne SG. Highly diastereoselective N-acyliminium ion cyclization reactions of a tethered furan. Tetrahedron. 2012;68(50):10280-5.
35. Zhang W, Franzén J. Diverse asymmetric quinolizidine synthesis: a stereodivergent one-pot approach. Advanced Synthesis & Catalysis. 2010;352(2-3):499-518.
36. Abe H, Miyagawa N, Hasegawa S, Kobayashi T, Aoyagi S, Kibayashi C, et al. Directed synthesis of 2-spiroindolines from indole derivatives by formic acid-induced N-acyliminium ion-conjugated diene spirocyclization. Tetrahedron Letters. 2015;56(7):921-4.
37. Yazici A, Pyne SG. Sequential 1, 4-and 1, 2-addition reactions to α, β-unsaturated N-acyliminium ions: a new strategy for the synthesis of spiro and bridged heterocycles. Organic letters. 2013;15(22):5878-81.
38. Shengule SR, Willis A, Pyne SG. Synthesis of spirocyclic azacycles from the cyclization of furan tethered N-acyliminium ions. Tetrahedron. 2012;68(4):1207-15.
39. Abe H, Takaya K-i, Watanabe K, Aoyagi S, Kibayashi C, Katoh T. Spirocyclization of an N-acyliminium ion with substituted pyridine: Synthesis of tricyclic spirolactams possessing pyridine or pyridone nucleus. Heterocycles. 2007;74:205-10.
40. Abe H, Takaya K-i, Watanabe K. Spirocyclization of an N-acyliminium ion with substituted pyridine: stereoselective synthesis of tetracyclic spirolactams possessing the pyridone nucleus. Heterocycles. 2010;82(1):257-61.
41. Bahajaj AA, Vernon JM, Wilson GD. Asymmetric synthesis of spiro 2-pyrrolidin-5-ones, 2-piperidin-6-ones and 1-isoindolin-3-ones. Part 2: N-Acyliminium ion cyclisations with an internal alkene nucleophile. Tetrahedron. 2004;60(5):1247-53.
42. Ascic E, Jensen JF, Nielsen TE. Synthesis of Heterocycles through a Ruthenium-Catalyzed Tandem Ring-Closing Metathesis/Isomerization/N-Acyliminium Cyclization Sequence. Angewandte Chemie. 2011;123(22):5294-7.
43. Muratore ME, Holloway CA, Pilling AW, Storer RI, Trevitt G, Dixon DJ. Enantioselective Brønsted acid-catalyzed N-acyliminium cyclization cascades. Journal of the American Chemical Society. 2009;131(31):10796-7.
44. Holloway CA, Muratore ME, Storer Rl, Dixon DJ. Direct enantioselective Brønsted acid catalyzed N-acyliminium cyclization cascades of tryptamines and ketoacids. Organic letters. 2010;12(21):4720-3.
45. Cai Q, Liang X-W, Wang S-G, Zhang J-W, Zhang X, You S-L. Ring-closing metathesis/isomerization/Pictet–Spengler cascade via ruthenium/chiral phosphoric acid sequential catalysis. Organic letters. 2012;14(19):5022-5.
46. Cincinelli R, Dallavalle S, Merlini L, Nannei R, Scaglioni L. Intramolecular N-acyliminium ion versus Friedel–Crafts cyclization onto 3-indoles: synthesis of the novel rings pyrrolizino [2, 1-b] indole and homologues. Tetrahedron. 2009;65(17):3465-72.
47. Grigg R, Sridharan V, Sykes DA. Sonogashira/N-acyliminium ion aromatic π-cyclisation processes: access to tetra-and pentacyclic lactams. Tetrahedron. 2008;64(37):8952-62.
48. Rose MD, Cassidy MP, Rashatasakhon P, Padwa A. Acid-promoted cyclization reactions of tetrahydroindolinones. Model studies for possible application in a synthesis

of selaginoidine. The Journal of organic chemistry. 2007;72(2):538-49.
49. Amat M, Santos MM, Gómez AM, Jokic D, Molins E, Bosch J. Enantioselective spirocyclizations from tryptophanol-derived oxazolopiperidone lactams. Organic Letters. 2007;9(15):2907-10.
50. Zhou L-M, Qu R-Y, Yang G-F. An overview of spirooxindole as a promising scaffold for novel drug discovery. Expert Opinion on Drug Discovery. 2020;15(5):603-25.
51. Gurevich P, Sattarova L, Petrovskiy A, Frolova N, Strunin B, Musin R. Interaction of spiro-heterocyclic oxindole system with sodium diformylimide. Chemistry of Heterocyclic Compounds. 2011;46(12):1527-30.
52. Hu Y, Wang M-M, Chen H, Shi D-Q. Efficient and convenient synthesis of spiroindolinone-quinazolines induced by stannous chloride. Tetrahedron. 2011;67(48):9342-6.
53. Bazgir A, Tisseh ZN, Mirzaei P. An efficient synthesis of spiro [dibenzo [b, i] xanthene-13, 3′-indoline]-pentaones and 5H-dibenzo [b, i] xanthene-tetraones. Tetrahedron Letters. 2008;49(35):5165-8.
54. Yeung BK, Zou B, Rottmann M, Lakshminarayana SB, Ang SH, Leong SY, et al. Spirotetrahydro β-carbolines (spiroindolones): a new class of potent and orally efficacious compounds for the treatment of malaria. Journal of medicinal chemistry. 2010;53(14):5155-64.
55. Nair V, Sethumadhavan D, Nair SM, Viji S, Rath NP. Reaction of nitrile ylides with isatins and o-benzoquinones: formation of novel spirooxazoline derivatives. Tetrahedron. 2002;58(15):3003-7.
56. Nair V, Sheela K, Sethumadhavan D, Bindu S, Rath NP, Eigendorf GK. Cycloaddition of Carbonyl Ylides to Isatins: Synthesis of Novel Spiro Oxindoles. Synlett. 2001;2001(02):0272-4.
57. Hosomi A, Hayashi S, Hoashi K, Kohra S, Tominaga Y. Unprecedented reaction of a thiocarbonyl ylide with carbonyl compounds: a novel synthesis of 1, 3-oxathiolanes. Journal of the Chemical Society, Chemical Communications. 1987(19):1442-3.
58. Lian Z, Shi M. Nitrogen-and Phosphorus-Containing Lewis Base Catalyzed [4+ 2] and [3+ 2] Annulation Reactions of Isatins with But-3-yn-2-one. Wiley Online Library; 2012.
59. Wang XN, Zhang YY, Ye S. Enantioselective synthesis of spirocyclic oxindole-β-lactones via n-heterocyclic carbene-catalyzed cycloaddition of ketenes and isatins. Advanced Synthesis & Catalysis. 2010;352(11-12):1892-5.
60. Sun L-H, Shen L-T, Ye S. Highly diastereo-and enantioselective NHC-catalyzed [3+ 2] annulation of enals and isatins. Chemical Communications. 2011;47(36):10136-8.
61. Basavaiah D, Rao JS, Reddy RJ, Rao AJ. TiCl 4 catalyzed tandem construction of C–C and C–O bonds: a simple and one-pot atom-economical stereoselective synthesis of spiro-oxindoles. Chemical communications. 2005(20):2621-3.
62. Badillo JJ, Arevalo GE, Fettinger JC, Franz AK. Titanium-catalyzed stereoselective synthesis of spirooxindole oxazolines. Organic Letters. 2011;13(3):418-21.
63. Hanhan NV, Ball-Jones NR, Tran NT, Franz AK. Catalytic asymmetric [3+ 2] annulation of allylsilanes with isatins: synthesis of spirooxindoles. Angewandte Chemie

International Edition. 2012;51(4):989-92.
64. Shintani R, Hayashi S-y, Murakami M, Takeda M, Hayashi T. Stereoselective Synthesis of spirooxindoles by palladium-catalyzed decarboxylative cyclization of γ-methylidene-δ-valerolactones with isatins. Organic Letters. 2009;11(16):3754-6.
65. Hojo D, Noguchi K, Hirano M, Tanaka K. Enantioselective Synthesis of Spirocyclic Benzopyranones by Rhodium-Catalyzed Intermolecular [4+ 2] Annulation. Angewandte Chemie. 2008;120(31):5904-6.
66. Cheng X, Vellalath S, Goddard R, List B. Direct catalytic asymmetric synthesis of cyclic aminals from aldehydes. Journal of the American Chemical Society. 2008;130(47):15786-7.
67. Jiang X, Cao Y, Wang Y, Liu L, Shen F, Wang R. A unique approach to the concise synthesis of highly optically active spirooxazolines and the discovery of a more potent oxindole-type phytoalexin analogue. Journal of the American Chemical Society. 2010;132(43):15328-33.
68. Grigg R, Aly MF, Sridharan V, Thianpatanagul S. Decarboxylative transamination. A new route to spirocyclic and bridgehead-nitrogen compounds. Relevance to α-amino acid decarboxylases. Journal of the Chemical Society, Chemical Communications. 1984(3):182-3.
69. Nair V, Sheela K, Rath NP. Dipolar Cycloaddition Reactions of Isatin Derived Azomethine Ylide with 3, 4-Diphenylcyclobutene-1, 2-dione: Synthesis of Novel Spiro [oxindole-3, 2′-pyrrolidine] Derivatives. Chemistry Letters. 2000;29(9):980-1.
70. Hu XF, Feng YQ. Synthesis of Novel Spiroheterocyclic Framework via the Regioselective 1, 3-Dipolar Cycloaddition Reaction of Azomethine Ylides. Synthetic communications. 2005;35(13):1747-52.
71. Zhang X-N, Li Y-X, Zhang Z-H. Nickel chloride-catalyzed one-pot three-component synthesis of pyrazolophthalazinyl spirooxindoles. Tetrahedron. 2011;67(38):7426-30.
72. Macaev F, Sucman N, Shepeli F, Zveaghintseva M, Pogrebnoi V. Facile and convenient one-pot process for the synthesis of spirooxindole derivatives in high optical purity using (−)-(S)-Brevicolline as an organocatalyst. Symmetry. 2011;3(2):165-70.
73. Liang B, Kalidindi S, Porco Jr JA, Stephenson CR. Multicomponent reaction discovery: three-component synthesis of spirooxindoles. Organic letters. 2010;12(3):572-5.
74. Balamurugan K, Perumal S, Menendez JC. New four-component reactions in water: a convergent approach to the metal-free synthesis of spiro [indoline/acenaphthylene-3, 4′-pyrazolo [3, 4-b] pyridine derivatives. Tetrahedron. 2011;67(18):3201-8.
75. Chen H, Shi D. Efficient one-pot synthesis of spiro [indoline-3, 4′-pyrazolo [3, 4-e][1, 4] thiazepine] dione via three-component reaction. Tetrahedron. 2011;67(31):5686-92.
76. Chen W-B, Wu Z-J, Pei Q-L, Cun L-F, Zhang X-M, Yuan W-C. Highly enantioselective construction of spiro [4H-pyran-3, 3′-oxindoles] through a domino Knoevenagel/Michael/cyclization sequence catalyzed by cupreine. Organic Letters. 2010;12(14):3132-5.
77. Singh G, Singh T, Lakhan R. Synthesis, C-13 NMR and anticonvulsant activity of new isatin-based spiroazetidinones. 1997.
78. Jarrahpour A, Khalili D. Synthesis of some mono-and bis-spiro-β-lactams of

benzylisatin. Tetrahedron Letters. 2007;48(40):7140-3.
79. Mulwad V, Mir AA. Synthesis and antibacterial screening of N-[coumarin-6-yl] spiro-indoloazetidin-2-ones/thiazolidin-4-ones. Journal of the Korean Chemical Society. 2008;52(6):649-56.
80. Marti C, Carreira EM. Construction of Spiro [pyrrolidine-3, 3′-oxindoles]− recent applications to the synthesis of oxindole alkaloids. European Journal of Organic Chemistry. 2003;2003(12):2209-19.
81. PONGLUX D, WONGSERIPIPATANA S, AIMI N, NISHIMURA M, ISHIKAWA M, SADA H, et al. Structure and synthesis of two new types of oxindole alkaloids found from Uncaria salaccensis. Chemical and pharmaceutical bulletin. 1990;38(2):573-5.
82. Bascop S, Sapi J, Laronze J, Levy J. On the synthesis of the oxindole alkaloid:(±)-Horsfiline. Heterocycles. 1994;38(4):725-32.
83. von Nussbaum F, Danishefsky SJ. A rapid total synthesis of spirotryprostatin B: proof of its relative and absolute stereochemistry. Angewandte Chemie International Edition. 2000;39(12):2175-8.
84. Pictet A, Spengler T. Über die Bildung von Isochinolin-derivaten durch Einwirkung von Methylal auf Phenyl-äthylamin, Phenyl-alanin und Tyrosin. Berichte der deutschen chemischen Gesellschaft. 1911;44(3):2030-6.
85. Shavel J, Zinnes H. Oxindole Alkaloids. I. Oxidative-Rearrangement of Indole Alkaloids to their Oxindole Analogs. Journal of the American Chemical Society. 1962;84(7):1320-1.
86. Pellegrini C, Strässler C, Weber M, Borschberg H-J. Synthesis of the oxindole alkaloid (−)-horsfiline. Tetrahedron: Asymmetry. 1994;5(10):1979-92.
87. Edmondson S, Danishefsky SJ, Sepp-Lorenzino L, Rosen N. Total synthesis of spirotryprostatin A, leading to the discovery of some biologically promising analogues. Journal of the American Chemical Society. 1999;121(10):2147-55.
88. Wang H, Ganesan A. A biomimetic total synthesis of (−)-spirotryprostatin B and related studies. The Journal of organic chemistry. 2000;65(15):4685-93.
89. Somei M, Noguchi K, Yamagami R, Kawada Y, Yamada K, Yamada F. Preparation and a Novel Rearrangement Reaction of 1, 2, 3, 4-tetrahydro-9-hydroxy-β-carboline, and Their Applications for the Total Synthesis of (±)-Coerulescine. Heterocycles. 2000;53(1):7-10.
90. Finch N, Gemenden C, Hsu IH-C, Taylor W. Oxidative transformations of indole alkaloids. II. The preparation of oxindoles from cis-DE-Yohimbinoid alkaloids. The partial synthesis of carapanaubine. Journal of the American Chemical Society. 1963;85(10):1520-3.
91. Jossang A, Jossang P, Hadi HA, Sevenet T, Bodo B. Horsfiline, an oxindole alkaloid from Horsfieldia superba. The Journal of Organic Chemistry. 1991;56(23):6527-30.
92. Wearing XZ, Cook JM. Enantiospecific, stereospecific total synthesis of the oxindole alkaloid alstonisine. Organic letters. 2002;4(24):4237-40.
93. Palmisano G, Annunziata R, Papeo G, Sisti M. Oxindole alkaloids. A novel non-biomimetic entry to (−)-Horsfiline. Tetrahedron: Asymmetry. 1996;7(1):1-4.
94. Sebahar PR, Osada H, Usui T, Williams RM. Asymmetric, stereocontrolled total synthesis of (+) and (−)-spirotryprostatin B via a diastereoselective azomethine ylide [1, 3]-dipolar cycloaddition reaction. Tetrahedron. 2002;58(32):6311-22.

95. Jones K, Wilkinson J. A total synthesis of horsfiline via aryl radical cyclisation. Journal of the Chemical Society, Chemical Communications. 1992(24):1767-9.
96. Lizos D, Tripoli R, Murphy JA. A novel and economical route to (±)-horsfiline using an aryl iodoazide tandem radical cyclisation strategy. Chemical Communications. 2001(24):2732-3.
97. Overman LE, Rosen MD. Total synthesis of (−)-spirotryprostatin B and three stereoisomers. Angewandte Chemie International Edition. 2000;39(24):4596-9.
98. Alper PB, Meyers C, Lerchner A, Siegel DR, Carreira EM. Facile, novel methodology for the synthesis of spiro [pyrrolidin-3, 3′-oxindoles]: catalyzed ring expansion reactions of cyclopropanes by aldimines. Angewandte Chemie International Edition. 1999;38(21):3186-9.
99. Altowyan MS, Barakat A, Al-Majid AM, Al-Ghulikah H. Spiroindolone analogues as potential hypoglycemic with dual inhibitory activity on α-amylase and α-glucosidase. Molecules. 2019;24(12):2342.
100. Elya B, Basah K, Mun'im A, Yuliastuti W, Bangun A, Septiana EK. Screening of α-glucosidase inhibitory activity from some plants of Apocynaceae, Clusiaceae, Euphorbiaceae, and Rubiaceae. Journal of Biomedicine and Biotechnology. 2012;2012.
101. Zhou J, Zhou S. Antihypertensive and neuroprotective activities of rhynchophylline: the role of rhynchophylline in neurotransmission and ion channel activity. Journal of ethnopharmacology. 2010;132(1):15-27.
102. BAN Y, SETO M, OISHI T. The synthesis of 3-spirooxindole derivatives. VII. Total synthesis of alkaloids (±)-rhynchophylline and (±)-isorhynchophylline. Chemical and Pharmaceutical Bulletin. 1975;23(11):2605-13.
103. Deiters A, Pettersson M, Martin SF. General strategy for the syntheses of corynanthe, tacaman, and oxindole alkaloids. The Journal of Organic Chemistry. 2006;71(17):6547-61.
104. Nagata K, Ishikawa H, Tanaka A. Formal syntheses of dihydrocorynantheine and isorhynchophylline via proline catalyzed Mannich-Michael reaction. Heterocycles. 2010;81(8):1791-8.
105. Zhang H, Ma X, Kang H, Hong L, Wang R. The enantioselective formal synthesis of rhynchophylline and isorhynchophylline. Chemistry–An Asian Journal. 2013;8(3):542-5.
106. Amat M, Ramos C, Pérez M, Molins E, Florindo P, Santos MM, et al. Enantioselective formal synthesis of ent-rhynchophylline and ent-isorhynchophylline. Chemical Communications. 2013;49(19):1954-6.
107. Wanner MJ, Ingemann S, van Maarseveen JH, Hiemstra H. Total synthesis of the spirocyclic oxindole alkaloids Corynoxine, Corynoxine B, Corynoxeine, and Rhynchophylline. European Journal of Organic Chemistry. 2013;2013(6):1100-6.
108. Xu J, Shao L-D, Shi X, Ren J, Xia C, Zhao Q-S. Collective formal synthesis of (±)-rhynchophylline and homologues. RSC advances. 2016;6(68):63131-5.
109. Zhang Z, Zhang W, Kang F, Ip FC, Ip NY, Tong R. Asymmetric total syntheses of rhynchophylline and isorhynchophylline. The Journal of Organic Chemistry. 2019;84(17):11359-65.
110. Lounasmaa M. Preparation of (±)-hirsutine and (±)-isocorynantheidine. Heterocycles. 1998;49:445-50.
111. Villa RA, Xu Q, Kwon O. Total synthesis of (±)-hirsutine: application of phosphine-catalyzed imine–allene [4+ 2] annulation. Organic letters. 2012;14(17):4634-

7.
112. Mali PR, Shirsat PK, Khomane N, Nayak L, Nanubolu JB, Meshram H. 1, 3-dipolar cycloaddition reactions for the synthesis of novel oxindole derivatives and their cytotoxic properties. ACS Combinatorial Science. 2017;19(10):633-9.
113. Hati S, Tripathy S, Dutta PK, Agarwal R, Srinivasan R, Singh A, et al. Spiro [pyrrolidine-3, 3-oxindole] as potent anti-breast cancer compounds: Their design, synthesis, biological evaluation and cellular target identification. Scientific reports. 2016;6(1):1-10.
114. Liu S-J, Zhao Q, Peng C, Mao Q, Wu F, Zhang F-H, et al. Design, synthesis, and biological evaluation of nitroisoxazole-containing spiro [pyrrolidin-oxindole] derivatives as novel glutathione peroxidase 4/mouse double minute 2 dual inhibitors that inhibit breast adenocarcinoma cell proliferation. European Journal of Medicinal Chemistry. 2021;217:113359.
115. Kuntiyong P, Piboonsrinakara N, Bunrod P. Synthesis of Quinolizidinone and Indolizidinone Using N-Acyliminium Ion Cyclization and a One-Pot Procedure for Preparation of Benzoquinolizidinone. Heterocycles: an international journal for reviews and communications in heterocyclic chemistry. 2014;89(2):437-52.

มหาวิทยาลัยศิลปากร

VITA

NAME	Mr. Artid Buaphan
DATE OF BIRTH	28 September 1986
PLACE OF BIRTH	Nakhon Pathom, Thailand
INSTITUTIONS ATTENDED	2005 - 2008 Bachelor of Science in Chemistry, Silpakorn University, Thailand 2012 - 2014 Master of Science in Organic Chemistry, Silpakorn University, Thailand 2017-present Doctor of Philosophy (Organic Chemistry), Silpakorn University, Thailand
HOME ADDRESS	10/2 Village No.2, Thammasala Sub-district, Muang District, Nakorn Pathom, Thailand, 73000
PUBLICATION	1. Kuntiyong, P., Piboonsrinakara, N., Bunrod, P., Namborisut, D., Akkarasamiyo, S., Songthammawat, P., Hemmara, C., Buaphan, A., Kongkathip, B. "Synthesis of Quinolizidinone and Indolizidinone Using N-Acyliminium Ion Cyclization and a One-Pot Procedure for Preparation of Benzoquinolizidinone". HETEROCYCLES, 2014, 89(2), 437. 2. Kuntiyong, P.; Inprung, N.; Phakdeeyothin, K.; Buaphan, A.; Thammapichai, K. "Synthesis of spiro[indolizidine-1,3'oxindole] from L-glutamic acid", Tetrahedron, 2020, 76 (24), 131261